Neural Plasticity

Role of Visual Cortical Plasticity in the Development and Treatment of Amblyopia and other Neurodevelopmental Disorders

Lead Guest Editor: Kathryn Murphy
Guest Editors: Claudia Lunghi, Hirofumi Morishita, Elizabeth Quinlan, and Ben Thompson

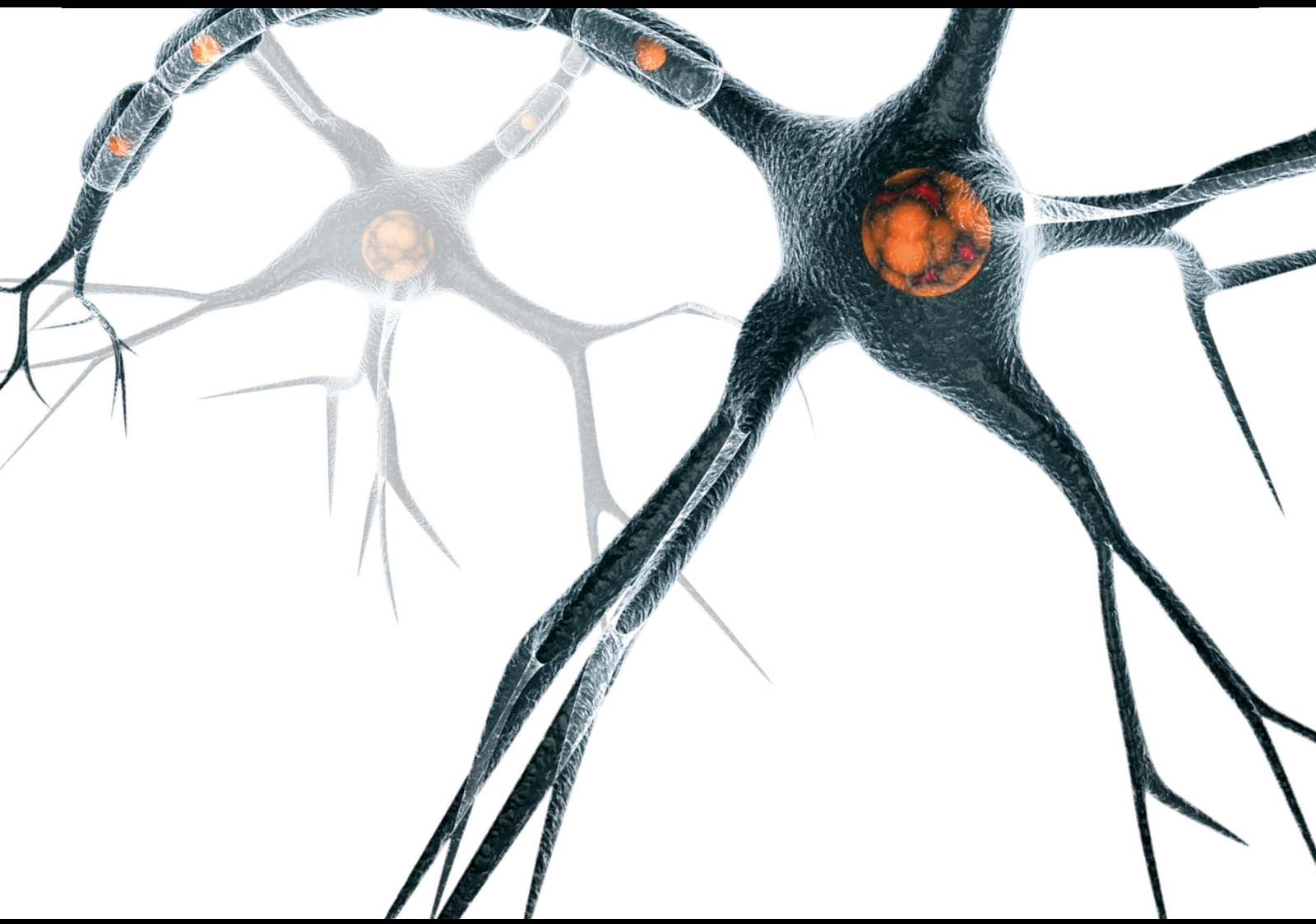

Role of Visual Cortical Plasticity in the Development and Treatment of Amblyopia and other Neurodevelopmental Disorders

Neural Plasticity

Role of Visual Cortical Plasticity in the Development and Treatment of Amblyopia and other Neurodevelopmental Disorders

Lead Guest Editor: Kathryn Murphy
Guest Editors: Claudia Lunghi, Hirofumi Morishita, Elizabeth Quinlan, and Ben Thompson

Contents

Hindawi
Neural Plasticity
Volume 2020, Article ID 1673897, 10 pages
https://doi.org/10.1155/2020/1673897

Research Article

Systematic Analysis of Environmental Chemicals That Dysregulate Critical Period Plasticity-Related Gene Expression Reveals Common Pathways That Mimic Immune Response to Pathogen

Milo R. Smith,[1,2,3,4,5,6,7] Priscilla Yevoo,[1,3,4,6,7] Masato Sadahiro,[1,3,4,6,7] Ben Readhead,[5,8] Brian Kidd,[2,5] Joel T. Dudley,[2,5] and Hirofumi Morishita[1,3,4,6,7]

[1]*Department of Psychiatry, Icahn School of Medicine at Mount Sinai, 1 Gustave L Levy Place, New York NY 10029, USA*
[2]*Department of Genetics and Genomic Sciences, Icahn School of Medicine at Mount Sinai, 1 Gustave L Levy Place, New York NY 10029, USA*
[3]*Nash Family Department of Neuroscience, Icahn School of Medicine at Mount Sinai, 1 Gustave L Levy Place, New York NY 10029, USA*
[4]*Department of Ophthalmology, Icahn School of Medicine at Mount Sinai, 1 Gustave L Levy Place, New York NY 10029, USA*
[5]*Institute for Next Generation Healthcare, Icahn School of Medicine at Mount Sinai, 1 Gustave L Levy Place, New York NY 10029, USA*
[6]*Friedman Brain Institute, Icahn School of Medicine at Mount Sinai, 1 Gustave L Levy Place, New York NY 10029, USA*
[7]*Mindich Child Health & Development Institute, Icahn School of Medicine at Mount Sinai, 1 Gustave L Levy Place, New York NY 10029, USA*
[8]*ASU-Banner Neurodegenerative Disease Research Center, Biodesign Institute, Building A, 1001 S McAllister Ave, Tempe, AZ 85281, USA*

Correspondence should be addressed to Joel T. Dudley; joel.dudley@gmail.com
and Hirofumi Morishita; hirofumi.morishita@mssm.edu

Received 22 May 2019; Accepted 4 February 2020; Published 5 May 2020

Academic Editor: Alfredo Berardelli

The tens of thousands of industrial and synthetic chemicals released into the environment have an unknown but potentially significant capacity to interfere with neurodevelopment. Consequently, there is an urgent need for systematic approaches that can identify disruptive chemicals. Little is known about the impact of environmental chemicals on critical periods of developmental neuroplasticity, in large part, due to the challenge of screening thousands of chemicals. Using an integrative bioinformatics approach, we systematically scanned 2001 environmental chemicals and identified 50 chemicals that consistently dysregulate two transcriptional signatures of critical period plasticity. These chemicals included pesticides (e.g., pyridaben), antimicrobials (e.g., bacitracin), metals (e.g., mercury), anesthetics (e.g., halothane), and other chemicals and mixtures (e.g., vehicle emissions). Application of a chemogenomic enrichment analysis and hierarchical clustering across these diverse chemicals identified two clusters of chemicals with one that mimicked an immune response to pathogen, implicating inflammatory pathways and microglia as a common chemically induced neuropathological process. Thus, we established an integrative bioinformatics approach to systematically scan thousands of environmental chemicals for their ability to dysregulate molecular signatures relevant to critical periods of development.

1. Introduction

Millions of newly synthesized chemical substances are added to the global inventory each year [1]. Tens of thousands of these are commercially produced and may be exposed to human beings [2]. Our dedication to generating this impressive chemical inventory has not been matched by our capacity to screen these chemicals for their impact on human brain

development. Neurodevelopmental disorders are highly prevalent, occurring in 17% of children, and this rate may be increasing [3], demanding serious consideration of how synthetic chemicals introduced into the human environment impact brain development. Human and animal studies have demonstrated that a number of environmental chemicals profoundly disrupt prenatal neural events such as proliferation, migration, and differentiation, leading to severe neurodevelopmental disorder [4]. In contrast, identification of chemicals impacting postnatal and childhood neurodevelopment has received less effort.

During childhood, the human brain undergoes refinement and reorganization during windows of heightened brain plasticity. These critical periods allow refinement of brain circuits by sensory and social experiences, which helps to establish normal perception and higher cognitive function [5–10]. Disruption of these critical periods can alter neural circuits that shape function and behavior, which may in turn contribute to neurodevelopmental disorders such as autism [11, 12].

Despite the potential for deleterious impacts on health, the role of environmental chemicals on critical period neuroplasticity has received minimal attention, although a few disruptors of developmental plasticity have been identified, including alcohol and bisphenol A [13, 14]. However, given the number of synthetic chemicals present in the environment, we need systematic approaches in order to accelerate the discovery of chemicals that damage brain development.

In our proof-of-principle study, we applied an integrative bioinformatics approach to assess hundreds of known neurotoxicants; using this strategy, we were able to rapidly identify and demonstrate that lead (Pb) disrupts critical period brain plasticity [15]. In this study, we built on that proof-of-principle, scanning across thousands of environmental chemicals to identify those that dysregulate two gene signatures of visual cortex critical period plasticity in mice. Among the 50 chemicals that dysregulated both gene signatures, we identified enrichments of common immune pathways, implicating microglia and inflammatory pathways in the pathology induced by exposure to these chemicals. Our findings show that an integrative bioinformatics approach is well suited to systematically assess the vast chemical space to identify candidate compounds that disrupt brain development.

2. Methods

2.1. Critical Period Plasticity-Related Signatures. Critical period signatures were generated from publicly available data obtained from juvenile and Lynx1-/- mice ([16]; GSE89757). Briefly, transcriptomes from the primary visual cortex (V1) in juvenile C57BL/6 mice on postnatal day (P) 29, adult Lynx1-/- mice (>P60), and adult C57BL/6 (>P60) mice ($n = 3$ each group) were profiled by microarray. Probe-level data were background corrected, quantile-normalized, and log2-transformed with Limma [17], yielding 9657 genes that mapped to human orthologues according to the Mouse Genome Informatics homology reference. Critical period signatures were defined as differential gene expression across the 9657-gene transcriptome in juvenile wild-type or Lynx1-/- adult vs. wild-type adult.

2.2. Environmental Chemical Signatures. Chemical signatures were derived as gene sets from Comparative Toxicogenomics Database (CTD) data. Only the chemical-mRNA relationships but not the chemical-protein relationships were extracted from 1.25 million CTD relationships between chemicals and 33 biological substrates (protein, DNA, mRNA, etc.). We only kept the chemical-mRNA relationships associated with PubMed references. To maximize power to detect biological and chemical characteristics in downstream analysis, all chemicals, including biologics and chemicals with unknown relevance to human exposure, were retained. Three gene set libraries consisting of groups of genes differentially expressed by a given chemical were created, limiting gene members to those also expressed in the critical period transcriptomes consisting of the 9657 genes after filtering for a minimum gene number filter of 3 genes: (1) CHEM composite (2001 chemicals; 3–750 genes per gene set), consisting of genes whose expression was either increased or decreased by a given chemical; (2) CHEM up (1742 chemicals; 3–726 genes per gene set), consisting of genes that were increased by a given chemical; and (3) CHEM down (1242 chemicals; 3–653 genes per gene set), consisting of genes that are decreased by a given chemical. Note that there are overlaps of chemicals among three libraries as CHEM composite gene sets were split into CHEM up and CHEM down libraries.

2.3. Molecular Matching. Gene Set Enrichment Analysis (GSEA) was used to assess the transcriptional similarity between a given chemical and the critical period signatures. GSEA was selected over other methods, such as the Connectivity Map approach [18], because GSEA controls the size of the input gene set (e.g., chemical gene sets) in its false discovery rate (FDR) calculation, which otherwise generally correlates with a P value; this is ideal in this context given the wide range of our chemical signature sizes (3 to 750 genes). Molecular matches using GSEA were computed between the CHEM composite, CHEM up, and CHEM down libraries and the juvenile and Lynx1-/- signatures; matches were considered significant if $P < 0.05$ and FDR < 0.25. An FDR of 0.25 was chosen for this exploratory discovery study to find candidate hypothesis to be further validated as a result of future research while avoiding overlooking potentially significant results. An initial exploratory GSEA was performed to assess whether CHEM composite signatures tended to impact expression of genes up- or downregulated in the juvenile and Lynx1-/- critical period signatures, as determined by the binomial test. Given that genes belonging to the CHEM composite signatures were much more likely to yield negative GSEA scores, indicating that they were among the downregulated genes in both juvenile and Lynx1-/- signatures, we then assessed separately if chemicals increased or decreased these genes applying GSEA to the 1742 CHEM up signatures and the 1242 CHEM down signatures.

2.4. Chemogenomic Enrichment Analysis. To uncover neurobiology of the 50 candidate plasticity-disrupting chemicals, we applied chemogenomic enrichment analysis (CGEA) to identify biological pathways overrepresented among the 50 chemicals relative to the remaining 1692 CHEM up signatures. To do so, we calculated gene set enrichment for 5191 Gene Ontology (GO) Biological Processes (BP) and for 96 Library of Integrated Network-based Cellular Signatures (LINCS) ligand expression profiles, using Fisher's exact test to assess the likelihood that genes overlapped between a given CHEM up signature and a given GO BP or ligand pathway. Enrichments were binarized to 1 if Padj < 0.05 and to 0 otherwise, and a hypergeometric test as implemented in the hypergea R package [19] was performed for each of 5191 GO BP and 96 LINCS ligand profiles to determine whether a given pathway was more likely to have a chance to be enriched in the 50 CHEM up signatures compared to the 1692 chemicals in the background.

2.5. Human Exposure Annotations. The risk of human exposure for a given chemical was determined from the literature, using the PubMed and Google Scholar search tools. Specifically, each name of the 50 chemicals derived from informatics analysis was searched in combination with other key terms such as "neurodevelopment", "neurotoxin", "neurotoxicity", "neurological side effects", and "cognitive development". We added more explanation to this section in Discussion. We identified 11 chemicals as high exposure risk, 14 as medium exposure risk, and 25 as low exposure risk. For example, chemicals like pyridaben, which are commonly detected on agricultural produce consumed by humans [20], were considered a high risk for exposure. In contrast, tool chemicals that are only used in the laboratory, such as SB-431542, were considered low risk. Medium risk included chemicals such as medications that are no longer the primary prescription for a given indication.

2.6. Activated Microglia Gene Set Enrichment. A total of 72 genes that increased by lipopolysaccharide- (LPS-) activated microglia were identified from the supplementary tables of a previous study [21]. Enrichments between the activated microglia genes and each of the 50 CHEM up signatures were calculated using Fisher's exact test, using as a background 15071 genes expressed in both microglia and CTD chemicals.

2.7. Statistical Analyses. Statistical analyses were completed in the R programming language (v 3.2.2). In cases of multiple hypothesis testing, P values were corrected using the false discovery rate (FDR) approach [22]; the corrected values are referred to as P adjusted (Padj) throughout the manuscript.

3. Results

3.1. Molecular Matching of Critical Period and Environmental Chemical Signatures. We generated two critical period signatures from transcriptomes of the primary visual cortex (V1) of juvenile wild-type mice during the peak of the critical period for visual cortex-mediated ocular dominance plasticity at postnatal day (P) 26 [23] or adult Lynx1-/- mice that have open-ended critical period plasticity throughout life [24] in comparison with adult wild type, revealing differential expression of 9657 genes (signatures derived from GSE89757 [16]) (Figure 1(a)). To determine the impact of environmental chemicals on juvenile and Lynx1-/- plasticity signatures, we used GSEA [25] to compute molecular matches of chemical gene expression signatures derived from the Comparative Toxicogenomics Database (CTD) to critical period signatures. Using 2001 composite chemical signatures (i.e., genes either increased or decreased by a given chemical, referred to as CHEM composite) (Figure 1(b)), we found that chemicals were more likely to impact the expression of genes that were downregulated in juvenile and Lynx1-/- critical period signatures, rather than genes that were upregulated (binomial tests: $P = 1.8 \times 10^{-4}$ and $P < 2.2 \times 10^{-16}$) (Figure 1(c)). Because environmental chemicals preferentially impact genes downregulated in the critical period signatures, we used GSEA to compute molecular matches between the directional chemical signatures (CHEM up: sets of genes increased by 1742 chemicals; CHEM down: sets of genes decreased by 1242 chemicals) and assessed only negative GSEA scores (reflecting a chemical's impact on downregulated critical period genes) to find that chemicals tended to preferentially increase, as opposed to decrease, the expression of genes downregulated in both juvenile and Lynx1-/- signatures (binomial tests: $P = 2.3 \times 10^{-12}$ and $P < 2.2 \times 10^{-16}$) (Figures 2(a) and 2(b)). We focused our subsequent analysis on 50 chemicals (of a total of 1742) that increased genes whose expression was downregulated in both of the critical period signatures, which was a significant overlap (Fisher's exact test: $P = 2.2 \times 10^{-16}$, OR = 14.4) (Figure 2(b)). Genes downregulated in the critical period signatures are putative "brakes" on developmental brain plasticity, suggesting that these 50 chemicals may disrupt neurodevelopment by prematurely expressing plasticity-dampening molecules.

3.2. Chemicals That Dysregulate Critical Period Signatures Converge on Pathogen Response Inflammatory Pathways. The 50 chemicals shown by GSEA to impact both juvenile and Lynx1-/- signatures were diverse and included pesticides (e.g., pyridaben), antimicrobials (e.g., bacitracin), metals (e.g., mercury), anesthetics (e.g., halothane), and other compounds or mixtures (e.g., vehicle emissions) (Supplementary Table 1). To gain insight into biological effects that might be shared by these diverse chemicals, we applied chemogenomic enrichment analysis (CGEA) by calculating overrepresentation of biological pathways in each of the 50 chemical signatures, relative to the remaining 1692 chemical signatures (see Figure 3 for the workflow). Using 5191 Gene Ontology (GO) Biological Process (BP) gene sets, we identified 33 BPs overrepresented in the 50 chemical signatures (at Padj < 0.05). CGEA enrichments of GO BPs were overwhelmingly associated to response to pathogen, immune cell chemotaxis, and inflammation (Figure 4(a)).

To understand the potential cytokine signaling by which these chemicals induce inflammatory responses, we computed overrepresentations for 96 ligand gene sets derived from the Enrichr library (http://amp.pharm.mssm.edu/Enrichr/) [26] which includes the Library of Integrated

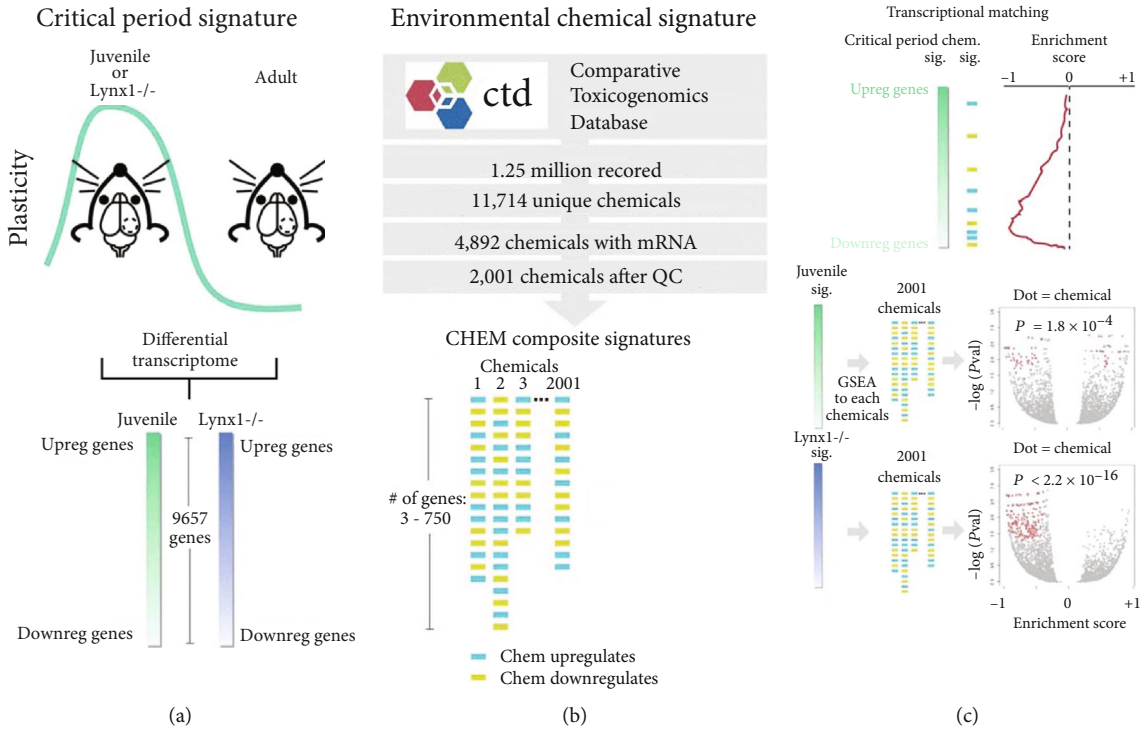

Figure 1: Environmental chemicals preferentially impact expression of genes downregulated in the critical period brain plasticity signatures of juvenile and Lynx1-/- mice. (a) We generated two in vivo critical period transcriptome signatures (juvenile at the peak of the endogenous critical period at P26 and Lynx1-/- adult mice, which maintain critical period-like plasticity) from public data. (b) Environmental chemical signatures using genes either increased or decreased by a given chemical (CHEM composite) were derived from the Comparative Toxicogenomics Database. (c) Molecular matches were computed to the critical period signatures using Gene Set Enrichment Analysis (GSEA) to identify that chemicals preferentially impact genes downregulated in the critical period signatures.

Network-based Cellular Signatures (LINCS) database, comprising genes upregulated after exposure to cytokines or growth factors. Consistent with the GO overrepresentations, we observed consistent overrepresentations of genes increased by IL-1 (5/7 IL-1 gene sets) and TNF-α (5/5 TNF-α gene sets), suggesting that these chemicals mimic an immune response to pathogen at the level of cytokine signaling (Figure 4(b)).

To determine whether these enrichments were consistent across all 50 chemicals, we performed hierarchical clustering on the negative log Padj values of the BP and ligand enrichments. This analysis yielded two primary clusters: Cluster A (29 chemicals) with few enrichments for inflammatory pathways and instead enriched in antimicrobials and Cluster B (21 chemicals) enriched in inflammatory pathways and more likely to be exposed to humans (Cluster B has 15/21 chemicals with medium or high exposure likelihood versus 10/29 chemicals in Cluster A; 2.07-fold enrichment; binomial test expecting equal likelihood: $P = 0.103$) (Figure 5 and Supplementary Table 1). These results suggest that 50 chemicals that dysregulate critical period signatures segregate into two major clusters; the members of one of these clusters are more likely to be exposed to humans and mimic an immune response to pathogen.

3.3. Chemicals That Dysregulate Critical Period Signatures Mimic Lipopolysaccharide-Activated Microglia. Given that CGEA identified enrichments of response to pathogen, immune cell chemotaxis, and inflammatory pathways, including the IL-1 and TNF-α pathways, we sought to determine whether these chemicals induce a peripheral pathogen-like inflammatory response in microglia. Microglia, the resident immune cells of the brain, not only survey the landscape for pathogens and cellular detritus but also support neural function and are required for critical period plasticity [27].

We hypothesized that these chemicals activate microglia, shifting them from the "resting-state" phenotype necessary to facilitate plasticity to a vigilant, activated state. To test this hypothesis, we generated a transcriptional signature of lipopolysaccharide- (LPS-) activated microglia, comprising 72 genes increased by LPS [21]. We then assessed this signature for overlap with the genes in a given CHEM up signature. The majority of chemicals (58%) mimicked an activated microglia phenotype at the transcriptional level, and Cluster B was more likely than Cluster A to display this phenotype (Fisher's exact test: OR = 3.8, $^*P = 0.26$) (Figure 6(a) and Supplementary Table 2), indicating that a subset of these chemicals activates microglia in a similar manner to LPS. These analyses indicate that a subset of chemicals that increase the expression of putative brakes on critical period plasticity, and whose gene expression signatures are enriched for inflammatory pathways, induces a transcriptional response similar to that of microglial activation, suggesting that exposure of these environmental chemicals during the critical period could activate microglia, shifting them from

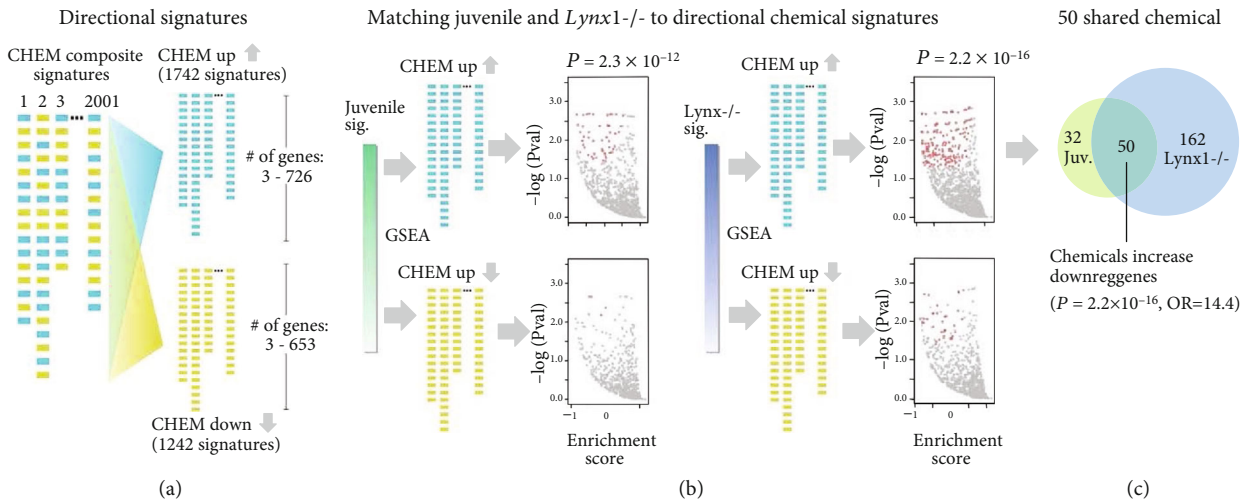

Figure 2: Molecular matching via GSEA identifies 50 chemicals that increase expression of genes downregulated in the juvenile and Lynx1-/- critical period transcriptome signatures. (a) 2001 CHEM composite gene sets were split into CHEM up (1742 signatures) and CHEM down (1242 signatures) libraries to assess the directional impact of each chemical on critical period gene expression. (b) GSEA was used to assess negative scores (reflecting a chemical's impact on downregulated critical period genes) for CHEM up and CHEM down signatures against the critical period signatures and the binomial test to assess a bias to up or down library. (c) Fifty chemicals increase downregulated critical period genes. See Supplementary Table 1 for a list of all 50 chemicals.

their physiological role in plasticity to a state of active watchfulness and disrupting critical period plasticity.

4. Discussion

Building on our recent proof-of-principle study [15], we established a transcriptome-based integrative bioinformatics approach to systematically identify environmental chemicals that dysregulate transcriptional signatures of critical periods of cortical plasticity. Previous high-throughput approaches typically used biochemical and cell-based experimental assays focused on a limited number of gene/protein expression or enzymatic activities. Although these assays may themselves be straightforward, they do not necessarily reflect more complex in vivo neurodevelopmental events. On the other hand, in vivo animal assays are low-throughput and only appropriate for the validation of screening results. Due to these limitations, no previous studies have attempted to systematically identify environmental chemicals that disrupt complex in vivo phenomenon such as critical periods of plasticity. Here, leveraging the utility of transcriptional signature matching to identify functional and mechanistic relationships [28], we matched multiple signatures of in vivo critical period plasticity to thousands of chemical signatures derived from public transcriptional data to systematically identify novel childhood critical period toxicant candidates.

The developmental consequences of disruption by these chemicals could be far-reaching. Disruption of the critical period for visual cortex plasticity prevents the development of an important visual function termed binocular matching of orientation preference [29], resulting in a disordered visual experience. Moreover, due to the hierarchical dependency of multiple critical periods (i.e., hearing, vision, language, and cognitive processes) across development, disruption of a sensory-specific critical period might ultimately interfere with higher-order cognitive functions [12]. In addition, given the fact that the mechanisms of plasticity identified in the visual critical period have been generalized to other brain regions and functions [30–32], critical period toxicants identified using the visual model may disrupt plasticity and neurodevelopment in other brain regions and for other functions.

Included among the 50 plasticity-disrupting chemical candidates we identified were both known and novel neurotoxicants with high exposure likelihood including inorganic metals (mercury, sodium arsenate), pesticides (pyridaben, chlorpyrifos, and carbofuran), anesthetics (chloroform and halothane), antimicrobials (bacitracin+nine others), and other chemicals (vehicle emissions, cyanuric acid—a common swimming pool water additive). There is evidence consistent with the ability of these chemicals to disrupt critical periods. For example, mercury levels have increased by 3-fold over the past 100 years, in large part due to power plant emissions and industrial byproducts [33]. Human exposure is primarily through the microorganism-processed methylated form (MeHg), which is found in aquatic organisms consumed as food, such as fish. Perinatal treatment of MeHg to mouse dams (embryonic day 7 (E7) to P7) at a dose of 0.59 mg/kg/day suggested a potential decrease in the maturation of parvalbumin-expressing neurons in the hippocampus of juvenile animals [34], suggesting that MeHg could delay the opening of critical periods, which requires the normal maturation of inhibitory neurons, such as parvalbumin-expressing cells [35]. Moreover, mercury, arsenic, chlorpyrifos, pyridaben, and vehicle emissions have been implicated in the neurodevelopmental disorder autism [20, 36–39], for which the critical period is emerging as a potential period of risk [15].

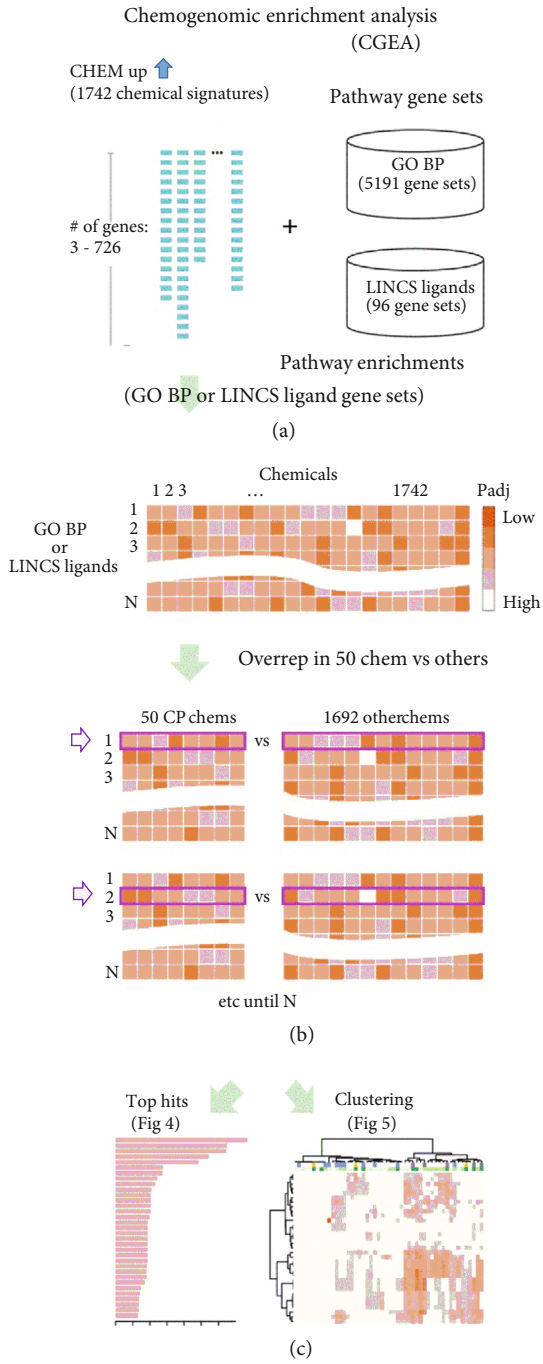

Figure 3: Chemogenomic enrichment analysis (CGEA) workflow. (a) Enrichments of 5191 Gene Ontology (GO) Biological Process (BP) and 96 Library of Integrated Network-based Cellular Signatures (LINCS) ligand gene sets were calculated for 1742 CHEM up signatures. (b) We calculated overrepresentation of pathways in each of 50 chemical signatures that impact critical period signatures, relative to the remaining 1692 chemical signatures. (c) Top overrepresentation hits were calculated (Figure 4), and hierarchical clustering was performed on enrichment Padj values (Figure 5).

A large portion of critical period-disrupting candidates were antimicrobials (10 of 50) indicating that the downstream pathways of antimicrobials may ultimately impact brain development. Bacitracin is used in humans as an antibiotic as well as in commercial farming practices to control microbes and in the feed of swine, chickens, and other livestock to promote growth [40]. Given the widespread administration of antibiotics to livestock for human consumption, there is considerable concern about the impact of residual antibiotic in animal products and its impact on human health [41]. Moreover, there is a growing recognition of the importance of the microbiome-immune-neural axis on health and disease and antibiotics can profoundly disrupt healthy microbiomes [42]. Bacitracin disrupts the microbiome and impacts BDNF levels [43], a growth factor involved in the opening of the visual critical period [35].

Given the diversity of the 50 candidate plasticity disruptors, we applied a chemogenomic enrichment analysis (CGEA) approach to identify shared pathways among these chemicals, which included response to pathogen, immune cell chemotaxis, and inflammatory pathways including IL-1 and TNF-α cytokine signaling. This suggests that chemicals that disrupt critical period plasticity may be perceived as invaders by the immune system, leading to induction of an inflammatory response. In the brain, this may involve activation of microglia. Should this occur during the critical period, it might shift microglia away from their physiological role in experience-dependent critical period plasticity [27] to a state of active watchfulness in which they are not able to facilitate experience-dependent brain development. Upon exposure to toxicants such as ozone and acetaminophen, peripheral immune cells (e.g., macrophages) activate and induce an inflammatory response that includes cytokines such as TNF, mimicking the response to Gram-negative bacterial pathogens [44]. Given the role of TNF in activating microglia [45–47], soluble transport of TNF across the blood-brain barrier [48] from peripherally stimulated immune cells could activate the stimulus. Future studies should assess the ability of individual chemicals to activate microglia and disrupt critical period plasticity.

This study was limited by the quality and breadth of available chemical data, and a future work will benefit from the toxicology in the 21st Century (Tox21) program, an ongoing effort to systematically profile the effect of tens of thousands of chemicals on the expression of 1500 genes in cell lines [49]. The chemical data used here were derived from heterogeneous tissues in multiple animal and cell models, not specifically focused on neurons or the brain [50]. Hence, specificity for neuronal phenotypes could be improved by extending current efforts to screen for damaging effects of toxicants in human cell lines [51] to neurons derived from human-induced pluripotent stem cells (iPSCs). Finally, we limited ourselves to two models of critical period plasticity; additional models, such as voluntary exercise-induced plasticity [52], may reveal additional insight regarding the mechanisms that can disrupt critical period plasticity.

In summary, we established an integrative bioinformatics paradigm for generating rational hypotheses about the impact of environmental chemicals on critical periods of brain plasticity, as well as their underlying mechanisms, with the goal of identifying targets for therapeutic intervention. This approach could be generalized to other brain

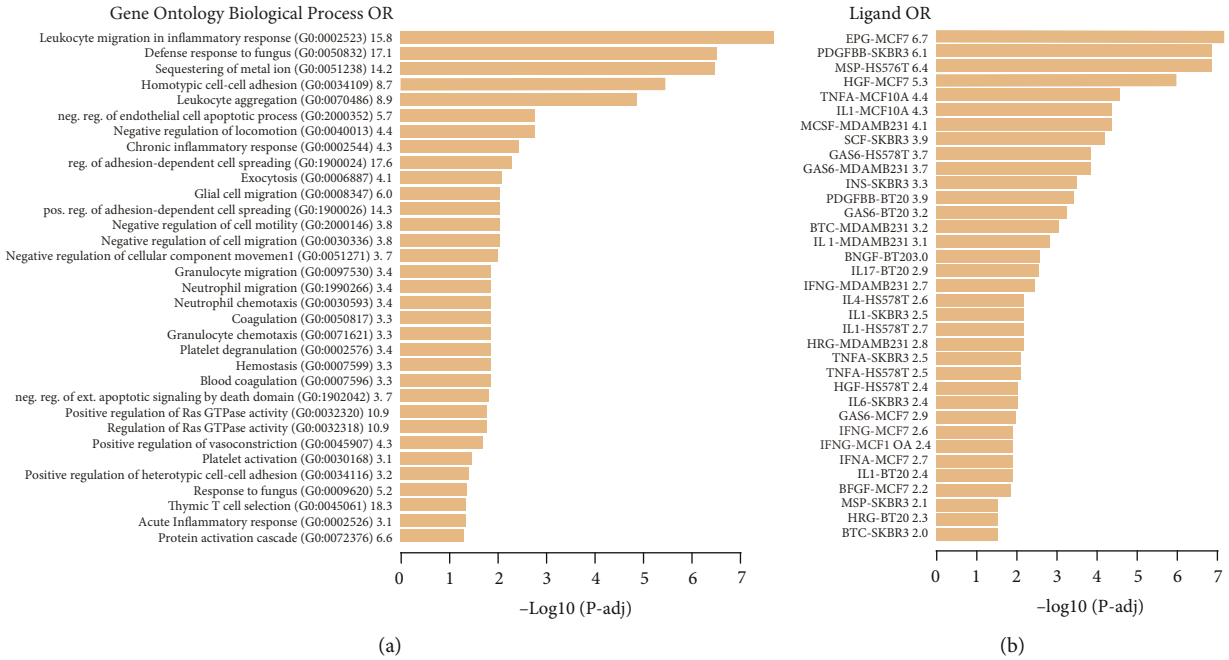

Figure 4: Chemogenomic enrichment analysis of 50 chemicals that increase expression of genes downregulated in the critical period signatures reveals inflammatory, response to pathogen, and immune cell chemotaxis pathways. We computed gene set enrichments for the CHEM up library (1742 chemical signatures) across 5191 Gene Ontology (GO) Biological Process (BP) gene sets and 96 LINCS ligand gene sets to yield 9,042,722 and 167,232 enrichment *P* values, which were corrected for multiple testing using the Benjamini and Hochberg approach. For each biological process or ligand, we calculated the overrepresentation of that gene set (if it was significant after multiple test correction) among the 50 chemicals identified as impacting both juvenile and Lynx1-/- critical period signatures, in comparison to the remaining 1692 chemicals, using a hypergeometric test (hypergea R package implementation). A pathway was considered associated with a chemical if the enrichment Padj < 0.05, yielding (a) 33 GO BP gene sets and (b) 48 LINCS ligand gene sets.

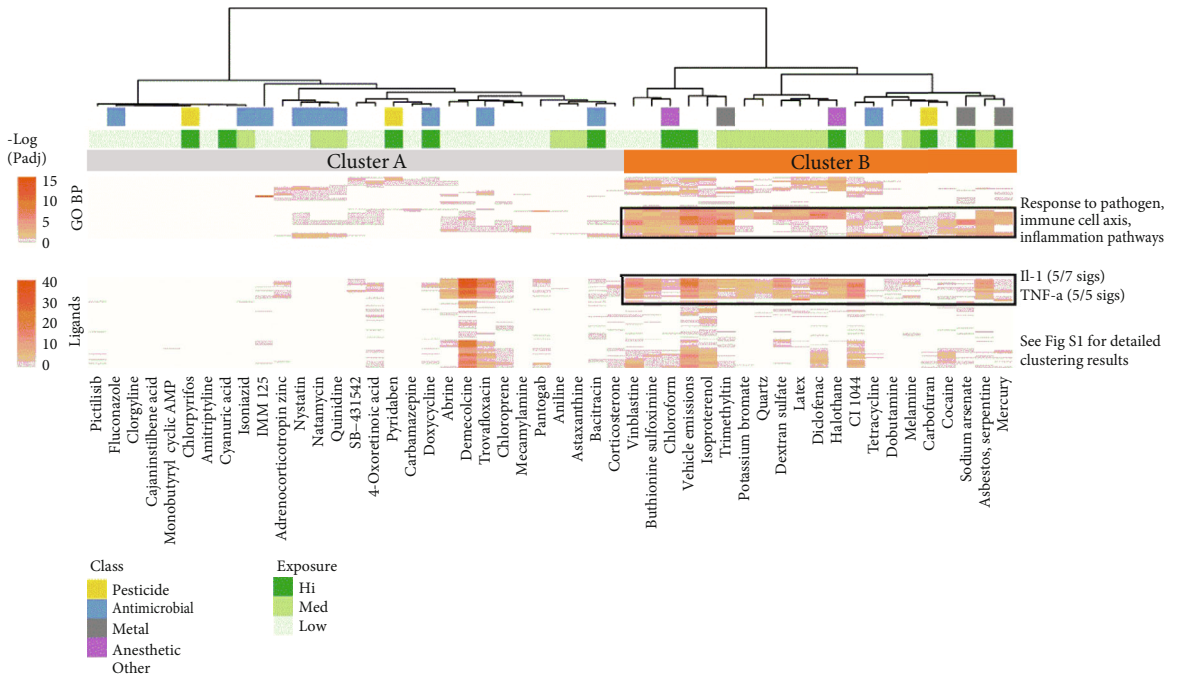

Figure 5: Clustering of chemical pathway enrichments identifies antimicrobial and inflammatory clusters. Hierarchical clustering (Ward D method) on the negative log Padj values of Gene Ontology (GO) Biological Process (BP) and LINCS ligand enrichment analysis revealed two clusters of chemicals. Cluster A (29 chemicals) contains few inflammatory pathway enrichments and 9 of the 10 antimicrobials in the set of 50 chemicals examined, whereas Cluster B contains the majority of enrichments for response to pathogen, inflammation, immune cell chemotaxis, and IL-1/TNF-α. See Supplementary Figure 1 for detailed enrichment information.

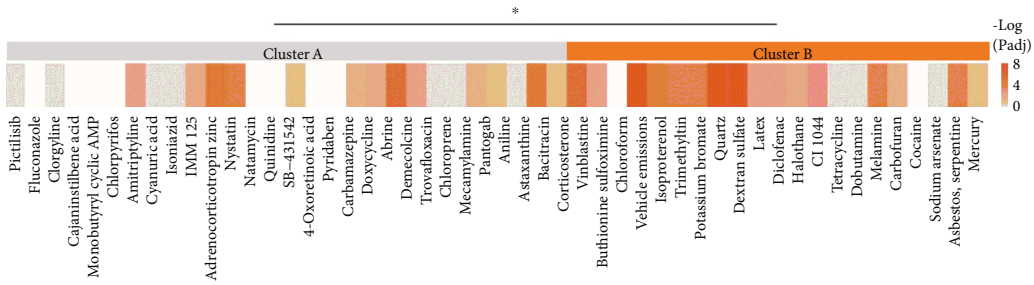

Figure 6: Fifty chemicals mimic the gene expression phenotype induced by LPS-activated microglia. We used Fisher's exact test to calculate the overlap of microglia genes increased by LPS activation to the genes in a given CHEM up signature. 58% of all chemicals were enriched (at Padj < 0.05), and Cluster B was more likely than Cluster A to display this phenotype (Fisher's exact test: OR = 3.8, $^{*}P = 0.26$). Chemicals ordered as in Figure 5.

phenotypes, allowing systematic assessment of the impact of chemicals on a wide array of brain development phenotypes.

Data Availability

The data used to support the findings of this study are included within the article.

Conflicts of Interest

The authors declare no competing interests.

Authors' Contributions

MRS, JTD, and HM designed the study; MRS, PY, and BR performed the analyses; MRS, BK, JTD, and HM provided the principal interpretations; MRS, JTD, and HM wrote the manuscript; and all authors approved the final manuscript.

Acknowledgments

This work was funded by a Traineeship, National Institute of Child Health and Human Development-Interdisciplinary Training in Systems and Developmental Biology and Birth Defects Grant T32H-D0-75735 (to M.R.S.); the Mindich Child Health and Development Institute Pilot Fund (to J.T.D. and H.M.); the Knights Templar Eye Foundation (to H.M.); the March of Dimes (to H.M.); the Whitehall Foundation (to H.M.); the Harris Family Foundation (to J.T.D.); and the National Institutes of Health Grants P30-ES-023515 (to J.T.D. and H.M.), R01-DK-098242, U54-CA189201, and R56-AG058469 (to J.T.D.), and R01-EY-024918, R01-EY-026053, and R21 MH106919 (to H.M.).

Supplementary Materials

Supplementary Table 1: chemicals that commonly increase putative brakes of both juvenile and Lynx1-KO transcriptome signatures. Supplementary Table 2: enrichment statistics for fifty chemicals that mimic the gene expression phenotype induced by LPS-activated microglia (sorted by an ascending *P* value). Supplementary Figure 1: expanded results of hierarchical clustering of GO BP and LINCS ligand CGEA for each of the 50 plasticity-disrupting candidate compounds (related to Figure 5). *(Supplementary Materials)*

References

[1] CAS, *CAS REGISTRY - the gold standard for chemical substance information*, American Chemical Society, 2018.

[2] D. Markell, "An overview of TSCA, its history and key underlying assumptions, and its place in environmental regulation," *Washington University Journal of Law & Policy*, vol. 32, pp. 333–375, 2010.

[3] C. A. Boyle, S. Boulet, L. A. Schieve et al., "Trends in the prevalence of developmental disabilities in US children, 1997–2008," *Pediatrics*, vol. 127, no. 6, pp. 1034–1042, 2011.

[4] D. Rice and S. Barone Jr., "Critical periods of vulnerability for the developing nervous system: evidence from humans and animal models," *Environmental Health Perspectives*, vol. 108, Suppl 3, pp. 511–533, 2000.

[5] S. E. Fox, P. Levitt, and C. A. Nelson III, "How the timing and quality of early experiences influence the development of brain architecture," *Child Development*, vol. 81, no. 1, pp. 28–40, 2010.

[6] J. S. Johnson and E. L. Newport, "Critical period effects in second language learning: the influence of maturational state on the acquisition of English as a second language," *Cognitive Psychology*, vol. 21, no. 1, pp. 60–99, 1989.

[7] T. L. Lewis and D. Maurer, "Multiple sensitive periods in human visual development: evidence from visually deprived children," *Developmental Psychobiology*, vol. 46, no. 3, pp. 163–183, 2005.

[8] C. A. Nelson, C. H. Zeanah, N. A. Fox, P. J. Marshall, A. T. Smyke, and D. Guthrie, "Cognitive recovery in socially deprived young children: the Bucharest Early Intervention Project," *Science*, vol. 318, no. 5858, pp. 1937–1940, 2007.

[9] T. P. Nikolopoulos, G. M. O'Donoghue, and S. Archbold, "Age at implantation: its importance in pediatric cochlear implantation," *The Laryngoscope*, vol. 109, no. 4, pp. 595–599, 1999.

[10] E. A. Schorr, N. A. Fox, V. van Wassenhove, and E. I. Knudsen, "Auditory-visual fusion in speech perception in children with cochlear implants," *Proceedings of the National Academy of Sciences of the United States of America*, vol. 102, no. 51, pp. 18748–18750, 2005.

[11] J. J. LeBlanc and M. Fagiolini, "Autism: a "critical period" disorder?," *Neural Plasticity*, vol. 2011, Article ID 921680, 17 pages, 2011.

[12] A. E. Takesian and T. K. Hensch, "Chapter 1 - balancing plasticity/stability across brain development," in *Progress in Brain Research*, M. N. M. M. Merzenich and M. V. V. Thomas, Eds., pp. 3–34, Elsevier, 2013.

[13] E. A. Kelly, L. A. Opanashuk, and A. K. Majewska, "The effects of postnatal exposure to low-dose bisphenol-A on activity-dependent plasticity in the mouse sensory cortex," *Frontiers in Neuroanatomy*, vol. 8, 2014.

[14] A. E. Medina and A. S. Ramoa, "Early alcohol exposure impairs ocular dominance plasticity throughout the critical period," *Developmental Brain Research*, vol. 157, no. 1, pp. 107–111, 2005.

[15] M. R. Smith, P. Yevoo, M. Sadahiro et al., "Integrative bioinformatics identifies postnatal lead (Pb) exposure disrupts developmental cortical plasticity," *Scientific Reports*, vol. 8, no. 1, p. 16388, 2018.

[16] M. R. Smith, P. Burman, M. Sadahiro, B. A. Kidd, J. T. Dudley, and H. Morishita, "Integrative analysis of disease signatures shows inflammation disrupts juvenile experience-dependent cortical plasticity," *eNeuro*, vol. 3, no. 6, pp. ENEURO.0240–ENEU16.2016, 2016.

[17] G. K. Smyth, "Limma: linear models for microarray data," in *Bioinformatics and Computational Biology Solutions Using R and Bioconductor*, pp. 397–420, Springer, New York, 2005.

[18] J. Lamb, E. D. Crawford, D. Peck et al., "The connectivity map: using gene-expression signatures to connect small molecules, genes, and disease," *Science*, vol. 313, no. 5795, pp. 1929–1935, 2006.

[19] M. Bönn, *Hypergea: hypergeometric tests*, R Foundation, 2016.

[20] B. L. Pearson, J. M. Simon, E. S. McCoy, G. Salazar, G. Fragola, and M. J. Zylka, "Identification of chemicals that mimic transcriptional changes associated with autism, brain aging and neurodegeneration," *Nature Communications*, vol. 7, no. 1, 2016.

[21] M. L. Bennett, F. C. Bennett, S. A. Liddelow et al., "New tools for studying microglia in the mouse and human CNS," *Proceedings of the National Academy of Sciences*, vol. 113, no. 12, pp. E1738–E1746, 2016.

[22] Y. Benjamini and Y. Hochberg, "Controlling the false discovery rate: a practical and powerful approach to multiple testing," *Journal of the Royal Statistical Society. Series B (Methodological)*, vol. 57, no. 1, pp. 289–300, 1995.

[23] J. A. Gordon and M. P. Stryker, "Experience-dependent plasticity of binocular responses in the primary visual cortex of the mouse," *The Journal of Neuroscience*, vol. 16, no. 10, pp. 3274–3286, 1996.

[24] H. Morishita, J. M. Miwa, N. Heintz, and T. K. Hensch, "Lynx1, a cholinergic brake, limits plasticity in adult visual cortex," *Science*, vol. 330, no. 6008, pp. 1238–1240, 2010.

[25] A. Subramanian, P. Tamayo, V. K. Mootha et al., "Gene set enrichment analysis: a knowledge-based approach for interpreting genome-wide expression profiles," *Proceedings of the National Academy of Sciences*, vol. 102, no. 43, pp. 15545–15550, 2005.

[26] E. Y. Chen, C. M. Tan, Y. Kou et al., "Enrichr: interactive and collaborative HTML5 gene list enrichment analysis tool," *BMC Bioinformatics*, vol. 14, no. 1, p. 128, 2013.

[27] G. O. Sipe, R. L. Lowery, M. È. Tremblay, E. A. Kelly, C. E. Lamantia, and A. K. Majewska, "Microglial P2Y12 is necessary for synaptic plasticity in mouse visual cortex," *Nature Communications*, vol. 7, no. 1, 2016.

[28] R. A. Hodos, B. A. Kidd, K. Shameer, B. P. Readhead, and J. T. Dudley, "In silico methods for drug repurposing and pharmacology," *Wiley Interdisciplinary Reviews: Systems Biology and Medicine*, vol. 8, no. 3, pp. 186–210, 2016.

[29] B.-S. Wang, R. Sarnaik, and J. Cang, "Critical period plasticity matches binocular orientation preference in the visual cortex," *Neuron*, vol. 65, no. 2, pp. 246–256, 2010.

[30] C. N. Levelt and M. Hübener, "Critical-period plasticity in the visual cortex," *Annual Review of Neuroscience*, vol. 35, no. 1, pp. 309–330, 2012.

[31] E. M. Nabel and H. Morishita, "Regulating critical period plasticity: insight from the visual system to fear circuitry for therapeutic interventions," *Frontiers in Psychiatry*, vol. 4, 2013.

[32] J. F. Werker and T. K. Hensch, "Critical periods in speech perception: new directions," *Annual Review of Psychology*, vol. 66, no. 1, pp. 173–196, 2015.

[33] P. W. Davidson, G. J. Myers, and B. Weiss, "Mercury exposure and child development outcomes," *Pediatrics*, vol. 113, 4 Suppl, pp. 1023–1029, 2004.

[34] J. Umemori, F. Winkel, E. Castrén, and N. N. Karpova, "Distinct effects of perinatal exposure to fluoxetine or methylmercury on parvalbumin and perineuronal nets, the markers of critical periods in brain development," *International Journal of Developmental Neuroscience*, vol. 44, no. C, pp. 55–64, 2015.

[35] Z. J. Huang, A. Kirkwood, T. Pizzorusso et al., "BDNF regulates the maturation of inhibition and the critical period of plasticity in mouse visual cortex," *Cell*, vol. 98, no. 6, pp. 739–755, 1999.

[36] P. J. Landrigan, L. Lambertini, and L. S. Birnbaum, "A research strategy to discover the environmental causes of autism and neurodevelopmental disabilities," *Environmental Health Perspectives*, vol. 120, no. 7, pp. a258–a260, 2012.

[37] K. Thirtamara Rajamani, S. Doherty-Lyons, C. Bolden et al., "Prenatal and early-life exposure to high-level diesel exhaust particles leads to increased locomotor activity and repetitive behaviors in mice," *Autism Research*, vol. 6, no. 4, pp. 248–257, 2013.

[38] H. E. Volk, I. Hertz-Picciotto, L. Delwiche, F. Lurmann, and R. McConnell, "Residential proximity to freeways and autism in the CHARGE study," *Environmental Health Perspectives*, vol. 119, no. 6, pp. 873–877, 2011.

[39] G. C. Windham, L. Zhang, R. Gunier, L. A. Croen, and J. K. Grether, "Autism spectrum disorders in relation to distribution of hazardous air pollutants in the San Francisco Bay Area," *Environmental Health Perspectives*, vol. 114, no. 9, pp. 1438–1444, 2006.

[40] C. E. Dewey, B. D. Cox, B. E. Straw, E. J. Bush, and S. Hurd, "Use of antimicrobials in swine feeds in the United States," *Journal of Swine Health and Production*, vol. 7, no. 1, pp. 19–25, 1999.

[41] M. D. Barton, "Antibiotic use in animal feed and its impact on human healt," *Nutrition Research Reviews*, vol. 13, no. 2, pp. 279–299, 2000.

[42] T. C. Fung, C. A. Olson, and E. Y. Hsiao, "Interactions between the microbiota, immune and nervous systems in health and disease," *Nature Neuroscience*, vol. 20, no. 2, pp. 145–155, 2017.

[43] P. Bercik, E. Denou, J. Collins et al., "The intestinal microbiota affect central levels of brain-derived neurotropic factor and behavior in mice," *Gastroenterology*, vol. 141, no. 2, pp. 599–609.e3, 2011.

[44] D. L. Laskin and J. D. Laskin, "Role of macrophages and inflammatory mediators in chemically induced toxicity," *Toxicology*, vol. 160, no. 1-3, pp. 111–118, 2001.

[45] A. J. Bruce, W. Boling, M. S. Kindy et al., "Altered neuronal and microglial responses to excitotoxic and ischemic brain injury in mice lacking TNF receptors," *Nature Medicine*, vol. 2, no. 7, pp. 788–794, 1996.

[46] R. Kuno, J. Wang, J. Kawanokuchi, H. Takeuchi, T. Mizuno, and A. Suzumura, "Autocrine activation of microglia by tumor necrosis factor-α," *Journal of Neuroimmunology*, vol. 162, no. 1-2, pp. 89–96, 2005.

[47] K. Sriram, J. M. Matheson, S. A. Benkovic, D. B. Miller, M. I. Luster, and J. P. O'Callaghan, "Deficiency of TNF receptors suppresses microglial activation and alters the susceptibility of brain regions to MPTP-induced neurotoxicity: role of TNF-α1," *The FASEB Journal*, vol. 20, no. 6, pp. 670–682, 2006.

[48] W. A. Banks, A. J. Kastin, and R. D. Broadwell, "Passage of cytokines across the blood-brain barrier," *Neuroimmunomodulation*, vol. 2, no. 4, pp. 241–248, 1995.

[49] D. Mav, R. R. Shah, B. E. Howard et al., "A hybrid gene selection approach to create the S1500+ targeted gene sets for use in high-throughput transcriptomics," *PLoS One*, vol. 13, no. 2, article e0191105, 2018.

[50] A. P. Davis, C. J. Grondin, K. Lennon-Hopkins et al., "The comparative toxicogenomics database's 10th year anniversary: update 2015," *Nucleic Acids Research*, vol. 43, no. D1, pp. D914–D920, 2014.

[51] F. Eduati, L. M. Mangravite, T. Wang et al., "Prediction of human population responses to toxic compounds by a collaborative competition," *Nature Biotechnology*, vol. 33, no. 9, pp. 933–940, 2015.

[52] E. Kalogeraki, F. Greifzu, F. Haack, and S. Löwel, "Voluntary physical exercise promotes ocular dominance plasticity in adult mouse primary visual cortex," *Journal of Neuroscience*, vol. 34, no. 46, pp. 15476–15481, 2014.

Hindawi
Neural Plasticity
Volume 2019, Article ID 2724101, 12 pages
https://doi.org/10.1155/2019/2724101

Review Article

Studying Cortical Plasticity in Ophthalmic and Neurological Disorders: From Stimulus-Driven to Cortical Circuitry Modeling Approaches

Joana Carvalho,[1] **Remco J. Renken**,[1,2] **and Frans W. Cornelissen**[1]

[1]*Laboratory of Experimental Ophthalmology, University Medical Center Groningen, University of Groningen, Groningen, Netherlands*
[2]*Cognitive Neuroscience Center, University Medical Center Groningen, University of Groningen, Netherlands*

Correspondence should be addressed to Joana Carvalho; j.c.de.oliveira.carvalho@rug.nl

Received 31 May 2019; Accepted 5 August 2019; Published 3 November 2019

Guest Editor: Kathryn Murphy

Unsolved questions in computational visual neuroscience research are whether and how neurons and their connecting cortical networks can adapt when normal vision is compromised by a neurodevelopmental disorder or damage to the visual system. This question on neuroplasticity is particularly relevant in the context of rehabilitation therapies that attempt to overcome limitations or damage, through either perceptual training or retinal and cortical implants. Studies on cortical neuroplasticity have generally made the assumption that neuronal population properties and the resulting visual field maps are stable in healthy observers. Consequently, differences in the estimates of these properties between patients and healthy observers have been taken as a straightforward indication for neuroplasticity. However, recent studies imply that the modeled neuronal properties and the cortical visual maps vary substantially within healthy participants, e.g., in response to specific stimuli or under the influence of cognitive factors such as attention. Although notable advances have been made to improve the reliability of stimulus-driven approaches, the reliance on the visual input remains a challenge for the interpretability of the obtained results. Therefore, we argue that there is an important role in the study of cortical neuroplasticity for approaches that assess intracortical signal processing and circuitry models that can link visual cortex anatomy, function, and dynamics.

1. Introduction

Unravelling the organization of the visual cortex is fundamental for understanding the foundations of vision in health and disease. A prominent feature of this organization is the presence of a multitude of visual field maps. These maps are spatially and hierarchically organized representations of the retinal image and are often specialized to encode specific environmental visual attributes. Studying these cortical visual maps is relevant as it enables the characterization of the structure and function of the visual cortex and therefore the study of the neuroplastic capacity of the brain. With the latter, we refer to the ability of the brain to adapt its function and structure in response to either injury or to a treatment designed to recover visual function.

Over the last two decades, visual field mapping has been extensively used to infer neuronal reorganization resulting from visual field defects or neuroophthalmologic diseases. For a review, see Wandell and Smirnakis [4]. Because of its focus on the analysis of individual participants and the relative amount of detail provided, the pRF model seems ideal to study questions on neuroplasticity—at least in theory. Some of the hypotheses that can be tested with pRF mapping are as follows: are the neurons within the lesion projection zone active? Is there a displacement in position or enlargement of the pRF size during development, following a retinal or cortical lesion? Do the pRF properties change in response to monocular treatments that promote the use of the amblyopic eye, e.g., patching or blurring therapy?

Noninvasive measurement of receptive fields.
The visual maps result from a combination of the receptive fields (RF) of individual neurons. In vision, a RF corresponds to the portion of the visual field that a neuron responds to. A fundamental property of the visual cortex is that visual neurons are retinotopically organized (neighboring visual neurons respond to nearby portions of the visual field). Currently, it is not possible to measure the activity of single neurons noninvasively; however, the development of noninvasive neuroimage techniques, such as functional magnetic resonance imaging (fMRI), combined with computational neural models have been used to characterize RF properties at a larger scale. Briefly, fMRI uses a magnetic field to detect changes in blood oxygenation, a proxy of neural activity. This activity is coupled to oxygen consumption, which is why fMRI is also called blood oxygen level-dependent (BOLD) imaging. In fMRI, a standard voxel of 3 mm^3 captures the aggregate activity of ~1 million neurons [1, 2].
Therefore, the notion of the RF is extended to the collective RF of a population of neurons, the population receptive field (pRF). By applying biologically plausible models to describe the structure of this collective RF at a recording site, pRF mapping became a popular technique for the detailed characterization of visual cortical maps at the level of neuronal populations [3]. In essence, this method models the pRF as a two-dimensional Gaussian, of which the center and width correspond to the pRF's position and size, respectively. The model pipeline and description are presented in Figure 1.

Box 1

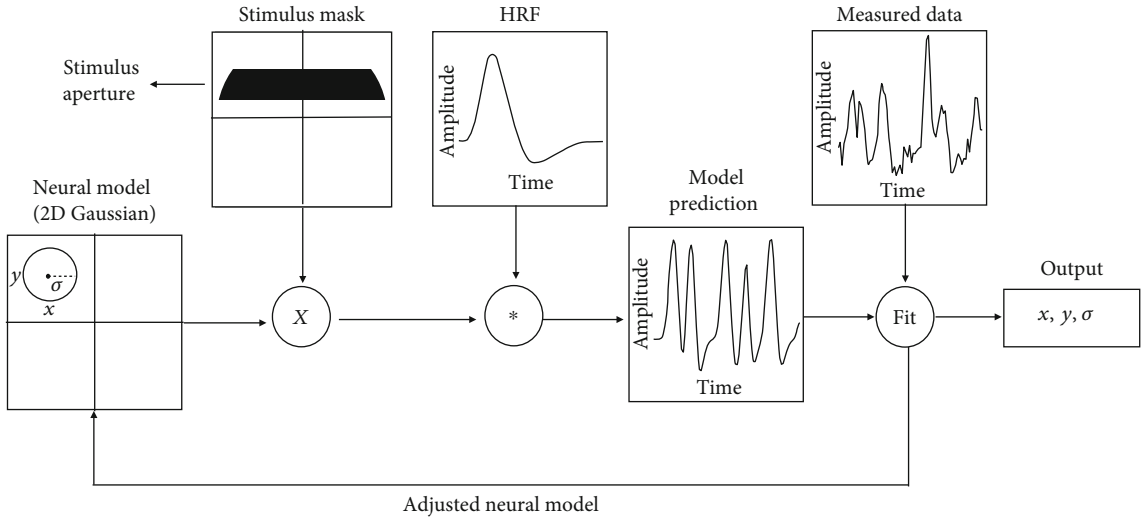

Figure 1: The population receptive field (pRF) modeling procedure. A pRF model describes, per voxel, the estimated pRF properties position (x, y) and size (σ). A voxel's response to the stimulus is calculated as the overlap between the stimulus mask (the binary image of the stimulus aperture: a moving bar) at each time point and the receptive field model. Following this, the delay in hemodynamic response is accounted for by convolving the predicted time courses with the hemodynamic response function. Finally, the pRF model parameters are adjusted for each voxel to minimize the difference between the prediction and the measured BOLD signal. The best fitting parameters are the output of the analysis. Figure adapted from Dumoulin and Wandell [3].

Given that visual neuroplasticity is greatest during early stages of development (childhood), the characterization of the pRF properties has special relevance to determine, in vivo, the presence of atypical properties of the visual cortex during development and plasticity. In particular, changes in pRF size have been reported in a series of studies on developmental disorders. Clavagnier and colleagues measured enlarged pRF sizes in primary visual areas (V1-V3) in the cortical projection from the amblyopic eye as compared to the fellow eye [5]. Schwarzkopf and colleagues reported that individuals with autism spectrum disorder (ASD) have larger pRFs as compared to controls [6]. Anderson and colleagues found smaller pRF sizes in the early visual cortex of individuals with schizophrenia compared to controls, using a specific pRF model that takes into account the center surround structure of the RF [7].

In the case of congenital visual pathway abnormalities that affect the optic nerve crossing at the chiasm, e.g., achiasma, albinism, and hemi-hydranencephaly, several studies revealed overlapping visual fields and bilateral vertical symmetric pRF representations [8–12]. This contrasts with the case of a single patient that had her left hemisphere removed at the age of three, who did show the expected right hemifield blindness, even though she had larger representations of the central visual field in extrastriate visual maps, which was particularly apparent in area LO1 in the right hemisphere [13].

Hence, the pRF modeling approach has been applied with at least some degree of success to reveal neuroplastic changes at the level of the visual cortex. Nevertheless, in the present paper, we will briefly indicate issues with the current pRF approach as it relates to neuroplasticity and ways to

improve the methods. Finally, we will argue that we should also look beyond it to fully address questions on neuroplasticity.

2. Limitations of Current Stimulus-Driven Approaches When Studying Neuroplasticity

We address the question to what extent population receptive field mapping is actually a suitable tool to capture cortical plasticity. We point out various limitations. The most important one is that the assumption of the receptive field and map stability in healthy controls is largely untenable.

The most common and straightforward manner in which the pRF approach has been applied is to compare model parameters between either two groups of participants—usually a patient group and matched controls [8, 14], or between the affected eye and the normal fellow eye, which can be done in the case of monocular developmental conditions such as amblyopia [5]. In both types of studies, it is commonly assumed that the differences in pRF estimates are caused by differences in brain organization and eye-brain connectivity of the two groups or the two eyes. However, there are various issues that complicate the interpretation of pRF differences in health and disease. A number of these limitations were recently discussed by Dumoulin and Knapen [15], and for this reason, we will only reiterate the most critical ones.

2.1. Changes at the Level of the Eye Limit the Use of pRF Mapping to Study Neuroplasticity in Both Ophthalmic and Neurological Diseases. Estimates of pRFs are based on the stimulus input. In numerous ophthalmic diseases, changes at the level of the eye—such as cataract or retinal lesions—strongly modify the visual input. This could be a decrease in visual acuity, contrast sensitivity, or the entire loss of vision in part of the visual field. Consequently, in many of such diseases, the stimulus-driven input to the brain will be different and usually deteriorated. In neurological conditions such as in hemianopia, retrograde degeneration of the retina [16, 17] gives rise to a similar concern. As changes in the visual input have a direct effect on the signal amplitude, straightforward differences in BOLD signal cannot be taken as an indicator of neuroplasticity or degeneration at the level of the cortex.

The retinotopic maps of healthy adults with normal or corrected to normal vision are stable over time when measured under similar environmental and cognitive factors [18, 19]. Hence, it would appear that changes in maps or population properties should be a good indication for the presence of neuroplasticity. Indeed, it was found that in patients with long-term visual impairment due to macular degeneration, the pRF of voxels representing both the scotomatic area and neighboring regions are displaced and changed in size [20].

However, there is mounting evidence that simple stimulus manipulations, e.g., masks mimicking retinal lesions, can have a large effect on the population-receptive field estimates in healthy participants. Estimated pRF properties (position shift and scaled size), similar to those in patients with retinal lesions, were observed in healthy adults in whom a visual field defect was simulated [20–22]. Comparable shifts in pRF position and scaling of pRF size were also found in an experiment that used scotopic illumination levels to examine the "rod scotoma" in the central visual field [23]. In other words, changes in visual input can mimic the consequences of lesions due to ophthalmic disease in healthy observers. This implies that observed differences in pRF properties in patients relative to controls may simply reflect normal responses to a lack in visual input rather than a reorganization of the visual cortex. Therefore, just by themselves, changes in pRF measures are insufficient to decide on the presence of neuroplasticity.

The feasibility to use pRF estimates to topographically map visual field defects in the cortex, particularly in early-stage disease, is further complicated by two aspects. First, neurons near the border of either the scotoma or the edge of the visual stimulus field may be partially stimulated. In such cases, the stimulus aperture partially activates receptive fields that belong to voxels whose pRF center would ordinarily be outside the stimulus presentation zone [21, 24]. Second, the presence or absence of a scotoma affects mostly the signal amplitude while the temporal dynamics of the modulation pattern are not affected. As pRF estimates are mostly invariant to the BOLD amplitude, the pRF model does not properly capture the effect of the scotoma. These two factors induce biases in the pRF estimates that can be wrongly interpreted as signs of neuroplasticity (see Box 2).

Nevertheless, changes in the BOLD signal may be used as an alternative assessment for nonfunctional parts of the visual system in patients that are unable to perform standard ophthalmic examinations, e.g., infants or patients with nystagmus [25–27]. However, because of the above aspects, caution is warranted when interpreting such data. Eye movements may affect the pRF estimates substantially, resulting in noisy maps and increased pRF sizes [28–30]. This is particularly relevant for developmental disorders such as amblyopia [5, 31–33]. In addition, pRF mapping is most accurate at an advanced stage of ophthalmologic disease where the visual field defects are relatively large and the scotomatic edge (i.e., the transition between healthy visual cortex and damaged visual cortex) is sharp [34, 35]. Overall, this inability to accurately detect small visual field defects implies that the sensitivity of the pRF approach is too limited to monitor the effects of slow retinal degeneration or slow cortical changes that would presumably be associated with rehabilitation therapies or other procedures to restore visual functioning.

2.2. Different Stimulus Properties Result in Distinct pRF Properties in Healthy Human Observers. An additional factor to be considered when interpreting pRF estimates is that the pRF represents the cumulative response across all neuronal subpopulations within a voxel. These subpopulations are selectively sensitive to spatial properties, such as orientation, color, luminance, and temporal and spatial frequencies. Hence, their activity can be driven by specific stimuli. In pRF mapping, manipulating the carrier—the stimulus aperture which drives the neuronal activity—elicits responses from a particular neuronal population. By selectively

A bias in pRF estimates induced by the presence of real and simulated scotomas.
To show how the presence of a scotoma may affect the pRF estimates, we simulated the pRF behavior in healthy vision (absence of scotoma) and in the presence of a scotoma (either due to a retinal or cortical lesion). The simulated circular scotoma is located in the horizontal meridian at 5 degrees of eccentricity, and it has a 3-degree radius. Figures 2(a) and 2(d) depict the overlap between the pRF model (in red) and the stimulus in the absence and presence of a scotoma (circular region within the bar aperture), respectively. Figures 2(b) and 2(e) show the respective simulations of the predicted pRF response resulting from convolving the stimulus with the pRF model (first part in Figure 1) and subsequent addition of noise. A similar level of noise was added to both simulations. The noise simulates any nonbiological signals captured with MRI. Note that the modulation pattern of the time series only differs between both conditions on the basis of the artificial noise added. The difference is mostly visible in the signal amplitude (note the different scales of the y-axes). When applying the pRF model, we need to define a stimulus mask which, ideally, should match the stimulus displayed during retinotopic mapping. Figure 2(c) shows the pRF-estimated properties in the absence of scotoma. Figures 2(f) and 2(g) depict the pRF estimates in the presence of a scotoma, using a stimulus mask that does not (Figure 2(f)) and that does (Figure 2(g)) take the scotoma into account. When we model the stimulus mask without taking the scotoma into account, this results in a bias, as pRF are enlarged and displaced towards the artificial lesion projection zone border (Figure 2(f)).When the presence of the scotoma is taken into account in the pRF model, the estimated properties of the pRF closely match the simulated ones. Note that the variance explained of pRF estimates in the three situations (normal vision (Figure 2(c)), lesion modelled without scotoma (Figure 2(f)), and lesion modelled with a scotoma (Figure 2(g))) is very similar. This shows that the pRF mapping approach is invariant to the BOLD amplitude, which hinders the detection of small scotomas. Additionally, in clinical cases where the extent of the scotoma is not fully established, it is thus impossible to accurately account for the presence of a scotoma in the pRF mapping.

Box 2

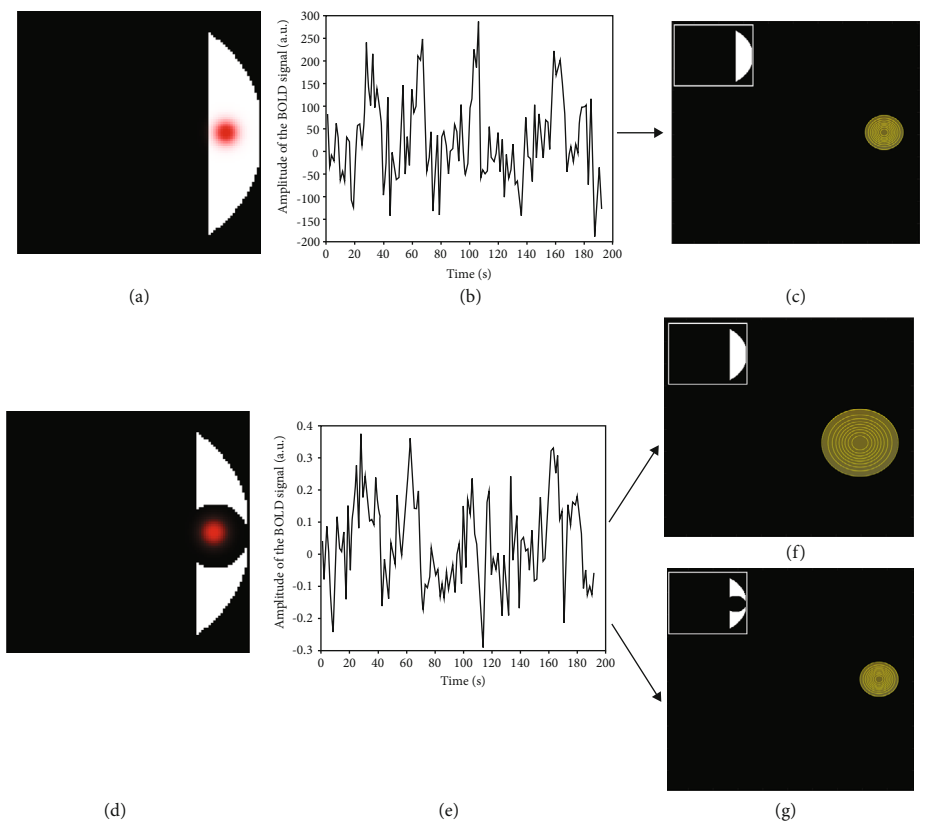

Figure 2: Simulated pRF time series and the associated estimated pRF properties: (a) simulation of a pRF (red) located at a specific region of the visual field ($x = 5, y = 0$) and with a size of $\sigma = 0.5$ deg assuming normal vision (i.e., no scotoma); (b) simulated fMRI response given the retinotopic stimulus (a) modelled with added noise (signal to noise ratio of 1 : 1); (c) estimated pRF using the normal vision simulated time series (b). The mask used in the pRF model is presented in the upper left corner. The estimated properties were identical to the simulated ones: $x = 5$, $y = 0$, $\sigma = 0.5$ deg, and a variance explained of 0.46. (d, e) are analogues to (a, b), but for a simulated pRF located in the lesion projection zone (thus inside the simulated scotoma); (f) estimated pRF based of the scotoma simulated time series (e) using a mask that assumes normal vision. The estimated pRF shifted in position and increased in size (estimated position shifted towards $x = 4$ and $y = -1$ and the size was enlarged, $\sigma = 1$ deg). The variance explained obtained was 0.45; (f) estimated pRF based of the scotoma simulated time series (e) and taking into account the lesion by using a mask that includes the scotoma (upper left corner). The estimated pRF properties are now again identical to the simulated ones ($x = 5$, $y = 0$, $\sigma = 0.5$ deg, and variance explained = 0.44).

stimulating these neuronal populations, a number of recent studies have shown that compared to the standard stimulus (flickering luminance contrast checkerboard bar), pRF estimates shift in position and change their size [36–39]. These studies indicate that the recruitment of neural resources depends on the task and that there is a dependency of the retinotopic maps on the task or stimulus. This type of stimulus selectivity captures the neuronal population characteristics for features such as luminance, orientation, or words. In contrast, Welbourne and colleagues [40] found no difference in pRF estimates when using chromatic and achromatic stimuli. This implies that for color, there may be a decoupling between the pRF measurement and the underlying neuronal populations [40].

The spatial distribution of the receptive fields can also be modelled by attention. A series of studies manipulating spatial and feature-based attention found that the neuronal resources are shifted towards the attended positions [30, 41, 42].

These findings imply one of two things: (1) the topography of the visual cortex is flexible and may change in response to environmental (stimulus, task) as well as cognitive factors such as attention or (2) pRF measures are inaccurate and may change in response to spatial and cognitive factors. Either of these explanations limits the ability of the pRF approach to provide a straightforward assessment of neuroplasticity.

3. Improving Stimulus-Driven Approaches

We consider various ways in which the pRF method might be improved to study neuroplasticity. Of note are models that provide information on the reliability of the pRF-estimated properties. As a further incentive, we propose a new pRF model that incorporates cortical temporal dynamics and which integrates connectivity and topography.

Given the limitations mentioned above, this raises the question whether and how the pRF approach can be modified to render it more suitable to track neuroplastic changes. As was indicated, mimicking visual field defects can alter pRF properties in a similar manner to patients. At the minimum, this requires creating elaborated control stimulus conditions (simulations) that exactly mimic patient conditions. Unfortunately, this is often impossible to achieve. Deviations of parameter estimates in the patient group from those control values could be an indication of neuroplasticity. However, obtaining good simulations is not trivial. Thus far, the simulations that have been used have generally been quite simple, i.e., mimicking scotomas in which no light sensitivity remained—usually simulated as a region without signal modulation. However, the perceptual awareness of natural scotomas may be substantially different from that of artificial ones. For example, when the visual input is incomplete, the visual system appears to fill in any missing features (through prediction and interpolation) in order to build a stable percept. Moreover, scotomas in patients are usually more complex than simulated ones, both in their shape and their depth (reduced sensitivity). Finally, the scotoma may also change the attentional deployment by the patient, potentially affecting the estimated pRF properties [30, 41, 42].

In order to accurately measure neuronal reorganization, it is crucial to overcome the abovementioned limitations. A significant amount of work has been directed towards the development of more reliable models of retinotopic mapping. The methodological advances serve three different goals, which may be useful in studying neuroplasticity: (1) improve the reliability of the estimates using more informative pRF shapes and more complex computational models, (2) measure stimulus-selective maps, which allow to capture the reorganization of specific neuronal populations, and (3) measure spatial modulation and dynamics of neuronal populations, potentially reflecting short-term neuroplastic changes.

3.1. Computational and Model Advances. Computational and model advances have been made to (a) improve the pRF shape so that it better reflects the biological structure of the RF, e.g., using a difference of Gaussian model allows to account for surround suppression [43], and (b) account for nonlinearities, provide distributions of property magnitudes, and capture neuronal characteristics, such as tuning curves. Such models add new pRF features which may be important to infer functional reorganization and provide a measure of the reliability of the estimates.

A different pRF shape can be an indication of neuroplasticity. Several models have been developed to account for various possible receptive field shapes: circular symmetric difference of Gaussian (DoG) functions [43], bilateral pRF [10], elliptic shape [34], Gabor wavelet pyramids [34, 44], and compressive spatial summation [45]. Some reviews have discussed these methods in detail [15, 46]. However, the above models all assume some form of symmetry. Recently, data-driven models were developed that do not assume any a priori shape [47–49]. These model-free approaches are particularly relevant to measure the functioning of the visual system in patients, as plasticity may manifest as a differently shaped pRF without affecting its position or size. An example is that asymmetrical shapes capture best the pRF properties of any skewed distributions of RF within a voxel. However, even in these data-driven approaches, the estimated shape of the receptive fields remains dependent on the stimulus used.

Extending the pRF model to account for more complex RF shapes will improve its explanatory power—the model can better predict the BOLD response. However, this will not remove the issue of model bias, mentioned in Box 2. In various attempts to resolve this, computational advances were made which can be categorized into four different classes. The first class comprises nonlinear pRF models, such as a compressive spatial summation model and convex optimized pRF, which substantially increases the range of shapes that the model can describe [45]. The second class is the development of Bayesian models. For each property, these models do not only estimate the best fitting value but a full posterior distribution as well [50, 51]. This serves several needs: (a) it indicates the uncertainty associated with each estimate (Figure 3). Such uncertainty maps are of particular importance when a visual field defect is present, as higher uncertainty will most likely be associated with model biases, (b)

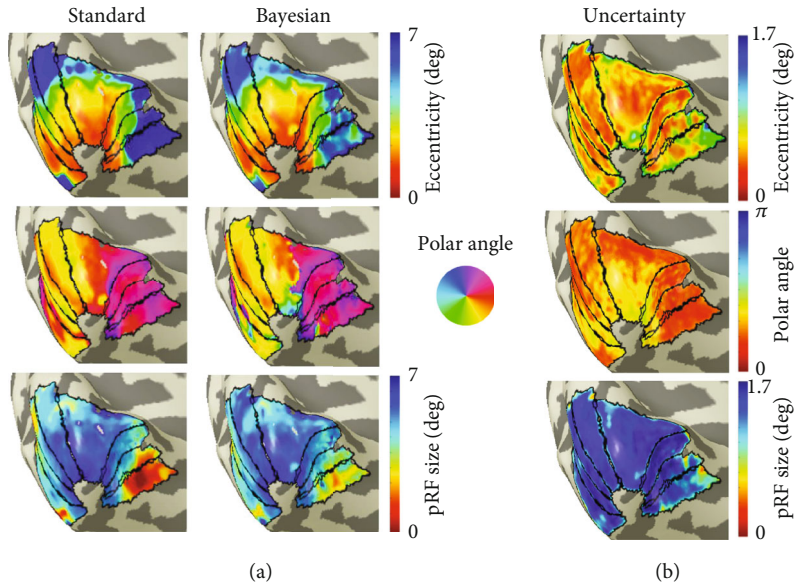

Figure 3: Mapping the uncertainty of model estimates: (a) maps obtained using conventional pRF mapping [3] and a custom implementation of the Monte Carlo Markov chain Bayesian pRF approach [50, 51]. Both methods result in similar visual field maps. However, the latter method also enables the estimation of the uncertainty associated with each parameter; (b) eccentricity, phase, and pRF size uncertainty maps obtained for the left hemisphere of a single healthy participant. The uncertainty maps describe how reliable each estimate is. For example, we see that the polar angle estimates for the central fovea (near fixation) are less reliable than those measured in the periphery. The uncertainty associated for each estimate was calculated as the difference between the 75% and 25% quantiles of the Bayesian Markov chain pRF distribution.

it facilitates the statistical analysis, and (c) it allows one to incorporate additional biological knowledge by providing prior information. An example of such a biologically based prior is that the density of cortical neurons is higher in the fovea than in the periphery [50, 51]. In combination, the above-referred three factors improve the interpretability of pRF estimates. The third class comprises the development of the feature-weighted receptive field (fwRF) models that allow capturing additional pRF parameters—such as neuronal tuning curves (e.g., the spatial frequency tuning)—through the combination of measured neural activity and visual features [52]. Finally, the fourth class relates to methods that allow to enhance the resolution at which we can detail RF properties. Of relevance are the approaches that allow to estimate the average single-unit RF size (suRF) [49, 53] or multiunit RF (muRF) properties that can without restriction uncover the size, position, and shape of neuronal subpopulations, also when these are fragmented and dispersed in visual space [49, 53].

3.2. Models of Perception: Spatial Modulation and Dynamics. Specific models have been developed to capture short-term plasticity. Such models take into account cognitive and/or perceptual factors such as attention [30, 54] or crowding [55, 56] to understand changes in observed spatial properties or perception. Recently, Dumoulin and Knapen proposed a more complex pRF model that relates pRF changes to the underlying neural mechanisms [15]. This very general model allows modeling and predicting dynamic changes that result from changes in the visual input. In particular, they proposed an extension of the pRF model to account for multiple neural subpopulations responding to different properties of the stimulus. Their expectation is that this will enable unravelling of the different sources of pRF plasticity.

Although there have been significant improvements in pRF models which may be able to aid in charting neuroplastic changes, in our view, this is still insufficient. There are still many constraints to be addressed, in particular, the fact that a voxel may contain a mixture of neurons with spatially distinct receptive fields. This is particularly relevant in developmental disorders such as albinism and achiasma [9, 10] or for voxels located in sulci. In those cases, the measured pRF properties will either represent the strongest contributing RF or be erroneously large.

In our view, the neuronal spatiotemporal dynamics can be better captured if we would take into account the interactions with nearby linked populations. The connectivity-weighted pRF, described next, is a first attempt to integrate models of cortical organization with cortical connectivity. This further encourages the development of new models that integrate stimulus- and cortex-referred methods.

3.3. The Connectivity-Weighted pRF Integrates Cortical Organization and Connectivity. Current analytical approaches to track retinotopic changes are voxel based. This limits their accuracy, as the visual system is dynamic and the activity of one population of neurons is influenced by nearby connected populations. Ideally, a more complete model should reflect the balance between inhibitory and excitatory processes and account for various cortico-cortical interactions.

Here—as an example of such a model—we propose a stimulus-driven pRF model, in which the estimated parameters, pRF_j, depend upon the unique activity of the neuronal population $pRFu_j$ and the activity of interacting cortical neuronal populations, weighted by the strength of their connections, C_{jk}. Note that e_j is the error associated with voxel j.

$$pRF_j = pRFu_j * \left(\sum_{k \neq j} C_{jk} * pRF_k \right) + e_j. \quad (1)$$

Depending on the goal of the study and the design of the experiment, the connectivity (C) can be based either on the structure (anatomically connected neighbors), on function (neuronal populations which exhibit specific correlated activity during the resting state), or on effective connectivity [57]. Here, we treat it as effective connectivity given that it accounts for dynamic interactions and the model of coupling between neuronal populations.

Such a model can describe the spatiotemporal dynamics of neuronal populations. It is sensitive to the recurrent flow of synchronized activity between connected neurons. Using such a connectivity-weighted model, we may—in the future—assess brain plasticity based on both structural reorganization and functional reorganization.

4. Cortical Circuitry Models Look beyond the Stimulus

We suggest that models that can be estimated without requiring visual stimulation, which we refer to as cortical circuitry models (CCM), may be highly suitable to measure cortical reorganization. While not without potential pitfalls themselves, such approaches avoid many of the complications associated with the stimulus-driven pRF approach. Additionally, we indicate various other avenues that may improve our ability to quantitatively assess neuroplastic changes in the visual cortex.

4.1. Studying Neuroplasticity Using Intrinsic Signals and Cortical Circuitry Models. The fMRI signal is a mixture of stimulus-specific and intrinsic signals [57, 58]. As a result, it is plausible to assume that intrinsic generated signals may influence stimulus-driven signals [57, 58]. Therefore, the study of brain plasticity may be ameliorated and/or complemented if the dependence on stimuli is reduced. For this reason, estimates based on intrinsic signals rather than task responses are potentially a very suitable source of information on the presence or absence of cortical plasticity. Intrinsic signals are commonly obtained in a "resting-state" condition in which participants are not required to do anything in particular and usually have their eyes closed. Resting-state fMRI signal fluctuations have been shown to correlate with anatomically and functionally connected areas of the brain. In particular, specialized networks have been found in cortical and subcortical areas in sensory systems [59–64]. Based on resting-state data, CCMs can be used to infer the integration of feedback and feedforward information [65]. However, one important limitation is that currently, the directionality of information flow cannot be directly inferred from the BOLD signal. Therefore, primarily because of the limited temporal resolution of fMRI, it remains to be determined whether CCMs can be used to assess this aspect.

Nonetheless, CCMs have the potential to capture the effects of structural reorganization and can inform about which neural circuits have the potential to reorganize and which are stable. An example of this type of model is the connective field (CF) model, which applies the notion of a receptive field to cortico-cortical connections [66]. Another example is the connectopic model which combines voxel-wise connectivity "fingerprints" with spatial statistical inference to detail multiple overlapping connection topographies (connectopies) in the human brain [66, 67]. Ultimately, in our view, it will be essential to combine retinotopic and neural circuitry models, such that their combination can be used to fully describe the dynamics of the visual cortex [68]. To accomplish this, models will have to be developed that can capture the (dynamic) adaptation of feedback, feedforward, and lateral connections in the functional networks underlying visual processing and cognition. Such models may be implemented by calculating the correlation between neuronal populations taking time lags into account or by using CCM to describe connections across cortical layers (see also below).

4.2. The Connective Field Defines a Receptive Field in Cortical Surface Space. Connective field (CF) modeling predicts the neuronal activity in a target area (e.g., V2) based on the activity in a source area (e.g., V1). In a similar way that a neuron has a preferred location and size in visual space (its receptive field), it also will have a preferred location and size on the cortical surface of a region that it is connected with [65, 66, 68]. Based on retinotopic mapping, the visual field coordinates of the target area can be inferred from the preferred locations in the source region. In this way, the connective field—when combined with pRF mapping—can link a CF's position in cortical surface space also to a position in visual space. The connective field model is briefly described in Box 3.

There are several advantages of CCMs when compared to pRF models. First, the ability to assess and compare the fine-grained topographic organization of cortical areas promotes the comparison of connectivity patterns between groups of participants with different health conditions and between experimental conditions [67, 70]. Second, CCMs can even be applied to data that was acquired in the absence of any sensory input, enabling the reconstruction of visuotopic maps even in the absence of a stimulus and in blind people. Several studies have shown that cortical connectivity during the resting state reflects the visuotopic organization of the visual cortex [65, 67, 70–73]. A comparison between stimulus-driven and resting-state CCMs may also convey information on the influence of retinal waves and prior visual experience in the cortical circuitry. For example, larger CF sizes were measured with visual stimulation when compared to the resting state [65, 73, 74]. Third, CCMs provide insight into the anatomical and functional neuronal circuitry that enables the visual system to integrate information across

Connective field modeling.
The CF model, as originally proposed by Haak and colleagues, assumes a circularly symmetric 2D Gaussian model on the surface of the source region as the integration field from the source to the target [66]. This 2D Gaussian is defined by its position ($v0$) and size (σ), where $d(v,v0)$ is the shortest distance between the voxel v and the connective field center $v0$ and σ is the Gaussian spread (mm). Distances are calculated across the cortical surface, using Dijkstra's algorithm [66, 69]. The connective field pipeline is described in Figure 4.

Box 3

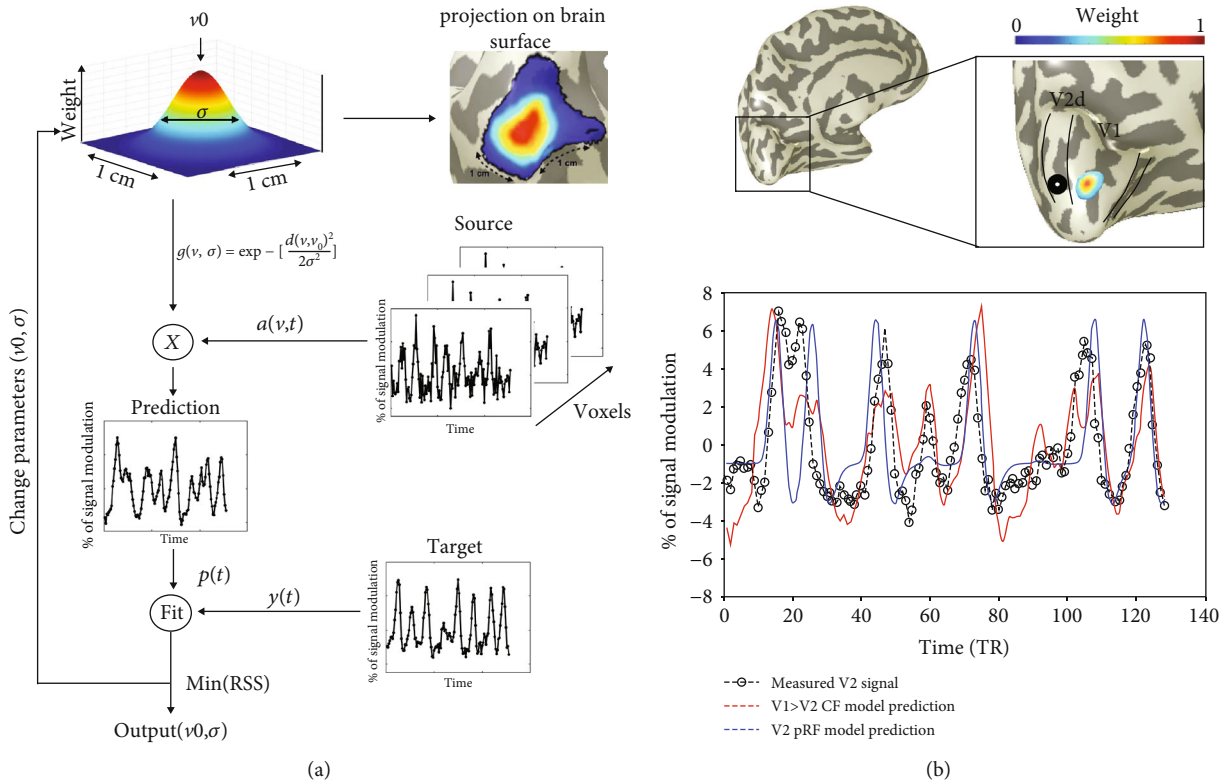

FIGURE 4: (a) CF pipeline as described by Haak and colleagues [66]. The model comprises two steps: (1) predict the fMRI response, $p(t)$, by multiplying the CF model $g(v0, \sigma)$ with the measured source fMRI signal $a(v, t)$, and (2) the CF position (v) and size (σ) are estimated by varying parameters and selecting the best fit between the predicted time series and the measured BOLD signal $y(t)$. Then this procedure is repeated for every voxel in the target region. (b) The V2 response is predicted based on the pRF (stimulus-driven, in blue) and connective field (cortical-driven, in red) model. The color map on the brain shows the V1>V2 CF model weights for a specific voxel.

different cortical areas. They can reveal the presence or absence of a change therein following a disease [74–76]. Fourth, CCMs, in particular when assessed in the resting state, are less affected by various intrinsic and extrinsic factors such as the type of task and stimulus [37–39], patient performance, optical properties and health condition of the eye [77], or stimulus-related model-fitting biases [22, 77].

Despite these important advantages, the current CCM approaches also have their limitations. First, the reliability of CCM parameters, such as the CF size, is affected by the signal-to-noise ratio. Fortunately, the signal-to-noise ratio does not introduce a systematic bias in the estimated parameters [74–76]. Second, the current iteration of CCM models does not capture causal interactions between different cortical visual areas. Third, like pRF estimates, it is likely that the accuracy of the CCM-related estimates depends on the spatial and temporal resolution, the distortion and spatial spread of the BOLD signal, and the distribution of dural venous sinuses and vessel artifacts. Fourth, although there is no need for stimulus-driven signals, resting state signals—and thus also any estimated CCM properties—are influenced by the environmental conditions under which they were acquired. Factors such as eye movements and exterior luminance may also influence estimates. These limitations demonstrate that although the CCM approach seems suitable to infer the presence or absence of plasticity by associating connectivity strength with cortical degeneration [75], it still requires careful experimentation as well.

Some of the above limitations have recently been addressed. For example, global search algorithms that help to avoid local minima have also been applied to CCMs

[74, 75]. Furthermore, new data-driven methods are able to measure multiple and even overlapping connectopies [67]. Although, currently establishing these connectopic maps requires a very large number of participants, they hold a promise of being able to reveal cortical and network reorganization and plasticity one day [67].

4.3. Cortical Circuitry Models in Ophthalmic or Neurological Diseases. The development of CCMs is a sequel to the classical pRF mapping. Hence, the available literature is still relatively small. Nonetheless, the existing studies give a good impression of the possible applications and the type of information that these models can provide.

At this point in time, in particular, the CF modeling approach has been applied in several ophthalmic disorders, in which visual perception was either impaired or completely absent. A study by Haak and colleagues found that in macular degeneration, long-term deprivation of visual input had not affected the underlying cortical circuitry [75]. This suggests that the visual cortex retains the ability to process visual information. In principle, following the restoration of visual input, i.e., via retinal implants, such patients may thus recuperate from vision loss. Papanikolaou and collaborators applied CF modeling to study the organization of area hV5/MT+ in five patients with large visual field defects resulting from either early visual areas or optic radiation lesions [76]. They showed that in three of the five subjects, the CFs between areas V1 and hV5/MT+ covered visual field locations that overlapped with the scotoma. This indicates that activity in the lesion projection zone in hV5/MT+ may originate from spared V1. Bock and collaborators applied the CF model to resting-state BOLD data acquired from normally sighted, early blind, and monocular patients in which one of the eyes had failed to develop [74]. All subjects showed retinotopic organization between V1 and V2/V3. Butt and colleagues studied the cortical circuitry of the visual cortex in blind observers and compared this to that of sighted controls [70, 74]. They found a very minute change in the pattern of fine-scale striate correlations between hemispheres, in contrast to the highly similar connectivity pattern within hemisphere. They concluded that the cortical connections within a region (which can be a hemisphere) are independent of visual experience. The above-cited studies show that, in general, the visuotopic organization of the cortical circuitry is maintained even after prolonged visual deprivation or blindness, supporting that the plasticity of the adult visual brain is limited (see Wandell and Smirnakis for a similar conclusion based on stimulus-driven mapping [4]). Moreover, these studies suggest that CCMs may be able to capture the integrity of cortical connections using both stimulus-driven and resting-state data. This encourages the development of new CCMs that can be applied to study how connected neurons in different layers and columns interact.

4.4. Mesoscale Plasticity: Layer- and Column-Based Cortical Circuitry Models. Measuring cortical reorganization at a finer scale might reveal changes that are invisible or masked at a coarser scale. With the recent advance in ultra-high field functional MRI, the tools to examine the human brain at a mesoscale in vivo have become available. This enables assessing the presence of cortical reorganization across cortical depth to measure the flow of information across different cortical laminae—in particular feedback and lateral inputs—and to infer the microcortical circuits by studying their columnar organization.

Many of the opportunities and challenges in visual neuroscience provided by increases in MRI field strength have been described in a recent review, to which we refer [78]. With respect to the topic of neuroplasticity, a study that showed that pRF in the input (middle) layer have a smaller RF than those in superficial and deeper intracortical layers is of particular interest [79]. Although this study provides hints about cortical organization, it exclusively relied on stimulus-based modelling and thus does not truly inform about the underlying circuitry. In order to bridge this gap, we propose that the application of CCM-like approaches to study short-range connections at laminar and columnar levels is warranted.

The development of methods that reflect the mesoscale circuitry should be able to answer various outstanding critical questions in visual neuroscience and contribute with new fundamental and clinically relevant insights into cortical functioning and neuroplasticity. For example, following a visual field defect, is the input/feedforward layer the one that is most affected? Do neurons in the upper and deepest layers of the lesion projection zone establish new connections to healthy neurons in the input layer? At what level of cortical processing do feedback and feedforward signals modulate our conscious percepts? Are putative overlapping representations in ventral areas [38] perhaps encoded in distinct layers of the visual cortex?

5. Conclusion

In this paper, we discussed (a) the role of pRF mapping to cortically characterize visual areas and extrinsic and intrinsic factors that influence the pRF estimates, (b) methodological advances in retinotopic and connectopic mapping, and (c) stimulus-driven and cortical circuitry models that can link visual cortex organization, dynamics, and plasticity.

Although we fully acknowledge the important contribution of pRF mapping towards understanding the structure and functioning of the visual cortex, we strongly argue against a "blind" reliance on this technique when studying neuroplasticity. The degree to which a change in signal amplitude or pRF measurements—by themselves—reflects that cortical reorganization remains to be determined: even in the presence of a presumed stable cortical organization in healthy participants, different pRF estimates may be elicited due to a change in the task at hand, cognitive factors, and the type of stimulus used. For this reason, we have stressed that prior to deciding that pRF changes are the result of reorganization, one has to exclude that these are due to different inputs, (implicit) task conditions, or cognitive demands.

To improve the reliability of retinotopic mapping, more complex models and computational approaches have been developed with a noticeable trend to move from stimulus-

driven to data-driven techniques. These efforts have resulted in a multitude of new methods. Their specific use depends upon the goal of the study and the neuronal population of interest. Nevertheless, although these newer techniques provide clear improvements, they potentially retain the issues associated with stimulus-driven approaches. Therefore, we argue in favor of also considering alternative techniques to study brain plasticity, in particular ones that directly assess the neural circuitry rather than stimulus-driven responses to estimate the extent of neuronal reorganization. As an exemplary incentive, we propose a model that combines connectivity with spatial sampling. In theory, such a model will not only inform about the spatial sampling but also about interactions between the linked neuronal populations. Finally, we encourage the development and application of models to capture the plasticity of layer-based circuitry at the mesoscale.

Disclosure

The funding organizations had no role in the design, conduct, analysis, or publication of this research.

Conflicts of Interest

The authors declare that they have no conflicts of interest.

Acknowledgments

JC was supported by the European Union's Horizon 2020 research and innovation programme under the Marie Sklodowska-Curie grant agreement no 641805. FWC was supported by the Netherlands Organization for Scientific Research (NWO Brain and Cognition grant 433-09-233).

References

[1] A. J. ROCKEL, R. W. HIORNS, and T. P. S. POWELL, "The basic uniformity in structure of the neocortex," *Brain*, vol. 103, no. 2, pp. 221–244, 1980.

[2] G. Leuba and L. J. Garey, "Comparison of neuronal and glial numerical density in primary and secondary visual cortex of man," *Experimental Brain Research*, vol. 77, no. 1, pp. 31–38, 1989.

[3] S. O. Dumoulin and B. A. Wandell, "Population receptive field estimates in human visual cortex," *NeuroImage*, vol. 39, no. 2, pp. 647–660, 2008.

[4] B. A. Wandell and S. M. Smirnakis, "Plasticity and stability of visual field maps in adult primary visual cortex," *Nature Reviews Neuroscience*, vol. 10, no. 12, pp. 873–884, 2009.

[5] S. Clavagnier, S. O. Dumoulin, and R. F. Hess, "Is the cortical deficit in amblyopia due to reduced cortical magnification, loss of neural resolution, or neural disorganization?," *Journal of Neuroscience*, vol. 35, no. 44, pp. 14740–14755, 2015.

[6] D. S. Schwarzkopf, E. J. Anderson, B. de Haas, S. J. White, and G. Rees, "Larger extrastriate population receptive fields in autism spectrum disorders," *The Journal of Neuroscience*, vol. 34, no. 7, pp. 2713–2724, 2014.

[7] E. J. Anderson, M. S. Tibber, D. S. Schwarzkopf et al., "Visual population receptive fields in people with schizophrenia have reduced inhibitory surrounds," *The Journal of Neuroscience*, vol. 37, no. 6, pp. 1546–1556, 2017.

[8] K. Ahmadi, A. Fracasso, J. A. van Dijk et al., "Altered organization of the visual cortex in FHONDA syndrome," *NeuroImage*, vol. 190, pp. 224–231, 2019.

[9] M. B. Hoffmann, D. J. Tolhurst, A. T. Moore, and A. B. Morland, "Organization of the visual cortex in human albinism," *The Journal of Neuroscience*, vol. 23, no. 26, pp. 8921–8930, 2003.

[10] M. B. Hoffmann, F. R. Kaule, N. Levin et al., "Plasticity and stability of the visual system in human achiasma," *Neuron*, vol. 75, no. 3, pp. 393–401, 2012.

[11] A. Fracasso, Y. Koenraads, G. L. Porro, and S. O. Dumoulin, "Bilateral population receptive fields in congenital hemihydranencephaly," *Ophthalmic & Physiological Optics*, vol. 36, no. 3, pp. 324–334, 2016.

[12] L. Muckli, M. J. Naumer, and W. Singer, "Bilateral visual field maps in a patient with only one hemisphere," *Proceedings of the National Academy of Sciences*, vol. 106, no. 31, pp. 13034–13039, 2009.

[13] K. V. Haak, D. R. M. Langers, R. Renken, P. van Dijk, J. Borgstein, and F. W. Cornelissen, "Abnormal visual field maps in human cortex: a mini-review and a case report," *Cortex*, vol. 56, pp. 14–25, 2014.

[14] I. P. Conner, J. V. Odom, T. L. Schwartz, and J. D. Mendola, "Retinotopic maps and foveal suppression in the visual cortex of amblyopic adults," *The Journal of Physiology*, vol. 583, no. 1, pp. 159–173, 2007.

[15] S. O. Dumoulin and T. Knapen, "How visual cortical organization is altered by ophthalmologic and neurologic disorders," *Annual Review of Vision Science*, vol. 4, no. 1, pp. 357–379, 2018.

[16] A. Herro and B. L. Lam, "Retrograde degeneration of retinal ganglion cells in homonymous hemianopsia," *Clinical Ophthalmology*, vol. 2015, no. 9, pp. 1057–1064, 2015.

[17] A. Cowey, I. Alexander, and P. Stoerig, "Transneuronal retrograde degeneration of retinal ganglion cells and optic tract in hemianopic monkeys and humans," *Brain*, vol. 134, no. 7, pp. 2149–2157, 2011.

[18] M. Senden, J. Reithler, S. Gijsen, and R. Goebel, "Evaluating population receptive field estimation frameworks in terms of robustness and reproducibility," *PLoS One*, vol. 9, no. 12, article e114054, 2014.

[19] J. A. van Dijk, B. de Haas, C. Moutsiana, and D. S. Schwarzkopf, "Intersession reliability of population receptive field estimates," *NeuroImage*, vol. 143, pp. 293–303, 2016.

[20] H. A. Baseler, A. Gouws, K. V. Haak et al., "Large-scale remapping of visual cortex is absent in adult humans with macular degeneration," *Nature Neuroscience*, vol. 14, no. 5, pp. 649–655, 2011.

[21] K. V. Haak, F. W. Cornelissen, and A. B. Morland, "Population receptive field dynamics in human visual cortex," *PLoS One*, vol. 7, no. 5, article e37686, 2012.

[22] P. Binda, J. M. Thomas, G. M. Boynton, and I. Fine, "Minimizing biases in estimating the reorganization of human visual areas with BOLD retinotopic mapping," *Journal of Vision*, vol. 13, no. 7, p. 13, 2013.

[23] B. Barton and A. A. Brewer, "fMRI of the rod scotoma elucidates cortical rod pathways and implications for lesion

measurements," *Proceedings of the National Academy of Sciences of the United States of America*, vol. 112, no. 16, pp. 5201–5206, 2015.

[24] M. Senden, "Real Time Estimation of Population Receptive Fields Using Gradient Descent," *bioRxiv*, p. 194621, 2017.

[25] M. M. Souweidane, K. H. S. Kim, R. McDowall et al., "Brain mapping in sedated infants and young children with passive-functional magnetic resonance imaging," *Pediatric Neurosurgery*, vol. 30, no. 2, pp. 86–92, 1999.

[26] G. Qing, S. Zhang, B. Wang, and N. Wang, "Functional MRI signal changes in primary visual cortex corresponding to the central normal visual field of patients with primary open-angle glaucoma," *Investigative Ophthalmology & Visual Science*, vol. 51, no. 9, pp. 4627–4634, 2010.

[27] K. N. Engin, B. Yemişci, S. T. Bayramoğlu et al., "Structural and functional evaluation of glaucomatous neurodegeneration from eye to visual cortex using 1.5T MR imaging: A Pilot Study," *Journal of Clinical & Experimental Ophthalmology*, vol. 05, no. 03, 2014.

[28] A. Hummer, M. Ritter, M. Tik et al., "Eyetracker-based gaze correction for robust mapping of population receptive fields," *NeuroImage*, vol. 142, pp. 211–224, 2016.

[29] N. Levin, S. O. Dumoulin, J. Winawer, R. F. Dougherty, and B. A. Wandell, "Cortical maps and white matter tracts following long period of visual deprivation and retinal image restoration," *Neuron*, vol. 65, no. 1, pp. 21–31, 2010.

[30] B. P. Klein, B. M. Harvey, and S. O. Dumoulin, "Attraction of position preference by spatial attention throughout human visual cortex," *Neuron*, vol. 84, no. 1, pp. 227–237, 2014.

[31] G. Gingras, D. E. Mitchell, and R. F. Hess, "Haphazard neural connections underlie the visual deficits of cats with strabismic or deprivation amblyopia," *The European Journal of Neuroscience*, vol. 22, no. 1, pp. 119–124, 2005.

[32] X. Li, S. O. Dumoulin, B. Mansouri, and R. F. Hess, "The fidelity of the cortical retinotopic map in human amblyopia," *European Journal of Neuroscience*, vol. 25, no. 5, pp. 1265–1277, 2007.

[33] R. Farivar, J. Zhou, Y. Huang, L. Feng, Y. Zhou, and R. F. Hess, "Two cortical deficits underlie amblyopia: a multifocal fMRI analysis," *NeuroImage*, vol. 190, pp. 232–241, 2019.

[34] E. H. Silson, T. S. Aleman, A. Willett et al., "Comparing clinical perimetry and population receptive field measures in patients with choroideremia," *Investigative Ophthalmology & Visual Science*, vol. 59, no. 8, pp. 3249–3258, 2018.

[35] M. Ritter, A. Hummer, A. A. Ledolter, G. E. Holder, C. Windischberger, and U. M. Schmidt-Erfurth, "Correspondence between retinotopic cortical mapping and conventional functional and morphological assessment of retinal disease," *The British Journal of Ophthalmology*, vol. 103, no. 2, pp. 208–215, 2019.

[36] T. S. Lee and M. Nguyen, "Dynamics of subjective contour formation in the early visual cortex," *Proceedings of the National Academy of Sciences of the United States of America*, vol. 98, no. 4, pp. 1907–1911, 2001.

[37] S. O. Dumoulin, R. F. Hess, K. A. May, B. M. Harvey, B. Rokers, and M. Barendregt, "Contour extracting networks in early extrastriate cortex," *Journal of Vision*, vol. 14, no. 5, p. 18, 2014.

[38] F. Yildirim, J. Carvalho, and F. W. Cornelissen, "A second-order orientation-contrast stimulus for population-receptive-field-based retinotopic mapping," *NeuroImage*, vol. 164, pp. 183–193, 2018.

[39] R. Le, N. Witthoft, M. Ben-Shachar, and B. Wandell, "The field of view available to the ventral occipito-temporal reading circuitry," *Journal of Vision*, vol. 17, no. 4, p. 6, 2017.

[40] L. E. Welbourne, A. B. Morland, and A. R. Wade, "Population receptive field (pRF) measurements of chromatic responses in human visual cortex using fMRI," *NeuroImage*, vol. 167, pp. 84–94, 2018.

[41] B. P. Klein, A. Fracasso, J. A. van Dijk, C. L. E. Paffen, S. F. Te Pas, and S. O. Dumoulin, "Cortical depth dependent population receptive field attraction by spatial attention in human V1," *NeuroImage*, vol. 176, pp. 301–312, 2018.

[42] D. M. van Es, J. Theeuwes, and T. Knapen, "Spatial sampling in human visual cortex is modulated by both spatial and feature-based attention," *eLife*, vol. 7, 2018.

[43] W. Zuiderbaan, B. M. Harvey, and S. O. Dumoulin, "Modeling center-surround configurations in population receptive fields using fMRI," *Journal of Vision*, vol. 12, no. 3, p. 10, 2012.

[44] K. N. Kay, T. Naselaris, R. J. Prenger, and J. L. Gallant, "Identifying natural images from human brain activity," *Nature*, vol. 452, no. 7185, pp. 352–355, 2008.

[45] K. N. Kay, J. Winawer, A. Mezer, and B. A. Wandell, "Compressive spatial summation in human visual cortex," *Journal of Neurophysiology*, vol. 110, no. 2, pp. 481–494, 2013.

[46] B. A. Wandell and J. Winawer, "Computational neuroimaging and population receptive fields," *Trends in Cognitive Sciences*, vol. 19, no. 6, pp. 349–357, 2015.

[47] C. A. Greene, S. O. Dumoulin, B. M. Harvey, and D. Ress, "Measurement of population receptive fields in human early visual cortex using back-projection tomography," *Journal of Vision*, vol. 14, no. 1, 2014.

[48] S. Lee, A. Papanikolaou, N. K. Logothetis, S. M. Smirnakis, and G. A. Keliris, "A new method for estimating population receptive field topography in visual cortex," *NeuroImage*, vol. 81, pp. 144–157, 2013.

[49] J. Carvalho, A. Invernizzi, K. Ahmadi, M. B. Hoffmann, and F. W. Cornelissen, "Micro-probing enables high-resolution mapping of neuronal subpopulations using fMRI," *BioRxiv*, p. 709006, 2019.

[50] P. Zeidman, E. H. Silson, D. S. Schwarzkopf, C. I. Baker, and W. Penny, "Bayesian population receptive field modelling," *NeuroImage*, vol. 180, pp. 173–187, 2018.

[51] S. Adaszewski, D. Slater, L. Melie-Garcia, B. Draganski, and P. Bogorodzki, "Simultaneous estimation of population receptive field and hemodynamic parameters from single point BOLD responses using Metropolis-Hastings sampling," *NeuroImage*, vol. 172, pp. 175–193, 2018.

[52] G. St-Yves and T. Naselaris, "The feature-weighted receptive field: an interpretable encoding model for complex feature spaces," *NeuroImage*, vol. 180, pp. 188–202, 2017.

[53] G. A. Keliris, Q. Li, A. Papanikolaou, N. K. Logothetis, and S. M. Smirnakis, "Estimating average single-neuron visual receptive field sizes by fMRI," *Proceedings of the National Academy of Sciences of the United States of America*, vol. 116, no. 13, pp. 6425–6434, 2019.

[54] A. Yoonessi and A. Yoonessi, "Functional assessment of magno, parvo and konio-cellular pathways; current state and future clinical applications," *Journal of Ophthalmic & Vision Research*, vol. 6, no. 2, pp. 119–126, 2011.

[55] R. van den Berg, J. B. T. M. Roerdink, and F. W. Cornelissen, "A neurophysiologically plausible population code model for

feature integration explains visual crowding," *PLoS Computational Biology*, vol. 6, no. 1, article e1000646, 2010.

[56] A. Grillini, R. Renken, N. Jansonius, and F. Cornelissen, "Perceptual learning following visual search decreases peripheral visual crowding," *Perception*, vol. 45, p. 226, 2016.

[57] M. Gilson, R. Moreno-Bote, A. Ponce-Alvarez, P. Ritter, and G. Deco, "Estimation of directed effective connectivity from fMRI functional connectivity hints at asymmetries of cortical connectome," *PLoS Computational Biology*, vol. 12, no. 3, article e1004762, 2016.

[58] A. M. Albers, T. Meindertsma, I. Toni, and F. P. de Lange, "Decoupling of BOLD amplitude and pattern classification of orientation-selective activity in human visual cortex," *NeuroImage*, vol. 180, pp. 31–40, 2018.

[59] C. F. Beckmann, M. DeLuca, J. T. Devlin, and S. M. Smith, "Investigations into resting-state connectivity using independent component analysis," *Philosophical Transactions of the Royal Society of London. Series B, Biological Sciences*, vol. 360, no. 1457, pp. 1001–1013, 2005.

[60] B. Biswal, F. Zerrin Yetkin, V. M. Haughton, and J. S. Hyde, "Functional connectivity in the motor cortex of resting human brain using echo-planar mri," *Magnetic Resonance in Medicine*, vol. 34, no. 4, pp. 537–541, 1995.

[61] D. Cordes, V. M. Haughton, K. Arfanakis et al., "Mapping functionally related regions of brain with functional connectivity MR imaging," *AJNR. American Journal of Neuroradiology*, vol. 21, no. 9, pp. 1636–1644, 2000.

[62] J. S. Damoiseaux, S. A. R. B. Rombouts, F. Barkhof et al., "Consistent resting-state networks across healthy subjects," *Proceedings of the National Academy of Sciences of the United States of America*, vol. 103, no. 37, pp. 13848–13853, 2006.

[63] T. Stein, C. Moritz, M. Quigley, D. Cordes, V. Haughton, and E. Meyerand, "Functional connectivity in the thalamus and hippocampus studied with functional MR imaging," *AJNR. American Journal of Neuroradiology*, vol. 21, no. 8, pp. 1397–1401, 2000.

[64] D. M. Cole, S. M. Smith, and C. F. Beckmann, "Advances and pitfalls in the analysis and interpretation of resting-state FMRI data," *Frontiers in Systems Neuroscience*, vol. 4, p. 8, 2010.

[65] N. Gravel, B. Harvey, B. Nordhjem et al., "Cortical connective field estimates from resting state fMRI activity," *Frontiers in Neuroscience*, vol. 8, p. 339, 2014.

[66] K. V. Haak, J. Winawer, B. M. Harvey et al., "Connective field modeling," *NeuroImage*, vol. 66, pp. 376–384, 2013.

[67] K. V. Haak, A. F. Marquand, and C. F. Beckmann, "Connectopic mapping with resting-state fMRI," *NeuroImage*, vol. 170, pp. 83–94, 2018.

[68] B. A. Wandell and R. K. Le, "Diagnosing the neural circuitry of reading," *Neuron*, vol. 96, no. 2, pp. 298–311, 2017.

[69] E. W. Dijkstra, "A note on two problems in connexion with graphs," *Numerische Mathematik*, vol. 1, no. 1, pp. 269–271, 1959.

[70] O. H. Butt, N. C. Benson, R. Datta, and G. K. Aguirre, "The fine-scale functional correlation of striate cortex in sighted and blind people," *The Journal of Neuroscience*, vol. 33, no. 41, pp. 16209–16219, 2013.

[71] J. Heinzle, T. Kahnt, and J.-D. Haynes, "Topographically specific functional connectivity between visual field maps in the human brain," *NeuroImage*, vol. 56, no. 3, pp. 1426–1436, 2011.

[72] T. H. Donner, D. Sagi, Y. S. Bonneh, and D. J. Heeger, "Retinotopic patterns of correlated fluctuations in visual cortex reflect the dynamics of spontaneous perceptual suppression," *The Journal of Neuroscience*, vol. 33, no. 5, pp. 2188–2198, 2013.

[73] M. Raemaekers, W. Schellekens, R. J. A. van Wezel, N. Petridou, G. Kristo, and N. F. Ramsey, "Patterns of resting state connectivity in human primary visual cortical areas: a 7T fMRI study," *NeuroImage*, vol. 84, pp. 911–921, 2014.

[74] A. S. Bock, P. Binda, N. C. Benson, H. Bridge, K. E. Watkins, and I. Fine, "Resting-state retinotopic organization in the absence of retinal input and visual experience," *The Journal of Neuroscience*, vol. 35, no. 36, pp. 12366–12382, 2015.

[75] K. V. Haak, A. B. Morland, G. S. Rubin, and F. W. Cornelissen, "Preserved retinotopic brain connectivity in macular degeneration," *Ophthalmic & Physiological Optics*, vol. 36, no. 3, pp. 335–343, 2016.

[76] A. Papanikolaou, G. A. Keliris, T. Dorina Papageorgiou, U. Schiefer, N. K. Logothetis, and S. M. Smirnakis, "Organization of Area hV5/MT+ in Subjects with Homonymous Visual Field Defects," *NeuroImage*, vol. 190, no. 15, pp. 254–268, 2018.

[77] Â. S. C. Miranda, A. d. F. Martins Rosa, M. J. Patrício Dias et al., "Optical properties influence visual cortical functional resolution after cataract surgery and both dissociate from subjectively perceived quality of vision," *Investigative Opthalmology & Visual Science*, vol. 59, no. 2, pp. 986–994, 2018.

[78] S. O. Dumoulin, A. Fracasso, W. van der Zwaag, J. C. W. Siero, and N. Petridou, "Ultra-high field MRI: advancing systems neuroscience towards mesoscopic human brain function," *NeuroImage*, vol. 168, pp. 345–357, 2018.

[79] A. Fracasso, N. Petridou, and S. O. Dumoulin, "Systematic variation of population receptive field properties across cortical depth in human visual cortex," *NeuroImage*, vol. 139, pp. 427–438, 2016.

Hindawi
Neural Plasticity
Volume 2019, Article ID 6067871, 15 pages
https://doi.org/10.1155/2019/6067871

Research Article

Stimulus- and Neural-Referred Visual Receptive Field Properties following Hemispherectomy: A Case Study Revisited

Hinke N. Halbertsma,[1] **Koen V. Haak**,[2] **and Frans W. Cornelissen**[1]

[1]*Laboratory of Experimental Ophthalmology-Visual Neurosciences, University Medical Center Groningen, 9713 GZ Groningen, Netherlands*
[2]*Donders Institute of Brain, Cognition and Behavior, Radboud University Medical Center, 6525 GA Nijmegen, Netherlands*

Correspondence should be addressed to Hinke N. Halbertsma; h.n.halbertsma@umcg.nl

Received 25 March 2019; Revised 21 June 2019; Accepted 4 July 2019; Published 3 September 2019

Guest Editor: Benjamin Thompson

Damage to the visual system can result in (a partial) loss of vision, in response to which the visual system may functionally reorganize. Yet the timing, extent, and conditions under which this occurs are not well understood. Hence, studies in individuals with diverse congenital and acquired conditions and using various methods are needed to better understand this. In the present study, we examined the visual system of a young girl who received a hemispherectomy at the age of three and who consequently suffered from hemianopia. We did so by evaluating the corticocortical and retinocortical projections in the visual system of her remaining hemisphere. For the examination of these aspects, we analyzed the characteristics of the connective fields ("neural-referred" receptive fields) based on both resting-state (RS) and retinotopy data. The evaluation of RS data, reflecting brain activity independent from visual stimulation, is of particular interest as it is not biased by the patient's atypical visual percept. We found that, primarily when the patient was at rest, the connective fields between V1 and both early and late visual areas were larger than normal. These abnormally large connective fields could be a sign either of functional reorganization or of unmasked suppressive feedback signals that are normally masked by interhemispheric signals. Furthermore, we confirmed our previous finding of abnormal retinocortical or "stimulus-referred" projections in both early and late visual areas. More specifically, we found an enlarged foveal representation and smaller population receptive fields. These differences could also be a sign of functional reorganization or rather a reflection of the interruption visual information that travels, via the remainder of the visual pathway, from the retina to the visual cortex. To conclude, while we do find indications for relatively subtle changes in visual field map properties, we found no evidence of large-scale reorganization—even though the patient could have benefitted from this. Our work suggests that at a later developmental stage, large-scale reorganization of the visual system no longer occurs, while small-scale properties may still change to facilitate adaptive processing and viewing strategies.

1. Introduction

Damage to critical components of its circuitry can have major consequences for the visual system. For example, lesions at the level of the optic radiation or early visual cortex can result in visual field defects spanning part of, or the entire, hemifield. Evidence supporting a reorganizatory potential of the visual system following both early and late acquired brain damage is now emerging (see for reviews [1–6]). For rehabilitation purposes, it is critical to understand the degree to which this potential can be deployed to restore lost function. For this reason, detailed studies on the organization of the visual system in patients and healthy observers are essential.

In the present study, we revisited the case of a girl who, at the age of three, received hemispherectomy as a treatment for Rasmussen syndrome (chronic focal encephalitis) and intractable epilepsy [7]. Her left hemisphere had been removed completely, which resulted in a full right homonymous visual field defect. The acquired visual field defect allowed us to

examine the potential reorganization of functional regions through examination of the properties of the visual field maps in her remaining hemisphere. Specifically, it allowed us to examine the effects of an interrupted processing of half of the retinal output (i.e., visual information coming from the left visual field) and the deprivation of interhemispheric inputs on the visual field map (VFM) properties.

We originally examined the VFM using retinotopy based on functional magnetic resonance imaging (fMRI) and established an absence of large-scale reorganization. However, using a specific analysis technique called population receptive field (pRF) modeling, we were able to assess more detailed properties of the underlying neuronal architecture. These pRF properties describe how the visual field is neuronally represented in the visual cortex. Because pRFs are modeled based on signals acquired during active stimulation, they are also referred to as "stimulus-referred" receptive fields. The application of pRF modelling to this patient suggested the presence of abnormal pRF properties in the visual areas [7]. Due to methodological developments since that study, we now had the opportunity to investigate this patient more extensively using connective field (CF) modeling. CF modeling, as an extension of the pRF technique, assesses the intracortical receptive fields, which are therefore also called "neural-referred" receptive fields [8]. The properties of the CFs describe how the visual field representations are projected from one region in the brain to another. A particular interesting aspect of CFs and the resulting CF maps is that we can estimate these, in addition to "active" stimulus-driven data, also based on resting-state data [9]. This has the advantage that the underlying signals are based on spontaneous fluctuations in brain activity and thus do not rely on visual input, which in neurological or ophthalmic patients may already be altered due to changes at the level of the eye or elsewhere in the brain [10].

In addition to the detailed evaluation of the CF maps, we also revisited pRF mapping (based on the "active" stimulus-driven data). Where our previous work focused on pRF modeling using a single unilateral pRF model, we additionally applied bilateral pRF modelling to examine a potential ipsilateral contribution to the patient's cortical VFMs. Ipsilateral VFM representations have been reported in cases with a congenital absence of or acquired damage to one of the two cerebral hemispheres [11–13]. In the interest of replication, and as a further improvement on our previous report, we also reevaluated the unilateral pRF model parameters of the patient. Yet, in addition to examining only differences in average or median values, we also compared parameter distributions between the patient and controls to assess whether changes occurred in specific parameter ranges.

2. Evaluation of Visual Field Map Properties

2.1. Materials and Methods

2.1.1. Participants. In this case-control study, the VFM properties of the right hemisphere of a 16-year-old female hemispherectomy patient were investigated. At the age of three, the girl's left hemisphere was removed completely (see Figure 1(a) for an anatomical MRI image of her brain). This surgical procedure resulted in a full right homonymous visual field defect without macular sparing (see Figure 1(b) for the results of a Goldmann perimetry). In spite of her visual defect, the girl was able to fixate reliably (as can also been seen from the straight visual field boundary along the vertical meridian of the Goldmann perimetry). At the same time, despite an initial major impact on her motoric and linguistic abilities, the girl partially recovered her motor control and speaks bilingually.

Twelve young healthy female participants (mean age = 22, sd = 1.8 years), of whom data was already acquired for a different project [14], with normal or corrected-to-normal visual acuity served as a control group. An additional four young healthy female participants (mean age = 27.5, sd = 1.7 years) with normal or corrected-to-normal visual acuity were recruited. This additional cohort served to control for the effect of different viewing instructions during RS on the estimation of the CF properties (see last paragraph of Data Acquisition).

For each participant, a high-resolution structural magnetic resonance (MR) image and a series of functional MR images were made available or newly collected. Informed written consent was obtained from all observers in accordance with the study procedures and protocols approved by the Medical Ethical Committee of the University Medical Center Groningen, the Netherlands. As the patient and the control participants were scanned at different points in time and initially for two different project, there were slight differences in the MR acquisition and visual stimulation protocols.

2.1.2. Stimulus. Visual field maps (VFM) were localized using a retinotopic mapping paradigm. The stimulus used was a drifting bar with a high-contrast checkerboard pattern and was presented on a grey (mean luminance) background. The bar had a radius of 12 or 10.21 degrees of visual angle and width of 3 and 2.75 degrees of visual angle, for the patient and controls, respectively. The full stimulus presentation (192 seconds) consisted of a sequence of eight bar apertures with four different orientations and two opposite motion directions (motion step every 1.5 seconds). Four 12-second mean-luminance periods ("blank periods") were inserted that replaced the bar presentation when it traversed the visual field along the diagonals. To ensure participants' central fixation, a small dot was presented in the center of the screen. Participants were asked to press a button on a button box whenever the dot changed color. The full stimulus cycle was presented to the participants either four or six times, for the patient and the controls, respectively, during separate scans. The VISTADISP toolbox (VISTA Lab, Stanford University) and PsychToolbox (https://github.com/Psychtoolbox-3/Psychtoolbox-3/) were used for stimulus control and display. For the patient, the stimulus was back-projected on a translucent display (44×34 cm) using a Barco LCD projector G300 set at a resolution of 800×600 pixels. For the control participants, the stimulus was presented on a 24-inch BOLD screen, an MRI-compatible full-color H-IPS LCD, and set at a resolution of 1920×1200

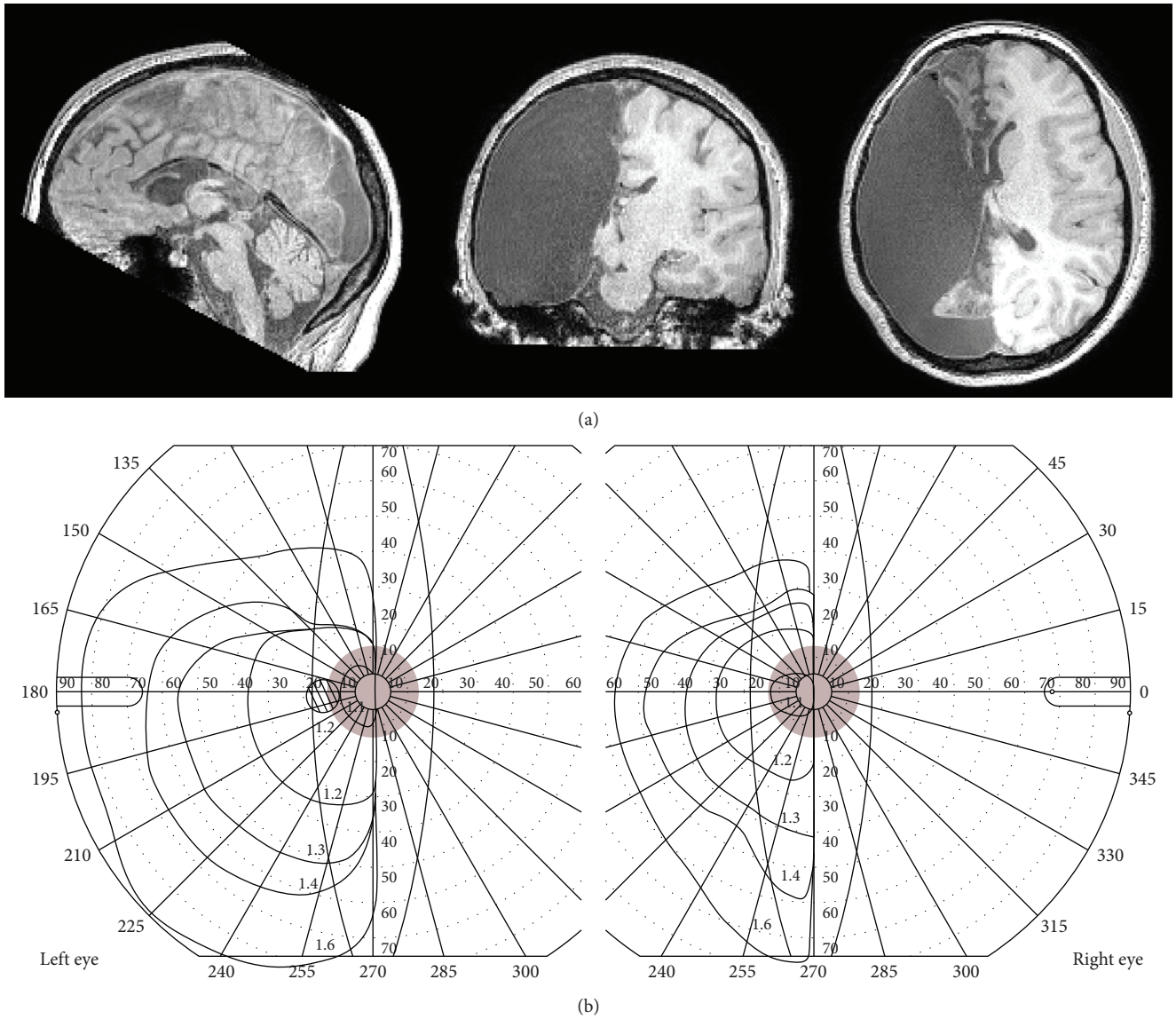

Figure 1: Anatomical MRI and Goldmann perimetry of the hemispherectomised patient. (a) High-resolution anatomical MRI scan showing the absence of the left hemispheres from a sagittal (left), coronal (middle), and axial (right) view. (b) Goldmann perimetry of both the left and right eyes showing a complete right-sided homonymous visual field defect, without macular sparing. The red patch indicates the size of the visual field that was stimulated during the fMRI experiment.

pixels. All participants viewed the display through a mirror placed at 11 cm from the eyes, with a viewing distance of 64 cm and 118 cm, for the patient and the controls, respectively.

2.1.3. Data Acquisition. All MRI images were acquired, using a 32-channel head coil, using a 3T Philips Intera MRI scanner (Philips; Best, the Netherlands) at the Neuroimaging Center in Groningen, the Netherlands.

For the patient, six functional scans (i.e., four retinotopy (RET) and two resting-state (RS) scans) were obtained using echo-planar imaging (EPI; $TR_{ret} = 1500$ ms/$TR_{rs} = 2000$ ms, $FOV_{ret} = 194 \times 72 \times 244$ mm/$FOV_{rs} = 192 \times 144 \times 192$ mm, $\text{voxel} - \text{size}_{ret} = 2.33 \times 2.33 \times 3$ mm/voxel $- \text{size}_{rs} = 3 \times 3 \times 3$ mm). During the RS scans, the patient was instructed to keep her eyes open and do nothing. Each RS scan had a duration of 370 seconds during which 181 volumes of each 48 slices were obtained. Both RS scans were obtained after the four RET scans. During retinotopy, the patient was instructed to pay attention to the stimulus and maintain fixation. In principle, each RET scan had a duration of 204 seconds (including a prescan period of twelve seconds), during which 136 volumes of each 24 slices were obtained. For some RET scans, the scanner was on longer than the actual experiment duration lasted; hence, additional acquired volumes were discarded.

For every control participant, seven EPI scans (i.e., one RS scan and six RET scans) were obtained or were made available ($TR_{rs} = 2000$ ms/$TR_{ret} = 1500$ ms, $FOV_{rs} = 220 \times 121 \times 220$ mm/$FOV_{ret} = 224 \times 72 \times 193.5$ mm, $\text{voxel} - \text{size}_{rs} = 3.44 \times 3.44 \times 3.29$ mm/voxel $- \text{size}_{ret} = 2.33 \times 2.33 \times 3$ mm). During the RS scan, control participants were instructed to

keep their eyes closed and do nothing. The RS scan had a duration of 708 seconds, during which 350 volumes of each 37 slices were obtained. During retinotopy, the control participants were instructed to pay attention to the stimulus and maintain fixation. Each RET scan had a duration of 204 seconds (including a prescan period of twelve seconds), during which 136 volumes of each 24 slices were obtained. However, due to technical issues, some scans lasted for only 198 seconds. As a consequence, no BOLD responses to the last two frames of the stimulus presentation (corresponding to a blank period) were recorded. A correction for this has been implemented in the pRF model.

The cohort of twelve control participants was initially scanned with a different project in mind [14]. As a result, the patient and the control subjects had received different instructions during the acquisition of the RS scans. Even though the scanner room was dimmed, the patient was instructed to fixate yet allowed to keep her eyes open. However, no eye tracking was performed leaving some room for fixation instability as a factor, and there was no control on whether she had in fact kept her eyes open during the entire RS scans. The participants that now serve as controls were instructed to keep their eyes closed. It cannot be excluded that these differences in instruction or their execution may have influenced the CF estimates. To verify this, in four additional female control participants, three six-minute EPI RS scans were collected during which participants were instructed, in successive scans, to keep their eyes closed (EC), fixated on a centered cross (FIX), or open (EO). The scanning parameters for these scans were identical to those used for the original control group. Furthermore, in this group of controls, six RET scans were also collected following the same scanning protocol and procedure as the other control participants in order to localize the visual areas.

For each participant, a T1-weighted high-resolution three-dimensional scan was obtained ($TR = 9.00$ ms, $TE = 3.5$ ms, flip angle $= 8^{\circ}$, acquisition matrix $= 251 \times 251 \times 170$ mm, $FOV = 256 \times 170 \times 232$, $voxel - size = 1 \times 1 \times 1$ mm) over a duration of 251 seconds, with a maximum number of 170 slices. Additionally, a short T1-weighted anatomical scan, with the same inplane resolution and orientation as the RET scans, was acquired for registration purposes of the retinotopy data.

2.1.4. Data Preprocessing. The T1-weighted anatomical scans were reoriented to AC-PC space and subsequently automatically segmented into grey and white matter using FreeSurfer (http://surfer.nmr.mgh.harvard.edu/), the results of which were manually refined using ITK-SNAP 3.6.0 (http://www.itksnap.org). To obtain a cortical reconstruction of the patient's brain, the intact hemisphere was copied and flipped along the x-axis to mimic a normal brain. Furthermore, because the tissue contrast in the patient's anatomical scan was suboptimal, we used a white matter (WM) mask created by FSL (https://fsl.fmrib.ox.ac.uk/fsl/fslwiki) FAST to decrease the intensity values for non-WM tissue, which significantly improved the automated cortical reconstruction done by FreeSurfer. All functional data were then preprocessed and analyzed at the individual level using FSL and the mrVista toolbox (https://github.com/vistalab/vistasoft) in MATLAB 2012b. RS data were first corrected for motion using FSL MCFLIRT and then denoised using ICA AROMA [15], a tool for head-motion-related artefact identification and removal. Using mrVista, RS data were interpolated to 1 mm structural data. The time series of the two, six-minute, consecutively collected RS scans of the patient were first normalized over time and then concatenated. This created a time series that matched the length of the RS time series of the controls.

RET data were preprocessed in mrVista. As the RET scans included a prescan of 12 seconds, the first eight volumes were removed from further analysis. Motion correction was applied to every scan; head movements within and between scans were calculated and corrected for (using rigid-body motion compensation [16]). Scans containing sudden head displacements larger than 1.5 voxels were discarded from further analyses. Functional scans were then averaged, interpolated to 1 mm structural data, and projected onto a mesh representation of the cortical surface.

2.1.5. Population Receptive Field Mapping (pRF Mapping). Population receptive fields (pRFs) were estimated using a model-based analysis (i.e., population receptive field mapping), by fitting 2D Gaussian pRFs to the data, as described in [17]. Parameters of interest were pRF eccentricity, polar angle, and size, where a voxel's pRF size reflects the size of the region of visual space that the voxel responds to and polar angle and eccentricity represent that voxel's pRF center location. The best-fitting models with a variance explained of at least 10% were then projected on an inflated representation of the visual cortex, on which early visual areas (V1, V2, and V3) and late visual areas (V3A, hV4, LO1, and LO2) were delineated based on their retinotopic properties (i.e., polar angle and eccentricity) using standard criteria [17–20]. More specifically, boundaries of the VFMs were based on phase reversals (i.e., reversals in polar angle value) and a maximum eccentricity of 10.2 degrees of visual angle. Furthermore, from every voxel within each ROI, its estimated pRF eccentricity and size were extracted for further analyses (see Section 2.1.8).

2.1.6. Connective Field Mapping (CF Mapping). Connective fields (CF) measure interareal spatial integration (as reflected by measures of corticocortical correlations) and were estimated using a model-based analysis (i.e., connective field mapping), as described by [8]. Parameters of interest derived were CF size and eccentricity. CF size reflects the size of the cortical surface area within a source region from which a target region samples its information. CF eccentricity equals the pRF eccentricity corresponding to the center of the sampled cortical area. Hence, the smaller the radius of the sampled area of the source region (i.e., the CF size), the higher the sampling resolution from cortical space. Using this CF-mapping approach, the functional connectivity profiles between the different VFMs were charted.

Six "source > target" CF maps (representing either CF eccentricity or size estimations) were computed with V1 as the source ROI and V2, V3, V3A, hV4, LO1, and LO2 as

the six target ROIs (tROIs). These CF maps were estimated (separately) from both signals under visual stimulation and spontaneous (resting-state) BOLD signals. For each participant, this resulted in one "active-state" CF (CF_{AS}) map and one "resting-state" CF (CF_{RS}) map per tROI. From every voxel within the tROIs, its estimated CF eccentricity and size were extracted for further analysis.

Similarly, for the additional four control participants, the CF field parameters were estimated per tROI and for the three viewing conditions (i.e., eyes closed, fixated, and open) separately. This resulted in three CF maps per tROI: CF_{EO}, CF_{FIX}, and CF_{EC}. Again, for each tROI, the estimated CF eccentricity and size were extracted for further analysis.

2.1.7. Bilateral pRF Mapping. In order to test whether each cortical location processes information from a single region of the visual field (as assumed with the conventional one Gaussian pRF model mentioned above) or from two bilateral regions of the visual field, two additional pRF models were run. With these bilateral pRF models, the time series predictions based on two, rather than one single, 2D Gaussians are fitted to the data. The Gaussians were mirrored around either the horizontal meridian (second fit in the ipsilateral hemifield) or the vertical meridian (second fit in the contralateral hemifield). This allowed us to examine the additional value of the second fit to the model prediction (see also [21]). Note that due to the mirroring, the unilateral and both bilateral models have the same number of parameters and can therefore be directly compared in terms of the explained variance in the fMRI time series.

2.1.8. Data Analyses. The derived VFM parameter estimates (i.e., CF size and eccentricity and pRF size and eccentricity) were thresholded at a variance explained (VE) level of 20%. Furthermore, we restricted our analyses to the VFM parameters corresponding to the stimulated region of the visual field of the controls. Hence, CFs and pRFs with eccentricity values larger than 10.2 degrees of visual angle were excluded from further analysis. Regions of interest were grouped into early (i.e., V1, V2, and V3) and late (i.e., V3A, LO1, LO2, and hV4) visual areas, and the CF and pRF parameter estimates were aggregated accordingly. Subsequent analyses were performed on the grouped areas, representing either early or late visual areas.

To examine whether the VFM parameter estimates differed between the patient and the control participants, several comparisons were performed. First, per area group, participants' CF and pRF sizes were plotted against the corresponding eccentricity estimates to examine the relationship between the two parameters. Per bin of 1 degree of CF_{AS}, CF_{RS}, and pRF eccentricity, the corresponding median sizes were calculated. Linear fits were computed for the median size vs. eccentricity relationship. Furthermore, the 95% confidence intervals (CIs) of the median were computed using a bootstrapping procedure with 1000 iterations.

Second, as a summarizing descriptive, participants' median CF and pRF eccentricities and sizes were computed per area group. Difference scores for each of the parameter's median were calculated for each possible "patient minus control" comparison. Obtained difference scores were statistically tested for deviating from zero with a one-sample t-test (p values of <0.0125 were considered significant after Bonferroni correction).

Lastly, per area group, relative frequency distributions were computed for all CF and pRF parameters, with bin sizes of 0.5 deg for CF eccentricity and pRF eccentricity/size or 0.5 mm for CF size. Obtained relative frequency distributions of the controls were averaged, and the 95% CIs of the mean were computed. This allowed us to examine, in addition to their medians, the distributions of the different VFM parameters.

In case relevant differences in CF_{RS} parameters between the patient and the controls were revealed by any of the above comparisons, a similar comparison was made between the CF estimates of the three viewing conditions. In this way, we were able to assess whether the apparent difference between patient and the controls could be potentially attributed to the different viewing instructions they received. For that reason, of primary interest were the comparisons of CF_{EO} vs. CF_{EC} and CF_{FIX} vs. CF_{EC}. For each of these comparisons, only those voxels were considered for which the models explained at least 20% of the variance in the time series of both viewing conditions to ensure an evaluation of the same set of voxels. For the CF_{EC}, this resulted in two sets of voxels: one for the comparison with CF_{EO} (i.e., $CF_{EC(EO)}$) and one for the comparison with CF_{FIX} (i.e., $CF_{EC(FIX)}$).

To examine the presence of ipsilateral visual field representations in the right hemisphere, a comparison was made between the two bilateral pRF models and the unilateral pRF model by comparing their VE distributions. Here, we limited ourselves to V1, since bilateral representations have been shown before for V1 [11–13] and since late visual areas are already known to sometimes possess large pRFs that overlap with the ipsilateral visual field [16, 21]. Only those voxels were considered for which all models explained at least 20% of the variance in the time series, ensuring evaluation of the same set of voxels for each model. The three models were compared in pairs, with the VE distribution of the first model taken as the test distribution, and the VE distribution of the second model taken as the baseline distribution. By iteratively changing the VE threshold (varying from 0.20 up to 0.99), the hit (HIT) rates (proportion of the test distribution passing the threshold) and false alarm (FA) rates (proportion of the baseline distribution passing the threshold) were computed. For each of the participants, and each of the model comparisons, isosensitivity curves were created by plotting the HIT rates against the FA rates. The area under the curve (AUC) of each of the isosensitivity lines described which model predicted the data best. AUC values above 0.5 indicated that the test model predicted the data better than the baseline model and vice versa. An AUC value of 0.5 indicated that the test and baseline model predicted the data equally well. For each of the model comparisons, a 95% CI was computed by bootstrapping the test and baseline distribution 2000 times with replacement.

Table 1: Median eccentricity and size estimates for CF_{AS} and CF_{RS} per area group, for the patient and averaged across controls. The medians' 1st and 3rd quartiles are presented between brackets.

	CF_{AS} ecc	CF_{AS} size	CF_{RS} ecc	CF_{RS} size	pRF ecc	pRF size
Early visual areas						
Patient	4.73 (2.4–7.5)	3.27 (1.8–5.1)	3.96 (2.9–7.2)	4.69 (1.4–8.6)	3.63 (2.3–5.8)	0.61 (0.2–3.6)
Controls	4.28 (2.4–6.9)	2.04 (0.8–3.9)	4.04 (2.4–6.8)	1.02 (0.4–2.4)	3.89 (2.2–6.2)	2.26 (1.5–3.2)
Late visual areas						
Patient	2.11 (1.6–4.1)	5.10 (1.6–8.0)	3.36 (2.2–4.0)	3.06 (1.0–9.2)	1.90 (0.9–4.2)	1.36 (0.2–5.0)
Controls	4.38 (2.5–6.7)	2.86 (1.0–7.3)	4.83 (2.8–8.0)	1.02 (0.4–2.2)	3.36 (1.7–6.1)	4.30 (2.7–6.5)

3. Results

We evaluated the visual field map properties in a hemispherectomy patient, using fMRI, to seek for the presence of functional reorganization of her visual system. More specifically, we evaluated CF properties both when at rest (resting-state (RS)) (CF_{RS}) and when visually stimulated (active-state (AS)) (CF_{AS}). Median values of the CF_{AS}, CF_{RS}, and pRF size and eccentricity estimates are presented in Table 1, for the patient and across the controls. These indicate that various differences exist between the patient and the controls.

3.1. Connective Field (CF) Eccentricity and Size

3.1.1. Patient vs. Controls. Figure 2(a) shows the relationship between eccentricity and size for CF_{AS} for both area groups. In the early visual areas, the patient shows an increase in CF_{AS} size with the eccentricity bin ($\beta = 3.09$, $p = 0.007$, df = 8), which is much larger ($\Delta\beta = 14.52$, $F = 19.01$, $p < 0.001$) than that of controls in the controls ($\beta = -11.43$, $p = 0.008$, df = 8). For the late visual areas, we found larger median CF_{AS} overall (mean $\Delta = 2.00$, paired t-test: $t = 4.62$, $p = 0.0013$, df = 9). Figure 2(b) shows the relationship between eccentricity and size of CF_{RS}. For both area groups, the CF_{RS} of the patient is larger at all eccentricities (paired t-test; early visual areas: mean $\Delta = 3.41$, $t = 9.145$, $p < 0.001$, df = 9; late visual areas: mean $\Delta = 3.20$, $t = 3.73$, $p = 0.0047$, df = 9).

Figure 3 compares, per area group, the difference in median eccentricity (Figure 3(a)) and size (Figure 3(b)) for CF_{AS} (purple) and CF_{RS} (blue) between the patient and the controls. This revealed various differences between the patient and controls. Namely, we found a lower median CF_{AS} eccentricity for the late visual areas (one-sample t-test: $t = -7.10$, $p < 0.001$, df = 11) and a larger median CF_{AS} for early visual areas (one-sample t-test: $t = 6.23$, $p < 0.001$, df = 11). Furthermore, we found larger median CF_{RS} for both early and late visual areas (one-sample t-test: $t = 38.9$, $p < 0.001$, and df = 11 and $t = 16.0$, $p < 0.001$, and df = 11, respectively).

Figure 4 shows the associated relative frequency-distributions for CF eccentricity (Figure 4(a)) and size (Figure 4(b)) to illustrate the origin of the differences described above. The distributions for CF_{AS} eccentricity indicate that the patient has a larger proportion of voxels with low eccentricities (range 1-2 deg) in late visual areas. Furthermore, it shows a smaller proportion of voxels with small CF_{AS} (up to 2 mm) in the patient, in early visual areas. This is accompanied by a larger proportion of CF_{AS} in the range of 3-7 mm. For CF_{RS}, we found smaller proportions of small CF_{RS} (<2 mm) for both area groups, which are accompanied by larger proportions of large CF_{RS} (>9 mm).

3.1.2. Eyes Closed vs. Fixated and Eyes Closed vs. Open. Our primary finding revealed larger CF_{RS} in the patient compared to the controls, in both early and late visual areas. To assess whether these observations could potentially be attributed to differences in viewing behavior, we compared the CF sizes in three viewing conditions (eyes open (EO), eyes fixated (FIX), and eyes closed (EC)) in four additional control participants. Table 2 shows the median values of CF_{EO}, CF_{FIX}, $CF_{EC(EO)}$, and $CF_{EC(FIX)}$. The median CF_{EO} and CF_{FIX} are slightly higher than $CF_{EC(EO)}$ and $CF_{EC(FIX)}$, respectively. Pairwise comparisons of the CF size for the early visual areas revealed no difference between CF_{EO} and $CF_{EC(EO)}$ (paired t-test; $t = -0.95$, df = 1142, $p = 0.34$) but did reveal a difference between CF_{FIX} and $CF_{EC(FIX)}$ (paired t-test; $t = 2.09$, df = 989, $p = 0.04$). Furthermore, we found a difference between CF_{EO} and $CF_{EC(EO)}$ (paired t-test; $t = 4.16$, df = 647, $p < 0.001$) and a difference between CF_{FIX} and $CF_{EC(FIX)}$ (paired t-test; $t = 2.61$, df = 443, $p = 0.0095$) for the late visual areas. p values are uncorrected for spatial autocorrelation and the upsampling that has been applied to the data during the CF modelling.

Figure 5 shows the associated relative frequency distributions of CF sizes for each of the three viewing conditions. This illustrates the origin of the differences in CF size between viewing conditions as described above. In both area groups, the distributions show a slightly larger proportion of voxels with small CFs (2-4 mm) for both the CF_{EO} and CF_{FIX} compared to CF_{EC}. In addition, the distribution of the patient (solid black line) and the mean distribution of the original group of controls (dashed black line) are presented that allowed for a direct comparison of all CF size distributions. From this, it can be noted that the origin of the CF size difference for CF_{EO} and CF_{FIX} is different from that of the patient (i.e., she has a smaller proportion of CF sizes in the 0-2 mm range and a larger proportion of CF sizes in the 9-10 mm range).

3.2. Population Receptive Field (pRF) Eccentricity and Size.

Figure 6 shows the relationship between pRF eccentricity and size for both area groups. In the patient, in both early and late visual areas, we found smaller pRFs at the low

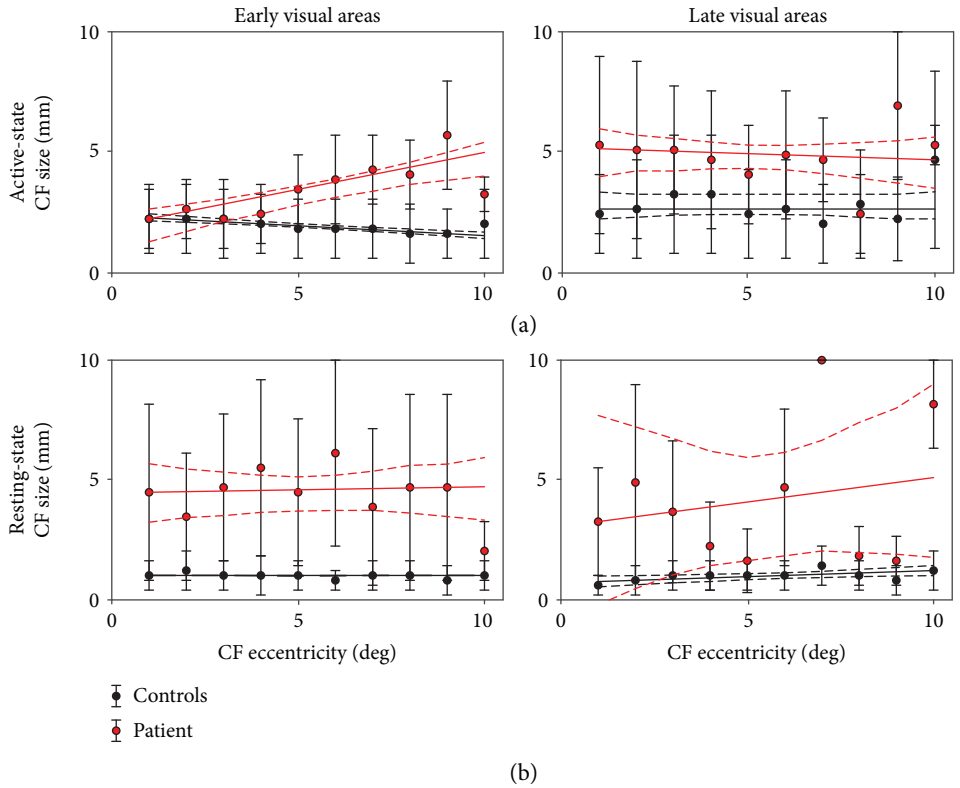

Figure 2: Relationship between eccentricity and size for CF_{AS} (a) and CF_{RS} (b). Data for both area groups of interest, grouped over controls and for the patient (red). CF eccentricity was binned in intervals of 1 deg. Median CF eccentricities are plotted, for which quantile regression fits were calculated (solid red line). Dashed lines represent the 95% bootstrapped confidence intervals for the fit of the median (1000 iterations).

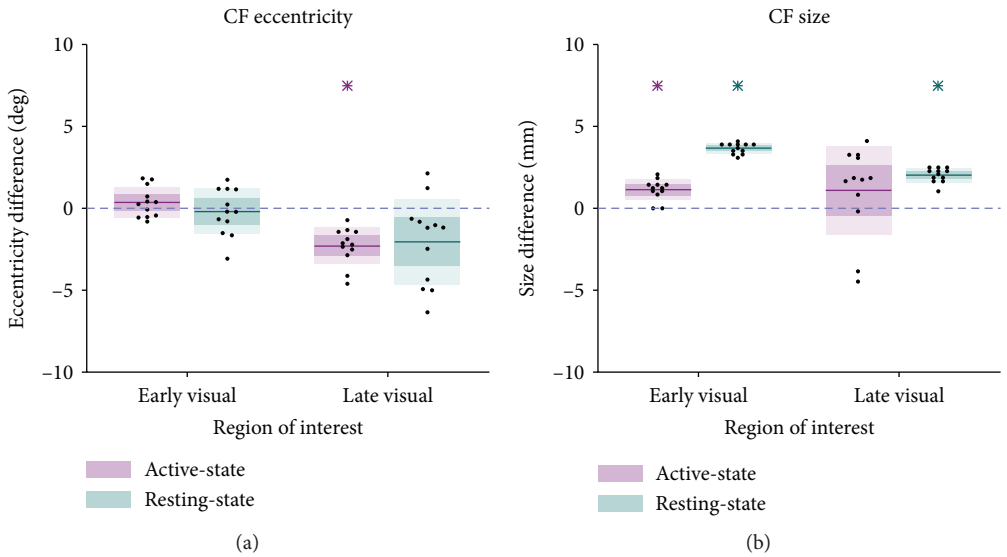

Figure 3: Difference distributions of the medians (patient – $control_n$). (a) Differences in median CF eccentricity (deg) per area group. (b) Differences in median CF size (in mm) per area group. Pink: CF_{AS} data; blue: CF_{RS} data; thick line: mean difference over all participants, with the dark and lighter shaded areas representing one SD and the 95% confidence interval of the mean, respectively. Blue dashed line at zero indicates no difference between the patient and control. An asterisk indicates a distribution deviating significantly from zero ($p < 0.0125$).

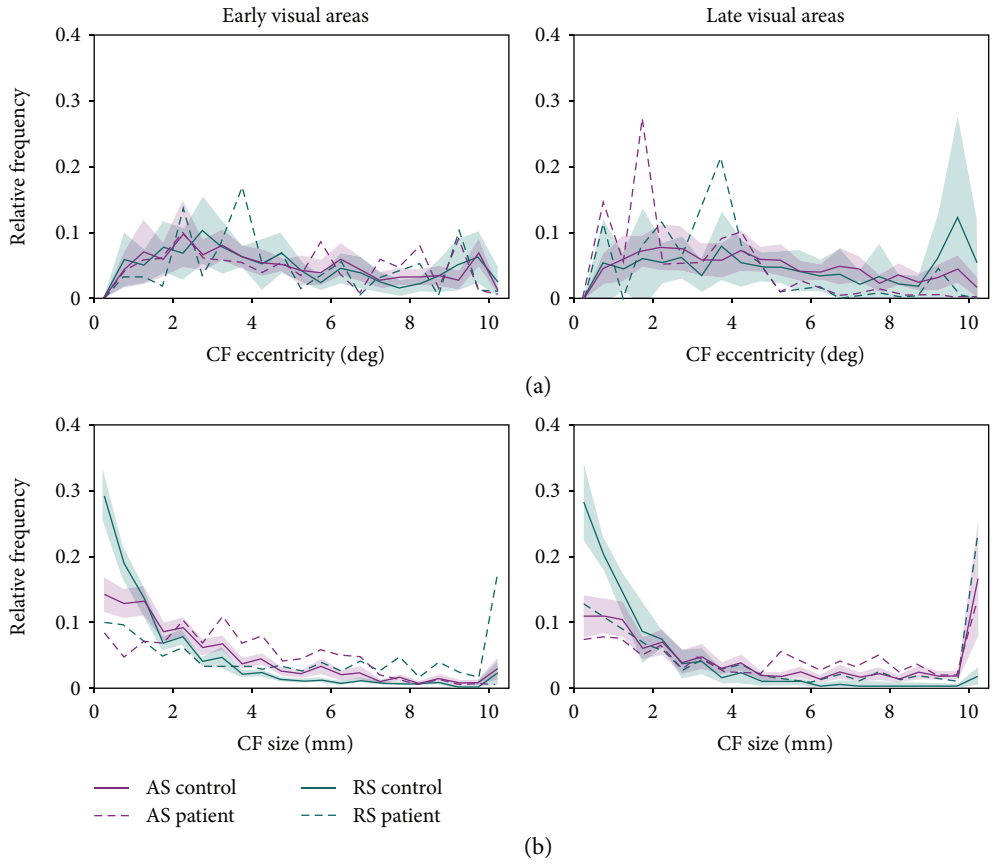

Figure 4: Relative frequency distributions of CF_{AS} (pink) and CF_{RS} (green) eccentricity (a) and size (b), per area group. Solid lines: average across controls ($n = 12$); shaded areas: 95% CI; dashed lines: patient.

Table 2: Median CF size estimates across subjects of the selected voxels per viewing condition. Interquartile ranges are presented in brackets.

Condition	Early visual	Late visual
CF_{FIX}	1.43 (0.61–2.65) ($n = 990$)	1.22 (0.61–2.65) ($n = 444$)
$CF_{EC(FIX)}$	0.82 (0.41–2.25) ($n = 990$)	0.82 (0.20–2.040) ($n = 444$)
CF_{EO}	1.22 (0.61–2.45) ($n = 1143$)	1.22 (0.82–2.65) ($n = 648$)
$CF_{EC(EO)}$	1.02 (0.41–2.60) ($n = 1143$)	0.61 (0.20–1.43) ($n = 648$)

eccentricities. At higher eccentricities, pRFs are within the normal range. These observations are in line with the previous observations of deviating pRF parameters in this patient [7].

Figure 7 compares the median eccentricity and size in both area groups for the patient and control. In the patient, for the late visual areas, we found a lower median pRF eccentricity. In addition, we found a smaller median pRF size in the early visual cortex and a substantially smaller median pRF size in the late visual areas (all $p < 0.01$).

To enable a more detailed evaluation of the differences between the patient and the control, Figure 8 shows the relative frequency distributions for pRF eccentricity (Figure 8(a)) and size (Figure 8(b)). The distributions for pRF eccentricity indicate that the patient has a larger proportion of voxels with low pRF eccentricities in the late visual areas (at 1 deg). Furthermore, it shows a larger proportion of voxels with small pRF sizes (up to 1 deg) in the patient, in both early and late visual areas. This is accompanied by a smaller proportion of pRFs in the range of 1-3 deg.

3.3. Follow-Up Analyses. Previous literature on CFs for V1 established that the sampling from V1 does not vary as a function of eccentricity [8, 22, 23]. To facilitate the interpretation of the (thus unexpected) increase in CF size with eccentricity in the early visual areas of the patient, we separately examined the pRF sizes of the source (i.e., V1) and the target regions of these CFs (i.e., V2 and V3). For the patient, we found a smaller median pRF size in V1 ($p < 0.01$), but not in V2 and V3, compared to controls. A larger CF size (i.e., a higher interareal sampling resolution) in the early visual areas of the patient may have given rise to this change in pRF size (from smaller to normal) from V1 to V2 and V3 that was observed at the lower eccentricities.

3.4. Single versus Bilateral pRF Model Comparison. We evaluated a possible ipsilateral contribution to the patient's

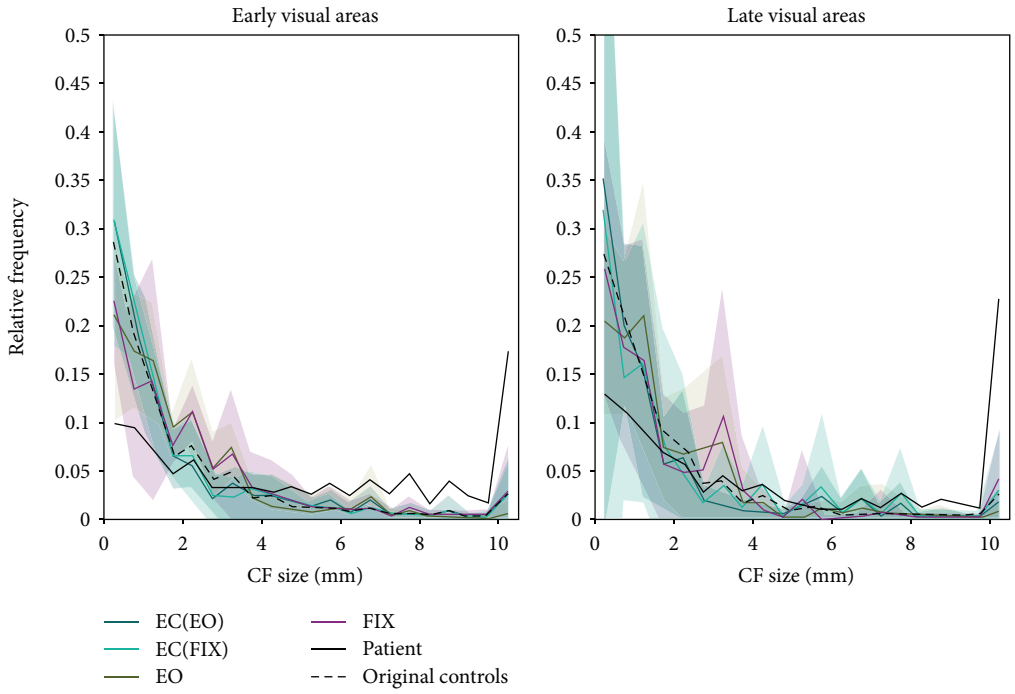

Figure 5: Relative frequency distributions of both CF_{EC} samples (blue lines), CF_{EO} (green), and CF_{FIX} purple size, per area group. Solid colored lines: average across controls ($n = 4$); shaded areas: 95% CI. Additionally, the CF size distribution of the patient (solid black) and the average distribution of the original groups of controls (dashed black, $n = 12$) are plotted.

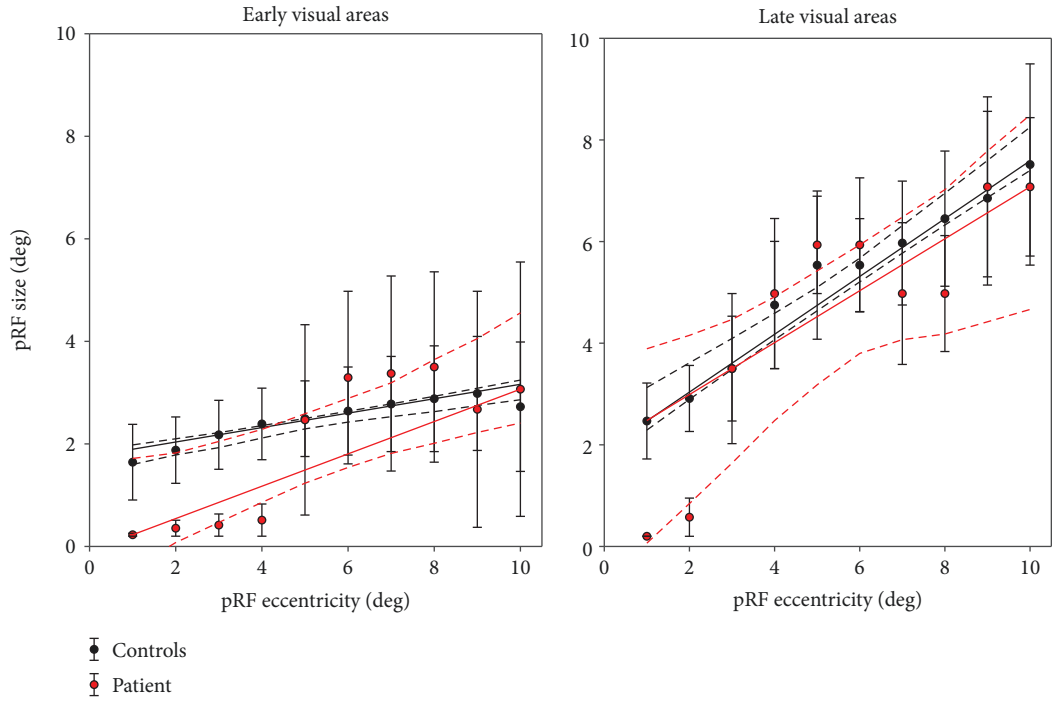

Figure 6: Relationship between pRF eccentricity and size. Data are presented for both area groups of interest, grouped over controls (black) versus the patient (red). PRF eccentricity was binned in intervals of 1 deg. Median pRF eccentricities are plotted, for which quantile regression fits were calculated (solid red line). Dashed lines represent the 95% bootstrapped confidence intervals for the fit of the median (1000 iterations).

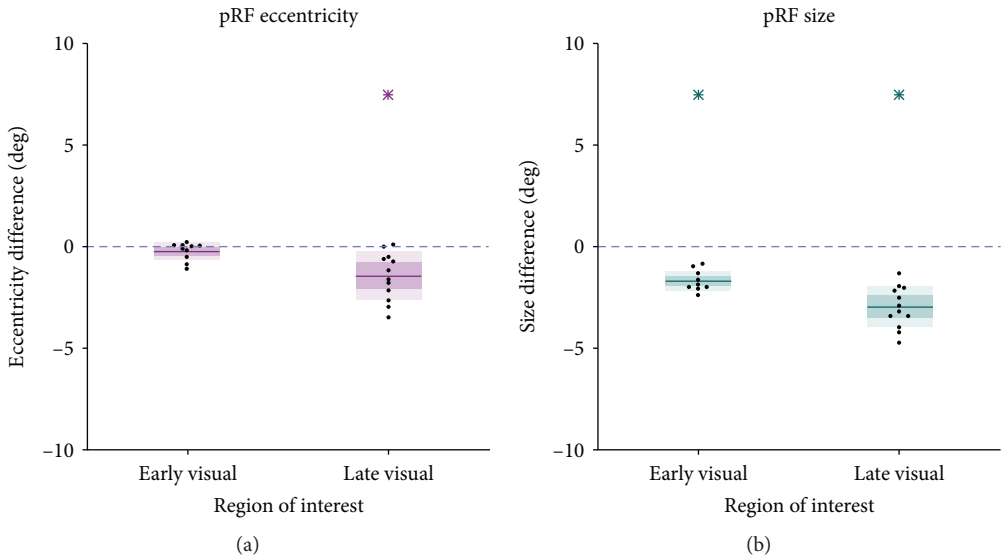

Figure 7: Difference distributions of the medians (patient − control$_n$). (a) Difference in pRF eccentricity per area group. (b) Same for pRF size. Thick line: mean difference over all participants, the dark and lighter shaded areas representing one SD and the 95% confidence interval of the mean, respectively. Blue dashed line at zero indicates no difference between the patient and control. Asterisk indicates a distribution deviating significantly from zero ($p < 0.01$).

cortical VFM by applying bilateral pRF modelling. In V1, the three different models (one unilateral and two bilateral) were evaluated using the isosensitivity curves. The isosensitivity lines for the patient showed a similar course as those of the controls, for the two single-versus-bilateral model comparisons (see Figures 9(a1), 9(b1), and 9(c1)). Specifically, they lie below the bisection line (the blue dotted line), suggesting that the single pRF model outperformed both the bilateral models. Bootstrapping analyses of the AUCs showed that the single pRF model performed better than the bilateral models for the majority of the participants (see Figures 9(a2), 9(b2), and 9(c2)), as indicated by the confidence intervals that do not overlap with 0.5. Nevertheless, for none of the participants, the AUC value was significantly larger than 0.5. Thus, by Occam's razor, the unilateral model was adopted as it is the simplest (i.e., with the fewest parameters) and performs at least as well as the more complex model (i.e., with more parameters). The isosensitivity lines of the vertically versus the horizontally mirrored pRF model lie around the bisection line, suggesting that one model did not perform better than the other. This was confirmed by the bootstrapping analyses that showed no AUC values significantly deviating from 0.5.

4. Discussion

Our main finding of the evaluation of the VFM properties of a hemispherectomy patient is that both the early and late visual areas contained larger CFs; this is most evident when in a resting-state condition. Additionally, we found smaller pRFs at low eccentricity, primarily for the late visual areas. Lastly, unlike what has been reported for cases with a congenital cause for an absence of a hemisphere, we found no evidence that V1 processes information from two bilateral regions of the visual field. This indicates a strictly contralateral processing of visual spatial information, in line with the patient's perimetrically established homonymous hemianopia.

4.1. Enlarged CFs in the Case of a Single Hemisphere. The main advance of this study, compared to our previous report [7], is that we were able to analyze the CF properties in the patient, both for active- and resting-state acquired signals. For the active-state condition, we found an increase in CF size with eccentricity in the early visual areas of the patient. In line with previous findings [7], this increase was absent in the controls. The decreased slope in the patient's later visual areas, compared to her early visual areas, suggests that the nonconstant sampling in these areas is largely inherited from V2/V3. For the resting-state condition, we also found larger CFs, this time in both area groups and over practically the entire range of eccentricities.

To our knowledge, our study is the first to find abnormally large CFs in a clinical case to date. Three other studies have examined CF parameters in a clinical population with a visual deficit. In patients with macular degeneration, Haak et al. showed preserved corticocortical organization, when visually stimulated, between input-deprived portions of V1 > V2/V3 [24]. In early blind and anophthalmia cases, Bock et al. found an intact corticocortical organization between V1 > V2/V3, even despite a complete absence of visual experience and retinal input [25]. Recently, Ahmadi et al. [26] showed changes in corticocortical connections for V1 > V3 in albinotic participants. Hence, this raises the question whether the abnormally large CF in our case is a sign of functional reorganization. While the absence of one hemisphere and half of the visual field might be a strong incentive for reorganization to occur [11, 12], it may also change the processing in the remaining hemisphere without reorganization per se. Therefore, before interpreting the observed differences

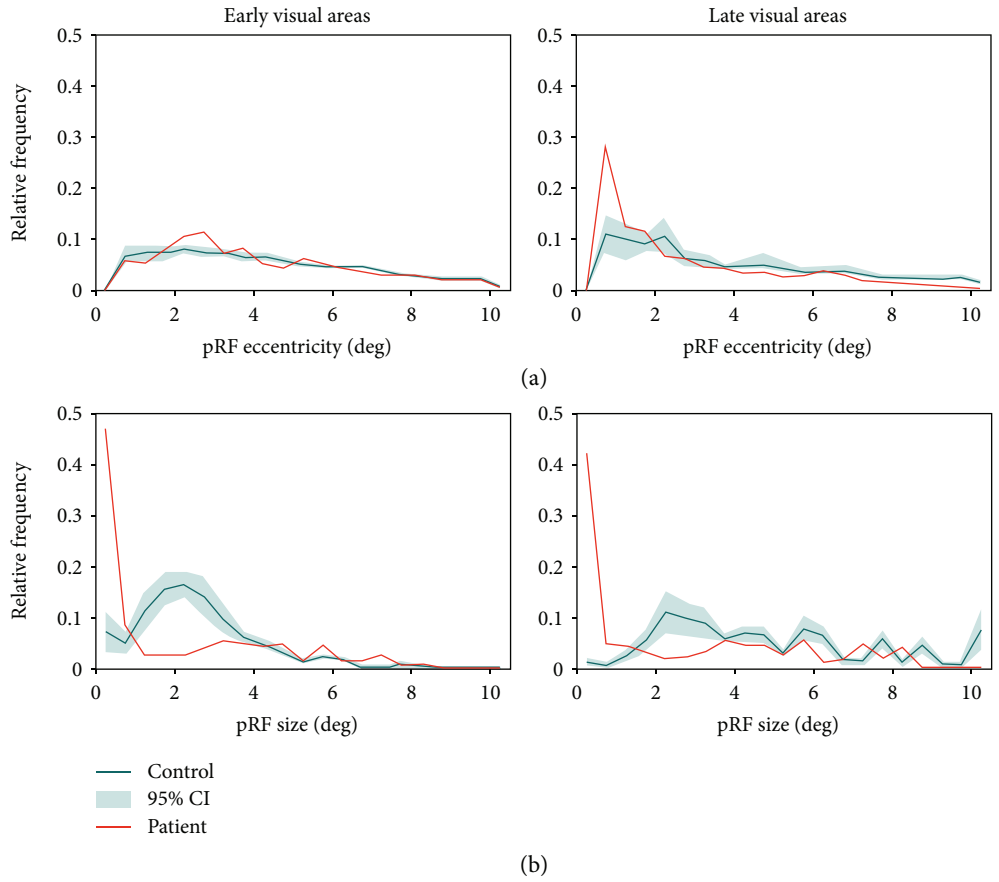

Figure 8: Relative frequency distribution for pRF eccentricity (a) and size (b). Green line: average of controls ($n = 12$); green shaded area: 95% CI; red line: patient.

in terms of functional reorganization, we should be able to rule out other possible causes [27].

Rather than the other two studies, ours presents the CF estimates in the case of a single hemisphere in the absence of the other one. What might explain the enlarged CFs in our case? And how can the enlarged CFs be reconciled with the observed pRF sizes, which were smaller than normal in foveal regions and roughly normal in the visual periphery? Indeed, it seems reasonable to expect that the pRF size scales with the CF size because larger CFs cover a larger cortical area and therefore cover a wider range of visual field locations. For example, if a voxel in V3 samples from a large area of V1 (i.e., it has a large CF), it intrinsically represents a large area of visual field. However, unlike the stimulus-referred pRF, the neural-referred CF captures both excitatory and suppressive responses [8]. Receptive fields can be conceptualized as spatial tuning curves with an excitatory center and a suppressive surround, the latter of which is thought to consist of a classical surround underpinned by lateral (intra-areal) connections and a wider extraclassical surround linked to feedback connections from higher order visual areas [8, 26–29]. The single Gaussian pRF model used in the present work captures only the excitatory responses and therefore reflects the center of the spatial tuning curve [27]. Since the pRF was not enlarged in the patient, and given that the CFs model interareal connectivity, we speculate that the enlarged CFs reflect a change in the extraclassical suppressive surround underpinned by modulatory feedback connections from later visual areas. This account suggests that the absence of the opposing cerebral hemisphere perturbs the feedback connectivity between V1 and later visual areas, the function of which is normally highly dependent on interhemispheric interactions (e.g., they have large receptive fields that overlap with the vertical meridian of the visual field). The account is also consistent with the observation that the CF enlargement is most profound in the absence of visual stimulation. When visually stimulated, the brain's activity is largely dominated by feed forward processes [29]. This makes the neural-referred receptive fields, estimated when visually active, less susceptible to feedback perturbations. This is in contrast with their estimations at rest and thus based on intrinsic brain activity. Whether these perturbations are the result of plastic reorganization or a consequence of unmasked suppressive feedback signals that are normally masked by interhemispheric signaling is an open question that remains to be addressed in future work.

However, the larger CFs in the early visual areas may also be a response to the smaller pRFs found in the early visual areas. In this case, their increased size may compensate for a lack of signal integration at this earlier level of processing in the cortical hierarchy. Indeed, detailed inspection of the

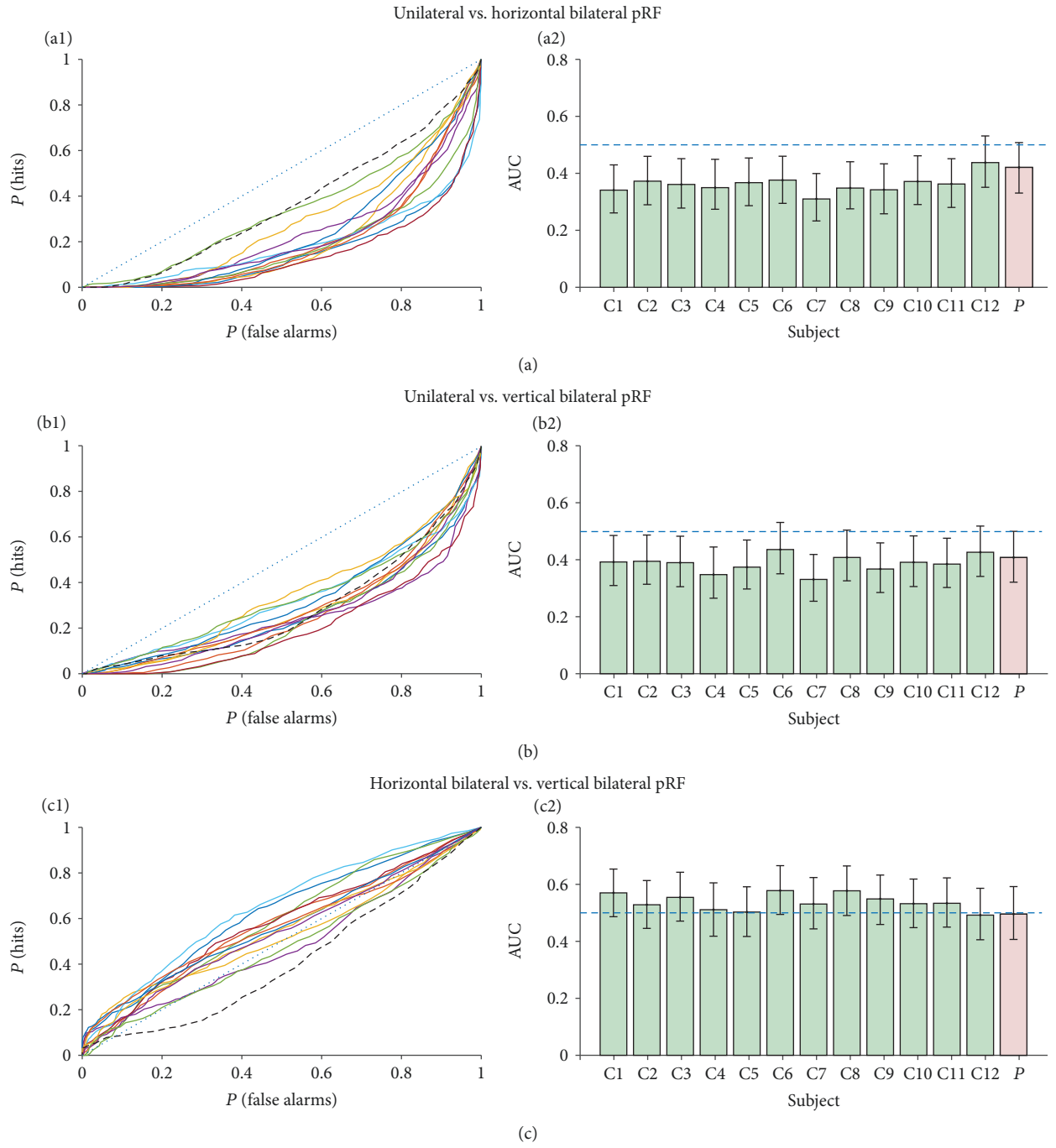

Figure 9: Isosensitivity and AUC plots for model comparison. (a1, b1, c1) Isosensitivity lines for the different model comparisons. Control participants are presented in colored solid lines and the patient in a dashed black line. Bisection line (AUC = 0.5) is plotted in dotted blue. (a2, b2, c2) A bar graph of the AUC values per participant. Error bars represent the 95% CI.

pRF sizes in the source (i.e., V1) and target regions (i.e., V2 and V3) of these CF estimations revealed smaller pRFs in the patient, exclusive to V1. While one would expect that these smaller V1 pRFs would be carried over to later visual areas, this is not what we found. A possible explanation is that the relatively large CFs of the patient for early visual areas V2 and V3 compensate for the small pRFs in V1. In this way, the pRF sizes of later stages of visual processing would be normalized.

4.2. CF Differences during Resting-State Cannot Be Attributed to Differences in Viewing Behavior. To investigate whether the observed increase in CF_{RS} size for the patient might be explained by a difference in viewing behavior, we compared the estimates from RS data acquired under three different viewing conditions (EC, FIX, and EO). Of primary interest were the comparisons of the eyes-open and eyes-fixated (most closely resembling the patient's condition) to the eyes-closed (identical to the controls) condition. Differences

between these conditions could affect the interpretation of the enlarged CF_{RS} as found in the patient.

For both the eyes-open and the eyes-fixated condition, we found a slightly larger median CF compared to the eyes-closed condition, in both area groups. Note that since uncorrected statistics have been reported, this difference found is most likely an overestimation of the actual difference. Nevertheless, these differences were much smaller (i.e., ~0.5 mm) than the difference we observed when comparing the patient to the controls (i.e., 3.20 mm). Furthermore, from the relative frequency distribution of CF size, we can conclude that the slight "viewing-condition-dependent" increase in CF size originated from a larger proportion of 2-4 mm range CFs. This is very different from the patient, who had primarily smaller proportions of small range CFs (<2 mm) and larger proportions of large range CFs (>9 mm), compared to controls.

To conclude, the differences in CF observed between the patient and the controls are much larger than can be explained by differences in viewing behavior and also occur in different parts of the CF size spectrum. Therefore, we conclude that the enlarged CFs of the patient are genuine.

4.3. Enlarged and More Detailed Foveal Processing. Our pRF modelling revealed a larger proportion of voxels with a low pRF eccentricity (foveal—parafoveal) for the late visual areas. Furthermore, we found larger proportions of small pRFs for both the early and late visual areas. These smaller than normal pRFs were found at a low eccentricity and are hence associated with a (para)foveal vision. These findings are in line with, and complement, previous observations on this patient of an enlarged foveal representation and smaller pRFs in the lateral occipital cortex as compared to controls [7]. This difference in pRF cannot be attributed to poor fixation as the patient was able fixate well. Furthermore, poor fixation would have resulted in larger pRF estimates, whereas in the patient, we found smaller pRF estimates.

Deviating pRF properties have been reported in a number of studies in patients with homonymous hemianopia. In another hemispherectomy patient, compared to controls, larger pRFs and increased eccentricity for dorsal V2 and V3 were found [30]. In a subset of hemianopic patients, Papanikolaou et al. [31] found a slight increase in pRF size in V1 of the intact hemisphere. This contrasts our finding of smaller pRFs at lower and approximately normal-sized pRFs at higher eccentricities in the early visual areas. All studies reported that polar angle representations remained unchanged [7, 29, 30].

Our pRF data implies that in the late visual areas, the patient shows an enlarged foveal representation (as reflected by the larger proportions of low pRF eccentricities), with a detailed processing of the visual field (as reflected by smaller pRFs). Similarly, the patient's early visual areas also possess a more detailed processing of spatial information (as reflected by the smaller pRFs). These findings might be explained as a functional response to the homonymous hemianopia (which was without macular sparing). Patients with central vision loss—for example, due to macular degeneration—often adopt an eccentric preferred retinal locus (PRL; see [31, 32]), which they use as a kind of pseudofovea. We speculate that our patient might have developed such a PRL as well and, in response to that, also a more extended (para)foveal processing in certain brain areas. Unfortunately, at present, we have no means to clinically verify this interpretation.

Haak et al. [7] attributed the unusually small pRFs in the patient's late visual cortex to a lack of input from the opposite cerebral hemisphere. At the same time, both Georgy et al. [30] and Papanikolaou et al. [31] attributed the increase in pRF size in the early visual cortex in their patients to a loss of interhemispheric input as well. Hence, there is no indication that the condition of hemianopia leads to consistent deviations in either field map representations or pRF properties. Differences in cause and onset of the hemianopia may be factors that affect what type of change will occur. At the same time, we should note that the number of cases studied is still very small, which prevents us from drawing firmer conclusions.

4.4. No Evidence for Representations of the Ipsilateral Visual Field. We also examined whether the V1 in the remaining hemisphere represented the ipsilateral visual field. Comparison of the three different pRF-mapping models showed no better model fit for the bilateral pRF models compared to the single pRF model, neither for the controls nor the patient. This suggests that the V1 of the patient, like the controls, primarily represented the contralateral visual field. This finding is consistent with the patient's perimetric results (i.e., a homonymous hemianopia).

Despite being described as infrequent, cases of bilateral visual field representations have been reported before in the literature, with patients possessing bilateral visual field representations despite having only one (intact) hemisphere [12] or two underdeveloped hemispheres [33], suggesting functional reorganization of the visual system. More recently, another case of congenital unilateral loss of the cerebral cortex (hemihydranencephaly) with a preserved visual field was investigated [11]. In particular, using the same bilaterally pRF-modelling approach as presented here, they tested for the presence of both ipsilateral and contralateral visual field representations in this patient. Data revealed interleaved representations of both the ipsilateral and the contralateral visual hemifield located in the early visual cortex of the intact hemisphere.

These studies show that in cases of major cortical damage to the visual system, there is a potential for functional reorganization that supports an improved perceptual performance. Yet, no bilateral processing was found in our hemispherectomy patient. It must be noted that most of the cases described above concern congenitally hemiblind observers whereas our case has an acquired cortical hemiblindness. An explanation for this discrepancy could thus be that in the congenitally unihemispheric patient, the abnormal functional organization could be attributed to the fact that there is an absence of the molecular gradient directing the growth of white matter fibers that normally cross the corpus callosum. Without this gradient and with no hemisphere to grow to, white matter fibers remain in the ipsilateral hemisphere

allowing for ipsilateral projections. In the case of a hemispherectomy, however, such fibers have already been grown and cut away during surgery. Additionally, molecular gradients are no longer present after the critical period (the present case had her hemispherectomy at the age of three).

5. Conclusion

The case presented here provides signs of relatively subtle functional reorganization. The patient's visual system did not recover from her acquired visual hemifield defect that emerged after removal of the left hemisphere. On the other hand, despite the initial major impact of the hemispheric removal on her motoric and linguistic abilities, the girl partially recovered her motor control and speaks bilingually. These aspects do indicate that functional reorganization has taken place after the surgery but not so obviously in the visual domain. In line with this, evaluation of the patient's visual field maps indeed did not reveal any major remapping, in that the remaining hemisphere does not contain representations of the ipsilateral visual field. Hence, we conclude that no large-scale reorganization has taken place.

At the same time, the chronic visual field defect allowed us to examine the effects of an interrupted processing of half of the retinal output and deprivation of interhemispheric inputs on the VFM map properties in the remaining hemisphere. This led to the observation of abnormal VFM properties in both the early and late visual areas. Specifically, we found larger than normal CFs for the patient. These larger CFs may be considered a form of subtle functional reorganization. The more detailed spatial processing and, in the late visual areas, the additional enlarged foveal representation found in the patient could be interpreted as a functional reorganization as well. In particular, in the context of a possible PRL, the brain might have adaptively reorganized itself in response to the development of such eccentric fixation. However, the interpretation of these deviating properties should be done with caution. Often other explanations are able to account for the abnormal maps that do not require assuming cortical reorganization. For example, abnormal visual maps may be reflections of (partially) absent visual inputs [7].

To conclude, in the absence of large-scale functional reorganization, we do find indications for relatively subtle changes in VFM organization, which might facilitate adaptive processing and viewing strategies. This evaluation contributes to the understanding of the consequences of removing a hemisphere at an early developmental stage for the functional organization of the visual system.

Data Availability

The data used to support the findings of this study are available from the corresponding author upon request.

Conflicts of Interest

The authors declare no conflict of interests.

Acknowledgments

We thank J.B.C Marsman for collecting the data of the hemispherectomy patient and B. Nordhjem for collecting the data of the control participants. HNH was supported by the Research Institute of Brain and Cognition of the Graduate School of Medical Sciences, Universitair Medisch Centrum Groningen, the Netherlands. HNH and FWC have been supported by the European Union's Horizon 2020 research and innovation programme under the Marie Sklodowska-Curie grant agreement No. 641805. KVH gratefully acknowledges funding from the Netherlands Organisation for Scientific Research (NWO VENI grant no. 016.Veni.171.068).

References

[1] R. Werth, "Visual functions without the occipital lobe or after cerebral hemispherectomy in infancy," *European Journal of Neuroscience*, vol. 24, no. 10, pp. 2932–2944, 2006.

[2] K. R. Huxlin, "Perceptual plasticity in damaged adult visual systems," *Vision Research*, vol. 48, no. 20, pp. 2154–2166, 2008.

[3] B. A. Wandell and S. M. Smirnakis, "Plasticity and stability of visual field maps in adult primary visual cortex," *Nature Reviews Neuroscience*, vol. 10, no. 12, pp. 873–884, 2009.

[4] A. Guzzetta, G. D'Acunto, S. Rose, F. Tinelli, R. Boyd, and G. Cioni, "Plasticity of the visual system after early brain damage," *Developmental Medicine & Child Neurology*, vol. 52, no. 10, pp. 891–900, 2010.

[5] C. D. Gilbert and W. Li, "Adult visual cortical plasticity," *Neuron*, vol. 75, no. 2, pp. 250–264, 2012.

[6] D. C. Reitsma, J. Mathis, J. L. Ulmer, W. Mueller, M. J. Maciejewski, and E. A. DeYoe, "Atypical retinotopic organization of visual cortex in patients with central brain damage: congenital and adult onset," *The Journal of Neuroscience*, vol. 33, no. 32, pp. 13010–13024, 2013.

[7] K. V. Haak, D. R. M. Langers, R. Renken, P. van Dijk, J. Borgstein, and F. W. Cornelissen, "Abnormal visual field maps in human cortex: a mini-review and a case report," *Cortex*, vol. 56, pp. 14–25, 2014.

[8] K. V. Haak, J. Winawer, B. M. Harvey et al., "Connective field modeling," *NeuroImage*, vol. 66, pp. 376–384, 2013.

[9] N. Gravel, B. Harvey, B. Nordhjem et al., "Cortical connective field estimates from resting state FMRI activity," *Frontiers in Neuroscience*, vol. 8, p. 339, 2014.

[10] Carvalho, Renken, and Cornelissen, "Studying cortical plasticity in ophthalmic and neurological disorders: from stimulus-driven to cortical circuitry approaches," Submitted to Neural Plasticity's special issue "Role of Visual Cortical Plasticity in the Development and Treatment of Amblyopia and other Neurodevelopmental Disorders".

[11] A. Fracasso, Y. Koenraads, G. L. Porro, and S. O. Dumoulin, "Bilateral population receptive fields in congenital hemihydranencephaly," *Ophthalmic & Physiological Optics*, vol. 36, no. 3, pp. 324–334, 2016.

[12] L. Muckli, M. J. Naumer, and W. Singer, "Bilateral visual field maps in a patient with only one hemisphere," *Proceedings of the National Academy of Sciences of the United States of America*, vol. 106, no. 31, pp. 13034–13039, 2009.

[13] L. Henriksson, A. Raninen, R. Nasanen, L. Hyvarinen, and S. Vanni, "Training-induced cortical representation of a

hemianopic hemifield," *Journal of Neurology, Neurosurgery & Psychiatry*, vol. 78, no. 1, pp. 74–81, 2007.

[14] N. Gravel, *The Neuroanatomical Organization of Intrinsic Brain Activity Measured by FMRI Activity in the Human Visual Cortex, Gravel Araneda, Nicolas Gaspar, [Ph.D. thesis]*, University of Groningen, Groningen, Netherlands, 2019, http://hdl.handle.net/11370/94e84a60-f7d2-4e40-afd8-814e03772d9a.

[15] R. H. R. Pruim, M. Mennes, D. van Rooij, A. Llera, J. K. Buitelaar, and C. F. Beckmann, "ICA-AROMA: a robust ICA-based strategy for removing motion artifacts from fMRI data," *NeuroImage*, vol. 112, pp. 267–277, 2015.

[16] O. Nestares and D. J. Heeger, "Robust multiresolution alignment of MRI brain volumes," *Magnetic Resonance in Medicine*, vol. 43, no. 5, pp. 705–715, 2000.

[17] S. O. Dumoulin and B. A. Wandell, "Population receptive field estimates in human visual cortex," *NeuroImage*, vol. 39, no. 2, pp. 647–660, 2008.

[18] S. A. Engel, G. H. Glover, and B. A. Wandell, "Retinotopic organization in human visual cortex and the spatial precision of functional MRI," *Cerebral Cortex*, vol. 7, no. 2, pp. 181–192, 1997.

[19] B. A. Wandell, S. O. Dumoulin, and A. A. Brewer, "Visual field maps in human cortex," *Neuron*, vol. 56, no. 2, pp. 366–383, 2007.

[20] M. I. Sereno, C. T. Mcdonald, and J. M. Allman, "Analysis of retinotopic maps in extrastriate cortex," June 2019, https://www.cogsci.ucsd.edu/~sereno/107B-201/readings/04.07-analysisretinmap.pdf.

[21] M. B. Hoffmann, F. R. Kaule, N. Levin et al., "Plasticity and stability of the visual system in human achiasma," *Neuron*, vol. 75, no. 3, pp. 393–401, 2012.

[22] R. B. H. Tootell, J. D. Mendola, N. K. Hadjikhani, A. K. Liu, and A. M. Dale, "The representation of the ipsilateral visual field in human cerebral cortex," *Proceedings of the National Academy of Sciences of the United States of America*, vol. 95, no. 3, pp. 818–824, 1998.

[23] B. M. Harvey and S. O. Dumoulin, "The relationship between cortical magnification factor and population receptive field size in human visual cortex: constancies in cortical architecture," *The Journal of Neuroscience*, vol. 31, no. 38, pp. 13604–13612, 2011.

[24] A. S. Bock, P. Binda, N. C. Benson, H. Bridge, K. E. Watkins, and I. Fine, "Resting-state retinotopic organization in the absence of retinal input and visual experience," *The Journal of Neuroscience*, vol. 35, no. 36, pp. 12366–12382, 2015.

[25] K. Ahmadi, A. Herbik, M. Wagner, M. Kanowski, H. Thieme, and M. B. Hoffmann, "Population receptive field and connectivity properties of the early visual cortex in human albinism," *bioRxiv*, 2019, article 627265.

[26] K. V. Haak, F. W. Cornelissen, and A. B. Morland, "Population receptive field dynamics in human visual cortex," *PLoS One*, vol. 7, no. 5, article e37686, 2012.

[27] L. Schwabe, J. M. Ichida, S. Shushruth, P. Mangapathy, and A. Angelucci, "Contrast-dependence of surround suppression in macaque V1: experimental testing of a recurrent network model," *NeuroImage*, vol. 52, no. 3, pp. 777–792, 2010.

[28] L. Schwabe, K. Obermayer, A. Angelucci, and P. C. Bressloff, "The role of feedback in shaping the extra-classical receptive field of cortical neurons: a recurrent network model," *The Journal of Neuroscience*, vol. 26, no. 36, pp. 9117–9129, 2006.

[29] V. A. F. Lamme and P. R. Roelfsema, "The distinct modes of vision offered by feedforward and recurrent processing," *Trends in Neurosciences*, vol. 23, no. 11, pp. 571–579, 2000.

[30] L. Georgy, B. Jans, M. Tamietto, and A. Ptito, "Functional reorganization of population receptive fields in a Hemispherectomy patient with blindsight," *Neuropsychologia*, vol. 128, pp. 198–203, 2019.

[31] A. Papanikolaou, G. A. Keliris, T. D. Papageorgiou et al., "Population receptive field analysis of the primary visual cortex complements perimetry in patients with homonymous visual field defects," *Proceedings of the National Academy of Sciences of the United States of America*, vol. 111, no. 16, pp. E1656–E1665, 2014.

[32] G. K. Von Noorden and G. Mackensen, "Phenomenology of eccentric fixation," *American Journal of Ophthalmology*, vol. 53, no. 4, pp. 642–661, 1962.

[33] M. Ptito, M. Dalby, and A. Gjedde, "Visual field recovery in a patient with bilateral occipital lobe damage," *Acta Neurologica Scandinavica*, vol. 99, no. 4, pp. 252–254, 1999.

Hindawi
Neural Plasticity
Volume 2019, Article ID 2564018, 23 pages
https://doi.org/10.1155/2019/2564018

Research Article

Classification of Visual Cortex Plasticity Phenotypes following Treatment for Amblyopia

Justin L. Balsor,[1] David G. Jones,[2] and Kathryn M. Murphy[1,3]

[1]*McMaster Integrative Neuroscience Discovery and Study (MiNDS) Program, McMaster University, Hamilton, ON, Canada L8S 4K1*
[2]*Pairwise Affinity Inc., Dundas, ON, Canada L9H 2R9*
[3]*Department of Psychology, Neuroscience & Behavior, McMaster University, Hamilton, ON, Canada L8S 4K1*

Correspondence should be addressed to Kathryn M. Murphy; kmurphy@mcmaster.ca

Received 24 December 2018; Revised 4 April 2019; Accepted 13 May 2019; Published 3 September 2019

Academic Editor: Malgorzata Kossut

Monocular deprivation (MD) during the critical period (CP) has enduring effects on visual acuity and the functioning of the visual cortex (V1). This experience-dependent plasticity has become a model for studying the mechanisms, especially glutamatergic and GABAergic receptors, that regulate amblyopia. Less is known, however, about treatment-induced changes to those receptors and if those changes differentiate treatments that support the recovery of acuity versus persistent acuity deficits. Here, we use an animal model to explore the effects of 3 visual treatments started during the CP ($n = 24$, 10 male and 14 female): binocular vision (BV) that promotes good acuity versus reverse occlusion (RO) and binocular deprivation (BD) that causes persistent acuity deficits. We measured the recovery of a collection of glutamatergic and GABAergic receptor subunits in the V1 and modeled recovery of kinetics for NMDAR and $GABA_AR$. There was a complex pattern of protein changes that prompted us to develop an unbiased data-driven approach for these high-dimensional data analyses to identify plasticity features and construct plasticity phenotypes. Cluster analysis of the plasticity phenotypes suggests that BV supports adaptive plasticity while RO and BD promote a maladaptive pattern. The RO plasticity phenotype appeared more similar to adults with a high expression of GluA2, and the BD phenotypes were dominated by $GABA_A\alpha1$, highlighting that multiple plasticity phenotypes can underlie persistent poor acuity. After 2-4 days of BV, the plasticity phenotypes resembled normals, but only one feature, the GluN2A:GluA2 balance, returned to normal levels. Perhaps, balancing Hebbian (GluN2A) and homeostatic (GluA2) mechanisms is necessary for the recovery of vision.

1. Introduction

Since the earliest demonstrations that monocular deprivation (MD) during a critical period (CP) causes ocular dominance plasticity and acuity loss [1–3], this model has been used to deepen our understanding of the neural changes associated with amblyopia. There have been fewer studies, however, about cortical changes associated with the acuity deficits that often persist after treatment for amblyopia [4–8]. Here, we use an animal model to classify the expression patterns (phenotypes) of a collection of synaptic proteins that regulate experience-dependent plasticity and explored if treatments that promote good versus poor acuity reinstate CP-like plasticity phenotypes in the visual cortex (V1).

Many animal studies have highlighted the roles of glutamatergic and GABAergic mechanisms for regulating plasticity during the CP [9–15]. For example, the subunit composition of AMPA, NMDA, and $GABA_A$ receptors regulates the bidirectional nature of ocular dominance plasticity [16–21]. Some of the changes caused by MD include delaying the maturational shift to more GluN2A-containing NMDARs [22, 23] and accelerating the expression of $GABA_A\alpha1$-containing $GABA_A$Rs [20, 23]. Together, those changes likely decrease signal efficacy and dysregulate the spike-timing-dependent plasticity that drives long-term depression (LTD) and weakens deprived-eye response [24]. Furthermore, silencing activity engages homeostatic mechanisms that scale the responsiveness of V1 neurons by inserting GluA2-containing AMPAR into the synapse [25]. Importantly, many of the receptor changes have been linked with specific acuity deficits [26, 27] suggesting that visual outcomes may reflect changes to a collection of

glutamatergic and GABAergic receptor subunits that together represent a plasticity phenotype for the V1.

Animal studies of amblyopia have also identified treatments that promote good versus poor recovery of acuity after MD. For example, reverse occlusion (RO) gives a competitive advantage to the deprived eye that promotes an ocular dominance shift, but the acuity recovered by the deprived eye is transient and can be lost within hours of introducing binocular vision [6–8]. Similarly, closing both eyes after MD to test a form of binocular deprivation therapy (BD) leads to poor acuity in both eyes that does not recover even after months of binocular vision [28]. In contrast, just opening the deprived eye to give binocular vision (BV) after MD appears to engage cooperative plasticity that promotes both physiological recovery [29] and long-lasting visual recovery in both eyes [27].

Here, we quantified the expression of glutamatergic and GABAergic receptor subunits in the V1 of animals reared with MD and then treated to promote either good visual recovery (BV) or persistent bilateral amblyopia (RO, BD). Next, we developed an unbiased high-dimensional analysis approach to identify plasticity features in the pattern of subunit expression and to construct plasticity phenotypes. Finally, we used cluster analysis to classify plasticity phenotypes associated with good versus poor acuity and analyzed those to determine which features suggest the recovery of adaptive versus maladaptive plasticity mechanisms.

2. Materials and Methods

2.1. Animals and Rearing Conditions. All experimental procedures were approved by the McMaster University Animal Research Ethics Board. We quantified the expression of 7 glutamatergic and GABAergic synaptic proteins in the V1 of cats reared with MD from eye opening until 5 weeks of age and then given one of the 3 treatments: RO for 18 d, BD for 4 d, or BV for either short-term (ST-BV; 1 hr, 6 hrs) or long-term (LT-BV; 1 d, 2 d, or 4 d) ($n = 7$, 4 male and 3 female) (Figure 1). The lengths of RO and BD were selected because they have well-documented and consistent visual changes that result in poor acuity in both eyes [7, 8, 30]. The BV periods were selected to match the lengths used previously to study rapid and dynamic changes caused by MD in both cat and mouse V1 [27, 31, 32]. Also, the short- and long-term BV groups were based on the data-driven analysis of protein expression described in detail below and that analysis placed the samples from ST-BV (1 hr or 6 hrs) versus LT-BV (1 d, 2 d, or 4 d) rearing conditions into separate clusters. The raw data collected previously [23] from animals reared with normal binocular vision until 2, 3, 4, 5, 6, 8, 12, 16, or 32 wks of age ($n = 9$ animals, 2 male and 7 female) or MD from eye opening (6-11 d) to 4, 5, 6, 9, or 32 wks ($n = 8$ animals, 4 male and 4 female) were used for comparison.

MD was started at the time of eye opening by suturing together the eyelid margins of one eye (5-0 Coated VICRYL Ethicon P-3) using surgical procedures described previously [8]. Sutures were inspected daily to ensure the eyelids remained closed. At 5 weeks of age, the period of MD was stopped and either BV was started by carefully parting the fused eyelid margins, RO was started by opening the closed eye and closing the open eye, or BD was started by closing the open eye. All of these surgical procedures were done using gaseous anesthesia (isoflurane, 1.5-5%, in oxygen) and aseptic surgical techniques.

At the end of the rearing condition, animals were euthanized using sodium pentobarbital injection (165 mg/kg, IV) and transcardially perfused with cold 0.1 M phosphate-buffered saline (PBS) (4°C; 80-100 ml/min) until the circulating fluid ran clear. The brain was removed from the skull and placed in cold PBS. A number of tissue samples (2 mm × 2 mm) were taken from the regions of the V1 representing the central (C), peripheral (P), and monocular (M) visual fields (Figure 1(c)). Each tissue sample was placed in a cold microcentrifuge tube, flash frozen on dry ice, and stored in a -80°C freezer.

2.2. Synaptoneurosome Preparation. Synaptoneurosomes were prepared according to a subcellular fractionation protocol [16, 33]. The tissue samples were suspended in 1 ml of cold homogenization buffer (10 mM HEPES, 1 mM EDTA, 2 mM EGTA, 0.5 mM DTT, 10 mg/l leupeptin, 50 mg/l soybean trypsin inhibitor, 100 nM microcystin, and 0.1 mM PMSF) and homogenized in a glass-glass Dounce tissue homogenizer (Kontes, Vineland, NJ, USA). Homogenized tissue was passed through a 5 μm pore hydrophobic mesh filter (Millipore, Billerica, MA), centrifuged at low-speed (1,000x*g*) for 20 min, the supernatant was discarded, and the pellet was resuspended in 1 ml of cold homogenization buffer. The sample was centrifuged for 10 min (1,000x*g*), the supernatant was discarded, and the pellet was resuspended in 100 μl boiling 1% sodium-dodecyl-sulfate (SDS). Samples were heated for 10 min and then stored at -80°C.

Total protein concentrations were determined for each sample and a set of protein standards using the bicinchoninic acid (BCA) assay (Pierce, Rockford, IL, USA). A linear function was fit to the observed absorbance values of the protein standards relative to their expected protein concentrations. If the fit was less than $R^2 = 0.99$, the assay was redone. The slope and the offset of the linear function were used to determine the protein concentration of each sample, and then the samples were diluted to 1 μg/μl with sample (M260 Next Gel Sample loading buffer 4x, Amresco) and Laemmli buffer (Cayman Chemical). A control sample was made by combining a small amount from each sample to create an average sample that was run on every gel. Each sample was run twice in the experiment.

2.3. Immunoblotting. Synaptoneurosome samples and a protein ladder were separated on 4-20% SDS-PAGE gels (Pierce, Rockford, IL) and transferred to polyvinylidene fluoride (PVDF) membranes (Millipore, Billerica, MA). The blots were blocked in PBS containing 0.05% Triton-x (Sigma, St. Louis, MO) (PBS-T) and 5% skim milk (wt/vol) for 1 hour. Blots were then incubated overnight at 4°C with constant agitation in one of the 7 primary antibodies (Table 1) and washed with PBS-T (Sigma, St. Louis, MO) (3 × 10 min).

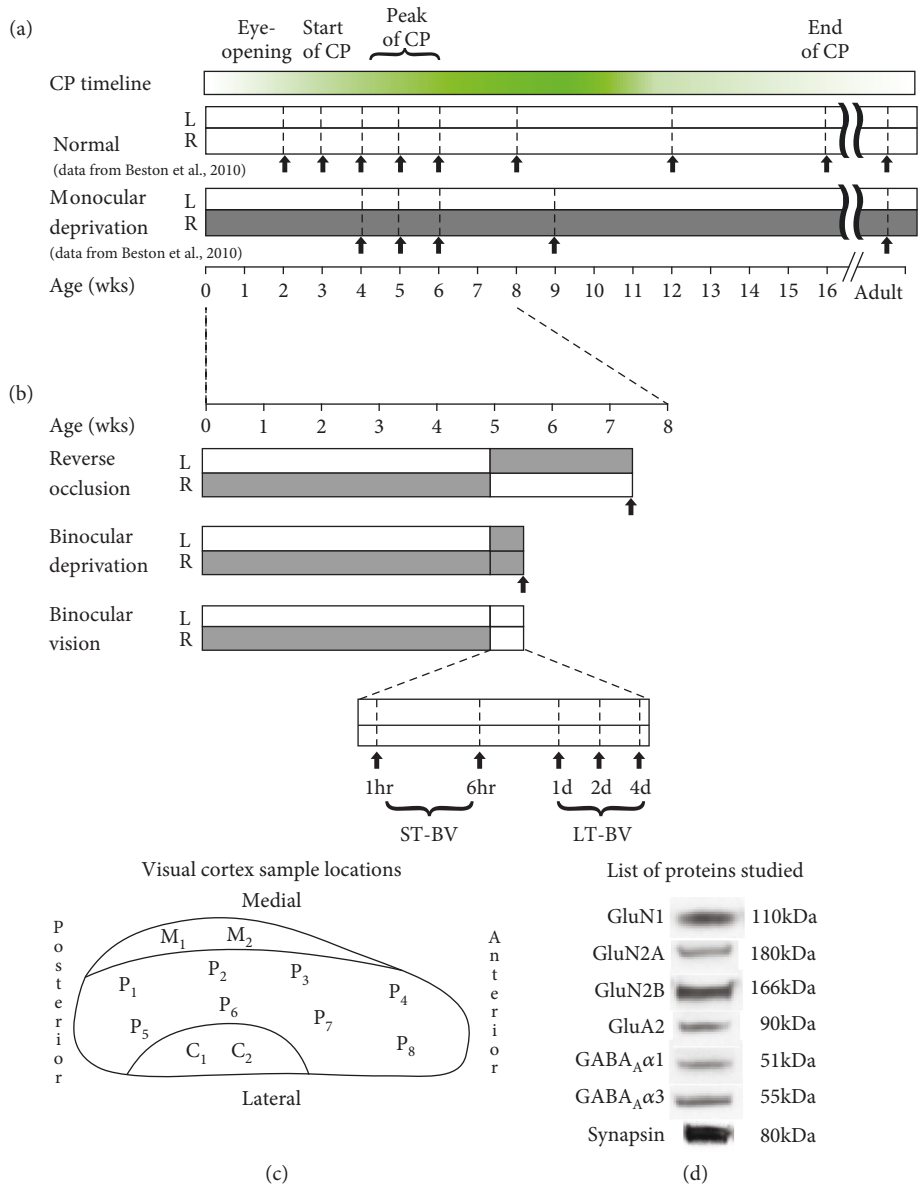

Figure 1: Study design diagram. Timelines for the rearing conditions used in this study. (a) Normal visual experience and monocular deprivation (MD), (b) treatment conditions (RO, BD, and BV) after MD to 5 wks. Filled bars indicate that an eye was closed. Black arrows indicate the age of animals used in the study. A timeline for the critical period (CP) in cat visual cortex [34] highlights the peak of the CP between 4 and 6 weeks of age. (c) Map of the sampling regions in the V1 representing the central (C, $n = 2$), peripheral (P, $n = 8$), and monocular (M, $n = 2$) visual fields. (d) Representative bands from the Western blots for the 7 proteins quantified in the study and the molecular weights (kDa).

The appropriate secondary antibody conjugated to horseradish peroxidase (HRP) (1 : 2,000; Cedarlane Laboratories LTD, Hornby, ON) was applied to membranes for 1 hour at room temperature, then blots were washed in PBS (3×10 min). Bands were visualized using enhanced chemiluminescence (Amersham, Pharmacia Biotech, Piscataway, NJ) and exposed to autoradiographic film (X-Omat, Kodak, Rochester, NY). After each exposure, blots were stripped (Blot Restore Membrane Rejuvenation kit (Chemicon International, Temecula, CA, USA)) and probed with the next antibody so each blot was probed for all 7 antibodies (Figure 1(d)).

2.4. Analysis of Protein Expression. The autoradiographic film and an optical density wedge (Oriel Corporation, Baltimore, MD) were scanned (16 bit, AGFA Arcus II, Agfa, Germany), and the bands were identified based on molecular weight. The bands were quantified using densitometry, and the integrated grey level of the band was converted into optical density units (OD) using custom software (MATLAB, The MathWorks Inc., Natick, Massachusetts). The background density between the lanes was subtracted from each band, and the density of each sample was normalized relative to the control sample run on each gel (sample band density/-control band density).

Table 1: List of primary antibody concentrations.

Antibody	Concentration	Company	Lot number	Location	RRID
Anti-GluN1	1 : 2,000	BD Biosciences Pharmingen	556308	San Diego, CA	RRID: AB_396353
Anti-GluN2A	1 : 2,000	MilliporeSigma	24826	Burlington, MA	RRID: AB_95169
Anti-GluN2B	1 : 2,000	MilliporeSigma	28629	Burlington, MA	RRID: AB_2112925
Anti-GluA2	1 : 1,000	Thermo Fisher		Waltham, MA	RRID: AB_2533058
Anti-$GABA_A\alpha1$	1 : 500	Santa Cruz Biotechnology	L3102	Santa Cruz, CA	
Anti-$GABA_A\alpha3$	1 : 2,000	MilliporeSigma		Burlington, MA	
Anti-Synapsin	1 : 2,000	Thermo Fisher		Waltham, MA	

Table 2: The number of animals, cortical tissue pieces, and WB measurements for each condition and V1 region. Rows summarize the number of runs from the central (C), peripheral (P), and monocular (M) regions of the V1 within a rearing condition. The columns list each of the 7 proteins analyzed using Western blotting. Column sums detail the number of runs across rearing conditions and cortical areas. The information for normal animals is in Table 2-1 and for MD animals is in Table 2-2.

Condition	Number of animals	Region	Number of cortical pieces	Number of Western blot measurements after 2 replications						
				GluN1	GluN2A	GluN2B	$GABA_A\alpha1$	$GABA_A\alpha3$	GluA2	Synapsin
Normal (5 wks)	1	C	2	4	4	4	4	4	4	4
		P	8	16	16	16	15	16	16	16
		M	2	4	4	4	4	4	4	4
MD (5 wks)	2	C	3	6	6	6	6	6	6	4
		P	9	18	18	18	18	18	18	12
		M	3	5	5	5	5	5	5	4
RO (18 d)	1	C	2	4	4	4	4	4	4	4
		P	8	19	19	19	19	19	14	14
		M	2	3	3	3	3	3	2	2
BD (4 d)	1	C	3	6	6	5	6	5	6	5
		P	9	18	18	17	16	18	18	17
		M	2	4	4	3	4	4	4	3
ST-BV (1 hr, 6 hr)	2	C	4	8	8	8	8	8	8	8
		P	16	32	32	32	32	32	32	32
		M	4	8	8	8	8	8	8	7
LT-BV (1 d, 2 d, and 4 d)	3	C	6	12	10	12	11	12	12	10
		P	24	43	40	43	43	42	43	40
		M	6	12	12	12	12	12	12	12
Sum				222	217	219	218	220	216	198

The data were normalized relative to the average expression of the 5 wk normal cases. Table 2 summarizes the number of tissue samples and replication of runs for the 5 wk normal, 5 wk MD, and recovery conditions across the 3 regions of the V1 and 7 proteins that were studied. Descriptions of the expression for the individual proteins in each of the conditions can be found in [35]. Those univariate comparisons confirmed the complex nature of these data and led us to develop and implement the data analysis workflow that is summarized in Figure 2.

2.5. Protein Network Analysis. A network analysis of protein expression was done for each rearing condition by calculating the pairwise Pearson's *R* correlations among the 7 proteins using the *rcorr* function in the Hmisc package in *R* [36]. The networks were visualized as correlation matrices (*heatmap2* function in *gplots* [37]), and the proteins were ordered using the dendextend [38] and seriation [39] packages to place proteins with similar patterns of correlations nearby in the dendrogram. Significant correlations were identified using the Bonferroni-corrected *p* values and indicated by asterisks on the cell in the correlation matrix.

2.6. Principal Component Analysis. We used principal component analysis (PCA) to reduce the dimensionality of the data, identify potential biological features, and create plasticity phenotypes. We applied the PCA following the procedures we used previously [23, 40, 41] and included data from all of the normal animals and MDs as well as the 3 recovery conditions. We assembled the protein expression for GluA2, GluN1, GluN2A, GluN2B, $GABA_A\alpha1$, $GABA_A\alpha3$, and synapsin into an *mxn* matrix. The *m* columns

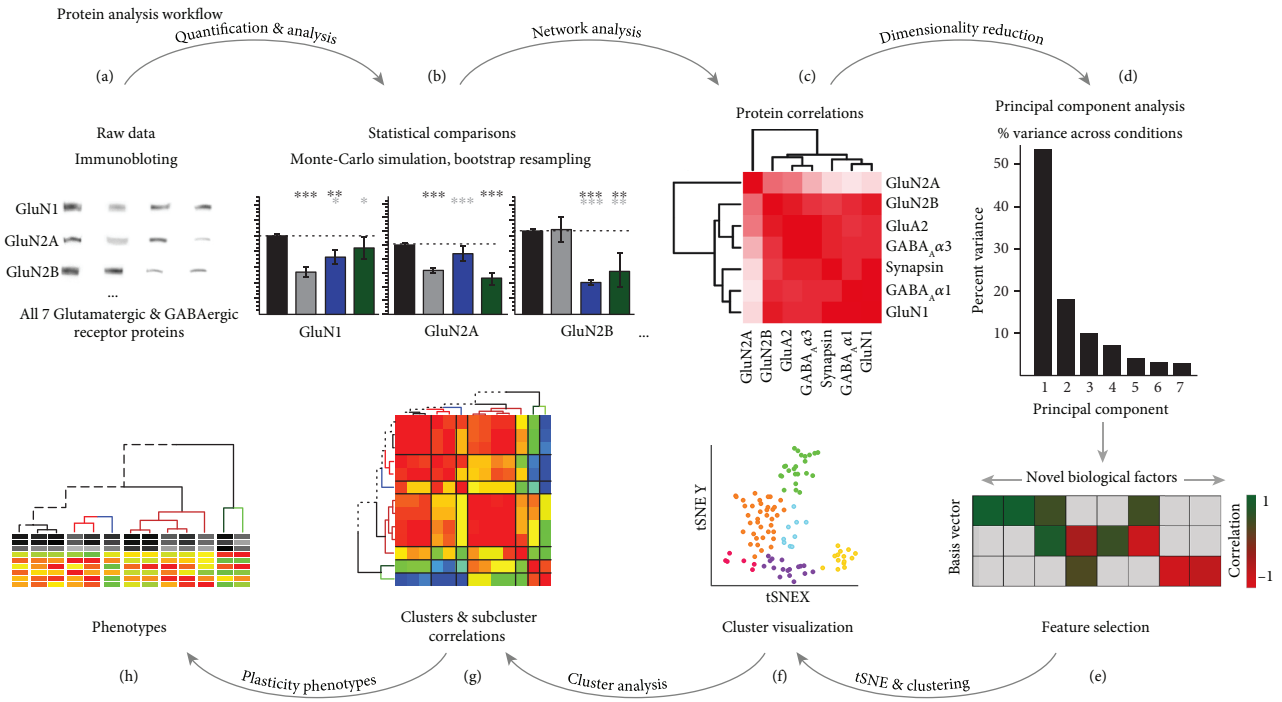

FIGURE 2: Analysis workflow. The analysis workflow for data in the study. (a) Immunoblots were quantified using densitometry. (b) Comparisons among rearing conditions were made [35]. (c) Pairwise correlations were calculated for the 7 proteins for each rearing condition. (d) Next, a series of steps were done beginning with dimension reduction (PCA). (e) Feature selection. (f) Cluster visualization based on the features (tSNE). (g) Correlation between features or the clusters and subclusters. (h) Construction and visualization of the plasticity phenotypes for each subcluster.

represented the 7 proteins, and the n rows were the average protein expression for each of the 12-14 samples from an animal. For a few of the rows, data was missing from a single cell, and so those samples were omitted for a total of $n = 279$ rows in the matrix and 1,953 observations.

The data were centered by subtracting the mean column vector and applying singular value decomposition (SVD) to calculate the principal components (RStudio). SVD represents the expression of all 7 proteins within a single tissue sample as a vector in a high dimensional space, and the PCA identifies variance captured by each dimension in that "protein expression space." The first 3 dimensions accounted for 82% of the total variance and were used for the next analyses.

We plotted the basis vectors for the first 3 dimensions (Dim) and used the weight, quality ($\cos^2$), and directionality of each protein, as well as known protein interactions, to help identify potential biological features accounting for the variance. We identified 9 potential features, calculated those features for each sample, and correlated each feature with Dim1, Dim2, and Dim3 to create a correlation matrix (see results). The p values for the correlations were Bonferroni corrected, and significant correlations were used to identify the features that would be part of the plasticity phenotype.

Eight of the features were significantly correlated with at least one of the first 3 dimensions. A measure associated with the E:I balance was not significantly correlated with the dimensions, and so it was not included in the tSNE or cluster analysis. The E:I measure, however, was used for analyzing the composition of the clusters and as a component of the plasticity phenotype because of the importance of the E:I balance for experience-dependent plasticity.

2.7. tSNE Dimension Reduction and Cluster Analysis. The average expression for the 8 features (Table 3) was compiled into an mxn matrix, with m columns ($m = 8$) representing the significant features and n rows representing each sample from the 3 V1 regions (central, peripheral, and monocular) for 5 wk normal, 5 wk MD, RO, BD, and BV animals ($n = 109$). t-distributed stochastic neighbor embedding (tSNE) was used to reduce this matrix to 2-dimensions (2D). tSNE was implemented in R [42], and the tSNE output was sorted using k-means to assign each sample to a cluster. To determine the optimal number of clusters (k), we calculated the within-groups sum of squares for increasing values of k, fit a single-exponential tau decay function to those data, found the "elbow point" at 4τ which was 6, and used that as the optimal number of clusters. The clusters were visualized by color-coding the dots in the tSNE plot, and the composition of the clusters was analyzed.

To facilitate analysis of the tSNE clusters, we grouped the BV cases into short-term BV (1 hr and 6 hr) (ST-BV) or long-term BV (1 d, 2 d, and 4 d) (LT-BV), color-coded the samples by rearing condition, and used different symbols to indicate the V1 region. For each cluster, we annotated the composition based on the rearing condition of the samples to create "subclusters" (e.g., LT-BV 1) that were used for the next analyses.

We evaluated the similarity/dissimilarity among the subclusters by calculating the pairwise correlations (Pearson's R)

Table 3: Formulas and Pearson's R correlation between the features and principal components. The formulas for PCA-identified features, including protein sums (Figure 5) and receptor indices (Figure 6), along with corresponding correlation (R^2) values for each of the first 3 principal components. The GluN1:GluA2 and $GABA_AR$ sum:GlutR sum were not significantly correlated with any of these 3 components.

PCA-identified features	Formula	R^2 Dim1	R^2 Dim2	R^2 Dim3
All protein sum	(GluA2 + GluN1 + GluN2A + GluN2B + $GABA_A\alpha1$ + $GABA_A\alpha3$ + synapsin) ÷ 7	0.983	0.134	0.039
GlutR sum	(GluA2 + GluN1 + GluN2A + GluN2B) ÷ 4	0.746	-0.160	0.573
$GABA_AR$ sum	($GABA_A\alpha1$ + $GABA_A\alpha3$) ÷ 2	0.478	0.819	-0.047
$GABA_AR$ sum:GlutR sum (EI index)	(GlutR sum − $GABA_AR$ sum) ÷ (GlutR sum + $GABA_AR$ sum)	0.036	-0.064	0.012
$GABA_A\alpha1$:GluN2A	(GluN2A − $GABA_A\alpha1$) ÷ (GluN2A + $GABA_A\alpha1$)	0.437	-0.743	-0.070
GluN2B:GluN2A	(GluN2A − GluN2B) ÷ (GluN2A + GluN2B)	0.044	-0.421	0.338
$GABA_A\alpha1$:$GABA_A\alpha3$	($GABA_A\alpha1$ − $GABA_A\alpha3$) ÷ ($GABA_A\alpha1$ + $GABA_A\alpha3$)	-0.176	0.504	0.194
GluN2B:GluA2	(GluN2B − GluA2) ÷ (GluN2B + GluA2)	0.058	0.209	-0.798
GluN2A:GluA2	(GluN2A − GluA2) ÷ (GluN2A + GluA2)	0.113	-0.172	-0.643

between subclusters using the features identified by the PCA as input to the R package *rcorr*. The correlations were visualized in a matrix with the cells color-coded to indicate the strength of the correlation [37]. The order of the subcluster in the matrix was optimized using hierarchical clustering, and a dendrogram was created based on the pattern of correlations (using dendextend and seriation packages in R) so that subclusters with strong correlations were nearby in the dendrogram.

2.8. Visualization and Comparison of Plasticity Phenotype. The features identified in the PCA were used to indicate the plasticity phenotype for each of the subclusters. In addition to the 8 significant features, the E:I measure was included in the visualization of the plasticity phenotype. The features were color-coded using grey scale for the 3 protein sum features and a color gradient (red = -1, yellow = 0, and green = +1) for the 6 protein indices. The plasticity phenotypes were displayed as a stack of color-coded bars with one bar for each feature. For the subclusters, the plasticity phenotypes were ordered by the dendrogram to facilitate comparison among subclusters that were similar versus dissimilar. We also calculated the plasticity phenotypes for the full complement of normally reared and MD animals and displayed those in a developmental sequence to facilitate age-related comparisons with the recovery subclusters. Finally, we did a bootstrap analysis to determine which features of the plasticity phenotypes were different from 5 wk normals and used Bonferroni correction to adjust the significance for the multiple comparisons. This analysis was displayed in 2 ways: first, each of the 9 feature bands for the dendrogram-ordered subclusters was color-coded with white if it was not different, red if it was greater, and blue if it was less than 5 wk normals; second, boxplots were made to show the value for each of the 9 features and to identify the subclusters that were different from 5 wk normals.

A detailed description of the network analysis, PCA, tSNE, clustering, and phenotype construction, along with the example code for each of these steps, can be found in [43].

2.9. Modeling Population Receptor Decay Kinetics for NMDARs and $GABA_AR$s. The subunit composition of NMDARs and $GABA_AR$s determines the decay kinetics of the receptor [44, 45], and so we used that information to build a model for the decay kinetics of a population of receptors for each of the rearing conditions. The decay kinetics of the most common NMDAR composition, triheteromeric receptors containing GluN2A and 2B, is 50 ms ± 3 ms, while diheteromers NMDARs containing only GluN2B are slower (2B = 333 ms ± 17 ms) and those containing only GluN2A are faster (2A = 36 ms ± 1 ms) [44]. The decay kinetics of $GABA_AR$s with both $\alpha1$ and $\alpha3$ subunits is 49 ms ± 23 ms while receptors with only the $\alpha3$ subunit are slower (129.0 ms ± 54.0 ms) and only $\alpha1$ are faster (42.2 ms ± 20.5 ms) [45].

We used the relative amounts of GluN2A and 2B, or $GABA_A\alpha1$ and $\alpha3$, as inputs to the model. Receptors containing GluN2A and 2B or $GABA_A\alpha1$ and $\alpha3$ are the most common in the cortex, so the model maximized the number of these pairs which was limited by the subunit with less expression. The remaining proportion of the highly expressed subunit was divided by 2 and used to model the number of pairs for those receptors (2A:2A or 2B:2B; $\alpha1$:$\alpha1$ or $\alpha3$:$\alpha3$) in the population. The population decay kinetics were then modeled by inserting the relative amounts of the subunits into these formulas:

$$\begin{aligned}\text{NMDAR kinetics}\,&\frac{(([2A:2B]\times 50\,\text{ms})+([2A]\times 36\,\text{ms})+([2B]\times 333\,\text{ms}))}{([2A:2B]+[2A]+[2B])};\\ \text{GABA}_A\text{R kinetics}\,&\frac{(([\alpha1:\alpha3]\times 49\,\text{ms})+([\alpha1]\times 42.2\,\text{ms})+([\alpha3]\times 129\,\text{ms}))}{([\alpha1:\alpha3]+[\alpha1]+[\alpha3])}.\end{aligned} \quad (1)$$

For example, a sample where GluN2A was 35% and 2B was 65% of the total NMDAR subunit population and would have population kinetics of 135 ms.

$$\frac{(([(0.65-0.35)/2]\times 50\,\text{ms})+([(0)/2]\times 36\,\text{ms})+([0.35/2]\times 333\,\text{ms}))}{([(0.65-0.35)]+[(0)/2]+[0.35])}=135\,\text{ms}. \quad (2)$$

First, we plotted scattergrams of the average NMDAR and $GABA_AR$ decay kinetics for normal animals and each treatment condition. The development of decay kinetics for normal animals was described using an exponential decay function, while changes in kinetics with increasing lengths of BV were fit by either exponential decay or sigmoidal curves. Then, we compared the relationship between NMDAR and $GABA_AR$ kinetics by plotting both on one graph.

2.10. Statistical Analyses. We used the bootstrap resampling method to compare the features because it is a conservative approach to analyzing small sample sizes when standard parametric or nonparametric statistical tests are not appropriate. Here, bootstrapping was used to estimate the confidence intervals (CI) for each feature in the subcluster, and a Monte Carlo simulation was run to determine if the 5 wk normal subcluster fell outside those CIs. The statistical software package *R* was used to simulate normal distributions with 1,000,000 points using the mean and standard deviation from the subcluster. Next, a Monte Carlo simulation was randomly sampled with replacement from the simulated distribution n times, where n was the number of observations made from the normal subcluster. The resampling procedure was repeated 100,000 times to determine the 95%, 99%, and 99.9% CIs. The subcluster feature was considered significantly different from normal (e.g., $p < 0.05$, $p < 0.01$, or $p < 0.001$) if the feature mean fell outside these CIs. When a subcluster was significantly greater than normal ($p < 0.05$), the boxplot was colored red; when it was less than normal ($p < 0.05$), the boxplot was colored blue; and if it was not different from normal ($p > 0.05$), the boxplot was colored grey.

All of the bootstrap statistical comparisons for the plasticity features (Table 5-1 and 6-1) are presented in the Supplemental material.

The p values for Pearson's correlations were calculated using the rcorr package [36], and the significance levels were adjusted using the Bonferroni correction for multiple comparisons. Pearson's Rs and p values for the protein networks (Table 3-1), plasticity features with PCA dimensions (Table 4-1), and association between clusters (Tables 8-1, 8-2) are included in the Supplemental material.

We tested if recovery during BV followed either an exponential decay or a sigmoidal pattern by fitting curves to the data using Kaleidagraph (Synergy Software, Reading, PA). Significant curve fits were plotted on the graphs to describe the trajectory of recovery.

3. Results

3.1. Analyzing the Pairwise Similarity between Protein Expression Profiles. First, we wanted to identify pairs of proteins with similar or opposing expression profiles and compare them among the rearing conditions. For each condition, we collapsed the data from the 3 regions of the V1, calculated the matrix of pairwise correlations between the 7 proteins, ordered the protein correlations using a hierarchical dendrogram, and used 2D heatmaps to visualize the correlations (Figure 3). The order of proteins in the dendrogram indicated which ones had similar (e.g., on the same branch of the dendrogram) or different patterns of expression, and the color of the cell illustrated the strength of the correlation. For 5 wk normal animals (Figure 3(a)), there were strong positive correlations (red cells) among all proteins except GluN2A, which was weakly correlated and not clustered with the other proteins. A different pattern of correlations was found after MD (Figure 3(b)); here, glutamatergic proteins were weakly or even negatively correlated (blue cells) with $GABA_A\alpha 1$, $GABA_A\alpha 3$, and synapsin. These results suggest that MD drives a decoupling of these excitatory and inhibitory mechanisms. RO also separated glutamatergic and GABAergic proteins into different clusters at the first branch (Figure 3(c)); however, the correlations were weaker, suggesting that RO reduced the MD-driven decoupling of these mechanisms. After BD, the correlation matrix had mostly positive correlations (Figure 3(d)) except for synapsin which was negatively correlated and not clustered with the other proteins. BV treatment highlighted the dynamic nature of this recovery (Figures 3(e)–3(i)). Just 1 hr of BV was enough to change the correlation matrix from the MD pattern, but even after 4 d of BV, the correlation matrix still appeared different from the normal 5 wk pattern of correlations.

These matrices suggest different patterns of correlations depending on the condition, but this analysis treats each comparison with the same weighting and it is likely that some proteins contribute more than others to the variance in the data. To assess this, we used the PCA to identify individual proteins and combinations of proteins that capture the variance in the data and may represent plasticity features reflecting differences among the treatment conditions.

3.2. Using Principal Component Analysis to Reduce Dimensionality and Identify Plasticity Features. We used the PCA to reduce the dimensionality, transform the data, and find features that define the covariance among the proteins.

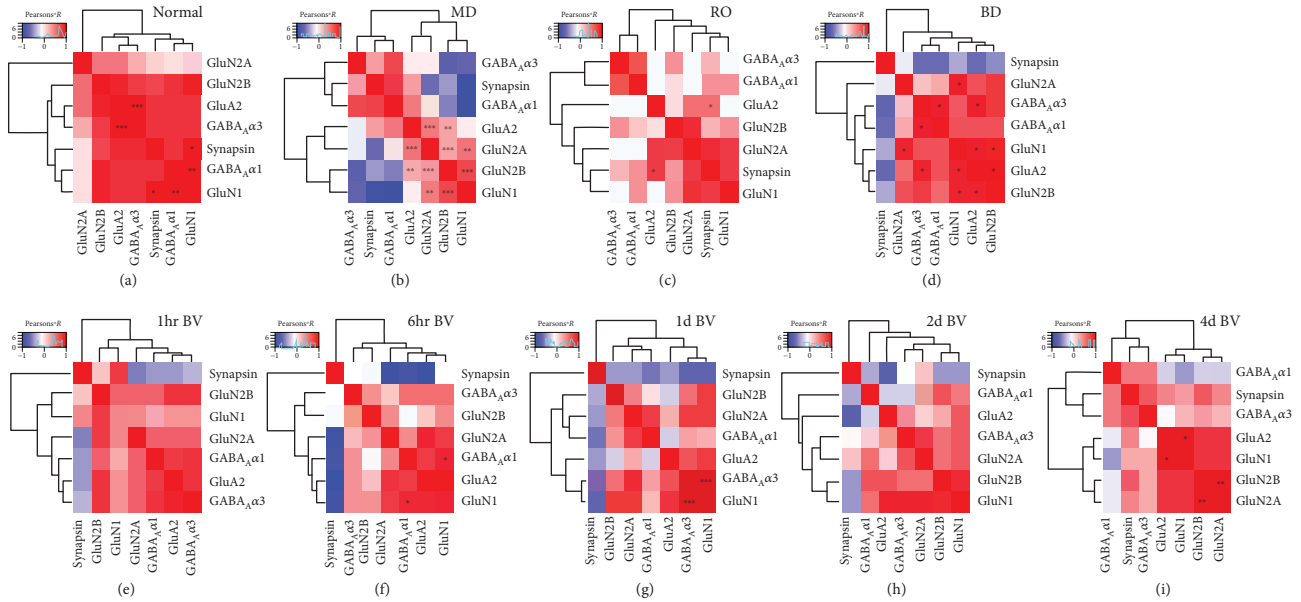

FIGURE 3: Visualizing pairwise correlations between proteins. Correlation matrices are plotted showing the strength (saturation) and direction (blue: negative; red: positive) of the pairwise Pearson's R correlations between proteins for each condition: (a) 5 wk normal, (b) 5 wk MD, (c) RO, (d) BD, and (e-i) BV. The order of proteins was determined using hierarchical clustering so proteins with stronger correlations were nearby in the matrix. Significant correlations are denoted by an asterisk ($^{*}p < 0.05$, $^{**}p < 0.01$, and $^{***}p < 0.001$). For the table of Pearson's R values and Bonferroni-corrected p values, see Supplemental Table 3-1.

An mxn matrix was made using protein expression, where the m columns were the 7 proteins and the n rows (109) were the tissue samples from all the animals and regions of the V1 used in this study. This matrix was analyzed using singular value decomposition (SVD), and the first 3 dimensions explained most of the variance (82%) in the data (Dim1: 54%, Dim2: 18%, and Dim3: 10%) (Figure 4(a)).

To understand which proteins contributed to each dimension, we addressed the quality of the representation for each protein using the $\cos^2$ metric and found that the glutamatergic proteins were well represented by Dim1, $GABA_A\alpha1$ by Dim2, and GluA2 and GluN2B by Dim3, but synapsin and $GABA_A\alpha3$ were weakly represented in the first 3 dimensions (Figures 4(b) and 4(c)). Next, we compared the vectors for each protein (Figures 4(d) and 4(f)) and the PCA space occupied by the rearing conditions (Figures 4(e) and 4(g)). The protein vectors show that GluN1, GluN2A, GluN2B, and GluA2 extended along Dim1, $GABA_A\alpha1$ along Dim2, and GluA2 and GluN2B were in different directions along Dim3. The PCA space occupied by the conditions suggest some differences: BD was separated on Dim2 in the same direction as $GABA_A\alpha1$, but the center of gravity for the other conditions overlapped the space occupied by normal samples.

The overlap among conditions raised the possibility that higher dimensions may separate the conditions. To begin to assess higher dimensional contributions, we examined the basis vectors (Figure 4(h)) and the correlations between individual proteins and PCA dimensions (Figure 4(i)) to identify combinations of proteins that might reflect higher dimension features. For example, all proteins had positive amplitudes for the Dim1 basis vector (Figure 4(h)), and positive correlations with Dim1 (Figure 4(i)) suggested that protein sums may be higher dimensional features. In addition, weights for GluN2A and $GABA_A\alpha1$ on Dim2 were opposite, suggesting that when one protein increased the other decreased, and this could be a novel feature of these data. Continuing with this approach, we identified 9 putative plasticity features: protein sums (all protein sum, GlutR sum, and $GABA_AR$ sum) or indices (GlutR:$GABA_AR$, GluN2A:GluN2B, $GABA_A\alpha1$:$GABA_A\alpha3$, GluN2A:$GABA_A\alpha1$, GluA2:GluN2B, and GluN2A:GluA2). All of the protein sums and 4 of the indices were features not analyzed with the univariate statistics; however, each had a strong biological basis in previous research. For example, the new indices paired the mature GluN2A with the mature $GABA_A\alpha1$ or GluA2 subunit and GluN2B with GluA2 which is known to regulate the development of AMPARs [46]. Finally, we calculated the 9 features and determined if at least one of the first 3 dimensions was correlated with the features (Figure 4(j)). Only the GlutR:$GABA_AR$ balance was not correlated with any of the first 3 dimensions, but because those mechanisms are related to the E:I balance [47], we included that measure in the next analysis.

3.3. Comparing Plasticity Features. We plotted the plasticity features and saw that the GlutR and $GABA_AR$ sums and indices identified various differences among the treatment conditions (Figures 5 and 6). There were, however, consistent changes after BV in the binocular regions with a loss of the total amount of $GABA_AR$ expression (44% ± 12) and a shift of the GlutR:$GABA_AR$ balance to favor GlutR (Figure 5(d)). The remaining indices in the feature list also identified differences (Figure 6) including the $GABA_A\alpha1$:GluN2A balance shifting to more GluN2A after BV (in binocular regions) but more $GABA_A\alpha1$ after BD. RO flipped the 2A:2B balance

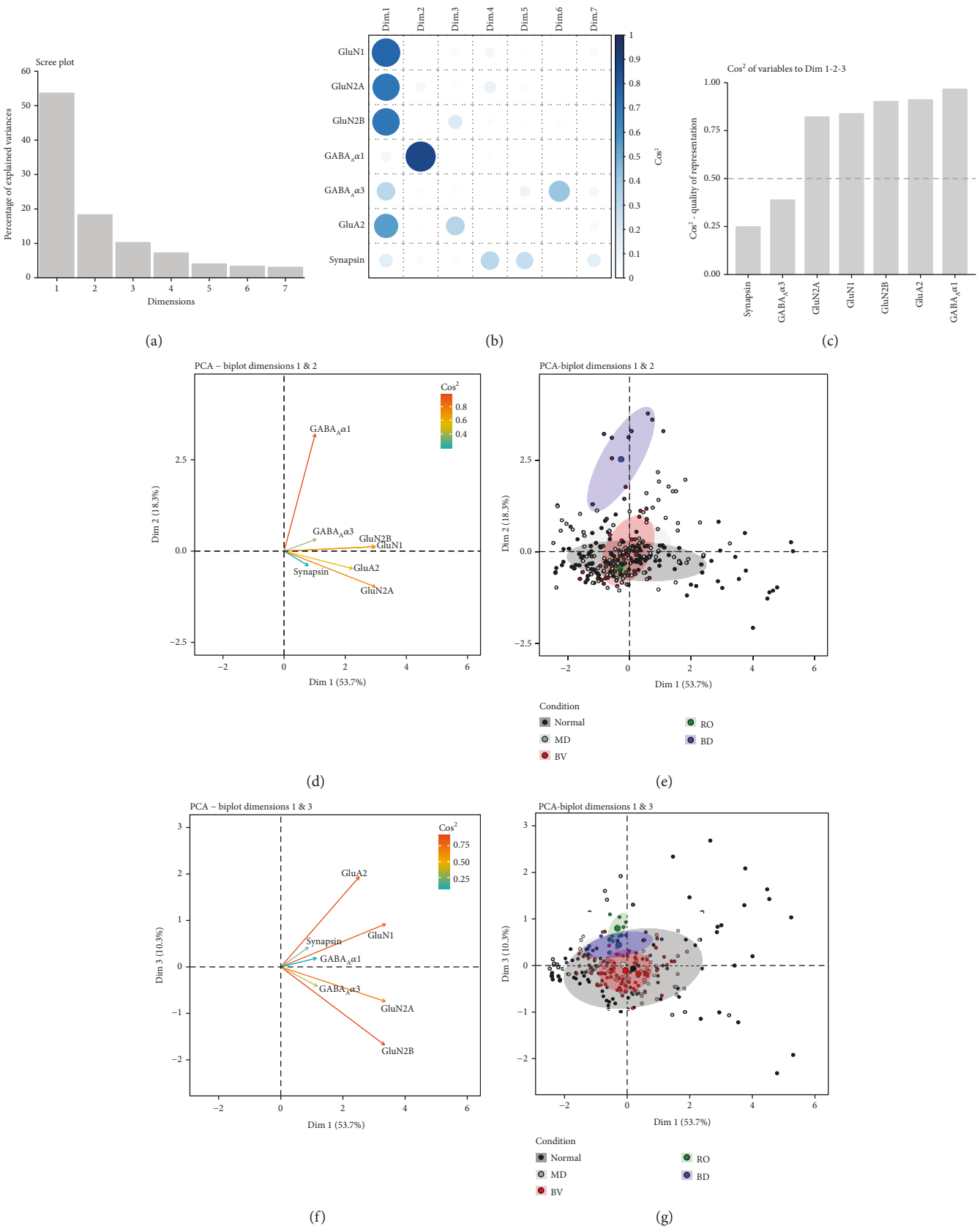

Figure 4: Continued.

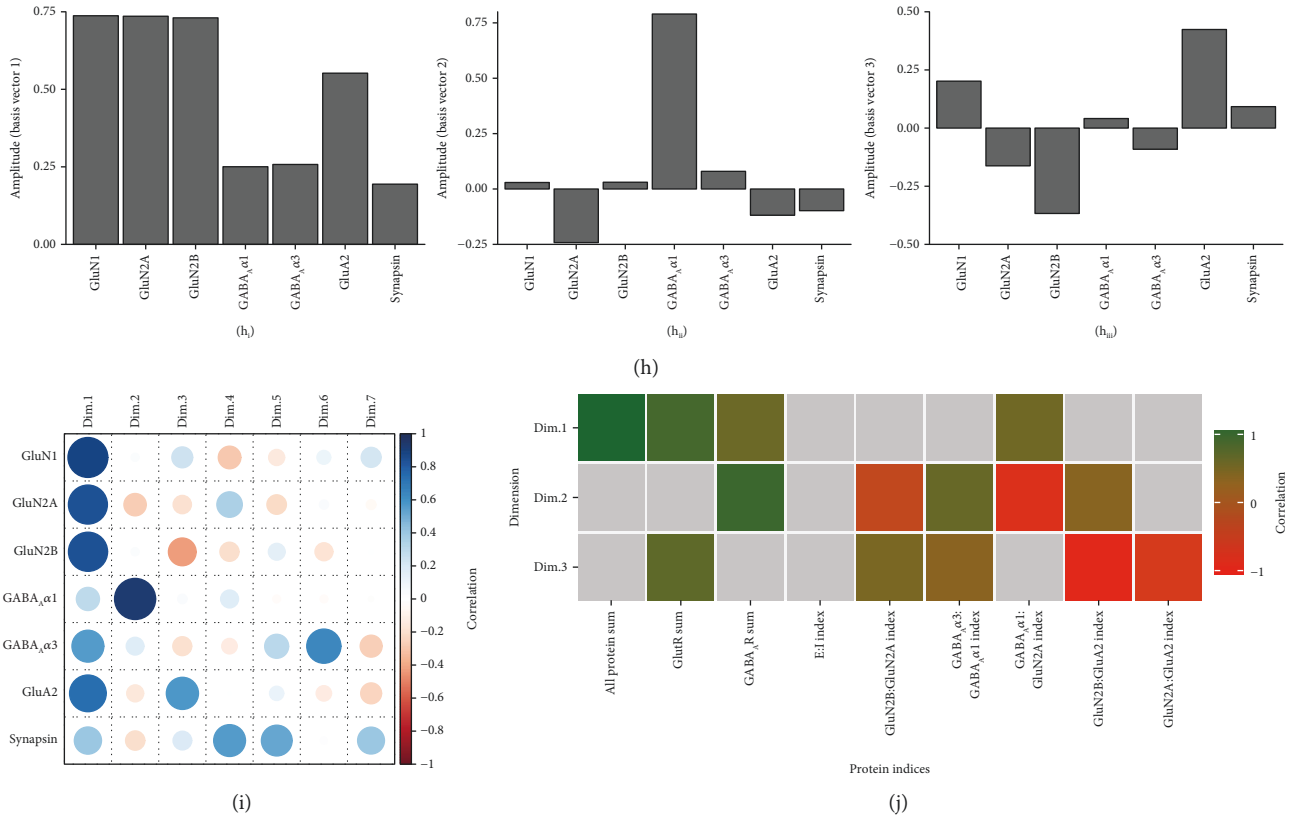

Figure 4: Identifying plasticity features using the principal component analysis. (a) .The percentage of variance captured by each principal component by singular value decomposition (SVD) applied using all of the protein expression data. The first 3 principal components capture 54%, 18%, and 10% of the variance, respectively, totalling >80% and thus representing the significant dimensions. (b). The quality of the representation, $\cos^2$, for the proteins is plotted for each dimension (small/white: low $\cos^2$; large/blue: high $\cos^2$). (c). The sum of $\cos^2$ values for the first 3 dimensions for each protein. (d, e). Biplots of PCA dimensions 1 and & 2 and (f, g). 1 and & 3. These plots show the vector for each protein (d, f) and the data (small dots) plus the average (large dots) for each condition with the best-fitting ellipse (e, g). (h). The basis vectors for dimensions 1-3 showing the amplitude of each protein in the vector. (i). The strength (circle size) and direction (blue-positive, red-negative) of the correlation (R^2) between each protein and the PCA dimensions. (j). Correlation between the plasticity features (columns) identified using the basis vectors (see Results) and then PCA dimensions 1-3. Filled cells are significant, Bonferroni- corrected correlations (green = positive, red = negative). For the table of Pearson's R values and significant p- values for these associations, see Supplemental Table 4-1.

to favor more GluN2A as did BD in the central region. In contrast, BV shifted the 2A:2B balance towards normal CP levels in all of the V1. The GABA$_A\alpha$1:GABA$_A\alpha$3 balance shifted towards the normal level after BV but strongly in favor of GABA$_A\alpha$3 after BD. The GluN2B:GluA2 balance shifted to substantially more GluA2 after RO while the GluN2A:GluA2 index shifted to more GluA2 outside the central region after RO and BD. Together, these features provide evidence of glutamatergic versus GABAergic differences among the treatment conditions.

3.4. Using tSNE to Transform and Visualize Clustering in the Pattern of Plasticity Features. We used tSNE to transform the plasticity features and visualize them in 2D (Figure 7(a)), then k-means and the "elbow method" (Supplemental Figure 7-1) to identify the number of clusters. For these analyses, the BV samples were grouped into ST-BV (1-6 hrs) and LT-BV (1-4 d) groups, and the plasticity features were calculated for all samples from the 3 V1 regions.

Six clusters were visualized with tSNE (Figure 7), and the composition of the clusters was analyzed to determine the V1 regions and rearing conditions in each cluster. Cluster 1 was the largest with 39 samples ($C = 26\%$; $P = 54\%$; and $M = 21\%$) and had the greatest number of samples from the central region (Figures 7(b) and 7(d)). Cluster 3 also had samples from the central, peripheral, and monocular regions while clusters 4, 5, and 6 were dominated by peripheral samples with few or no central region samples. Thus, there was some clustering by the V1 region, but more apparent clustering emerged when the samples were color-coded by rearing condition (Figures 7(c) and 7(d)). All but one of the normal samples were in cluster 1, all of the RO samples were in cluster 2, most of the BD samples were in cluster 3 with a few in cluster 6, and most of the MD samples were in clusters 1 or 3. The BV samples, however, were found in 5 of the clusters with the greatest number of BV central samples (83%) grouped with normals in cluster 1.

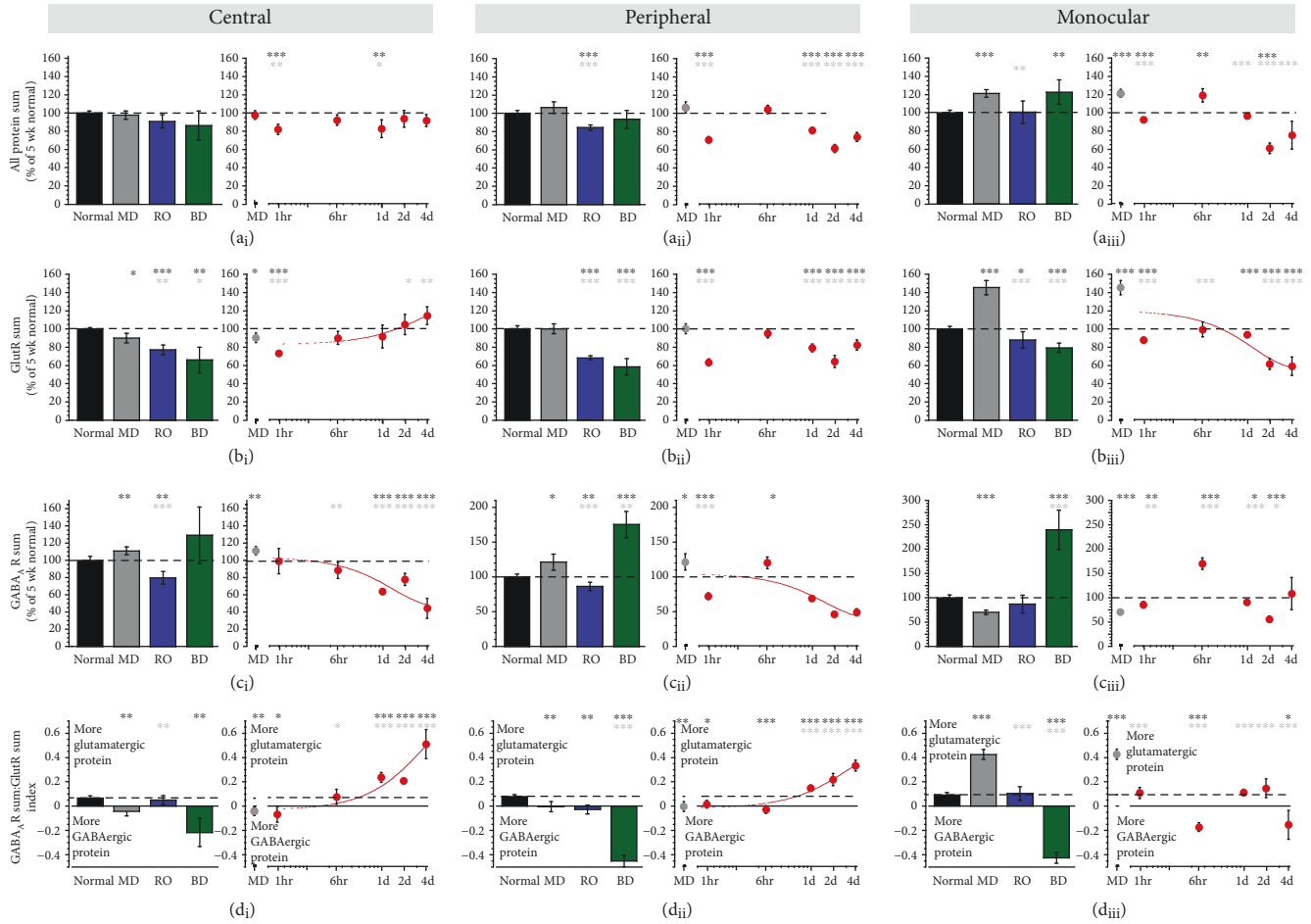

FIGURE 5: Expression of plasticity features for protein sums identified using the principal component analysis. Histograms and scatterplots showing the protein sums and a new protein sum index (GABAR sum:GlutR sum, rows) that were identified using the PCA basis vectors (Figure 4(j)) and plotted for each region of the V1 (columns). For exact p values, Pearson's R, and equations for the curve-fits, see Supplemental Table 5-1.

Further analysis of cluster 1 showed that the majority of LT-BV and ST-BV samples from the central region clustered with the normals (Figure 7(d)). Interestingly, some of the MD samples were also in cluster 1; however, those samples were from the peripheral and monocular regions which are known to be less affected by MD than the central region [48]. Together, these results show that the data are clustered and that the clustering was driven by both the rearing condition and the region of the V1.

3.5. Correlating Plasticity Features among Subclusters. We annotated the samples in each cluster using the rearing condition and V1 region and used that information to identify 13 subclusters where at least one region per condition had $n \geq 2$ and >20% of the samples in that cluster (Figure 7(d), black font). A correlation matrix was calculated (Figure 8) to assess the similarity between subclusters (see Supplemental Table 8-1 for R values and 8-2 for Bonferroni-adjusted p values), and the order of the subclusters in the correlation matrix was optimized by hierarchical clustering so subclusters with similar patterns of features were nearby in the dendrogram. Bonferroni-adjusted p value was used to determine the significant correlations ($0.05/78 = 0.0006$) (Figure 8). This analysis showed that 3 of the 4 LT-BV subclusters (LT-BV 1: $R = 0.98$; LT-BV 5: $R = 0.98$; and LT-BV 4: $R = 0.96$) and the MD 1_{PM} subcluster ($R = 0.98$) were strongly correlated with normals. The other MD subcluster with central samples (MD 3_{CP}) was on a separate branch of the dendrogram and was strongly correlated with the 3 ST-BV subclusters (ST-BV 1: $R = 0.98$; ST-BV 3: $R = 0.99$; and ST-BV 5: $R = 0.98$). The ST-BV subclusters were also correlated with normals (ST-BV 1: $R = 0.96$; ST-BV 3: $R = 0.94$; and ST-BV 5: $R = 0.97$), LT-BV 1 (ST-BV 1: $R = 0.98$; ST-BV 3: $R = 0.94$; and ST-BV 5: $R = 0.98$), and MD1 (ST-BV 1: $R = 0.98$; ST-BV 3: $R = 0.94$; and ST-BV 5: $R = 0.99$) but weaker correlations with LT-BV 4 (ST-BV 1: $R = 0.94$; ST-BV 5: $R = 0.95$) and no significant correlations with LT-BV 5. RO was correlated with normal ($R = 0.96$) but only one of the LT-BV subclusters (LT-BV 5: $R = 0.96$) and none of the ST-BV subclusters. The two BD subclusters were correlated ($R = 0.94$) but none of the other correlations were significant. The pattern of strong correlations in this matrix and the

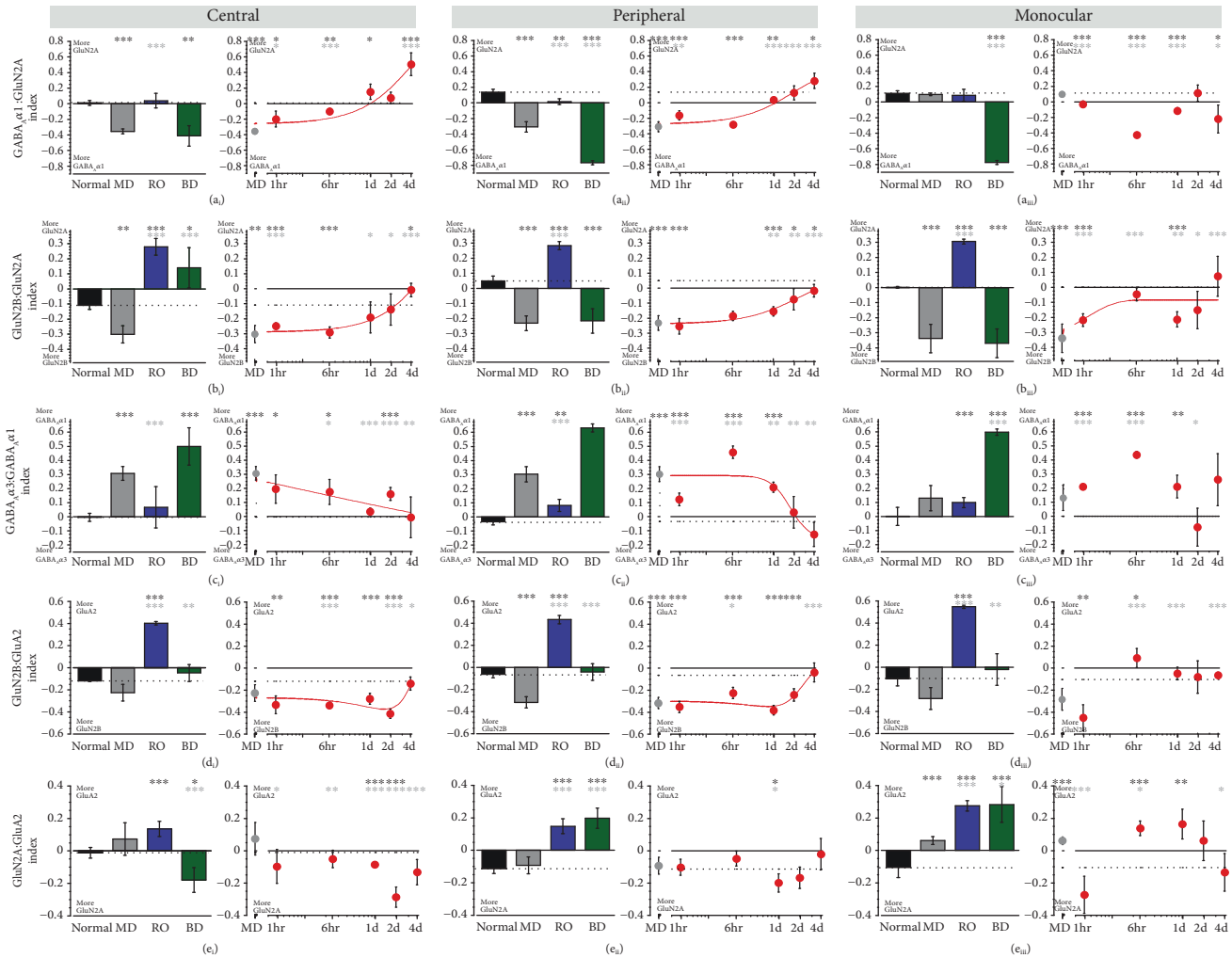

FIGURE 6: Expression of plasticity feature for indices identified using the principal component analysis. Histograms and scatterplots showing the plasticity features (rows) that were identified using the PCA basis vectors (Figure 4(j)) and plotted for each region of the V1 (columns). The conventions are the same as in Figure 5. For exact p values, Pearson's R, and equations for the curve-fits, see Supplemental Table 6-1.

resulting dendrogram suggested that the subclusters might form 4 groups that have similar plasticity features (1: normal, LT-BV, $MD_{P \text{ or } M}$; 2: RO; 3: ST-BV, MD_C; and 4: BD).

3.6. Constructing Plasticity Phenotypes and Comparing among the Subclusters. To compare the pattern of plasticity features among the subclusters, we visualized the average for each feature as a color-coded horizontal band, stacked the bands to illustrate the pattern that we called the plasticity phenotype (Figure 9(a)), and ordered the phenotypes using the same dendrogram as the correlation matrix (Figure 9(b)). In addition, we visualized the plasticity phenotypes for normal development and MD (using the data from [23]) to compare the treatment subclusters with a broad range of ages that had developed with either normal or abnormal visual experience (Figures 9(c) and 9(d)).

Inspection of the plasticity phenotypes identified some obvious and other subtler differences among the subclusters (Figure 9(b)). Indeed, the pattern of red and green bands in the BD phenotypes was different from 5 wk normals (Figure 9) and showed the shift to more GABA$_A$α1 and less GluN2A. For the RO subcluster, the light grey bands and number of green bands identified loss of protein expression and a shift to more GluN2A than 2B and more GluA2 than 5 wk normals. The RO pattern, however, appeared similar to an older (e.g., 12 wk) normally reared animal suggesting that RO may accelerate maturation of these proteins. Thus, these BD and RO treatments led to distinct plasticity phenotypes.

The pattern of red and green bands in the plasticity phenotype for LT-BV and some of the ST-BV subclusters (ST-BV1, ST-BV5) appeared similar to the 5 wk normals (Figure 9(b)), but many of the features were still significantly different from the age-matched normals (Figure 10(a), Supplemental Table 10-1). Nonetheless, these subclusters had some consistent differences with less GABA$_A$Rs and more GluN2B than 5 wk normals. Interestingly, one of the novel features found by the PCA, the GluN2A:GluA2 balance, was the only measure where all of the LT-BV subclusters were not different from 5 wk normals, but both

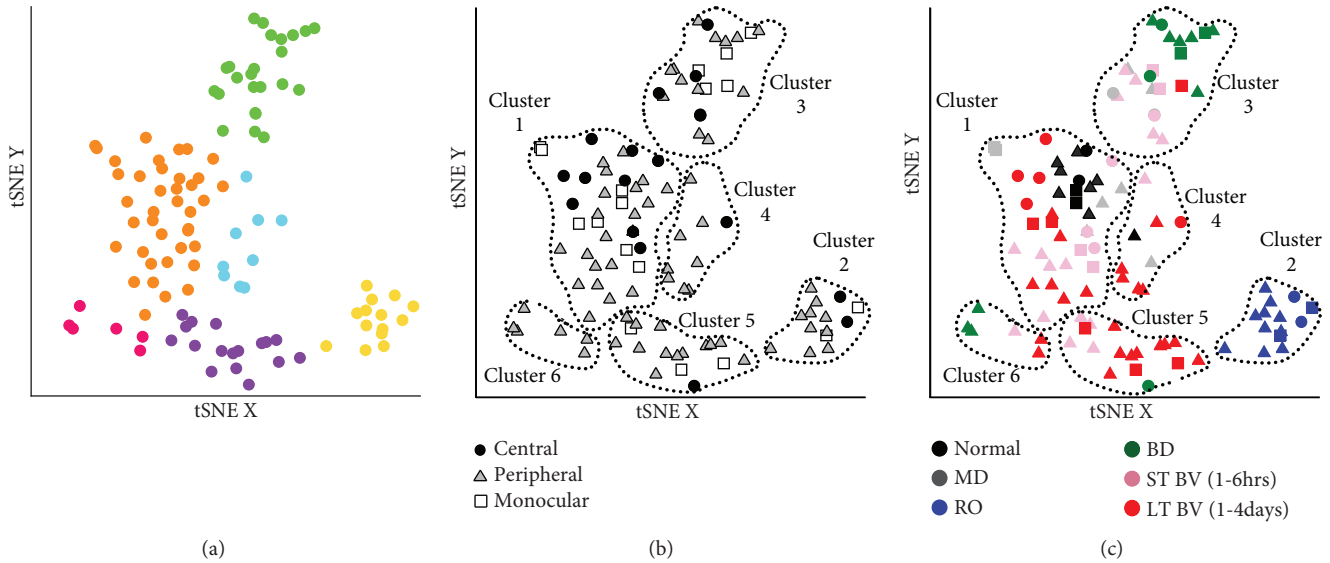

(a) (b) (c)

		Normal	MD	ST BV (1-6 h)	LT BV (1-4 d)	BD	RO
Cluster 1	C	100		75	83		
	P	88	50	31	27		
	M	100	100	50	33		
Cluster 2	C						100
	P						100
	M						100
Cluster 3	C		100	25		67	
	P		33	31		67	
	M			50	17	100	
Cluster 4	C				17		
	P	13	17	6	23		
	M						
Cluster 5	C					33	
	P			25	41		
	M				50		
Cluster 6	C						
	P			6	9	33	
	M						

(d)

Figure 7: Clustering of samples with similar plasticity features identified using *t*-distributed stochastic neighbor embedding (tSNE) and *k*-means clustering. (a) Using tSNE to visualize clustering of samples (109 tissue samples from animals reared to 5 wk normal, 5 wk MD, RO, BD, and BV) calculated from *k*-means analysis of the 8 plasticity features identified by PCA. The optimal number of clusters ($k = 6$) was identified by measuring the within groups sum of squares at intervals between 2 and 9 clusters (Figure 7-1). (b) The content of each cluster was visualized for the region (central, peripheral, and monocular) (c) or treatment condition. (d) The table summarizes the percentage of samples for each region and condition in clusters 1-6. For example, 100% of the samples from the central region of the V1 in normal animals were in cluster 1 while 100% of the samples from all regions of RO were in cluster 2. This information was used to annotate subclusters based on the cluster membership (1-6), rearing condition, and region of the V1.

RO and BD were different. Thus, this visualization of the plasticity phenotypes illustrated that the pattern promoted by BV, and LT-BV in particular, was most similar to the normal CP phenotype.

3.7. Modeling NMDAR and $GABA_AR$ Population Kinetics. The subunit composition of NMDARs and $GABA_A$Rs helps to regulate the threshold for experience-dependent plasticity, in part by controlling receptor kinetics [44, 45]. We used the

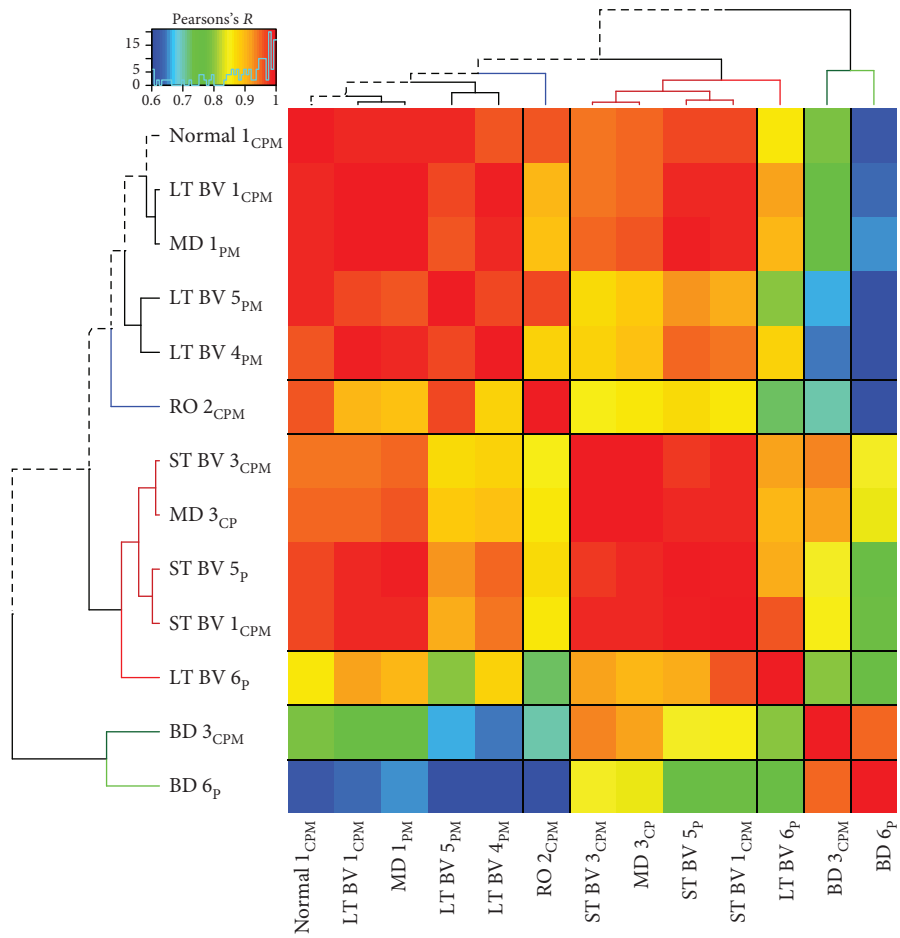

Figure 8: Visualizing pairwise correlations between treatment subclusters. The matrix is showing the strength (0.6 = blue; 1 = red) of correlation between the subclusters identified in Figure 7(d) and annotated here using the rearing condition, cluster (1-6), and region of the V1. Hierarchical clustering was used to order the data so that subclusters with strong correlations were nearby in the matrix. The subclusters formed 5 groups using the height of the dendrogram that is denoted by a change in the color of the dendrogram. The dotted black line in the dendrogram highlights the path to the normal subcluster. The black lines in the matrix identify the 5 groupings of the subclusters. For exact Bonferroni-corrected p values, see Supplemental Table 8-1, and for Pearson's R values, see Supplemental Table 8-2.

information about receptor kinetics with different subunit compositions to make a model that predicts the average population kinetics and applied it to normal development and the rearing conditions studied here. First, we transformed the 2A:2B and α1:α3 balances into predicted population kinetics (see Methods) and plotted the normal postnatal development (Figures 11(a) and 11(b)). Both the NMDA and $GABA_A$ kinetics rapidly speed up between 2 and 6 weeks of age. Next, we compared the predicted kinetics among the rearing conditions (Figures 11(c) and 11(d)). The pattern of results is necessarily similar to the balances presented for the indices (Figure 6); however, the predicted kinetics suggests a compression of differences between conditions when the balances favor the mature subunits (2A or α1) versus an accentuation of differences with much slower kinetics when the immature subunits (2B or α3) dominated.

To address how treatment-induced changes to NMDAR and $GABA_AR$ composition might affect the relationship between glutamatergic and GABAergic transmission timing, we made XY scatterplots using the predicted kinetics (Figure 11(e)). During normal development (black line), both balances progressed from slow kinetics at 2 wks to faster kinetics through the peak of the CP (Figure 11(e), yellow zone; 4-6 wks) to reach adult levels. The NMDAR:$GABA_AR$ kinetics for MD, RO, and BD fell outside the window predicted for the normal CP but in different directions. MD had slower NMDAR (C: 135 ms ± 16 ms; P: 121 ms ± 12 ms; and M: 146 ms ± 27 ms) but faster $GABA_AR$ kinetics (C: 47 ms ± 0.3 ms; P: 48 ms ± 1 ms; and M: 51 ms ± 4 ms), RO had faster NMDAR (C: 46 ms ± 0.8 ms; P: 46 ms ± 0.4 ms; and M: 46 ms ± 0.2 ms) but normal CP range for $GABA_AR$ (C:54 ms ± 6 ms; P:51 ms ± 2 ms; and M: 48 ms ± 0.2 ms), and BD had faster $GABA_AR$ (C: 46 ms ± 0.9 ms; P: 44 ms ± 0.2 ms; and M : 45 ms ± 0.2 ms) but normal CP range NMDAR kinetics in the central region only (C: 61 ms ± 12 ms; P: 130 ms ± 12 ms; and M: 155 ms ± 27 ms).

The introduction of BV caused a progressive change in the predicted NMDAR:$GABA_AR$ kinetics suggesting an initial speeding up of the NMDAR kinetics over the first 1 d to 2 d followed by a slowing of the $GABA_AR$ kinetics, especially in the central region. Taken together, the predicted NMDAR:$GABA_AR$ kinetics provided additional evidence

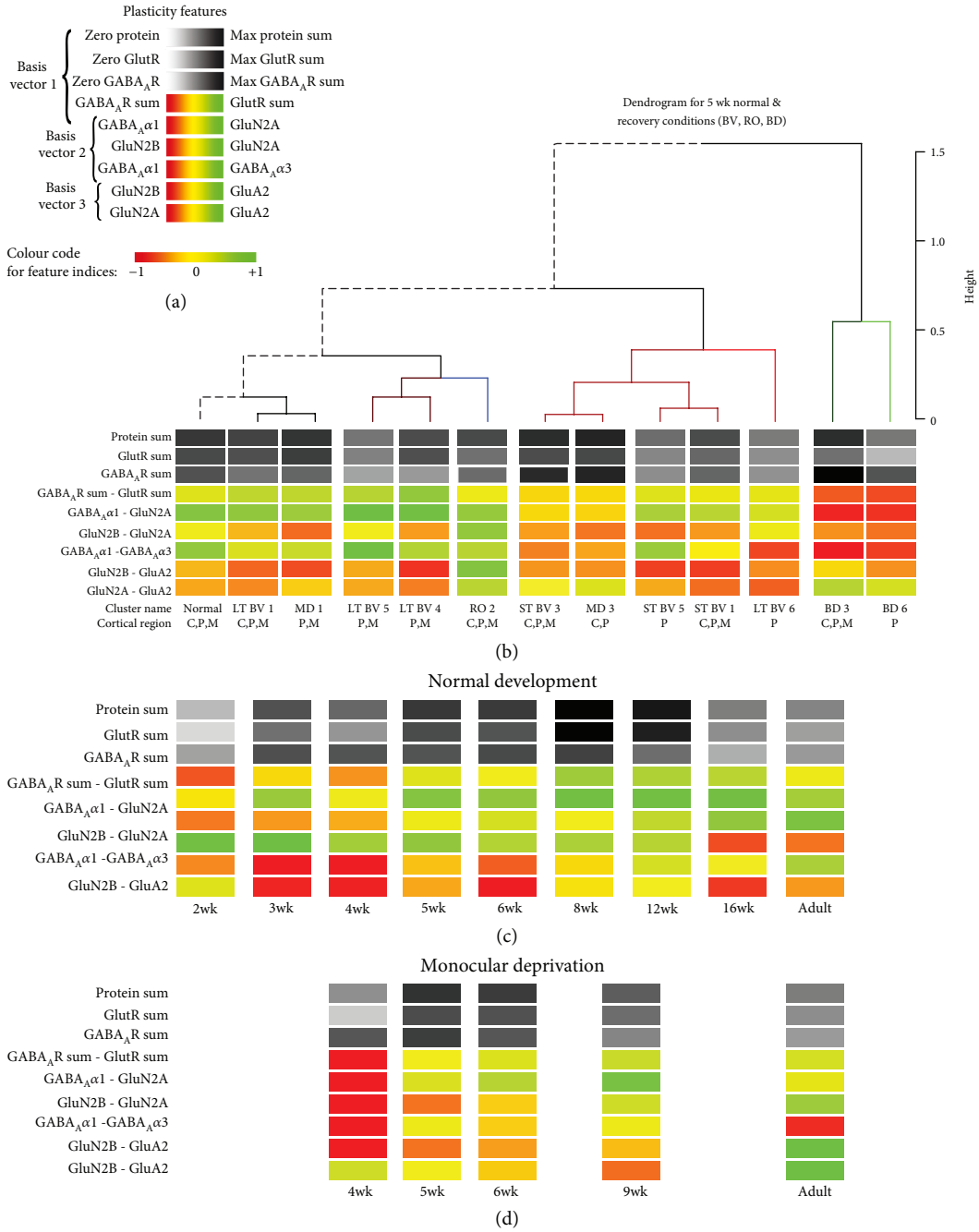

Figure 9: Visualizing the plasticity features and phenotypes for each subclusters. (a) We visualized the plasticity features as a stack of color-coded horizontal bars that together comprise the plasticity phenotype. The 3 grey scale bars represent the protein sums, and the 6 red-green color-coded bars represent the protein indices identified by the PCA. (b) The plasticity phenotypes were calculated for each subcluster and ordered using the same dendrogram as described in Figure 8. (c) For comparison, the plasticity phenotypes were calculated using previously published data [23] for normal development (2 – 32 wks) (d) and animals MDed from eye open until either 4, 5, 6, 9, or 32 wks.

that BV shifts protein expression towards a normal CP balance, but none of the treatments reinstated normal kinetics.

4. Discussion

Here, we studied a set of glutamatergic and GABAergic receptor subunits in the V1 that regulate plasticity and explored classifying treatments that cause either persistent bilateral amblyopia (RO or BD) or good acuity in both eyes (BV). Not surprisingly, there was a complex pattern of changes that varied by treatment and region within the V1. Applying a new analysis approach, however, using the PCA and cluster analysis, identified higher dimensional features and subclusters with different plasticity phenotypes for

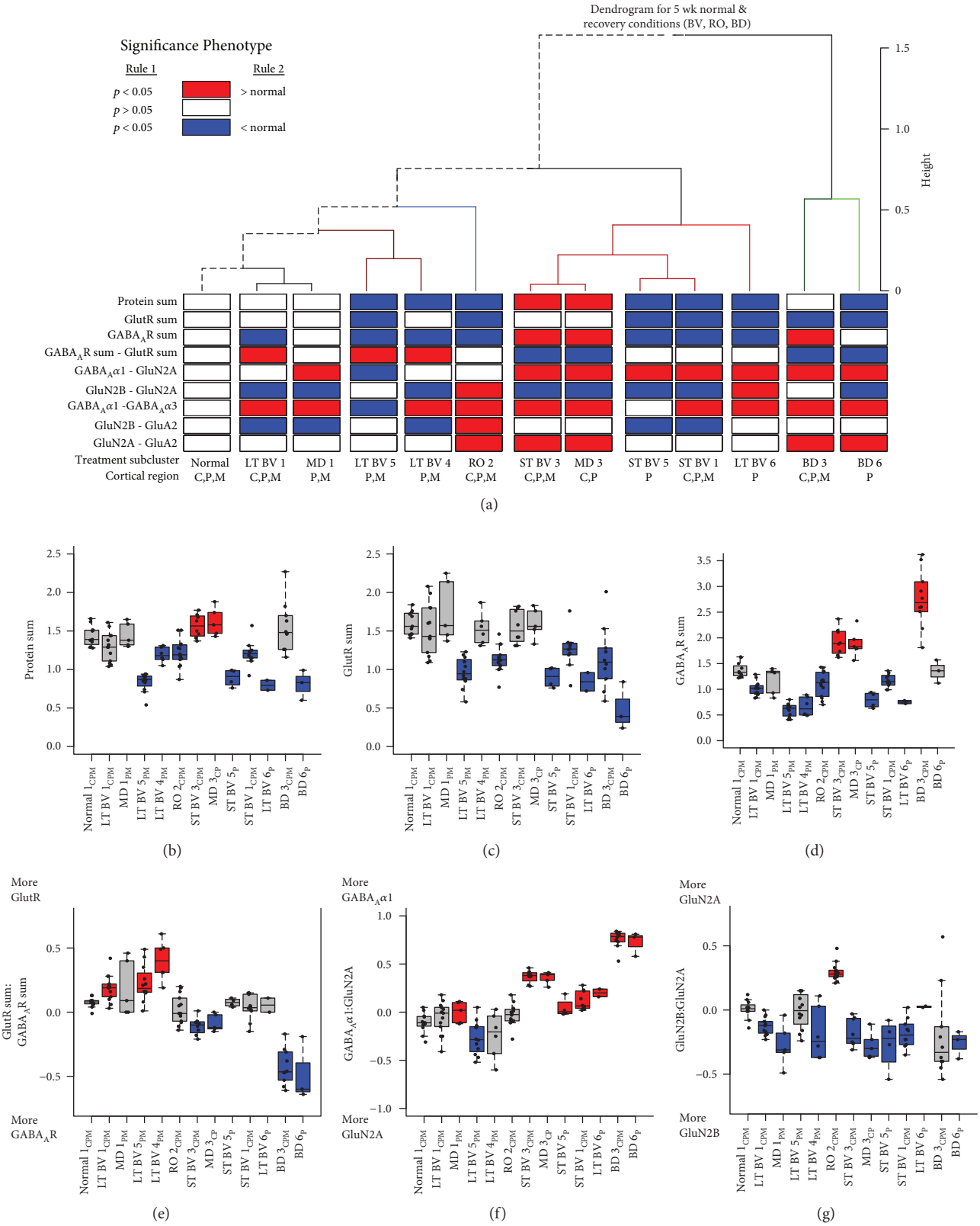

Figure 10: Continued.

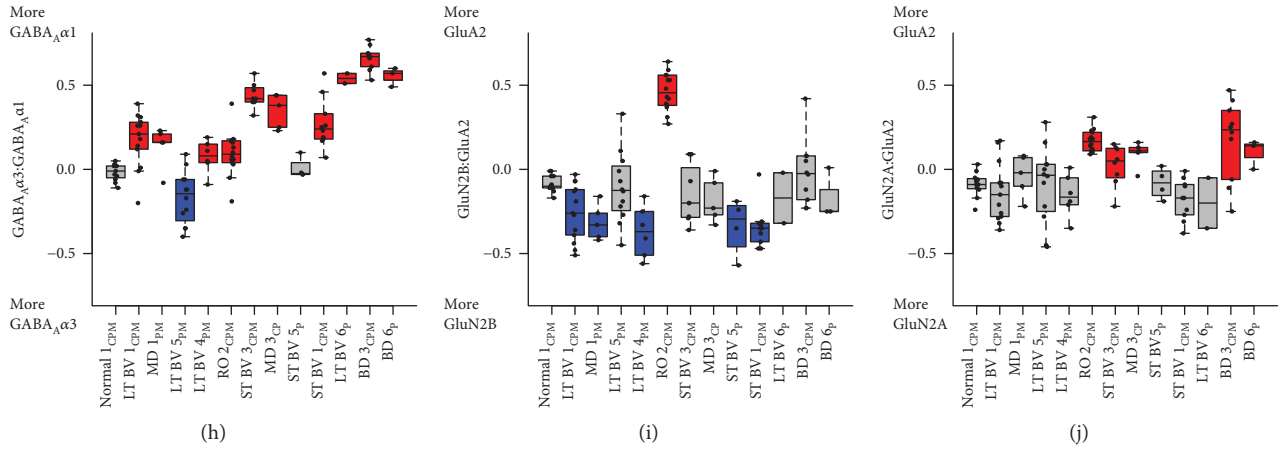

FIGURE 10: Significant plasticity features. (a) We used bootstrap analysis to identify plasticity features that were significantly different from 5 wk normal animals and color-coded the horizontal bars red if the feature was >normal and blue if it was <normal ($p < 0.05$). (b-j) The boxplots show the average protein sum (b-d) and an average index value (e-j) for each of the subclusters. Boxes were colored red if significantly greater than 5 wk normals, blue if significantly less than 5 wk normals, and grey if not significantly different from 5 wk normals. For exact Bonferroni-corrected p values, see Supplemental Table 10-1.

treatments that promote good versus poor recovery of acuity. The LT-BV plasticity phenotypes were closest to the normal CP pattern while the RO phenotype appeared more similar to an older pattern dominated by GluA2. In contrast, the BD phenotypes were dominated by GABA$_A\alpha$1 making it distinct from RO and illustrating that multiple plasticity phenotypes can underlie persistent bilateral amblyopia. The PCA identified an understudied feature, the balance between mature glutamate receptor subunits (GluN2A:GluA2 balance), as a marker that might differentiate treatments supporting good acuity (BV), from those that lead to persistent bilateral amblyopia (RO, BD). Finally, modeling kinetics for NMDAR and GABA$_A$R provided additional evidence that BV can return CP-like balances, especially in the central region of the V1.

4.1. Study Limitations and Design. The exploratory nature of the design used here was limited because the small number of animals used leaves unanswered how much variation there is in response to the treatments. The visual manipulations (MD, RO, BD, and BV), however, are known to cause consistent changes in visual perception [7, 8, 49–52], physiology [7, 29, 31, 53], and molecular mechanisms [23, 27, 54–59] that have been reliably measured in a number of laboratories using the cat to study visual system plasticity. Thus, these treatment-induced changes provide an understanding about the pattern of recovery that will be useful for formulating new hypotheses about the links between these proteins and persistent amblyopia.

The study design had some strengths including that (i) the animal model has excellent spatial vision, with a central visual field, so we could compare changes in the regions of the V1 that represent different parts of the visual field [27], (ii) the treatments were initiated and completed within the CP [34], (iii) there is detailed information about the recovery of physiology for RO and BV [7, 29, 32, 53] and acuity for all 3 treatments [7, 8, 27, 29, 30], (iv) both RO and BD cause persistent bilateral amblyopia [8, 30], and (v) the treatments engage different forms of experience-dependent plasticity (RO: competitive; BD: cooperative with degraded visual input; and BV: cooperative with normal visual input).

We observed that only one feature (GluN2A:GluA2 balance) returned to normal after LT-BV treatment raising the hypothesis that it is necessary for good recovery. We were not able to test that question because the molecular tools are not available for manipulating proteins in the cat cortex so it will be important to replicate that finding in the mouse and then test the question by directly manipulating those proteins. In addition, a large number of other treatments have been tested to improve recovery after MD, including a brief period of dark-rearing [30, 60], fluoxetine administration [61], perceptual learning [27, 62], or targeting specific molecular mechanisms (e.g., perineuronal nets [63]). Undoubtedly, the timing, length, and type of treatment influence recovery, but the conditions used here were necessarily limited because of the labor-intensive nature of this study. Notwithstanding these limitations, the plasticity phenotypes identified RO and BD as different from each other and from normals, but the LT-BV subclusters were remarkably similar to the 5 wk normal pattern.

Finally, the design took advantage of the reliability and multiplexing capabilities of Western blotting to obtain a large dataset of plasticity proteins from multiple V1 regions and rearing conditions. Western blotting, however, does not provide information about the cell types, layers, cortical columns, or subcellular localization of these proteins that would reveal which circuits are involved in recovery or persistent amblyopia. Even without that information, the application of high dimensional analyses led to the characterization of features and treatment-based clusters with unique plasticity phenotypes. The phenotyping approach developed here is scalable for studying more proteins or genes, cortical areas, and treatment conditions. Taken together, we think that

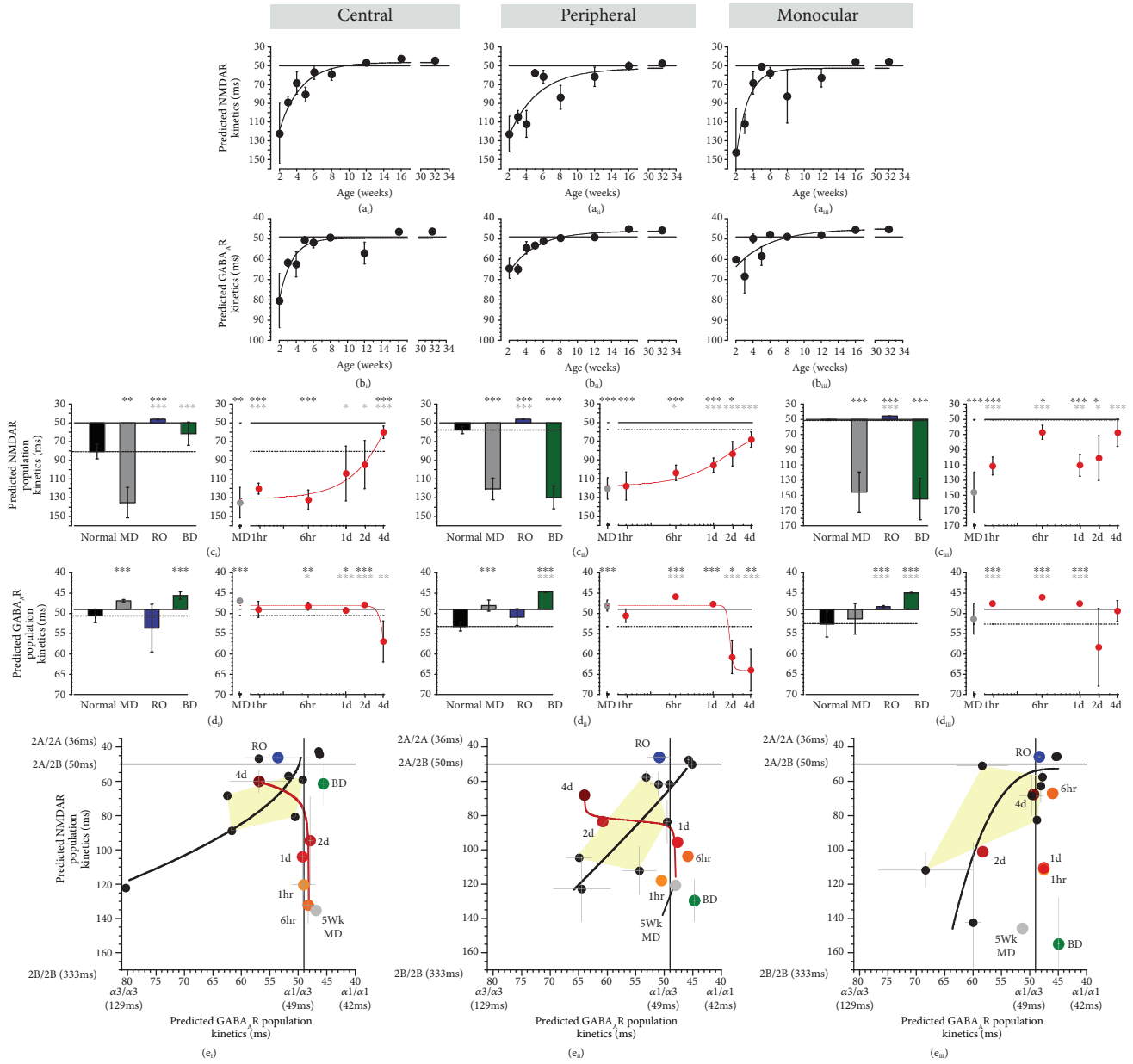

Figure 11: Indices for pairs of receptor subunits and modeling of predicted decay kinetics for a population of NMDARs and GABA$_A$Rs. Scatterplots showing the average expression of the predicted population kinetics ((a) NMDAR, (b) GABA$_A$R) for the regions of the V1 (columns) across normal development. Histograms and scatterplots showing the average expression of the predicted population kinetics ((c) NMDAR, (d) GABA$_A$R) for the regions of the V1 (columns) across treatment conditions. (e) The predicted population kinetics are plotted for both GABA$_A$Rs (x-values) and NMDARs (y-values) for normally reared animals age range 2 wks adult with the curve representing the trajectory of the relationship between these features (black dots and line, see (a) and (b)). Also, the data are plotted for 5 wk MD (grey dot), RO (blue dot), and BD (green dot). The relationship between NMDAR and GABA$_A$R kinetics during BV treatment for 1 hr (orange) to 4 d (red) is plotted, and the line uses the functions fit to the data in (c) and (d). For exact p values, Pearson's R, and equations for the curve-fits, see Supplemental Table 11-1.

this approach can be used in other animal models where molecular tools can be combined with visual testing to identify the features and phenotypes necessary for optimal visual recovery.

4.2. BV Promoted Recovery of CP-Like Plasticity Phenotype and Identified GluA2:GluN2A as a Balance That Differentiated BV Treatment. We explored BV treatment because it promotes long-lasting recovery of good acuity in both eyes [27], and those findings are similar to promising results of binocular therapies for treating amblyopia in children [64]. Furthermore, there is good physiological recovery with BV [29, 32]. Thus, it was not surprising to find that LT-BV subclusters had the strongest correlations with normals or that those subclusters had CP-like phenotypes. However, only one of the features, the GluA2:GluN2A balance, returned

to normal levels. Those findings suggest that it may not be necessary to recapitulate every detail of the normal phenotype to support good visual recovery and that the GluA2:-GluN2A balance may be a characteristic feature for tracking functional recovery. Although that balance is not commonly quantified, both proteins are critical components of mechanisms regulating experience-dependent plasticity, and that balance might signify the adaptive engagement of multiple plasticity mechanisms. For example, the delayed increase in visual responses during ocular dominance plasticity is part of a homeostatic plasticity mechanism regulated by trafficking GluA2-containing AMPARs into the synapse [65, 66]. Meanwhile, the initiation of ocular dominance plasticity requires GluN2A expression [22], and when GluN2A is deleted or reduced, MD does not depress deprived eye responses but instead causes enhancement of activity driven by the open eye [21]. Our finding that LT-BV returned a CP-like GluA2:GluN2A balance suggests that BV may prime GluN2A-dependent Hebbian plasticity to consolidate deprived-eye connections while GluA2-dependent homeostatic plasticity enhances deprived-eye responsiveness without triggering runaway excitation [67–71]. Thus, the GluA2:GluN2A balance may reflect the idea that during BV treatment the nondeprived eye acts as a *teacher* guiding both cooperative and competitive plasticity mechanisms [29].

4.3. RO versus BD Plasticity Phenotypes. Because RO and BD treatments cause persistent bilateral amblyopia [7, 8, 30], we expected these conditions to have abnormal phenotypes. We were surprised, however, to find very different phenotypes for these conditions, showing that more than one plasticity phenotype can account for persistent acuity deficits.

RO samples were in a single cluster dominated by an overabundance of GluA2 and more GluN2A than 2B. Together, those changes made the RO phenotype appear more similar to an adult than the CP pattern. The increase in GluA2 was in sharp contrast to the loss after BV treatment and suggests that RO may scale up AMPAR-dependent homeostatic mechanisms to drive recovery [25] without engaging NMDAR-dependent mechanisms to consolidate those changes [72]. Since AMPAR-mediated homeostasis promotes rapid but transient gains in responsiveness [25, 65, 73–76], this might explain the labile acuity recovered with RO [7, 8]. Interestingly, the overrepresentation of GluA2 promoted by RO implicates the dense expression of GluA2-containing synapses at feedback connections onto parvalbumin-positive (PV+) neurons [77]. The feedforward connections onto PV+ neurons may also be involved in RO circuit abnormalities because the labile acuity and early shift to GluN2A after RO are similar to changes found in MeCP2 KOs where an abnormally early shift to GluN2A at synapses onto PV+ neurons that halts acuity development [78, 79]. Taken together, these findings provide preliminary evidence that RO may leave behind feedforward (GluN2A subunits) and feedback abnormalities (GluA2) in PV+ neuron circuits in the V1.

Although various models of neural plasticity predict that decreasing firing rates will enhance plasticity, that idea has not translated to using BD treatment to improve recovery from MD [30]. BD for weeks or months during the CP has a range of effects on the V1 including enhancing the appearance of cytochrome oxidase blobs [80], weakening stimulus-evoked activity of PV+ neurons [81], and delaying the developmental increase in the GAD65 expression [82]. Here, we found that a few days of BD treatment caused an abnormal increase in the expression of $GABA_A\alpha1$ throughout the V1 and a shift to more GluN2A in the central region. $GABA_A\alpha1$ receptors are found on pyramidal cell bodies where PV+ neurons synapse, and they serve as regulators of ocular dominance plasticity [20] and the window for coincident spike-time-dependent plasticity [24]. A recent study has shown that the loss of PV+ activity caused by BD depends on $GABA_A\alpha1$ mechanisms and that blocking this subunit increases BD-evoked activity allowing for LTP of PV+ neurons [83]. Our observation of increased $GABA_A\alpha1$ expression suggests that BD treatment may further reduce visually evoked activity in the V1 that is compounded by the shift to more GluN2A reducing the availability of the NMDA-dependent mechanism needed to consolidate visual recovery.

4.4. Modeling Recovery of NMDAR and $GABA_AR$ Kinetics. Our modeling of population kinetics suggests that different physiological changes accompany the 3 treatments. During normal development, the increases in NMDAR and $GABA_AR$ kinetics progress in concert. Physiological studies [84] and our modeling show that this fine balance is decoupled by MD because the delayed shift to GluN2A has slower NMDAR kinetics, but the premature increase of $GABA_A\alpha1$ has faster $GABA_AR$ kinetics. Neither RO nor BD treatment corrected that decoupling and the modeling suggests that those treatments accelerate the shift to faster adult-like kinetics for NMDARs after RO or $GABA_ARs$ after BD. Modeling the kinetics for BV treatment identified 2 phases of recovery especially in the binocular regions of the V1. First, between 0 and 2 days of BV, there was a rapid increase in the predicted NMDAR kinetics that was similar to changes that occur between 2 and 4 weeks of age in normal cats. Second, between 2 and 4 days of BV, there was a slowing of the predicted $GABA_AR$ kinetics and that was opposite to the normal developmental increase in kinetics. These sequential phases of BV treatment do not recapitulate normal development. These results raise the question of whether the BV-driven increase in NMDAR kinetics needs to reach a certain level before triggering the slowing of $GABA_AR$ kinetics to rebalance these mechanisms. This modeling, however, was based on population data about the expression of the receptor subunits and cannot be extrapolated to individual receptors. Nonetheless, the rapid changes with BV treatment suggest that some aspects of normal development may be missed, and it will be important to determine what those are.

4.5. How Might These Plasticity Phenotypes be Used for Developing and Testing Treatments for Persistent Amblyopia? The distinct plasticity phenotypes classified for RO and BD treatments provide preliminary evidence that multiple neural changes can account for persistent amblyopia and

highlight the need to know which mechanisms to target when trying to engage neuroplasticity mechanisms to improve acuity. Whether the treatment should focus on AMPARs, NMDARs, $GABA_A$Rs, or some combination of those receptors will depend on the underlying plasticity phenotype. Insights into those questions can be addressed in animal models using modern molecular tools and vision testing, but translating those findings into treatments for humans will depend on noninvasive ways to determine an individual's plasticity phenotype. For example, magnetic resonance spectroscopy has been used to measure changes in glutamate or GABA concentrations in human V1 after different types of visual experience (e.g., MD [85]), and receptor expression can be quantified by radioligands labeled for SPECT and PET [86]. New molecular imaging techniques hold the promise of even greater detail with the ability to measure the concentration of receptor subunits [87–89]. That information may be comparable to protein analysis in animal models and suitable for constructing plasticity phenotypes for human V1 to facilitate the translation of new treatments. Furthermore, behavioral paradigms linked with specific plasticity mechanisms (e.g., stimulus-selective response plasticity [90]) may further aid in characterizing human plasticity phenotypes. Thus, selecting a treatment to prevent or correct persistent amblyopia may benefit from *in vivo* steps to classify an individual's plasticity phenotype.

5. Conclusions

This exploration of glutamatergic and GABAergic receptor subunit changes in the V1 after treatment that promotes either good (BV) or poor (RO, BD) recovery of vision provides a better understanding of the complexity of this problem. Of the treatments studied here, only BV provided evidence for recovery of a CP-like plasticity phenotype in the V1. However, only one feature, the GluA2:GluN2A balance, returned to normal levels after BV, and that balance is noteworthy because the proteins are regulators of homeostatic and Hebbian plasticity, respectively. The modeling of NMDAR and $GABA_A$R kinetics suggests two stages for BV recovery: a rapid increase in NMDAR kinetics, followed by slowing of the predicted $GABA_A$R kinetics which together move that balance into the CP range. We identified features of the plasticity phenotypes that may guide future studies on persistent amblyopia to look for high levels of GluA2 and GluN2A following RO and high levels of $GABA_A\alpha 1$ after BD treatment. Finally, the plasticity phenotyping is a good approach for uncovering novel neurobiological features that may be important for the recovery of acuity and new treatment targets.

Data Availability

The data used to support the findings of this study are available from the corresponding author upon request.

Conflicts of Interest

The authors declare that they have no conflicts of interest.

Authors' Contributions

JB designed and performed research, analyzed data, and wrote/revised the paper; DJ analyzed data and revised the paper; KM designed and performed research, analyzed data, and wrote/revised the paper.

Acknowledgments

We thank Kyle Hornby and Dr. Brett Beston for assistance with data collection. NSERC Grant RGPIN-2015-06215 awarded to KM; Woodburn Heron OGS awarded to JB.

Supplementary Materials

Supplemental Tables 2-1 and 2-2 expand on the descriptive statistics for the rearing conditions outlined in Table 2 in the main text. Supplemental Figure 7 describes the method used to determine the number of clusters identified after tSNE analysis. The remaining tables in the supplemental material contain supporting statistics that accompany Figures 3–6, 8, 10, and 11. *(Supplementary Materials)*

References

[1] T. N. Wiesel and D. H. Hubel, "Single-cell responses in striate cortex of kittens deprived of vision in one eye," *Journal of Neurophysiology*, vol. 26, no. 6, pp. 1003–1017, 1963.

[2] D. H. Hubel and T. N. Wiesel, "The period of susceptibility to the physiological effects of unilateral eye closure in kittens," *The Journal of Physiology*, vol. 206, no. 2, pp. 419–436, 1970.

[3] P. B. Dews and T. N. Wiesel, "Consequences of monocular deprivation on visual behaviour in kittens," *The Journal of Physiology*, vol. 206, no. 2, pp. 437–455, 1970.

[4] E. E. Birch, D. R. Stager Sr., J. Wang, and A. O'Connor, "Longitudinal changes in refractive error of children with infantile esotropia," *Eye*, vol. 24, no. 12, pp. 1814–1821, 2010.

[5] D. K. Wallace, Pediatric Eye Disease Investigator Group, A. R. Edwards et al., "A randomized trial to evaluate 2 hours of daily patching for strabismic and anisometropic amblyopia in children," *Ophthalmology*, vol. 113, no. 6, pp. 904–912, 2006.

[6] D. E. Mitchell, K. M. Murphy, and M. G. Kaye, "Labile nature of the visual recovery promoted by reverse occlusion in monocularly deprived kittens," *Proceedings of the National Academy of Sciences of the United States of America*, vol. 81, no. 1, pp. 286–288, 1984.

[7] K. M. Murphy and D. E. Mitchell, "Bilateral amblyopia after a short period of reverse occlusion in kittens," *Nature*, vol. 323, no. 6088, pp. 536–538, 1986.

[8] K. M. Murphy and D. E. Mitchell, "Reduced visual acuity in both eyes of monocularly deprived kittens following a short or long period of reverse occlusion," *Journal of Neuroscience*, vol. 7, no. 5, pp. 1526–1536, 1987.

[9] L. N. Cooper and M. F. Bear, "The BCM theory of synapse modification at 30: interaction of theory with experiment," *Nature Reviews Neuroscience*, vol. 13, no. 11, pp. 798–810, 2012.

[10] T. K. Hensch, "Critical period plasticity in local cortical circuits," *Nature Reviews Neuroscience*, vol. 6, no. 11, pp. 877–888, 2005.

[11] A. Maffei and G. Turrigiano, "Chapter 12 The age of plasticity: developmental regulation of synaptic plasticity in neocortical microcircuits," *Progress in Brain Research*, vol. 169, pp. 211–223, 2008.

[12] G. B. Smith, A. J. Heynen, and M. F. Bear, "Bidirectional synaptic mechanisms of ocular dominance plasticity in visual cortex," *Philosophical Transactions of the Royal Society B: Biological Sciences*, vol. 364, no. 1515, pp. 357–367, 2009.

[13] K. Yashiro and B. D. Philpot, "Regulation of NMDA receptor subunit expression and its implications for LTD, LTP, and metaplasticity," *Neuropharmacology*, vol. 55, no. 7, pp. 1081–1094, 2008.

[14] T. K. Hensch and E. M. Quinlan, "Critical periods in amblyopia," *Visual Neuroscience*, vol. 35, article E014, 2018.

[15] J. A. Heimel, D. van Versendaal, and C. N. Levelt, "The role of GABAergic inhibition in ocular dominance plasticity," *Neural Plasticity*, vol. 2011, Article ID 391763, 11 pages, 2011.

[16] E. M. Quinlan, D. H. Olstein, and M. F. Bear, "Bidirectional, experience-dependent regulation of N-methyl-D-aspartate receptor subunit composition in the rat visual cortex during postnatal development," *Proceedings of the National Academy of Sciences of the United States of America*, vol. 96, no. 22, pp. 12876–12880, 1999.

[17] B. D. Philpot, A. K. Sekhar, H. Z. Shouval, and M. F. Bear, "Visual experience and deprivation bidirectionally modify the composition and function of NMDA receptors in visual cortex," *Neuron*, vol. 29, no. 1, pp. 157–169, 2001.

[18] B. D. Philpot, J. S. Espinosa, and M. F. Bear, "Evidence for altered NMDA receptor function as a basis for metaplasticity in visual cortex," *Journal of Neuroscience*, vol. 23, no. 13, pp. 5583–5588, 2003.

[19] A. J. Heynen, B.-J. Yoon, C.-H. Liu, H. J. Chung, R. L. Huganir, and M. F. Bear, "Molecular mechanism for loss of visual cortical responsiveness following brief monocular deprivation," *Nature Neuroscience*, vol. 6, no. 8, pp. 854–862, 2003.

[20] M. Fagiolini, J.-M. Fritschy, K. Löw, H. Möhler, U. Rudolph, and T. K. Hensch, "Specific GABAA circuits for visual cortical plasticity," *Science*, vol. 303, no. 5664, pp. 1681–1683, 2004.

[21] K. K. A. Cho, L. Khibnik, B. D. Philpot, and M. F. Bear, "The ratio of NR2A/B NMDA receptor subunits determines the qualities of ocular dominance plasticity in visual cortex," *Proceedings of the National Academy of Sciences of the United States of America*, vol. 106, no. 13, pp. 5377–5382, 2009.

[22] M. Fagiolini, H. Katagiri, H. Miyamoto et al., "Separable features of visual cortical plasticity revealed by N-methyl-D-aspartate receptor 2A signaling," *Proceedings of the National Academy of Sciences of the United States of America*, vol. 100, no. 5, pp. 2854–2859, 2003.

[23] B. R. Beston, D. G. Jones, and K. M. Murphy, "Experience-dependent changes in excitatory and inhibitory receptor subunit expression in visual cortex," *Frontiers in Synaptic Neuroscience*, vol. 2, p. 138, 2010.

[24] R. C. Froemke and Y. Dan, "Spike-timing-dependent synaptic modification induced by natural spike trains," *Nature*, vol. 416, no. 6879, pp. 433–438, 2002.

[25] M. A. Gainey, J. R. Hurvitz-Wolff, M. E. Lambo, and G. G. Turrigiano, "Synaptic scaling requires the GluR2 subunit of the AMPA receptor," *Journal of Neuroscience*, vol. 29, no. 20, pp. 6479–6489, 2009.

[26] K. Iny, A. J. Heynen, E. Sklar, and M. F. Bear, "Bidirectional modifications of visual acuity induced by monocular deprivation in juvenile and adult rats," *Journal of Neuroscience*, vol. 26, no. 28, pp. 7368–7374, 2006.

[27] K. Williams, J. L. Balsor, S. Beshara, B. R. Beston, D. G. Jones, and K. M. Murphy, "Experience-dependent central vision deficits: neurobiology and visual acuity," *Vision Research*, vol. 114, pp. 68–78, 2015.

[28] K. R. Duffy, D. H. Bukhamseen, M. J. Smithen, and D. E. Mitchell, "Binocular eyelid closure promotes anatomical but not behavioral recovery from monocular deprivation," *Vision Research*, vol. 114, pp. 151–160, 2015.

[29] P. C. Kind, D. E. Mitchell, B. Ahmed, C. Blakemore, T. Bonhoeffer, and F. Sengpiel, "Correlated binocular activity guides recovery from monocular deprivation," *Nature*, vol. 416, no. 6879, pp. 430–433, 2002.

[30] K. R. Duffy and D. E. Mitchell, "Darkness alters maturation of visual cortex and promotes fast recovery from monocular deprivation," *Current Biology*, vol. 23, no. 5, pp. 382–386, 2013.

[31] S. D. Faulkner, V. Vorobyov, and F. Sengpiel, "Visual cortical recovery from reverse occlusion depends on concordant binocular experience," *Journal of Neurophysiology*, vol. 95, no. 3, pp. 1718–1726, 2006.

[32] D. S. Schwarzkopf, V. Vorobyov, D. E. Mitchell, and F. Sengpiel, "Brief daily binocular vision prevents monocular deprivation effects in visual cortex," *European Journal of Neuroscience*, vol. 25, no. 1, pp. 270–280, 2007.

[33] E. B. Hollingsworth, E. T. McNeal, J. L. Burton, R. J. Williams, J. W. Daly, and C. R. Creveling, "Biochemical characterization of a filtered synaptoneurosome preparation from guinea pig cerebral cortex: cyclic adenosine $3'$:$5'$-monophosphate- generating systems, receptors, and enzymes," *The Journal of Neuroscience*, vol. 5, no. 8, pp. 2240–2253, 1985.

[34] C. R. Olson and R. D. Freeman, "Profile of the sensitive period for monocular deprivation in kittens," *Experimental Brain Research*, vol. 39, no. 1, 1980.

[35] J. L. Balsor, D. G. Jones, and K. M. Murphy, "Recovery of Glutamatergic and GABAergic Protein Expression in Visual Cortex after Monocular Deprivation," 2019, bioRxiv, 684191.

[36] F. E. Harrell Jr. and M. C. Dupont, "The Hmisc package," *R Package, version*, 2006.

[37] G. R. Warnes, B. Bolker, L. Bonebakker et al., "gplots: various R programming tools for plotting data. R package version 3.0.1.1," 2015, https://CRAN.R-project.org/package=gplots.

[38] T. Galili, "dendextend: an R package for visualizing, adjusting and comparing trees of hierarchical clustering," *Bioinformatics*, vol. 31, no. 22, pp. 3718–3720, 2015.

[39] M. Hahsler, K. Hornik, and C. Buchta, "Getting things in order: an introduction to the R package seriation," *Journal of Statistical Software*, vol. 25, no. 3, pp. 1–34, 2008.

[40] J. G. A. Pinto, K. R. Hornby, D. G. Jones, and K. M. Murphy, "Developmental changes in GABAergic mechanisms in human visual cortex across the lifespan," *Frontiers in Cellular Neuroscience*, vol. 4, p. 16, 2010.

[41] J. G. A. Pinto, D. G. Jones, C. K. Williams, and K. M. Murphy, "Characterizing synaptic protein development in human visual cortex enables alignment of synaptic age with rat visual cortex," *Frontiers in Neural Circuits*, vol. 9, p. 3, 2015.

[42] J. Donaldson, "tsne: t-distributed stochastic neighbor embedding for R (t-SNE). R package version 0.1-3," 2016, https://CRAN.R-project.org/package=tsne.

[43] J. L. Balsor, D. G. Jones, and K. M. Murphy, "A Primer on High-Dimensional Data Analysis Workflows for Studying Visual Cortex Development and Plasticity," 2019, bioRxiv, 554378.

[44] W. Sun, K. B. Hansen, and C. E. Jahr, "Allosteric interactions between NMDA receptor subunits shape the developmental shift in channel properties," *Neuron*, vol. 94, no. 1, pp. 58–64.e3, 2017.

[45] M. D. Eyre, M. Renzi, M. Farrant, and Z. Nusser, "Setting the time course of inhibitory synaptic currents by mixing multiple GABA(A) receptor α subunit isoforms," *Journal of Neuroscience*, vol. 32, no. 17, pp. 5853–5867, 2012.

[46] B. J. Hall, B. Ripley, and A. Ghosh, "NR2B signaling regulates the development of synaptic AMPA receptor current," *Journal of Neuroscience*, vol. 27, no. 49, pp. 13446–13456, 2007.

[47] D. Keith and A. El-Husseini, "Excitation control: balancing PSD-95 function at the synapse," *Frontiers in Molecular Neuroscience*, vol. 1, p. 4, 2008.

[48] K. M. Murphy, K. R. Duffy, and D. G. Jones, "Experience-dependent changes in NMDAR1 expression in the visual cortex of an animal model for amblyopia," *Visual Neuroscience*, vol. 21, no. 4, pp. 653–670, 2004.

[49] D. E. Mitchell, "The long-term effectiveness of different regimens of occlusion on recovery from early monocular deprivation in kittens," *Philosophical Transactions of the Royal Society of London. Series B: Biological Sciences*, vol. 333, no. 1266, pp. 51–79, 1991.

[50] K. Burnat, E. Vandenbussche, and B. Zernicki, "Global motion detection is impaired in cats deprived early of pattern vision," *Behavioural Brain Research*, vol. 134, no. 1-2, pp. 59–65, 2002.

[51] K. Burnat, P. Stiers, L. Arckens, E. Vandenbussche, and B. Zernicki, "Global form perception in cats early deprived of pattern vision," *NeuroReport*, vol. 16, no. 7, pp. 751–754, 2005.

[52] M. Zapasnik and K. Burnat, "Binocular pattern deprivation with delayed onset has impact on motion perception in adulthood," *Neuroscience*, vol. 255, pp. 99–109, 2013.

[53] J. A. Movshon, "Reversal of the physiological effects of monocular deprivation in the kitten's visual cortex," *The Journal of Physiology*, vol. 261, no. 1, pp. 125–174, 1976.

[54] L. Chen, N. G. Cooper, and G. D. Mower, "Developmental changes in the expression of NMDA receptor subunits (NR1, NR2A, NR2B) in the cat visual cortex and the effects of dark rearing," *Molecular Brain Research*, vol. 78, no. 1-2, pp. 196–200, 2000.

[55] S. Jaffer, V. Vorobyov, P. C. Kind, and F. Sengpiel, "Experience-dependent regulation of functional maps and synaptic protein expression in the cat visual cortex," *European Journal of Neuroscience*, vol. 35, no. 8, pp. 1281–1294, 2012.

[56] L. Cnops, T.-T. Hu, J. Vanden Broeck, K. Burnat, G. Van Den Bergh, and L. Arckens, "Age- and experience-dependent expression of Dynamin I and Synaptotagmin I in cat visual system," *The Journal of Comparative Neurology*, vol. 504, no. 3, pp. 254–264, 2007.

[57] L. Cnops, T.-T. Hu, K. Burnat, and L. Arckens, "Influence of binocular competition on the expression profiles of CRMP2, CRMP4, Dyn I, and Syt I in developing cat visual cortex," *Cerebral Cortex*, vol. 18, no. 5, pp. 1221–1231, 2008.

[58] K. Laskowska-Macios, L. Arckens, M. Kossut, and K. Burnat, "BDNF expression in cat striate cortex is regulated by binocular pattern deprivation," *Acta Neurobiologiae Experimentalis*, vol. 77, no. 3, pp. 199–204, 2017.

[59] K. Laskowska-Macios, J. Nys, T.-T. Hu et al., "Binocular pattern deprivation interferes with the expression of proteins involved in primary visual cortex maturation in the cat," *Molecular Brain*, vol. 8, no. 1, p. 48, 2015.

[60] E. M. Quinlan, B. D. Philpot, R. L. Huganir, and M. F. Bear, "Rapid, experience-dependent expression of synaptic NMDA receptors in visual cortex *in vivo*," *Nature Neuroscience*, vol. 2, no. 4, pp. 352–357, 1999.

[61] J. F. Maya-Vetencourt, A. Sale, A. Viegi et al., "The antidepressant fluoxetine restores plasticity in the adult visual cortex," *Science*, vol. 320, no. 5874, pp. 385–388, 2008.

[62] K. M. Murphy, G. Roumeliotis, K. Williams, B. R. Beston, and D. G. Jones, "Binocular visual training to promote recovery from monocular deprivation," *Journal of Vision*, vol. 15, no. 1, pp. 2–2, 2015.

[63] D. Carulli, T. Pizzorusso, J. C. F. Kwok et al., "Animals lacking link protein have attenuated perineuronal nets and persistent plasticity," *Brain*, vol. 133, no. 8, pp. 2331–2347, 2010.

[64] K. R. Kelly, R. M. Jost, Y.-Z. Wang et al., "Improved binocular outcomes following binocular treatment for childhood amblyopia," *Investigative Opthalmology & Visual Science*, vol. 59, no. 3, pp. 1221–1228, 2018.

[65] M. E. Lambo and G. G. Turrigiano, "Synaptic and intrinsic homeostatic mechanisms cooperate to increase L2/3 pyramidal neuron excitability during a late phase of critical period plasticity," *Journal of Neuroscience*, vol. 33, no. 20, pp. 8810–8819, 2013.

[66] B.-J. Yoon, G. B. Smith, A. J. Heynen, R. L. Neve, and M. F. Bear, "Essential role for a long-term depression mechanism in ocular dominance plasticity," *Proceedings of the National Academy of Sciences of the United States of America*, vol. 106, no. 24, pp. 9860–9865, 2009.

[67] T. Keck, T. Toyoizumi, L. Chen et al., "Integrating Hebbian and homeostatic plasticity: the current state of the field and future research directions," *Philosophical Transactions of the Royal Society B: Biological Sciences*, vol. 372, no. 1715, article 20160158, 2017.

[68] M. A. Gainey and D. E. Feldman, "Multiple shared mechanisms for homeostatic plasticity in rodent somatosensory and visual cortex," *Philosophical Transactions of the Royal Society B: Biological Sciences*, vol. 372, no. 1715, article 20160157, 2017.

[69] J. Lisman, "Glutamatergic synapses are structurally and biochemically complex because of multiple plasticity processes: long-term potentiation, long-term depression, short-term potentiation and scaling," *Philosophical Transactions of the Royal Society B: Biological Sciences*, vol. 372, no. 1715, article 20160260, 2017.

[70] A. X. Yee, Y.-T. Hsu, and L. Chen, "A metaplasticity view of the interaction between homeostatic and Hebbian plasticity," *Philosophical Transactions of the Royal Society B: Biological Sciences*, vol. 372, no. 1715, article 20160155, 2017.

[71] F. Zenke and W. Gerstner, "Hebbian plasticity requires compensatory processes on multiple timescales," *Philosophical Transactions of the Royal Society B: Biological Sciences*, vol. 372, no. 1715, article 20160259, 2017.

[72] B. D. Philpot, K. K. A. Cho, and M. F. Bear, "Obligatory role of NR2A for metaplasticity in visual cortex," *Neuron*, vol. 53, no. 4, pp. 495–502, 2007.

[73] S.-H. Shi, Y. Hayashi, R. S. Petralia et al., "Rapid spine delivery and redistribution of AMPA receptors after synaptic NMDA

receptor activation," *Science*, vol. 284, no. 5421, pp. 1811–1816, 1999.

[74] G. G. Turrigiano, K. R. Leslie, N. S. Desai, L. C. Rutherford, and S. B. Nelson, "Activity-dependent scaling of quantal amplitude in neocortical neurons," *Nature*, vol. 391, no. 6670, pp. 892–896, 1998.

[75] A. Maffei and G. G. Turrigiano, "Multiple modes of network homeostasis in visual cortical layer 2/3," *Journal of Neuroscience*, vol. 28, no. 17, pp. 4377–4384, 2008.

[76] V. Tatavarty, Q. Sun, and G. G. Turrigiano, "How to scale down postsynaptic strength," *Journal of Neuroscience*, vol. 33, no. 32, pp. 13179–13189, 2013.

[77] R. N. Kooijmans, M. W. Self, F. G. Wouterlood, J. A. M. Beliën, and P. R. Roelfsema, "Inhibitory interneuron classes express complementary AMPA-receptor patterns in macaque primary visual cortex," *Journal of Neuroscience*, vol. 34, no. 18, pp. 6303–6315, 2014.

[78] S. Durand, A. Patrizi, K. B. Quast et al., "NMDA receptor regulation prevents regression of visual cortical function in the absence of Mecp2," *Neuron*, vol. 76, no. 6, pp. 1078–1090, 2012.

[79] S. B. Mierau, A. Patrizi, T. K. Hensch, and M. Fagiolini, "Cell-specific regulation of N-methyl-D-aspartate receptor maturation by Mecp2 in cortical circuits," *Biological Psychiatry*, vol. 79, no. 9, pp. 746–754, 2016.

[80] K. M. Murphy, K. R. Duffy, D. G. Jones, and D. E. Mitchell, "Development of cytochrome oxidase blobs in visual cortex of normal and visually deprived cats," *Cerebral Cortex*, vol. 11, no. 2, pp. 122–135, 2001.

[81] B. D. Feese, D. E. Pafundo, M. N. Schmehl, and S. J. Kuhlman, "Binocular deprivation induces both age-dependent and age-independent forms of plasticity in parvalbumin inhibitory neuron visual response properties," *Journal of Neurophysiology*, vol. 119, no. 2, pp. 738–751, 2018.

[82] Y. Guo, I. V. Kaplan, N. G. Cooper, and G. D. Mower, "Expression of two forms of glutamic acid decarboxylase (GAD67 and GAD65) during postnatal development of cat visual cortex," *Developmental Brain Research*, vol. 103, no. 2, pp. 127–141, 1997.

[83] M. C. Bridi, R. de Pasquale, C. L. Lantz et al., "Two distinct mechanisms for experience-dependent homeostasis," *Nature Neuroscience*, vol. 21, no. 6, pp. 843–850, 2018.

[84] A. Maffei, S. B. Nelson, and G. G. Turrigiano, "Selective reconfiguration of layer 4 visual cortical circuitry by visual deprivation," *Nature Neuroscience*, vol. 7, no. 12, pp. 1353–1359, 2004.

[85] C. Lunghi, U. E. Emir, M. C. Morrone, and H. Bridge, "Short-term monocular deprivation alters GABA in the adult human visual cortex," *Current Biology*, vol. 25, no. 11, pp. 1496–1501, 2015.

[86] W.-D. Heiss and K. Herholz, "Brain receptor imaging," *Journal of Nuclear Medicine*, vol. 47, no. 2, pp. 302–312, 2006.

[87] J. van der Aart, M. Yaqub, E. J. M. Kooijman et al., "Evaluation of the novel PET tracer [^{11}C]HACH242 for imaging the GluN2B NMDA receptor in non-human primates," *Molecular Imaging and Biology*, vol. 14, p. 383, 2018.

[88] A. Haider, I. Iten, H. Ahmed et al., "Identification and preclinical evaluation of a radiofluorinated benzazepine derivative for imaging the GluN2B subunit of the ionotropic NMDA receptor," *The Journal of Nuclear Medicine*, vol. 60, no. 2, pp. 259–266, 2019.

[89] S. D. Krämer, T. Betzel, L. Mu et al., "Evaluation of ^{11}C-Me-NB1 as a Potential PET Radioligand for Measuring GluN2B-Containing NMDA Receptors, Drug Occupancy, and Receptor Cross Talk," *The Journal of Nuclear Medicine*, vol. 59, no. 4, pp. 698–703, 2018.

[90] S. F. Cooke and M. F. Bear, "Stimulus-selective response plasticity in the visual cortex: an assay for the assessment of pathophysiology and treatment of cognitive impairment associated with psychiatric disorders," *Biological Psychiatry*, vol. 71, no. 6, pp. 487–495, 2012.

Hindawi
Neural Plasticity
Volume 2019, Article ID 3198285, 10 pages
https://doi.org/10.1155/2019/3198285

Research Article

Modification of Peak Plasticity Induced by Brief Dark Exposure

Alexander J. Lingley, Donald E. Mitchell, Nathan A. Crowder, and Kevin R. Duffy

Department of Psychology & Neuroscience, Dalhousie University, Halifax, NS, Canada B3H 4R2

Correspondence should be addressed to Kevin R. Duffy; kevin.duffy@dal.ca

Received 1 February 2019; Revised 13 May 2019; Accepted 22 May 2019; Published 3 September 2019

Guest Editor: Elizabeth Quinlan

The capacity for neural plasticity in the mammalian central visual system adheres to a temporal profile in which plasticity peaks early in postnatal development and then declines to reach enduring negligible levels. Early studies to delineate the critical period in cats employed a fixed duration of monocular deprivation to measure the extent of ocular dominance changes induced at different ages. The largest deprivation effects were observed at about 4 weeks postnatal, with a steady decline in plasticity thereafter so that by about 16 weeks only small changes were measured. The capacity for plasticity is regulated by a changing landscape of molecules in the visual system across the lifespan. Studies in rodents and cats have demonstrated that the critical period can be altered by environmental or pharmacological manipulations that enhance plasticity at ages when it would normally be low. Immersion in complete darkness for long durations (dark rearing) has long been known to alter plasticity capacity by modifying plasticity-related molecules and slowing progress of the critical period. In this study, we investigated the possibility that brief darkness (dark exposure) imposed just prior to the critical period peak can enhance the level of plasticity beyond that observed naturally. We examined the level of plasticity by measuring two sensitive markers of monocular deprivation, namely, soma size of neurons and neurofilament labeling within the dorsal lateral geniculate nucleus. Significantly larger modification of soma size, but not neurofilament labeling, was observed at the critical period peak when dark exposure preceded monocular deprivation. This indicated that the natural plasticity ceiling is modifiable and also that brief darkness does not simply slow progress of the critical period. As an antecedent to traditional amblyopia treatment, darkness may increase treatment efficacy even at ages when plasticity is at its highest.

1. Introduction

Disruption of normal binocular vision during critical periods early in postnatal development can provoke anatomical and physiological alterations to neurons within the primary visual pathway. Monocular deprivation (MD) by eyelid closure can elicit a shift in cortical responsivity so that most neurons come to be excited only by stimulation of the nondeprived eye [1], leaving the deprived eye able to control few neurons and with a visual acuity deficit, called amblyopia [2], that is most severe in the central visual field [3]. This deprivation-induced shift in ocular dominance is consequent to a reduction in the number and strength of cortical neural connections serving the deprived eye [4–6], which is reflected by a reduction in the cross-sectional soma area of neurons within deprived-eye recipient layers of the dorsal lateral geniculate nucleus (dLGN) in the thalamus [7, 8].

The capacity of the visual system to be modified by imbalanced visual experience is regulated by age, reaching peak plasticity levels early in the postnatal life and thereafter declining through adolescence and into early adulthood [9–12]. In cats, the critical period for susceptibility to MD (Figure 1(a)) reaches its peak at about 4 weeks of age [9–11] and is then followed by a decline to low levels by about 12-16 postnatal weeks [9, 10] followed again by an even slower decay to negligible levels at about 10 months [11, 12]. The capacity for recovery from the effects of MD likewise adheres to a critical period, but with a shorter timespan and with little recovery observed when MD is followed by reverse occlusion beyond about 12 weeks postnatal [13, 14].

The notion that plasticity capacity is rigidly associated with age is at odds with a growing number of studies on mice, rats, and cats demonstrating that the critical period profile is itself plastic, a concept referred to as *metaplasticity* [16].

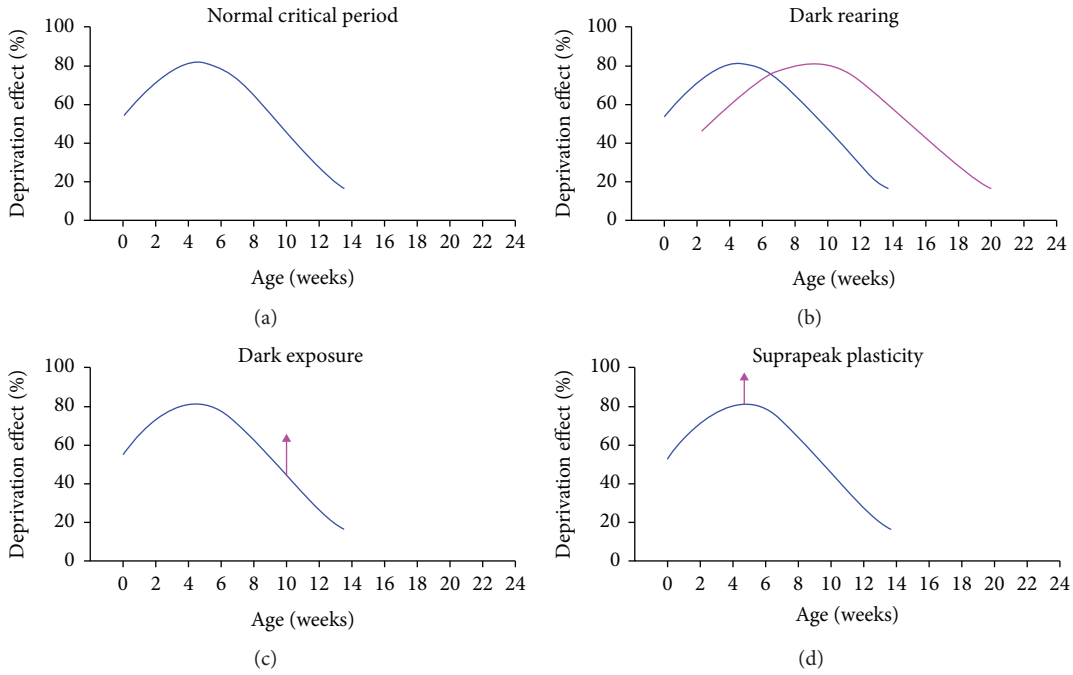

Figure 1: Illustration of the effect on plasticity capacity following immersion in complete darkness. Profile of the critical period in normally reared cats (based on data from [9]) demonstrates peak plasticity at about 4 weeks of age followed by a progressive decline to low levels that are maintained into adolescence (a). Dark rearing from near birth and for long durations has been postulated to slow the overall time course of the critical period (magenta profile in (b)) so that enhanced plasticity can be observed at ages when normally reared animals exhibit lower plasticity capacity (based on [15]). More recently, short durations of darkness (dark exposure) in rodents and cats have been employed to raise plasticity levels beyond that observed from age-matched controls (c). In the current study, we investigated the possibility that 10 days of dark exposure imposed just prior to the critical period peak can enhance plasticity capacity beyond its natural maximum (d).

Genetic, molecular, and experiential interventions have been employed to alter key critical period parameters that have enabled manipulation of plasticity levels in the visual system [17, 18]. In rodents, critical period timing can be modified through manipulation of GABAergic [19–21] or glutamatergic signalling [22, 23], by alteration of the neurotrophin expression [24] or the expression of protein constituents of the extracellular matrix [25–28], as well as by the tweaking of epigenetic targets [29–31]. In aggregate, these studies demonstrate that plasticity capacity in the visual system can be adjusted beyond what would be available in age-matched normally reared animals.

Immersing young cats in complete darkness has long been known to extend the critical period [32–36] and has provided a means of modifying a variety of neural plasticity regulators to bring about high levels of visual plasticity [37–43]. Kittens reared from near birth in complete darkness maintain sensitivity to MD in the visual cortex even when dark rearing extends to 10 months of age at which time the cortex of normal animals is immutable [33]. A prominent theory of how long durations of darkness (called dark rearing) modify plasticity levels in the visual system postulates that dark rearing slows the time course of the critical period (Figure 1(b)), with both its onset and decay being delayed relative to animals reared under normal conditions [15]. More recent research in mice, rats, and cats has demonstrated that long durations of dark rearing are not necessary to provoke enhanced plasticity capacity and that much shorter durations of darkness (called dark exposure) can significantly elevate plasticity levels in the visual system [39, 41, 44]. The notion that darkness acts to slow the progress of the critical period profile is incongruent with rodent research showing plasticity enhancement following dark exposure in juveniles and adults [39, 44] and also with cat research showing a modest plasticity boost when dark exposure is imposed past the critical period peak (Figure 1(c); [45]). The ability for dark exposure to raise the level of plasticity capacity rather than simply slow its progression implies that there are differences between the mechanisms mediating the effects of long- and short-term dark immersion and suggests that dark exposure does not alter plasticity levels simply by slowing progress of the critical period. In this study, we examined whether the plasticity enhancement conferred by dark exposure occurs when darkness is imposed at the peak of the critical period, a time when plasticity capacity is at its natural maximum (Figure 1(d)). A modification of peak plasticity would indicate that dark exposure does not cause a protraction of the critical period but rather alters the constellation of plasticity-related molecules enabling enhanced plasticity even from its natural maximum. We demonstrate that 10 days of dark exposure applied immediately prior to the peak of the critical period can enhance the effect of a week-long period of MD. These results indicate that dark exposure does not simply slow the temporal progression of the critical period, but is efficacious even when applied within the first postnatal month and can elevate plasticity levels beyond natural limits.

2. Materials and Methods

2.1. Animals and Rearing Histories. Eight animals were reared from birth in a closed cat breeding colony at Dalhousie University for the purposes of this study. In summary, four animals were monocularly deprived for 7 days at postnatal day 30 (MD-only group), and four animals were immersed in darkness for 10 days from postnatal day 20 to 30 and then removed from darkness and immediately monocularly deprived for 7 days (dark exposure+MD group). All experimental procedures adhered to protocols that were approved by the Dalhousie University Committee on Laboratory Animals in accordance with policies established by the Canadian Council on Animal Care.

2.2. Monocular Deprivation. Monocular deprivation was performed under general gaseous anesthetic using 3-4% isoflurane in oxygen. The upper and lower palpebral conjunctivae of the left eye were sutured with vicryl suture material, followed by closure of the overlying eyelids with silk suture, as has been described in detail previously [46]. The surgery lasted approximately 15 minutes after which anesthetized animals were administered a subcutaneous injection of Anafen for postoperative analgesia, as well as topical ophthalmic Alcaine (proparacaine hydrochloride) to mitigate postprocedural discomfort. A broad-spectrum topical antibiotic (1% Chloromycetin) was also given postprocedurally to mitigate infection.

2.3. Dark Exposure. Kittens indicated for darkness exposure were housed for 10 days in a darkness facility that has been in use for many decades and has been described in detail previously [47]. In brief, the darkness facility contains three darkrooms accessible only via a series of completely dark anterooms, each segregated by doors sealed at all margins to prevent any entrance of light. The central darkroom is used to house the communal cage containing kittens and their mother, with the dark anterooms used as transfer space to facilitate cleaning and husbandry. Daily feeding, cleaning, and social interaction were provided by experienced technicians. The appearance, health, weight, and well-being of animals in the dark were monitored through the use of a CCD camera and infrared illumination system (>820 nm) that remained off when not in use. Animals destined to be monocularly deprived following 10 days of dark exposure were transported to a nearby surgical suite within an opaque, light-impermeable chamber that was designed to allow for the administration of gaseous anesthetic while mitigating exposure to light.

2.4. Histology. Histological procedures were the same for all animals in this study. Kittens were anesthetized with isoflurane (5% in oxygen) and euthanized with an intraperitoneal lethal dose of sodium pentobarbital (Euthanyl; 150 mg/kg). Subsequently, animals were transcardially perfused with 150 mL of phosphate-buffered saline (PBS) followed by 150 mL of 4% dissolved paraformaldehyde in PBS. Brain tissue was immediately extracted following perfusion, and the thalamus containing the dLGN was carefully dissected from the overlying cortex using a scalpel. The block of tissue containing the dLGN was immersed in a PBS solution containing 30% sucrose for cryoprotection. Five days later, sections of the dLGN were sliced into 50 μm thick coronal sections using a freezing microtome (Leica SM2000R; Germany). A portion of the cut sections were stained for Nissl substance by mounting them onto glass sides, immersing them in a graded series of ethanol concentrations, followed by immersion in a solution of 0.1% cresyl violet acetate dye dissolved in distilled water. A separate set of sections was labeled for neurofilament protein via immersion in PBS containing a mouse monoclonal antibody targeting the heavy chain subunit of neurofilament (1 : 1000 dilution; SMI-32; BioLegend, San Diego, CA). Sections were left overnight, then thoroughly washed in PBS, and immersed in a PBS solution containing goat-anti-mouse secondary antibody for 1 hour (1 : 500; Jackson Immunoresearch, West Grove, PA). Following another wash with PBS, sections were placed in an avidin and peroxidase-conjugated biotin solution for one hour (PK6100; Vector Labs, Burlingame, CA). Neurofilament labelling was visualized through reaction with 3,3′-diaminobenzidine. Tissue sections stained for Nissl substance or labelled for neurofilament protein were immersed in a graded series of ethanol concentrations, cleared using Histoclear (DiaMed Lab Supplies Inc.; Canada) and coverslipped using Permount (Fisher Scientific; Canada). Tissue from one MD-only animal and one animal immersed in darkness before MD was fixed suboptimally following perfusion and exhibited pale reactivity for neurofilament within and beyond the dLGN. Although excellent Nissl staining enabled soma size quantification from these animals, the quality of neurofilament labeling was insufficient for quantification so they were excluded from our quantification.

The specificity of the primary antibody, SMI-32 (Table 1), for the nonphosphorylated heavy-chain subunit of neurofilament was verified with an immunoblot of homogenized normal cat primary visual cortex. The labelled blots revealed bands corresponding with the expected mass of NF-H [48].

2.5. Quantification. Quantification of neuron soma size and neurofilament immunoreactivity in the dLGN was performed blind to animal rearing condition. Quantification was performed using a BX-51 microscope (Olympus; Markham, Ottawa, Canada) fitted with a DP-70 digital camera (Olympus; Markham, Ottawa, Canada) and a computerized stereology software package (newCast; Visiopharm, Denmark). The cross-sectional area of neuron somata within A and A1 layers of the left and right dLGN was measured from Nissl-stained sections using the "nucleator" stereology probe, whereas the density of neurofilament immunoreactive neurons in separate sections was measured using the "optical dissector" stereology probe. Neurons in Nissl-stained sections were distinguished from glial cells by established selection criteria [1, 7, 8]. Cells characterized by dark cytoplasmic and nucleolar staining with light nuclear staining were considered admissible for quantification. These criteria help to reduce the chance of inadvertently quantifying cell caps, rather than cells cut through the somal midline. Cells within the dLGN labelled for neurofilament and selected for

Table 1: Antibody characterization.

Antigen	Immunogen	Source	Dilution
Neurofilament H	Homogenized rat hypothalamus	Covance (Princeton, NJ), mouse monoclonal, clone SMI-32, No. SMI-32. AB_509998	1 : 1000

quantification exhibited dark cytoplasmic reactivity with pale or absent labeling within the nucleus. A summary of measurements is presented in Table 2.

2.6. Statistics. A deprivation index (DI) was calculated to assess the within-animal percent difference ((nondeprived layer A1 + nondeprived layer A)-(deprived layer A1 + deprived layer A)/(nondeprived layer A1 + nondeprived layer A)) in neuronal somal size and density of neurofilament immunoreactivity between deprived- and non-deprived-eye layers [43, 49, 50]. All statistical analyses and data visualizations were performed using Prism (GraphPad, USA). Statistical comparisons between deprived and nondeprived layers within each rearing condition were performed using Mann-Whitney U tests. Statistical comparisons between rearing conditions were made using Permutation tests for a difference in means, and we applied the Benjamini-Hochberg procedure for controlling false discovery rate (6 total comparisons). Adjusted p values are reported [51].

3. Results

3.1. Within Condition Effects. Low-power (4x objective) microscopic examination of Nissl-stained dLGN sections from animals in the 7-day MD-only group revealed a clear deprivation effect characterized by smaller neuron somata and reduced staining intensity within deprived-eye layers (Figure 2(a), a1 and a2; Table 2). Nissl-stained sections of dLGN from animals that received 10 days of darkness before 7 days of MD also showed an obvious reduction in the size of neuron somata that was accompanied by a loss of staining intensity within deprived-eye layers (Figure 2(b), b1 and b2). From our initial low-power observations of staining intensity reduction induced by MD, we noted that the contrast between deprived and nondeprived layers appeared slightly greater in the group subjected to darkness before MD, suggestive of a larger deprivation effect relative to the MD-only group; this difference was also revealed by our *Between Condition* analysis below. Observations of the anatomical differences that were evident at low magnification were reflected in the quantification of the cross-sectional area of somata from both groups. In the MD-only group, there was a clear difference in the average size of deprived relative to nondeprived neurons, with deprived neurons (average = 147.8 μm^2; SD = 16 μm^2) 17% smaller than nondeprived neurons (average = 178.8 μm^2; SD = 23 μm^2; Figure 2(a), a3). Deprived neurons were significantly smaller than nondeprived neurons in this MD-only group ($p < 0.02$; Mann-Whitney U test; $n = 16$ layers). In the group of animals that received darkness prior to MD, the size of deprived neurons (average = 134.5 μm^2; SD = 21 μm^2) was also measured to be smaller, by an average of 22%, compared to nondeprived neurons (average = 172.5 μm^2; SD = 26 μm^2; Figure 2(b), b3). Statistical analysis revealed this difference was also significant ($p < 0.02$; Mann-Whitney U test; $n = 16$ layers).

Similar to the reduction of soma size precipitated by MD, loss of neurofilament protein in the dLGN has emerged as a sensitive means of measuring the effect of visual deprivation [52, 53]. In the current study, we observed a considerable loss of neurofilament labeling in the dLGN following MD for 7 days (Figure 3(a), a1–a3), with deprived layers having significantly fewer ($p < 0.02$; Mann-Whitney U test; $n = 12$ layers) immunopositive neurons (average = 115 neurons/mm^2; SD = 54 neurons/mm^2) compared to nondeprived layers (average = 230 neurons/mm^2; SD = 99 neurons/mm^2), which corresponded to a 51% reduction in immunopositive cells. Animals that received darkness prior to MD also showed a strong deprivation effect (Figure 3(b), b1–b3), with deprived layers having significantly fewer ($p < 0.02$; Mann-Whitney U test; $n = 12$ layers) immunopositive neurons (average = 67 neurons/mm^2; SD = 15 neurons/mm^2) relative to nondeprived layers (average = 142 neurons/mm^2; SD = 35 neurons/mm^2), which corresponded to a 52% reduction in immunopositive cells.

3.2. Between Condition Effects. Next, we sought to quantify whether the deprivation effect was greater for the group subjected to darkness before MD relative to the MD-only group. Within-animal percent differences (DI) in density of neurofilament immunoreactivity and neuron soma size were used to test for group effects between the MD-only condition and darkness prior to MD condition. DIs were similar for neurofilament immunoreactivity between the MD-only condition and darkness prior to MD condition (Figure 4(a)), indicating that on this measure dark exposure did not produce an exaggerated effect. This conclusion was supported by a statistical test of DIs between groups, which revealed that the magnitude of neurofilament loss was not significantly larger in the group that received dark exposure prior to MD ($p = 0.4286$; Permutation test; $n = 6$ cats). Conversely, when changes in soma size were compared between the two groups, the animals where darkness preceded MD showed changes that were approximately 23% larger than MD-only animals (Figure 4(b)), and this difference was significant ($p = 0.02$; Permutation test; $n = 8$ cats).

4. Discussion

In this study, we demonstrate that a short period of darkness preceding a week of MD initiated at the peak of the critical period can produce a modest increase in the effect of MD on the difference between deprived and nondeprived soma size in the dLGN. However, we did not observe a difference in the magnitude of neurofilament loss within deprived-eye layers between MD-only and MD following darkness conditions. The enhanced MD effect with darkness indicates that

Table 2: Measurements of the average soma area (μm^2) and neurofilament-positive cell density (cells/mm^2) presented for animals across both rearing conditions in this study. Deprivation index (DI) represents the percentage difference between deprived and nondeprived layers for each animal studied. Asterisks indicate measurements that were not collected because immunolabelling was insufficient for quantification.

Cat #	Condition	Soma area nondeprived	Soma area deprived	DI (%)	Neurofilament nondeprived	Neurofilament deprived	DI (%)
#100	MD	180	150	16	342	176	49
#101	MD	176	145	17	195	95	51
#102	MD	208	168	19	153	73	52
#103	MD	151	128	15	*	*	*
#110	DR+MD	162	129	21	114	61	46
#111	DR+MD	211	166	22	181	84	54
#112	DR+MD	165	123	25	131	56	57
#113	DR+MD	152	120	21	*	*	*

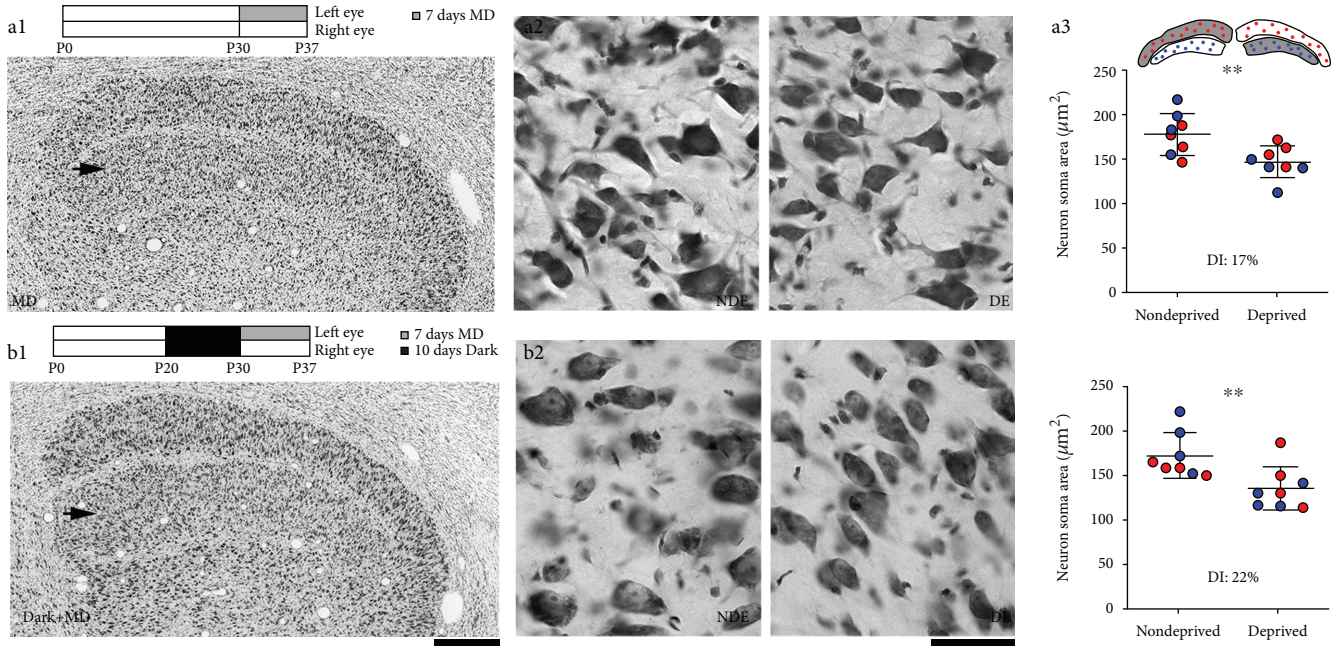

Figure 2: The effect on neuron size of a 7-day duration of MD imposed at the peak of the critical period with and without a prior 10-day period of darkness. Schematic at the top of (a1) and (b1) indicate the rearing history and timeline of procedures for each group. The effect of 7 days of MD imposed at postnatal day 30 was obvious upon gross examination of the eye-specific layers of the dLGN (a1), as well as at higher magnification where neurons within deprived-eye (DE) layers were smaller than neurons within non-deprived-eye (NDE) counterpart layers. Stereological quantification of soma size revealed that deprived neurons were rendered 17% smaller than nondeprived neurons, which represented a significant difference. When the same MD was imposed immediately following 10 continuous days of dark exposure started at postnatal day 20, there was an obvious reduction in the staining intensity within deprived-eye layers compared to non-deprived-eye layers (b1). The paler staining within deprived-eye layers was accompanied by a reduction in the size of deprived neurons when compared to nondeprived neurons (b2). Quantification of neuron cross-sectional soma size revealed that deprived neurons were significantly smaller than nondeprived neurons by an average of 22%. Drawing in (a3) represents eye-specific layers of the dLGN with red and blue circles indicating measurements from A and A1 layers, respectively. Scale bars = 500 μm (1) and 50 μm (2). Arrows in (a1) and (b1) indicate the deprived-eye layer. Asterisks indicate statistical significance at probability < 0.05.

the natural peak of plasticity is malleable on some measures and suggests that brief dark exposure, unlike longer dark rearing, does not act by delaying both the onset and decay of the critical period. This result, as well as studies demonstrating enhanced plasticity following dark exposure long after the critical period has waned [39, 40, 44], is inconsistent with the suggestion that darkness slows the entire profile of the critical period but instead suggests that brief darkness can alter key plasticity parameters [54] to rejuvenate the visual system and bring about heightened plasticity capacity.

The absence of an increased effect of MD following dark exposure on neurofilament labeling may be due to neurofilament loss reaching saturation faster than the effect that MD exerts on soma size. Examination of effect sizes with shorter

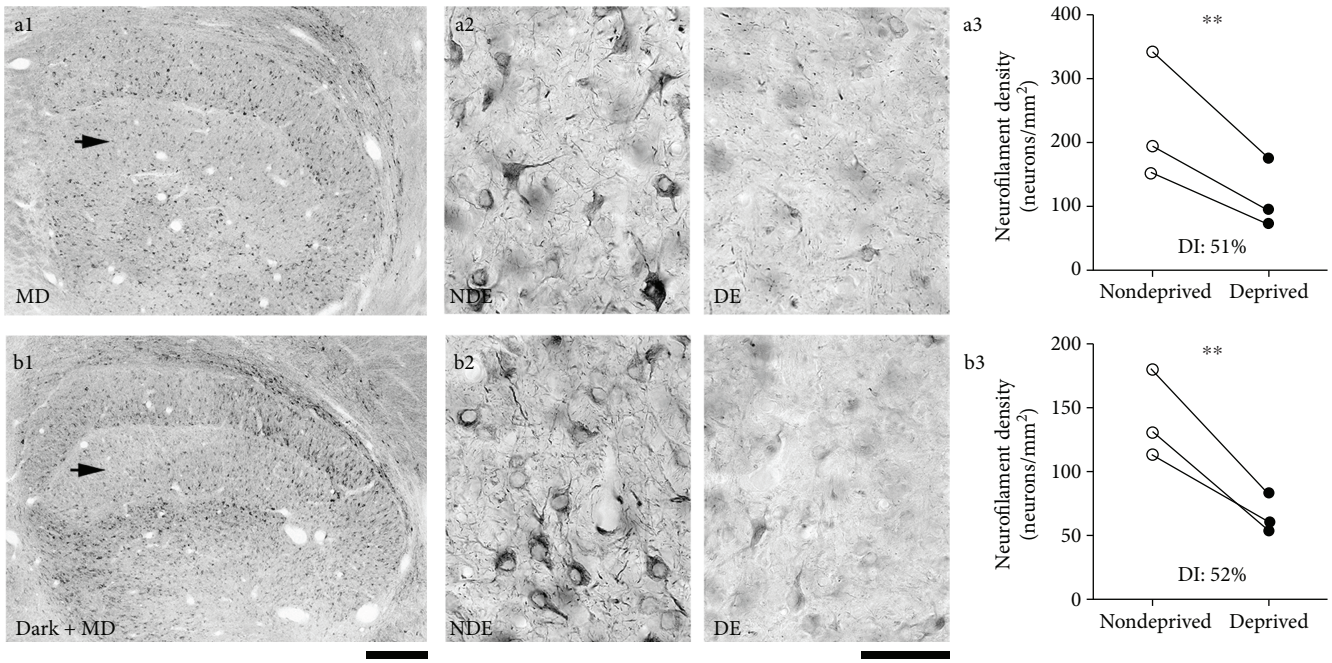

Figure 3: Examination of the magnitude of neurofilament loss in the dLGN from animals that were either monocularly deprived for 7 days at the peak of the critical period or else received 10 days of dark exposure before the same length of MD. Monocular deprivation alone produced a substantial reduction in the amount of neurofilament labeling within deprived-eye dLGN layers (a1). At high magnification, the loss of labeling was evident as a reduced number of immunopositive neurons, as well as a reduction in labeling intensity (a2) in deprived-eye (DE) relative to non-deprived-eye (NDE) layers. When the same MD was preceded by 10 days of darkness, a similar reduction in neurofilament within deprived-eye layers was observed at low (b1) as well as at high magnification (b2). Stereological quantification of the density of neurofilament-positive neurons revealed that MD-only (a3) and MD preceded by dark exposure (b3) produced a similar deprivation effect, each with a significant reduction in deprived layers. Arrows in (a1) and (b1) indicate the deprived-eye layer. Asterisks indicate statistical significance at probability < 0.05. Scale bars = 500 μm (1) and 50 μm (2).

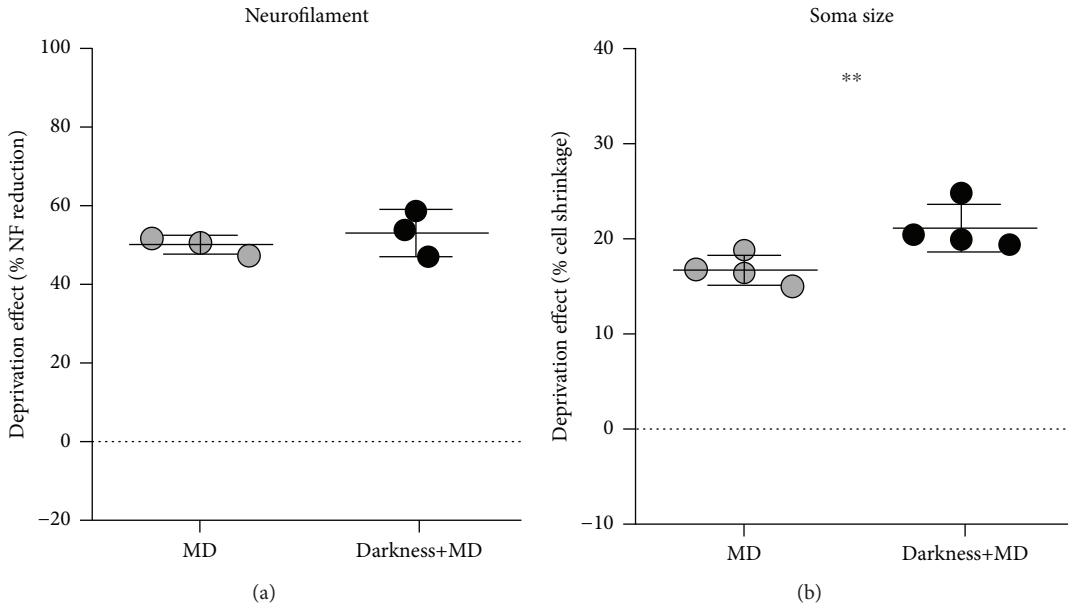

Figure 4: Comparison of the MD effect between MD-only and dark exposure followed by MD conditions. Whereas comparison of the effect of MD on neurofilament labeling across conditions indicated that the loss in the dLGN was similar with or without darkness (a), the effect on soma size was significantly larger in the group of animals that received dark exposure prior to MD (b). Asterisks indicate statistical significance at probability < 0.05.

durations of MD may have revealed a difference between the two groups with regard to neurofilament labeling. This dichotomy between the effect of MD on neurofilament and soma size is mirrored in a study conducted on cats that examined the effect of dark exposure beyond the critical period peak, which showed a slight plasticity boost with measurements of soma size but not with changes in neurofilament labeling [45]. Shifts in cortical ocular dominance measured physiologically elicited by MD can also emerge and saturate quickly, with shifts occurring within 1-2.5 days of MD onset and saturation by about a week of MD [55–57]. Interestingly, a study that examined ocular dominance shifts in kittens that were monocularly deprived after receiving a prior period of dark rearing from birth revealed a slightly exaggerated ocular dominance shift when darkness occurred from birth to 50 days and was followed by 2.5 days of MD compared to the MD-only group (see Figure 3 in [57]); though with longer MD, there was no difference between groups.

The enhancement of plasticity observed in the group of animals subjected to dark exposure may originate from a reduction in deprived neuron size, a hypertrophy of nondeprived neuron size, or a combination of the two effects. The effect of monocular deprivation on cells within the dLGN includes both a shrinkage of neurons innervated by the deprived eye and hypertrophy of neurons connected to the nondeprived eye. The atrophy and hypertrophy of neurons in the context of monocular deprivation are both manifestations of neural plasticity. The magnitude of nondeprived neuron hypertrophy has been estimated to be about 10% [58]. The hypertrophy of nondeprived neurons likely derives from an expansion of nondeprived terminal fields, as has been demonstrated previously [5]. Darkness beginning at birth and lasting 3 weeks does not reduce the size of neurons within the dLGN; however, further dark exposure up to 12 weeks does reduce the size of dLGN neurons relative to normal controls [59]. It is possible that in our study, dark exposure for 10 days resulted in smaller dLGN neurons relative to controls, meaning that the enhanced deprivation effect may derive from nondeprived neuron hypertrophy. Examination of a darkness-only group would address this possibility. Irrespective of the size of neurons immediately following dark exposure, the enhanced DI observed when MD follows darkness demonstrates a higher level of neural plasticity compared to the MD-only condition.

In rodents, the enhancement of neural plasticity produced by dark exposure is thought to partly originate from a shift in NMDA receptor subunits toward the neonatal isoform [60, 61], as well as a rejuvenation of inhibitory synaptic transmission [21]. Examination of the effects of inhibitory neural transmission and plasticity capacity following dark exposure applied at different ages has revealed in rodents a refractory period for plasticity enhancement [21]. The enhancement of ocular dominance plasticity observed in very young or adult rodents following 10 days of dark exposure is not observed during a refractory period that occurs between postnatal days 35 and 55 [21]. It is possible that such a refractory period also exists for cats that are subjected to dark exposure beyond the critical period peak, which in cats occurs at about postnatal day 30 [9]. Given that adult cats exposed to darkness do not exhibit the same enhancement in plasticity that younger cats demonstrate [62], it is alternatively possible that the cat visual system exhibits a progressive decline in the capacity for dark exposure to enhance plasticity in the visual system.

The natural peak of the critical period for ocular dominance plasticity emerges as a consequence of a molecular balance between plasticity facilitators and inhibitors. While the stages of development and maturity of the visual system are characterized by a changing landscape of molecules [63, 64], it appears that dark exposure can have an effect across a broad collection of molecular arrangements and does not seem to effect influence upon a single molecular conglomeration. This confers broad applicability to dark exposure as a means of promoting plasticity at various stages during postnatal development. Although dark exposure imposed in adult cats does not produce elevated plasticity levels [62], dark exposure is efficacious at ages past the critical period peak [41, 45], and results from the current study demonstrate that elevated plasticity can also be elicited very early in postnatal development when plasticity is naturally at its highest.

That the natural peak of the critical period is modifiable through dark exposure raises the intriguing possibility that darkness could be used as an auxiliary to gold standard treatments for human amblyopia with the aim of expediting the recovery of visual function and perhaps producing superior outcomes for vision. The use of dark exposure in conjunction with other treatments for amblyopia such as occlusion therapy, perceptual learning, or video game play may provide a means of enhancing recovery outcomes early in development and not just when the efficacy of conventional treatments fades with age. Visual training has emerged as a robust approach to promote recovery from amblyopia in rats, cats, and humans [65–68], and a recent rat study has examined recovery outcomes when dark exposure was immediately followed by visual training in rodents [68]. Visual training that quickly followed dark exposure promoted recovery from severe amblyopia in rats, whereas amblyopia was not reversed with visual training alone [68]. It was suggested that this form of recovery occurs in a two-step process that involves a reactivation of synaptic plasticity mediated by dark exposure, followed by visual training that instructs synaptic modifications and promotes visual recovery. The plasticity enhancement that we demonstrate in the current study raises the possibility that such combinatorial therapy may prove beneficial not only when applied beyond the critical period but also when applied at younger ages that may benefit from an increase in the speed and or amount of recovery.

Data Availability

The data used to support the findings of this study are available from the corresponding author upon request.

Conflicts of Interest

The authors declare that they have no conflicts of interest.

Acknowledgments

This study was supported by the Natural Science and Engineering Research Council to KRD (2015-05320), DEM (2015-03819), and NAC (2015-06761) and the Canadian Institutes of Health Research (PJT-153333) to KRD, DEM, and NAC.

References

[1] T. N. Wiesel and D. H. Hubel, "Single-cell responses in striate cortex of kittens deprived of vision in one eye," *Journal of Neurophysiology*, vol. 26, no. 6, pp. 1003–1017, 1963.

[2] P. B. Dews and T. N. Wiesel, "Consequences of monocular deprivation on visual behaviour in kittens," *The Journal of Physiology*, vol. 206, no. 2, pp. 437–455, 1970.

[3] K. Williams, J. L. Balsor, S. Beshara, B. R. Beston, D. G. Jones, and K. M. Murphy, "Experience-dependent central vision deficits: neurobiology and visual acuity," *Vision Research*, vol. 114, pp. 68–78, 2015.

[4] R. W. Guillery, "Binocular competition in the control of geniculate cell growth," *The Journal of Comparative Neurology*, vol. 144, no. 1, pp. 117–129, 1972.

[5] A. Antonini and M. P. Stryker, "Rapid remodeling of axonal arbors in the visual cortex," *Science*, vol. 260, no. 5115, pp. 1819–1821, 1993.

[6] M. F. Bear and H. Colman, "Binocular competition in the control of geniculate cell size depends upon visual cortical N-methyl-D-aspartate receptor activation," *Proceedings of the National Academy of Sciences of the United States of America*, vol. 87, no. 23, pp. 9246–9249, 1990.

[7] T. N. Wiesel and D. H. Hubel, "Effects of visual deprivation on morphology and physiology of cells in the cats lateral geniculate body," *Journal of Neurophysiology*, vol. 26, no. 6, pp. 978–993, 1963.

[8] R. W. Guillery and D. J. Stelzner, "The differential effects of unilateral lid closure upon the monocular and binocular segments of the dorsal lateral geniculate nucleus in the cat," *The Journal of Comparative Neurology*, vol. 139, no. 4, pp. 413–421, 1970.

[9] C. R. Olson and R. D. Freeman, "Profile of the sensitive period for monocular deprivation in kittens," *Experimental Brain Research*, vol. 39, no. 1, pp. 17–21, 1980.

[10] K. R. Jones, P. D. Spear, and L. Tong, "Critical periods for effects of monocular deprivation: differences between striate and extrastriate cortex," *The Journal of Neuroscience*, vol. 4, no. 10, pp. 2543–2552, 1984.

[11] N. W. Daw, K. Fox, H. Sato, and D. Czepita, "Critical period for monocular deprivation in the cat visual cortex," *Journal of Neurophysiology*, vol. 67, no. 1, pp. 197–202, 1992.

[12] D. H. Hubel and T. N. Wiesel, "The period of susceptibility to the physiological effects of unilateral eye closure in kittens," *The Journal of Physiology*, vol. 206, no. 2, pp. 419–436, 1970.

[13] C. Blakemore and R. C. Van Sluyters, "Reversal of the physiological effects of monocular deprivation in kittens: further evidence for a sensitive period," *The Journal of physiology*, vol. 237, no. 1, pp. 195–216, 1974.

[14] J. A. Movshon, "Reversal of the physiological effects of monocular deprivation in the kitten's visual cortex," *The Journal of Physiology*, vol. 261, no. 1, pp. 125–174, 1976.

[15] G. D. Mower, "The effect of dark rearing on the time course of the critical period in cat visual cortex," *Developmental Brain Research*, vol. 58, no. 2, pp. 151–158, 1991.

[16] W. C. Abraham and M. F. Bear, "Metaplasticity: the plasticity of synaptic plasticity," *Trends in Neurosciences*, vol. 19, no. 4, pp. 126–130, 1996.

[17] H. Morishita, J. M. Miwa, N. Heintz, and T. K. Hensch, "Lynx1, a cholinergic brake, limits plasticity in adult visual cortex," *Science*, vol. 330, no. 6008, pp. 1238–1240, 2010.

[18] M. Fong, D. E. Mitchell, K. R. Duffy, and M. F. Bear, "Rapid recovery from the effects of early monocular deprivation is enabled by temporary inactivation of the retinas," *Proceedings of the National Academy of Sciences of the United States of America*, vol. 113, no. 49, pp. 14139–14144, 2016.

[19] T. K. Hensch, M. Fagiolini, N. Mataga, M. P. Stryker, S. Baekkeskov, and S. F. Kash, "Local GABA circuit control of experience-dependent plasticity in developing visual cortex," *Science*, vol. 282, no. 5393, pp. 1504–1508, 1998.

[20] M. Fagiolini and T. K. Hensch, "Inhibitory threshold for critical-period activation in primary visual cortex," *Nature*, vol. 404, no. 6774, pp. 183–186, 2000.

[21] S. Huang, Y. Gu, E. M. Quinlan, and A. Kirkwood, "A refractory period for rejuvenating GABAergic synaptic transmission and ocular dominance plasticity with dark exposure," *The Journal of Neuroscience*, vol. 30, no. 49, pp. 16636–16642, 2010.

[22] M. F. Bear, A. Kleinschmidt, Q. A. Gu, and W. Singer, "Disruption of experience-dependent synaptic modifications in striate cortex by infusion of an NMDA receptor antagonist," *The Journal of Neuroscience*, vol. 10, no. 3, pp. 909–925, 1990.

[23] N. W. Daw, B. Gordon, K. D. Fox et al., "Injection of MK-801 affects ocular dominance shifts more than visual activity," *Journal of Neurophysiology*, vol. 81, no. 1, pp. 204–215, 1999.

[24] Z. J. Huang, A. Kirkwood, T. Pizzorusso et al., "BDNF regulates the maturation of inhibition and the critical period of plasticity in mouse visual cortex," *Cell*, vol. 98, no. 6, pp. 739–755, 1999.

[25] X. Hou, N. Yoshioka, H. Tsukano et al., "Chondroitin sulfate is required for onset and offset of critical period plasticity in visual cortex," *Scientific Reports*, vol. 7, no. 1, article 12646, 2017.

[26] T. Pizzorusso, P. Medini, N. Berardi, S. Chierzi, J. W. Fawcett, and L. Maffei, "Reactivation of ocular dominance plasticity in the adult visual cortex," *Science*, vol. 298, no. 5596, pp. 1248–1251, 2002.

[27] T. Pizzorusso, P. Medini, S. Landi, S. Baldini, N. Berardi, and L. Maffei, "Structural and functional recovery from early monocular deprivation in adult rats," *Proceedings of the National Academy of Sciences of the United States of America*, vol. 103, no. 22, pp. 8517–8522, 2006.

[28] D. Carulli, T. Pizzorusso, J. C. F. Kwok et al., "Animals lacking link protein have attenuated perineuronal nets and persistent plasticity," *Brain*, vol. 133, no. 8, pp. 2331–2347, 2010.

[29] E. Putignano, G. Lonetti, L. Cancedda et al., "Developmental downregulation of histone posttranslational modifications regulates visual cortical plasticity," *Neuron*, vol. 53, no. 5, pp. 747–759, 2007.

[30] D. Silingardi, M. Scali, G. Belluomini, and T. Pizzorusso, "Epigenetic treatments of adult rats promote recovery from visual acuity deficits induced by long-term monocular deprivation,"

European Journal of Neuroscience, vol. 31, no. 12, pp. 2185–2192, 2010.

[31] L. Baroncelli, M. Scali, G. Sansevero et al., "Experience affects critical period plasticity in the visual cortex through an epigenetic regulation of histone post-translational modifications," *Journal of Neuroscience*, vol. 36, no. 12, pp. 3430–3440, 2016.

[32] M. Cynader, N. Berman, and A. Hein, "Recovery of function in cat visual cortex following prolonged deprivation," *Experimental Brain Research*, vol. 25, no. 2, pp. 139–156, 1976.

[33] M. Cynader and D. E. Mitchell, "Prolonged sensitivity to monocular deprivation in dark-reared cats," *Journal of Neurophysiology*, vol. 43, no. 4, pp. 1026–1040, 1980.

[34] B. Timney, D. E. Mitchell, and F. Giffin, "The development of vision in cats after extended periods of dark-rearing," *Experimental Brain Research*, vol. 31, no. 4, pp. 547–560, 1978.

[35] G. D. Mower, J. L. Burchfiel, and F. H. Duffy, "The effects of dark-rearing on the development and plasticity of the lateral geniculate nucleus," *Developmental Brain Research*, vol. 1, no. 3, pp. 418–424, 1981.

[36] G. D. Mower, D. Berry, J. L. Burchfiel, and F. H. Duffy, "Comparison of the effects of dark rearing and binocular suture on development and plasticity of cat visual cortex," *Brain Research*, vol. 220, no. 2, pp. 255–267, 1981.

[37] E. Castrén, F. Zafra, H. Thoenen, and D. Lindholm, "Light regulates expression of brain-derived neurotrophic factor mRNA in rat visual cortex," *Proceedings of the National Academy of Sciences of the United States of America*, vol. 89, no. 20, pp. 9444–9448, 1992.

[38] E. M. Quinlan, B. D. Philpot, R. L. Huganir, and M. F. Bear, "Rapid, experience-dependent expression of synaptic NMDA receptors in visual cortex in vivo," *Nature Neuroscience*, vol. 2, no. 4, pp. 352–357, 1999.

[39] H.-Y. He, B. Ray, K. Dennis, and E. M. Quinlan, "Experience-dependent recovery of vision following chronic deprivation amblyopia," *Nature Neuroscience*, vol. 10, no. 9, pp. 1134–1136, 2007.

[40] K. L. Montey and E. M. Quinlan, "Recovery from chronic monocular deprivation following reactivation of thalamocortical plasticity by dark exposure," *Nature Communications*, vol. 2, no. 1, p. 317, 2011.

[41] K. R. Duffy and D. E. Mitchell, "Darkness alters maturation of visual cortex and promotes fast recovery from monocular deprivation," *Current Biology*, vol. 23, no. 5, pp. 382–386, 2013.

[42] P. C. Kind, F. Sengpiel, C. J. Beaver et al., "The development and activity-dependent expression of aggrecan in the cat visual cortex," *Cerebral Cortex*, vol. 23, no. 2, pp. 349–360, 2013.

[43] K. R. Duffy, D. H. Bukhamseen, M. J. Smithen, and D. E. Mitchell, "Binocular eyelid closure promotes anatomical but not behavioral recovery from monocular deprivation," *Vision Research*, vol. 114, pp. 151–160, 2015.

[44] I. Erchova, A. Vasalauskaite, V. Longo, and F. Sengpiel, "Enhancement of visual cortex plasticity by dark exposure," *Philosophical Transactions of the Royal Society B: Biological Sciences*, vol. 372, no. 1715, article 20160159, 2017.

[45] K. R. Duffy, A. J. Lingley, K. D. Holman, and D. E. Mitchell, "Susceptibility to monocular deprivation following immersion in darkness either late into or beyond the critical period," *Journal of Comparative Neurology*, vol. 524, no. 13, pp. 2643–2653, 2016.

[46] K. M. Murphy and D. E. Mitchell, "Reduced visual acuity in both eyes of monocularly deprived kittens following a short or long period of reverse occlusion," *The Journal of Neuroscience*, vol. 7, no. 5, pp. 1526–1536, 1987.

[47] D. E. Mitchell, "A shot in the dark: the use of darkness to investigate visual development and as a therapy for amblyopia," *Clinical and Experimental Optometry*, vol. 96, no. 4, pp. 363–372, 2013.

[48] M. E. Goldstein, N. H. Sternberger, and L. A. Sternberger, "Phosphorylation protects neurofilaments against proteolysis," *Journal of Neuroimmunology*, vol. 14, no. 2, pp. 149–160, 1987.

[49] K. R. Duffy, M. F. Fong, D. E. Mitchell, and M. F. Bear, "Recovery from the anatomical effects of long-term monocular deprivation in cat lateral geniculate nucleus," *Journal of Comparative Neurology*, vol. 526, no. 2, pp. 310–323, 2018.

[50] K. R. Duffy, K. D. Holman, and D. E. Mitchell, "Shrinkage of X cells in the lateral geniculate nucleus after monocular deprivation revealed by FoxP2 labeling," *Visual Neuroscience*, vol. 31, no. 3, pp. 253–261, 2014.

[51] Y. Benjamini and Y. Hochberg, "Controlling the false discovery rate: a practical and powerful approach to multiple testing," *Journal of the Royal Statistical Society: Series B (Methodological)*, vol. 57, no. 1, pp. 289–300, 1995.

[52] M. E. Bickford, W. Guido, and D. W. Godwin, "Neurofilament proteins in Y-cells of the cat lateral geniculate nucleus: normal expression and alteration with visual deprivation," *The Journal of Neuroscience*, vol. 18, no. 16, pp. 6549–6557, 1998.

[53] M. R. Kutcher and K. R. Duffy, "Cytoskeleton alteration correlates with gross structural plasticity in the cat lateral geniculate nucleus," *Visual Neuroscience*, vol. 24, no. 6, pp. 775–785, 2007.

[54] S. Murase, C. L. Lantz, and E. M. Quinlan, "Light reintroduction after dark exposure reactivates plasticity in adults via perisynaptic activation of MMP-9," *eLife*, vol. 6, 2017.

[55] L. Mioche and W. Singer, "Chronic recordings from single sites of kitten striate cortex during experience-dependent modifications of receptive-field properties," *Journal of Neurophysiology*, vol. 62, no. 1, pp. 185–197, 1989.

[56] R. Malach, R. Ebert, and R. C. Van Sluyters, "Recovery from effects of brief monocular deprivation in the kitten," *Journal of Neurophysiology*, vol. 51, no. 3, pp. 538–551, 1984.

[57] C. R. Olson and R. D. Freeman, "Progressive changes in kitten striate cortex during monocular vision," *Journal of Neurophysiology*, vol. 38, no. 1, pp. 26–32, 1975.

[58] T. L. Hickey, P. D. Spear, and K. E. Kratz, "Quantitative studies of cell size in the cat's dorsal lateral geniculate nucleus following visual deprivation," *The Journal of Comparative Neurology*, vol. 172, no. 2, pp. 265–281, 1977.

[59] R. Kalil, "Dark rearing in the cat: effects on visuomotor behavior and cell growth in the dorsal lateral geniculate nucleus," *Journal of Comparative Neurology*, vol. 178, no. 3, pp. 451–467, 1978.

[60] H.-Y. He, W. Hodos, and E. M. Quinlan, "Visual deprivation reactivates rapid ocular dominance plasticity in adult visual cortex," *The Journal of Neuroscience*, vol. 26, no. 11, pp. 2951–2955, 2006.

[61] E. M. Quinlan, D. H. Olstein, and M. F. Bear, "Bidirectional, experience-dependent regulation of N-methyl-D-aspartate receptor subunit composition in the rat visual cortex during postnatal development," *Proceedings of the National Academy of Sciences of the United States of America*, vol. 96, no. 22, pp. 12876–12880, 1999.

[62] K. D. Holman, K. R. Duffy, and D. E. Mitchell, "Short periods of darkness fail to restore visual or neural plasticity in adult cats," *Visual Neuroscience*, vol. 35, article E002, 2018.

[63] S. Song, D. E. Mitchell, N. A. Crowder, and K. R. Duffy, "Postnatal accumulation of intermediate filaments in the cat and human primary visual cortex," *The Journal of Comparative Neurology*, vol. 523, no. 14, pp. 2111–2126, 2015.

[64] C. R. Siu and K. M. Murphy, "The development of human visual cortex and clinical implications," *Eye and Brain*, vol. 10, pp. 25–36, 2018.

[65] R. F. Hess and B. Thompson, "Amblyopia and the binocular approach to its therapy," *Vision Research*, vol. 114, pp. 4–16, 2015.

[66] R. W. Li and D. M. Levi, "Characterizing the mechanisms of improvement for position discrimination in adult amblyopia," *Journal of Vision*, vol. 4, no. 6, p. 7, 2004.

[67] K. M. Murphy, G. Roumeliotis, K. Williams, B. R. Beston, and D. G. Jones, "Binocular visual training to promote recovery from monocular deprivation," *Journal of Vision*, vol. 15, no. 1, p. 2, 2015.

[68] N. C. Eaton, H. M. Sheehan, and E. M. Quinlan, "Optimization of visual training for full recovery from severe amblyopia in adults," *Learning and Memory*, vol. 23, no. 2, pp. 99–103, 2016.

Hindawi
Neural Plasticity
Volume 2019, Article ID 1538137, 9 pages
https://doi.org/10.1155/2019/1538137

Review Article

Emerging Roles of Synapse Organizers in the Regulation of Critical Periods

Adema Ribic[1] **and Thomas Biederer**[1,2]

[1]*Department of Neuroscience, Tufts University School of Medicine, Boston, MA 02111, USA*
[2]*Department of Neurology, Yale University School of Medicine, New Haven, CT 06511, USA*

Correspondence should be addressed to Adema Ribic; adema.ribic@gmail.com and Thomas Biederer; thomas.biederer@tufts.edu

Received 29 March 2019; Revised 9 July 2019; Accepted 25 July 2019; Published 3 September 2019

Guest Editor: Hirofumi Morishita

Experience remodels cortical connectivity during developmental windows called critical periods. Experience-dependent regulation of synaptic strength during these periods establishes circuit functions that are stabilized as critical period plasticity wanes. These processes have been extensively studied in the developing visual cortex, where critical period opening and closure are orchestrated by the assembly, maturation, and strengthening of distinct synapse types. The synaptic specificity of these processes points towards the involvement of distinct molecular pathways. Attractive candidates are pre- and postsynaptic transmembrane proteins that form adhesive complexes across the synaptic cleft. These synapse-organizing proteins control synapse development and maintenance and modulate structural and functional properties of synapses. Recent evidence suggests that they have pivotal roles in the onset and closure of the critical period for vision. In this review, we describe roles of synapse-organizing adhesion molecules in the regulation of visual critical period plasticity and we discuss the potential they offer to restore circuit functions in amblyopia and other neurodevelopmental disorders.

1. Introduction

Sensitive periods for the development of brain function have been described in different species and brain areas, but it was the work of Hubel and Wiesel in cat and primate visual cortexes during the 1970s and 1980s that first shed light on the underlying circuit principles [1–4]. This enabled studies of cellular mechanisms, leading to the recognition of synapses in the visual cortex as cellular substrates for critical period plasticity [5–9]. These studies showed that balanced visual input is accompanied by stereotypic developmental remodeling and pruning of synapses in the primary visual cortex, whereas visual deprivation results in synapse loss and shrinkage of axonal and dendritic arbors [5, 10–17]. The application of genetic, chemo-, and optogenetic tools in mice later revealed how vision shapes cortical connectivity during development and how the establishment of cortical connectivity instructs visual function [18–23]. These approaches have also shed light on synaptic mechanisms that control critical periods and actively restrict plasticity in the adult brain [18, 19]. This review is focused on the recently discovered roles of molecules that specify and assemble synaptic connectivity in the onset and closure of plasticity in the visual cortex, a model of cortical plasticity.

2. Synaptic Control of Critical Period Timing

Circuit functions emerge early in development and are shaped by the environment and patterns of activity during critical periods [24–27]. Heightened plasticity and adaptability of circuits during critical periods enable sensory input, vision included, to guide selective strengthening and refinement of different synapse types [22, 28]. This experience-dependent synaptic remodeling stabilizes the synaptic connectivity patterns that underlie mature circuit function. Notably, in the visual cortex, GABA(gamma-aminobutyric acid)-releasing inhibitory neurons are considered key for critical period timing [29–31]. The onset of synaptic integration of inhibitory neurons into local networks coincides with a rise in inhibitory synapse density and overall

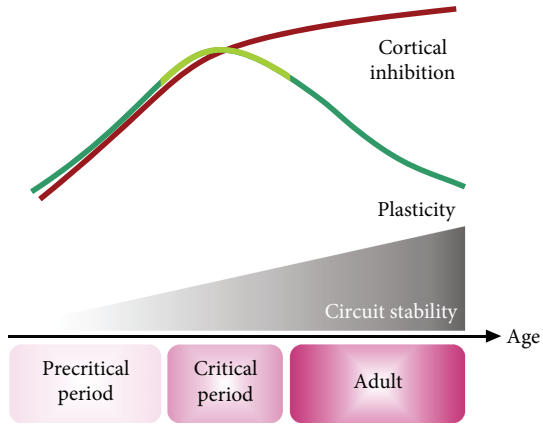

Figure 1: Circuit plasticity, stability, and levels of inhibition as functions of age. Circuit functions are shaped by external experiences during the critical period, when plasticity is high. Levels of cortical inhibitory neurotransmission rise through the critical period and, once optimal function is reached, contribute to the waning of plasticity and stabilization of circuit function in adults.

levels of inhibitory neurotransmitters in the brain [13, 22, 32–35]. A threshold level of cortical inhibition is necessary for the visual critical period to open, and manipulating GABAergic transmission with pharmacologic or genetic tools can either advance or prevent critical period opening [29–31]. As levels of cortical inhibition further rise in the maturing brain, the critical period closes and the potential for plasticity and remodeling wanes (Figure 1). In parallel, glutamatergic synapses onto both excitatory pyramidal and inhibitory neurons undergo vision-driven remodeling [22, 36]. The heightened circuit plasticity that is characteristic of critical periods is no longer present once mature circuit functions are established, and active stabilization and maintenance of function take over in the adult brain [18, 24, 26, 27] (Figure 1).

High levels of inhibition in adults are thought to contribute to the stabilization of mature brain function by limiting circuit plasticity (Figure 1) [24]. Indeed, acute reduction in levels of inhibitory neurotransmitters in the mature visual cortex can reinstate visual plasticity [37, 38]. On a cellular level, manipulation of activity of soma-targeting, fast-spiking Parvalbumin (PV) and dendrite-targeting, regular-spiking Somatostatin (SST) circuitry results in robust changes in visual plasticity [18, 39–47]. These interneuron classes exert powerful control over critical period onset: transplantation of embryonic PV and SST interneurons derived from medial ganglionic eminence into the adult visual cortex can trigger another visual critical period, with remarkably preserved timing of onset and closure [40, 48]. These precise developmental sequences indicate tight genetic control of interneuron maturation, which is well described for PV interneurons [49–52]. PV interneuron maturation is directed, at least in part, by the complex interplay of Orthodenticle Homeobox 2 (Otx2), a non-cell-autonomous transcription factor secreted from the retina and choroid plexus, and the extracellular matrix (ECM) deposited around interneurons [50, 51, 53–57]. The capture of Otx2 by the ECM that surrounds PV interneurons is essential for the onset of their maturation [57, 58], and misregulated Otx2 expression and localization lead to deficits in critical period plasticity [50, 51, 53, 57–60]. The stereotypic circuit integration of transplanted PV interneurons supports the additional involvement of cell-autonomous factors that control the development of synaptic connectivity of these cells [48]. Activity-driven assembly of local excitatory inputs onto PV interneurons prior to critical period opening in mice is pivotal for its onset [19]. The parallel increase in interneuron expression of synapse-organizing adhesion proteins such as Neuroligins and SynCAMs (see below) further supports that synaptogenesis is an important factor in PV cell maturation [61]. A recent study demonstrated that PV interneuron-expressed Synaptic Cell Adhesion Molecule 1 (SynCAM 1) is required for critical period closure, which involves the SynCAM 1-dependent formation of long-range excitatory inputs from the thalamus [18]. In the following sections, we describe known molecular regulators of synaptic connectivity in the visual cortex.

3. Roles of Synapse-Organizing Proteins in Visual Cortex Synaptogenesis and Plasticity

Cell adhesion proteins that instruct synapse assembly and their maintenance are expressed in diverse neuron types and in glial cells [62–66]. These proteins were initially identified as potent drivers of presynaptic differentiation in an *in vitro* heterologous system, and they form complexes in *trans* (for adhesion) and in *cis* (for lateral assembly) [66–70]. After instructing the assembly of pre- and postsynaptic specializations into functional synapses, these proteins can maintain synapses in the maturing brain [71–73]. Recent research suggests that distinct pairs of synaptic organizers impact different synapse types in the cortex [74, 75] as summarized below.

3.1. Neuroligins and Hevin. Neuroligins are prototypical postsynaptic synapse organizers and type 1 transmembrane proteins that interact with presynaptic Neurexins [67, 76, 77]. Neuroligins 1-4 are redundant for synapse assembly *in vivo* but are key for synapse maturation and function [65, 77]. Their interactions with α- and β-Neurexins affect both inhibitory and excitatory presynaptic functions, as well as recruitment of synapse scaffolding components and neurotransmitter receptors to the postsynapse [78–83]. Different combinations of Neuroligin/Neurexin complexes can potentially specify different synapse types, and the repertoire of these interactions is expanded by splicing isoforms [84] and accessory extracellular linker proteins, such as glia-expressed Hevin [85] (Figure 2). While cell-surface expression levels of Neuroligins can be regulated by visual activity [86], it is the removal of Hevin in the visual cortex that impairs Neuroligin 1/Neurexin interaction and reduces the density of thalamic inputs (Figure 2) [85, 87]. Mice that lack Hevin show impaired ocular dominance and critical period opening, suggesting that the assembly of thalamocortical synapses by Neuroligin 1/Neurexin/Hevin interactions controls the opening of the visual critical period [85]. Hevin

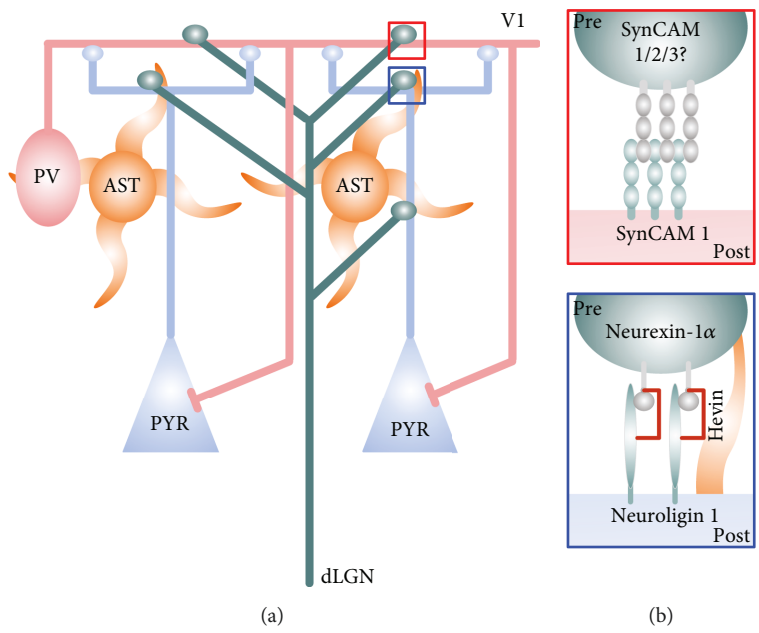

Figure 2: Synaptic connectivity of the visual thalamocortical circuit. (a) Excitatory inputs carrying visual information from the dorsal lateral geniculate nucleus (dLGN, green) in the thalamus innervate pyramidal (PYR, blue box) neurons and Parvalbumin (PV, red box) interneurons in thalamorecipient layers of the visual cortex (red box). PV interneurons receive inputs from neighbouring PYR neurons across cortical layers. Astrocytes (AST) express molecules that can act as synaptic bridges between thalamocortical axons and their postsynaptic targets (Hevin, blue box). (b) Red box: the synaptic immunoglobulin SynCAM 1 organizes thalamic inputs onto PV interneurons. Presynaptic interacting partners of SynCAM 1 at thalamocortical synapses are currently unknown, but other SynCAMs (2 and 3) are candidates. Blue box: Neuroligin 1 on PYR cells interacts with Neurexin-1α via the astrocytic Hevin (brown) to organize thalamic inputs onto PYR cells. Astrocytic process is depicted in orange. Presynapse (Pre) and postsynapse (Post) are indicated.

knockout mice display a compensatory increase in local, intracortical excitatory synapses that is insufficient to open the critical period, indicating that specific synapse types are key for different circuit functions [85].

3.2. SynCAMs. Similar to Neuroligins, SynCAM cell adhesion complexes are prominently expressed in the visual cortex and recent research highlighted their role in timing the onset and offset of cortical critical periods [18, 88, 89]. SynCAMs are potent inducers of synapse differentiation *in vitro* [68, 90] that contribute to excitatory synapse formation and maintenance *in vivo* across different brain regions [18, 72, 91, 92]. SynCAMs 1-4 are immunoglobulin domain type-1 transmembrane proteins, whose homo- and heterophilic interactions across the synaptic cleft organize excitatory synapses [90, 93]. The most studied family member is SynCAM 1 that interacts with itself and SynCAMs 2 and 3 in *cis* and *trans* [90, 93–95]. SynCAM 1 controls both pre- and postsynaptic properties through its interactions across the synaptic cleft and affects cytoskeletal remodeling and receptor recruitment at the synapse through its intracellular partners [72, 88, 96, 97]. In the cortex, SynCAM 1 recruits large and potent long-range thalamocortical excitatory inputs onto PV interneurons (Figure 2) [18, 91]. Further, PV-expressed SynCAM 1 is regulated by visual activity [18]. In agreement with its role in PV maturation, SynCAM 1 is a regulatory target of Otx2 [52] and is essential for maturation of PV interneurons in the visual cortex. Similar to Hevin knockout mice, mice that lack SynCAM 1 have fewer thalamocortical synapses (Figure 2) [18]. This results in poorly developed binocular vision and an extended visual critical period [18]. SynCAM 1 is actively required to control plasticity and even a brief cell-specific removal of SynCAM 1 from PV interneurons results in increased levels of visual plasticity in the adult brain, pointing to a key role for thalamic inputs onto PV interneurons in the regulation of plasticity in mature circuits [18]. This cell-autonomous, postsynaptic requirement for SynCAM 1 in PV interneurons suggests that postsynaptic SynCAM 1 engages currently unknown transsynaptic partners in thalamic axons to assemble thalamocortical synapses (Figure 2) [18, 90].

3.3. Distinct Roles of Neuroligin/Hevin and SynCAM 1. As reviewed above, both Neuroligin/Neurexin interaction (through Hevin) and SynCAM 1 play a role in the formation of thalamocortical synapses but with opposing effects on visual plasticity [18, 85]. Lack of Hevin prevents the critical period from opening, whereas lack of SynCAM 1 prevents it from closure [18, 85]. However, Hevin appears to affect most, if not all, excitatory thalamocortical synapses formed across neuron types, while SynCAM 1 shows a PV-specific action on thalamocortical inputs [18, 85, 87]. It is possible that gross development of thalamocortical synapses mediated by Neuroligin 1/Neurexin-1α/Hevin interaction is a prerequisite for the critical period to open, and PV-specific recruitment and maintenance of thalamic inputs by SynCAM 1 is necessary for subsequent critical period closure. Future studies

can address whether any cross-talk between the two pathways exists in PV interneurons, as well as whether these molecules control plasticity through thalamocortical synapses in other sensory or association areas [98, 99].

3.4. Extracellular Matrix, LRRTMs, and NCAM. So far, only SynCAMs and Neuroligins (through Hevin) have demonstrated roles in visual plasticity, but recent research demonstrated that members of the leucine-rich repeat transmembrane (LRRTM) family of molecules can interact at synapses with the extracellular matrix (ECM), a powerful regulator of visual plasticity [34, 100]. LRRTMs 1-4 are another group of type 1 transmembrane proteins that bind Neurexins, potently induce excitatory presynaptic differentiation and regulate receptor composition at the synapse [70, 101, 102]. LRRTM-deficient mice show defects in both pre- and postsynaptic functions, and their repertoire of interactions with Neurexins can impact diverse synapse types [70, 74, 103, 104]. LRRTMs bind Neurexins across the synaptic cleft similar to Neuroligins, but they can also instruct differential synapse formation through interactions with components of the ECM [100–102, 105]. As the ECM in the form of perineuronal nets exerts powerful control over the maturation of PV interneurons and critical period timing [34, 58, 106–111], the role of LRRTMs in visual plasticity warrants future investigation. An ECM-related protein modification, the polysialylation of neural cell adhesion molecule (NCAM), guides the development of inhibitory connections in the visual cortex [112]. NCAM is an immunoglobulin superfamily protein that regulates early synapse development and is mostly found in a glycan-bound state [113]. Visual activity-dependent polysialylation of NCAM affects its homophilic interactions across the synapse, and removal of PSA from NCAM can shift the critical period to an earlier time point through modulation of PV connectivity [112]. SynCAM 1 can also be found in the polysialylated state, pointing to yet another way to diversify the function and interactions of synapse organizers [114, 115].

4. Therapeutic Potential of Synapse-Organizing Molecules in Amblyopia and Neurodevelopmental Disorders

The diminished plasticity of mature circuits is thought to preclude recovery from early visual insults such as amblyopia. Patching or visual stimulation can provide therapeutic interventions before the critical period closes, but the reduced capacity of visual synapses for activity-driven remodeling likely interferes with the success of interventions later in life [116–118]. The reduced potential of the adult brain to rewire itself may also impede treatments for other neurodevelopmental disorders, such as autism-spectrum disorders (ASD) and schizophrenia [55, 119–122]. Studies of amblyopia and visual plasticity have identified promising interventions for recovering the potential for plasticity in the entire brain, such as neuromodulation of inhibitory connections [46, 123], systemic regulation of inhibitory neurotransmission [124], and sensory manipulations that may target the activity of thalamocortical synapses [125–127]. On a more specific level, recent research has demonstrated that the cell-specific manipulation of thalamocortical synapses reinstates plastic features to the adult visual cortex [18]. As distinct circuits regulate plasticity of binocularity and improvements in visual acuity in amblyopia models [128, 129], targeting synapses that organize different circuits may hence represent a way to precisely manipulate different brain functions.

How do we target specific synapse types? Transient genetic silencing tools in combination with cell-specific adenoviral vectors could allow manipulating synapse organizers in a cell type-and-region-specific manner [130–132]. Further, peptide fragments of extracellular domains of synapse organizers can impair their interactions *in vitro* and may have a similar effect *in vivo* [86, 93]. Indeed, a recent study using a combination of these approaches to manipulate signaling by a secreted molecule, semaphorin 3A, demonstrated its feasibility in rat models of amblyopia [133]. Such approaches may increase plasticity to a level sufficient for visual therapy to have effects in adult amblyopic patients [116–118, 133–136]. These tools could provide a localized therapy that can be restricted to the visual cortex alone, thus precluding systemic side-effects. A transient elevation of cortical plasticity may even improve therapeutic outcomes for other neurodevelopmental disorders [137–140]. Approaches that result in the elevated potential for plasticity in the mature brain could additionally enhance recovery after brain injury, including traumatic brain injury (TBI) and stroke [120, 141–147]. In combination with targeting mechanisms that control neuronal specification [148–152], tools that target specific synapse types hence offer highly specific therapeutic interventions for developmental brain disorders. Future studies on mechanisms of synapse specification within distinct circuits are likely to provide an avenue for progress in this area.

Conflicts of Interest

The authors declare that there is no conflict of interest regarding the publication of this paper.

Acknowledgments

This work was supported by a National Institute of Health grant (R01 DA018928, to T.B.) and the Knights Templar Eye Foundation Career Starter Grant in Paediatric Ophthalmology (to A.R.).

References

[1] D. H. Hubel and T. N. Wiesel, "The period of susceptibility to the physiological effects of unilateral eye closure in kittens," *The Journal of Physiology*, vol. 206, no. 2, pp. 419–436, 1970.

[2] D. H. Hubel, T. N. Wiesel, and S. LeVay, "Functional architecture of area 17 in normal and monocularly deprived macaque monkeys," *Cold Spring Harbor Symposia on Quantitative Biology*, vol. 40, pp. 581–589, 1976.

[3] D. H. Hubel, T. N. Wiesel, and S. LeVay, "Plasticity of ocular dominance columns in monkey striate cortex," *Philosophical Transactions of the Royal Society of London Series B: Biological Sciences*, vol. 278, no. 961, pp. 377–409, 1977.

[4] S. Le Vay, T. N. Wiesel, and D. H. Hubel, "The development of ocular dominance columns in normal and visually deprived monkeys," *The Journal of Comparative Neurology*, vol. 191, no. 1, pp. 1–51, 1980.

[5] A. Antonini, M. Fagiolini, and M. P. Stryker, "Anatomical correlates of functional plasticity in mouse visual cortex," *The Journal of Neuroscience*, vol. 19, no. 11, pp. 4388–4406, 1999.

[6] A. Antonini and M. P. Stryker, "Development of individual geniculocortical arbors in cat striate cortex and effects of binocular impulse blockade," *The Journal of Neuroscience*, vol. 13, no. 8, pp. 3549–3573, 1993.

[7] A. Antonini, D. C. Gillespie, M. C. Crair, and M. P. Stryker, "Morphology of single geniculocortical afferents and functional recovery of the visual cortex after reverse monocular deprivation in the kitten," *The Journal of Neuroscience*, vol. 18, no. 23, pp. 9896–9909, 1998.

[8] J. S. Lund, S. M. Holbach, and W. W. Chung, "Postnatal development of thalamic recipient neurons in the monkey striate cortex: Influence of afferent driving on spine acquisition and dendritic growth of layer 4c spiny stellate neurons," *The Journal of Comparative Neurology*, vol. 309, no. 1, pp. 129–140, 1991.

[9] E. A. Lachica, M. W. Crooks, and V. A. Casagrande, "Effects of monocular deprivation on the morphology of retinogeniculate axon arbors in a primate," *The Journal of Comparative Neurology*, vol. 296, no. 2, pp. 303–323, 1990.

[10] P. R. Huttenlocher, "Synapse elimination and plasticity in developing human cerebral cortex," *American Journal of Mental Deficiency*, vol. 88, no. 5, pp. 488–496, 1984.

[11] Y. Zhou, B. Lai, and W. B. Gan, "Monocular deprivation induces dendritic spine elimination in the developing mouse visual cortex," *Scientific Reports*, vol. 7, no. 1, article 4977, 2017.

[12] H. Yu, A. K. Majewska, and M. Sur, "Rapid experience-dependent plasticity of synapse function and structure in ferret visual cortex in vivo," *Proceedings of the National Academy of Sciences of the United States of America*, vol. 108, no. 52, pp. 21235–21240, 2011.

[13] J. De Felipe, P. Marco, A. Fairen, and E. G. Jones, "Inhibitory synaptogenesis in mouse somatosensory cortex," *Cerebral Cortex*, vol. 7, no. 7, pp. 619–634, 1997.

[14] M. E. Blue and J. G. Parnavelas, "The formation and maturation of synapses in the visual cortex of the rat. II. Quantitative analysis," *Journal of Neurocytology*, vol. 12, no. 4, pp. 697–712, 1983.

[15] P. R. Huttenlocher, C. de Courten, L. J. Garey, and H. Van der Loos, "Synaptogenesis in human visual cortex — evidence for synapse elimination during normal development," *Neuroscience Letters*, vol. 33, no. 3, pp. 247–252, 1982.

[16] A. Antonini and M. P. Stryker, "Rapid remodeling of axonal arbors in the visual cortex," *Science*, vol. 260, no. 5115, pp. 1819–1821, 1993.

[17] A. Antonini and M. P. Stryker, "Plasticity of geniculocortical afferents following brief or prolonged monocular occlusion in the cat," *The Journal of Comparative Neurology*, vol. 369, no. 1, pp. 64–82, 1996.

[18] A. Ribic, M. C. Crair, and T. Biederer, "Synapse-selective control of cortical maturation and plasticity by parvalbumin-autonomous action of SynCAM 1," *Cell Reports*, vol. 26, no. 2, pp. 381–393.e6, 2019.

[19] S. J. Kuhlman, N. D. Olivas, E. Tring, T. Ikrar, X. Xu, and J. T. Trachtenberg, "A disinhibitory microcircuit initiates critical-period plasticity in the visual cortex," *Nature*, vol. 501, no. 7468, pp. 543–546, 2013.

[20] C. E. Stephany, T. Ikrar, C. Nguyen, X. Xu, and A. W. McGee, "Nogo receptor 1 confines a disinhibitory microcircuit to the critical period in visual cortex," *The Journal of Neuroscience*, vol. 36, no. 43, pp. 11006–11012, 2016.

[21] Y. Sun, T. Ikrar, M. F. Davis et al., "Neuregulin-1/ErbB4 signaling regulates visual cortical plasticity," *Neuron*, vol. 92, no. 1, pp. 160–173, 2016.

[22] Q. Miao, L. Yao, M. J. Rasch, Q. Ye, X. Li, and X. Zhang, "Selective maturation of temporal dynamics of intracortical excitatory transmission at the critical period onset," *Cell Reports*, vol. 16, no. 6, pp. 1677–1689, 2016.

[23] H. Ko, L. Cossell, C. Baragli et al., "The emergence of functional microcircuits in visual cortex," *Nature*, vol. 496, no. 7443, pp. 96–100, 2013.

[24] A. E. Takesian and T. K. Hensch, "Balancing plasticity/stability across brain development," *Progress in Brain Research*, vol. 207, pp. 3–34, 2013.

[25] B. S. Wang, R. Sarnaik, and J. Cang, "Critical period plasticity matches binocular orientation preference in the visual cortex," *Neuron*, vol. 65, no. 2, pp. 246–256, 2010.

[26] N. W. Tien and D. Kerschensteiner, "Homeostatic plasticity in neural development," *Neural Development*, vol. 13, no. 1, p. 9, 2018.

[27] N. Vitureira, M. Letellier, and Y. Goda, "Homeostatic synaptic plasticity: from single synapses to neural circuits," *Current Opinion in Neurobiology*, vol. 22, no. 3, pp. 516–521, 2012.

[28] R. Chittajallu and J. T. R. Isaac, "Emergence of cortical inhibition by coordinated sensory-driven plasticity at distinct synaptic loci," *Nature Neuroscience*, vol. 13, no. 10, pp. 1240–1248, 2010.

[29] M. Fagiolini and T. K. Hensch, "Inhibitory threshold for critical-period activation in primary visual cortex," *Nature*, vol. 404, no. 6774, pp. 183–186, 2000.

[30] T. K. Hensch, M. Fagiolini, N. Mataga, M. P. Stryker, S. Baekkeskov, and S. F. Kash, "Local GABA circuit control of experience-dependent plasticity in developing visual cortex," *Science*, vol. 282, no. 5393, pp. 1504–1508, 1998.

[31] Y. Iwai, M. Fagiolini, K. Obata, and T. K. Hensch, "Rapid critical period induction by tonic inhibition in visual cortex," *The Journal of Neuroscience*, vol. 23, no. 17, pp. 6695–6702, 2003.

[32] Q. Ye and Q. L. Miao, "Experience-dependent development of perineuronal nets and chondroitin sulfate proteoglycan receptors in mouse visual cortex," *Matrix Biology*, vol. 32, no. 6, pp. 352–363, 2013.

[33] C. Ferrer, H. Hsieh, and L. P. Wollmuth, "Input-specific maturation of NMDAR-mediated transmission onto parvalbumin-expressing interneurons in layers 2/3 of the visual cortex," *Journal of Neurophysiology*, vol. 120, no. 6, pp. 3063–3076, 2018.

[34] K. K. Lensjo, M. E. Lepperod, G. Dick, T. Hafting, and M. Fyhn, "Removal of perineuronal nets unlocks juvenile plasticity through network mechanisms of decreased

inhibition and increased gamma activity," *The Journal of Neuroscience*, vol. 37, no. 5, pp. 1269–1283, 2017.

[35] D. van Versendaal and C. N. Levelt, "Inhibitory interneurons in visual cortical plasticity," *Cellular and Molecular Life Sciences*, vol. 73, no. 19, pp. 3677–3691, 2016.

[36] J. Lu, J. Tucciarone, Y. Lin, and Z. J. Huang, "Input-specific maturation of synaptic dynamics of parvalbumin interneurons in primary visual cortex," *Proceedings of the National Academy of Sciences of the United States of America*, vol. 111, no. 47, pp. 16895–16900, 2014.

[37] A. Harauzov, M. Spolidoro, G. DiCristo et al., "Reducing intracortical inhibition in the adult visual cortex promotes ocular dominance plasticity," *The Journal of Neuroscience*, vol. 30, no. 1, pp. 361–371, 2010.

[38] T. Pizzorusso, P. Medini, N. Berardi, S. Chierzi, J. W. Fawcett, and L. Maffei, "Reactivation of ocular dominance plasticity in the adult visual cortex," *Science*, vol. 298, no. 5596, pp. 1248–1251, 2002.

[39] P. Larimer, J. Spatazza, J. S. Espinosa et al., "Caudal ganglionic eminence precursor transplants disperse and integrate as lineage-specific interneurons but do not induce cortical plasticity," *Cell Reports*, vol. 16, no. 5, pp. 1391–1404, 2016.

[40] Y. Tang, M. P. Stryker, A. Alvarez-Buylla, and J. S. Espinosa, "Cortical plasticity induced by transplantation of embryonic somatostatin or parvalbumin interneurons," *Proceedings of the National Academy of Sciences of the United States of America*, vol. 111, no. 51, pp. 18339–18344, 2014.

[41] C. K. Pfeffer, M. Xue, M. He, Z. J. Huang, and M. Scanziani, "Inhibition of inhibition in visual cortex: the logic of connections between molecularly distinct interneurons," *Nature Neuroscience*, vol. 16, no. 8, pp. 1068–1076, 2013.

[42] Y. Fu, M. Kaneko, Y. Tang, A. Alvarez-Buylla, and M. P. Stryker, "A cortical disinhibitory circuit for enhancing adult plasticity," *eLife*, vol. 4, article e05558, 2015.

[43] R. Priya, B. Rakela, M. Kaneko et al., "Vesicular GABA transporter is necessary for transplant-induced critical period plasticity in mouse visual cortex," *The Journal of Neuroscience*, vol. 39, no. 14, pp. 2635–2648, 2019.

[44] C. E. Yaeger, D. L. Ringach, and J. T. Trachtenberg, "Neuromodulatory control of localized dendritic spiking in critical period cortex," *Nature*, vol. 567, no. 7746, pp. 100–104, 2019.

[45] M. P. Demars and H. Morishita, "Cortical parvalbumin and somatostatin GABA neurons express distinct endogenous modulators of nicotinic acetylcholine receptors," *Molecular Brain*, vol. 7, no. 1, p. 75, 2014.

[46] M. Sadahiro, M. P. Demars, P. Burman et al., *Activation of somatostatin inhibitory neurons by Lypd6-nAChRα2 system restores juvenile-like plasticity in adult visual cortex*, bioRxiv, 2017.

[47] M. Kaneko and M. P. Stryker, "Sensory experience during locomotion promotes recovery of function in adult visual cortex," *eLife*, vol. 3, article e02798, 2014.

[48] D. G. Southwell, R. C. Froemke, A. Alvarez-Buylla, M. P. Stryker, and S. P. Gandhi, "Cortical plasticity induced by inhibitory neuron transplantation," *Science*, vol. 327, no. 5969, pp. 1145–1148, 2010.

[49] J. Apulei, N. Kim, D. Testa et al., "Non-cell autonomous OTX2 homeoprotein regulates visual cortex plasticity through Gadd45b/g," *Cerebral Cortex*, vol. 29, no. 6, pp. 2384–2395, 2019.

[50] S. Sugiyama, A. A. Di Nardo, S. Aizawa et al., "Experience-dependent transfer of Otx2 homeoprotein into the visual cortex activates postnatal plasticity," *Cell*, vol. 134, no. 3, pp. 508–520, 2008.

[51] C. Bernard and A. Prochiantz, "Otx2-PNN interaction to regulate cortical plasticity," *Neural Plasticity*, vol. 2016, Article ID 7931693, 7 pages, 2016.

[52] A. Sakai, R. Nakato, Y. Ling et al., "Genome-wide target analyses of Otx2 homeoprotein in postnatal cortex," *Frontiers in Neuroscience*, vol. 11, p. 307, 2017.

[53] J. Spatazza, H. H. C. Lee, A. A. di Nardo et al., "Choroid-plexus-derived Otx2 homeoprotein constrains adult cortical plasticity," *Cell Reports*, vol. 3, no. 6, pp. 1815–1823, 2013.

[54] H. H. C. Lee, C. Bernard, Z. Ye et al., "Genetic Otx2 mislocalization delays critical period plasticity across brain regions," *Molecular Psychiatry*, vol. 22, no. 5, pp. 680–688, 2017.

[55] H. Morishita, J. H. Cabungcal, Y. Chen, K. Q. Do, and T. K. Hensch, "Prolonged period of cortical plasticity upon redox dysregulation in fast-spiking interneurons," *Biological Psychiatry*, vol. 78, no. 6, pp. 396–402, 2015.

[56] X. Hou, N. Yoshioka, H. Tsukano et al., "Chondroitin sulfate is required for onset and offset of critical period plasticity in visual cortex," *Scientific Reports*, vol. 7, no. 1, article 12646, 2017.

[57] S. Miyata, Y. Komatsu, Y. Yoshimura, C. Taya, and H. Kitagawa, "Persistent cortical plasticity by upregulation of chondroitin 6-sulfation," *Nature Neuroscience*, vol. 15, no. 3, pp. 414–422, 2012.

[58] M. Beurdeley, J. Spatazza, H. H. C. Lee et al., "Otx2 binding to perineuronal nets persistently regulates plasticity in the mature visual cortex," *The Journal of Neuroscience*, vol. 32, no. 27, pp. 9429–9437, 2012.

[59] G. Despras, C. Bernard, A. Perrot et al., "Toward libraries of biotinylated chondroitin sulfate analogues: From synthesis to in vivo studies," *Chemistry - A European Journal*, vol. 19, no. 2, pp. 531–540, 2013.

[60] E. Favuzzi, A. Marques-Smith, R. Deogracias et al., "Activity-dependent gating of parvalbumin interneuron function by the perineuronal net protein brevican," *Neuron*, vol. 95, no. 3, pp. 639–655.e10, 2017.

[61] E. Favuzzi, R. Deogracias, A. Marques-Smith et al., "Distinct molecular programs regulate synapse specificity in cortical inhibitory circuits," *Science*, vol. 363, no. 6425, pp. 413–417, 2019.

[62] M. Missler, T. C. Südhof, and T. Biederer, "Synaptic cell adhesion," *Cold Spring Harbor Perspectives in Biology*, vol. 4, no. 4, article a005694, 2012.

[63] T. Biederer, P. S. Kaeser, and T. A. Blanpied, "Transcellular nanoalignment of synaptic function," *Neuron*, vol. 96, no. 3, pp. 680–696, 2017.

[64] A. L. Kolodkin and M. Tessier-Lavigne, "Mechanisms and molecules of neuronal wiring: a primer," *Cold Spring Harbor Perspectives in Biology*, vol. 3, no. 6, 2011.

[65] T. C. Sudhof, "Towards an understanding of synapse formation," *Neuron*, vol. 100, no. 2, pp. 276–293, 2018.

[66] K. Shen and P. Scheiffele, "Genetics and cell biology of building specific synaptic connectivity," *Annual Review of Neuroscience*, vol. 33, no. 1, pp. 473–507, 2010.

[67] P. Scheiffele, J. Fan, J. Choih, R. Fetter, and T. Serafini, "Neuroligin expressed in nonneuronal cells triggers presynaptic development in contacting axons," *Cell*, vol. 101, no. 6, pp. 657–669, 2000.

[68] T. Biederer, Y. Sara, M. Mozhayeva et al., "SynCAM, a synaptic adhesion molecule that drives synapse assembly," *Science*, vol. 297, no. 5586, pp. 1525–1531, 2002.

[69] K. Czondor and O. Thoumine, "Synaptogenic assays using neurons cultured on micropatterned substrates," *Methods in Molecular Biology*, vol. 1538, pp. 29–44, 2017.

[70] M. W. Linhoff, J. Lauren, R. M. Cassidy et al., "An unbiased expression screen for synaptogenic proteins identifies the LRRTM protein family as synaptic organizers," *Neuron*, vol. 61, no. 5, pp. 734–749, 2009.

[71] N. Korber and V. Stein, "In vivo imaging demonstrates dendritic spine stabilization by SynCAM 1," *Scientific Reports*, vol. 6, no. 1, article 24241, 2016.

[72] E. M. Robbins, A. J. Krupp, K. Perez de Arce et al., "SynCAM 1 adhesion dynamically regulates synapse number and impacts plasticity and learning," *Neuron*, vol. 68, no. 5, pp. 894–906, 2010.

[73] P. Mendez, M. De Roo, L. Poglia, P. Klauser, and D. Muller, "N-cadherin mediates plasticity-induced long-term spine stabilization," *Journal of Cell Biology*, vol. 189, no. 3, pp. 589–600, 2010.

[74] A. Schroeder, J. Vanderlinden, K. Vints et al., "A modular organization of LRR protein-mediated synaptic adhesion defines synapse identity," *Neuron*, vol. 99, no. 2, pp. 329–344.e7, 2018.

[75] R. Sando, X. Jiang, and T. C. Sudhof, "Latrophilin GPCRs direct synapse specificity by coincident binding of FLRTs and teneurins," *Science*, vol. 363, no. 6429, article eaav7969, 2019.

[76] C. Dean, F. G. Scholl, J. Choih et al., "Neurexin mediates the assembly of presynaptic terminals," *Nature Neuroscience*, vol. 6, no. 7, pp. 708–716, 2003.

[77] P. Scheiffele, "Cell-cell signaling during synapse formation in the CNS," *Annual Review of Neuroscience*, vol. 26, no. 1, pp. 485–508, 2003.

[78] F. Varoqueaux, G. Aramuni, R. L. Rawson et al., "Neuroligins determine synapse maturation and function," *Neuron*, vol. 51, no. 6, pp. 741–754, 2006.

[79] A. Poulopoulos, G. Aramuni, G. Meyer et al., "Neuroligin 2 drives postsynaptic assembly at perisomatic inhibitory synapses through gephyrin and collybistin," *Neuron*, vol. 63, no. 5, pp. 628–642, 2009.

[80] J. S. Martenson, T. Yamasaki, N. H. Chaudhury, D. Albrecht, and S. Tomita, "Assembly rules for GABAA receptor complexes in the brain," *Elife*, vol. 6, 2017.

[81] G. S. Maro, S. Gao, A. M. Olechwier et al., "MADD-4/punctin and neurexin organize *C. elegans* GABAergic postsynapses through neuroligin," *Neuron*, vol. 86, no. 6, pp. 1420–1432, 2015.

[82] B. Chih, H. Engelman, and P. Scheiffele, "Control of excitatory and inhibitory synapse formation by neuroligins," *Science*, vol. 307, no. 5713, pp. 1324–1328, 2005.

[83] M. Heine, O. Thoumine, M. Mondin, B. Tessier, G. Giannone, and D. Choquet, "Activity-independent and subunit-specific recruitment of functional AMPA receptors at neurexin/neuroligin contacts," *Proceedings of the National Academy of Sciences of the United States of America*, vol. 105, no. 52, pp. 20947–20952, 2008.

[84] B. Chih, L. Gollan, and P. Scheiffele, "Alternative splicing controls selective trans-synaptic interactions of the neuroligin-neurexin complex," *Neuron*, vol. 51, no. 2, pp. 171–178, 2006.

[85] S. K. Singh, J. A. Stogsdill, N. S. Pulimood et al., "Astrocytes assemble thalamocortical synapses by bridging NRX1α and NL1 via hevin," *Cell*, vol. 164, no. 1-2, pp. 183–196, 2016.

[86] R. T. Peixoto, P. A. Kunz, H. Kwon et al., "Transsynaptic signaling by activity-dependent cleavage of neuroligin-1," *Neuron*, vol. 76, no. 2, pp. 396–409, 2012.

[87] W. C. Risher, S. Patel, I. H. Kim et al., "Astrocytes refine cortical connectivity at dendritic spines," *Elife*, vol. 3, 2014.

[88] L. A. Thomas, M. R. Akins, and T. Biederer, "Expression and adhesion profiles of SynCAM molecules indicate distinct neuronal functions," *The Journal of Comparative Neurology*, vol. 510, no. 1, pp. 47–67, 2008.

[89] A. W. Lyckman, S. Horng, C. A. Leamey et al., "Gene expression patterns in visual cortex during the critical period: synaptic stabilization and reversal by visual deprivation," *Proceedings of the National Academy of Sciences of the United States of America*, vol. 105, no. 27, pp. 9409–9414, 2008.

[90] A. I. Fogel, M. R. Akins, A. J. Krupp, M. Stagi, V. Stein, and T. Biederer, "SynCAMs organize synapses through heterophilic adhesion," *The Journal of Neuroscience*, vol. 27, no. 46, pp. 12516–12530, 2007.

[91] K. A. Park, A. Ribic, F. M. Laage Gaupp et al., "Excitatory synaptic drive and feedforward inhibition in the hippocampal CA3 circuit are regulated by SynCAM 1," *The Journal of Neuroscience*, vol. 36, no. 28, pp. 7464–7475, 2016.

[92] A. Ribic, X. Liu, M. C. Crair, and T. Biederer, "Structural organization and function of mouse photoreceptor ribbon synapses involve the immunoglobulin protein synaptic cell adhesion molecule 1," *The Journal of Comparative Neurology*, vol. 522, no. 4, pp. 900–920, 2014.

[93] A. I. Fogel, M. Stagi, K. Perez de Arce, and T. Biederer, "Lateral assembly of the immunoglobulin protein SynCAM 1 controls its adhesive function and instructs synapse formation," *The EMBO Journal*, vol. 30, no. 23, pp. 4728–4738, 2011.

[94] J. A. Frei, I. Andermatt, M. Gesemann, and E. T. Stoeckli, "The SynCAM synaptic cell adhesion molecules are involved in sensory axon pathfinding by regulating axon-axon contacts," *Journal of Cell Science*, vol. 127, no. 24, pp. 5288–5302, 2014.

[95] F. M. Ranaivoson, L. S. Turk, S. Ozgul et al., "A proteomic screen of neuronal cell-surface molecules reveals IgLONs as structurally conserved interaction modules at the synapse," *Structure*, vol. 27, no. 6, pp. 893–906.e9, 2019.

[96] L. Cheadle and T. Biederer, "The novel synaptogenic protein Farp1 links postsynaptic cytoskeletal dynamics and transsynaptic organization," *Journal of Cell Biology*, vol. 199, no. 6, pp. 985–1001, 2012.

[97] J. L. Hoy, J. R. Constable, S. Vicini, Z. Fu, and P. Washbourne, "SynCAM1 recruits NMDA receptors via protein 4.1B," *Molecular and Cellular Neurosciences*, vol. 42, no. 4, pp. 466–483, 2009.

[98] J. A. Blundon, N. C. Roy, B. J. W. Teubner et al., "Restoring auditory cortex plasticity in adult mice by restricting thalamic

adenosine signaling," *Science*, vol. 356, no. 6345, pp. 1352–1356, 2017.

[99] A. Barre, C. Berthoux, D. De Bundel et al., "Presynaptic serotonin 2A receptors modulate thalamocortical plasticity and associative learning," *Proceedings of the National Academy of Sciences of the United States of America*, vol. 113, no. 10, pp. E1382–E1391, 2016.

[100] T. J. Siddiqui, P. K. Tari, S. A. Connor et al., "An LRRTM4-HSPG complex mediates excitatory synapse development on dentate gyrus granule cells," *Neuron*, vol. 79, no. 4, pp. 680–695, 2013.

[101] R. T. Roppongi, B. Karimi, and T. J. Siddiqui, "Role of LRRTMs in synapse development and plasticity," *Neuroscience Research*, vol. 116, pp. 18–28, 2017.

[102] T. J. Siddiqui, R. Pancaroglu, Y. Kang, A. Rooyakkers, and A. M. Craig, "LRRTMs and neuroligins bind neurexins with a differential code to cooperate in glutamate synapse development," *The Journal of Neuroscience*, vol. 30, no. 22, pp. 7495–7506, 2010.

[103] M. Bhouri, W. Morishita, P. Temkin et al., "Deletion of *LRRTM1* and *LRRTM2* in adult mice impairs basal AMPA receptor transmission and LTP in hippocampal CA1 pyramidal neurons," *Proceedings of the National Academy of Sciences of the United States of America*, vol. 115, no. 23, pp. E5382–E5389, 2018.

[104] J. Ko, G. J. Soler-Llavina, M. V. Fuccillo, R. C. Malenka, and T. C. Sudhof, "Neuroligins/LRRTMs prevent activity- and Ca^{2+}/calmodulin-dependent synapse elimination in cultured neurons," *Journal of Cell Biology*, vol. 194, no. 2, pp. 323–334, 2011.

[105] P. Zhang, H. Lu, R. T. Peixoto et al., "Heparan sulfate organizes neuronal synapses through neurexin partnerships," *Cell*, vol. 174, no. 6, pp. 1450–1464.e23, 2018.

[106] D. Carulli, J. C. F. Kwok, and T. Pizzorusso, "Perineuronal nets and CNS plasticity and repair," *Neural Plasticity*, vol. 2016, Article ID 4327082, 2 pages, 2016.

[107] D. Carulli, T. Pizzorusso, J. C. F. Kwok et al., "Animals lacking link protein have attenuated perineuronal nets and persistent plasticity," *Brain*, vol. 133, no. 8, pp. 2331–2347, 2010.

[108] G. Cornez, F. N. Madison, A. Van der Linden et al., "Perineuronal nets and vocal plasticity in songbirds: a proposed mechanism to explain the difference between closed-ended and open-ended learning," *Developmental Neurobiology*, vol. 77, no. 8, pp. 975–994, 2017.

[109] C. De Luca and M. Papa, "Looking inside the matrix: perineuronal nets in plasticity, maladaptive plasticity and neurological disorders," *Neurochemical Research*, vol. 41, no. 7, pp. 1507–1515, 2016.

[110] K. Ohira, R. Takeuchi, T. Iwanaga, and T. Miyakawa, "Chronic fluoxetine treatment reduces parvalbumin expression and perineuronal nets in gamma-aminobutyric acidergic interneurons of the frontal cortex in adult mice," *Molecular Brain*, vol. 6, no. 1, p. 43, 2013.

[111] B. A. Sorg, S. Berretta, J. M. Blacktop et al., "Casting a wide net: role of perineuronal nets in neural plasticity," *The Journal of Neuroscience*, vol. 36, no. 45, pp. 11459–11468, 2016.

[112] G. Di Cristo, B. Chattopadhyaya, S. J. Kuhlman et al., "Activity-dependent PSA expression regulates inhibitory maturation and onset of critical period plasticity," *Nature Neuroscience*, vol. 10, no. 12, pp. 1569–1577, 2007.

[113] J. Z. Kiss and D. Muller, "Contribution of the neural cell adhesion molecule to neuronal and synaptic plasticity," *Reviews in the Neurosciences*, vol. 12, no. 4, pp. 297–310, 2001.

[114] R. Guirado, D. La Terra, M. Bourguignon et al., "Effects of PSA removal from NCAM on the critical period plasticity triggered by the antidepressant fluoxetine in the visual cortex," *Frontiers in Cellular Neuroscience*, vol. 10, p. 22, 2016.

[115] M. Muhlenhoff, M. Rollenhagen, S. Werneburg, R. Gerardy-Schahn, and H. Hildebrandt, "Polysialic acid: versatile modification of NCAM, SynCAM 1 and neuropilin-2," *Neurochemical Research*, vol. 38, no. 6, pp. 1134–1143, 2013.

[116] D. M. Levi and R. W. Li, "Perceptual learning as a potential treatment for amblyopia: a mini-review," *Vision Research*, vol. 49, no. 21, pp. 2535–2549, 2009.

[117] Y. Zhou, C. Huang, P. Xu et al., "Perceptual learning improves contrast sensitivity and visual acuity in adults with anisometropic amblyopia," *Vision Research*, vol. 46, no. 5, pp. 739–750, 2006.

[118] U. Polat, T. Ma-Naim, M. Belkin, and D. Sagi, "Improving vision in adult amblyopia by perceptual learning," *Proceedings of the National Academy of Sciences of the United States of America*, vol. 101, no. 17, pp. 6692–6697, 2004.

[119] H. K. Chang, J. W. Hsu, J. C. Wu et al., "Traumatic brain injury in early childhood and risk of attention-deficit/hyperactivity disorder and autism spectrum disorder: a nationwide longitudinal study," *The Journal of Clinical Psychiatry*, vol. 79, no. 6, 2018.

[120] F. Y. Ismail, A. Fatemi, and M. V. Johnston, "Cerebral plasticity: windows of opportunity in the developing brain," *European Journal of Paediatric Neurology*, vol. 21, no. 1, pp. 23–48, 2017.

[121] J. J. LeBlanc and M. Fagiolini, "Autism: a "critical period" disorder?," *Neural Plasticity*, vol. 2011, Article ID 921680, 17 pages, 2011.

[122] S. D. Greenhill, K. Juczewski, A. M. de Haan, G. Seaton, K. Fox, and N. R. Hardingham, "Neurodevelopment. Adult cortical plasticity depends on an early postnatal critical period," *Science*, vol. 349, no. 6246, pp. 424–427, 2015.

[123] H. Morishita, J. M. Miwa, N. Heintz, and T. K. Hensch, "Lynx1, a cholinergic brake, limits plasticity in adult visual cortex," *Science*, vol. 330, no. 6008, pp. 1238–1240, 2010.

[124] J. F. M. Vetencourt, A. Sale, A. Viegi et al., "The antidepressant fluoxetine restores plasticity in the adult visual cortex," *Science*, vol. 320, no. 5874, pp. 385–388, 2008.

[125] S. Murase, C. L. Lantz, and E. M. Quinlan, "Light reintroduction after dark exposure reactivates plasticity in adults via perisynaptic activation of MMP-9," *Elife*, vol. 6, 2017.

[126] K. L. Montey and E. M. Quinlan, "Recovery from chronic monocular deprivation following reactivation of thalamocortical plasticity by dark exposure," *Nature Communications*, vol. 2, no. 1, p. 317, 2011.

[127] G. Rodriguez, D. Chakraborty, K. M. Schrode et al., "Cross-modal reinstatement of thalamocortical plasticity accelerates ocular dominance plasticity in adult mice," *Cell Reports*, vol. 24, no. 13, pp. 3433–3440.e4, 2018.

[128] C.-E. Stephany, L. L. H. Chan, S. N. Parivash et al., "Plasticity of binocularity and visual acuity are differentially limited by Nogo receptor," *The Journal of Neuroscience*, vol. 34, no. 35, pp. 11631–11640, 2014.

[129] C. E. Stephany, X. Ma, H. M. Dorton et al., "Distinct circuits for recovery of eye dominance and acuity in murine amblyopia," *Current Biology*, vol. 28, no. 12, pp. 1914–1923.e5, 2018.

[130] J. Dimidschstein, Q. Chen, R. Tremblay et al., "A viral strategy for targeting and manipulating interneurons across vertebrate species," *Nature Neuroscience*, vol. 19, no. 12, pp. 1743–1749, 2016.

[131] L. T. Graybuck, A. Sedeño-Cortés, T. N. Nguyen et al., *Prospective, brain-wide labeling of neuronal subclasses with enhancer-driven AAVs*, bioRxiv, 2019.

[132] J. Jüttner, A. Szabo, B. Gross-Scherf et al., "Targeting neuronal and glial cell types with synthetic promoter AAVs in mice, non-human primates and humans," *Nature Neuroscience*, vol. 22, no. 8, pp. 1345–1356, 2019.

[133] E. M. Boggio, E. M. Ehlert, L. Lupori et al., "Inhibition of semaphorin3A promotes ocular dominance plasticity in the adult rat visual cortex," *Molecular Neurobiology*, vol. 56, no. 9, pp. 5987–5997, 2019.

[134] J. Bonaccorsi, N. Berardi, and A. Sale, "Treatment of amblyopia in the adult: insights from a new rodent model of visual perceptual learning," *Frontiers in Neural Circuits*, vol. 8, p. 82, 2014.

[135] Z. Hussain, B. S. Webb, A. T. Astle, and P. V. McGraw, "Perceptual learning reduces crowding in amblyopia and in the normal periphery," *The Journal of Neuroscience*, vol. 32, no. 2, pp. 474–480, 2012.

[136] X. Y. Liu, T. Zhang, Y. L. Jia, N. L. Wang, and C. Yu, "The therapeutic impact of perceptual learning on juvenile amblyopia with or without previous patching treatment," *Investigative Ophthalmology & Visual Science*, vol. 52, no. 3, pp. 1531–1538, 2011.

[137] C. L. Gatto and K. Broadie, "Genetic controls balancing excitatory and inhibitory synaptogenesis in neurodevelopmental disorder models," *Frontiers in Synaptic Neuroscience*, vol. 2, p. 4, 2010.

[138] S. B. Nelson and V. Valakh, "Excitatory/inhibitory balance and circuit homeostasis in autism spectrum disorders," *Neuron*, vol. 87, no. 4, pp. 684–698, 2015.

[139] L. Baroncelli, C. Braschi, M. Spolidoro, T. Begenisic, L. Maffei, and A. Sale, "Brain plasticity and disease: a matter of inhibition," *Neural Plasticity*, vol. 2011, Article ID 286073, 11 pages, 2011.

[140] O. Marin, "Developmental timing and critical windows for the treatment of psychiatric disorders," *Nature Medicine*, vol. 22, no. 11, pp. 1229–1238, 2016.

[141] M. Nahmani and G. G. Turrigiano, "Adult cortical plasticity following injury: recapitulation of critical period mechanisms?," *Neuroscience*, vol. 283, pp. 4–16, 2014.

[142] T. K. Hensch and P. M. Bilimoria, "Re-opening windows: manipulating critical periods for brain development," *Cerebrum*, vol. 2012, p. 11, 2012.

[143] J. C. F. Kwok, G. Dick, D. Wang, and J. W. Fawcett, "Extracellular matrix and perineuronal nets in CNS repair," *Developmental Neurobiology*, vol. 71, no. 11, pp. 1073–1089, 2011.

[144] S. C. Cramer, M. Sur, B. H. Dobkin et al., "Harnessing neuroplasticity for clinical applications," *Brain*, vol. 134, no. 6, pp. 1591–1609, 2011.

[145] S. Prilloff, P. Henrich-Noack, S. Kropf, and B. A. Sabel, "Experience-dependent plasticity and vision restoration in rats after optic nerve crush," *Journal of Neurotrauma*, vol. 27, no. 12, pp. 2295–2307, 2010.

[146] J. Fawcett, "Molecular control of brain plasticity and repair," *Progress in Brain Research*, vol. 175, pp. 501–509, 2009.

[147] M. Spolidoro, A. Sale, N. Berardi, and L. Maffei, "Plasticity in the adult brain: lessons from the visual system," *Experimental Brain Research*, vol. 192, no. 3, pp. 335–341, 2009.

[148] B. Tasic, Z. Yao, L. T. Graybuck et al., "Shared and distinct transcriptomic cell types across neocortical areas," *Nature*, vol. 563, no. 7729, pp. 72–78, 2018.

[149] T. L. Daigle, L. Madisen, T. A. Hage et al., "A suite of transgenic driver and reporter mouse lines with enhanced brain-cell-type targeting and functionality," *Cell*, vol. 174, no. 2, pp. 465–480.e22, 2018.

[150] A. B. Rosenberg, C. M. Roco, R. A. Muscat et al., "Single-cell profiling of the developing mouse brain and spinal cord with split-pool barcoding," *Science*, vol. 360, no. 6385, pp. 176–182, 2018.

[151] J. F. Poulin, B. Tasic, J. Hjerling-Leffler, J. M. Trimarchi, and R. Awatramani, "Disentangling neural cell diversity using single-cell transcriptomics," *Nature Neuroscience*, vol. 19, no. 9, pp. 1131–1141, 2016.

[152] A. Paul, M. Crow, R. Raudales, M. He, J. Gillis, and Z. J. Huang, "Transcriptional architecture of synaptic communication delineates GABAergic neuron identity," *Cell*, vol. 171, no. 3, pp. 522–539.e20, 2017.

Hindawi
Neural Plasticity
Volume 2019, Article ID 6208414, 12 pages
https://doi.org/10.1155/2019/6208414

Research Article

Contribution of Short-Time Occlusion of the Amblyopic Eye to a Passive Dichoptic Video Treatment for Amblyopia beyond the Critical Period

Lauren Sauvan,[1,2] Natacha Stolowy,[1,2] Danièle Denis,[1] Frédéric Matonti,[2,3] Frédéric Chavane,[2] Robert F. Hess,[4] and Alexandre Reynaud[4]

[1]*Department of Ophthalmology, CHU NORD, Marseille, France*
[2]*Institut de Neurosciences de la Timone (INT), Centre National de la Recherche Scientifique (CNRS) and Aix-Marseille Université (AMU), Marseille, France*
[3]*Centre Paradis Monticelli, Marseille, France*
[4]*McGill Vision Research, Department of Ophthalmology and Visual Sciences, McGill University, Montreal, Quebec, Canada*

Correspondence should be addressed to Alexandre Reynaud; alexandre.reynaud@mail.mcgill.ca

Received 22 January 2019; Revised 29 April 2019; Accepted 17 June 2019; Published 28 August 2019

Guest Editor: Claudia Lunghi

Dichoptic movie viewing has been shown to significantly improve visual acuity in amblyopia in children. Moreover, short-term occlusion of the amblyopic eye can transiently increase its contribution to binocular fusion in adults. In this study, we first asked whether dichoptic movie viewing could improve the visual function of amblyopic subjects beyond the critical period. Secondly, we tested if this effect could be enhanced by short-term monocular occlusion of the amblyopic eye. 17 subjects presenting stable functional amblyopia participated in this study. 10 subjects followed 6 sessions of 1.5 hour of dichoptic movie viewing (nonpatched group), and 7 subjects, prior to each of these sessions, had to wear an occluding patch over the amblyopic eye for two hours (patched group). Best-corrected visual acuity, monocular contrast sensitivity, interocular balance, and stereoacuity were measured before and after the training. For the nonpatched group, mean amblyopic eye visual acuity significantly improved from 0.54 to 0.46 logMAR ($p < 0.05$). For the patched group, mean amblyopic eye visual acuity significantly improved from 0.62 to 0.43 logMAR ($p < 0.05$). Stereoacuity improved significantly when the data of both groups were combined. No significant improvement was observed for the other visual functions tested. Our training procedure combines modern video technologies and recent fundamental findings in human plasticity: (i) long-term plasticity induced by dichoptic movie viewing and (ii) short-term adaptation induced by temporary monocular occlusion. This passive dichoptic movie training approach is shown to significantly improve visual acuity of subjects beyond the critical period. The addition of a short-term monocular occlusion to the dichoptic training shows promising trends but was not significant for the sample size used here. The passive movie approach combined with interocular contrast balancing even over such a short period as 2 weeks has potential as a clinical therapy to treat amblyopia in older children and adults.

1. Introduction

Amblyopia is a neurodevelopmental disorder arising from abnormal visual experience during childhood over a period called "the period of susceptibility" or "the critical period" [1–5]. It mainly manifests itself by a loss of binocular function, reduced visual acuity in one eye, the amblyopic eye, and it is the most frequent cause of unilateral visual loss in childhood. Its prevalence is around 1-3% of the general population [6–12]. The presently accepted treatment for amblyopia consists of full optical correction [13] and monocular patching of the nonamblyopic eye to force the use of the amblyopic eye [14]. This treatment is only successful for young children, and it has been assumed that older children

and particularly adults lack sufficient brain plasticity. Thus, no treatment is offered to these older patients as their amblyopia is thought to be fixed [1–5, 15, 16].

It is now well established that amblyopia is associated with cortical dysfunction at monocular and binocular sites [17–21]. One binocular theory suggested that it is the consequence of an excess of interocular suppression [22–24]. Therefore, binocular training strategies have emerged, focusing on treating the primary binocular disorder [25–37]. These are based on dichoptic image presentation that the subject needs to binocularly combine to have full information content of a global motion stimulus [24], a video game [27, 28, 38], a movie [36, 39, 40], or an altered reality device [25, 41]. Binocular fusion only occurs if the contrast of the image seen by the nonamblyopic eye is reduced sufficiently to address the interocular imbalance resulting from suppression. At first, such strategies involved an active participation of the subjects playing a dichoptic video game where success depended on using information simultaneously presented to each eye [27, 28, 31, 35, 38, 42–46]. There is also evidence that video game training in general can aid bilateral amblyopia [47].

However, not all patients want to play video games, and some children/adults are so amblyopic that it is not possible to resolve the features necessary to play video games. Hence, more recently, a general application of the same contrast balancing principles has been applied to natural scene stimuli with either passive dichoptic movie watching [36, 37] or augmented reality [25]. These procedures are based on the presentation of complementary images in the two eyes. Passive dichoptic movie watching resulted in benefits for visual acuity in children [36, 39] but has not been tested on adults yet. In principle, this method could be applied to the passive viewing of any video content such as sporting programs, movies, or children's animations [40]. Here, we tested this procedure for the first time on amblyopic adults and children with stable and resistant amblyopia which could not be treated with standard procedures.

Binocular training methods are an improvement on the current patching approach because they are better accepted [31, 37] and they aim to obtain a better binocular outcome. They engage binocular viewing and in doing so improve the visual acuity of the amblyopic eye. They are thought to operate by utilizing the residual brain plasticity that remains after the critical period of visual development. Recently, another approach has also demonstrated the residual visual plasticity in normal adults [38, 39]. This involves changes in ocular dominance that occur after just 1-2 hours of monocular occlusion. Interestingly, this short-term monocular occlusion results in a strengthening of the deprived eye which is the opposite of what occurs during the critical period in early life. This shift in dominance is only transient, lasting about 1 hour [48–51]. This has also been shown in adults with amblyopia [52]. The dominance shift for amblyopes is in the same direction as that found for normals, namely, the deprived eye becomes stronger, but it can be of larger magnitude and longer duration. Thus, the binocular imbalance that characterizes amblyopia can be manipulated for a certain duration by occluding the amblyopic eye, the opposite of classical patching therapy. The hypothesis is that the decrease in sensory stimulation during the deprivation induces a contrast gain increment to boost the sensitivity of the patched eye. Since it occurs rapidly, the mechanism underlying this contrast gain increment is suspected to involve a change of the excitatory/inhibitory balance [48–54]. However, this relatively rapid patching effect (few hours) may be quite different to more standard binocular training procedures which operate on a relatively long timescale (weeks). These long-term training procedures may involve a different plasticity mechanism, for example, by establishing new synaptic connections [55, 56].

In this study, we ask whether binocular training based on passive dichoptic movie viewing could, by way of a change in brain plasticity, increase the visual function of subjects with a stable amblyopia who are beyond the normal treatment period for classical patching. Secondly, we wondered if the effects of such a dichoptic treatment protocol could be enhanced by short-term monocular occlusion, specifically carrying out the training during the time window where the occlusion has temporarily rebalanced the excitation-inhibition ratio. To answer this question, we combined these two approaches and asked the subjects to wear an eye patch for two hours prior to undergoing binocular training sessions involving passive dichoptic movie watching.

2. Material and Methods

2.1. Participants. 17 amblyopic subjects were included in our study aged from 9 to 67 yo, mean age 34 yo. The criteria for including subjects in the experiment were the following. Subjects had to present with functional amblyopia, secondary to strabismus or anisometropia or both. Their visual acuity had to be stable for at least one year before inclusion, and children under 12 years old had to go through at least six months of conventional occlusion therapy to make sure that amblyopia was stable and resistant. Best-corrected visual acuity (BCVA) in the amblyopic eye had to be higher or equal to 0.2 logMAR, or BCVA difference between the two eyes had to be at least equal to 0.2 logMAR. The strabismus angle had to be lower or equal to 15 prism diopters. We excluded subjects with organic amblyopia, congenital strabismus, presenting any visual or neurologic disease or presenting developmental delay. For the first examination, each participant had to fill out a questionnaire about his/her medical history, and more specifically on the previous treatments, he/she might have had for amblyopia and the observance of these treatments optical correction, occlusion therapy, and strabismus surgery. Clinical details of the amblyopic subjects are reported in Table 1.

Subjects had to wear their full optical correction for all the testing and training procedures. Five subjects who had anisometropia (S1, S7, S8, S9, and S17) did not wear any optical correction before inclusion. For these subjects, we made them wear their adapted optical correction only during testings and dichoptic movie viewing sessions, which was equivalent in total to approximately 12 hours with an optical correction (see Table 1). This is insufficient itself to explain

Table 1: Characteristics of amblyopic subjects.

#id	Sex	Age	Group	Type of amblyopia	History of occlusion therapy	Hours/day watching a screen	AE BCVA	TNO (arcsec)	Number of training sessions	Total time of visioning	Follow-up (in days)
1	M	19	P	Mixed	No	3	0.92	NA	6	8.45	NA
2	F	11	NP	Anisometropia	No	2	0.22	60	6	9.12	48
3	F	13	P	Anisometropia	Yes	2	0.42	60	6	9.12	32
4	M	42	P	Strabismus	Yes	5	1.12	NA	6	8.78	40
5	M	47	NP	Anisometropia	Yes	2.5	0.22	120	6	8.38	35
6	M	21	NP	Anisometropia	No	6	0.72	NA	6	9.86	34
7	M	45	NP	Anisometropia	Yes	2	0.92	NA	6	7.55	38
8	F	32	P	Anisometropia	No	2	1.01	NA	6	8.7	NA
9	F	67	P	Strabismus	No	4	0.52	NA	6	8.96	42
10	M	35	NP	Anisometropia	No	15	0.12	60	6	8.8	51
11	M	10	NP	Mixed	Yes	1	0.32	240	6	9.06	NA
12	F	47	NP	Anisometropia	Yes	4	0.22	240	6	8.81	33
13	F	9	NP	Anisometropia	Yes	NA	0.22	NA	6	8.8	NA
14	M	38	P	Anisometropia	No	2.5	0.22	NA	6	10.11	42
15	M	62	NP	Mixed	No	3	1.12	NA	6	10.46	NA
16	F	46	NP	Anisometropia	No	2.5	0.42	NA	6	8.45	NA
17	M	42	NP	Mixed	No	5	1.01	NA	4	7.71	NA

Group assignment: P = patched, NP = nonpatched.

any improvement in the visual functions in terms of spectacle adaptation [13].

Subjects were allocated into one of two intervention groups: the nonpatched group (10 subjects, see details in Table 1), who only followed the dichoptic movie training (see procedures), and the patched group (7 subjects, details in Table 1), who were subjected to monocular occlusion of the amblyopic eye prior to each training session with the dichoptic movies. Subject allocation to each group was mainly determined by their ability to be patched two hours before coming to the lab.

The study took place in the Ophthalmology Department of La Timone Hospital in Marseille. Written informed consent was obtained from all patients or parents/guardians.

2.2. Procedures. Subjects underwent a binocular training procedure. The nonpatched group followed a procedure of six 1.5 hour sessions of dichoptic movie viewing to train their binocular vision similar as in Li et al. [36] (one subject could only undergo 5 sessions, see exact duration per subject in Table 1). The patched group followed the same procedure except that they had to wear an occluding patch over their amblyopic eye for two hours prior to each training session which was removed right before the dichoptic movie viewing. The patch was a standard occlusive adhesive-on-skin Ortopad patch. The patients were shown how to wear the patch in the assessment session. Then, they had to put them on by themselves two hours before they came to the lab for the dichoptic movie viewing session.

A battery of visual function tests detailed below was used to examine the effects of binocular training. It involved monocular visual acuity, contrast sensitivity, interocular balance, and stereosensitivity, tested in that order, each test lasting 5 to 10 minutes. The baseline measures were assessed during a first preliminary assessment session, a few days before the actual beginning of the training. The training outcome measures were realized at the end of the last training session. A follow-up test was also performed approximately one month after the training, but only 10 subjects could come back for this test (see details in Table 1).

2.3. Dichoptic Movie Design. Patients strengthened their binocular vision by passively watching dichoptic movies. A digital mask composed of irregularly shaped blobs was applied on the images seen by the amblyopic eye, and the inverse mask was applied to the images seen by the fellow eye (Figure 1(a) and example Supplementary Movie 1). Therefore, parts of the image were only seen by one eye and complementary parts were only seen by the other eye [36]. Therefore, to perceive a completed coherent picture, it was necessary to combine information seen by both eyes. The shapes and locations of the masks were varied over time. The contrast of the image seen by the amblyopic eye was fixed to its maximum, and the contrast of the image seen by the fellow eye was based on the results of the binocular balance contrast sensitivity baseline measure (Figure 1(b) and example Supplementary Movie 2). Under these conditions of unequal interocular contrasts, suppression is reduced to the point where information can be combined between the two eyes and the videos perceived stably as a coherent whole. These movies were displayed on a linearized wide passive 3D LG 32LB650V 32″ screen, 1920 × 1080 px, 60 Hz (LG Electronics USA; Englewood, NJ) with polarized glasses at a distance of 120 cm, spanning 32° of visual angle.

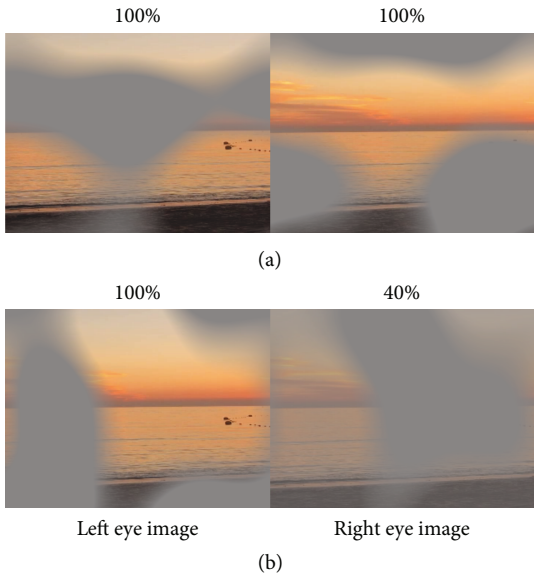

Figure 1: Illustration of the dichoptic movies. The two eyes' views are shown side by side. Complementary patterned image masks composed of irregularly shaped blobs were overlaid over the images seen by the two eyes. The shape and location of the blobs were varied dynamically every 10 seconds. (a) 100% contrast images were presented to the two eyes. (b) A 100% contrast image is presented to the left eye, and an image with a contrast reduced to 40% is presented to the right eye. Movie examples are available as supplementary material. Source video: Lauren Sauvan, wikimedia commons/CC-0.

If the subject perceived the full picture of the movie during a session, then, the contrast in the fellow eye was increased by 10% for the next session. In practice, all subjects always perceived the full picture, and so the contrast was increased in each session. Thus, it happened that it reached the maximal value of 100% for some subjects before the end of the training. Participants confirmed that they could still see the two eye images during each session. This follows the dichoptic balancing principles that have been validated by video games in a number of different studies [26–33, 35–37].

2.4. Visual Function Assessment

2.4.1. Visual Acuity. Visual acuity was measured using a logarithmic letter chart in standardized conditions (logarithmic visual acuity chart "2000").

2.4.2. Contrast Sensitivity Function. Monocular contrast sensitivity as a function of spatial frequency was measured using the quick contrast sensitivity function [57]. This is a Bayesian adaptive method which determines the optimal pair of spatial frequency and contrast to test at each trial in order to maximize the information about the contrast sensitivity function. Over the course of 100 trials, the participant had to identify in a single-interval identification task the orientation (horizontal or vertical) of a spatially filtered noise pattern at these set spatial frequencies and contrasts (Figure 2(a)). This method has already been validated on amblyopic subjects [58, 59]. This test was performed on the same equipment as the movie viewing except that participants wore an eyepatch to test monocular vision. Full details of the procedure are given in Reynaud et al. [60].

2.4.3. Interocular Balance. Interocular balance was measured with the dichoptic letter chart developed by Kwon et al. [61]. This procedure has already been validated on amblyopic subjects [61, 62]. Five letters spatially filtered to a peak spatial frequency of 2 c/d were presented at various contrasts to the left eye and 5 different letters with complementary contrasts to the right eye at the same spatial locations. Therefore, when viewed binocularly, the letters appeared superimposed. The subject had to report the five most visible letters for 10 trials (Figure 2(b)). The relative contrast of the letters seen by each eye was adjusted by an adaptive method [61, 62] in order to determine the interocular balance point for contrast sensitivity. The interocular balance point is expressed as the ratio in dB between the amblyopic and nonamblyopic eye, so a negative value means that the nonamblyopic eye is stronger, a value close to 0 means that the eyes are well-balanced, and a positive value would indicate that the amblyopic eye is stronger. This test was performed on the same equipment as the movie viewing.

2.4.4. Stereosensitivity. Disparity thresholds were measured using the TNO test (Netherlands Organisation for Applied Scientific Research, distributed by Lameris Ootech BV). It is a duochrome test without monocular clue, based on the principles of Julesz's tests [63], allowing the measurement of stereoscopic acuity from 480 to 15 seconds of arc.

3. Results

We trained 17 subjects, distributed in patched and nonpatched groups (see Materials and Methods) following our protocol to assess the improvement of visual acuity (VA). For most subjects, the VA of the amblyopic eye (AE) improved (lower value in logMAR) at the completion of training compared to before training (the baseline) (see Figure 3(a)). For the nonpatched group (open black symbols), the average value at baseline was 0.54 ± 0.37 logMAR and 0.46 ± 0.38 logMAR at the completion of training. This is a significant improvement of 0.08 logMAR (one-sided Wilcoxon signed rank test, $p < 0.01$), which is equivalent to almost one line on the visual acuity chart. For the patched group (filled grey symbols), the average visual acuity of the amblyopic eye was 0.62 ± 0.40 logMAR at baseline and 0.43 ± 0.28 logMAR at the end of training, resulting in an average improvement of 0.19 logMAR, equivalent to almost two lines on the chart. This improvement is also significant (one-sided Wilcoxon signed rank test, $p < 0.01$) and remained significant at the one-month follow-up (one-sided Wilcoxon signed rank test, $p < 0.05$) whereas it did not quite reach significance for the nonpatched group. To better appreciate these improvements, the difference in VA from baseline is reported in Figure 3(b). The improvement in visual acuity of the amblyopic eye of the participants in the patched group is slightly greater, although this difference is

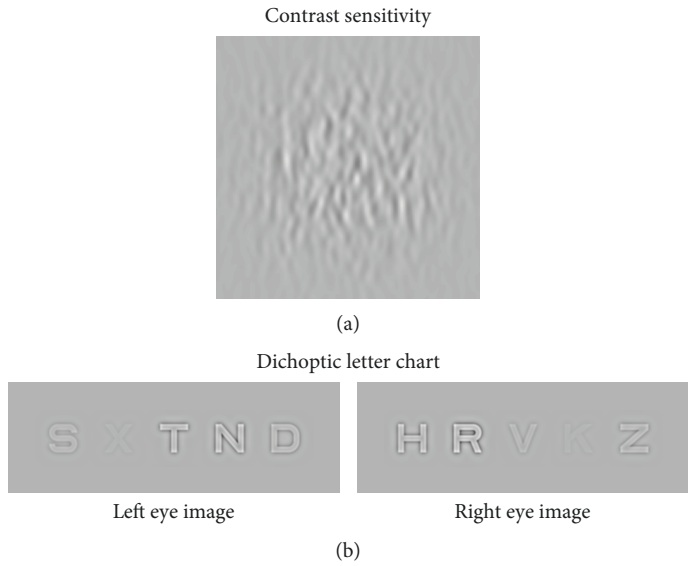

Figure 2: Test stimuli illustrations. (a) qCSF stimulus illustration. In a single-interval identification task, the subject had to judge the orientation (horizontal or vertical) of a filtered noise pattern of varying spatial frequency and contrast. (b) Dichoptic letter chart illustration. Five letters of 2 c/d were presented at various contrasts to the left eye and 5 different letters with complementary contrasts to the right eye at the same spatial locations. So when viewed with both eyes, letters appeared overlapping on screen. Adapted from Kwon et al. [61]; Birch et al. [62].

not significant (two-sided Wilcoxon rank sum test, $p = 0.06$) and is more long lasting (because it is still significant at the one month follow-up, whereas it is not for the nonpatched group). In both groups, the training did not affect the VA of the nonamblyopic eye with an average improvement of 0.04 and 0.05 logMAR in the patched and nonpatched groups, respectively (two-sided Wilcoxon signed rank test, $p = 0.31$ and $p = 0.06$, respectively), thus verifying that the improvement was not induced by any learning of the visual acuity measurement itself.

In order to test whether the amplitude of the effect we observe depends on the severity of amblyopia, we plot in Figure 3(c) the difference in VA from baseline as a function of the initial acuity of the amblyopic eye. There is no link between the degree of improvement and the initial severity of amblyopia in the nonpatched group (coefficient of determination $r^2 = 0.005$, $p = 0.84$). However, there is a significant correlation between the degree of improvement and the acuity of the AE at baseline in the patched group ($r^2 = 0.78$, $p < 0.01$). The effect is such that in this group, the stronger the amblyopia, the greater the improvement. We did not observe a significant correlation between the amplitude of the effect and the age of the participants in either group ($r^2 = 0.003$, $p = 0.87$ in the nonpatched group and $r^2 = 0.001$, $p = 0.94$ in the patched group).

Another monocular function we tested was contrast sensitivity. We measured the average contrast sensitivity of the amblyopic eye as a function of spatial frequency before and after training (Figure 4). For the nonpatched group (Figure 4)(a), the contrast sensitivity function at baseline peaks at approximately 1.5 c/d with an amplitude of 45 (solid line) which is in line with previous reports [58, 59]. At the completion of training, the amplitude reaches 78. For the patched group (Figure 4(b)), the contrast sensitivity function at baseline peaks at approximately 1.5 c/d with an amplitude of 84 (solid line). After training, the amplitude reached 134 with a peak shifted to higher frequencies at 3 c/d. In order to test the significance of these improvements, we reported the gain parameter of the sensitivity function as estimated by the qCSF method [57] for each participant at baseline, at the completion of training, and at the follow-up control, after training had been completed in Figure 4(c). This training improvement is not significant for either the nonpatched or the patched group (one-sided Wilcoxon signed rank test, $p = 0.21$ and $p = 0.34$, respectively). It is not different between the two groups either (two-sided Wilcoxon rank sum test, $p = 0.58$). And there is no significant correlation between the amplitude of the improvement and the gain at baseline in either group (respective $r^2 = 0.46$, $p = 0.10$ and $r^2 = 0.10$, $p = 0.41$ in the patched and nonpatched group).

Finally, we tested the effect of the training on two binocular functions: the interocular balance and the stereosensitivity (Figure 5). The interocular balance expressed as the ratio in dB between the amblyopic and nonamblyopic eye is reported for each participant in Figure 5(a). The averages of the balance over the nonpatched group at baseline and at the completion of training are, respectively, -22.67 ± 13.76 and -21.61 ± 12.68 dB. The fact that the value gets closer to zero indicates a small improvement in the balance, although it is not significant (one-sided Wilcoxon signed rank test, $p = 0.71$). For the patched group, a better improvement from -21.16 ± 15.44 to -19.57 ± 19.12 dB was observed; however, this is not significant either (one-sided Wilcoxon signed rank test, $p = 0.66$). Even merging, the two groups, this improvement remained not significant (one-sided Wilcoxon signed rank test, $p = 0.68$).

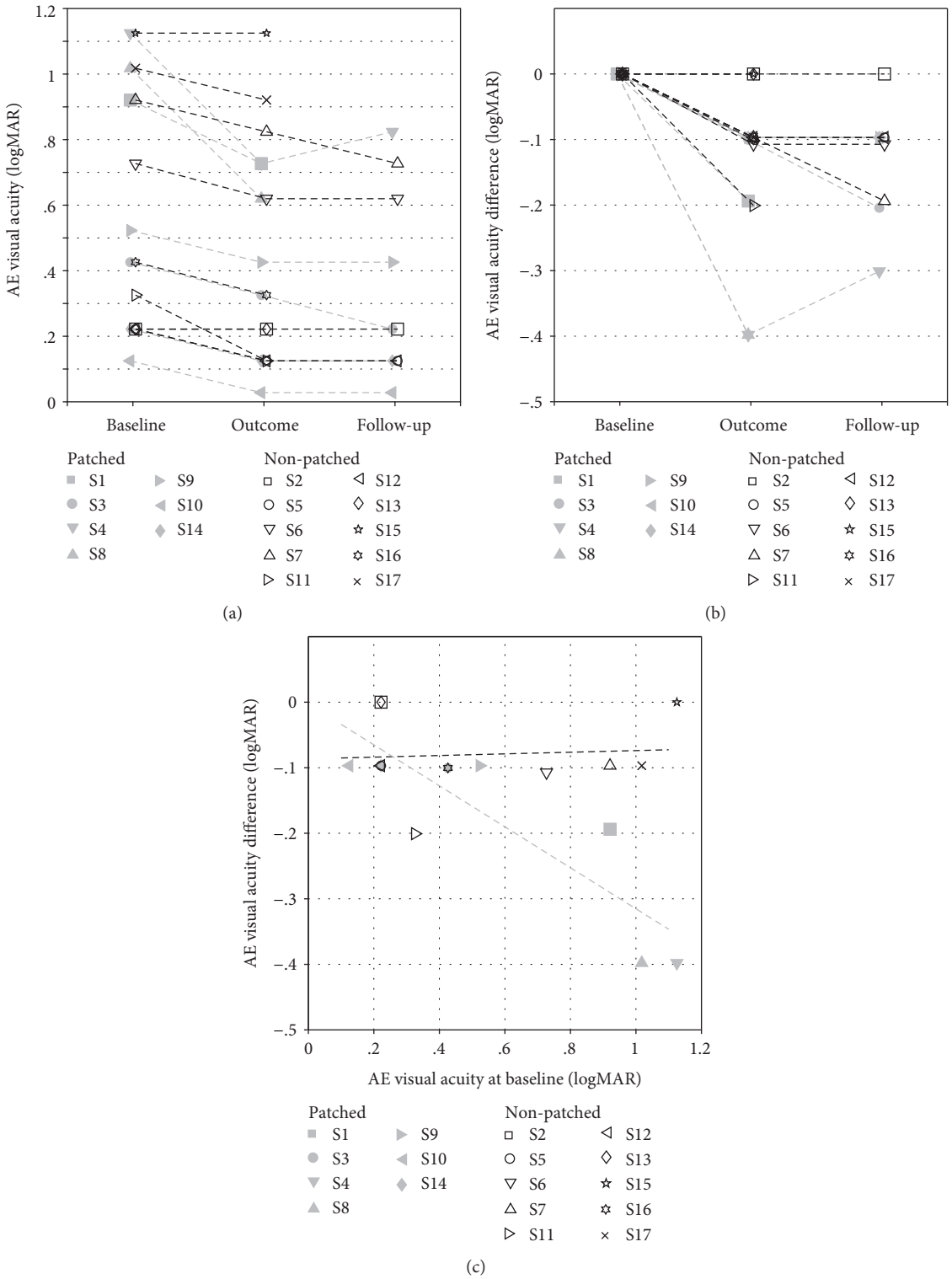

Figure 3: Visual acuity improvement. (a) Visual acuity of the amblyopic eye (AE) of the participants reported at baseline, at the outcome of the training, and at the follow-up control one month later. (b) Visual acuity difference from the baseline of the amblyopic eye. (c) Visual acuity difference from baseline as a function of the initial acuity of the amblyopic eye. Participants from the patched group are indicated with filled grey symbols, and participants of the nonpatched group with open black symbols. Dashed lines represent linear regressions.

For stereosensitivity, among the subjects who initially had stereovision, in the nonpatched group, their average stereo threshold improved from 165 ± 90 arcmin at baseline to 64 ± 43 arcmin at the completion of training (Figure 5(b)). However, this improvement was not significant because only four subjects could initially perform the test (one-sided

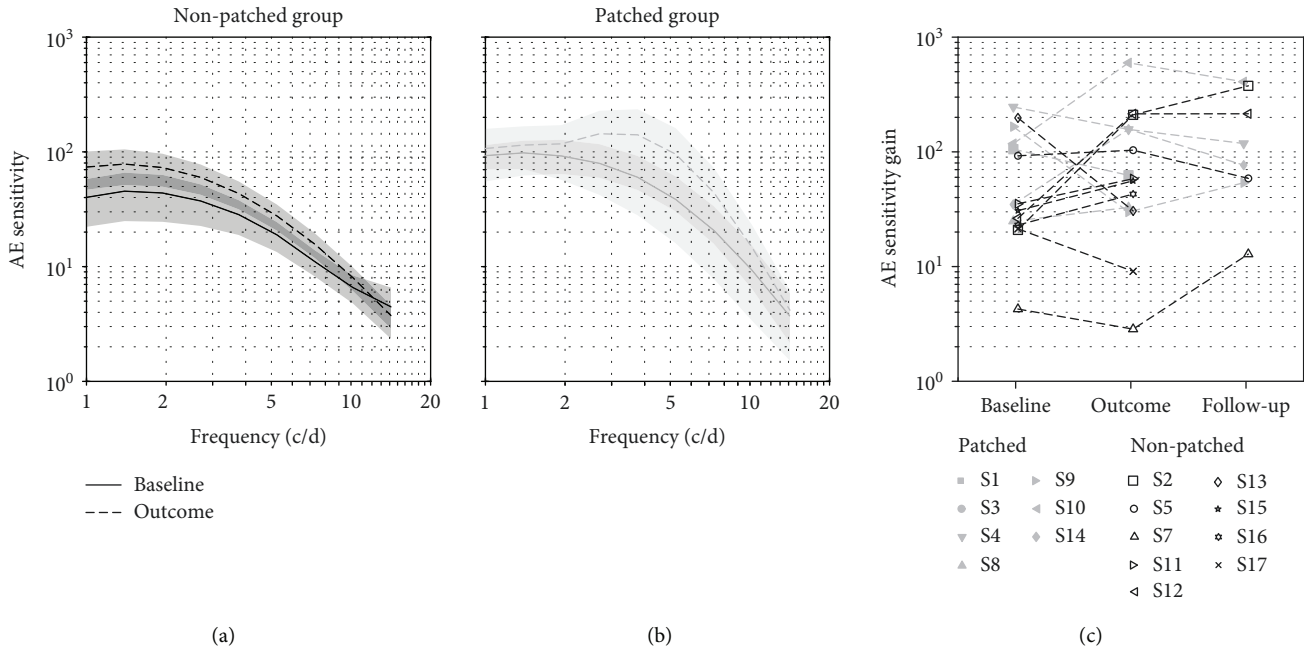

Figure 4: Contrast sensitivity improvement. (a) Contrast sensitivity of the amblyopic eye as a function of spatial frequency at baseline (solid line) and at the training outcome (dashed line) for the nonpatched group. Grey areas represent ±standard error. (b) Contrast sensitivity of the amblyopic eye as a function of spatial frequency at baseline and at the training outcome for the patched group. Same line style as (a). (c) Individual sensitivity gain of the participants at baseline, at the outcome of the training, and at the follow-up control one month later. Participants from the patched group are indicated with filled grey symbols, and participants of the nonpatched group with open black symbols.

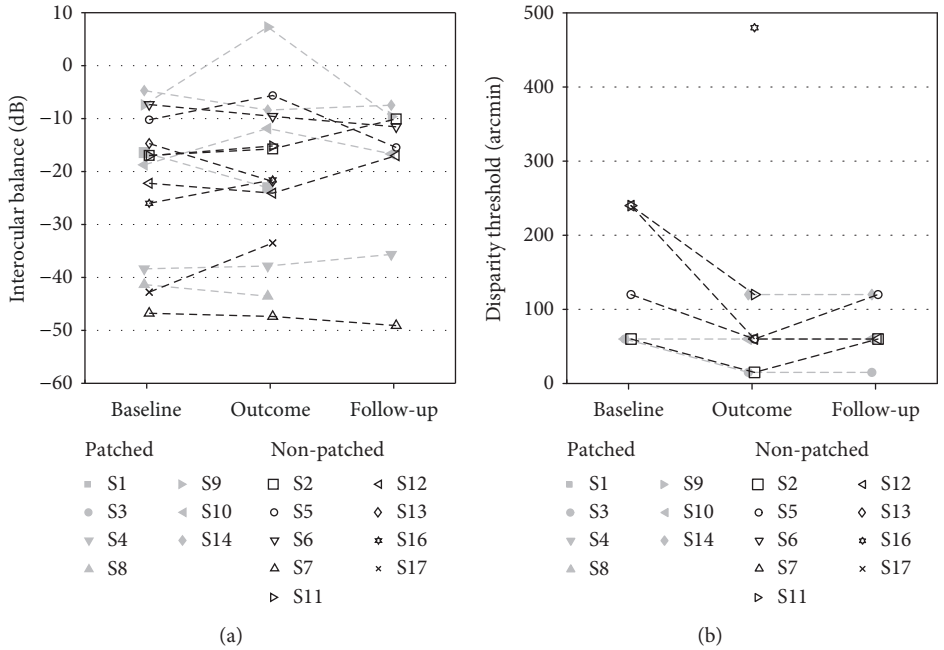

Figure 5: Effect of training on binocular vision. (a) Interocular balance amblyopic/nonamblyopic eye expressed in dB at baseline, at the outcome, and at the follow-up of the training. (b) Disparity sensitivity threshold at baseline, at the outcome, and at the follow-up of the training. Participants from the patched group are indicated with filled grey symbols, and participants of the nonpatched group with open black symbols.

Wilcoxon signed rank test, $p = 0.06$). Additionally, one subject (S16) who previously was not able to perform the TNO test showed a measurable stereosensitivity after training (480 arcmin). In the patched group, only two subjects had a measurable stereosensitivity at baseline. Their average stereo threshold improved from 60 ± 0 arcmin to 38 ± 32

arcmin, but again, this improvement was not significant due to the small sample size (one-sided Wilcoxon signed rank test, $p = 0.5$). Here again, one subject (S14) who was not able to perform the TNO test initially showed a measurable stereosensitivity after training (120 arcmin).

Since there was no statistically significant difference in any measure between the patched and nonpatched groups and since they both were subjected to the same passive dichoptic movie treatment, in order to get more statistical power, we combined the results from the two groups to address the question of whether the treatment per se leads to improvements in visual function in older children and adults with amblyopia. Statistically significant improvements were found in both visual acuity (average improvement from 0.58 to 0.45 logMAR: one-sided Wilcoxon signed rank test, $p < 0.001$) and stereopsis (130 ± 88 arcmin to 55 ± 39 arcmin: one-sided Wilcoxon signed rank test, $p = 0.03$). This is the first report of the successful application of this passive approach in amblyopic older children and adults which complements a previous report of its success in younger amblyopic children [36].

4. Discussion

The primary objective of our study was to evaluate the effect of binocular training with passive dichoptic movie viewing on subjects with a stable resistant amblyopia. The training intervention was very minimal compared with classical patching therapy: 9 hours compared with many months. Our results showed that even very short dichoptic movie viewing significantly improved visual acuity of about one line after approximately 9 hours of training over a two-week period; the maximum visual acuity improvement measured was of 3 lines. This improvement is consistent with the results of Bao et al. [25] on teenagers and adults using an altered reality system and Li et al. [36] and Mezad-Koursh et al. [39] on children using passive movie viewing. The visual acuity improvements we observe are comparable with those of Bao et al. (0.08 logMAR improvement in both studies). Although not unexpectedly, they are lower compared to those obtained in children (0.20 logMAR for Li et al. and 0.26 logMAR for Mezad-Koursh et al.). This difference may be explained by the fact that subjects in these studies were children whereas in our study, they were mostly adults, hence showing less plasticity [64].

We also observed an improvement in the monocular peak contrast sensitivity function amplitude, but it was not significant due to the small sample size [25]. Despite the subjects' ability to appreciate the full picture of the movie while we increased the contrast seen by the fellow eye by 10% for each session, the interocular contrast sensitivity balance remained quite stable after training. Bossi et al. [40] and Li et al. [36] observed similar results, contrary to Hess et al. [26], Li et al. [28], and Kelly et al. [37] who observed a reweighting of this balance proportional to the visual gain. The reason for this is unclear; each of the above studies used a different test for binocular balance. The method used in the study by Kelly et al. [37] is similar to that used in the present study; however, they studied children and we studied adults. It may be possible to improve acuity in the absence of any change in binocular function [36, 40].

Most subjects who had measurable stereoscopic vision with the TNO test at inclusion showed an improvement of it although this was not significant due to the small sample of subjects and the fact that disparities larger than 480 arc seconds could not be measured with the TNO test. Indeed, among the 10 subjects of the nonpatched group, only 4 of them had measurable stereoscopic vision at baseline and all of them improved after training. In this nonpatched group, one patient without measurable stereoscopic vision with the TNO test at baseline exhibited measurable stereopsis after training. Only 2 subjects had measurable stereoscopic vision at baseline in the patched group. One improved and one remained constant after training. In this group, one patient without measurable stereoscopic vision at baseline exhibited measurable stereopsis at final evaluation too. The trend is for stereopsis to improve although owing to limitations in our stereo test [65–68] and the reduced stereopsis of our patients. When the results of the two groups were combined, this improvement became statistically significant (130 ± 88 arcmin to 55 ± 39 arcmin: one-sided Wilcoxon signed rank test, $p = 0.03$). This is the first evidence that passive dichoptic movie training improves stereovision in older children and adults with amblyopia.

Our study shows for the first time that a very short period (9 hours) of passive dichoptic movie viewing can improve visual function in adult subjects presenting with a stable and resistant amblyopia. Previously, a similar improvement was shown for an altered reality system in teenagers and adults [25]. One interest of dichoptic movie viewing is its potential to increase compliance in comparison to patching or to other forms of dichoptic training [25, 31, 35, 41, 45, 69, 70]. First of all, because dichoptic movie viewing is passive, it does not require any active participation of the subject, unlike perceptual learning or dichoptic video game play. This is a crucial advantage especially for older subjects who do not want to play video games or even for younger children who may not have the necessary cognitive capabilities. Furthermore, dichoptic movie viewing is very flexible in that it can be used at home and can be adapted to any video content such as virtual or augmented reality approaches [25, 41, 71–74].

The secondary objective of our study was to evaluate if the mechanisms involved in short-term monocular occlusion and dichoptic movie training could be complementary and synergistic and, if combined together, result in a larger therapeutic effect. Short-term monocular deprivation might activate binocular brain plasticity mechanisms via changes in the excitatory/inhibitory balance [48–50, 52, 75, 76] and that could enhance dichoptic training-based improvements.

We observed a trend that such prior monocular occlusion could enhance the effect of training on visual acuity: our results showed a larger improvement of visual acuity in the patched group (0.19 logMAR, almost 2 lines, maximum gain in this subgroup: 4 lines), in comparison to the nonpatched group (0.08 logMAR, almost 1 line, maximum gain in this subgroup: 2 lines); however, the difference was not significant for our sample size.

Two recent studies examined the effect of intermittent monocular patching of the amblyopic eye 2 h per day as a treatment for amblyopia with procedures comparable to our patching [77, 78]. The Lunghi et al. study also involved physical exercise, and the Zhou et al. study involved more patching sessions. They, respectively, reported improvements of 0.15 and 0.13 logMAR in the acuity of the amblyopic eye which is less than the 0.19 logMAR improvement we observed with the combined patching and dichoptic movie viewing procedure.

We do not observe any correlation between the acuity of the amblyopic eye at baseline and the improvement in the nonpatched group (Figure 3(c)). This could indicate that the dichoptic movie training effect in itself does not depend on the strength of amblyopia and that the difference we observe in the improvement between the two groups is not due to their initial acuity differences. Lunghi et al. [77] do not report such correlation either in their patching combined with exercise study. However, we observe a correlation in the patched group such that the stronger the amblyopia, the greater the improvement. This would indicate that the preliminary patching mostly affects severe cases of amblyopia. One explanation could be that the improvement reaches a saturation level in mild cases whereas the combined patching and dichoptic training method would be the only one powerful enough to show a greater improvement in severe cases.

This trend should be investigated with a much larger sample size and possibly a crossover design because there is a good reason to think that these two approaches (ocular dominance plasticity and dichoptic training) may, because of their different dynamics, be mutually beneficial. Preliminary monocular patching might act on short-term adaptation by altering the inhibitory/excitatory balance allowing a rapid change in contrast gain [48–50, 52–54]. On the other hand, dichoptic movie training follows a slower course, probably by involving binocular mechanisms similar to perceptual learning [25, 79] resulting in the longer term establishment of new synaptic connections [55, 56, 80–82]. Thus, there is every reason to think that the change in the excitatory/inhibitory balance may accelerate and/or amplify the plasticity effect induced by the dichoptic training by inducing a more plastic state in the brain before each training session.

There were trends that did not reach significance between either groups for other visual functions: monocular contrast sensitivity, interocular contrast balance, and stereoscopic vision. The results in each group should be considered independently because the two groups were not homogeneous. Indeed, randomization was not possible because of logistic issues (i.e., preliminary patching was not possible for subjects who were coming to the hospital by car or who were coming very early in the morning). In both groups, the subjects can be considered as their own controls because training did not affect the VA of the nonamblyopic eye; this rules out any hypothesis based on the fact that the improvement could have been a consequence of task learning. Furthermore, all participants were used to watching screens (TV or computer) at least one hour a day (average 3.8 hours a day, see Table 1). Hence, adding 1.5 hour of TV watching every 2-3 days did not drastically change their exposure to digital screens, and so it is very unlikely that the improvement we observe could be solely due to the increased time of screen exposure per se.

Apart from these inconveniences, preliminary monocular patching did not really decrease compliance (qualitative report) to the training because it was the amblyopic eye that was patched [77, 78]; hence, it was much less disabling than patching the fellow eye, and the patching was for a much shorter duration compared to what the subjects were used to.

Our training method shows promising results and could be used to power larger scale *randomized controlled trials* to validate this type of treatment. These results were obtained in only six sessions over a 2-week period of training. There are a number of recommendations: extend the training to a longer period than 2 weeks, develop a better measure of stereopsis in the coarse disparity range, one that can provide an individual variability measure for better statistical evaluation, produce a more sensitive test of binocular balance, and extend the periods of monocular occlusion to see if its benefits for dichoptic training can be enhanced.

Data Availability

The data used to support the findings of this study are available from the corresponding author upon request.

Conflicts of Interest

McGill University holds two patents related to this dichoptic movie treatment. Drs. Reynaud and Hess are the named inventors. Other authors have no commercial relationships to disclose.

Acknowledgments

This work was supported by a grant from the Agence Régionale de la Santé to LS, a grant from the Fondation de France–Berthe Fouassier to NS, grants from the Canadian Institutes of Health Research (228103) and ERA-NET NEURON (JTC 2015) to RFH, and a FRQS Vision Health Research Network of Quebec networking grant to RFH, FC, and AR.

Supplementary Materials

Supplementary 1. Supplementary Movie 1: example movie with 100% contrast images presented to the two eyes. Source video: Lauren Sauvan, wikimedia commons/CC-0.

Supplementary 2. Supplementary Movie 2: example movie with 100% contrast image presented to the left eye and 40% contrast image presented to the right eye. Source video: Lauren Sauvan, wikimedia commons/CC-0.

References

[1] D. H. Hubel and T. N. Wiesel, "Receptive fields of single neurones in the cat's striate cortex," *The Journal of Physiology*, vol. 148, no. 3, pp. 574–591, 1959.

[2] D. H. Hubel and T. N. Wiesel, "Shape and arrangement of columns in cat's striate cortex," *The Journal of Physiology*, vol. 165, no. 3, pp. 559–568, 1963.

[3] D. H. Hubel and T. N. Wiesel, "Effects of monocular deprivation in kittens," *Naunyn-Schmiedebergs Archiv für experimentelle Pathologie und Pharmakologie*, vol. 248, no. 6, pp. 492–497, 1964.

[4] D. H. Hubel and T. N. Wiesel, "Binocular interaction in striate cortex of kittens reared with artificial squint," *Journal of Neurophysiology*, vol. 28, no. 6, pp. 1041–1059, 1965.

[5] D. H. Hubel and T. N. Wiesel, "The period of susceptibility to the physiological effects of unilateral eye closure in kittens," *The Journal of Physiology*, vol. 206, no. 2, pp. 419–436, 1970.

[6] K. Attebo, P. Mitchell, R. Cumming, W. Smith, N. Jolly, and R. Sparkes, "Prevalence and causes of amblyopia in an adult population," *Ophthalmology*, vol. 105, no. 1, pp. 154–159, 1998.

[7] D. S. Friedman, M. X. Repka, J. Katz et al., "Prevalence of amblyopia and strabismus in white and African American children aged 6 through 71 months: the Baltimore Pediatric Eye Disease Study," *Ophthalmology*, vol. 116, no. 11, pp. 2128–2134.e2, 2009.

[8] S. Ganekal, V. Jhanji, Y. Liang, and S. Dorairaj, "Prevalence and etiology of amblyopia in southern India: results from screening of school children aged 5-15 years," *Ophthalmic Epidemiology*, vol. 20, no. 4, pp. 228–231, 2013.

[9] J. H. Groenewoud, A. M. Tjiam, V. K. Lantau et al., "Rotterdam AMblyopia screening effectiveness study: detection and causes of amblyopia in a large birth cohort," *Investigative Ophthalmology & Visual Science*, vol. 51, no. 7, pp. 3476–3484, 2010.

[10] D. Magdalene, H. Bhattacharjee, M. Choudhury et al., "Community outreach: an indicator for assessment of prevalence of amblyopia," *Indian Journal of Ophthalmology*, vol. 66, no. 7, pp. 940–944, 2018.

[11] A. S.-I. Pai, K. A. Rose, J. F. Leone et al., "Amblyopia prevalence and risk factors in Australian preschool children," *Ophthalmology*, vol. 119, no. 1, pp. 138–144, 2012.

[12] C. Wu and D. G. Hunter, "Amblyopia: diagnostic and therapeutic options," *American Journal of Ophthalmology*, vol. 141, no. 1, pp. 175–184.e2, 2006.

[13] S. A. Cotter, A. R. Edwards, D. K. Wallace et al., "Treatment of anisometropic amblyopia in children with refractive correction," *Ophthalmology*, vol. 113, no. 6, pp. 895–903, 2006.

[14] S. E. Dorey, G. G. Adams, J. P. Lee, and J. J. Sloper, "Intensive occlusion therapy for amblyopia," *The British Journal of Ophthalmology*, vol. 85, no. 3, pp. 310–313, 2001.

[15] W. E. Scott and C. F. Dickey, "Stability of visual acuity in amblyopic patients after visual maturity," *Graefe's Archive for Clinical and Experimental Ophthalmology*, vol. 226, no. 2, pp. 154–157, 1988.

[16] C. E. Stewart, M. J. Moseley, D. A. Stephens, and A. R. Fielder, "Treatment dose-response in amblyopia therapy: the Monitored Occlusion Treatment of Amblyopia Study (MOTAS)," *Investigative Opthalmology & Visual Science*, vol. 45, no. 9, pp. 3048–3054, 2004.

[17] H. M. Eggers and C. Blakemore, "Physiological basis of anisometropic amblyopia," *Science*, vol. 201, no. 4352, pp. 264–267, 1978.

[18] L. Kiorpes and J. A. Movshon, "Neural limitations on visual development," in *The Visual Neurosciences*, L. M. Calupa and J. S. Werner, Eds., pp. 159–173, MIT Press, Cambridge, MA, USA, 2004.

[19] L. Kiorpes, D. C. Kiper, L. P. O'Keefe, J. R. Cavanaugh, and J. A. Movshon, "Neuronal correlates of amblyopia in the visual cortex of macaque monkeys with experimental strabismus and anisometropia," *The Journal of Neuroscience*, vol. 18, no. 16, pp. 6411–6424, 1998.

[20] S. LeVay, M. Connolly, J. Houde, and D. C. V. Essen, "The complete pattern of ocular dominance stripes in the striate cortex and visual field of the macaque monkey," *The Journal of Neuroscience*, vol. 5, no. 2, pp. 486–501, 1985.

[21] C. Shooner, L. E. Hallum, R. D. Kumbhani et al., "Asymmetric dichoptic masking in visual cortex of amblyopic macaque monkeys," *The Journal of Neuroscience*, vol. 37, no. 36, pp. 8734–8741, 2017.

[22] R. F. Hess and B. Thompson, "Amblyopia and the binocular approach to its therapy," *Vision Research*, vol. 114, pp. 4–16, 2015.

[23] D. H. Baker, T. S. Meese, B. Mansouri, and R. F. Hess, "Binocular summation of contrast remains intact in strabismic amblyopia," *Investigative Ophthalmology & Visual Science*, vol. 48, no. 11, pp. 5332–5338, 2007.

[24] B. Mansouri, B. Thompson, and R. F. Hess, "Measurement of suprathreshold binocular interactions in amblyopia," *Vision Research*, vol. 48, no. 28, pp. 2775–2784, 2008.

[25] M. Bao, B. Dong, L. Liu, S. A. Engel, and Y. Jiang, "The best of both worlds: adaptation during natural tasks produces long-lasting plasticity in perceptual ocular dominance," *Psychological Science*, vol. 29, no. 1, pp. 14–33, 2018.

[26] R. F. Hess, B. Mansouri, and B. Thompson, "A new binocular approach to the treatment of amblyopia in adults well beyond the critical period of visual development," *Restorative Neurology and Neuroscience*, vol. 28, no. 6, pp. 793–802, 2010.

[27] L. To, B. Thompson, J. R. Blum, G. Maehara, R. F. Hess, and J. R. Cooperstock, "A game platform for treatment of amblyopia," *IEEE Transactions on Neural Systems and Rehabilitation Engineering*, vol. 19, no. 3, pp. 280–289, 2011.

[28] J. Li, B. Thompson, D. Deng, L. Y. L. Chan, M. Yu, and R. F. Hess, "Dichoptic training enables the adult amblyopic brain to learn," *Current Biology*, vol. 23, no. 8, pp. R308–R309, 2013.

[29] D. P. Spiegel, J. Li, R. F. Hess et al., "Transcranial direct current stimulation enhances recovery of stereopsis in adults with amblyopia," *Neurotherapeutics*, vol. 10, no. 4, pp. 831–839, 2013.

[30] B. Mansouri, P. Singh, A. Globa, and P. Pearson, "Binocular training reduces amblyopic visual acuity impairment," *Strabismus*, vol. 22, no. 1, pp. 1–6, 2014.

[31] R. F. Hess, R. J. Babu, S. Clavagnier, J. Black, W. Bobier, and B. Thompson, "The iPod binocular home-based treatment for amblyopia in adults: efficacy and compliance," *Clinical and Experimental Optometry*, vol. 97, no. 5, pp. 389–398, 2014.

[32] P. J. Knox, A. J. Simmers, L. S. Gray, and M. Cleary, "An exploratory study: prolonged periods of binocular stimulation can provide an effective treatment for childhood amblyopia," *Investigative Ophthalmology & Visual Science*, vol. 53, no. 2, pp. 817–824, 2012.

[33] S. L. Li, R. M. Jost, S. E. Morale et al., "A binocular iPad treatment for amblyopic children," *Eye*, vol. 28, no. 10, pp. 1246–1253, 2014.

[34] E. E. Birch, S. L. Li, R. M. Jost et al., "Binocular iPad treatment for amblyopia in preschool children," *Journal of American*

Association for Pediatric Ophthalmology and Strabismus, vol. 19, no. 1, pp. 6–11, 2015.

[35] K. R. Kelly, R. M. Jost, L. Dao, C. L. Beauchamp, J. N. Leffler, and E. E. Birch, "Binocular iPad game vs patching for treatment of amblyopia in children: a randomized clinical trial," *JAMA Ophthalmology*, vol. 134, no. 12, pp. 1402–1408, 2016.

[36] S. L. Li, A. Reynaud, R. F. Hess et al., "Dichoptic movie viewing treats childhood amblyopia," *Journal of American Association for Pediatric Ophthalmology and Strabismus*, vol. 19, no. 5, pp. 401–405, 2015.

[37] K. R. Kelly, R. M. Jost, Y.-Z. Wang et al., "Improved binocular outcomes following binocular treatment for childhood amblyopia," *Investigative Opthalmology & Visual Science*, vol. 59, no. 3, pp. 1221–1228, 2018.

[38] R. W. Li, C. Ngo, J. Nguyen, and D. M. Levi, "Video-game play induces plasticity in the visual system of adults with amblyopia," *PLoS Biology*, vol. 9, no. 8, article e1001135, 2011.

[39] D. Mezad-Koursh, A. Rosenblatt, H. Newman, and C. Stolovitch, "Home use of binocular dichoptic video content device for treatment of amblyopia: a pilot study," *Journal of American Association for Pediatric Ophthalmology and Strabismus*, vol. 22, no. 2, pp. 134–138.e4, 2018.

[40] M. Bossi, V. K. Tailor, E. J. Anderson et al., "Binocular therapy for childhood amblyopia improves vision without breaking interocular suppression," *Investigative Ophthalmology & Visual Science*, vol. 58, no. 7, pp. 3031–3043, 2017.

[41] B. Dong, Y. Jiang, S. A. Engel, and M. Bao, "Adaptation to patch-wise complementary video reduces perceptual ocular dominance," *Journal of Vision*, vol. 14, no. 10, 2014.

[42] C. Gambacorta, M. Nahum, I. Vedamurthy et al., "An action video game for the treatment of amblyopia in children: a feasibility study," *Vision Research*, vol. 148, pp. 1–14, 2018.

[43] R. F. Hess, B. Thompson, J. M. Black et al., "An iPod treatment of amblyopia: an updated binocular approach," *Optometry*, vol. 83, no. 2, pp. 87–94, 2012.

[44] S. L. Li, R. M. Jost, S. E. Morale et al., "Binocular iPad treatment of amblyopia for lasting improvement of visual acuity," *JAMA Ophthalmology*, vol. 133, no. 4, pp. 479-480, 2015.

[45] S. Noah, J. Bayliss, I. Vedamurthy, M. Nahum, D. Levi, and D. Bavelier, "Comparing dichoptic action video game play to patching in adults with amblyopia," *Journal of Vision*, vol. 14, no. 10, p. 691, 2014.

[46] P. E. Waddingham, T. K. H. Butler, S. V. Cobb et al., "Preliminary results from the use of the novel interactive binocular treatment (I-BiT) system, in the treatment of strabismic and anisometropic amblyopia," *Eye*, vol. 20, no. 3, pp. 375–378, 2006.

[47] S. T. Jeon, D. Maurer, and T. L. Lewis, "The effect of video game training on the vision of adults with bilateral deprivation amblyopia," *Seeing and Perceiving*, vol. 25, no. 5, pp. 493–520, 2012.

[48] C. Lunghi, D. C. Burr, and C. Morrone, "Brief periods of monocular deprivation disrupt ocular balance in human adult visual cortex," *Current Biology*, vol. 21, no. 14, pp. R538–R539, 2011.

[49] E. Chadnova, A. Reynaud, S. Clavagnier, and R. F. Hess, "Short-term monocular occlusion produces changes in ocular dominance by a reciprocal modulation of interocular inhibition," *Scientific Reports*, vol. 7, no. 1, article 41747, 2017.

[50] J. Zhou, S. Clavagnier, and R. F. Hess, "Short-term monocular deprivation strengthens the patched eye's contribution to binocular combination," *Journal of Vision*, vol. 13, no. 5, 2013.

[51] C. Lunghi, D. C. Burr, and M. C. Morrone, "Long-term effects of monocular deprivation revealed with binocular rivalry gratings modulated in luminance and in color," *Journal of Vision*, vol. 13, no. 6, p. 1, 2013.

[52] J. Zhou, B. Thompson, and R. F. Hess, "A new form of rapid binocular plasticity in adult with amblyopia," *Scientific Reports*, vol. 3, no. 1, article 2638, 2013.

[53] J. Zhou, A. Reynaud, and R. F. Hess, "Real-time modulation of perceptual eye dominance in humans," *Proceedings of the Royal Society B: Biological Sciences*, vol. 281, no. 1795, article 20141717, 2014.

[54] T. K. Hensch and M. Fagiolini, "Excitatory-inhibitory balance and critical period plasticity in developing visual cortex," *Progress in Brain Research*, vol. 147, pp. 115–124, 2005.

[55] E. Zohary, S. Celebrini, K. H. Britten, and W. T. Newsome, "Neuronal plasticity that underlies improvement in perceptual performance," *Science*, vol. 263, no. 5151, pp. 1289–1292, 1994.

[56] T. H. Brown, E. W. Kairiss, and C. L. Keenan, "Hebbian synapses: biophysical mechanisms and algorithms," *Annual Review of Neuroscience*, vol. 13, no. 1, pp. 475–511, 1990.

[57] L. A. Lesmes, Z.-L. Lu, J. Baek, and T. D. Albright, "Bayesian adaptive estimation of the contrast sensitivity function: the quick CSF method," *Journal of Vision*, vol. 17, no. 3, pp. 1–21, 2010.

[58] F. Hou, C.-B. Huang, L. Lesmes et al., "qCSF in clinical application: efficient characterization and classification of contrast sensitivity functions in amblyopia," *Investigative Opthalmology & Visual Science*, vol. 51, no. 10, pp. 5365–5377, 2010.

[59] Y. Gao, A. Reynaud, Y. Tang, L. Feng, Y. Zhou, and R. F. Hess, "The amblyopic deficit for 2nd order processing: generality and laterality," *Vision Research*, vol. 114, pp. 111–121, 2015.

[60] A. Reynaud, Y. Tang, Y. Zhou, and R. F. Hess, "A normative framework for the study of second-order sensitivity in vision," *Journal of Vision*, vol. 14, no. 9, 2014.

[61] M. Kwon, E. Wiecek, S. C. Dakin, and P. J. Bex, "Spatial-frequency dependent binocular imbalance in amblyopia," *Scientific Reports*, vol. 5, no. 1, article 17181, 2015.

[62] E. E. Birch, S. E. Morale, R. M. Jost et al., "Assessing suppression in amblyopic children with a dichoptic eye chart," *Investigative Ophthalmology & Visual Science*, vol. 57, no. 13, pp. 5649–5654, 2016.

[63] B. Julesz, "Stereoscopic vision," *Vision Research*, vol. 26, no. 9, pp. 1601–1612, 1986.

[64] J. M. Holmes and D. M. Levi, "Treatment of amblyopia as a function of age," *Visual Neuroscience*, vol. 35, article E015, 2018.

[65] D. M. Levi, D. C. Knill, and D. Bavelier, "Stereopsis and amblyopia: a mini-review," *Vision Research*, vol. 114, pp. 17–30, 2015.

[66] A. Reynaud and R. F. Hess, "Interocular correlation sensitivity and its relationship with stereopsis," *Journal of Vision*, vol. 18, no. 1, p. 11, 2018.

[67] R. W. Li, K. So, T. H. Wu et al., "Monocular blur alters the tuning characteristics of stereopsis for spatial frequency and size," *Royal Society Open Science*, vol. 3, no. 9, article 160273, 2016.

[68] J. Tittes, A. S. Baldwin, R. F. Hess et al., "Digital or analogue? First assessment of a newly developed digital stereotest in

adults and children with and without amblyopia," in *European Conference on Visual Perception*, Trieste, 2018.

[69] J. M. Holmes, V. M. Manh, E. L. Lazar et al., "Effect of a binocular iPad game vs part-time patching in children aged 5 to 12 years with amblyopia: a randomized clinical trial," *JAMA Ophthalmology*, vol. 134, no. 12, pp. 1391–1400, 2016.

[70] J. Wang, "Compliance and patching and atropine amblyopia treatments," *Vision Research*, vol. 114, pp. 31–40, 2015.

[71] W. Wen, X. Sun, H. Liu, and X. Li, "A dichoptic augmented-reality paradigm as a treatment for adult amblyopes," *Investigative Ophthalmology & Visual Science*, vol. 58, no. 8, article 3829, 2017.

[72] A. D. Deemer, C. K. Bradley, N. C. Ross et al., "Low vision enhancement with head-mounted video display systems: are we there yet?," *Optometry and Vision Science*, vol. 95, no. 9, pp. 694–703, 2018.

[73] M. Falconbridge, D. Wozny, L. Shams, and S. A. Engel, "Adapting to altered image statistics using processed video," *Vision Research*, vol. 49, no. 14, pp. 1757–1764, 2009.

[74] P. Zhang, M. Bao, M. Kwon, S. He, and S. A. Engel, "Effects of orientation-specific visual deprivation induced with altered reality," *Current Biology*, vol. 19, no. 22, pp. 1956–1960, 2009.

[75] G. C. DeAngelis, A. Anzai, I. Ohzawa, and R. D. Freeman, "Receptive field structure in the visual cortex: does selective stimulation induce plasticity?," *Proceedings of the National Academy of Sciences of the United States of America*, vol. 92, no. 21, pp. 9682–9686, 1995.

[76] B. Boroojerdi, F. Battaglia, W. Muellbacher, and L. G. Cohen, "Mechanisms underlying rapid experience-dependent plasticity in the human visual cortex," *Proceedings of the National Academy of Sciences*, vol. 98, no. 25, pp. 14698–14701, 2001.

[77] C. Lunghi, A. T. Sframeli, A. Lepri et al., "A new counterintuitive training for adult amblyopia," *Annals of Clinical and Translational Neurology*, vol. 6, no. 2, pp. 274–284, 2018.

[78] J. Zhou, Z. He, Y. Wu et al., "Inverse occlusion: a binocularly motivated treatment for amblyopia," *Neural Plasticity*, vol. 2019, Article ID 5157628, 12 pages, 2019.

[79] A. Karni and D. Sagi, "The time course of learning a visual skill," *Nature*, vol. 365, no. 6443, pp. 250–252, 1993.

[80] F. Sengpiel, "Plasticity of the visual cortex and treatment of amblyopia," *Current Biology*, vol. 24, no. 18, pp. R936–R940, 2014.

[81] M. Scali, L. Baroncelli, M. C. Cenni, A. Sale, and L. Maffei, "A rich environmental experience reactivates visual cortex plasticity in aged rats," *Experimental Gerontology*, vol. 47, no. 4, pp. 337–341, 2012.

[82] L. Baroncelli, A. Sale, A. Viegi et al., "Experience-dependent reactivation of ocular dominance plasticity in the adult visual cortex," *Experimental Neurology*, vol. 226, no. 1, pp. 100–109, 2010.

Hindawi
Neural Plasticity
Volume 2019, Article ID 3681430, 10 pages
https://doi.org/10.1155/2019/3681430

Research Article

Altered Spontaneous Brain Activity of Children with Unilateral Amblyopia: A Resting State fMRI Study

Peishan Dai,[1,2] **Jinlong Zhang**,[1,2] **Jing Wu**,[1] **Zailiang Chen**,[1,2] **Beiji Zou**,[1,2] **Ying Wu**,[3,4] **Xin Wei**,[3,4] **and Manyi Xiao**[3,4]

[1]*School of Computer Science and Engineering, Central South University, Changsha, Hunan 410083, China*
[2]*Hunan Engineering Research Center of Machine Vision and Intelligent Medicine, Central South University, Changsha 410083, China*
[3]*Department of Ophthalmology, Second Xiangya Hospital, Central South University, Changsha, Hunan 410083, China*
[4]*Hunan Clinical Research Center of Ophthalmic Disease, Changsha, Hunan 410083, China*

Correspondence should be addressed to Manyi Xiao; 13973119862@163.com

Received 27 December 2018; Revised 1 May 2019; Accepted 27 June 2019; Published 25 July 2019

Guest Editor: Benjamin Thompson

Objective. This study is aimed at investigating differences in local brain activity and functional connectivity (FC) between children with unilateral amblyopia and healthy controls (HCs) by using resting state functional magnetic resonance imaging (rs-fMRI). *Methods.* Local activity and FC analysis methods were used to explore the altered spontaneous brain activity of children with unilateral amblyopia. Local brain function analysis methods included the amplitude of low-frequency fluctuation (ALFF). FC analysis methods consisted of the FC between the primary visual cortex (PVC-FC) and other brain regions and the FC network between regions of interest (ROIs-FC) selected by independent component analysis. *Results.* The ALFF in the bilateral frontal, temporal, and occipital lobes in the amblyopia group was lower than that in the HCs. The weakened PVC-FC was mainly concentrated in the frontal lobe and the angular gyrus. The ROIs-FC between the default mode network, salience network, and primary visual cortex network (PVCN) were significantly reduced, whereas the ROIs-FC between the PVCN and the high-level visual cortex network were significantly increased in amblyopia. *Conclusions.* Unilateral amblyopia may reduce local brain activity and FC in the dorsal and ventral visual pathways and affect the top-down attentional control. Amblyopia may also alter FC between brain functional networks. These findings may help understand the pathological mechanisms of children with amblyopia.

1. Introduction

Amblyopia is a neurodevelopmental disorder of the visual cortex characterized by visual deficiency in an eye that is otherwise physically normal or by a deficiency that is out of proportion with the structural abnormalities of the eyes [1–3], thereby affecting 2%–4% of the general population [4]. Amblyopia is believed to be caused by an abnormal visual experience during the critical visual development period in childhood [5]. Amblyopia is generally correlated with an abnormal ocular alignment (strabismus) or an unequal refractive error between the two eyes (anisometropia) in early life [6]. The peak of brain plasticity is in early childhood [7], so the brain functional mechanism of amblyopia in children should be investigated to administer treatments timely and accurately.

Functional magnetic resonance imaging (fMRI) can be applied to investigate brain activity noninvasively; as such, fMRI is widely used to reveal neuropathological mechanisms in amblyopia [8, 9]. Amblyopia is considered a visual cortex but not a retinal dysfunction [10]. For this reason, brain areas on the vision pathway have been widely explored. Task-related fMRI, which is obtained by stimulating with a visual task, has been used to investigate local brain activities. The

lateral geniculate nucleus (LGN) is a relay center in the visual pathway. Miki et al. [11] used task-related fMRI and revealed that LGN activation is diminished during monocular viewing by an eye with anisometropic amblyopia. Hess et al. [12] found functional deficits in the LGN by employing visual stimulus fMRI in human adults. The primary visual cortex (PVC) (V1) has also been widely explored. Goodyear et al. [13] selected a region of interest (ROI) around the V1 and confirmed that the activation region of the amblyopic eye is smaller than that of the normal eye with the same stimulus. Barnes et al. [14] reported a reduced fMRI activation in the V1 and V2 regions. These findings confirmed that the visual impairment of amblyopia may be related to the functional changes in neurons in the V1 region [15–18]. Further research has indicated that the abnormal brain function of amblyopia is not limited to the PVC. Muckli et al. [19] reported that responses of amblyopic eye were progressively reduced on the central visual pathway (V3a/VP, V4/V8, lateral occipital complex (LOC)) compared with the low-level visual areas (V1/V2) when grating stimuli were presented, suggesting that the vision pathway from the PVC to the high-level visual areas of the amblyopic eye may have been impaired. Spiegel et al. [3] used checkerboard stimulation and found a reduced fMRI activation in the V2 and V3 in amblyopia. Simmers et al. [20–22] employed psychophysical methods and revealed that the ventral and dorsal extrastriate functions are affected by amblyopia. These studies have suggested that amblyopia affects the visual pathway, including primary and high-level visual areas.

rs-fMRI can investigate the spontaneous neuronal activity of the human brain [23, 24]. In comparison with task-related fMRI, rs-fMRI is easily performed, is simple in design, and can be easily obtained for most children [9, 25]. Several scholars investigated the spontaneous brain activity and FC of amblyopia through rs-fMRI. Tang et al. [9] and Liang et al. [26] revealed that the amplitude of low-frequency fluctuation (ALFF) of spontaneous brain activity changes in the anisometropic amblyopia group. Lin et al. [1] observed that regional homogeneity (ReHo) value changes in individuals with anisometropic amblyopia. Wang et al. [27, 28] and Ding et al. [29] found decreased FC in the visual pathway in amblyopia. These studies have revealed functional changes in the visual pathway from the ALFF, ReHo, and FC analysis in amblyopia. In addition, they also found functional changes in nonvisual pathway areas. But there were few commonalities between the results. The reasons may be as follows: first, sample characteristics are different. Second, rs-fMRI may reflect spontaneous brain activity, and the noise may be greater than task-related fMRI. Lastly, the effect of amblyopia may not be limited to visual pathways because of neuroplasticity.

In previous rs-fMRI studies, the amblyopia group usually includes a mixture of left eye, right eye, and bilateral amblyopia. But in this study, we chose unilateral amblyopia as a research object to reduce the sample interference between left, right, and bilateral amblyopia. Our hypothesis was that unilateral amblyopia might alter local brain activity and FC, and such an alteration might not completely focus on the visual pathway. To confirm this hypothesis, we analyzed spontaneous brain activity from multiple perspectives, including ALFF, FC in the primary visual cortex (PVC-FC), and FC network between regions of interest (ROIs-FC) analysis.

2. Materials and Methods

2.1. Participants. The inclusion criteria for the amblyopia group were as follows: the best-corrected visual acuity of 0.3 logMAR (3 years), 0.2 logMAR (4–7 years), 0.1 logMAR (more than 7 years), or two-line (0.2 logMAR) interocular optotype acuity differences without pathology and history of treatment. The inclusion criteria for HCs were as follows: without amblyopia-related diseases and history of treatment. There was no significant difference in age and gender to the amblyopia group.

This study was approved by the Ethics Committee of the Second Xiangya Hospital, Central South University, and in accordance with the Declaration of Helsinki. A written informed consent was obtained from all participants enrolled in the study or from their legal guardians. All participants received detailed eye examinations that included assessments of visual acuity, intraocular pressure and refraction, slit lamp examination, ophthalmoscopy, binocular alignment, ocular motility, and random dot butterfly stereograms.

The participants included 17 individuals with normal vision and 17 individuals with amblyopia, and they were enrolled as two groups of subjects in the study. From each group, 4 individuals whose data contained consistent outliers likely due to excessive head motion were excluded from the analysis. As a result, 13 individuals were retained in the amblyopia group, and the same number of age-matched normally sighted individuals remained in the control group. The individuals in the amblyopia group had left eye amblyopia. Those in the control group had normal or corrected to normal visual acuity in both eyes and reported no history of visual disorders. The demographic information of the participants is summarized in Table 1.

2.2. Magnetic Resonance Imaging Data Acquisition. Scans were conducted using a Philips Achieva 3-T magnetic resonance scanner at Trinity MRI, with a Philips 8 Channel head coil. The scanning session included a T1-weighted anatomical scan (TE, 2.7 ms; TR, 5.8 ms; flip angle, 8; voxel size, 1 mm^3) followed by a blood oxygenation level-dependent fMRI (BOLD-fMRI) scan (single-shot spin-echo echo-planar imaging, parallel imaging [36 slices]). BOLD-fMRI scans were measured with transverse orientation; AP fold-over direction; TE, 2000 ms; TR, 30 s; flip angle, 90°; isotropic 3.5 mm × 3.5 mm × 3.5 mm resolution; FOV, 240 mm × 240 mm × 144 mm; acquisition matrix $M \times P$, 64×64; REC voxel MPS, 1.67 mm × 1.67 mm × 4.0 mm; and time points = 189.

2.3. Data Processing. Preprocessing steps were generated using the Data Processing and Analysis for Brain Imaging (DPABI) software package [30]. The steps included DICOM-to-NIFTI transformation, removal of 10 time points, slice timing correction, head motion correction, nuisance covariate regression (six head motion signals, white matter, averaged cerebrospinal

Table 1: Demographic information of subjects.

Subject	Gender	Age	Amblyopic type	Amblyopic eye	CVA (logMAR)		History of treatment
					OD	OS	
Amb 01	F	12	ANA	OS	-0.1	0.7	None
Amb 02	M	5	ANA	OS	0.1	0.4	None
Amb 03	F	14	ANA	OS	0.0	1.0	None
Amb 04	M	8	AMA	OS	-0.1	0.5	None
Amb 05	M	6	ANA; AMA	OS	0.0	1.0	None
Amb 06	M	13	ANA	OS	0.0	0.4	None
Amb 07	M	8	ANA; AMA	OS	0.1	0.7	None
Amb 08	M	10	ANA; AMA	OS	0.0	0.7	None
Amb 09	F	14	ANA; AMA	OS	0.0	0.5	None
Amb 10	M	12	ANA	OS	0.0	1.2	None
Amb 11	F	8	ANA	OS	0.0	0.7	None
Amb 12	M	24	AMA	OS	0.0	0.2	None
Amb 13	M	15	AMA	OS	0.0	0.5	None
Control 01	F	6	None	None	0.2	0.1	None
Control 02	F	24	None	None	0.0	0.0	None
Control 03	F	12	None	None	0.0	0.0	None
Control 04	F	12	None	None	0.0	0.0	None
Control 05	M	9	None	None	0.0	0.0	None
Control 06	F	8	None	None	0.0	0.0	None
Control 07	M	13	None	None	0.0	0.0	None
Control 08	M	14	None	None	0.0	0.0	None
Control 09	F	14	None	None	-0.2	-0.1	None
Control 10	F	11	None	None	0.0	0.0	None
Control 11	M	10	None	None	-0.1	-0.2	None
Control 12	M	7	None	None	0.0	-0.1	None
Control 13	M	10	None	None	-0.2	-0.1	None

Note: Amb: amblyopia group; F: female; M: male; CVA: corrected visual acuity; OD: oculus dexter; OS: oculus sinister; ANA: anisometropic amblyopia; AMA: ametropic amblyopia.

flow, and global), standard space normalization (based on the Montreal Neurological Institute coordinate system), smoothing with a 4 mm full width at a half maximum of Gaussian kernel to decrease the spatial noise, and band-pass filtering ($0.01\,\text{Hz} < f < 0.08\,\text{Hz}$) of the waveform of each voxel to reduce the effects of low-frequency drift and high-frequency noise [31]. Head motion parameters had no significant difference between the two groups.

2.4. ALFF Analysis. After preprocessing, ALFF was computed on each individual's data. The ALFF of the rs-fMRI signal has been widely used to measure the intensity of regional spontaneous brain activity [24, 32–36]. ALFF analysis does not depend on prior knowledge and model, thus avoiding the possible errors in the model and hypothesis dependency. ALFF analysis is conducted to measure the magnitude of the energy from the BOLD signal intensity and indirectly measure the relative activity of the local brain area in the resting state. Such a spontaneous activity in the brain area is generally due to the rhythmic activity of the brain region functionally associated with other brain regions. The brain areas with a high ALFF may indicate an increased spontaneous neuronal activity, whereas the brain areas with a low ALFF may correspond to a decreased spontaneous neuronal activity.

2.5. PVC-FC Analysis

2.5.1. ROI Identification. The ROIs of the PVC were defined as the intersections of the gray matter cortex and 17 bilateral Brodmann's areas according to the WFU-atlas [37, 38]. Therefore, two ROIs represent the PVC on the left and right hemispheres.

2.5.2. FC Analysis. The PVC-FC analyis was performed with DPABI. The regional rs-fMRI time series was computed for each ROI by averaging all the voxels within each region at each time point in the time series, resulting in 189 time points for each ROI. The correlation coefficient between the average time series of each ROI and other voxels of the brain was calculated as the connection strength. A two-sample t-test was conducted to compare the differences in FC between the amblyopia group and the healthy controls (HCs) at $P \leq 0.05$ by using GRF correction with a cluster size of >85.

Table 2: Key nodes of each network.

Network	Region	BA	Peak MNI coordinates (mm)			z-scores
			X	Y	Z	
SN	rFIC	47	38	20	1	14.32
	lFIC	47	-33	19	-1	12.21
	ACC	24	-2.5	11.5	38.5	14.48
CEN	rDPC	9	48	22	45	15.64
	lDPC	9	-43.5	23.5	41.5	12.35
	rPPC	40	56	-50	43	14.87
	lPPC	40	-43.5	-52.5	49.5	11.41
DMN	VPC	11	0	-48	-15	14.08
	PCC	23/30	-6	-49	29	13.36
PVCN	rCAL	17	17.5	-99.5	4.5	12.10
	lCAL	17	-17.5	-99.5	4.5	13.65
HVCN	rLING	19	13	-55	-2	14.54
	rFFG	19	41	-62	-18	13.54
	rFFG	37	30	-47	-12	10.96
	lFFG	37	-30	-47	-12	12.05

Note: BA: Brodmann's area; MNI: Montreal neurological institute; SN: salience network; CEN: cerebellum network; DMN: default mode network; PVCN: primary visual cortex network; HVCN: higher visual cortex network; rFIC: right frontoinsular cortex; lFIC: left frontoinsular cortex; ACC: anterior cingulate cortex; rDPC: right dorsolateral prefrontal cortex; lDPC: left dorsolateral prefrontal cortex; rPPC: right posterior parietal cortex; lPPC: left posterior parietal cortex; VPC: ventromedial prefrontal cortex; PCC: posterior cingulate cortex; rCAL: right calcarine cortex; lCAL: left calcarine cortex; rLING: right lingual gyrus; rFFG: fusiform gyrus; lFFC: fusiform gyrus.

2.6. FC Network among ROIs

2.6.1. ROI Selection. Independent component analysis (ICA) was conducted on each participant's smoothened, normalized images by using GIFT v3.0a (Group ICA of fMRI Toolbox) [39]. This analysis was limited to 25 output-only components of the group. From these components, networks of interest (salience network (SN), default mode network (DMN), primary visual cortex network (PVCN), high visual cortex network (HVCN), cerebellum network (CEN), right frontoparietal network (rFPN), and left frontoparietal network (lFPN)) were selected. A nonlinear template matching was conducted to select the "best fit" or the most suitable network component. The template matching steps were as follows: for each component, the average z-score of the voxels of the component falling within and outside the template was calculated. Then, the component from the 25 components with the maximum difference in the average z-score of voxels falling within and outside the template was selected as the network component that most closely matched the template. The z-scores here reflected the degree to which the time series of a given voxel was correlated with the time series corresponding to the specific ICA component. A combined group analysis was performed using the individual best fit network components for the three networks. Individual t-statistic images from both groups were used to determine the combined group-level statistical maps by using a single-sample t-test. Significant clusters were identified using a voxel-wise statistical height ($P \leq 0.01$) and extent ($P \leq 0.01$) thresholds corrected at the whole-brain level.

According to previous results on resting state networks [40], the classical resting state networks were selected from the ICA components. The seed of ROIs of each network was defined on the basis of the peaks of z-scores of the ICA clusters and selected (Table 2). The final ROIs were drawn as spheres with a radius of 8 mm centered on the given nodes. The ROIs were created correspondingly on both hemispheres. These ROI selection procedures are widely used in functional and effective connectivity studies [41–44].

2.6.2. FC Analysis. The regionally averaged rs-fMRI time series of each ROI was contracted to calculate the connections between the ROIs, and the correlation between the time series was computed by DPARSF software. Fisher's r to z transformation was applied to ensure a normal distribution. A single-sample t-test was conducted to analyze the FC at a group level, and a two-sample t-test was performed to examine the between-group differences ($P \leq 0.01$, FDR correction, and cluster size > 85).

3. Results

3.1. Comparison of ALFF in Amblyopia versus HCs. The ALFF values were computed at a voxel level to assess the difference in the intensity of the local brain activity between the two groups.

The differences in ALFF between the amblyopia group and HCs are illustrated in the 3D gray cortical model in Figure 1. The differences in ALFF values between both groups as revealed by using the two-sample t-test are presented in Table 3.

ALFF analysis showed that the brain regions with lower ALFF values in the amblyopia group than those in the HCs were distributed in the bilateral brain, including frontal, temporal, and occipital lobes. The middle temporal gyrus is a high-level functional area in the visual dorsal information processing stream, and the low ALFF may be related to the attention deficit of amblyopia. The brain regions with higher ALFF values in the amblyopia group than those in HCs were distributed in the right fusiform gyrus, the right caudate nucleus, and the right superior parietal gyrus.

3.2. Comparison of PVC-FC in Amblyopia versus HCs. The FC results between the left PVC and the whole brain are shown in Figure 2(a), and the brain area statistics are provided in Table 4. In comparison with the HCs, the amblyopia group revealed that the brain regions with strong FC were mainly in the bilateral fusiform gyrus, but brain regions with a weak connectivity were mainly in the right middle frontal and angular gyri.

The results of FC between the right PVC and the whole brain are shown in Figure 2(b), and the brain area statistics are listed in Table 5. In comparison with HCs, the amblyopia group indicated that the brain regions with a strong FC were only in the right fusiform gyrus, but the brain regions with a

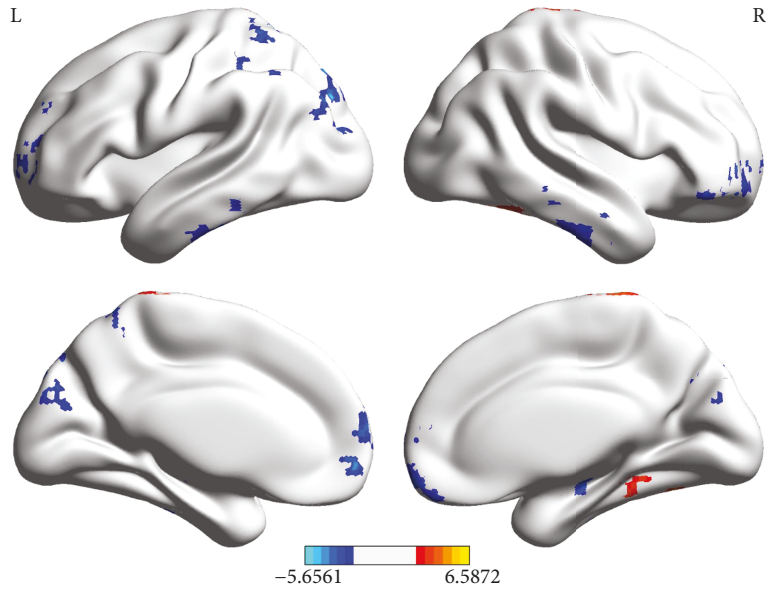

Figure 1: Differences in ALFF between the amblyopia group and HCs ($P \leq 0.05$, alphasim corrected, and cluster size > 85). The red region indicates that the ALFF of the amblyopia group is significantly higher than that of HCs. The blue region implies that the ALFF of the amblyopia group is significantly lower than that of HCs.

Table 3: Differences in ALFF between the amblyopia group and HCs.

Region	BA	Peak MNI coordinates (mm)			Cluster size	*T* value
		X	*Y*	*Z*		
rITG	20	48	-33	-18	231	-4.0713
lMTG	20	-45	-24	-18	192	-4.4553
lMFG	10	-6	57	-6	103	-4.2173
rMFG	—	39	54	-15	159	-4.2101
lMOG	19	-27	-81	9	242	-5.6561
lSFG	—	-18	63	3	149	-4.5657
lCUN	—	0	-84	42	122	-3.6131
lIPG	40	-48	-54	48	136	-3.867
lIPG	—	-24	-51	54	93	-4.5914
lPreCG	—	-24	-15	54	75	-4.3692
rPreCG	7	12	-60	63	35	-3.5482
lPCL	6	-6	-27	69	15	-2.4483
rFFG	—	33	-60	-18	222	4.881
rCAU	—	12	18	3	279	5.0006
rSPG	—	16	-63	72	322	6.5872

Note: BA: Brodmann's area; MNI: Montreal neurological institute; rITG: right inferior temporal gyrus; lMTG: left middle temporal gyrus; lMFG: left middle frontal gyrus; rMFG: right middle frontal gyrus; lMOG: left middle occipital gyrus; lSFG: left superior frontal gyrus; lCUN: left cuneus; lIPG: left inferior parietal gyrus; lPreCG: left precentral gyrus; rPreCG: right precentral gyrus; lPCL: left paracentral lobule; rFFG: right fusiform gyrus; rCAU: right caudate nucleus; rSPG: right superior parietal gyrus.

weak connectivity were mainly in the right putamen, left orbital inferior frontal gyrus, dorsolateral superior frontal gyrus, left medial superior frontal, right angular gyrus, and right middle frontal gyrus.

The bilateral PVC had a weak connectivity with the right angular and right middle frontal gyri in amblyopia.

3.3. Comparison of FC between ROIs in Amblyopia versus HCs. Pearson's correlation was conducted for each ROI pair to assess the strength of functional coupling among network nodes. Figure 3 illustrates the results of the two-sample *t*-test for the FC of ROIs between amblyopia and HCs. Table 6 shows the statistical information.

In comparison with HCs, the amblyopia group possessed a weak FC between the following ROIs: left frontoinsular cortex-ventromedial prefrontal cortex, left frontoinsular cortex-left calcarine cortex, left frontoinsular cortex-right calcarine cortex, ventromedial prefrontal cortex-anterior cingulate cortex, ventromedial prefrontal cortex-right frontoinsular cortex, and right frontoinsular cortex-right fusiform gyrus. Strong FC existed between the PVCN and HVCN (left calcarine cortex-right fusiform gyrus, right calcarine cortex-left frontoinsular cortex, and right calcarine cortex-right frontoinsular cortex).

4. Discussion

Amblyopia shows evident visual function impairment but does not have typical ocular organic changes, although previous rs-fMRI studies have found alteration of spontaneous brain activity in amblyopia. However, fMRI studies focusing on unilateral amblyopia is limited. Here, we examined the brain functional differences between the amblyopia group and the HCs from multiple level analysis.

As a local method, ALFF analysis was conducted to locate the dysfunctional brain regions of amblyopia. In comparison with HCs, the amblyopia group indicated low ALFF in the bilateral frontal, temporal, and occipital lobes. This result

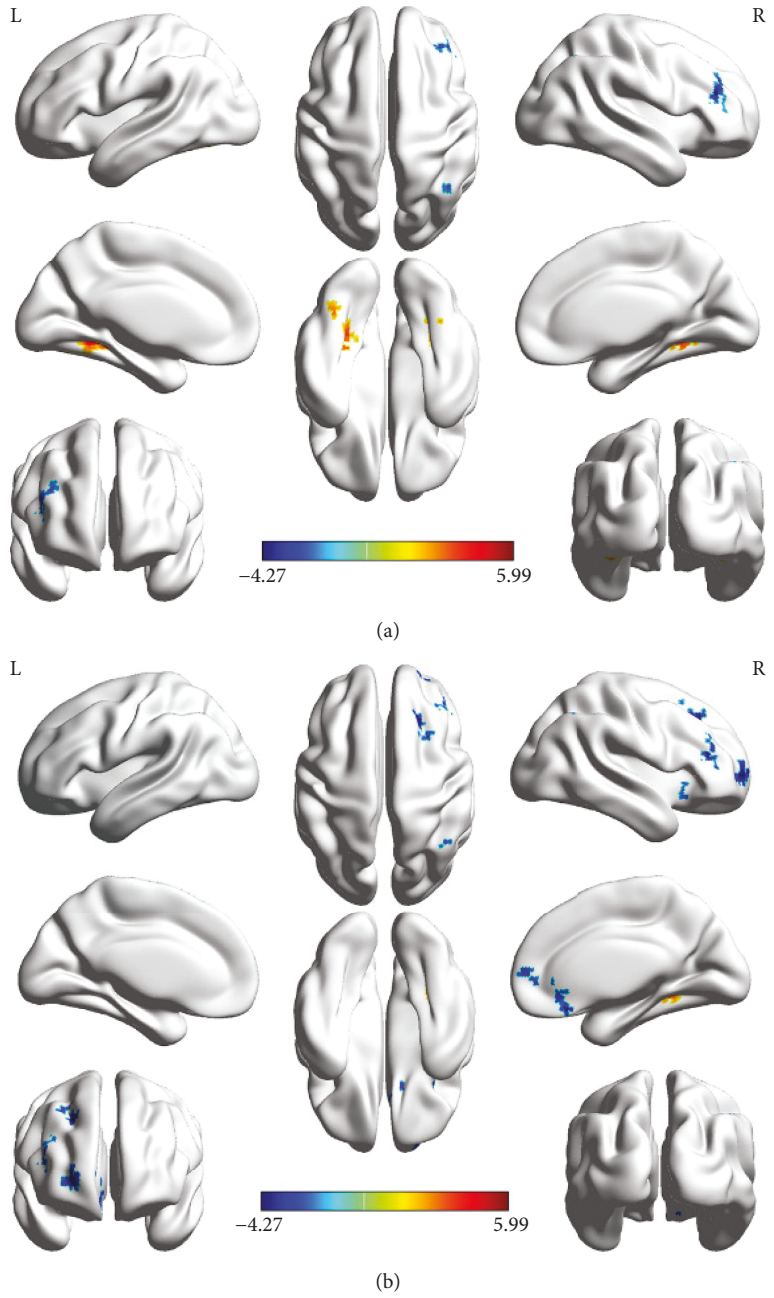

Figure 2: FC between the PVC and other brain regions ($P \leq 0.05$, GRF corrected, and cluster size > 85). (a) FC between the left PVC and other brain regions. (b) FC between the right PVC and other brain regions. The red region indicates that the ALFF of the amblyopia group is significantly higher than that of the HCs. The blue region indicates that the ALFF of the amblyopia group is significantly lower than that of the HCs.

was consistent with a task-related fMRI study in amblyopia [45]. The three lobes play important roles in the visual pathway. ALFF reduction in these regions may indicate a change in visual function in amblyopia. The frontal lobe plays a significant role in visual information perception, memory, and regulation [46]. The temporal lobe plays an important role in visual perception, facial recognition, and memory association and formation [47]. The occipital lobe is mainly responsible for the functions of visual and motion perception, and occipital lobe damage may cause partial or complete blindness [48, 49]. Bilateral middle temporal and middle occipital gyri are involved in the visual spatial information processing network.

The brain regions, including the fusiform gyrus, caudate nucleus, and superior parietal gyrus, with higher ALFF than HCs were on the right. Our results were different from those of Liang et al. [26], except for the left middle occipital gyrus. However, our values were reduced in the left middle occipital gyrus, whereas those of Liang et al. were increased possibly because our subjects were having unilateral left eye amblyopia, and those of Liang et al. [26] were having a mixture of unilateral left and right eye amblyopia.

Table 4: Regions with statistically significant FC to the left PVC between the amblyopia group and HCs.

Region	BA	Peak MNI coordinates (mm)			Cluster size	*T* value
		X	*Y*	*Z*		
rFFG	37	36	-48	-12	72	5.9695
lFFG	37	-33	-51	-6	85	5.1071
rMFG	—	39	39	33	82	-4.1831
rANG	—	42	-69	54	72	-4.3852

Note: BA: Brodmann's area; MNI: Montreal neurological institute; rFFG: right fusiform gyrus; lFFG: left fusiform gyrus; rMFG: right middle frontal gyrus; rANG: right angular gyrus.

Table 5: Regions with statistically significant FC to the right PVC between the amblyopia group and HCs.

Region (aal)	BA	Peak MNI coordinates (mm)			Cluster size	*T* value
		X	*Y*	*Z*		
rFFG	37	36	-48	-9	82	6.6431
rPUT	—	18	9	-6	178	-3.8243
lORBinf	—	-39	42	-6	91	-3.8903
rSFG	—	21	57	3	353	-4.718
lSFGmed	—	-9	30	51	130	-6.1944
rANG	40	42	-69	54	95	-4.1872
rMFG	8	21	27	42	215	-5.6782

Note: BA: Brodmann's area; MNI: Montreal neurological institute; rFFG: right fusiform gyrus; rPUT: right lenticular nucleus-putamen; lORBinf: left orbital part inferior frontal gyrus; rSFG: right superior frontal gyrus; lSFGmed: right medial superior frontal gyrus; rANG: right angular gyrus; rMFG: right middle frontal gyrus.

We investigated whether the left/right PVC-FC with the whole brain is also altered. Our results revealed that the FC of the PVC to the right angular gyrus and the right middle frontal gyrus were significantly reduced. These regions were all in the visual pathways, possibly indicating the alteration of the PVC-FC in amblyopia. The fMRI analysis in another study [29] also showed that the FC between the PVC and angular gyrus was significantly reduced.

We used the ROIs-FC to analyze whether left eye amblyopia altered the typical brain functional networks. The results showed six reduced FC and three increased FC for amblyopia. The reduced FC was mainly located in the left hemisphere, whereas the increased FC was in the right hemisphere. A bilateral PVC has a weak connectivity with the frontoinsular cortex of the SN. The frontoinsular cortex is regarded as an information integration hub of the SN [14, 50]. The ventral stream passes through the PVC to the frontoinsular cortex. Therefore, the weak connectivity between the bilateral PVC and the frontal-insular cortex of the SN might indicate that the information integration hub of the brain was affected in amblyopia. Moreover, amblyopia might alter the FC of the DMN, SN, PVCN, and HVCN.

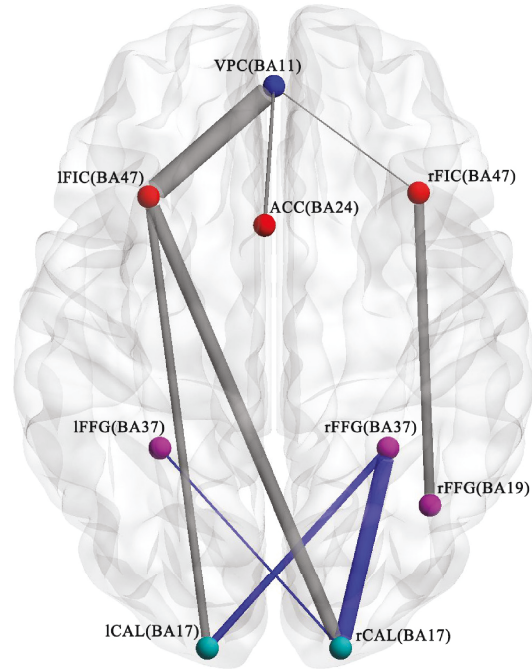

Figure 3: Differences in the FC of ROIs between the amblyopia group and HCs ($P \leq 0.05$, FDR corrected, and cluster size > 85). Blue indicates that the FC strength in the amblyopia group is enhanced compared with that in HCs. Gray implies that the FC strength in the amblyopia group is weakened compared with that in HCs. VPC: ventromedial prefrontal cortex; lFIC: left frontoinsular cortex; rFIC: right frontoinsular cortex; ACC: anterior cingulate cortex; lFFG: left fusiform gyrus; rFFG: right fusiform gyrus; lCAL: left calcarine cortex; rCAL: right calcarine cortex.

The results of these analyses revealed that unilateral amblyopia might alter local brain activity and FC. Amblyopia affects the dorsal and ventral stream of the visual pathway. The findings of the ALFF and PVC-FC analyses showed the reduced ALFF and FC of the angular gyrus of amblyopia. The angular gyrus is a key region of the temporoparietal junction (TPJ) [51], though no standardized anatomical definitions exist in TPJ localization [52]. As TPJ plays a critical role in the integration of top-down and bottom-up attentional controls [53], the reduced ALFF values and FC of the angular gyrus might indicate that amblyopia affected the top-down attentional control.

The PVC-FC and ROIs-FC analyses also confirmed an increased FC between the PVC and the fusiform gyrus. Similarly, the ALFF values in the right fusiform gyrus increased. These results were different from our expectations, and one possible explanation was that PVC belonged to the PVCN, whereas the fusiform gyrus belonged to the HVCN. These results might indicate that FC between the PVCN and HVCN increased. Our hypothesis was that a normal FC between the PVCN and HVCN could form a normal visual perception when visual information arrived at the PVCN for people with normal vision. However, an increased FC between the PVCN and HVCN might be necessary to form a near-normal visual perception when visual information arrived at the PVCN for the amblyopia group.

Table 6: Difference in FC between ROIs in important networks of amblyopia.

	VPC (BA11)	lFIC (BA47)	rFIC (BA47)	ACC (BA24)	lFFG (BA37)	rFFG (BA37)	lCAL (BA17)	rCAL (BA17)	rFFG (BA19)
VPC (BA11)		↓	↓	↓					
lFIC (BA47)	↓						↓	↓	
rFIC (BA47)	↓								↓
ACC (BA24)	↓								
lFFG (BA37)								↑	
rFFG (BA37)							↑	↑	
lCAL (BA17)		↓				↑			
rCAL (BA17)		↓			↑	↑			
rFFG (BA19)			↓						

Note: "↓" indicates a decrease in FC in the amblyopia relative to the HCs. "↑" denotes an increase in FC in the amblyopia relative to the HCs. VPC: ventromedial prefrontal cortex; lFIC: left frontoinsular cortex; rFIC: right frontoinsular cortex; ACC: anterior cingulate cortex; lFFG: left fusiform gyrus; rFFG: right fusiform gyrus; lCAL: left calcarine cortex; rCAL: right calcarine cortex.

The present study has several limitations. First, the number of people enrolled in the experiment was relatively small because of the difficulty in recruiting participants and the poor controllability of the test data of children's test subjects. In the future, we can increase the sample size to reduce the possibility of making a type 1 error. Second, the current study only included left eye amblyopia, which might reduce the inferential effect on amblyopia in the right eye. In future studies, the right eye amblyopia should also be examined to compare the differences between the two groups and HCs. Thus, additional data can be provided to help understand amblyopia and neuroplasticity. These limitations are all aspects of improvement in future research.

5. Conclusions

Our multiple level analysis of rs-fMRI reveals that unilateral amblyopia may alter local brain activity and FC. A reduced activity in the angular gyrus may indicate that amblyopia affects the top-down attentional control. Our study may also help elucidate the neurological mechanisms of amblyopia.

Data Availability

The resting state fMRI data used to support the findings of this study were supplied by the Ethics Committee of the Second Xiangya Hospital under license and so cannot be made freely available. Requests for access to these data should be made to Professor Xiao (13973119862@163.com).

Conflicts of Interest

The authors declare that they have no conflicts of interest.

Acknowledgments

This work was supported by the National Natural Science Foundation of China (grant numbers 81171420 and 61672542), the Hunan Provincial Natural Science Foundation of China (grant number 2019JJ40387), the Science and Technology Planning Project of Hunan Province (grant numbers 2015TP2007 and 2015SK2031), the Changsha Science and Technology Research Program (grant number kc1702033), and the Fundamental Research Funds for the Central Universities of Central South University (grant number 2019zzts595).

References

[1] X. Lin, K. Ding, Y. Liu, X. Yan, S. Song, and T. Jiang, "Altered spontaneous activity in anisometropic amblyopia subjects: revealed by resting-state FMRI," *PLoS One*, vol. 7, no. 8, article e43373, 2012.

[2] D. M. Levi, D. C. Knill, and D. Bavelier, "Stereopsis and amblyopia: a mini-review," *Vision Research*, vol. 114, pp. 17–30, 2015.

[3] D. P. Spiegel, W. D. Byblow, R. F. Hess, and B. Thompson, "Anodal transcranial direct current stimulation transiently improves contrast sensitivity and normalizes visual cortex activation in individuals with amblyopia," *Neurorehabilitation and Neural Repair*, vol. 27, no. 8, pp. 760–769, 2013.

[4] C. Williams, K. Northstone, M. Howard, I. Harvey, R. A. Harrad, and J. M. Sparrow, "Prevalence and risk factors for common vision problems in children: data from the ALSPAC study," *The British Journal of Ophthalmology*, vol. 92, no. 7, pp. 959–964, 2008.

[5] O. Joly and E. Frankó, "Neuroimaging of amblyopia and binocular vision: a review," *Frontiers in Integrative Neuroscience*, vol. 8, p. 62, 2014.

[6] Y. Lerner, P. Pianka, B. Azmon et al., "Area-specific amblyopic effects in human occipitotemporal object representations," *Neuron*, vol. 40, no. 5, pp. 1023–1029, 2003.

[7] D. Bavelier, D. M. Levi, R. W. Li, Y. Dan, and T. K. Hensch, "Removing brakes on adult brain plasticity: from molecular to behavioral interventions," *The Journal of Neuroscience*, vol. 30, no. 45, pp. 14964–14971, 2010.

[8] H. D. H. Brown, R. L. Woodall, R. E. Kitching, H. A. Baseler, and A. B. Morland, "Using magnetic resonance imaging to assess visual deficits: a review," *Ophthalmic & Physiological Optics*, vol. 36, no. 3, pp. 240–265, 2016.

[9] A. Tang, T. Chen, J. Zhang, Q. Gong, and L. Liu, "Abnormal spontaneous brain activity in patients with anisometropic amblyopia using resting-state functional magnetic resonance

imaging," *Journal of Pediatric Ophthalmology and Strabismus*, vol. 54, no. 5, pp. 303–310, 2017.

[10] S. Clavagnier, S. O. Dumoulin, and R. F. Hess, "Is the cortical deficit in amblyopia due to reduced cortical magnification, loss of neural resolution, or neural disorganization?," *The Journal of Neuroscience*, vol. 35, no. 44, pp. 14740–14755, 2015.

[11] A. Miki, G. T. Liu, Z. G. Goldsmith, C.-S. J. Liu, and J. C. Haselgrove, "Decreased activation of the lateral geniculate nucleus in a patient with anisometropic amblyopia demonstrated by functional magnetic resonance imaging," *Ophthalmologica*, vol. 217, no. 5, pp. 365–369, 2003.

[12] R. F. Hess, B. Thompson, G. Gole, and K. T. Mullen, "Deficient responses from the lateral geniculate nucleus in humans with amblyopia," *The European Journal of Neuroscience*, vol. 29, no. 5, pp. 1064–1070, 2009.

[13] B. G. Goodyear, D. A. Nicolle, G. K. Humphrey, and R. S. Menon, "BOLD fMRI response of early visual areas to perceived contrast in human amblyopia," *Journal of Neurophysiology*, vol. 84, no. 4, pp. 1907–1913, 2000.

[14] G. R. Barnes, R. F. Hess, S. O. Dumoulin, R. L. Achtman, and G. B. Pike, "The cortical deficit in humans with strabismic amblyopia," *The Journal of Physiology*, vol. 533, no. 1, pp. 281–297, 2001.

[15] A. Algaze, C. Roberts, L. Leguire, P. Schmalbrock, and G. Rogers, "Functional magnetic resonance imaging as a tool for investigating amblyopia in the human visual cortex: a pilot study," *Journal of AAPOS*, vol. 6, no. 5, pp. 300–308, 2002.

[16] J. Körtvélyes, E. M. Bankó, A. Andics et al., "Visual cortical responses to the input from the amblyopic eye are suppressed during binocular viewing," *Acta Biologica Hungarica*, vol. 63, Supplement 1, pp. 65–79, 2012.

[17] R. Farivar, B. Thompson, B. Mansouri, and R. F. Hess, "Interocular suppression in strabismic amblyopia results in an attenuated and delayed hemodynamic response function in early visual cortex," *Journal of Vision*, vol. 11, no. 14, p. 16, 2011.

[18] X. Li, K. T. Mullen, B. Thompson, and R. F. Hess, "Effective connectivity anomalies in human amblyopia," *NeuroImage*, vol. 54, no. 1, pp. 505–516, 2011.

[19] L. Muckli, S. Kiess, N. Tonhausen, W. Singer, R. Goebel, and R. Sireteanu, "Cerebral correlates of impaired grating perception in individual, psychophysically assessed human amblyopes," *Vision Research*, vol. 46, no. 4, pp. 506–526, 2006.

[20] A. J. Simmers, T. Ledgeway, B. Mansouri, C. V. Hutchinson, and R. F. Hess, "The extent of the dorsal extra-striate deficit in amblyopia," *Vision Research*, vol. 46, no. 16, pp. 2571–2580, 2006.

[21] A. J. Simmers, T. Ledgeway, and R. F. Hess, "The influences of visibility and anomalous integration processes on the perception of global spatial form versus motion in human amblyopia," *Vision Research*, vol. 45, no. 4, pp. 449–460, 2005.

[22] A. J. Simmers, T. Ledgeway, R. F. Hess, and P. V. McGraw, "Deficits to global motion processing in human amblyopia," *Vision Research*, vol. 43, no. 6, pp. 729–738, 2003.

[23] M. E. Raichle, A. M. MacLeod, A. Z. Snyder, W. J. Powers, D. A. Gusnard, and G. L. Shulman, "A default mode of brain function," *Proceedings of the National Academy of Sciences of the United States of America*, vol. 98, no. 2, pp. 676–682, 2001.

[24] B. Biswal, F. Z. Yetkin, V. M. Haughton, and J. S. Hyde, "Functional connectivity in the motor cortex of resting human brain using echo-planar MRI," *Magnetic Resonance in Medicine*, vol. 34, no. 4, pp. 537–541, 1995.

[25] Y. Wu and L. Q. Liu, "Research advances on cortical functional and structural deficits of amblyopia," *Chinese Journal of Ophthalmology*, vol. 53, no. 5, pp. 392–395, 2017.

[26] M. Liang, B. Xie, H. Yang et al., "Distinct patterns of spontaneous brain activity between children and adults with anisometropic amblyopia: a resting-state fMRI study," *Graefe's Archive for Clinical and Experimental Ophthalmology*, vol. 254, no. 3, pp. 569–576, 2016.

[27] J. Wang, L. Hu, W. Li, J. Xian, L. Ai, and H. He, "Alternations of functional connectivity in amblyopia patients: a resting-state fMRI study," in *Medical Imaging 2014: Biomedical Applications in Molecular, Structural, and Functional Imaging*, p. 8, San Diego, CA, USA, March 2014.

[28] T. Wang, Q. Li, M. Guo et al., "Abnormal functional connectivity density in children with anisometropic amblyopia at resting-state," *Brain Research*, vol. 1563, pp. 41–51, 2014.

[29] K. Ding, Y. Liu, X. Yan, X. Lin, and T. Jiang, "Altered functional connectivity of the primary visual cortex in subjects with amblyopia," *Neural Plasticity*, vol. 2013, Article ID 612086, 8 pages, 2013.

[30] C.-G. Yan, X.-D. Wang, X.-N. Zuo, and Y.-F. Zang, "DPABI: data processing & analysis for (resting-state) brain imaging," *Neuroinformatics*, vol. 14, no. 3, pp. 339–351, 2016.

[31] L. Tian, T. Jiang, Y. Wang et al., "Altered resting-state functional connectivity patterns of anterior cingulate cortex in adolescents with attention deficit hyperactivity disorder," *Neuroscience Letters*, vol. 400, no. 1-2, pp. 39–43, 2006.

[32] Y.-F. Zang, Y. He, C.-Z. Zhu et al., "Altered baseline brain activity in children with ADHD revealed by resting-state functional MRI," *Brain and Development*, vol. 29, no. 2, pp. 83–91, 2007.

[33] Q.-H. Zou, C.-Z. Zhu, Y. Yang et al., "An improved approach to detection of amplitude of low-frequency fluctuation (ALFF) for resting-state fMRI: fractional ALFF," *Journal of Neuroscience Methods*, vol. 172, no. 1, pp. 137–141, 2008.

[34] M. J. Hoptman, X.-N. Zuo, P. D. Butler et al., "Amplitude of low-frequency oscillations in schizophrenia: a resting state fMRI study," *Schizophrenia Research*, vol. 117, no. 1, pp. 13–20, 2010.

[35] Z. Zhang, G. Lu, Y. Zhong et al., "fMRI study of mesial temporal lobe epilepsy using amplitude of low-frequency fluctuation analysis," *Human Brain Mapping*, vol. 31, no. 12, pp. 1851–1861, 2010.

[36] Y. Han, J. Wang, Z. Zhao et al., "Frequency-dependent changes in the amplitude of low-frequency fluctuations in amnestic mild cognitive impairment: a resting-state fMRI study," *NeuroImage*, vol. 55, no. 1, pp. 287–295, 2011.

[37] J. A. Maldjian, P. J. Laurienti, and J. H. Burdette, "Precentral gyrus discrepancy in electronic versions of the Talairach atlas," *NeuroImage*, vol. 21, no. 1, pp. 450–455, 2004.

[38] J. A. Maldjian, P. J. Laurienti, R. A. Kraft, and J. H. Burdette, "An automated method for neuroanatomic and cytoarchitectonic atlas-based interrogation of fMRI data sets," *NeuroImage*, vol. 19, no. 3, pp. 1233–1239, 2003.

[39] S. Rachakonda, E. Egolf, N. Correa, and V. Calhoun, "Group ICA of fMRI toolbox (GIFT) manual," 2007, http://www.nitrc.org/docman/view.php/55/295/v1.3d_GIFTManual.pdf.

[40] M. P. van den Heuvel and H. E. Hulshoff Pol, "Exploring the brain network: a review on resting-state fMRI functional connectivity," *European Neuropsychopharmacology*, vol. 20, no. 8, pp. 519–534, 2010.

[41] M. D. Fox, A. Z. Snyder, J. L. Vincent, M. Corbetta, D. C. Van Essen, and M. E. Raichle, "The human brain is intrinsically

organized into dynamic, anticorrelated functional networks," *Proceedings of the National Academy of Sciences of the United States of America*, vol. 102, no. 27, pp. 9673–9678, 2005.

[42] D. A. Fair, A. L. Cohen, N. U. F. Dosenbach et al., "The maturing architecture of the brain's default network," *Proceedings of the National Academy of Sciences of the United States of America*, vol. 105, no. 10, pp. 4028–4032, 2008.

[43] A. K. Roy, Z. Shehzad, D. S. Margulies et al., "Functional connectivity of the human amygdala using resting state fMRI," *NeuroImage*, vol. 45, no. 2, pp. 614–626, 2009.

[44] K. Supekar, L. Q. Uddin, K. Prater, H. Amin, M. D. Greicius, and V. Menon, "Development of functional and structural connectivity within the default mode network in young children," *NeuroImage*, vol. 52, no. 1, pp. 290–301, 2010.

[45] X. H. Yin, M. X. Guo, Y. T. Zhang, Q. J. Li, Y. Fu, and Q. Y. Jiang, "Observation of brain activity on anisometropic amblyopia with fMRI based on amplitude of low frequency fluctuation," *Chinese Journal of Medical Imaging Technology*, vol. 39, no. 5, pp. 855–859, 2010.

[46] N. J. Majaj, M. Carandini, and J. A. Movshon, "Motion integration by neurons in macaque MT is local, not global," *The Journal of Neuroscience*, vol. 27, no. 2, pp. 366–370, 2007.

[47] Y. Shrager, J. J. Gold, R. O. Hopkins, and L. R. Squire, "Intact visual perception in memory-impaired patients with medial temporal lobe lesions," *The Journal of Neuroscience*, vol. 26, no. 8, pp. 2235–2240, 2006.

[48] K. Grill-Spector, T. Kushnir, T. Hendler, S. Edelman, Y. Itzchak, and R. Malach, "A sequence of object-processing stages revealed by fMRI in the human occipital lobe," *Human Brain Mapping*, vol. 6, no. 4, pp. 316–328, 1998.

[49] D. L. Schacter, D. T. Gilbert, and D. M. Wegner, *Psychology*, Worth, New York, NY, USA, 2nd edition, 2011.

[50] X. Li, D. Coyle, L. Maguire, T. M. McGinnity, and R. F. Hess, "Long timescale fMRI neuronal adaptation effects in human amblyopic cortex," *PLoS One*, vol. 6, no. 10, article e26562, 2011.

[51] M. Schurz, M. G. Tholen, J. Perner, R. B. Mars, and J. Sallet, "Specifying the brain anatomy underlying temporo-parietal junction activations for theory of mind: a review using probabilistic atlases from different imaging modalities," *Human Brain Mapping*, vol. 38, no. 9, pp. 4788–4805, 2017.

[52] S. Vossel, J. J. Geng, and G. R. Fink, "Dorsal and ventral attention systems: distinct neural circuits but collaborative roles," *The Neuroscientist*, vol. 20, no. 2, pp. 150–159, 2014.

[53] Q. Wu, C.-F. Chang, S. Xi et al., "A critical role of temporoparietal junction in the integration of top-down and bottom-up attentional control," *Human Brain Mapping*, vol. 36, no. 11, pp. 4317–4333, 2015.

Hindawi
Neural Plasticity
Volume 2019, Article ID 6817839, 18 pages
https://doi.org/10.1155/2019/6817839

Review Article

Visuomotor Behaviour in Amblyopia: Deficits and Compensatory Adaptations

Ewa Niechwiej-Szwedo,[1] **Linda Colpa**,[2] **and Agnes M. F. Wong**[2,3]

[1]*Department of Kinesiology, University of Waterloo, Waterloo, Canada*
[2]*Department of Ophthalmology and Vision Sciences, The Hospital for Sick Children, Toronto, Canada*
[3]*University of Toronto, Toronto, Canada*

Correspondence should be addressed to Ewa Niechwiej-Szwedo; eniechwi@uwaterloo.ca

Received 25 March 2019; Accepted 28 May 2019; Published 9 June 2019

Guest Editor: Claudia Lunghi

Amblyopia is a neurodevelopmental visual disorder arising from decorrelated binocular experience during the critical periods of development. The hallmark of amblyopia is reduced visual acuity and impairment in binocular vision. The consequences of amblyopia on various sensory and perceptual functions have been studied extensively over the past 50 years. Historically, relatively fewer studies examined the impact of amblyopia on visuomotor behaviours; however, research in this area has flourished over the past 10 years. Therefore, the aim of this review paper is to provide a comprehensive review of current knowledge about the effects of amblyopia on eye movements, upper limb reaching and grasping movements, as well as balance and gait. Accumulating evidence indicates that amblyopia is associated with considerable deficits in visuomotor behaviour during amblyopic eye viewing, as well as adaptations in behaviour during binocular and fellow eye viewing in adults and children. Importantly, due to amblyopia heterogeneity, visuomotor development in children and motor skill performance in adults may be significantly influenced by the etiology and clinical features, such as visual acuity and stereoacuity. Studies with larger cohorts of children and adults are needed to disentangle the unique contribution of these clinical characteristics to the development and performance of visuomotor behaviours.

1. Introduction

Amblyopia is a common neurodevelopmental disorder clinically defined as reduced visual acuity that cannot be immediately corrected using optical refraction [1]. The current gold-standard treatment for amblyopia involves occlusion therapy; that is, patching the eye with better acuity to force the use of the amblyopic eye. However, monocular acuity deficits persist in 15-50% of children after treatment, and patients often have deficits in binocular visual function, such as reduced or absent stereopsis, interocular suppression, and gaze instability [2]. Importantly, in addition to the sensory visual deficits, there are a variety of changes in the perceptual, cognitive, and motor functions in children and adults with amblyopia (for reviews, see [3–5]).

The widespread effects of amblyopia on perceptual and sensorimotor functions are not surprising given that vision provides a key sensory input necessary for the optimal development of neural circuits and behavioural functions [3, 6–8]. Abnormal visual experience due to amblyopia during the sensitive periods of development has a direct effect on the morphology and neurophysiological responses of neurons in the striate and extrastriate cortex and the functional connectivity of cortical networks [9–14]. Because the primary visual cortex is the origin of two anatomically and functionally distinct neural pathways, i.e., the ventral stream that projects to the inferior temporal cortex and the dorsal stream that projects to the posterior parietal cortex [15], abnormalities in early visual processing can lead to profound changes in neural processing in cortical areas receiving inputs from the visual cortex [10, 16–18]. Support for the widespread cortical reorganization was recently shown in a study with 5 to 15-year-old children, which reported reduced functional connectivity density at rest in the anisometropic amblyopia

group compared to an age- and gender-similar control group [19]. This study found decreased strength of both short- and long-range connections, which included pathways extending from the occipital cortex to the inferior temporal area, parietal cortex, and the prefrontal cortex. The authors suggested that the abnormal development of long-range connectivity could be the underlying neurophysiological cause of visuomotor deficits in amblyopia.

Visual perceptual changes in amblyopia have been studied extensively (for recent reviews, see [4, 20, 21]). In contrast, the effects of amblyopia on motor function have historically received relatively less attention, with most studies and new insights emerging in the last 10 years. Therefore, the purpose of this paper is to provide a comprehensive review of the literature that advanced our understanding of the neuroplastic changes in visuomotor behaviour in humans with amblyopia. To highlight the changes in motor function associated with decorrelated binocular visual experience during development, we begin by introducing the key components of visuomotor control.

2. Visuomotor Coupling during Goal-Directed Action

The only way to interact with our environment is through action: making eye movements while reading or looking for relevant objects, performing goal-directed reaching and grasping movements with our hands, or navigating to a target destination while avoiding obstacles. The intricate link between vision and movement was first revealed by Held and Hein [22] in a seminal study which demonstrated that normal development of functional vision requires specific experiences where visual and motor inputs are coupled during a particular behaviour. It is now widely accepted that vision provides a key sensory input during the performance of most daily activities, including reaching, grasping, and navigation [23–26].

Reaching and grasping is a complex behaviour, which requires spatial and temporal coordination among multiple sensory and motor systems. For example, following the decision to drink a cup of coffee, the action sequence requires coordinated movements of the eyes to fixate the cup, and then the arm to reach and grasp the cup without knocking it over or spilling its contents. This seemingly simple action requires extensive processing of the visual input along the dorsal cortical stream where neurons are preferentially activated by binocular inputs [27–30]. The first step requires localization of the object in three-dimensional (3D) space with respect to the body [31]. If the object falls on the peripheral retina, saccadic and/or vergence eye movements, as well as head movements, are executed to bring the image onto the fovea of both eyes. The fovea has the highest density of photoreceptors, and correspondingly, the largest representation in the primary visual cortex, which correlates with acuity thresholds [32]. In general, arm movements are initiated following object fixation [33–37], and this temporal coupling could reduce the sensory uncertainty about the object's extrinsic (i.e., 3D location) and intrinsic (i.e., material) properties. Reducing sensory uncertainty about an object's location and properties is important for planning efficient reach and grasp movements (i.e., feedforward control). Importantly, once the reach is initiated, online visual feedback provides information about the ongoing action, and can be used to amend the trajectory when errors are detected [38]. Prior experience and current visual information about an object's material properties are used to plan the grasp by predicting the amount of force necessary to grasp and lift the object [39, 40]. At the time of hand contact, haptic feedback becomes available and can be used to adjust the grip force when the initial visual information is not reliable [41, 42]. Establishing a stable grasp of the object is performed under visual control while fixating the object; however, as soon as the grasp is stable, the eyes move on to the next target [43].

As discussed above, vision thus provides important sensory input for optimal performance of goal-directed behaviours. When visual feedback is restricted or eliminated, movements become slower, less accurate, and more variable. For example, visuomotor performance is significantly diminished when adults with normal vision are forced to perform a task under monocular compared to binocular viewing [44–47]. Similarly, binocular vision provides an important sensory input for the performance of fine motor skills in typically developing children [48]. For example, lower stereoacuity thresholds (i.e., better stereoacuity) are associated with improved grasping performance in school-aged children [49]. On the other hand, children diagnosed with a developmental coordination disorder, which is characterized by reduced motor function, also exhibit abnormal binocular vision [50]. Given that the hallmark of amblyopia is a disruption in binocular visual function, it is important to understand the type and extent of neuroplastic changes in visuomotor behaviour in adults and children with this neurodevelopmental disorder. It is also important to note that neuroplastic changes can be negative, which would manifest as deficits, as well as positive, which would manifest as compensatory adaptations that allow individuals with amblyopia to function normally. Investigating the effects of amblyopia on the oculomotor, manual, and postural systems could provide insight into the neural adaptation of the brain networks involved in sensorimotor transformations underlying the performance of functional behaviours.

3. Profile of Amblyopia

Population studies in children estimate the prevalence of amblyopia to be between 1.3% and 3.6% [2]. Amblyopia arises when children experience decorrelated binocular visual input due to strabismus (i.e., eye misalignment), anisometropia (i.e., unequal refractive error), and strabismus and anisometropia (i.e., mixed mechanism) or form vision deprivation (e.g., infantile cataracts). In children younger than 3 years old, amblyopia is associated with strabismus in 82% of the cases, whereas in older children (3-7 years old), both anisometropia and strabismus each account for ~40% of amblyopia [2]. The clinical profile of visual deficits varies with the etiology of amblyopia. For example, strabismic amblyopia is associated with greater deficits in binocular visual function, including poorer stereoacuity and greater

interocular suppression [51, 52]. A distinct pattern of visual deficits was also found among strabismic, anisometropic, and mixed mechanism amblyopia in a large cohort of adults [53]. Specifically, individuals with strabismus had reduced optotype acuity, as compared to grating acuity, and better than normal contrast sensitivity at low spatial frequencies. In contrast, adults with anisometropic amblyopia had comparable optotype and grating acuity but reduced contrast sensitivity. Because amblyopia etiology is associated with a different age of onset and differential effects on spatial vision, it is important to consider the role of amblyogenic factors on visuomotor development in children, and on motor performance in adults with amblyopia.

4. Effects of Amblyopia on the Oculomotor System

4.1. Fixation Stability. Periods of attempted fixation consist of fixational eye movements that include (slow drift velocity < 2 deg/sec), microsaccades, and high-frequency tremor [54]. The rate of microsaccades in visually normal adults is ~1-2 per second, and they tend to have a small amplitude, typically <0.5° with an asymptote at approximately 1°. The contribution of fixational eye movements to perceptual, cognitive, and motor functions is still under investigation. To date, studies with visually normal adults demonstrated that microsaccades prevent fading during a prolonged fixation (i.e., the Troxler effect) [55], they are associated with better performance during a high-acuity task (i.e., simulated needle threading) [56], and their rate increases during visual search [57]. These studies indicate that microsaccades play an important role in visual information processing. Consequently, abnormal fixational eye movements may contribute to deficits in performance of perceptual, cognitive, and motor tasks.

The effects of amblyopia on fixational eye movements have been studied for over 40 years, and several abnormalities have been documented in both adults and children with different amblyopia etiologies. The early studies included relatively small sample sizes, and they quantified fixation instability by reporting the frequency and amplitude of microsaccades, as well as amplitude and rate of ocular drift [58–61]. They showed that amblyopia etiology was associated with different patterns of fixation instability. Specifically, adults with strabismic amblyopia had an increased frequency of microsaccades (referred to as "saccadic intrusions" by the authors) in the amblyopic eyes, whereas individuals with anisometropic amblyopia had a comparable frequency of microsaccades to the control group [59]. In contrast, a higher amplitude and velocity of drift were evident in the amblyopic eyes regardless of etiology, but not in patients with intermittent strabismus without amblyopia [61]. Due to the small sample size, these studies could not disentangle the association between fixation instability and visual acuity.

Advancements in eye-tracking technology have led to larger studies in children and adults, providing insight into the association between fixation instability and visual acuity deficits. Recent studies quantified fixation instability using a variable called bivariate contour ellipse area (BCEA), which provides a measure of dispersion of the eyes during a fixation interval. Therefore, BCEA is a global measure of fixation instability influenced by the presence of microsaccades and ocular drift, so a larger BCEA could be due to an increased drift or more frequent and/or larger microsaccades. Results from two recent studies with adults are in agreement with the earlier reports. First, Gonzalez et al. [62] tested 13 patients with various amblyopia etiologies and found increased BCEA in the amblyopic eye, which was evident even during binocular viewing. In this small sample, amblyopic eye fixation instability was not associated with the etiology or visual acuity loss. In the second study, Chung et al. [63] assessed fixation instability in a larger cohort that included 14 adults with anisometropic and 14 adults with strabismic amblyopia. In agreement with the earlier studies [58, 59], they found a significantly higher rate and larger amplitude of microsaccades only in patients with strabismic amblyopia. Also consistent with previous studies [59], the amplitude of slow drift was greater during amblyopic eye viewing in all patients, regardless of amblyopia etiology. This was the first study in adults to show that microsaccade amplitude and slow drift amplitude are both associated with reduced visual acuity, and they explain 14% and 30% of total variance, respectively, in amblyopic eye acuity [63].

Several recent studies examined fixation instability in children with amblyopia. Subramanian et al. [64] assessed 52 children with amblyopia due to anisometropia, strabismus, or the mixed mechanism and compared their BCEA with those of nonamblyopic children (i.e., typically developing: $n = 40$ and nonamblyopic strabismus and anisometropia: $n = 37$). Fixation instability during amblyopic eye viewing was almost three times greater in comparison to fellow eye viewing in children with amblyopia, which in turn was comparable to the fixation stability found in the nonamblyopic children viewing with either eye and the left eye of a visually normal control group. This study did not report whether any of the children presented with latent nystagmus; however, fixation instability was larger in the horizontal axis, which is consistent with the presence of fusion maldevelopment nystagmus syndrome. Similarly to adults with amblyopia [63], amblyopic eye fixation instability in children was associated with poorer visual acuity ($r = 0.60$). Interestingly, this correlation was high in a subset of children with strabismic amblyopia ($r = 0.94$) but not statistically significant in the anisometropic amblyopia group ($r = 0.26$). Finally, although there was no significant difference in fixation instability among the subtypes of amblyopia, a trend towards significance was reported ($p = 0.07$). Several reasons could contribute to the lack of significant difference due to etiology in this study with children, which was clearly evident in the adult studies [58, 60]. First, the group with strabismic amblyopia consisted of only 7 children (6 with accommodative esotropia), whereas the anisometropic group included 21 children and the combined mechanism group included 24 children. Second, as mentioned previously, BCEA is a global measure of fixation instability influenced by microsaccades and drift. Based on the results from adult studies, it could be hypothesized that a larger BCEA in children with strabismic amblyopia is due to a larger microsaccade amplitude, whereas in

children with anisometropic amblyopia the larger BCEA is due to larger drift amplitude.

Two additional studies provide further insight into the contribution of microsaccades and drift to fixation instability in the pediatric population. First, Shi et al. [65] tested 28 children with anisometropic amblyopia and compared their performance with an age-matched control group. They found a reduced rate of small-amplitude (i.e. <0.6 deg) microsaccades and an increased rate of larger-amplitude microsaccades during amblyopic eye viewing in comparison to fellow eye viewing, and when compared to children in the control group. These larger microsaccades also had significantly greater amplitude and peak velocity. The association with visual acuity was not examined in that study, presumably because all children had relatively mild amblyopia (range 20/30-20/60). The second study included 36 children with amblyopia and 11 visually normal children; however, 17 children were excluded from the analysis because they presented with latent nystagmus or unreliable eye-tracking data [66]. Therefore, the final sample included 19 children with amblyopia (9 with anisometropia, 4 with strabismus, and 6 with the mixed mechanism), and the severity of amblyopia ranged from mild (20/30) to severe (20/400). Results were in agreement with Shi et al. [65] and showed decreased frequency but increased microsaccade amplitude during amblyopic eye viewing. This behaviour was associated with amblyopia severity: microsaccade amplitude was approximately twice as large in children with severe compared to those with mild amblyopia. Surprisingly, there was no association with amblyopia etiology, which may be due to a relatively small sample size that included only 4 children with strabismic amblyopia. Interestingly, drift variance was higher in both the amblyopic and fellow eyes of children with amblyopia compared to the control group. Furthermore, the extent of drift variance was not associated with microsaccade amplitude or amblyopia severity in this particular study. It is difficult to directly compare these results with adult studies because Shi et al. reported the variance of composite eye position during the intersaccadic interval rather than the amplitude or velocity of slow drift.

The increased drift variance in both eyes of children with amblyopia might have implications for binocular oculomotor control, which was investigated by Kelly et al. [67]. They examined fixation instability of the amblyopic (nonpreferred) and fellow (preferred) eyes, as well as vergence instability during binocular viewing in a large cohort of children (amblyopic: $n = 98$ (49 anisometropic, 15 strabismic, and 34 mixed mechanism); nonamblyopic: $n = 62$ (15 anisometropic, 29 strabismic, and 18 mixed mechanism), and control: $n = 46$). Increased fixation instability (i.e., larger BCEA) was found in the amblyopic and nonamblyopic groups compared to the control group when viewing with the amblyopic or nonpreferred eyes. Moreover, vergence instability was associated with the presence of strabismus in both the amblyopic and nonamblyopic children. Further analysis showed that fixation and vergence instability were both associated with worse stereoacuity ($r = 0.31$). These results indicate that fixation instability is not a unique feature of amblyopia as children with different nonamblyopic visual and oculomotor deficits have significant fixation instability as compared to a visually normal control group.

To summarize, amblyopic eye fixation instability has been found in adults and children. Notably, most studies found no significant difference in BCEA between the control eyes and patients viewing with the fellow eye [62–65]. Comparing the results of studies with children and adults with amblyopia can reveal important insights about developmental plasticity. In particular, three studies with children found no significant association between etiology and fixation instability during monocular viewing [64–66]. In contrast, adults with strabismic amblyopia tend to exhibit significantly larger instability, which is mainly due to the increased frequency and amplitude of microsaccades [63]. One interpretation for these results could be that children with anisometropic amblyopia are able to improve their fixation stability during the course of development. In contrast, the presence of strabismus interferes with the normal development of oculomotor control. Therefore, the potential for positive plasticity may depend on the etiology of amblyopia.

Fixation instability has been associated with poorer visual acuity [63, 64, 66] and worse stereoacuity [61, 64], and these changes could have a negative impact on visuomotor behaviours, such as reading or visual search. This hypothesis was examined by two recent studies. First, Kelly et al. reported a moderate correlation between fellow eye fixation instability (i.e., BCEA) during binocular viewing and binocular reading speed ($r = -0.52$) in a cohort of 20 children with anisometropic amblyopia [68]. In contrast, the association between binocular reading speed and amblyopic eye fixation instability or stereoacuity did not reach significance ($r = -0.32$ and $r = 0.22$, respectively) in that study. Importantly, results from that study showed that children with anisometropia without amblyopia were reading at a comparable speed to a visually normal control group. Unfortunately, the fixation instability measures were not reported for that group. The second study by Chen et al. examined microsaccades during a visual search task in 21 children with amblyopia while viewing was monocular with either the amblyopic or fellow eye; however, binocular viewing was not assessed [69]. Visual search was significantly less accurate and longer during amblyopic eye viewing when compared to the control group. Although search accuracy was comparable between the groups when viewing with the fellow eye, search time remained significantly longer in children with amblyopia. Deficits were further exacerbated in children with latent nystagmus. Collectively, emerging studies suggest that fixation instability may influence functional tasks such as reading and visual search in individuals with amblyopia; however, more studies are needed to assess the role of etiology, visual acuity, and stereoacuity in the performance of these complex tasks.

4.2. Saccades. Voluntary saccades are quick, conjugate eye movements performed to explore the environment in a task-dependent manner [70]. Saccade metrics and their underlying neural networks have been studied extensively, and the subcortical and cortical areas involved in saccade planning and generation are well established [71–75]. At

the behavioural level, saccades can be described by the "main sequence," which quantifies the relation between saccade amplitude and peak velocity and amplitude and duration [76]. Saccades are often studied by asking participants to fixate a target presented in the periphery. The two outcome measures commonly used to assess oculomotor processing are saccade latency (i.e., reaction time) and amplitude, which provide a measure of a decision-making process, specifically, the time needed to detect and initiate a response towards a peripheral target and the accuracy and precision of target localization [77, 78].

The effects of amblyopia on saccadic eye movements were first characterized by Schor [79] in a small sample of five adults with strabismic amblyopia. Using a stimulus that stepped predictably along the horizontal meridian, results showed more variable saccade latency when viewing with the amblyopic eye; however, there was no significant difference in mean latency between the two eyes. The lack of difference was most likely due to the predictable nature of stimulus presentation because a subsequent study reported significant delays in saccade initiation for the amblyopic eye when a stimulus was presented with temporal and spatial uncertainty [80].

Building on these pioneering studies, research into saccadic eye movements has flourished over the past 10 years. Recent studies assessed larger cohorts of patients, and showed that clinical characteristics, such as amblyopia etiology, acuity, and stereoacuity have a significant influence on saccade latency and kinematics. The effects of etiology were clearly demonstrated in a large cohort ($n = 393$) of adults with abnormal vision [81]. The interocular saccade latency difference was 40-80 ms in adults with strabismic and mixed mechanism amblyopia and 25 ms in adults with anisometropic amblyopia. Perdziak et al. [82, 83] reported comparable differences in interocular saccade latency in a smaller cohort of patients with strabismic ($n = 10$) and anisometropic amblyopia ($n = 16$). In contrast, the cohorts assessed by Niechwiej-Szwedo et al. showed a different pattern of results [84, 85]. The mean latency difference between the amblyopic and fellow eye was ~45 ms in both anisometropic and strabismic amblyopia groups. It is possible that the discrepancy between this and other studies is due to patient characteristics; for example, 4 out of 13 anisometropic patients (31% of the sample) had a severe acuity loss and negative stereopsis [85], whereas only 1 of the 16 patients tested by Perdziak et al. in 2014 lacked stereopsis. In general, patients with anisometropic amblyopia have better binocular vision compared to those with strabismic amblyopia; however, nonbinocular observers with anisometropia show a similar pattern of visual deficits to the strabismic group [53]. Thus, it is possible that the increased interocular latency difference in a cohort of anisometropic amblyopia assessed by Niechwiej-Szwedo et al. was due to a greater number of nonbinocular participants.

A detailed regression analysis of patient characteristics, including acuity, stereoacuity, and ocular deviation, on saccade latency was performed in a cohort of 55 adults with various amblyopia etiology (22 anisometropic, 18 strabismic, and 15 mixed mechanism) [86]. The study also included a group of patients with strabismus only ($n = 14$) to disentangle the effects of ocular deviation (tropia) and amblyopia. Multiple regression analysis revealed that visual acuity loss was the strongest predictor of amblyopic eye saccade latency delay, explaining 28% of the total variance. These results are consistent with the McKee et al. study [81], which found a correlation of 0.75 between interocular saccade latency difference and interocular acuity difference.

It is important to mention that subtle, but significant saccade latency deficits may also be present when viewing binocularly or monocularly with the fellow eye. For example, binocular compared to monocular viewing is associated with superior performance on various perceptual and motor tasks in visually normal participants (i.e., binocular summation) [87–90]. Consistent with this literature, a significant, albeit small (~20 ms), binocular advantage was found for saccade latency in the control group, but not in the anisometropic or strabismic groups, where a comparable saccade latency was found during fellow eye and binocular viewing [84, 85]. In general, saccade latency elicited by a sudden onset of a peripheral stimulus is comparable between patients' fellow eye and a monocularly viewing control group [81]. Superficially, these results may seem at odds with a recent study that reported significantly longer saccade latency in strabismic amblyopes viewing with the fellow eye when compared to a monocularly viewing control group [82]. This discrepancy can be explained by considering the experimental paradigms used to assess saccades. Perdziak et al. used the disappearance of a central stimulus as the "go" signal to initiate saccades, which is in contrast to the other studies that used a peripheral stimulus to elicit reflexive saccades. These results provide the first evidence to suggest that strabismic amblyopia may affect saccade initiation when viewing with the fellow eye.

It is well known that saccade latency is task dependent; for example, latency is shorter when the fixation target disappears 50-200 ms prior to the presentation of a peripheral target, which is referred to as the gap effect [77]. It has been suggested that the reduced saccade latency in gap trials is due to the reduced activity of fixation neurons in the superior colliculus [91]. Two recent studies examined the gap effect in adults with amblyopia [92, 93]. Results showed faster saccade latency for gap trials across all viewing conditions suggesting that disengagement of visual attention is not affected by amblyopia. Notably, the delays for saccade initiation during amblyopic eye viewing persisted during the gap trials. In other words, during amblyopic eye viewing saccades were initiated faster during gap trials compared to overlap trials, but the latency was still longer compared to fellow eye viewing.

The accuracy and precision of saccade amplitude are important measures of performance; however, only one study to date assessed these outcomes in a cohort of 55 adults with amblyopia [84–86]. The study found no significant differences in saccade accuracy (i.e., mean amplitude or gain) between the patient and control groups. In contrast, saccade endpoint precision was significantly reduced across all viewing conditions in the anisometropic group [85], and a strong trend towards significance ($p = 0.06$) was found in the strabismic amblyopia group [84]. A detailed regression analysis revealed that 25% of the total variance in saccade amplitude

precision was explained by visual acuity loss [86]. Finally, the presence of amblyopia was associated with the increased frequency of secondary, corrective saccades. It is plausible that these secondary saccades represent a compensatory/adaptive mechanism to correct for the spatial error following the primary saccade.

Reduced saccade precision and an increased number of secondary saccades could impact reading, which is an important daily activity that requires accurate and precise control of eye movements. Several studies that examined reading in amblyopia reported significantly lower reading speeds in children and adults, even during binocular viewing. For example, the reading speed of adults with strabismic amblyopia during binocular viewing was ~67% of that found in an education-matched control group [94]. Reading deficits were associated with a greater frequency of saccades [94, 95]. Studies with children indicate that reading speed is reduced by ~25% in the amblyopic eye compared to the fellow eye, even in the case when the acuity recovers to normal [96]. Two other studies assessed reading during binocular viewing and reported an ~33% reduction in reading speed in the amblyopia group when compared to a visually normal control group as well as children with strabismus only or anisometropia without amblyopia [68, 97]. These studies stress that it is amblyopia, rather than other oculomotor or visual problems, that has a negative impact on reading speed. Importantly, using eye-tracking during the reading task revealed differences in oculomotor behaviour, including greater frequency of regressive or forward saccades [68, 97]. These changes in saccadic behaviour during reading are consistent with studies that reported reduced saccade precision and an increased number of secondary saccades in a single target task [84, 85].

In summary, accumulating evidence demonstrates a significant saccade-related deficit in the amblyopic eye, which is evident regardless of amblyopia etiology. The impairment manifests as a delay in movement initiation and reduced precision of target localization. Moreover, saccade deficits are associated with acuity loss, and may be greater in adults with strabismic and mixed amblyopia [81, 86]. These behavioural deficits could arise as a result of difficulties in processing the sensory information and/or planning the motor response. Several lines of evidence suggest that oculomotor deficits arise from delays in the processing of sensory input. First, studies using electroencephalography and magnetoencephalography showed delayed responses in the visual cortex during amblyopic eye viewing in comparison to fellow eye or binocular viewing [98, 99]. Second, Perdziak et al. used a computational model approach to show that increased latency in amblyopia is due to a slower accumulation of visual information [83, 100]. It has also been argued that fixation instability could contribute to increased saccade latency [81, 92, 101]; however, this hypothesis has not been directly tested in amblyopia. Finally, it is important to note that although saccade deficits are largely confined to the amblyopic eye, some individuals may also exhibit subtle deficits in saccade latency and precision during binocular or fellow eye viewing, which could have a negative impact on visuomotor behaviours, such as reading.

4.3. Smooth Pursuit. Smooth pursuit involves conjugate eye movements that stabilize the image of a moving target on the fovea. Cortical networks involved in smooth pursuit include areas in the parietal and frontal, as well as subcortical areas, with some overlap with the saccade network [72, 102]. While saccades are initiated to reduce the retinal position error, the initiation of pursuit movements requires an estimate of the target's velocity based on retinal input and transformation of that sensory input into a motor output (i.e., matching eye velocity). A common metric used to evaluate the accuracy of smooth pursuit is gain, which is calculated as the ratio of eye velocity to target velocity. A gain of one indicates accurate tracking; that is, the image of a moving target is stabilized close to the fovea. The gain is dependent on a target's velocity, with values approaching 0.9 for target velocities between 10 and 90 deg/sec in visually normal humans [103]. Deficits in smooth pursuit may be expected in individuals with amblyopia given that disruption of the central vision is the hallmark of amblyopia.

Von Noorden led the first investigation into the effects of strabismic amblyopia on smooth pursuit and reported lower pursuit velocity and increased saccade frequency (i.e., catch-up saccades) [104]. These initial findings were corroborated by subsequent studies [79, 105, 106], which shed more light on the critical variables that impact smooth pursuit performance in amblyopia. First, a study that included strabismic and anisometropic groups reported that individuals with strabismic amblyopia exhibited greater deficits in the amblyopic eye, including reduced pursuit velocity, increased frequency of catch-up saccades, and nasal-temporal gain asymmetry [105]. These deficits were most pronounced for small-amplitude targets (<2 deg), where tracking was accomplished mainly with saccades rather than pursuit. Smooth pursuit was evident for larger target amplitude (4-8 deg); however, the gain was significantly lower than normal (0.4-0.7). Since individuals with strabismic amblyopia have increased fixation instability [58, 59, 63] with a strong bias for a nasalward drift [58], Bedell et al. assessed the influence of nasal drift on pursuit accuracy by subtracting the mean velocity of fixational drift from pursuit velocity [106]. Even after applying this correction for drift, results showed persistent reduction in pursuit gain for the amblyopic eyes. Overall, these studies provide clear evidence for smooth pursuit deficits in the amblyopic eye of strabismic amblyopes. In contrast, individuals with anisometropic amblyopia show relativity fewer deficits. Specifically, a recent study showed that the mean pursuit gain of both eyes was comparable to visually normal controls; however, pursuit initiation was slightly delayed (~20 ms), and the gain was more variable in the amblyopic eye [107].

4.4. Vergence. Vergence involves disjunctive eye movements to fixate objects presented at different viewing distances [108]. Disparity vergence is initiated during binocular viewing because objects nearer or farther from the fixation plane stimulate disparate retinal locations. Vergence eye movements are executed to reduce the disparity such that the images on both retinas fall on corresponding retinal points, and an object is perceived as single. Disparity vergence is

neurally coupled with accommodative vergence, which is activated by visual blur [109]. Therefore, vergence can be initiated by the accommodative system during monocular viewing.

The effect of amblyopia on vergence eye movements was examined by Kenyon et al. [110] in seven adult amblyopes (4 strabismic, 3 anisometropic). In comparison to the control group, which showed symmetric vergence during binocular viewing, the strabismic group had asymmetric vergence eye movements, which were accompanied by saccades. Moreover, vergence dynamics were similar during binocular and monocular viewing, indicating a deficit in disparity-driven vergence, and the use of accommodative vergence when viewing binocularly. There was a lack of consistency in vergence behaviour in the anisometropic group: one patient performed similarly to controls, another patient's vergence was highly variable, and one performed similarly to the strabismic group. Clearly, further research with a larger sample size is necessary to gain a better understanding of the effects of clinical characteristics associated with amblyopia on vergence eye movements. Understanding the deficits and adaptation of the vergence system has ecological significance because everyday behaviours involve binocular eye movements. Furthermore, ocular vergence provides an important distance cue about the location of a fixated object, which is critical for planning and executing goal-directed reaching and grasping movements.

To summarize, deficits in eye movements are mainly seen during amblyopic eye viewing for saccades and smooth pursuit in adults with amblyopia. Given that the hallmark of amblyopia is an impairment in binocular vision, vergence movements are also affected; however, this should be examined in more detail with a larger cohort of patients. Importantly, eye movements have not been examined in children with amblyopia, which presents a significant gap in our understanding of how abnormal visual experience affects oculomotor development. Examining eye movements in children with amblyopia during the course of development will provide insight into the plasticity of the visuomotor system.

5. Effects of Amblyopia on the Manual System

Investigating upper limb movements provides insight into the neural control of visuomotor behaviour. For example, simple motor responses, such as a button press, have been used to assess the speed of sensorimotor processing, whereas reaching movements have been used to examine visuomotor mapping, motor planning (i.e., feedforward control), and feedback control [23, 31, 111–114]. One approach to study upper limb movement control involves using a high-speed motion camera to assess three-dimensional (3D) kinematics, including limb trajectory, velocity, and acceleration. In addition to measures such as movement latency, duration, and accuracy, which provide an overall index of motor performance, 3D kinematics provide insight into motor planning and feedback control processes. For example, reaction time, peak acceleration, and peak velocity have been used to assess feedforward control, while the duration of the deceleration phase and limb trajectory path have been used to infer feedback processes [115–119]. The aim of Section 5.1 is to synthesize the current knowledge about the effect of amblyopia on various components of visuomotor behaviour.

5.1. Stimulus Detection. Visuomotor control has been first studied in amblyopia using a manual reaction time paradigm to assess the speed of information processing during a simple stimulus detection task. Results showed increased reaction time for centrally presented targets during amblyopic compared to fellow eye viewing [120–123]. Notably, Hamasaki and Flynn reported a high correlation between visual acuity loss and reaction time in a cohort of strabismic amblyopes ($n = 36$; $r = 0.82$) [122]. Reduced contrast sensitivity in the amblyopic eye has been documented extensively [53, 124–126], and it is well known that reaction time is influenced by stimulus strength (Pieron's Law [127],). Therefore, several studies examined whether equating signal strength (i.e., contrast) across the two eyes reduces the latency delay in the amblyopic eye. These studies highlight important differences as a result of amblyopia etiology. Specifically, in the case of anisometropic amblyopia, there was no significant difference in the manual reaction time between the amblyopic and fellow eyes after stimulus visibility was equated [128]. On the other hand, individuals with strabismic amblyopia exhibited persistent delays during amblyopic eye viewing even when stimulus contrast was equated between the two eyes [101]. The authors suggested that this latency delay could be due to fixation instability, which is greater in adults with strabismic amblyopia [63].

Given that central vision deficits are the hallmark of amblyopia, delayed response initiation for targets presented centrally is not surprising. The manual reaction time to peripheral targets was subsequently assessed during monocular viewing by Chelazzi et al. in a group of people with amblyopia and esotropia which ranged from 6 to 40 PD [129]. Results showed longer manual latency when viewing with the amblyopic eye for stimuli presented in the central 10 deg as compared to more peripheral targets, which was interpreted as a stronger suppression of the central visual field in strabismic amblyopia. Manual button press responses to peripheral targets have not been examined in anisometropic amblyopia. However, Niechwiej-Szwedo et al. investigated manual pointing responses to high-contrast targets presented at 5 and 10 deg eccentricity [130]. Comparing the reaction time of the anisometropic amblyopia group with that of the control group showed no significant difference between the groups or viewing conditions. In contrast, reach initiation was significantly delayed in the strabismic amblyopia group compared to the control group, particularly for the amblyopic eye viewing condition [131], which is consistent with the results from Chelazzi et al. Regression analysis that included the full cohort (i.e., anisometropic, strabismic, and mixed mechanism groups) showed that visual acuity loss explained only 10% of the total variance in reach latency (compared to 28% of variance that was explained by reduced visual acuity for saccade latency in the same cohort) [86].

Altogether, these studies provide important insight into the effect of amblyopia on the speed of target detection during visuomotor processing. First, the delay in motor response

initiation is longer in individuals with strabismic amblyopia compared to anisometropic amblyopia. Second, response initiation is delayed not only for centrally presented targets, but also for peripheral targets presented within 10 deg eccentricity. Third, poorer visual acuity is associated with increased manual response delay, but this relation appears to be stronger for centrally presented targets as compared to responses evoked by peripheral stimuli. Fourth, delays in response initiation persist in strabismic amblyopia after equating stimulus contrast between the two eyes. Overall, these results are consistent with studies that found increased saccade latency during amblyopic compared to fellow eye viewing. Importantly, the delay in both saccade and manual response initiation appears to be greater in individuals with strabismic compared to anisometropic amblyopia.

5.2. Spatial Localization. Abnormal space perception in humans with amblyopia has been documented using a variety of experimental tasks, such as stimulus bisection, alignment, drawing, or pointing [132–138]. Performance on these tasks provides information about the accuracy and precision of spatial localization, as well as spatial distortions. Despite the differences across experimental tasks used, results are remarkably consistent and indicate significant spatial localization deficits for the amblyopic eye, including systematic errors (i.e., lower accuracy) and increased uncertainty (i.e., reduced precision), as well as significant spatial distortions [136–139]. Although these spatial deficits seem to be most pronounced in central vision [140], some studies have reported abnormal spatial localization in the peripheral visual field by up to 15 deg eccentricity [141]. Interestingly, in the latter study, the distortions were highly heterogenous and not associated with clinical characteristics, such as visual acuity or strabismus. These results contrast with a study that examined spatial localization using an alignment task in children ($n = 32$) which showed that the group with strabismic amblyopia had larger constant and precision errors compared to the anisometropic and control groups [142]. Notably, reduced localization precision has been associated with poorer visual acuity in individuals with strabismic amblyopia ($r > 0.80$ for adults, $r = 0.56$ for children). Taken together, significantly greater perceptual spatial deficits have been reported for the amblyopic eye in strabismic compared to anisometropic amblyopia.

Most studies that examined spatial processing in amblyopia focused on perceptual alignment tasks, while only a few examined upper limb reaching/pointing responses. Given the dual visual processing streams [15, 143], it is important to examine the effects of amblyopia on spatial localization using both perceptual and motor tasks. Fronius and Sireteanu [134] examined pointing to targets presented briefly at 5-20 deg from fixation, with and without visual feedback of the arm in a cohort of 19 adults with amblyopia. They showed reduced accuracy and precision during amblyopic eye viewing in a group with strabismic amblyopia. In contrast, individuals with anisometropic amblyopia exhibited a relatively smaller increase in endpoint variability, and their overall performance was similar to the control group. Removing visual feedback of the arm was associated with increased endpoint variability, but this effect was similar across all groups. A more recent study also examined upper limb reaching movements in a large cohort of 55 adults with amblyopia during both monocular, as well as binocular viewing [86]. The main results showed reduced reach endpoint precision during amblyopic eye viewing as compared to monocular viewing in the control group and no differences during fellow eye or binocular viewing. Furthermore, a multivariate analysis revealed that amblyopic eye acuity and eye deviation accounted for 35% of the total variance in reach precision error.

In summary, two main findings emerge from studies that examined the effects of abnormal visual input during development on spatial processing. First, amblyopia is associated with spatial localization deficits across both perceptual (i.e., alignment) and motor (i.e., pointing) tasks. Second, spatial errors are greater in individuals with strabismic amblyopia. Two prominent models have been proposed to explain anomalous spatial processing in amblyopia. Hess et al. used the term "tarachopia" (i.e., scrambled vision) to describe the idea that neural representation of visual input from the amblyopic eye is distorted, which is also referred to as topographical disarray [125]. In contrast, Levi and Klein proposed that retinotopic undersampling of higher spatial frequencies could explain visual misperceptions [144]. These models were both developed to explain the perceptual deficits in spatial vision based on the results from stimulus alignment experiments. In order to explain the spatial deficits for a visuomotor pointing task, one must also consider the mapping of sensory input onto a motor response. In other words, the accurate and precise execution of upper limb movements requires the transformation of the sensory input, such as the spatial location of the target in egocentric coordinates, into an appropriate set of motor commands. Experimental evidence suggests that increased noise in the sensory signal representation due to topographical disarray or undersampling has a negative effect on the sensorimotor transformation process.

5.3. Feedforward and Feedback Control of Upper Limb Reaching and Grasping Movements. To gain a better understanding into how abnormal visual experience during development affects the control of upper limb movements, recent studies used kinematics to examine performance on reach-to-touch [130, 131, 145] and reach-to-grasp tasks [146–151]. The neural control of these movements is incredibly complex, and several theoretical models have been proposed in an attempt to explain the underlying mechanisms. Therefore, prior to considering the effects of amblyopia on upper limb movement performance, it is important to introduce a framework for sensorimotor control, and to define the kinematic outcome measures that provide insight into the control mechanism.

Optimal motor performance can be operationally defined as movements that are performed fast and accurately, while minimizing the energy and mental costs [152]. In order to perform the movement quickly, it is necessary to generate a large force (i.e., large impulse) to accelerate the limb towards the goal target. In general, increasing movement speed is

associated with increased endpoint variability, which leads to a well-known speed-accuracy trade-off described by Fitts' Law [153, 154]. However, it is widely accepted that trajectory errors associated with greater limb acceleration can be amended during movement execution, provided that the movement duration is long enough and sensory feedback is available [119, 155]. Therefore, in the case of reaching movements, optimal motor performance depends on the interaction between feedforward control (i.e., generate a large force to accelerate the limb ballistically towards the target) and feedback control (i.e., use sensory feedback to correct trajectory errors as the arm approaches the target) [23, 156]. Recording limb kinematics using a high-speed motion camera provides insight into feedforward and feedback control processes [117, 157]. For example, peak acceleration occurs within the first 100 ms after movement onset. Therefore, it cannot be modulated based on sensory feedback and consequently reflects aspects of feedforward control (i.e., open-loop control). Typical reaching movements are longer than 500 ms; therefore, the latter part of the limb trajectory can be controlled using sensory feedback. Extensive evidence for online control comes from studies which show a significant reduction in spatial variability of limb trajectory after peak velocity [118, 155, 158].

Feedforward and feedback control processes have been examined in adults with amblyopia using kinematics for two different experimental tasks: reach-to-touch [159] and reach-to-grasp [148]. In addition, the developmental aspects of upper limb control have been assessed using a reach-to-grasp task in children with amblyopia [149, 151]. Reach-to-touch movements were studied by asking participants to point to a peripheral visual target randomly presented at 5 or 10 deg to the left or right of fixation as fast and accurately as possible. This relatively simple motor task revealed that amblyopia is associated with adaptation of feedforward control [130, 131]. This conclusion is supported by the following evidence. First, the overall movement duration was approximately 100 ms longer in the amblyopic group compared to the control group, regardless of viewing condition. Critically, partitioning the total movement duration into the acceleration and deceleration intervals (i.e., the time spent in the acceleration and deceleration phase), revealed a significant increase in the duration of the acceleration interval, while duration of the deceleration was not statistically different from the control group. In addition, the magnitude of peak acceleration was significantly lower in the amblyopic groups compared to the control group, which was evident across all viewing conditions. These results clearly show that amblyopia mainly affects the early movement kinematics, which reflect changes in feedforward control of upper limb reaching movements. Notably, changes in feedforward control (i.e., longer acceleration duration and lower peak acceleration) were associated with improved reach endpoint precision during binocular and fellow eye viewing, but not during amblyopic eye viewing. In contrast, the control group displayed a different control strategy in which a longer deceleration interval duration was associated with a higher endpoint precision. Results from the control group are consistent with a large body of research, which shows that optimal movement execution depends on the interaction between feedforward and feedback control where trajectory errors, due to a large initial acceleration force, are seamlessly corrected online to achieve fast, accurate, and precise movements [155, 157, 160, 161]. Importantly, artificially reducing visual acuity in one eye using plus lenses to simulate mild amblyopia in adults with normal vision did not affect their reach kinematics significantly [162]. Specifically, there were no changes in the feedforward or feedback control processes of reaching associated with a short-term, transient visual disruption in adults.

To summarize, detailed kinematic analysis revealed that decorrelated binocular visual experience during development is associated with a neural adaptation of the motor control system that involves an adjustment of the speed-accuracy trade-off function [163]. In other words, the available data suggest that in order to achieve similar movement precision to visually normal controls, individuals with amblyopia execute slower movements by reducing the initial acceleration (i.e., the ballistic part of the movement). Importantly, this adaptation in movement planning and execution allowed patients to achieve a similar endpoint precision during fellow eye and binocular viewing, but deficits persisted during amblyopic eye viewing. Additional regression analysis showed that more effective online control during amblyopic eye viewing was associated with better stereoacuity and smaller ocular deviation [86]. Finally, a similar visuomotor adaptation of reaching was evident regardless of amblyopia etiology, as well as in a group of adults with strabismus only, without amblyopia, which strongly indicates that normal binocular experience during development is necessary for optimal development of the visuomotor control system.

The planning and execution of reach-to-grasp movements is more complex compared to reach-to-touch because in addition to the transport component, grasping involves interacting with an object. In other words, in addition to localizing the target in egocentric coordinates to plan the reach movement [31], the central nervous system must process relevant object features to program grip aperture and grasp forces [39]. Grip aperture is defined as the distance between the thumb and index finger, and maximum aperture occurs around the time of peak deceleration [164]. Extensive research has shown that maximum grip aperture is scaled precisely to object size, such that a larger aperture is associated with larger objects. The fact that maximum grip aperture occurs during reach execution and that it is scaled to an object's size indicates that this kinematic variable is planned based on the initial visual input prior to reach initiation. Once the hand contacts the object, grip and load forces need to be generated to lift and transport the object. Studies have also shown that these forces are generated predictively based on an object's properties, such as weight, friction, density, and texture, which are encoded by the visual modality [113, 165–170]. Therefore, visual input provides critical sensory input for efficient performance of prehension movements.

Precision grasping has been studied in adults and children with amblyopia using a task that involves gripping cylindrical objects. The first study included a group of 20 adults with amblyopia (10 with strabismus and 10 with

anisometropia; amblyopic eye acuity 0.20-2.80 logMAR) [148]. Movements performed during amblyopic eye viewing were slower, less accurate, and more inconsistent, and these deficits were apparent during transport and grasping. Although peak grip aperture was comparable between the groups during binocular and fellow eye viewing, impairment in grasp execution was evident once the hand contacted the object. Specifically, grasp application time was 22% longer, and grasping errors, defined as adjustments of the thumb and index finger around the object, were more than twice as high in the amblyopic group (control: 8.7% vs. amblyopia: 17.7%). In this study, visual acuity loss explained 50% of the total variance in grasp errors during binocular viewing. In contrast, etiology or stereo deficits were not significantly associated with prehension performance: grasping errors were similar in the groups with reduced and negative stereoacuity. A follow-up study used the same experimental approach to assess grasping in 20 individuals with a history of amblyopia, who had regained good visual acuity via occlusion therapy (i.e., 14 had normal acuity and 6 out of 20 had residual amblyopia with an acuity of 0.20-0.24) [150]. The results showed a similar pattern of prehension deficits during binocular viewing, with ~25% longer grasp application time and more than twice as many grasping errors. Consistent with Grant et al.'s study, no significant difference was found in grasp errors between the group with residual stereo and the stereo negative group. However, after removing a couple of outliers (2 out of 10), stereoacuity explained 63% of total variance in grasp application in the group with residual stereo. Overall, these studies provided the first insight into the effects of amblyopia on prehension performance using detailed kinematic measures. Both studies showed significant deficits during grasp application. Acuity and stereoacuity could be both contributing to these deficits; thus, a study with a larger sample size is required to disentangle their individual contributions.

Two other studies examined prehension in amblyopia while manipulating the environmental context. First, the effects of object contrast and lighting on prehension were examined in 13 adults with strabismic or mixed mechanism amblyopia [147]. The authors hypothesized that grasping deficits in amblyopia would be exacerbated when the task becomes more challenging; that is, when the object has low contrast or the task is performed in low lighting. Results from the study did not support this hypothesis: grasping performance was slower when the task became more challenging, but the relative changes were similar in both groups. In other words, the amblyopic group had a longer reaching and grasping duration even in the high-contrast and high-luminance condition, but when the task difficulty increased, they were not at a greater disadvantage in comparison to visually normal controls.

The second study examined prehension to objects surrounded by distractors/flankers in 20 adults with amblyopia. Using this experimental approach provides greater ecological insight into the effects of amblyopia on prehension because the objects that we interact with everyday are usually in proximity to other objects [146]. Results were consistent with previous studies showing slower overall performance, with a disproportionally greater deficit when the flanker objects were positioned in front or behind the target object as compared to either the left or right side. In contrast to the study by Grant et al., which found no significant difference in grip aperture between the groups during binocular viewing, aperture was significantly reduced in the presence of flanker objects in the amblyopic compared to the control group. These results indicate that patients with amblyopia adapted a more cautious approach strategy when reaching towards objects surrounded by flankers. It is possible that changes in prehension behaviour were due to visual crowding, which is one of the consequences of amblyopia [171]. On the other hand, changes in prehension could arise due to difficulties in estimating the depth of the target and flanker objects because the deficits were most pronounced when the flankers were presented in front or behind the object.

To summarize, significant prehension deficits have been found in adults with amblyopia during binocular viewing when interacting with high-contrast objects in a well-lit environment. In general, prehension was performed slower and the greatest impact was seen on grasp execution, rather than the reach component. The two measures commonly used to assess grasping are peak grip aperture and grasp duration. It is the latter measure that seems to be more impaired in amblyopia, which provides important insight into the nature of the control mechanism that is disrupted. First, results from Grant et al. [148] showed that peak grip aperture was scaled to object size and was comparable to the control group during binocular viewing. This suggests that despite having abnormal binocular input, individuals with amblyopia were able to extract the relevant visual information about the object's size to adjust their fingers appropriately during reaching. On the other hand, Buckley et al. [146] provided evidence to suggest that grip aperture was affected when the task became more challenging. Most importantly, all studies to date show significant grasping deficits after the hand contacts the object, which manifest as a prolonged handling duration. One interpretation for this finding is that patients have difficulty extracting, processing, or encoding specific object features that are critical for guiding the fingers' positioning around the object and/or for the programming of grip and lift forces. Because these forces are generated predictively based on the visual input acquired prior to contacting the object [39, 170], the specific pattern of grasping deficits in amblyopia indicates a compromised feedforward control of prehension. Prolonged grasping time while handling the object before the lift could be a compensatory strategy where haptic feedback plays a critical role in adjusting forces in order to grasp and lift the object successfully [172]. Several lines of evidence suggest that stereoacuity may play an important role in feedforward control of grasping forces [150]. First, grasping deficits persist in individuals with abnormal stereoacuity who "recovered" from amblyopia based on the current clinical definition (i.e., improved visual acuity). Second, reducing stereoacuity by simulating amblyopia with plus lenses leads to similar grasping deficits in visually normal individuals.

Results from adult studies are consistent with studies that examined prehension kinematics in a large cohort of 55

children with amblyopia aged 5 to 9 years old [149, 151]. Significant deficits, including longer movement duration and greater reach and grasp error rate, were found during binocular viewing in the younger group (5-6 yrs old), regardless of stereoacuity status. In contrast, stereoacuity was associated with improved grasping performance in the older group (7-9 yrs old). In fact, movement duration and grasping errors during binocular viewing were comparable in the control group and children with residual stereoacuity, but the group with negative stereopsis performed significantly worse. Most interestingly, a few longitudinal case studies presented in this paper showed that recovery of stereoacuity, but not just visual acuity, was associated with improved prehension kinematics. The results from this kinematic study suggest that children with better binocularity might be able to catch up to their peers, and with time develop appropriate sensorimotor strategies to perform similarly on this type of prehension task.

The fact that stereoacuity seems to be important for prehension and fine motor skills is also supported by a recent study that examined the effects of a newly developed binocular treatment (dichoptically presented iPod game) on fine motor skills in 18 children with mixed amblyopia etiology (mean age 8.5 yrs) [173]. Motor performance was assessed using a clinical test (the Bruininks-Oseretsky Test), which provides an overall, age-standardized score of motor proficiency. Following a 5-week training protocol, there was a significant improvement in stereoacuity (mean change 0.56 log arc sec) and an ~30% improvement in motor proficiency (mean change in standardized score 4.17). Interestingly, greater improvement in motor performance was associated with better baseline binocular vision ($r = 0.75$), rather than improvements in stereoacuity due to treatment. These results highlight the importance of binocular vision in the context of motor learning. Indeed, adults with poor stereovision show very little improvement after intensive training on a one-handed ball catching task [174].

Altogether, the accumulating evidence suggests that better binocular visual function, specifically stereoacuity, could provide a critical sensory input for the optimal development of prehension and other fine motor skills. Importantly, research shows that younger children seem to be affected to a greater extent compared to older children or adults. The improved performance of adults may be due to extensive practice and learning of compensatory strategies; for example, adaptation might involve relying on haptic feedback more when grasping and manipulating objects. However, studies with a larger sample size of adults and children over a larger age range (i.e., >9 yrs old) are required to establish a more definitive relation between stereoacuity and prehension performance, as well as the contribution of stereoacuity to motor learning. Using kinematics will provide useful insight into which aspects of sensorimotor control are affected, and how the system adapts to compensate for the abnormal visual experience during development.

6. Effects of Amblyopia on Balance and Gait

Maintaining postural stability while standing or navigating through the environment is of paramount importance for everyday function. Sensorimotor integration is key for postural stability control. Vision, along with vestibular and somatosensory inputs, provides sensory information about the position of the body in relation to the environment to ensure upright balance and forward progression during gait [175]. Postural stability during quiet stance is usually examined under increasingly challenging conditions, such as reduced base of support (i.e., standing on one leg) or reduced sensory cues (i.e., standing with eyes closed or on a soft surface). Similarly, obstacles have been used to assess walking in a more challenging environment [176].

There is a dearth of studies that examined the effect of amblyopia on balance and gait. Odenrick et al. provided the first report which included 23 children with strabismic amblyopia (the group also included 12 children with strabismus without amblyopia, aged 4.5-10.5 years) [177]. The results from the balance test showed that girls had significantly reduced postural stability, whereas boys performed similarly to the control group. Evaluation of gait parameters revealed that children with strabismus (and amblyopia) had significantly shorter stride length and shorter single-support time. This study found no association between binocular function and balance or gait measures.

The next study that examined the effect of impaired stereovision on adaptive gait included 16 adults (9 were amblyopic (5 had negative stereopsis), 7 were strabismic only (5 had negative stereopsis)) [178]. Gait parameters were assessed during an obstacle-crossing task where the task difficulty was manipulated using different obstacle heights, and the task was performed during binocular and monocular viewing. Detailed analysis of the gait pattern revealed that increasing the difficulty of the task by increasing obstacle height had a significantly greater impact in the stereo-deficient group that included individuals with amblyopia and strabismus. Specifically, increasing the obstacle's height was associated with slower gait velocity, a shorter step length when approaching the obstacle, and a higher toe clearance in the stereo-deficient group in comparison to the control group. Similar gait modifications were seen across all viewing conditions. The authors interpreted these results as a deficit in using visual input to plan the approach to the obstacle (i.e., feedforward regulation of the gait pattern). Other studies with visually normal subjects where binocular viewing was manipulated reached similar conclusions and suggested that monocular viewing disrupts the feedforward aspect of adaptive gait control [26, 179]. More specifically, increased uncertainty about an obstacle's height or location could lead to a more cautious approach that includes slower speed and higher toe clearance. Because the study did not report a separate analysis for subjects with and without amblyopia [178], it remains to be established whether amblyopia and strabismus have the same effect on adaptive gait, and the extent to which stereoacuity directly contributes to these changes in behaviour.

Finally, a recent study compared postural stability in a cohort of children with amblyopia ($n = 18$), strabismus without amblyopia ($n = 16$), and a visually normal control group ($n = 22$) [180]. Balance was assessed using the Bruininks-Oseretsky Test, and included standing tasks with increasing

levels of difficulty; for example, standing in tandem or on one leg with eyes open or closed. The standardized balance score was significantly lower in the amblyopia group (mean 9.0) and the strabismic group (mean 8.6) in comparison to the control group (mean 18.9). Detailed analysis revealed the greatest deficits in the most challenging tasks; that is, when the base of support was narrow and visual input was removed in the eyes-closed condition. These findings suggest that despite abnormal vision, children rely on this sensory input to maintain balance and there is no evidence indicating compensatory adaptation involving the use of other sensory inputs (i.e., relying more on the vestibular or somatosensory input). Notably, there was no significant relation between balance scores and clinical patient characteristics, such as visual acuity or stereoacuity.

To summarize, evidence from a limited number of studies indicates that decorrelated binocular experience during development has a significant impact on the control of postural stability in children. Parallel research in adults with strabismus revealed reduced stability during quiet stance in comparison to a control group [181]. Surprisingly, the study showed better balance control when patients were viewing with the nondominant eye, and while performing a cognitive task. In contrast, another study with a larger cohort of children and adults with strabismus showed that postural stability was significantly worse only in children with strabismus, while adults performed similarly to a visually normal control group [182]. It appears that standing balance has not been examined in adults with amblyopia. This gap in knowledge should be addressed to clarify whether the deficits seen in children with amblyopia persist into adulthood or resolve at some age. Importantly, the deficits in balance control and gait are unmasked under more challenging testing conditions.

7. Conclusion

The goal of this paper was to provide a synthesis of current knowledge highlighting the changes associated with amblyopia across the three motor systems: oculomotor, manual, and postural. The accumulating body of research indicates that decorrelated visual experience during the early childhood years has a significant impact on visuomotor behaviour, including eye movements and upper limb reaching and grasping, as well as postural stability control. Examination of performance measures across different tasks shows that deficits are clearly evident during amblyopic eye viewing. These deficits include increased latency, slower execution, and reduced movement precision. Importantly, binocular viewing is also associated with some behavioural deficits, such as reduced reading speed, slower prehension, and decreased postural stability. In-depth kinematic analysis revealed that patients adapt compensatory strategies to improve performance. These compensatory behaviours involve secondary corrective eye movements, adjustment of the speed-accuracy trade-off function, and increased reliance on somatosensory feedback when manipulating objects. It is possible that the compensatory behaviours that are seen during binocular and fellow eye viewing depend on higher level cortical plasticity involving changes in connectivity and function of large cortical networks beyond the primary visual areas [19]. Importantly, using these compensatory strategies is associated with improved movement accuracy and precision; however, the cost is time: motor tasks are performed significantly slower. Moreover, it seems that deficits become more apparent when the tasks become more difficult or challenging, and that individuals with strabismic amblyopia may be affected to a greater degree. In regard to the sensorimotor control mechanism, experimental results suggest that amblyopia impacts feedforward and feedback movement control processes. Changes in feedforward control were most apparent during the performance of simple reaching movements, while feedforward and feedback control processes were both affected during prehension. Specifically, grasp execution was slower because the initial movement plan (i.e., feedforward control) was less accurate, which consequently led to a prolonged execution time in order to correct the errors. Finally, the majority of research examining the consequences of amblyopia on visuomotor function in humans focused on adult behaviour; therefore, our understanding of the developmental changes during childhood is quite limited. Addressing this gap in knowledge will provide important insights into the extent of neural plasticity and the clinical characteristics that influence positive and negative plasticity (i.e., compensatory adaptations and deficits).

7.1. Clinical Implications for Assessment and Treatment. Accumulating evidence indicates that binocularity, rather than just monocular visual acuity, is the critical sensory input contributing to optimal development of the sensorimotor control system. Correlated binocular experience during sensitive periods of development may be necessary for the normal development of the sensorimotor systems involved in the execution of eye movements, upper limb movements, and postural stability. Most intriguingly, developing innovative therapies that target the visuomotor system might facilitate the recovery of binocularity [183]. Emerging research highlights the functional impact of amblyopia on behaviours that involve spatiotemporal coordination among the visual and motor systems [3, 5, 184]. Yet, the effects of amblyopia on motor skill performance are not currently assessed during routine clinical assessments. Given the experimental evidence reviewed in this paper and additional studies that reported motor deficits on clinical tests [185–187], it may be important to consider adding a visuomotor assessment in this population to have a more comprehensive phenotype profile of individuals affected by amblyopia.

Conflicts of Interest

The authors declare that there is no conflict of interest regarding the publication of this paper.

References

[1] D. K. Wallace, M. X. Repka, K. A. Lee et al., "Amblyopia Preferred Practice Pattern®," *Ophthalmology*, vol. 125, no. 1, pp. P105–P142, 2018.

[2] E. E. Birch, "Amblyopia and binocular vision," *Progress in Retinal and Eye Research*, vol. 33, pp. 67–84, 2013.

[3] S. Grant and M. J. Moseley, "Amblyopia and real-world visuomotor tasks," *Strabismus*, vol. 19, no. 3, pp. 119–128, 2011.

[4] D. M. Levi, D. C. Knill, and D. Bavelier, "Stereopsis and amblyopia: A mini-review," *Vision Research*, vol. 114, no. 30, pp. 17–30, 2015.

[5] A. L. Webber, "The functional impact of amblyopia," *Clinical and Experimental Optometry*, vol. 101, no. 4, pp. 443–450, 2018.

[6] O. Braddick and J. Atkinson, "Development of human visual function," *Vision Research*, vol. 51, no. 13, pp. 1588–1609, 2011.

[7] C. Siu and K. M. Murphy, "The development of human visual cortex and clinical implications," *Eye and Brain*, vol. Volume 10, pp. 25–36, 2018.

[8] J. Atkinson, "The Davida Teller Award Lecture, 2016: Visual Brain Development: a review of "Dorsal Stream Vulnerability"—motion, mathematics, amblyopia, actions, and attention," *Journal of Vision*, vol. 17, no. 3, p. 26, 2017.

[9] D. H. Hubel, T. N. Wiesel, and S. LeVay, "Plasticity of ocular dominance columns in monkey striate cortex," *Philosophical Transactions of the Royal Society, B: Biological Sciences*, vol. 278, no. 961, pp. 377–409, 1977.

[10] O. Joly and E. FrankÃ, "Neuroimaging of amblyopia and binocular vision: a review," *Frontiers in Integrative Neuroscience*, vol. 8, 2014.

[11] H. Bi, B. Zhang, X. Tao, R. S. Harwerth, E. L. Smith, and Y. M. Chino, "Neuronal responses in visual area V2 (V2) of macaque monkeys with strabismic amblyopia," *Cerebral Cortex*, vol. 21, no. 9, pp. 2033–2045, 2011.

[12] A. M. F. Wong, "New concepts concerning the neural mechanisms of amblyopia and their clinical implications," *Canadian Journal of Ophthalmology*, vol. 47, no. 5, pp. 399–409, 2012.

[13] B. T. Barrett, A. Bradley, and P. V. McGraw, "Understanding the neural basis of amblyopia," *The Neuroscientist*, vol. 10, no. 2, pp. 106–117, 2004.

[14] J. D. Mendola, J. Lam, M. Rosenstein, L. B. Lewis, and A. Shmuel, "Partial correlation analysis reveals abnormal retinotopically organized functional connectivity of visual areas in amblyopia," *NeuroImage: Clinical*, vol. 18, pp. 192–201, 2018.

[15] M. Mishkin and L. G. Ungerleider, "Contribution of striate inputs to the visuospatial functions of parieto-preoccipital cortex in monkeys," *Behavioural Brain Research*, vol. 6, no. 1, pp. 57–77, 1982.

[16] J. Hyvärinen, L. Hyvärinen, M. Färkkilä, S. Carlson, and L. Leinonen, "Modification of visual functions of the parietal lobe at early age in the monkey," *Medical Biology*, vol. 56, no. 2, pp. 103–109, 1978.

[17] S. Carlson, A. Pertovaara, and H. Tanila, "Late effects of early binocular visual deprivation on the function of Brodmann's area 7 of monkeys (*Macaca arctoides*)," *Developmental Brain Research*, vol. 33, no. 1, pp. 101–111, 1987.

[18] J. D. Mendola, I. P. Conner, A. Roy et al., "Voxel-based analysis of MRI detects abnormal visual cortex in children and adults with amblyopia," *Human Brain Mapping*, vol. 25, no. 2, pp. 222–236, 2005.

[19] T. Wang, Q. Li, M. Guo et al., "Abnormal functional connectivity density in children with anisometropic amblyopia at resting-state," *Brain Research*, vol. 1563, pp. 41–51, 2014.

[20] K. Meier and D. Giaschi, "Unilateral amblyopia affects two eyes: fellow eye deficits in amblyopia," *Investigative Ophthalmology & Visual Science*, vol. 58, no. 3, pp. 1779–1800, 2017.

[21] L. M. Hamm, J. Black, S. Dai, and B. Thompson, "Global processing in amblyopia: a review," *Frontiers in Psychology*, vol. 5, 2014.

[22] R. Held and A. Hein, "Movement-produced stimulation in the development of visually guided behavior," *Journal of Comparative and Physiological Psychology*, vol. 56, no. 5, pp. 872–876, 1963.

[23] D. Elliott, S. Hansen, L. E. M. Grierson, J. Lyons, S. J. Bennett, and S. J. Hayes, "Goal-directed aiming: two components but multiple processes," *Psychological Bulletin*, vol. 136, no. 6, pp. 1023–1044, 2010.

[24] M. A. Goodale, "Transforming vision into action," *Vision Research*, vol. 51, no. 13, pp. 1567–1587, 2011.

[25] M. M. Hayhoe, "Vision and action," *Annual Review of Vision Science*, vol. 3, no. 1, pp. 389–413, 2017.

[26] A. E. Patla, E. Niechwiej, V. Racco, and M. A. Goodale, "Understanding the contribution of binocular vision to the control of adaptive locomotion," *Experimental Brain Research*, vol. 142, no. 4, pp. 551–561, 2002.

[27] L. Minini, A. J. Parker, and H. Bridge, "Neural modulation by binocular disparity greatest in human dorsal visual stream," *Journal of Neurophysiology*, vol. 104, no. 1, pp. 169–178, 2010.

[28] R. M. Rutschmann and M. W. Greenlee, "BOLD response in dorsal areas varies with relative disparity level," *Neuroreport*, vol. 15, no. 4, pp. 615–619, 2004.

[29] B. G. Cumming and G. C. DeAngelis, "The physiology of stereopsis," *Annual Review of Neuroscience*, vol. 24, no. 1, pp. 203–238, 2001.

[30] A. J. Parker, "Binocular depth perception and the cerebral cortex," *Nature Reviews. Neuroscience*, vol. 8, no. 5, pp. 379–391, 2007.

[31] J. D. Crawford, W. P. Medendorp, and J. J. Marotta, "Spatial transformations for eye-hand coordination," *Journal of Neurophysiology*, vol. 92, no. 1, pp. 10–19, 2004.

[32] R. O. Duncan and G. M. Boynton, "Cortical magnification within human primary visual cortex correlates with acuity thresholds," *Neuron*, vol. 38, no. 4, pp. 659–671, 2003.

[33] H. Bekkering and U. Sailer, "Commentary: coordination of eye and hand in time and space," *Progress in Brain Research*, vol. 140, pp. 365–373, 2002.

[34] N. Mennie, M. Hayhoe, and B. Sullivan, "Look-ahead fixations: anticipatory eye movements in natural tasks," *Experimental Brain Research*, vol. 179, no. 3, pp. 427–442, 2007.

[35] R. S. Johansson, G. Westling, A. Backstrom, and J. R. Flanagan, "Eye-hand coordination in object manipulation," *The Journal of Neuroscience*, vol. 21, no. 17, pp. 6917–6932, 2001.

[36] R. A. Abrams, D. E. Meyer, and S. Kornblum, "Eye-hand coordination: oculomotor control in rapid aimed limb movements," *Journal of Experimental Psychology: Human Perception and Performance*, vol. 16, no. 2, pp. 248–267, 1990.

[37] U. Sailer, T. Eggert, J. Ditterich, and A. Straube, "Spatial and temporal aspects of eye-hand coordination across different tasks," *Experimental Brain Research*, vol. 134, no. 2, pp. 163–173, 2000.

[38] V. Gaveau, L. Pisella, A. E. Priot et al., "Automatic online control of motor adjustments in reaching and grasping," *Neuropsychologia*, vol. 55, pp. 25–40, 2014.

[39] J. R. Flanagan, M. C. Bowman, and R. S. Johansson, "Control strategies in object manipulation tasks," *Current Opinion in Neurobiology*, vol. 16, no. 6, pp. 650–659, 2006.

[40] R. S. Johansson, "Sensory control of dexterous manipulation in humans," in *Hand and Brain: the Neurophysiology and Psychology of Hand Movements*, vol. 1996, pp. 381–414, Academic Press, San Diego.

[41] R. S. Johansson and G. Westling, "Programmed and triggered actions to rapid load changes during precision grip," *Experimental Brain Research*, vol. 71, no. 1, pp. 72–86, 1988.

[42] K. J. Cole and J. H. Abbs, "Grip force adjustments evoked by load force perturbations of a grasped object," *Journal of Neurophysiology*, vol. 60, no. 4, pp. 1513–1522, 1988.

[43] D. A. Gonzalez and E. Niechwiej-Szwedo, "The effects of monocular viewing on hand-eye coordination during sequential grasping and placing movements," *Vision Research*, vol. 128, pp. 30–38, 2016.

[44] P. Servos, M. A. Goodale, and L. S. Jakobson, "The role of binocular vision in prehension: a kinematic analysis," *Vision Research*, vol. 32, no. 8, pp. 1513–1521, 1992.

[45] S. R. Jackson, C. A. Jones, R. Newport, and C. Pritchard, "A kinematic analysis of goal-directed prehension movements executed under binocular, monocular and memory-guided viewing conditions," *Visual Cognition*, vol. 4, no. 2, pp. 113–142, 1997.

[46] A. Loftus, P. Servos, M. A. Goodale, N. Mendarozqueta, and M. Mon-Williams, "When two eyes are better than one in prehension: monocular viewing and end-point variance," *Experimental Brain Research*, vol. 158, no. 3, pp. 317–327, 2004.

[47] D. R. Melmoth and S. Grant, "Advantages of binocular vision for the control of reaching and grasping," *Experimental Brain Research*, vol. 171, no. 3, pp. 371–388, 2006.

[48] F. Alramis, E. Roy, L. Christian, and E. Niechwiej-Szwedo, "Contribution of binocular vision to the performance of complex manipulation tasks in 5–13years old visually-normal children," *Human Movement Science*, vol. 46, pp. 52–62, 2016.

[49] E. Niechwiej-Szwedo, G. Thai, and L. Christian, "Contribution of binocular vision to the performance of a precision manipulation task in 8-14 years old visually normal children," *Investigative Ophthalmology & Visual Science*, vol. 59, no. 9, pp. 2961–2961, 2018.

[50] S. A. Rafique and N. Northway, "Relationship of ocular accommodation and motor skills performance in developmental coordination disorder," *Human Movement Science*, vol. 42, pp. 1–14, 2015.

[51] R. Harrad, "Psychophysics of suppression," *Eye*, vol. 10, no. 2, pp. 270–273, 1996.

[52] F. Sengpiel and C. Blakemore, "The neural basis of suppression and amblyopia in strabismus," *Eye*, vol. 10, no. 2, Part 2, pp. 250–258, 1996.

[53] S. P. McKee, D. M. Levi, and J. A. Movshon, "The pattern of visual deficits in amblyopia," *Journal of Vision*, vol. 3, no. 5, p. 5, 2003.

[54] S. Martinez-Conde, J. Otero-Millan, and S. L. Macknik, "The impact of microsaccades on vision: towards a unified theory of saccadic function," *Nature Reviews Neuroscience*, vol. 14, no. 2, pp. 83–96, 2013.

[55] S. Martinez-Conde, S. L. Macknik, X. G. Troncoso, and T. A. Dyar, "Microsaccades counteract visual fading during fixation," *Neuron*, vol. 49, no. 2, pp. 297–305, 2006.

[56] H.-k. Ko, M. Poletti, and M. Rucci, "Microsaccades precisely relocate gaze in a high visual acuity task," *Nature Neuroscience*, vol. 13, no. 12, pp. 1549–1553, 2010.

[57] J. Otero-Millan, X. G. Troncoso, S. L. Macknik, I. Serrano-Pedraza, and S. Martinez-Conde, "Saccades and microsaccades during visual fixation, exploration, and search: foundations for a common saccadic generator," *Journal of Vision*, vol. 8, no. 14, pp. 21.1–2118, 2008.

[58] C. Schor and W. Hallmark, "Slow control of eye position in strabismic amblyopia," *Investigative Ophthalmology & Visual Science*, vol. 17, no. 6, pp. 577–581, 1978.

[59] K. J. Ciuffreda, R. V. Kenyon, and L. Stark, "Fixational eye movements in amblyopia and strabismus," *Journal of the American Optometric Association*, vol. 50, no. 11, pp. 1251–1258, 1979.

[60] H. E. Bedell and M. C. Flom, "Bilateral oculomotor abnormalities in strabismic amblyopes: evidence for a common central mechanism," *Documenta Ophthalmologica*, vol. 59, no. 4, pp. 309–321, 1985.

[61] K. J. Ciuffreda, R. V. Kenyon, and L. Stark, "Increased drift in amblyopic eyes," *British Journal of Ophthalmology*, vol. 64, no. 1, pp. 7–14, 1980.

[62] E. G. González, A. M. F. Wong, E. Niechwiej-Szwedo, L. Tarita-Nistor, and M. J. Steinbach, "Eye Position Stability in Amblyopia and in Normal Binocular Vision," *Investigative Opthalmology & Visual Science*, vol. 53, no. 9, pp. 5386–5394, 2012.

[63] S. T. L. Chung, G. Kumar, R. W. Li, and D. M. Levi, "Characteristics of fixational eye movements in amblyopia: limitations on fixation stability and acuity?," *Vision Research*, vol. 114, pp. 87–99, 2015.

[64] V. Subramanian, R. M. Jost, and E. E. Birch, "A quantitative study of fixation stability in amblyopia," *Investigative Opthalmology & Visual Science*, vol. 54, no. 3, pp. 1998–2003, 2013.

[65] X. F. Shi, L. M. Xu, Y. Li, T. Wang, K. X. Zhao, and B. A. Sabel, "Fixational saccadic eye movements are altered in anisometropic amblyopia," *Restorative Neurology and Neuroscience*, vol. 30, no. 6, pp. 445–462, 2012.

[66] A. G. Shaikh, J. Otero-Millan, P. Kumar, and F. F. Ghasia, "Abnormal fixational eye movements in amblyopia," *PLoS One*, vol. 11, no. 3, article e0149953, 2016.

[67] K. R. Kelly, C. S. Cheng-Patel, R. M. Jost, Y.-Z. Wang, and E. E. Birch, "Fixation instability during binocular viewing in anisometropic and strabismic children," *Experimental Eye Research*, no. 18, 2018.

[68] K. R. Kelly, R. M. Jost, A. De La Cruz et al., "Slow reading in children with anisometropic amblyopia is associated with fixation instability and increased saccades," *Journal of American Association for Pediatric Ophthalmology and Strabismus*, vol. 21, no. 6, pp. 447–451.e1, 2017.

[69] D. Chen, J. Otero-Millan, P. Kumar, A. G. Shaikh, and F. F. Ghasia, "Visual search in amblyopia: abnormal fixational eye movements and suboptimal sampling strategies," *Investigative Opthalmology & Visual Science*, vol. 59, no. 11, pp. 4506–4517, 2018.

[70] A. L. Yarbus, "Saccadic Eye Movements," in *Eye Movements and Vision*, Springer US, Boston, MA, 1967.

[71] K. Johnston and S. Everling, "Neurophysiology and neuroanatomy of reflexive and voluntary saccades in non-human primates," *Brain and Cognition*, vol. 68, no. 3, pp. 271–283, 2008.

[72] R. J. Krauzlis, "The control of voluntary eye movements: new perspectives," *The Neuroscientist*, vol. 11, no. 2, pp. 124–137, 2005.

[73] P. J. May, "The mammalian superior colliculus: laminar structure and connections," *Progress in Brain Research*, vol. 151, pp. 321–378, 2006.

[74] J. E. McDowell, K. A. Dyckman, B. P. Austin, and B. A. Clementz, "Neurophysiology and neuroanatomy of reflexive and volitional saccades: evidence from studies of humans," *Brain and Cognition*, vol. 68, no. 3, pp. 255–270, 2008.

[75] D. L. Sparks, "The brainstem control of saccadic eye movements," *Nature Reviews Neuroscience*, vol. 3, no. 12, pp. 952–964, 2002.

[76] A. T. Bahill, A. Brockenbrough, and B. T. Troost, "Variability and development of a normative data base for saccadic eye movements," *Investigative Opthalmology & Visual Science*, vol. 21, no. 1, pp. 116–125, 1981.

[77] R. H. S. Carpenter, *Eye Movements*, CRC Press, Boca Raton, 1991.

[78] I. Noorani and R. H. S. Carpenter, "The LATER model of reaction time and decision," *Neuroscience & Biobehavioral Reviews*, vol. 64, pp. 229–251, 2016.

[79] C. Schor, "A directional impairment of eye movement control in strabismus amblyopia," *Investigative Opthalmology & Visual Science*, vol. 14, no. 9, pp. 692–697, 1975.

[80] K. J. Ciuffreda, R. V. Kenyon, and L. Stark, "Increased saccadic latencies in amblyopic eyes," *Investigative Opthalmology & Visual Science*, vol. 17, no. 7, pp. 697–702, 1978.

[81] S. P. McKee, D. M. Levi, C. M. Schor, and J. A. Movshon, "Saccadic latency in amblyopia," *Journal of Vision*, vol. 16, no. 5, p. 3, 2016.

[82] M. Perdziak, D. K. Witkowska, W. Gryncewicz, and J. K. Ober, "Not only amblyopic but also dominant eye in subjects with strabismus show increased saccadic latency," *Journal of Vision*, vol. 16, no. 10, p. 12, 2016.

[83] M. Perdziak, D. Witkowska, W. Gryncewicz, A. Przekoracka-Krawczyk, and J. Ober, "The amblyopic eye in subjects with anisometropia show increased saccadic latency in the delayed saccade task," *Frontiers in Integrative Neuroscience*, vol. 8, 2014.

[84] E. Niechwiej-Szwedo, M. Chandrakumar, H. C. Goltz, and A. M. F. Wong, "Effects of strabismic amblyopia and strabismus without amblyopia on visuomotor behavior, I: saccadic eye movements," *Investigative Opthalmology & Visual Science*, vol. 53, no. 12, pp. 7458–7545, 2012.

[85] E. Niechwiej-Szwedo, H. C. Goltz, M. Chandrakumar, Z. A. Hirji, and A. M. F. Wong, "Effects of anisometropic amblyopia on visuomotor behavior, I: saccadic eye movements," *Investigative Opthalmology & Visual Science*, vol. 51, no. 12, pp. 6348–6354, 2010.

[86] E. Niechwiej-Szwedo, H. C. Goltz, L. Colpa, M. Chandrakumar, and A. M. F. Wong, "Effects of reduced acuity and stereo acuity on saccades and reaching movements in adults with amblyopia and strabismus," *Investigative Opthalmology & Visual Science*, vol. 58, no. 2, pp. 914–921, 2017.

[87] R. K. Jones and D. N. Lee, "Why two eyes are better than one: the two views of binocular vision," *Journal of Experimental Psychology: Human Perception and Performance*, vol. 7, no. 1, pp. 30–40, 1981.

[88] R. Blake and R. Fox, "The psychophysical inquiry into binocular summation," *Perception & Psychophysics*, vol. 14, no. 1, pp. 161–185, 1973.

[89] R. Blake, M. Sloane, and R. Fox, "Further developments in binocular summation," *Perception & Psychophysics*, vol. 30, no. 3, pp. 266–276, 1981.

[90] R. Blake and H. R. Wilson, "Binocular vision," *Vision Research*, vol. 51, no. 7, pp. 754–770, 2011.

[91] M. C. Dorris and D. P. Munoz, "A neural correlate for the gap effect on saccadic reaction times in monkey," *Journal of Neurophysiology*, vol. 73, no. 6, pp. 2558–2562, 1995.

[92] C. Gambacorta, J. Ding, S. P. McKee, and D. M. Levi, "Both saccadic and manual responses in the amblyopic eye of strabismics are irreducibly delayed," *Journal of Vision*, vol. 18, no. 3, p. 20, 2018.

[93] M. Perdziak, W. Gryncewicz, D. Witkowska, P. Sawosz, and J. Ober, "Gap effect and express saccades generation in amblyopia," *Journal of Vision*, vol. 19, no. 4, p. 17, 2019.

[94] E. Kanonidou, F. A. Proudlock, and I. Gottlob, "Reading strategies in mild to moderate strabismic amblyopia: an eye movement investigation," *Investigative Opthalmology & Visual Science*, vol. 51, no. 7, pp. 3502–3508, 2010.

[95] E. Kanonidou, I. Gottlob, and F. A. Proudlock, "The effect of font size on reading performance in strabismic amblyopia: an eye movement investigation," *Investigative Opthalmology & Visual Science*, vol. 55, no. 1, pp. 451–459, 2014.

[96] E. Stifter, G. Burggasser, E. Hirmann, A. Thaler, and W. Radner, "Monocular and binocular reading performance in children with microstrabismic amblyopia," *The British Journal of Ophthalmology*, vol. 89, no. 10, pp. 1324–1329, 2005.

[97] K. R. Kelly, R. M. Jost, A. De La Cruz, and E. E. Birch, "Amblyopic children read more slowly than controls under natural, binocular reading conditions," *Journal of AAPOS*, vol. 19, no. 6, pp. 515–520, 2015.

[98] S. J. Anderson and J. B. Swettenham, "Neuroimaging in human amblyopia," *Strabismus*, vol. 14, no. 1, pp. 21–35, 2009.

[99] U. Yinon, L. Jakobovitz, and E. Auerbach, "The visual evoked response to stationary checkerboard patterns in children with strabismic amblyopia," *Investigative Ophthalmology*, vol. 13, no. 4, pp. 293–296, 1974.

[100] M. Perdziak, D. Witkowska, W. Gryncewicz, and J. Ober, "Strabismic amblyopia affects decision processes preceding saccadic response," *Biocybernetics and Biomedical Engineering*, vol. 38, no. 1, pp. 190–199, 2018.

[101] E. Niechwiej-Szwedo, E. Gonzalez, L. Tarita-Nistor, M. Chandrakumar, H. Goltz, and A. Wong, "Relationship between fixation stability and saccade initiation in patients with amblyopia," in *North American Neuro-Ophthalmology Society Annual Meeting*, San Antonio, TX, USA, 2012.

[102] S. G. Lisberger, "Visual guidance of smooth pursuit eye movements," *Annual Review of Vision Science*, vol. 1, no. 1, pp. 447–468, 2015.

[103] C. H. Meyer, A. G. Lasker, and D. A. Robinson, "The upper limit of human smooth pursuit velocity," *Vision Research*, vol. 25, no. 4, pp. 561–563, 1985.

[104] G. K. von Noorden and G. Mackensen, "Pursuit movements of normal and amblyopic eyes an electro-ophthalmographic study 1. physiology of pursuit movements," *American Journal of Ophthalmology*, vol. 53, no. 2, pp. 325–336, 1962.

[105] K. J. Ciuffreda, R. V. Kenyon, and L. Stark, "Abnormal saccadic substitution during small-amplitude pursuit tracking in amblyopic eyes," *Investigative Ophthalmology & Visual Science*, vol. 18, no. 5, pp. 506–516, 1979.

[106] H. E. Bedell, Y. L. Yap, and M. C. Flom, "Fixational drift and nasal-temporal pursuit asymmetries in strabismic amblyopes," *Investigative Ophthalmology & Visual Science*, vol. 31, no. 5, pp. 968–976, 1990.

[107] R. A. Raashid, I. Z. Liu, A. Blakeman, H. C. Goltz, and A. M. F. Wong, "The initiation of smooth pursuit is delayed in anisometropic amblyopia," *Investigative Opthalmology & Visual Science*, vol. 57, no. 4, pp. 1757–1764, 2016.

[108] I. P. Howard and B. Rogers, *Seeing in Depth*, Porteus, Toronto, 2002.

[109] P. D. R. Gamlin, "Subcortical neural circuits for ocular accommodation and vergence in primates," *Ophthalmic and Physiological Optics*, vol. 19, no. 2, pp. 81–89, 1999.

[110] R. V. Kenyon, K. J. Ciuffreda, and L. Stark, "Dynamic vergence eye movements in strabismus and amblyopia: symmetric vergence," *Investigative Ophthalmology & Visual Science*, vol. 19, no. 1, pp. 60–74, 1980.

[111] M. Jeannerod, M. A. Arbib, G. Rizzolatti, and H. Sakata, "Grasping objects: the cortical mechanisms of visuomotor transformation," *Trends in Neurosciences*, vol. 18, no. 7, pp. 314–320, 1995.

[112] J. F. Kalaska, S. H. Scott, P. Cisek, and L. E. Sergio, "Cortical control of reaching movements," *Current Opinion in Neurobiology*, vol. 7, no. 6, pp. 849–859, 1997.

[113] J. C. Culham and K. F. Valyear, "Human parietal cortex in action," *Current Opinion in Neurobiology*, vol. 16, no. 2, pp. 205–212, 2006.

[114] M. Desmurget and S. Grafton, "Forward modeling allows feedback control for fast reaching movements," *Trends in Cognitive Sciences*, vol. 4, no. 11, pp. 423–431, 2000.

[115] C. Glazebrook, D. Gonzalez, S. Hansen, and D. Elliott, "The role of vision for online control of manual aiming movements in persons with autism spectrum disorders," *Autism*, vol. 13, no. 4, pp. 411–433, 2009.

[116] L. E. Grierson and D. Elliott, "Goal-directed aiming and the relative contribution of two online control processes," *The American Journal of Psychology*, vol. 122, no. 3, pp. 309–324, 2009.

[117] V. Gritsenko, S. Yakovenko, and J. F. Kalaska, "Integration of predictive feedforward and sensory feedback signals for online control of visually guided movement," *Journal of Neurophysiology*, vol. 102, no. 2, pp. 914–930, 2009.

[118] S. Hansen, D. Elliott, and L. Tremblay, "Online control of discrete action following visual perturbation," *Perception*, vol. 36, no. 2, pp. 268–287, 2007.

[119] M. Khan, I. Franks, D. Elliott et al., "Inferring online and offline processing of visual feedback in target-directed movements from kinematic data," *Neuroscience and Biobehavioral Reviews*, vol. 30, no. 8, pp. 1106–1121, 2006.

[120] G. K. Von Noorden, "Reaction time in normal and amblyopic eyes," *JAMA Ophthalmology*, vol. 66, pp. 695–701, 1961.

[121] D. M. Levi, R. S. Harwerth, and R. E. Manny, "Suprathreshold spatial frequency detection and binocular interaction in strabismic and anisometropic amblyopia," *Investigative Ophthalmology & Visual Science*, vol. 18, no. 7, pp. 714–725, 1979.

[122] D. I. Hamasaki and J. T. Flynn, "Amblyopic eyes have longer reaction times," *Investigative Ophthalmology & Visual Science*, vol. 21, no. 6, pp. 846–853, 1981.

[123] G. Mackensen, "Reaktionsheitmessungen bei Amblyopie," *Albrecht von Graefe's Archiv für Ophthalmologie*, vol. 159, no. 6, pp. 636–642, 1958.

[124] D. M. Levi, "Visual processing in amblyopia: human studies," *Strabismus*, vol. 14, no. 1, pp. 11–19, 2009.

[125] R. F. Hess, F. W. Campbell, and T. Greenhalgh, "On the nature of the neural abnormality in human amblyopia: neural aberrations and neural sensitivity loss," *Pflügers Archiv*, vol. 377, no. 3, pp. 201–207, 1978.

[126] L. Kiorpes, R. G. Boothe, A. E. Hendrickson, J. A. Movshon, H. M. Eggers, and M. S. Gizzi, "Effects of early unilateral blur on the macaque's visual system. I. Behavioral observations," *The Journal of Neuroscience*, vol. 7, no. 5, pp. 1318–1326, 1987.

[127] H. Pieron, "II. Recherches sur les lois de variation des temps de latence sensorielle en fonction des intensités excitatrices," *L'Année Psychologique*, vol. 20, no. 1, pp. 17–96, 1913.

[128] M. J. Pianta and M. Kalloniatis, "Characteristics of anisometropic suppression: simple reaction time measurements," *Perception & Psychophysics*, vol. 60, no. 3, pp. 491–502, 1998.

[129] L. Chelazzi, C. A. Marzi, G. Panozzo, N. Pasqualini, G. Tassinari, and L. Tomazzoli, "Hemiretinal differences in speed of light detection in esotropic amblyopes," *Vision Research*, vol. 28, no. 1, pp. 95–104, 1988.

[130] E. Niechwiej-Szwedo, H. C. Goltz, M. Chandrakumar, Z. Hirji, J. D. Crawford, and A. M. F. Wong, "Effects of anisometropic amblyopia on visuomotor behavior, part 2: visually guided reaching," *Investigative Opthalmology & Visual Science*, vol. 52, no. 2, pp. 795–803, 2011.

[131] E. Niechwiej-Szwedo, H. C. Goltz, M. Chandrakumar, and A. M. F. Wong, "Effects of strabismic amblyopia on visuomotor behavior: part II. visually guided reaching," *Investigative Opthalmology & Visual Science*, vol. 55, no. 6, pp. 3857–3865, 2014.

[132] D. M. Levi and S. A. Klein, "Spatial localization in normal and amblyopic vision," *Vision Research*, vol. 23, no. 10, pp. 1005–1017, 1983.

[133] H. D. Bedell and M. C. Flom, "Monocular spatial distortion in strabismic amblyopia," *Investigative Ophthalmology & Visual Science*, vol. 20, no. 2, pp. 263–268, 1981.

[134] M. Fronius and R. Sireteanu, "Pointing errors in strabismics: complex patterns of distorted visuomotor coordination," *Vision Research*, vol. 34, no. 5, pp. 689–707, 1994.

[135] R. F. Hess and I. E. Holliday, "The spatial localization deficit in amblyopia," *Vision Research*, vol. 32, no. 7, pp. 1319–1339, 1992.

[136] B. T. Barrett, I. E. Pacey, A. Bradley, L. N. Thibos, and P. Morrill, "Nonveridical visual perception in human amblyopia," *Investigative Ophthalmology & Visual Science*, vol. 44, no. 4, pp. 1555–1567, 2003.

[137] R. Sireteanu, A. Thiel, S. Fikus, and A. Iftime, "Patterns of spatial distortions in human amblyopia are invariant to stimulus duration and instruction modality," *Vision Research*, vol. 48, no. 9, pp. 1150–1163, 2008.

[138] R. Sireteanu, W.-D. Lagreze, and D. H. Constantinescu, "Distortions in two-dimensional visual space perception in strabismic observers," *Vision Research*, vol. 33, no. 5-6, pp. 677–690, 1993.

[139] H. E. Bedell and M. C. Flom, "Normal and abnormal space perception," *Optometry and Vision Science*, vol. 60, no. 6, pp. 426–435, 1983.

[140] M. Fronius and R. Sireteanu, "Monocular geometry is selectively distorted in the central visual field of strabismic amblyopes," *Investigative Ophthalmology & Visual Science*, vol. 30, no. 9, pp. 2034–2044, 1989.

[141] B. Mansouri, B. C. Hansen, and R. F. Hess, "Disrupted retinotopic maps in amblyopia," *Investigative Ophthalmology & Visual Science*, vol. 50, no. 7, pp. 3218–3225, 2009.

[142] M. Fronius, R. Sireteanu, and A. Zubcov, "Deficits of spatial localization in children with strabismic amblyopia," *Graefe's Archive for Clinical and Experimental Ophthalmology*, vol. 242, no. 10, pp. 827–839, 2004.

[143] M. A. Goodale, G. Kroliczak, and D. A. Westwood, "Dual routes to action: contributions of the dorsal and ventral streams to adaptive behavior," *Progress in Brain Research*, vol. 149, pp. 269–283, 2005.

[144] D. M. Levi and S. A. Klein, "Sampling in spatial vision," *Nature*, vol. 320, no. 6060, pp. 360–362, 1986.

[145] E. Niechwiej-Szwedo, H. C. Goltz, M. Chandrakumar, and A. M. F. Wong, "The effect of sensory uncertainty due to amblyopia (lazy eye) on the planning and execution of visually-guided 3D reaching movements," *PLoS One*, vol. 7, no. 2, article e31075, 2012.

[146] J. G. Buckley, I. E. Pacey, G. K. Panesar, A. Scally, and B. T. Barrett, "Prehension of a flanked target in individuals with amblyopia," *Investigative Opthalmology & Visual Science*, vol. 56, no. 12, pp. 7568–7580, 2015.

[147] S. Grant and M. L. Conway, "Reach-to-precision grasp deficits in amblyopia: Effects of object contrast and low visibility," *Vision Research*, vol. 114, pp. 100–110, 2015.

[148] S. Grant, D. R. Melmoth, M. J. Morgan, and A. L. Finlay, "Prehension deficits in amblyopia," *Investigative Ophthalmology & Visual Science*, vol. 48, no. 3, pp. 1139–1148, 2007.

[149] S. Grant, C. Suttle, D. R. Melmoth, M. L. Conway, and J. J. Sloper, "Age- and stereovision-dependent eye–hand coordination deficits in children with amblyopia and abnormal binocularity," *Investigative Ophthalmology & Visual Science*, vol. 55, no. 9, pp. 5687–57015, 2014.

[150] D. R. Melmoth, A. L. Finlay, M. J. Morgan, and S. Grant, "Grasping deficits and adaptations in adults with stereo vision losses," *Investigative Ophthalmology & Visual Science*, vol. 50, no. 8, pp. 3711–3720, 2009.

[151] C. M. Suttle, D. R. Melmoth, A. L. Finlay, J. J. Sloper, and S. Grant, "Eye-hand coordination skills in children with and without amblyopia," *Investigative Ophthalmology & Visual Science*, vol. 52, no. 3, pp. 1851–1864, 2011.

[152] E. Todorov, "Optimality principles in sensorimotor control," *Nature Neuroscience*, vol. 7, no. 9, pp. 907–915, 2004.

[153] R. A. Schmidt, H. Zelaznik, B. Hawkins, J. S. Frank, and J. T. Quinn Jr, "Motor-output variability: a theory for the accuracy of rapid motor acts," *Psychological Review*, vol. 47, no. 5, pp. 415–451, 1979.

[154] P. M. Fitts, "The information capacity of the human motor system in controlling the amplitude of movement," *Journal of Experimental Psychology*, vol. 47, no. 6, pp. 381–391, 1954.

[155] D. Elliott, G. Binsted, and M. Heath, "The control of goal-directed limb movements: correcting errors in the trajectory," *Human Movement Science*, vol. 18, no. 2-3, pp. 121–136, 1999.

[156] D. Elliott, J. Lyons, S. J. Hayes et al., "The multiple process model of goal-directed reaching revisited," *Neuroscience & Biobehavioral Reviews*, vol. 72, pp. 95–110, 2017.

[157] M. A. Khan, D. Elliott, J. Coull, R. Chua, and J. Lyons, "Optimal control strategies under different feedback schedules: kinematic evidence," *Journal of Motor Behavior*, vol. 34, no. 1, pp. 45–57, 2002.

[158] D. C. Knill, L. T. Maloney, and J. Trommershauser, "Sensorimotor processing and goal-directed movement," *Journal of Vision*, vol. 7, no. 5, pp. 1-2, 2007.

[159] E. Niechwiej-Szwedo, H. Goltz, and A. M. F. Wong, "Deficits and adaptation of eye-hand coordination during visually guided reaching movements in people with amblyopia," in *Plasticity in Sensory Systems*, J. K. Steeves and L. R. Harris, Eds., vol. 2013, Cambridge University Press, New York, 2012.

[160] D. Elliott, R. G. Garson, D. Goodman, and R. Chua, "Discrete vs. continuous visual control of manual aiming," *Human Movement Science*, vol. 10, no. 4, pp. 393–418, 1991.

[161] D. Elliott, W. F. Helsen, and R. Chua, "A century later: Woodworth's (1899) two-component model of goal-directed aiming," *Psychological Bulletin*, vol. 127, no. 3, pp. 342–357, 2001.

[162] E. Niechwiej-Szwedo, S. A. Kennedy, L. Colpa, M. Chandrakumar, H. C. Goltz, and A. M. F. Wong, "Effects of induced monocular blur versus anisometropic amblyopia on saccades, reaching, and eye-hand coordination," *Investigative Opthalmology & Visual Science*, vol. 53, no. 8, pp. 4354–4362, 2012.

[163] M. Dean, S. W. Wu, and L. T. Maloney, "Trading off speed and accuracy in rapid, goal-directed movements," *Journal of Vision*, vol. 7, no. 5, pp. 10–12, 2007.

[164] M. Jeannerod, "The timing of natural prehension movements," *Journal of Motor Behavior*, vol. 16, no. 3, pp. 235–254, 1984.

[165] M. J. Grol, J. Majdandzic, K. E. Stephan et al., "Parieto-frontal connectivity during visually guided grasping," *The Journal of Neuroscience*, vol. 27, no. 44, pp. 11877–11887, 2007.

[166] L. Verhagen, H. C. Dijkerman, M. J. Grol, and I. Toni, "Perceptuo-motor interactions during prehension movements," *The Journal of Neuroscience*, vol. 28, no. 18, pp. 4726–4735, 2008.

[167] Y. Paulignan, C. MacKenzie, R. Marteniuk, and M. Jeannerod, "Selective perturbation of visual input during prehension movements. 1. The effects of changing object position," *Experimental Brain Research*, vol. 83, no. 3, pp. 502–512, 1991.

[168] J. J. Marotta and M. A. Goodale, "The role of familiar size in the control of grasping," *Journal of Cognitive Neuroscience*, vol. 13, no. 1, pp. 8–17, 2001.

[169] M. A. Goodale, J. P. Meenan, H. H. Bulthoff, D. A. Nicolle, K. J. Murphy, and C. I. Racicot, "Separate neural pathways for the visual analysis of object shape in perception and prehension," *Current Biology*, vol. 4, no. 7, pp. 604–610, 1994.

[170] G. Buckingham, J. S. Cant, and M. A. Goodale, "Living in a material world: how visual cues to material properties affect

the way that we lift objects and perceive their weight," *Journal of Neurophysiology*, vol. 102, no. 6, pp. 3111–3118, 2009.

[171] J. A. Stuart and H. M. Burian, "A study of separation difficulty. Its relationship to visual acuity in normal and amblyopic eyes," *American Journal of Ophthalmology*, vol. 53, no. 3, pp. 471–477, 1962.

[172] E. Niechwiej-Szwedo, J. Chin, P. J. Wolfe, C. Popovich, and W. R. Staines, "Abnormal visual experience during development alters the early stages of visual-tactile integration," *Behavioural Brain Research*, vol. 304, pp. 111–119, 2016.

[173] A. L. Webber, J. M. Wood, and B. Thompson, "fine motor skills of children with amblyopia improve following binocular treatment," *Investigative Opthalmology & Visual Science*, vol. 57, no. 11, pp. 4713–4720, 2016.

[174] L. I. N. Mazyn, M. Lenoir, G. Montagne, C. Delaey, and G. J. P. Savelsbergh, "Stereo vision enhances the learning of a catching skill," *Experimental Brain Research*, vol. 179, no. 4, pp. 723–726, 2007.

[175] M. H. Woollacott and A. Shumway-Cook, "Changes in posture control across the life span—a systems approach," *Physical Therapy*, vol. 70, no. 12, pp. 799–807, 1990.

[176] A. E. Patla, "Understanding the roles of vision in the control of human locomotion," *Gait & Posture*, vol. 5, no. 1, pp. 54–69, 1997.

[177] P. Odenrick, P. Sandstedt, and G. Lennerstrand, "Postural sway and gait of children with convergent strabismus," *Developmental Medicine and Child Neurology*, vol. 26, no. 4, pp. 495–499, 1984.

[178] J. G. Buckley, G. K. Panesar, M. J. MacLellan, I. E. Pacey, and B. T. Barrett, "Changes to control of adaptive gait in individuals with long-standing reduced stereoacuity," *Investigative Ophthalmology & Visual Science*, vol. 51, no. 5, pp. 2487–2495, 2010.

[179] M. Hayhoe, B. Gillam, K. Chajka, and E. Vecellio, "The role of binocular vision in walking," *Visual Neuroscience*, vol. 26, no. 1, pp. 73–80, 2009.

[180] A. B. Zipori, L. Colpa, A. M. F. Wong, S. L. Cushing, and K. A. Gordon, "Postural stability and visual impairment: assessing balance in children with strabismus and amblyopia," *PLoS One*, vol. 13, no. 10, article e0205857, 2018.

[181] A. Przekoracka-Krawczyk, P. Nawrot, M. Czaińska, and K. P. Michalak, "Impaired body balance control in adults with strabismus," *Vision Research*, vol. 98, pp. 35–45, 2014.

[182] A. Dickmann, E. Di Sipio, C. Simbolotti et al., "Balance in subjects with congenital or early onset strabismus: influence of age," *Neuroscience Letters*, vol. 623, pp. 28–35, 2016.

[183] I. Vedamurthy, D. C. Knill, S. J. Huang et al., "Recovering stereo vision by squashing virtual bugs in a virtual reality environment," *Philosophical Transactions of the Royal Society of London. Series B, Biological Sciences*, vol. 371, no. 1697, article 20150264, 2016.

[184] E. E. Birch and K. R. Kelly, "Pediatric ophthalmology and childhood reading difficulties," *Journal of AAPOS*, vol. 21, no. 6, pp. 442–444, 2017.

[185] S. Hrisos, M. P. Clarke, T. Kelly, J. Henderson, and C. M. Wright, "Unilateral visual impairment and neurodevelopmental performance in preschool children," *The British Journal of Ophthalmology*, vol. 90, no. 7, pp. 836–838, 2006.

[186] A. R. O'Connor, E. E. Birch, S. Anderson, and H. Draper, "The functional significance of stereopsis," *Investigative Opthalmology & Visual Science*, vol. 51, no. 4, pp. 2019–2023, 2010.

[187] A. L. Webber, J. M. Wood, G. A. Gole, and B. Brown, "The effect of amblyopia on fine motor skills in children," *Investigative Ophthalmology & Visual Science*, vol. 49, no. 2, pp. 594–603, 2008.

Hindawi
Neural Plasticity
Volume 2019, Article ID 5857243, 10 pages
https://doi.org/10.1155/2019/5857243

Clinical Study

The Effect of Combined Patching and Citalopram on Visual Acuity in Adults with Amblyopia: A Randomized, Crossover, Placebo-Controlled Trial

Alice K. Lagas,[1] Joanna M. Black,[1] Bruce R. Russell,[2] Robert R. Kydd,[3] and Benjamin Thompson[1,4]

[1]*School of Optometry and Vision Science, University of Auckland, New Zealand*
[2]*School of Pharmacy, University of Otago, New Zealand*
[3]*Department of Psychological Medicine, University of Auckland, New Zealand*
[4]*School of Optometry and Vision Science, University of Waterlo, Canada*

Correspondence should be addressed to Benjamin Thompson; ben.thompson@uwaterloo.ca

Received 25 March 2019; Accepted 14 May 2019; Published 9 June 2019

Academic Editor: Malgorzata Kossut

Nonhuman animal models have demonstrated that selective serotonin reuptake inhibitors (SSRIs) can enhance plasticity within the mature visual cortex and enable recovery from amblyopia. The aim of this study was to test the hypothesis that the SSRI citalopram combined with part-time patching of the fellow fixing eye would improve amblyopic eye visual acuity in adult humans. Following a crossover, randomized, double-blind, placebo-controlled design, participants completed two 2-week blocks of fellow fixing eye patching. One block combined patching with citalopram (20 mg/day) and the other with a placebo tablet. The blocks were separated by a 2-week washout period. The primary outcome was change in amblyopic eye visual acuity. Secondary outcomes included stereoacuity and electrophysiological measures of retinal and cortical function. Seven participants were randomized, fewer than our prespecified sample size of 20. There were no statistically significant differences in amblyopic eye visual acuity change between the active (mean ± SD change = 0.08 ± 0.16 logMAR) and the placebo (mean change = −0.01 ± 0.03 logMAR) blocks. No treatment effects were observed for any secondary outcomes. However, 3 of 7 participants experienced a 0.1 logMAR or greater improvement in amblyopic eye visual acuity in the active but not the placebo blocks. These results from a small sample suggest that larger-scale trials of SSRI treatment for adult amblyopia may be warranted. Considerations for future trials include drug dose, treatment duration, and recruitment challenges. This study was preregistered as a clinical trial (ACTRN12611000669998).

1. Introduction

Disruptions to binocular vision such as strabismus (an eye turn) or anisometropia (unequal refractive error between the two eyes) during the critical period of visual development can cause a neurodevelopmental disorder of vision called amblyopia [1, 2]. The deficits associated with amblyopia encompass a wide range of monocular and binocular visual functions [3, 4] and also extend to the fellow fixing eye [5]. Clinically, amblyopia is typically diagnosed on the basis of a monocular visual acuity loss that cannot be explained by ocular pathology combined with an amblyogenic factor [1]. Current treatments for amblyopia in childhood involve the provision of refractive correction followed by patching or penalization of the fellow fixing eye to promote use of the amblyopic eye. These treatments are effective [6–12], but efficacy appears to decline with increasing age in children [13–16], possibly due to a decline in neural plasticity as the visual cortex matures and exits the critical period for visual development [17–20]. A growing body of literature demonstrates that vision can improve in adult humans with amblyopia through interventions such as monocular [21, 22] and binocular [23–27] perceptual learning and noninvasive brain stimulation [28–32]. However, these approaches have

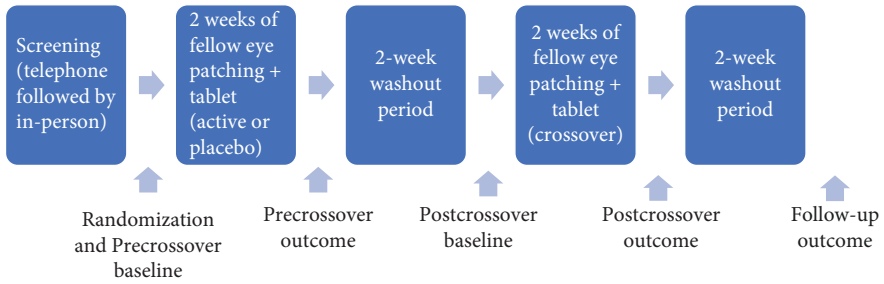

Figure 1: Schematic of the study protocol and the timing of baseline, outcome, and follow-up measures.

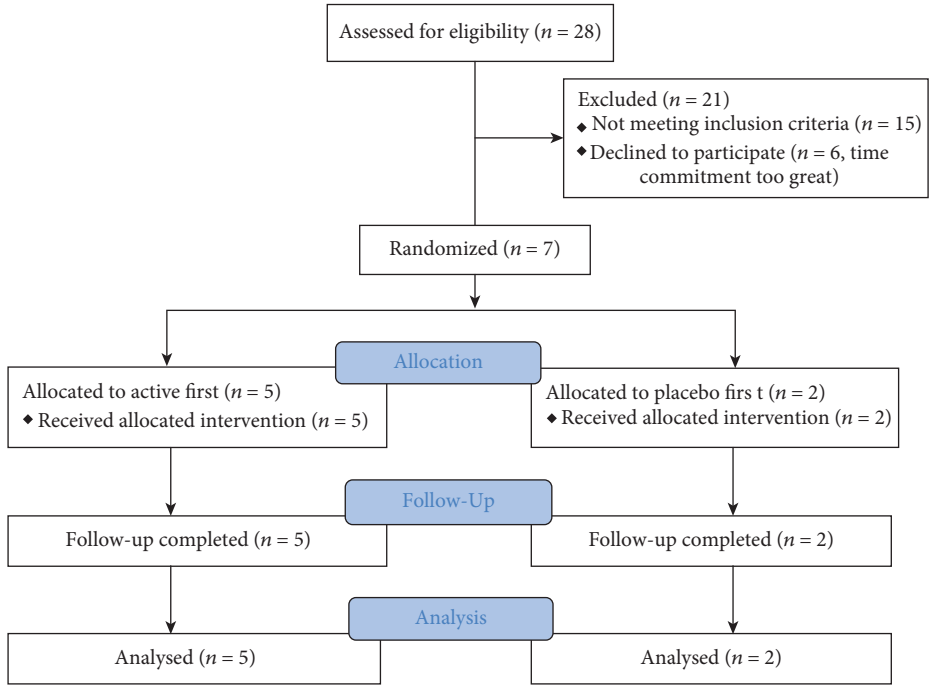

Figure 2: CONSORT diagram for the study.

not yet translated into positive randomized clinical trials in adult patients that are required for evidence-based clinical practice [33].

Amblyopia also forms the basis of a prominent nonhuman animal model for studying cortical development and plasticity [34]. Monocular amblyopia can be induced in nonhuman animals within the critical period of visual development using an eyelid suture, induction of strabismus, or provision of anisometropic refractive error [35]. Over the past decade or so, a considerable number of studies have used this model to explore postcritical period neuroplasticity [36]. Successful interventions for amblyopia recovery in postcritical period animal models include dark exposure [37, 38], enriched visual environments [39], food restriction [40], binocular training [41], physical exercise [42], and retinal inactivation [43].

Pharmaceutical interventions have also been investigated in rodent models of amblyopia. A particularly striking result was reported by Vetencourt et al. [44] whereby chronic administration of the selective serotonin reuptake inhibitor (SSRI) fluoxetine enabled recovery of normal visual cortex responses and visual acuity in mature rats with unilateral deprivation amblyopia. This effect occurred when fluoxetine was administered before and during eyelid suture of the nondeprived eye and opening of the deprived eye (a procedure known as a reverse suture). The improvements in visual function were linked to reduced GABA-mediated inhibition within the visual cortex and increased expression of brain-derived neurotrophic factor (BDNF). This finding is of particular interest in the context of amblyopia treatment in adult humans because SSRIs are widely available to clinicians. Furthermore, SSRIs may enhance plasticity within the human motor [45, 46] and visual [47] cortexes. Fluoxetine has also been found to enhance physiotherapy outcomes after stroke, possibly by increasing cortical plasticity [48]. However, fluoxetine did not enhance visual perceptual learning of a motion discrimination task or motor cortex plasticity in a study of healthy human adults [49].

Two studies have investigated the use of fluoxetine to treat human amblyopia. Sharif et al. [50] compared 3 months of fellow fixing eye patching plus fluoxetine (0.5 mg/kg/day, $n = 20$) to patching plus a placebo tablet placebo ($n = 15$) in

Table 1: Participant details.

	Age/sex	AME VA logMAR	FFE VA logMAR	Type	AME refraction	FFE refraction	Strab	Stereo (arc/sec)	Suppression	History	BDNF	First treatment
P1	43/F	1.00	0.00	Aniso	-0.25	+6.00/−2.25 × 180		Nil	Full	Patching age 7	Val66Met	Placebo
P2	32/M	1.20	-0.04	Mixed	+9.75	-0.25	Exo12Δ, hyper 11Δ	Nil	Full	Surgery 14 yrs, patching and spectacles 10-12 yrs	Val/val	Active
P3	47/M	0.64	-0.10	Mixed	Plano/−0.25 × 160	+1.75	Eso 10Δ	Nil	Full	Surgery 7 yrs	Val/val	Placebo
P4	19/F	0.34	-0.04	Aniso	+3.75/−1.75 × 180	+0.50/−0.25 × 180		60	Intermittent	Detected 11 yrs patching and VT	Val66Met	Active
P5	19/M	1.00	0.00	Strab	+4.50/−1.50 × 104	+3.50/−0.25 × 170	Eso 6Δ	Nil	Full	Spectacles and patching in childhood	Val/val	Active
P6	30/M	0.10	-0.08	Strab	Plano/−1.00 × 20	-2	Exo 20Δ	Nil	Full	Surgery 2 yrs, patching in childhood	Val/val	Active
P7	44/M	0.34	0.00	Mixed	+5.25/−1.25 × 90	+1.75/0.50 × 75	Exo 12Δ	Nil	Full	Surgery 2 and 10 yrs, spectacles until 15 yrs old	Val/val	Active

AME: amblyopic eye; FFE: fellow fixing eye; VA: visual acuity; exo: exotropia; eso: esotropia; hyper: hypertropia; aniso: anisometropic; strab: strabismic/strabismus; VT: vision training; BDNF: brain-derived neurotrophic factor.

Table 2: Amblyopic eye visual acuity results.

	Active baseline	Active outcome	Active change	Placebo baseline	Placebo outcome	Placebo change	Final washout
P1	0.94	0.82	0.12	1	0.97	0.03	0.87
P2	1.20	1.20	0.00	1	1	0	1.1
P3	0.73	0.60	0.13	0.64	0.67	-0.03	0.633
P4	0.34	0.36	-0.02	0.32	0.32	0	0.3
P5	1.00	0.60	0.40	0.866	0.9	-0.034	0.74
P6	0.10	0.10	0.00	0.1	0.08	0.02	0.14
P7	0.34	0.40	-0.06	0.32	0.36	-0.04	0.32
Mean (SD)	**0.66 (0.36)**	**0.58 (0.35)**	**0.08 (0.16)**	**0.61 (0.36)**	**0.61 (0.36)**	**-0.01 (0.03)**	**0.59 (0.35)**

Change values were calculated by subtracting the outcome from the baseline. All values are in logMAR.

Table 3: Self-reported patching adherence data sourced from participants' patching diaries.

	Active	Placebo	Difference
P1	116 (31)	114 (24)	2
P2	40 (19)	29 (21)	11
P3	55 (28)	55 (7)	1
P4	96 (38)	111 (32)	-15
P5	75 (0)	75 (0)	0
P6	111 (78)	111 (74)	0
P7	111 (32)	111 (32)	0
Mean (SD)	**86 (30)**	**87 (34)**	**0.1 (7.6)**

Data are shown as mean minutes of patching per day (SD). The prescribed dose was 120 minutes per day.

older children and adults (10-40 years) with amblyopia. A significantly greater amblyopic eye visual acuity improvement in the fluoxetine compared to the placebo group was observed. However, Huttunen et al. [51] found no differences in visual function improvement between a group of adults with amblyopia treated for 10 days with combined perceptual learning and fluoxetine (20 mg per day, $n = 22$) and a group treated with perceptual learning combined with a placebo tablet ($n = 20$).

In this study, we explored the effects of 2 weeks (14 days) of the SSRI citalopram combined with fellow fixing eye patching on visual acuity, stereopsis, and visually evoked retinal and cortical responses in adults with amblyopia. We anticipated that recruitment would be challenging due to the use of patching and the administration of an antidepressant drug. We therefore adopted a placebo-controlled, randomized, double-blind, crossover design. In this context, citalopram was chosen over fluoxetine (as used in prior studies) because citalopram has a shorter half-life [52] that allowed for a manageable washout period to be incorporated into the design of the study. No significant effects of citalopram were observed, although our study may have been underpowered due to recruitment challenges.

2. Methods

2.1. Trial Design. The single-site trial involved two blocks of fellow fixing eye patching each lasting two weeks separated by a two-week washout period. Participants were provided with citalopram (1 × 20 mg tablet per day) during one patching block and otherwise identical placebo tablets (sucrose) during the other block. Block order was randomized using a random number generator. The timing of the baseline and the outcome measures are shown in Figure 1. Only the pharmacist dispensing the tablets, who did not interact with study participants, was unmasked to block order. Study participants and all other members of the research team were masked to the randomization. The study was approved by the Northern X Regional Ethics Committee in New Zealand (NTX/11/06/044) and preregistered as a clinical trial (ACTRN12611000669998).

Participants completed a screening protocol consisting of a telephone interview followed by a full optometric examination, medical history, the Profile of Mood States Short Form (POMS-SF) questionnaire, and the Depression Anxiety and Stress Scale (DASS-21).

Study inclusion criteria were as follows: 18 years of age or over, 0.2 logMAR or worse visual acuity in the amblyopic eye, 0.0 logMAR or better visual acuity in the fellow fixing eye, an interocular acuity difference of at least 0.2 logMAR, and the presence of a strabismus and/or anisometropia defined as a difference in spherical equivalent refractive error of 1.5 dioptres or greater between the eyes. The exclusion criteria were as follows: the presence of ocular pathology, an explanation for the visual acuity loss other than amblyopia, personal or family history of a mood disorder, diabetes, history of addiction, current use of medications or supplements known to alter mood, medications that interact with SSRIs such as codeine, and abnormal mood states evident on the mood questionnaires as reviewed by a psychiatrist. Prior to randomization, participants who were not wearing optimal full correction for both eyes were provided with full correction (either spectacles or contact lenses) and were reviewed every four weeks until visual acuity was stable (<0.2 logMAR difference between visits). Participants were recruited through the University of Auckland Optometry Clinic, referral from eye care practitioners, word of mouth, and newspaper advertisements. Participants were compensated for their time.

2.2. Baseline and Outcome Measures. Visual acuity (VA) was assessed using a computerized ETDRS chart (Medmont) from 6 m. The right eye was tested first. Each correctly

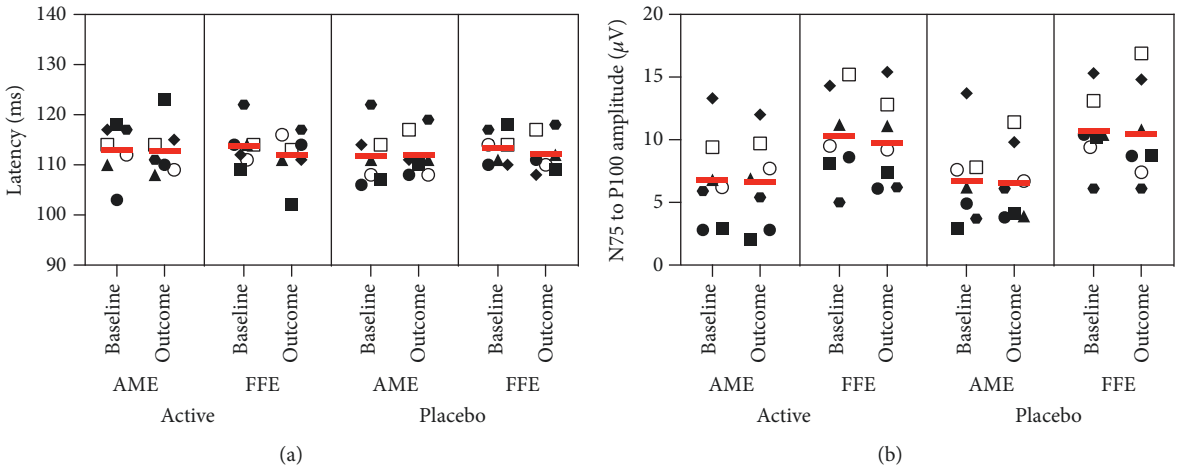

Figure 3: VEP results for the 1° check stimulus. Latencies for the P100 component are shown in (a), and amplitudes for the N57-P100 waveform component are in (b). Individual participants are shown with different symbols—P1-7 as follows: filled circle, filled square, filled triangle, filled diamond, filled hexagon, open circle, and open square, respectively. Horizontal lines depict group mean values.

identified letter was worth 0.02 logMAR. Binocular vision was assessed using a unilateral cover test, a prism cover test, the Worth 4-dot test (33 cm and 6 m), and the TNO stereoacuity test. Electrophysiological measurements of retinal and visual cortex function were made using ISCEV-standardized electrophysiological protocols on a Roland RETIscan system (software version 4.13.1.8). The following tests were applied monocularly (right eye first): pattern ERG (1° check size—modified from the 0.8° standard for direct comparison with the VEP stimuli), VEP (1° and 0.3° check sizes), and multifocal ERG with pupil dilation. ERG measures were included so that any retinal effects of citalopram could be accounted for if the trial was positive. The POMS-SF questionnaire was completed at each study visit, and participants completed a patching diary for each 2-week patching session. The brain-derived neurotrophic factor (BNDF) phenotype has been identified as a possible mediator of cortical plasticity [53], and BNDF upregulation has been identified as a mechanism for increased visual cortex plasticity following fluoxetine administration in rats [44]. To test for BDNF polymorphisms, participants provided a blood sample directly after the first two-week block of patching. Following a previously reported protocol [49], an Agena MassARRAY iPLEX assay (Agena Bioscience, San Diego, CA, USA) was used for genotyping. A Bruker Mass Spectrometer with optimized parameters for iPLEX chemistry was then used to resolve single base extensions. Typer 4 analysis software (Agena Bioscience) enabled visual inspection of generated peaks in comparison to the nontemplate control.

2.3. Statistical Analysis. At the time of study initiation, no previous studies of SSRIs in human amblyopia treatment were available. Therefore, we selected a sample size of 20 based on recruitment estimates for the study site. Outcome measures were analysed separately using mixed ANOVAs with within-subject factors of Session (baseline vs. outcome) and Treatment (active vs. placebo) and a between-subject factor of Group (active first vs. placebo first).

3. Results

Sixty-one participants expressed interest in the study and were sent a study information package. Twenty-eight participants responded and were assessed for eligibility. Seven participants were randomized. The CONSORT diagram for these participants is shown in Figure 2. Reasons for exclusion included time commitment too great, medical or recreational use of drugs, vision too good in the amblyopic eye, and diabetes. One participant who did not meet the visual acuity inclusion criteria was randomized (P6, see Table 1). Data from this participant were included in the final analysis due to the small sample size. Randomized participant details, including BDNF polymorphism, are shown in Table 1.

Baseline and outcome data for amblyopic eye visual acuity are shown in Table 2. There was no significant interaction between the Session and Treatment factors ($F_{1,5} = 1.7$, $p = 0.25$, and partial $\eta^2 = 0.26$) indicating no difference between the active and the placebo treatment. The Session factor also had no main effect indicating the absence of a visual acuity improvement across the two periods of patching ($F_{1,5} = 1.7$, $p = 0.25$, and partial $\eta^2 = 0.26$). Overall, no main effects or interactions were significant in the analysis (all $p > 0.25$). An inspection of individual data (Table 2) indicated that 3/7 participants improved by >0.1 logMAR in the active but not the placebo condition. One of these participants had a val66met BDNF polymorphism. The remaining two had val/val BNDF polymorphisms. No main effects or interactions were present for the fellow fixing eye visual acuity data (all $F < 3.9$, all $p > 0.1$, and all partial $\eta^2 < 0.4$).

Adherence data are shown in Table 3. Adherence did not differ significantly between active and placebo blocks ($t_6 = 1.0$, $p = 0.9$). On average, participants had approximately 70% adherence with the 120 minutes per day of prescribed patching. There was no correlation between patching adherence and visual acuity change in either the active ($r_7 = -0.2$, $p = 0.6$) or placebo ($r_7 = 0.3$, $p = 0.5$) blocks.

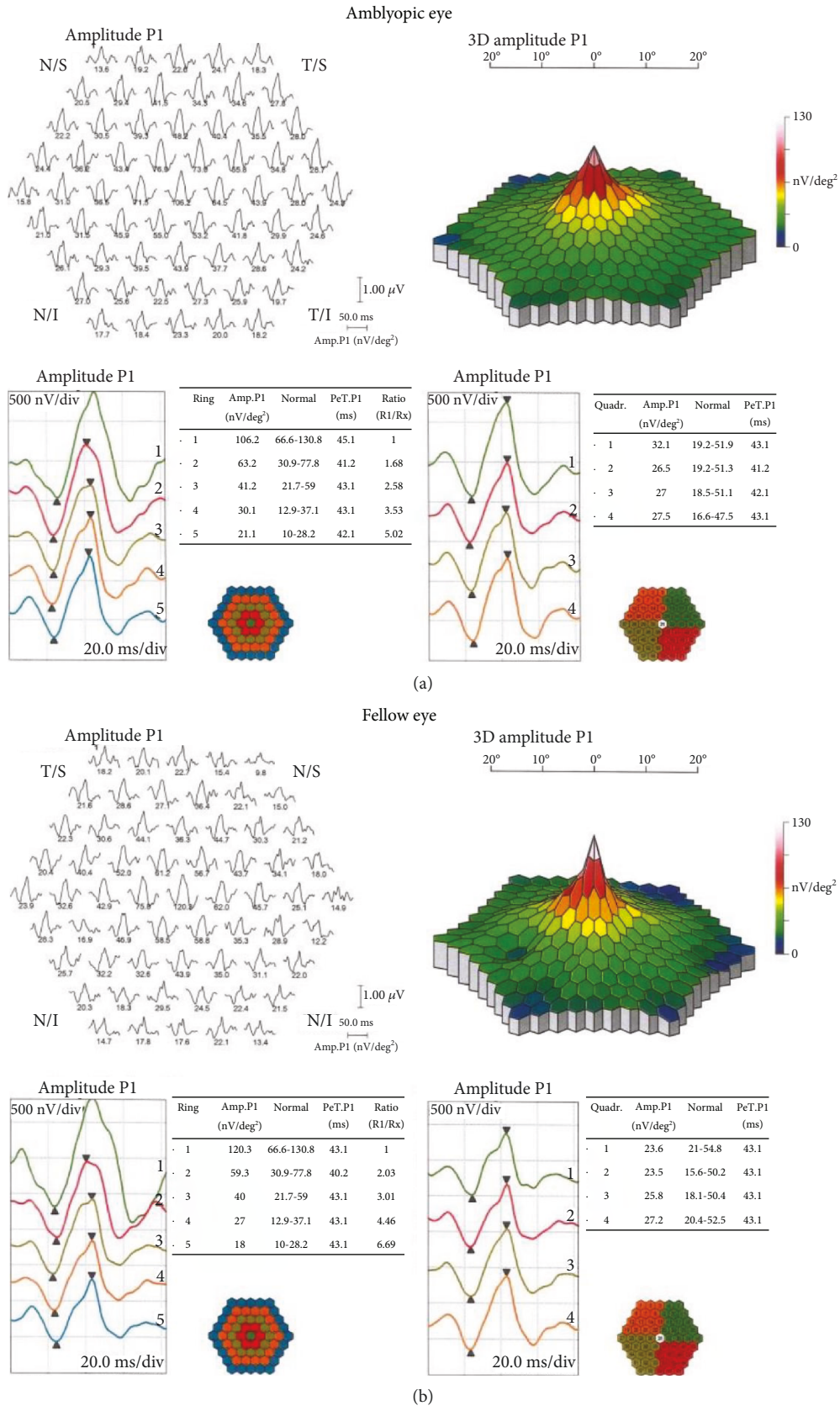

Figure 4: Multifocal ERG results for participant P7 (first baseline session).

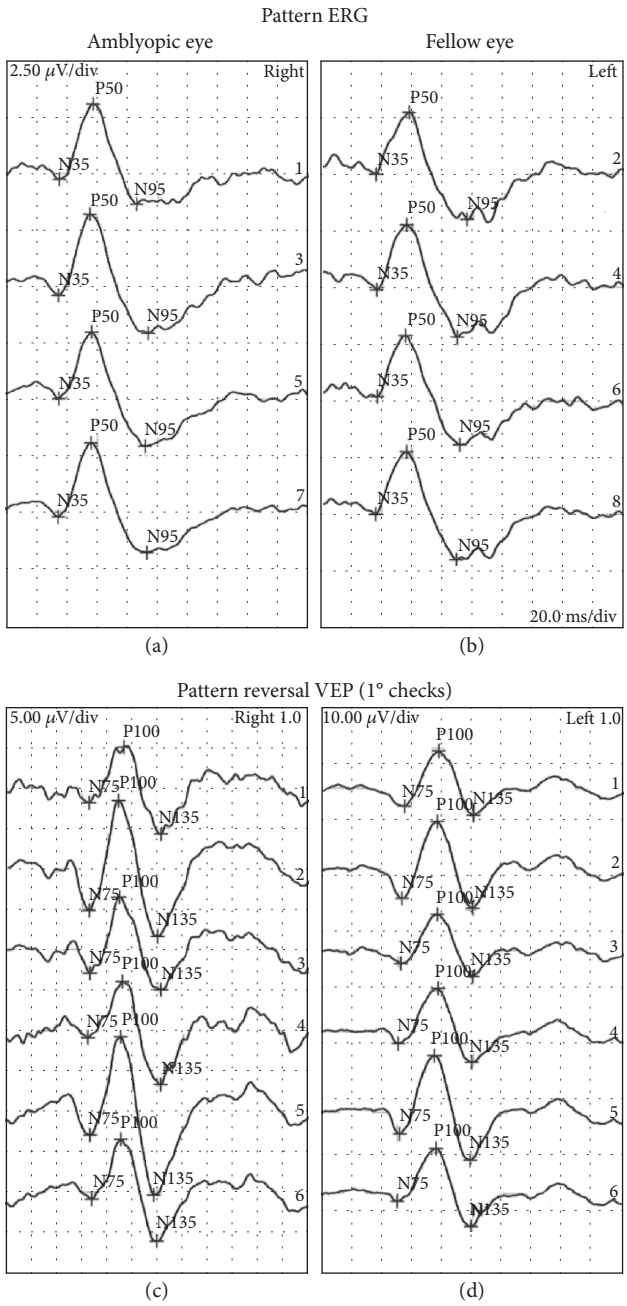

Figure 5: Pattern ERG (a, b) and pattern reversal VEP (c, d) results for the amblyopic (a, c) and fellow (b, d) eyes of participant P7 (first baseline session).

Only participant P6 exhibited a change in stereoacuity, improving from nil to 240 arc/sec in the active block and from nil to 480 arc/sec in the placebo block. Follow-up stereoacuity was nil. No significant treatment effects were evident for any of the electrophysiological measurements (all $F < 2.0$, all $p > 2$). Figure 3 shows 1° check stimulus VEP latencies (left) and N75-P100 amplitudes (right) for both the amblyopic and fellow fixing eyes. Figure 4 shows example multifocal ERG data for participant P7 (first baseline measure), and Figure 5 shows example pattern ERG and VEP data for the same participant. There were no treatment effects on POM-SF scores.

4. Discussion

The SSRI fluoxetine enabled recovery of vision in mature rats with amblyopia [44] and has recently been reported to enhance the effect of patching in older children and adults [50]. We found no effect of the SSRI citalopram combined with two weeks of patching on amblyopic eye visual acuity or a range of secondary outcome measures in adults with amblyopia. These results are broadly consistent with another recent study with a similar duration treatment period (10 days) that reported no advantage of combining fluoxetine with perceptual learning compared to perceptual learning alone in adults with amblyopia [51]. A preliminary study of donepezil [54] and a randomized clinical trial of levodopa [55] have also found no benefit of drug treatment in amblyopia therapy. In addition, we found no effect of two weeks of patching alone in adult patients despite reasonable self-reported adherence. This is expected based on the short treatment period and the reduced effect of patching with increasing age [15, 16, 56].

A number of factors may explain the lack of a drug treatment effect in our study. First, and perhaps most importantly, we did not achieve our planned sample size of 20 participants due to difficulties with recruitment. This led to a small sample with varied amblyopia etiology and treatment history. Barriers to recruitment included the time commitment required by the study and the stringent medical inclusion criteria. Therefore, our study may be underpowered to detect a treatment effect, although the sample size is within the range of previous case-series perceptual learning studies that have reported treatment effects [57]. It is intriguing that three participants exhibited an amblyopic eye visual acuity improvement of 0.1 logMAR or greater for the active but not the placebo treatment sessions. These participants had relatively poor baseline amblyopic eye visual acuity compared to most of the other participants. No participants exhibited any improvement for the placebo sessions. This observation suggests that further testing of SSRI treatment effects in adults with amblyopic may be warranted.

Whereas previous studies have used fluoxetine, we used citalopram because it has a short lead-in period of two hours [58]. Moreover, citalopram has a shorter half-life than fluoxetine; the distribution phase lasts about ten hours and the terminal half-life (T1/2) is 30-35 hours for citalopram [58] in contrast to two to four days' half-life for fluoxetine [59]. Citalopram and fluoxetine appear to have the same efficacy for treating major depression [60] and comparable effects on plasma GABA, glutamine, and glutamate levels in human patients [61]. However, citalopram and fluoxetine have different patterns of binding affinity within the human brain [62]. It is currently unknown whether the two drugs differ in the extent to which they promote visual cortex plasticity.

We used a 20 mg/day dose of citalopram over 2 weeks. It is possible that larger doses and longer treatment times are required to replicate the effects found in nonhuman animals. Supporting this idea, Sharif et al. [50] found a significant

effect of combined fluoxetine and patching with a dose of 0.5 mg/kg/day and a 3-month treatment period whereas Huttunen et al. [51] found no effect with 20 mg per day over 10 days. The parameter space for dosing and treatment duration is large for drug intervention studies of this type, and further work is required to identify optimal values. In addition, genotype may also influence an individual's response to a pharmacological intervention. In this study, we measured BDNF polymorphisms because they have been linked to neuroplasticity [53] and an increase in BDNF expression has been identified as a key mechanism in SSRI-induced recovery from amblyopia in mature rats [44]. There was no relationship between BDNF polymorphism and treatment response in this study with both val/val and val66met carriers improving by 1 logMAR line or more. However, the small sample size precludes any strong conclusions.

In agreement with Huttunen et al. [51], we found no effect of SSRI treatment on VEP parameters. This is in contrast to other emerging potential approaches to amblyopia treatment in adulthood such as the noninvasive brain stimulation technique anodal transcranial direct current stimulation that increases VEP amplitude [28]. The lack of any VEP changes is consistent with the lack of a treatment effect on any of the other outcome measures used within this study. Retinal electrophysiology was also conducted to rule out any retinal changes if a positive treatment effect was observed. No retinal changes were observed, in agreement with the overall study results.

In addition to the small sample size, a weakness of our study is that one participant (P6) did not meet the visual acuity inclusion criteria. We retained this participant in the study due to difficulties with recruitment. We note that excluding this participant from the sample does not change the pattern of results.

In conclusion, we found no effect of 2 weeks of combined citalopram and patching on amblyopic eye visual acuity in adults with amblyopia. This result may have been due to our study being underpowered as a result of recruitment challenges. Three out of seven participants did exhibit an amblyopic eye visual acuity improvement of 0.1 logMAR or more with combined citalopram and patching suggesting that further studies in this area may be warranted.

Data Availability

All clinical data are provided within the manuscript tables. Anonymized electrophysiological data are available from the authors upon request.

Conflicts of Interest

The authors have no conflicts of interest to declare.

Acknowledgments

This study was supported by grants to BT from the Marsden Fund of New Zealand and the Canadian Institutes of Health Research (CIHR 365136).

References

[1] J. M. Holmes and M. P. Clarke, "Amblyopia," *The Lancet*, vol. 367, no. 9519, pp. 1343–1351, 2006.

[2] D. Maurer and K. S. Mc, "Classification and diversity of amblyopia," *Visual Neuroscience*, vol. 35, article E012, 2018.

[3] L. M. Hamm, J. Black, S. Dai, and B. Thompson, "Global processing in amblyopia: a review," *Frontiers in Psychology*, vol. 5, p. 583, 2014.

[4] A. M. Wong, "New concepts concerning the neural mechanisms of amblyopia and their clinical implications," *Canadian Journal of Ophthalmology*, vol. 47, no. 5, pp. 399–409, 2012.

[5] K. Meier and D. Giaschi, "Unilateral amblyopia affects two eyes: fellow eye deficits in amblyopia," *Investigative Opthalmology & Visual Science*, vol. 58, no. 3, pp. 1779–1800, 2017.

[6] J. M. Holmes, "Designing clinical trials for amblyopia," *Vision Research*, vol. 114, pp. 41–47, 2015.

[7] C. E. Stewart, M. J. Moseley, D. A. Stephens, and A. R. Fielder, "Treatment dose-response in amblyopia therapy: the Monitored Occlusion Treatment of Amblyopia Study (MOTAS)," *Investigative Opthalmology & Visual Science*, vol. 45, no. 9, pp. 3048–3054, 2004.

[8] Pediatric Eye Disease Investigator Group Writing, "A randomized trial comparing Bangerter filters and patching for the treatment of moderate amblyopia in children," *Ophthalmology*, vol. 117, no. 5, pp. 998–1004.e6, 2010.

[9] M. X. Repka and J. M. Holmes, "Lessons from the amblyopia treatment studies," *Ophthalmology*, vol. 119, no. 4, pp. 657-658, 2012.

[10] M. M. Scheiman, R. W. Hertle, R. W. Beck et al., "Randomized trial of treatment of amblyopia in children aged 7 to 17 years," *Archives of Ophthalmology*, vol. 123, no. 4, pp. 437–447, 2005.

[11] Pediatric Eye Disease Investigator Group, "Patching vs atropine to treat amblyopia in children aged 7 to 12 years: a randomized trial," *Archives of Ophthalmology*, vol. 126, no. 12, pp. 1634–1642, 2008.

[12] D. K. Wallace and Pediatric Eye Disease Investigator Group, "A randomized trial to evaluate 2 hours of daily patching for strabismic and anisometropic amblyopia in children," *Ophthalmology*, vol. 113, no. 6, pp. 904–912, 2006.

[13] C. E. Stewart, D. A. Stephens, A. R. Fielder, M. J. Moseley, and M. Cooperative, "Modeling dose-response in amblyopia: toward a child-specific treatment plan," *Investigative Opthalmology & Visual Science*, vol. 48, no. 6, pp. 2589–2594, 2007.

[14] J. M. Holmes and D. M. Levi, "Treatment of amblyopia as a function of age," *Visual Neuroscience*, vol. 35, article E015, 2018.

[15] J. M. Holmes, E. L. Lazar, B. M. Melia et al., "Effect of age on response to amblyopia treatment in children," *Archives of Ophthalmology*, vol. 129, no. 11, pp. 1451–1457, 2011.

[16] M. Fronius, L. Cirina, H. Ackermann, T. Kohnen, and C. M. Diehl, "Efficiency of electronically monitored amblyopia treatment between 5 and 16 years of age: new insight into declining susceptibility of the visual system," *Vision Research*, vol. 103, pp. 11–19, 2014.

[17] C. Blakemore and R. C. Van Sluyters, "Reversal of the physiological effects of monocular deprivation in kittens: further evidence for a sensitive period," *The Journal of Physiology*, vol. 237, no. 1, pp. 195–216, 1974.

[18] D. H. Hubel and T. N. Wiesel, "The period of susceptibility to the physiological effects of unilateral eye closure in kittens," *The Journal of Physiology*, vol. 206, no. 2, pp. 419–436, 1970.

[19] J. A. Movshon, "Reversal of the physiological effects of monocular deprivation in the kitten's visual cortex," *The Journal of Physiology*, vol. 261, no. 1, pp. 125–174, 1976.

[20] N. W. Daw, *Visual development*, Springer, New York, NY, USA, 3rd edition edition, 2014.

[21] D. M. Levi, "Perceptual learning in adults with amblyopia: a reevaluation of critical periods in human vision," *Developmental Psychobiology*, vol. 46, no. 3, pp. 222–232, 2005.

[22] D. M. Levi and R. W. Li, "Perceptual learning as a potential treatment for amblyopia: a mini-review," *Vision Research*, vol. 49, no. 21, pp. 2535–2549, 2009.

[23] R. F. Hess and B. Thompson, "Amblyopia and the binocular approach to its therapy," *Vision Research*, vol. 114, pp. 4–16, 2015.

[24] R. F. Hess, B. Thompson, and D. H. Baker, "Binocular vision in amblyopia: structure, suppression and plasticity," *Ophthalmic and Physiological Optics*, vol. 34, no. 2, pp. 146–162, 2014.

[25] J. Li, D. P. Spiegel, R. F. Hess et al., "Dichoptic training improves contrast sensitivity in adults with amblyopia," *Vision Research*, vol. 114, pp. 161–172, 2015.

[26] J. Li, B. Thompson, D. Deng, L. Y. Chan, M. Yu, and R. F. Hess, "Dichoptic training enables the adult amblyopic brain to learn," *Current Biology*, vol. 23, no. 8, pp. R308–R309, 2013.

[27] I. Vedamurthy, M. Nahum, S. J. Huang et al., "A dichoptic custom-made action video game as a treatment for adult amblyopia," *Vision Research*, vol. 114, pp. 173–187, 2015.

[28] Z. Ding, J. Li, D. P. Spiegel et al., "The effect of transcranial direct current stimulation on contrast sensitivity and visual evoked potential amplitude in adults with amblyopia," *Scientific Reports*, vol. 6, no. 1, article 19280, 2016.

[29] B. Moret, R. Camilleri, A. Pavan et al., "Differential effects of high-frequency transcranial random noise stimulation (hf-tRNS) on contrast sensitivity and visual acuity when combined with a short perceptual training in adults with amblyopia," *Neuropsychologia*, vol. 114, pp. 125–133, 2018.

[30] D. P. Spiegel, W. D. Byblow, R. F. Hess, and B. Thompson, "Anodal transcranial direct current stimulation transiently improves contrast sensitivity and normalizes visual cortex activation in individuals with amblyopia," *Neurorehabil Neural Repair*, vol. 27, no. 8, pp. 760–769, 2013.

[31] D. P. Spiegel, J. Li, R. F. Hess et al., "Transcranial direct current stimulation enhances recovery of stereopsis in adults with amblyopia," *Neurotherapeutics*, vol. 10, no. 4, pp. 831–839, 2013.

[32] B. Thompson, B. Mansouri, L. Koski, and R. F. Hess, "Brain plasticity in the adult: modulation of function in amblyopia with rTMS," *Current Biology*, vol. 18, no. 14, pp. 1067–1071, 2008.

[33] T. Y. Gao, C. X. Guo, R. J. Babu et al., "Effectiveness of a binocular video game vs placebo video game for improving visual functions in older children, teenagers, and adults with amblyopia: a randomized clinical trial," *JAMA Ophthalmology*, vol. 136, no. 2, pp. 172–181, 2018.

[34] H. Morishita and T. K. Hensch, "Critical period revisited: impact on vision," *Current Opinion in Neurobiology*, vol. 18, no. 1, pp. 101–107, 2008.

[35] D. Mitchell and F. Sengpiel, "Animal models of amblyopia," *Visual Neuroscience*, vol. 35, article E017, 2018.

[36] M. P. Stryker and S. Löwel, "Amblyopia: new molecular/pharmacological and environmental approaches," *Visual Neuroscience*, vol. 35, article E018, 2018.

[37] H. Y. He, B. Ray, K. Dennis, and E. M. Quinlan, "Experience-dependent recovery of vision following chronic deprivation amblyopia," *Nature Neuroscience*, vol. 10, no. 9, pp. 1134–1136, 2007.

[38] K. R. Duffy and D. E. Mitchell, "Darkness alters maturation of visual cortex and promotes fast recovery from monocular deprivation," *Current Biology*, vol. 23, no. 5, pp. 382–386, 2013.

[39] A. Sale, J. F. Maya Vetencourt, P. Medini et al., "Environmental enrichment in adulthood promotes amblyopia recovery through a reduction of intracortical inhibition," *Nature Neuroscience*, vol. 10, no. 6, pp. 679–681, 2007.

[40] M. Spolidoro, L. Baroncelli, E. Putignano, J. F. Maya-Vetencourt, A. Viegi, and L. Maffei, "Food restriction enhances visual cortex plasticity in adulthood," *Nature Communications*, vol. 2, no. 1, p. 320, 2011.

[41] K. M. Murphy, G. Roumeliotis, K. Williams, B. R. Beston, and D. G. Jones, "Binocular visual training to promote recovery from monocular deprivation," *Journal of Vision*, vol. 15, no. 1, p. 2, 2015.

[42] M. Kaneko and M. P. Stryker, "Sensory experience during locomotion promotes recovery of function in adult visual cortex," *Elife*, vol. 3, article e02798, 2014.

[43] M. F. Fong, D. E. Mitchell, K. R. Duffy, and M. F. Bear, "Rapid recovery from the effects of early monocular deprivation is enabled by temporary inactivation of the retinas," *Proceedings of the National Academy of Sciences of the United States of America*, vol. 113, no. 49, pp. 14139–14144, 2016.

[44] J. F. Maya Vetencourt, A. Sale, A. Viegi et al., "The antidepressant fluoxetine restores plasticity in the adult visual cortex," *Science*, vol. 320, no. 5874, pp. 385–388, 2008.

[45] I. Loubinoux, J. Pariente, O. Rascol, P. Celsis, and F. Chollet, "Selective serotonin reuptake inhibitor paroxetine modulates motor behavior through practice. A double-blind, placebo-controlled, multi-dose study in healthy subjects," *Neuropsychologia*, vol. 40, no. 11, pp. 1815–1821, 2002.

[46] I. Loubinoux, D. Tombari, J. Pariente et al., "Modulation of behavior and cortical motor activity in healthy subjects by a chronic administration of a serotonin enhancer," *Neuroimage*, vol. 27, no. 2, pp. 299–313, 2005.

[47] C. Normann, D. Schmitz, A. Furmaier, C. Doing, and M. Bach, "Long-term plasticity of visually evoked potentials in humans is altered in major depression," *Biological Psychiatry*, vol. 62, no. 5, pp. 373–380, 2007.

[48] F. Chollet, J. Tardy, J. F. Albucher et al., "Fluoxetine for motor recovery after acute ischaemic stroke (FLAME): a randomised placebo-controlled trial," *The Lancet Neurology*, vol. 10, no. 2, pp. 123–130, 2011.

[49] A. K. Lagas, J. M. Black, W. D. Byblow et al., "Fluoxetine does not enhance visual perceptual learning and triazolam specifically impairs learning transfer," *Frontiers in Human Neuroscience*, vol. 10, 2016.

[50] M. H. Sharif, M. R. Talebnejad, K. Rastegar, M. R. Khalili, and M. H. Nowroozzadeh, "Oral fluoxetine in the management of amblyopic patients aged between 10 and 40 years old: a randomized clinical trial," *Eye*, 2019.

[51] H. J. Huttunen, J. M. Palva, L. Lindberg et al., "Fluoxetine does not enhance the effect of perceptual learning on visual function in adults with amblyopia," *Scientific Reports*, vol. 8, no. 1, article 12830, 2018.

[52] P. Baumann, "Pharmacology and pharmacokinetics of citalopram and other SSRIs," *International Clinical Psychopharmacology*, vol. 11, pp. 5–12, 1996.

[53] J. A. Kleim, S. Chan, E. Pringle et al., "BDNF val66met polymorphism is associated with modified experience-dependent plasticity in human motor cortex," *Nature Neuroscience*, vol. 9, no. 6, pp. 735–737, 2006.

[54] S. T. L. Chung, R. W. Li, M. A. Silver, and D. M. Levi, "Donepezil does not enhance perceptual learning in adults with amblyopia: a pilot study," *Frontiers in Neuroscience*, vol. 11, p. 448, 2017.

[55] Pediatric Eye Disease Investigator Group, M. X. Repka, R. T. Kraker et al., "A randomized trial of levodopa as treatment for residual amblyopia in older children," *Ophthalmology*, vol. 122, no. 5, pp. 874–881, 2015.

[56] M. Epelbaum, C. Milleret, P. Buisseret, and J. L. Dufier, "The sensitive period for strabismic amblyopia in humans," *Ophthalmology*, vol. 100, no. 3, pp. 323–327, 1993.

[57] D. M. Levi and U. Polat, "Neural plasticity in adults with amblyopia," *Proceedings of the National Academy of Sciences of the United States of America*, vol. 93, no. 13, pp. 6830–6834, 1996.

[58] K. Bezchlibnyk-Butler, I. Aleksic, and S. H. Kennedy, "Citalopram–a review of pharmacological and clinical effects," *Journal of Psychiatry and Neuroscience*, vol. 25, no. 3, pp. 241–254, 2000.

[59] C. Gury and F. Cousin, "Pharmacokinetics of SSRI antidepressants: half-life and clinical applicability," *Encephale*, vol. 25, no. 5, pp. 470–476, 1999.

[60] M. Patris, J. M. Bouchard, T. Bougerol et al., "Citalopram versus fluoxetine: a double-blind, controlled, multicentre, phase III trial in patients with unipolar major depression treated in general practice," *International Clinical Psychopharmacology*, vol. 11, no. 2, pp. 129–136, 1996.

[61] E. Kucukibrahimoglu, M. Z. Saygin, M. Caliskan, O. K. Kaplan, C. Unsal, and M. Z. Goren, "The change in plasma GABA, glutamine and glutamate levels in fluoxetine- or S-citalopram-treated female patients with major depression," *European Journal of Clinical Pharmacology*, vol. 65, no. 6, pp. 571–577, 2009.

[62] M. J. Owens, D. L. Knight, and C. B. Nemeroff, "Second-generation SSRIs: human monoamine transporter binding profile of escitalopram and R-fluoxetine," *Biological Psychiatry*, vol. 50, no. 5, pp. 345–350, 2001.

Hindawi
Neural Plasticity
Volume 2019, Article ID 5653180, 9 pages
https://doi.org/10.1155/2019/5653180

Review Article

From Basic Visual Science to Neurodevelopmental Disorders: The Voyage of Environmental Enrichment-Like Stimulation

Alan Consorti[1], **Gabriele Sansevero**[2], **Claudia Torelli**[3,4], **Nicoletta Berardi**[3,4] **and Alessandro Sale**[3]

[1]*University of Pisa, Pisa, Italy*
[2]*IRCCS Stella Maris, Calambrone, Pisa, Italy*
[3]*Neuroscience Institute, National Research Council (CNR), Pisa, Italy*
[4]*Department of Neuroscience, Psychology, Drug Research and Child Health NEUROFARBA, University of Florence, Florence, Italy*

Correspondence should be addressed to Alessandro Sale; sale@in.cnr.it

Received 22 January 2019; Revised 6 March 2019; Accepted 16 April 2019; Published 6 May 2019

Guest Editor: Elizabeth Quinlan

Genes and environmental stimuli cooperate in the regulation of brain development and formation of the adult neuronal architecture. Genetic alterations or exposure to perturbing environmental conditions, therefore, can lead to altered neural processes associated with neurodevelopmental disorders and brain disabilities. In this context, environmental enrichment emerged as a promising and noninvasive experimental treatment for favoring recovery of cognitive and sensory functions in different neurodevelopmental disorders. The aim of this review is to depict, mainly through the much explicative examples of amblyopia, Down syndrome, and Rett syndrome, the increasing interest in the potentialities and applications of enriched environment-like protocols in the field of neurodevelopmental disorders and the understanding of the molecular mechanisms underlying the beneficial effects of these protocols, which might lead to development of pharmacological interventions.

1. Introduction

The brain capability to adapt in response to environmental changes is called neural plasticity, which allows cerebral circuits to modify their structure and function in response to experience through changes occurring at the molecular, neuronal, and systemic level.

In all mammal species studied so far, major plastic changes are mostly confined to specific time windows, early in development, known as critical periods (CPs) [1, 2]. During these periods, different for distinct developing functions, the inner genetic plan and the external environmental influences cooperate, leading to the final unfolding and maturation of an adaptive individual body. At the end of CPs, neural plasticity levels decay, possibly as the result of evolutionary pressures towards a final stabilization and maintenance of the mature structural connections and of the ensuing sensory functions emerging from the developmental events.

A key consequence of the interplay between genes and environment underlying brain development is that genetic alterations and/or exposure to altered environmental conditions before the closure of CPs can lead to alterations of brain development, resulting in a number of different, moderate to severe, neurodevelopmental disorders [3, 4].

During the last decades, an increasing number of experimental researches have led to the discovery of molecular brakes that restrict neural plasticity within the temporal limits of the CPs [5–8]. The opportunity to regulate these molecules and to modulate the time course and closure of CPs have opened the possibility to ameliorate brain functioning in neurodevelopmental disorders even past the end of the CPs. In this context, the visual system emerges as a favorite model to probe cortical plasticity throughout and after the end of CPs, both in physiological and pathological conditions [9]. Indeed, since the original discovery by the Nobel Prize winners Wiesel and Hubel demonstrating the existence of a CP for ocular dominance plasticity in mammals with

binocular sight [10], the visual cortex has become the most widely employed system to investigate the mechanisms underlying cerebral plasticity and the possibility to restore or enhance it in adulthood. Beyond its impact on the treatment of neurodevelopmental visual disorders such as amblyopia [11], this seminal work has opened new perspectives in the field of neurodevelopmental disorders which are not considered, in their essential nature, visual ones, such as Rett syndrome (RTT), autism spectrum disorders (ASD; in particular X-fragile syndrome (FXS)), and Down syndrome (DS) [12–16].

In particular, the study of the mechanisms underlying visual system plasticity in animal models and the specific impact that EE exerts on them has provided insights for the development of possible pharmacological and nonpharmacological [17–19] interventions in human subjects with RTT, DS, and FXS. In some occasions, these applications have already moved forward to the phase 3 of clinical experimentation or randomized studies [17–19].

In this review, we shall discuss the translational route from basic studies focused on visual system plasticity to the application of possible EE interventions in human subjects. Wherever possible, we shall underscore the relevance of a better knowledge of the molecular mechanisms underlying the EE effects in animal models for the characterization of similar mechanisms underlying neural dysfunctions in humans and for the development of possible successful interventions.

2. Manipulating the Environment to Enhance Plasticity: The Environmental Enrichment Approach

The most direct approach to manipulate the environment in order to enhance neural plasticity is environmental enrichment (EE), introduced in the early 1960s by Rosenzweig and colleagues [20–22]. EE consists in rearing laboratory animals in cages wider and more attractive than those employed in the so-called standard conditions (SCs), with a variety of sensory, cognitive, motor, and social stimuli. Exposure to EE exerts profound effects on brain morphology and physiology, enhancing neural plasticity in different brain areas at all ages analyzed so far (for review, see [23–25]) and exerting beneficial effects in animal models of neurodegenerative diseases and brain injury [26].

The definition of EE is based on a comparison with a reference condition that, for laboratory animal models, is generally represented by SCs, in which the animals are reared in simple cages without any other object than litter, food, and water, and are hosted in very small social groups. Thus, one critical question is to what extent is the EE approach able to provide supernormal levels of stimulation or whether it should be better considered a way to compensate for sensory-motor deprivation associated with SCs. According to this criticism, the beneficial results obtained with EE in animal models might be of reduced interest in terms of their applicability to the clinic, as humans are generally considered already "enriched" in their living conditions (see also [27]). As originally stated by the first proposers of the EE approach, it is worth considering that, after hundreds of generations in SCs, a strong genetic drift with respect to wild natural populations may have rescaled neural development and basic brain functions in a new physiological and well-adapted dimension, without any pathological or aberrant side effect for brain development. Thus, measures collected in these simplified models may actually represent a suitable source for normative data, to be compared with the effects deriving from exposure to EE.

3. When Experience Affects Development: The Case of Amblyopia

An unbalanced stimulation of the two eyes during early postnatal development induced by variable causes such as congenital cataract, unequal refractive power, or strabismus can lead to a neurodevelopmental visual deficit known as amblyopia (lazy eye). This disease has an incidence of 1-5% in the worldwide population, and it is the most prevalent one-eye visual impairment, characterized by a loss in visual acuity, low contrast sensitivity, hampered stereopsis, and an impairment of the orientation tuning of cortical neurons (binocular matching) [28–30]. Amblyopia is considered a purely cortical deficit with no detectable impairments in peripheral regions, albeit the lateral geniculate nucleus may be anatomically and functionally involved [24, 31]. A timely patching of the spared eye performed during the CP for binocular vision and visual acuity development (approximately until 8 years of age in humans) is normally associated with a rescue from amblyopia. Nevertheless, the closure of CP turns amblyopia into an almost untreatable disease.

Amblyopia is easily modeled in animals, keeping one eye deprived of pattern vision via prolonged eyelid suture (monocular deprivation (MD)), started during the CP and protracted until adulthood [32, 33]. The procedure causes a marked ocular dominance shift towards the open eye in the binocular neurons of the primary visual cortex, determined by functional and structural empowering of the inputs emerging from the ipsilateral/spared eye, at the expense of those from the contralateral/deprived one [34].

In recent years, EE has proven successful in the treatment of amblyopia in adult animals. Adult amblyopic rats that were transferred to an EE setting for three weeks displayed a full recovery of visual acuity, ocular dominance, and depth perception [7, 35]. More selective EE conditions are also able to reproduce the beneficial effects elicited by the entire complex enriched experience, especially when motor or visual stimuli are specifically enhanced [36]. In particular, three weeks of voluntary physical exercise induced a full recovery of visual acuity and ocular dominance in adult amblyopic rats [36]. Also data from Stryker's lab confirmed the potential of motor activity as a booster of visual responsiveness and plasticity in the visual cortex, showing that running on a treadmill enhances visual cortical activity in mice [37] and promotes visual function recovery following monocular deprivation [38]. Another condition akin to EE, i.e., practicing in a two-choice active visual discrimination task, also resulted in an almost-full rescue of visual acuity and ocular dominance in adult amblyopic animals [36, 39].

Animal model data provided also information on the mechanisms underlying EE-like effects in promoting recovery from amblyopia. Data from Stryker's lab showed that enhancement of visual cortical activity [37] and visual function recovery following monocular deprivation [38] in running mice is associated with a disynaptic disinhibition involving activation of VIP+ interneurons and inhibition of SOM+ interneurons in the visual cortex [40]. Our work and other labs showed that exposure to EE reduces GABAergic inhibition in the visual cortex of enriched animals [7, 41]. Recovery of visual functions in enriched amblyopic rats was accompanied by increased expression of BDNF, reduction in the intracortical inhibition-excitation balance, and reduced density of perineuronal nets made by chondroitin sulphate proteoglycans enwrapping the terminals of GABAergic interneurons [7, 15]. Moreover, exposure to EE increased levels of serotonin in the adult visual cortex and a pharmacological blockade of this enhancement prevented EE-dependent restoration of visual cortex plasticity in adult animals [15]. Interestingly, both motor activity and PL also led to a reduced synaptic release of GABA in the visual cortex of adult amblyopic rats [36].

EE and physical exercise also contribute to increase insulin-like growth factor-1 (IGF-1) in the brain. IGF-1 has a crucial role in setting the pace of visual development and seems to be a "master mediator" of EE effects, upstream of BDNF, correcting, for instance, the mismatch between two visual developmental processes, ocular dominance development, and binocular matching of orientation selectivity development, caused by genetic overexpression of BDNF [42, 43]. This is important to underline, since the possibility that different molecules or the same molecule but in different neurons can differently affect developmental trajectories and functional recovery is now suggested not only by the effects of BDNF on binocular matching but also by Ngr1 deletion on visual acuity and ocular dominance recovery in amblyopic mice [31]. Confirming its nature of master experience mediator, the administration of IGF-1 in the adult visual cortex promoted recovery of visual acuity and ocular dominance in adult amblyopic rats, an effect paralleled by the reduction of intracortical GABA levels [44].

Given its noninvasive nature, the concept of EE appears as a promising strategy to counteract visual impairments in human amblyopia. The major challenge is how to transfer EE to human life conditions, setting up the best protocols to induce a suitable environmental stimulation for human patients. Recent papers show very encouraging data. Active videogames appear a clever trick to combine key EE components such as visual attention and enhanced sensory stimulation (see [45]), with promising results in adult subjects with amblyopia [46], but with apparently limited effects in children [47, 48]. In the same context, engagement in subtle visual discrimination tasks such as those associated with visual perceptual learning (see [39] for a recent review) can favor recovery of visual functions in adult amblyopia (e.g., [49–60]). Very recently, moderate levels of voluntary physical activity combined with short-term monocular deprivation have been shown to enhance homeostatic plasticity in the visual cortex of healthy human subjects, favoring the dominance of the briefly deprived eye [61]. Most importantly, brief occlusion of the amblyopic eye combined with enhanced physical activity promoted a remarkable and long-lasting recovery of visual acuity and stereopsis in adult amblyopic individuals [62].

Thus, basic studies on the impact of EE on visual system plasticity are currently leading to an increasing interest for the development of promising nonpharmacological interventions in amblyopic human subjects. Future research should try to provide evidence on the effectiveness of such active training on amblyopia recovery in different categories of human amblyopic subjects and to ascertain whether the documented beneficial effects in humans are due to the same mechanisms already verified in animal models.

4. When Genes Affect Development: The Case of Down Syndrome and Rett Syndrome

Differently from amblyopia, Down syndrome (DS) and Rett syndrome (RTT) are developmental disorders of genetic nature. Originally described by John Langdon Down, DS is the most widespread genetic form of intellectual disability and it is caused by the total or partial triplication in the genome of the chromosome 21 [63]. This has a dramatic impact on the central nervous system, with a disruption of the synaptic architectures leading to a failure in cognition, learning, memory, and language [64, 65]. The genetic imbalance does also result in severe consequences in extracognitive domains, such as in the visual system, with damaged spatial acuity and increased incidence of strabismus and cataract [66]. Moreover, since the gene encoding the amyloid precursor protein (APP) is located on the chromosome 21, trisomy induces an increase in the concentration of brain β-amyloid, and adult DS individuals of more than 40 years of age display early-onset Alzheimer-like neuropathology that additionally complicates their quality of life and independence possibilities [67, 68].

The complexity of the DS made its replication in animal models a highly demanding aim. Generated in the 1990 [69], the Ts65Dn mouse represents the most commonly used model to study this pathology. Ts65Dn mice bear a segmental triplication of the chromosome 16 that displays high degree of synteny with the human chromosome 21 [70]. The resulting mutation closely resembles the structural and behavioral features of the human disorder. Ts65Dn mice display decreased long-term hippocampal potentiation, defective neurogenesis, low synaptogenesis, and a generalized state of cerebral overactivation of GABAergic circuits [65, 71]. Remarkably, similarly to human subjects with DS, trisomic mice display severe visual deficits: the visual acuity is significantly impaired, visual evoked potentials are slower than normal, and the visual cortex responsiveness is anomalously shifted towards the ipsilateral inputs [72, 73].

RTT is a debilitating progressive disorder first noted by Andreas Rett in 1966 [74]. It is a rare pathology affecting quite exclusively females, with an incidence of about 1 over 10,000 births. With very few exceptions [75], the majority of males with RTT die soon after delivery. RTT remains mostly asymptomatic during the first months of postnatal growth. Thereafter, most of the skills already acquired by

an affected subject dramatically deteriorate. As RTT lacks a specific cortical localization, deficits involve the whole brain functionality, with some prototypical characteristics including severe motor deficits (stereotyped hand movements are the principal RTT hallmark), autonomic dysfunctions, and intellectual disability [76, 77]. Only in 1999 [78], these deficits were first associated to loss-of-function mutations in the gene encoding the methyl-CpG-binding protein (MeCP2) on the X chromosome, thus clarifying discrepancy in the incidence between females and males. The MeCP2 protein has a proven role as a master regulator of the chromatin state and gene expression (including the *BDNF* gene [79]), being involved in the formation of a multiprotein complex that binds methylated CpG regions and allows gene silencing [80]. Recent evidence expanded this view, suggesting that it could also activate the expression of several other genes, playing as an activator or a repressor depending on the type of proteins that join the complex [81]. The deletion of the MeCP2 gene in mouse models leads to a phenotype that closely recapitulates many features of the human disorder [82]; thus, employment of mouse models has become essential to study the mechanisms involved in RTT and to test the potential useful treatments. A recent paper documented, in girls with RTT, visual deficits similar to those found in Mecp2 heterozygous female mice, and underscored the possibility to successfully exploit visual evoked potentials (VEPs) as an unbiased, quantitative biomarker to monitor brain function in RTT [13].

Strikingly, the EE approach turned out to be very valuable in the context of these genetic disorders [83–86]. Exposure of either developing or adult Ts65Dn mice to EE induces a marked recovery of both cognitive and visual functions [72, 87], and middle aged Ts65Dn mice chronically maintained in EE conditions displayed a reduced amount of β-amyloid oligomers compared to trisomic mice reared in SCs [88]. In *Mecp2*mutant mice, EE ameliorated motor coordination and motor learning and rescued memory deficits and anxiety-related behavior, with gender differences [89].

As seen for visual disorders, physical exercise emerges as one critical component underlying the beneficial EE effects for DS, being specifically associated with an increased neurogenesis and gliogenesis in the hippocampus [90, 91]. Recently, the specific effect of physical exercise was also explored in the Mecp2(+/-) mouse model of RTT, with the demonstration that increased voluntary physical activity normalizes the physiology of the hypothalamic-pituitary-adrenal axis, providing a significant rescue from affective behavioral dysfunctions [92].

The positive impact of EE on both DS and RTT has been linked, in animal models, to modulation of GABAergic synaptic strength and to an increased BDNF expression [72, 87, 89, 93].

Based on the results obtained in animal models of DS and RTT, recent studies have started to apply the EE paradigm to infants and children with these disorders. Different kinds of early multisensory intervention have been associated with beneficial effects on the maturation of visual functions in infants with DS [19] and improved gross motor skills and increased blood BDNF levels in children with RTT [18].

Thus, as seen for amblyopia, a general picture emerges in which results obtained in animal models might orient future research in humans, with the aim to uncover shared molecular mechanisms that might be instrumental for the development of suitable pharmacological approaches.

5. Towards an Environment-Based Pharmacological Approach?

The remarkable capacity of the EE approach to trigger recovery in diseases as different as amblyopia or genetic intellectual disabilities could be due, at least in part, to its impact on the GABAergic circuitry. An increased activation of the GABAergic inhibitory system is widely considered as a common hallmark of many brain developmental pathologies [94, 95]. Unfortunately, availability of suitable therapeutic compounds that may safely act in decreasing the activation in the GABAergic system is scant, while most of the drugs have severe proconvulsive side effects, with consequent rejection by FDA.

In this context, fluoxetine, a selective serotonin reuptake inhibitor (SSRI) widely prescribed in the treatment of human depression, emerges as a potentially interesting candidate for drug repositioning, given its capability to increase levels and availability of serotonin, one key molecular factor underlying EE effects [15].

Adult amblyopic rats chronically treated with fluoxetine display robust recovery of visual cortex plasticity and visual functions, together with increased BDNF and a reduced GABAergic tone in the primary visual cortex [96]. A very recent study examined the effect of fluoxetine in adult amblyopic human subjects, without a significant improvement in visual performance compared to that obtained in subjects treated with placebo [97]. Since all patients did also perform, during the 10 weeks of pharmacological treatment, an intense perceptual training therapy, it remains unclear whether the lack of a specific effect of fluoxetine in this study was due to a ceiling effect of the training paradigm.

Administration of fluoxetine for eight weeks in the drinking water reduced brain GABA release and rescued hippocampal synaptic plasticity and spatial memory in DS mice [98]. Moreover, treating neonate Ts65Dn mice with fluoxetine led to a full recovery of dentate gyrus neurogenesis and hippocampus-dependent memory performance [99]. Based on these results, the effectiveness of fluoxetine in human subjects with DS is, at the moment, under evaluation in several clinical trials [100, 101].

It remains unclear whether the therapeutic effects of fluoxetine are due to its action on the GABAergic system or are also dependent on its recognized ability to increase BDNF levels [102, 103]. BDNF itself, indeed, could emerge as a helpful compound to treat amblyopia and genetic disorders like DS and RTT. The promising potential of BDNF, however, is thwarted by the impossibility for this neurotrophic factor to efficiently cross the blood-brain barrier when delivered via peripheral administration [104]. Recently, intranasal BDNF administration, a safe procedure considered quite effective to target proteins to the central nervous system [105], induced recovery of visual acuity, ocular dominance,

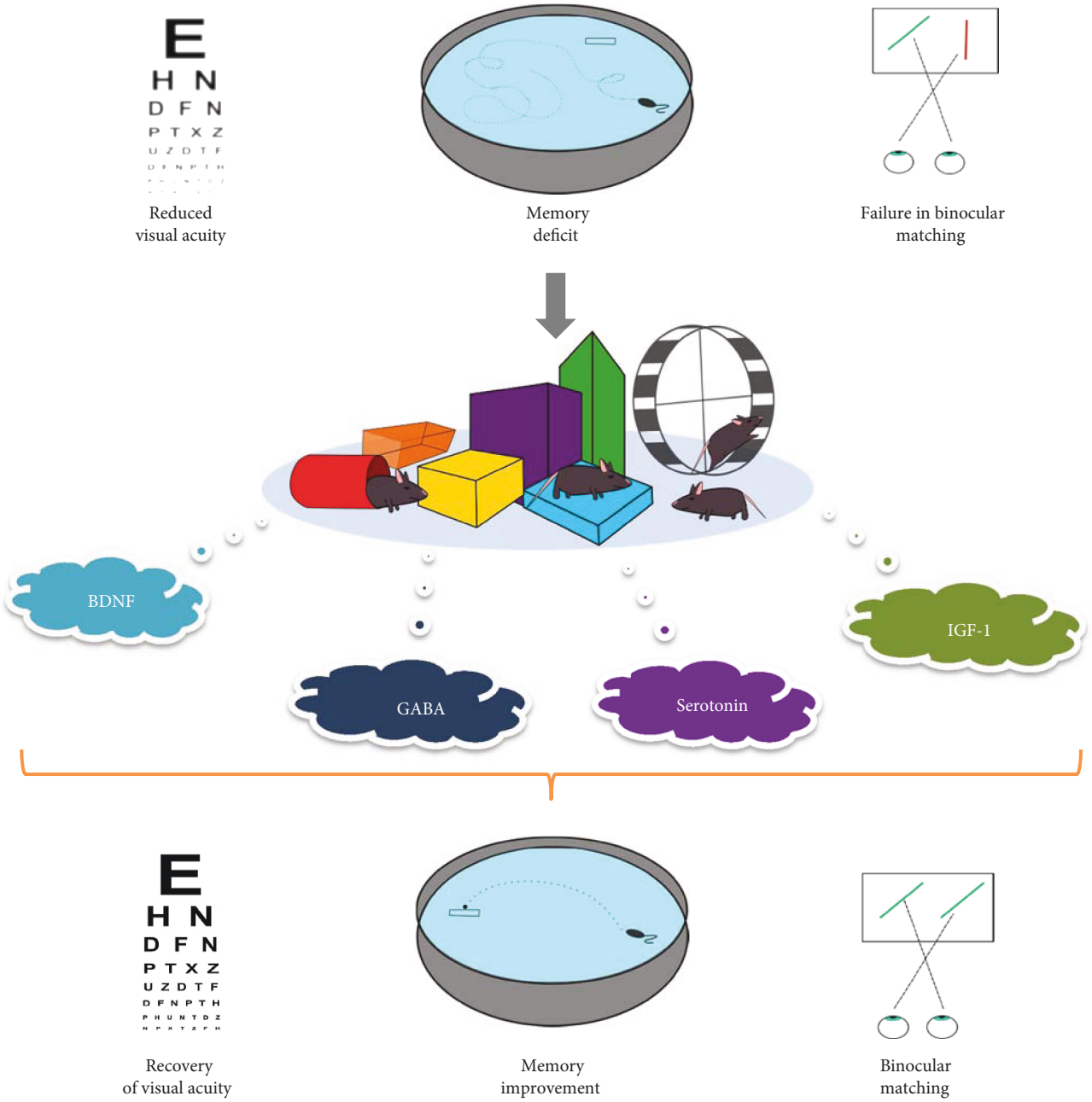

Figure 1: Exposure to conditions of environmental enrichment modulates a number of key molecular factors involved in brain plasticity and repair, favoring recovery of sensory functions (e.g., visual acuity and binocular matching) and improvement of learning/memory abilities in neurodevelopmental disorders. The molecular factors involved in the beneficial effects elicited by enrichment-like conditions can become the target for successful pharmacological manipulations and potential translational application to the clinic.

and visual depth perception in adult amblyopic rats. Moreover, the administration of 7,8-dihydroxyflavone, an agonist of the BDNF receptor TrkB, efficiently restored learning and memory abilities in Ts65Dn mice [106]. In heterozygous female *Mecp2* mutant mice, pharmacologic activation of the BDNF receptor TrkB ameliorated several biochemical and functional abnormalities, highlighting TrkB as a possible therapeutic target in this disease [107].

Several papers showed that treatment with either a fragment of IGF-1 or the full-length molecule can be effective in alleviating symptoms in RTT mouse models (reviewed in [108]). Based on these studies, the application of IGF-1 to RTT patients has recently started (e.g., [109, 110]).

In conclusion, combining EE with classical studies on visual system plasticity has led to the characterization of several potential molecular targets for successful translational applications (Figure 1). The therapeutic value of the emerging molecular pathways overcomes the boundaries of the visual system and opens the way for further testing in the treatment of several neurodevelopmental disorders of different genetic or environmental origin [104, 111–114]. Future studies should exploit the EE approach in animal

models (applied either as a multicomponent or as a channel-specific strategy) as a source for translational application to human patients. Knowledge about shared molecular pathways might inspire the development of new pharmacological strategies for still cureless developmental disorders.

Conflicts of Interest

The authors declare that they have no conflicts of interest.

Acknowledgments

This work was supported by ERANET-NEURODREAM funding, MIUR—Italian Ministry of Education, University and Research, and PRIN-2015 grant.

References

[1] N. Berardi, T. Pizzorusso, and L. Maffei, "Critical periods during sensory development," *Current Opinion in Neurobiology*, vol. 10, no. 1, pp. 138–145, 2000.

[2] T. K. Hensch, "Critical period plasticity in local cortical circuits," *Nature Reviews Neuroscience*, vol. 6, no. 11, pp. 877–888, 2005.

[3] E. I. Knudsen, "Experience alters the spatial tuning of auditory units in the optic tectum during a sensitive period in the barn owl," *Journal of Neuroscience*, vol. 5, no. 11, pp. 3094–3109, 1985.

[4] A. Antonini, M. Fagiolini, and M. P. Stryker, "Anatomical correlates of functional plasticity in mouse visual cortex," *Journal of Neuroscience*, vol. 19, no. 11, pp. 4388–4406, 1999.

[5] T. Pizzorusso, P. Medini, N. Berardi, S. Chierzi, J. W. Fawcett, and L. Maffei, "Reactivation of ocular dominance plasticity in the adult visual cortex," *Science*, vol. 298, no. 5596, pp. 1248–1251, 2002.

[6] D. Bavelier, D. M. Levi, R. W. Li, Y. Dan, and T. K. Hensch, "Removing brakes on adult brain plasticity: from molecular to behavioral interventions," *Journal of Neuroscience*, vol. 30, no. 45, pp. 14964–14971, 2010.

[7] A. Sale, J. F. Maya Vetencourt, P. Medini et al., "Environmental enrichment in adulthood promotes amblyopia recovery through a reduction of intracortical inhibition," *Nature Neuroscience*, vol. 10, no. 6, pp. 679–681, 2007.

[8] S. Sugiyama, A. Prochiantz, and T. K. Hensch, "From brain formation to plasticity: insights on Otx2 homeoprotein," *Development, Growth & Differentiation*, vol. 51, no. 3, pp. 369–377, 2009.

[9] M. Hübener and T. Bonhoeffer, "Neuronal plasticity: beyond the critical period," *Cell*, vol. 159, no. 4, pp. 727–737, 2014.

[10] T. N. Wiesel and D. H. Hubel, "Single-cell responses in striate cortex of kittens deprived of vision in one eye," *Journal of Neurophysiology*, vol. 26, no. 6, pp. 1003–1017, 1963.

[11] B. T. Barrett, A. Bradley, and P. V. McGraw, "Understanding the neural basis of amblyopia," *The Neuroscientist*, vol. 10, no. 2, pp. 106–117, 2004.

[12] T. Karaminis, C. Lunghi, L. Neil, D. Burr, and E. Pellicano, "Binocular rivalry in children on the autism spectrum," *Autism Research*, vol. 10, no. 6, pp. 1096–1106, 2017.

[13] J. J. LeBlanc, G. DeGregorio, E. Centofante et al., "Visual evoked potentials detect cortical processing deficits in Rett syndrome," *Annals of Neurology*, vol. 78, no. 5, pp. 775–786, 2015.

[14] F. M. John, N. R. Bromham, J. M. Woodhouse, and T. R. Candy, "Spatial vision deficits in infants and children with Down syndrome," *Investigative Ophthalmology & Visual Science*, vol. 45, no. 5, pp. 1566–1572, 2004.

[15] L. Baroncelli, A. Sale, A. Viegi et al., "Experience-dependent reactivation of ocular dominance plasticity in the adult visual cortex," *Experimental Neurology*, vol. 226, no. 1, pp. 100–109, 2010.

[16] E. M. Berry-Kravis, L. Lindemann, A. E. Jønch et al., "Drug development for neurodevelopmental disorders: lessons learned from fragile X syndrome," *Nature Reviews Drug Discovery*, vol. 17, no. 4, pp. 280–299, 2017.

[17] G. Pini, L. Congiu, A. Benincasa et al., "Illness severity, social and cognitive ability, and EEG analysis of ten patients with Rett syndrome treated with mecasermin (recombinant human IGF-1)," *Autism Research and Treatment*, vol. 2016, Article ID 5073078, 9 pages, 2016.

[18] J. Downs, J. Rodger, C. Li et al., "Environmental enrichment intervention for Rett syndrome: an individually randomised stepped wedge trial," *Orphanet Journal of Rare Diseases*, vol. 13, no. 1, 2018.

[19] G. Purpura, F. Tinelli, S. Bargagna, M. Bozza, L. Bastiani, and G. Cioni, "Effect of early multisensory massage intervention on visual functions in infants with Down syndrome," *Early Human Development*, vol. 90, no. 12, pp. 809–813, 2014.

[20] M. C. Diamond, F. Law, H. Rhodes et al., "Increases in cortical depth and glia numbers in rats subjected to enriched environment," *The Journal of Comparative Neurology*, vol. 128, no. 1, pp. 117–125, 1966.

[21] M. R. Rosenzweig, E. L. Bennett, and M. C. Diamond, "Effects of differential environments on brain anatomy and brain chemistry," *Proceedings of the Annual Meeting of the American Psychopathological Association*, vol. 56, pp. 45–56, 1967.

[22] M. R. Rosenzweig, D. Krech, E. L. Bennett, and J. F. Zolman, "Variation in environmental complexity and brain measures," *Journal of Comparative and Physiological Psychology*, vol. 55, no. 6, pp. 1092–1095, 1962.

[23] H. van Praag, G. Kempermann, and F. H. Gage, "Neural consequences of environmental enrichment," *Nature Reviews Neuroscience*, vol. 1, no. 3, pp. 191–198, 2000.

[24] A. Sale, N. Berardi, and L. Maffei, "Environment and brain plasticity: towards an endogenous pharmacotherapy," *Physiological Reviews*, vol. 94, no. 1, pp. 189–234, 2014.

[25] A. Sale, "A systematic look at environmental modulation and its impact in brain development," *Trends in Neurosciences*, vol. 41, no. 1, pp. 4–17, 2018.

[26] J. Nithianantharajah and A. J. Hannan, "Enriched environments, experience-dependent plasticity and disorders of the nervous system," *Nature Reviews Neuroscience*, vol. 7, no. 9, pp. 697–709, 2006.

[27] M. P. Stryker and S. Löwel, "Amblyopia: new molecular/-pharmacological and environmental approaches," *Visual Neuroscience*, vol. 35, article E018, 2018.

[28] J. M. Holmes and M. P. Clarke, "Amblyopia," *The Lancet*, vol. 367, no. 9519, pp. 1343–1351, 2006.

[29] D. M. Levi, D. C. Knill, and D. Bavelier, "Stereopsis and amblyopia: a mini-review," *Vision Research*, vol. 114, pp. 17–30, 2015.

[30] B.-S. Wang, R. Sarnaik, and J. Cang, "Critical period plasticity matches binocular orientation preference in the visual cortex," *Neuron*, vol. 65, no. 2, pp. 246–256, 2010.

[31] C.-É. Stephany, X. Ma, H. M. Dorton et al., "Distinct circuits for recovery of eye dominance and acuity in murine amblyopia," *Current Biology*, vol. 28, no. 12, pp. 1914–1923.e5, 2018.

[32] L. C. Sincich, C. M. Jocson, and J. C. Horton, "Neuronal projections from V1 to V2 in amblyopia," *Journal of Neuroscience*, vol. 32, no. 8, pp. 2648–2656, 2012.

[33] A. Antonini, D. C. Gillespie, M. C. Crair, and M. P. Stryker, "Morphology of single geniculocortical afferents and functional recovery of the visual cortex after reverse monocular deprivation in the kitten," *Journal of Neuroscience*, vol. 18, no. 23, pp. 9896–9909, 1998.

[34] T. N. WIESEL and D. H. HUBEL, "Effects of Visual Deprivation on Morphology and Physiology of Cells in the Cats Lateral Geniculate Body," *Journal of Neurophysiology*, vol. 26, no. 6, pp. 978–993, 1963.

[35] L. Baroncelli, C. Braschi, and L. Maffei, "Visual depth perception in normal and deprived rats: effects of environmental enrichment," *Neuroscience*, vol. 236, pp. 313–319, 2013.

[36] L. Baroncelli, J. Bonaccorsi, M. Milanese et al., "Enriched experience and recovery from amblyopia in adult rats: impact of motor, social and sensory components," *Neuropharmacology*, vol. 62, no. 7, pp. 2388–2397, 2012.

[37] C. M. Niell and M. P. Stryker, "Modulation of visual responses by behavioral state in mouse visual cortex," *Neuron*, vol. 65, no. 4, pp. 472–479, 2010.

[38] M. Kaneko and M. P. Stryker, "Sensory experience during locomotion promotes recovery of function in adult visual cortex," *eLife*, vol. 3, article e02798, 2014.

[39] J. Bonaccorsi, N. Berardi, and A. Sale, "Treatment of amblyopia in the adult: insights from a new rodent model of visual perceptual learning," *Frontiers in Neural Circuits*, vol. 8, 2014.

[40] Y. Fu, M. Kaneko, Y. Tang, A. Alvarez-Buylla, and M. P. Stryker, "A cortical disinhibitory circuit for enhancing adult plasticity," *eLife*, vol. 4, article e05558, 2015.

[41] F. Greifzu, J. Pielecka-Fortuna, E. Kalogeraki et al., "Environmental enrichment extends ocular dominance plasticity into adulthood and protects from stroke-induced impairments of plasticity," *Proceedings of the National Academy of Sciences of the United States of America*, vol. 111, no. 3, pp. 1150–1155, 2014.

[42] B.-S. Wang, L. Feng, M. Liu, X. Liu, and J. Cang, "Environmental enrichment rescues binocular matching of orientation preference in mice that have a precocious critical period," *Neuron*, vol. 80, no. 1, pp. 198–209, 2013.

[43] S. Landi, A. Sale, N. Berardi, A. Viegi, L. Maffei, and M. C. Cenni, "Retinal functional development is sensitive to environmental enrichment: a role for BDNF," *The FASEB Journal*, vol. 21, no. 1, pp. 130–139, 2007.

[44] J. F. Maya-Vetencourt, L. Baroncelli, A. Viegi et al., "IGF-1 restores visual cortex plasticity in adult life by reducing local GABA levels," *Neural Plasticity*, vol. 2012, Article ID 250421, 10 pages, 2012.

[45] C. S. Green and D. Bavelier, "Learning, attentional control, and action video games," *Current Biology*, vol. 22, no. 6, pp. R197–R206, 2012.

[46] R. W. Li, C. Ngo, J. Nguyen, and D. M. Levi, "Video-game play induces plasticity in the visual system of adults with amblyopia," *PLoS Biology*, vol. 9, no. 8, article e1001135, 2011.

[47] J. M. Holmes, V. M. Manh, E. L. Lazar et al., "Effect of a binocular iPad game vs part-time patching in children aged 5 to 12 years with amblyopia: a randomized clinical trial," *JAMA Ophthalmology*, vol. 134, no. 12, pp. 1391–1400, 2016.

[48] K. R. Kelly, R. M. Jost, L. Dao, C. L. Beauchamp, J. N. Leffler, and E. E. Birch, "Binocular iPad game vs patching for treatment of amblyopia in children," *JAMA Ophthalmology*, vol. 134, no. 12, pp. 1402–1408, 2016.

[49] D. M. Levi and U. Polat, "Neural plasticity in adults with amblyopia," *Proceedings of the National Academy of Sciences of the United States of America*, vol. 93, no. 13, pp. 6830–6834, 1996.

[50] D. M. Levi, U. Polat, and Y. S. Hu, "Improvement in Vernier acuity in adults with amblyopia. Practice makes better," *Investigative Ophthalmology & Visual Science*, vol. 38, no. 8, pp. 1493–1510, 1997.

[51] C.-B. Huang, Y. Zhou, and Z.-L. Lu, "Broad bandwidth of perceptual learning in the visual system of adults with anisometropic amblyopia," *Proceedings of the National Academy of Sciences*, vol. 105, no. 10, pp. 4068–4073, 2008.

[52] D. M. Levi and R. W. Li, "Perceptual learning as a potential treatment for amblyopia: a mini-review," *Vision Research*, vol. 49, no. 21, pp. 2535–2549, 2009.

[53] U. Polat, T. Ma-Naim, M. Belkin, and D. Sagi, "Improving vision in adult amblyopia by perceptual learning," *Proceedings of the National Academy of Sciences*, vol. 101, no. 17, pp. 6692–6697, 2004.

[54] R. W. Li and D. M. Levi, "Characterizing the mechanisms of improvement for position discrimination in adult amblyopia," *Journal of Vision*, vol. 4, no. 6, pp. 7–7, 2004.

[55] D. M. Levi, "Perceptual learning in adults with amblyopia: a reevaluation of critical periods in human vision," *Developmental Psychobiology*, vol. 46, no. 3, pp. 222–232, 2005.

[56] R. W. Li, K. G. Young, P. Hoenig, and D. M. Levi, "Perceptual learning improves visual performance in juvenile amblyopia," *Investigative Opthalmology & Visual Science*, vol. 46, no. 9, p. 3161, 2005.

[57] R. W. Li, A. Provost, and D. M. Levi, "Extended perceptual learning results in substantial recovery of positional acuity and visual acuity in juvenile amblyopia," *Investigative Opthalmology & Visual Science*, vol. 48, no. 11, p. 5046, 2007.

[58] S. T. L. Chung, R. W. Li, and D. M. Levi, "Identification of contrast-defined letters benefits from perceptual learning in adults with amblyopia," *Vision Research*, vol. 46, no. 22, pp. 3853–3861, 2006.

[59] S. T. L. Chung, R. W. Li, and D. M. Levi, "Learning to identify near-threshold luminance-defined and contrast-defined letters in observers with amblyopia," *Vision Research*, vol. 48, no. 27, pp. 2739–2750, 2008.

[60] Y. Zhou, C. Huang, P. Xu et al., "Perceptual learning improves contrast sensitivity and visual acuity in adults with anisometropic amblyopia," *Vision Research*, vol. 46, no. 5, pp. 739–750, 2006.

[61] C. Lunghi and A. Sale, "A cycling lane for brain rewiring," *Current Biology*, vol. 25, no. 23, pp. R1122–R1123, 2015.

[62] C. Lunghi, A. T. Sframeli, A. Lepri et al., "A new counterintuitive training for adult amblyopia," *Annals of Clinical and Translational Neurology*, vol. 6, no. 2, pp. 274–284, 2019.

[63] N. J. Roizen and D. Patterson, "Down's syndrome," *The Lancet*, vol. 361, no. 9365, pp. 1281–1289, 2003.

[64] A. Contestabile, F. Benfenati, and L. Gasparini, "Communication breaks-Down: from neurodevelopment defects to cognitive disabilities in Down syndrome," *Progress in Neurobiology*, vol. 91, no. 1, pp. 1–22, 2010.

[65] M. Dierssen, "Down syndrome: the brain in trisomic mode," *Nature Reviews Neuroscience*, vol. 13, no. 12, pp. 844–858, 2012.

[66] C. M. Suttle and A. M. Turner, "Transient pattern visual evoked potentials in children with Down's syndrome," *Ophthalmic and Physiological Optics*, vol. 24, no. 2, pp. 91–99, 2004.

[67] E. Head, I. T. Lott, D. M. Wilcock, and C. A. Lemere, "Aging in Down syndrome and the development of Alzheimer's disease neuropathology," *Current Alzheimer Research*, vol. 13, no. 1, pp. 18–29, 2016.

[68] G. Cenini, A. L. S. Dowling, T. L. Beckett et al., "Association between frontal cortex oxidative damage and beta-amyloid as a function of age in Down syndrome," *Biochimica et Biophysica Acta (BBA) - Molecular Basis of Disease*, vol. 1822, no. 2, pp. 130–138, 2012.

[69] M. T. Davisson, C. Schmidt, and E. C. Akeson, "Segmental trisomy of murine chromosome 16: a new model system for studying Down syndrome," *Progress in Clinical and Biological Research*, vol. 360, pp. 263–280, 1990.

[70] M. Gupta, A. R. Dhanasekaran, and K. J. Gardiner, "Mouse models of Down syndrome: gene content and consequences," *Mammalian Genome*, vol. 27, no. 11–12, pp. 538–555, 2016.

[71] R. Bartesaghi, S. Guidi, and E. Ciani, "Is it possible to improve neurodevelopmental abnormalities in Down syndrome?," *Reviews in the Neurosciences*, vol. 22, no. 4, pp. 419–455, 2011.

[72] T. Begenisic, M. Spolidoro, C. Braschi et al., "Environmental enrichment decreases GABAergic inhibition and improves cognitive abilities, synaptic plasticity, and visual functions in a mouse model of Down syndrome," *Frontiers in Cellular Neuroscience*, vol. 5, p. 29, 2011.

[73] J. J. Scott-McKean, B. Chang, R. E. Hurd et al., "The mouse model of Down syndrome Ts65Dn presents visual deficits as assessed by pattern visual evoked potentials," *Investigative Ophthalmology & Visual Science*, vol. 51, no. 6, pp. 3300–3308, 2010.

[74] A. Rett, "On a unusual brain atrophy syndrome in hyperammonemia in childhood," *Wiener Medizinische Wochenschrift*, vol. 116, no. 37, 1966.

[75] G. Chahil, A. Yelam, and P. C. Bollu, "Rett syndrome in males: a case report and review of literature," *Cureus*, vol. 10, no. 10, article e3414, 2018.

[76] M. Chahrour and H. Y. Zoghbi, "The story of Rett syndrome: from clinic to neurobiology," *Neuron*, vol. 56, no. 3, pp. 422–437, 2007.

[77] J. P. K. Ip, N. Mellios, and M. Sur, "Rett syndrome: insights into genetic, molecular and circuit mechanisms," *Nature Reviews Neuroscience*, vol. 19, no. 6, pp. 368–382, 2018.

[78] R. E. Amir, I. B. Van den Veyver, M. Wan, C. Q. Tran, U. Francke, and H. Y. Zoghbi, "Rett syndrome is caused by mutations in X-linked *MECP2*, encoding methyl-CpG-binding protein 2," *Nature Genetics*, vol. 23, no. 2, pp. 185–188, 1999.

[79] W. Li and L. Pozzo-Miller, "BDNF deregulation in Rett syndrome," *Neuropharmacology*, vol. 76, pp. 737–746, 2014.

[80] X. Nan, H.-H. Ng, C. A. Johnson et al., "Transcriptional repression by the methyl-CpG-binding protein MeCP2 involves a histone deacetylase complex," *Nature*, vol. 393, no. 6683, pp. 386–389, 1998.

[81] M. Chahrour, S. Y. Jung, C. Shaw et al., "MeCP2, a key contributor to neurological disease, activates and represses transcription," *Science*, vol. 320, no. 5880, pp. 1224–1229, 2008.

[82] J. Guy, B. Hendrich, M. Holmes, J. E. Martin, and A. Bird, "A mouse *Mecp2*-null mutation causes neurological symptoms that mimic Rett syndrome," *Nature Genetics*, vol. 27, no. 3, pp. 322–326, 2001.

[83] C. Martínez-Cué, C. Baamonde, M. Lumbreras et al., "Differential effects of environmental enrichment on behavior and learning of male and female Ts65Dn mice, a model for Down syndrome," *Behavioural Brain Research*, vol. 134, no. 1–2, pp. 185–200, 2002.

[84] C. Martínez-Cué, N. Rueda, E. García, M. T. Davisson, C. Schmidt, and J. Flórez, "Behavioral, cognitive and biochemical responses to different environmental conditions in male Ts65Dn mice, a model of Down syndrome," *Behavioural Brain Research*, vol. 163, no. 2, pp. 174–185, 2005.

[85] M. Dierssen, R. Benavides-Piccione, C. Martínez-Cué et al., "Alterations of neocortical pyramidal cell phenotype in the Ts65Dn mouse model of Down syndrome: effects of environmental enrichment," *Cerebral Cortex*, vol. 13, no. 7, pp. 758–764, 2003.

[86] M. Kondo, L. J. Gray, G. J. Pelka, J. Christodoulou, P. P. L. Tam, and A. J. Hannan, "Environmental enrichment ameliorates a motor coordination deficit in a mouse model of Rett syndrome *Mecp2* gene dosage effects and BDNF expression," *European Journal of Neuroscience*, vol. 27, no. 12, pp. 3342–3350, 2008.

[87] T. Begenisic, G. Sansevero, L. Baroncelli, G. Cioni, and A. Sale, "Early environmental therapy rescues brain development in a mouse model of Down syndrome," *Neurobiology of Disease*, vol. 82, pp. 409–419, 2015.

[88] G. Sansevero, T. Begenisic, M. Mainardi, and A. Sale, "Experience-dependent reduction of soluble β-amyloid oligomers and rescue of cognitive abilities in middle-age Ts65Dn mice, a model of Down syndrome," *Experimental Neurology*, vol. 283, Part A, pp. 49–56, 2016.

[89] G. Lonetti, A. Angelucci, L. Morando, E. M. Boggio, M. Giustetto, and T. Pizzorusso, "Early environmental enrichment moderates the behavioral and synaptic phenotype of MeCP2 null mice," *Biological Psychiatry*, vol. 67, no. 7, pp. 657–665, 2010.

[90] M. V. Llorens-Martín, N. Rueda, G. S. Tejeda, J. Flórez, J. L. Trejo, and C. Martínez-Cué, "Effects of voluntary physical exercise on adult hippocampal neurogenesis and behavior of Ts65Dn mice, a model of Down syndrome," *Neuroscience*, vol. 171, no. 4, pp. 1228–1240, 2010.

[91] L. Chakrabarti, J. Scafidi, V. Gallo, and T. F. Haydar, "Environmental enrichment rescues postnatal neurogenesis defect in the male and female Ts65Dn mouse model of Down syndrome," *Developmental Neuroscience*, vol. 33, no. 5, pp. 428–441, 2011.

[92] M. A. Kondo, L. J. Gray, G. J. Pelka et al., "Affective dysfunction in a mouse model of Rett syndrome: therapeutic effects of environmental stimulation and physical activity," *Developmental Neurobiology*, vol. 76, no. 2, pp. 209–224, 2016.

[93] L. Baroncelli, C. Braschi, M. Spolidoro, T. Begenisic, A. Sale, and L. Maffei, "Nurturing brain plasticity: impact of environmental enrichment," *Cell Death & Differentiation*, vol. 17, no. 7, pp. 1092–1103, 2017.

[94] F. Fernandez and C. C. Garner, "Over-inhibition: a model for developmental intellectual disability," *Trends in Neurosciences*, vol. 30, no. 10, pp. 497–503, 2007.

[95] L. Baroncelli, C. Braschi, M. Spolidoro, T. Begenisic, L. Maffei, and A. Sale, "Brain plasticity and disease: a matter of inhibition," *Neural Plasticity*, vol. 2011, Article ID 286073, 11 pages, 2011.

[96] J. F. M. Vetencourt, A. Sale, A. Viegi et al., "The antidepressant fluoxetine restores plasticity in the adult visual cortex," *Science*, vol. 320, no. 5874, pp. 385–388, 2008.

[97] H. J. Huttunen, J. M. Palva, L. Lindberg et al., "Fluoxetine does not enhance the effect of perceptual learning on visual function in adults with amblyopia," *Scientific Reports*, vol. 8, no. 1, article 12830, 2018.

[98] T. Begenisic, L. Baroncelli, G. Sansevero et al., "Fluoxetine in adulthood normalizes GABA release and rescues hippocampal synaptic plasticity and spatial memory in a mouse model of Down syndrome," *Neurobiology of Disease*, vol. 63, pp. 12–19, 2014.

[99] P. Bianchi, E. Ciani, S. Guidi et al., "Early pharmacotherapy restores neurogenesis and cognitive performance in the Ts65Dn mouse model for Down syndrome," *Journal of Neuroscience*, vol. 30, no. 26, pp. 8769–8779, 2010.

[100] C. Tamminga, M. E. Carlin, J. Giampaolo, S. Patel, and R. Horsager-Boehrer, *A Pilot Feasibility Trial of Prenatal and Early Postnatal Fluoxetine Treatment for Intellectual Impairments of Down Syndrome Study Doctors*, http://downsyndromedallas.org/Websites/downsyndromedallas/files/Content/3219874/Two_Page_Study_Summary_-_Clinician_Version_-_updated_1.24.2017.pdf.

[101] H. M. O'Leary, W. E. Kaufmann, K. V. Barnes et al., "Placebo-controlled crossover assessment of mecasermin for the treatment of Rett syndrome," *Annals of Clinical and Translational Neurology*, vol. 5, no. 3, pp. 323–332, 2018.

[102] E. Castrén, "Neurotrophins as mediators of drug effects on mood, addiction, and neuroprotection," *Molecular Neurobiology*, vol. 29, no. 3, pp. 289–302, 2004.

[103] A. C. Mondal and M. Fatima, "Direct and indirect evidences of BDNF and NGF as key modulators in depression: role of antidepressants treatment," *International Journal of Neuroscience*, vol. 129, no. 3, pp. 283–296, 2018.

[104] A. H. Nagahara and M. H. Tuszynski, "Potential therapeutic uses of BDNF in neurological and psychiatric disorders," *Nature Reviews Drug Discovery*, vol. 10, no. 3, pp. 209–219, 2011.

[105] F. Malerba, F. Paoletti, S. Capsoni, and A. Cattaneo, "Intranasal delivery of therapeutic proteins for neurological diseases," *Expert Opinion on Drug Delivery*, vol. 8, no. 10, pp. 1277–1296, 2011.

[106] M. Parrini, D. Ghezzi, G. Deidda et al., "Aerobic exercise and a BDNF-mimetic therapy rescue learning and memory in a mouse model of Down syndrome," *Scientific Reports*, vol. 7, no. 1, article 16825, 2017.

[107] D. A. Schmid, T. Yang, M. Ogier et al., "A TrkB small molecule partial agonist rescues TrkB phosphorylation deficits and improves respiratory function in a mouse model of Rett syndrome," *Journal of Neuroscience*, vol. 32, no. 5, pp. 1803–1810, 2012.

[108] N. Bray, "Righting Rett syndrome with IGF1," *Nature Reviews Drug Discovery*, vol. 13, no. 9, pp. 653–653, 2014.

[109] G. Pini, M. F. Scusa, L. Congiu et al., "IGF1 as a potential treatment for Rett syndrome: safety assessment in six Rett patients," *Autism Research and Treatment*, vol. 2012, Article ID 679801, 14 pages, 2012.

[110] G. Pini, M. F. Scusa, A. Benincasa et al., "Repeated insulin-like growth factor 1 treatment in a patient with Rett syndrome: a single case study," *Frontiers in Pediatrics*, vol. 2, p. 52, 2014.

[111] O. S. Khwaja, E. Ho, K. V. Barnes et al., "Safety, pharmacokinetics, and preliminary assessment of efficacy of mecasermin (recombinant human IGF-1) for the treatment of Rett syndrome," *Proceedings of the National Academy of Sciences*, vol. 111, no. 12, pp. 4596–4601, 2014.

[112] S. Guidi, F. Stagni, P. Bianchi et al., "Prenatal pharmacotherapy rescues brain development in a Down's syndrome mouse model," *Brain*, vol. 137, no. 2, pp. 380–401, 2014.

[113] C. Vahdatpour, A. H. Dyer, and D. Tropea, "Insulin-like growth factor 1 and related compounds in the treatment of childhood-onset neurodevelopmental disorders," *Frontiers in Neuroscience*, vol. 10, p. 450, 2016.

[114] A. De Giorgio, "The roles of motor activity and environmental enrichment in intellectual disability," *Somatosensory & Motor Research*, vol. 34, no. 1, pp. 34–43, 2017.

Hindawi
Neural Plasticity
Volume 2019, Article ID 7624837, 11 pages
https://doi.org/10.1155/2019/7624837

Research Article

Fast Recovery of the Amblyopic Eye Acuity of Kittens following Brief Exposure to Total Darkness Depends on the Fellow Eye

Donald E. Mitchell, Elise Aronitz, Philip Bobbie-Ansah, Nathan Crowder, and Kevin R. Duffy

Department of Psychology & Neuroscience, Dalhousie University, Halifax, NS, Canada B3H 4R2

Correspondence should be addressed to Donald E. Mitchell; d.e.mitchell@dal.ca

Received 18 January 2019; Accepted 12 March 2019; Published 24 April 2019

Guest Editor: Hirofumi Morishita

Recent studies conducted on kittens have revealed that the reduced visual acuity of the deprived eye following a short period of monocular deprivation imposed in early life is reversed quickly following a 10-day period spent in total darkness. This study explored the contribution of the fellow eye to the darkness-induced recovery of the acuity of the deprived eye. Upon emergence of kittens from darkness, the fellow eye was occluded for different lengths of time in order to investigate its effects on either the speed or the extent of the recovery of acuity of the deprived eye. Occlusion of the fellow eye for even a day immediately following the period spent in darkness blocked any recovery of the acuity of the deprived eye. Moreover, occlusion of the fellow eye two days after the period of darkness blocked any further visual recovery beyond that achieved in the short period when both eyes were open. The results imply that the darkness-induced recovery of the acuity of the deprived eye depends upon, and is guided by, neural activity in the mature neural connections previously established by the fellow eye.

1. Introduction

The extreme shift of eye preference of neurons in the visual cortex and the accompanying anatomical changes observed in kittens [1], infant monkeys [2], ferrets [3], and rodents [4, 5] that follow a brief postnatal period of monocular deprivation (MD) are widely touted as the quintessential demonstration of developmental cortical plasticity. Accompanying the physiological and anatomical sequelae of MD are severe behavioural deficits that are especially noteworthy in terms of changes to the visual ability of the deprived eye [6]. The consequences of MD occur only during certain critical periods of vulnerability that vary widely in their profile and duration across species. For kittens, susceptibility to the physiological consequences of MD within the visual cortex rises from low levels at the time of natural eye opening at about a week of age to a peak at 4 to 5 weeks followed by a gradual decline to negligible values at an age beyond 4 months but before 8 months [7–9]. Because of the large magnitude and highly reproducible consequences of MD, this form of early deprivation has been employed extensively to study the interaction between programs of gene expression and visually driven neural activity in the development of the central visual pathways (e.g., [10–14]). In addition, MD by eyelid suture has become a standard and convenient means to provide an animal model of human amblyopia and in particular the type referred to as deprivation amblyopia that is typically observed in children with a history of an early opacity of the optical media, such as a cataract, or other peripheral obstruction to clear imagery in one eye.

In addition to documentation of the visual deficits that are observed immediately upon cessation of a period of early MD, there have been many studies of the extent and pace of any recovery that occurs afterward in various situations. The simplest recovery situation, commonly referred to as binocular recovery, is where normal visual input is restored to the deprived eye to allow simultaneous visual input to both eyes without any other manipulation. All other recovery situations include additional manipulations beyond restoration of normal visual input to the deprived eye in an effort to promote greater recovery of the vision of this eye. The simplest

of these is reverse occlusion where at the time vision is restored to the deprived eye, the other eye is occluded. The improvement of the visual acuity of the deprived eye with binocular recovery can be substantial but never complete in cats, a result that is in general agreement with the physiological recovery observed in the visual cortex [15, 16]. However, in monkeys, very little behavioural or physiological recovery is observed in this recovery condition [17, 18]. Reverse occlusion can promote fast and substantial recovery of various visual functions of the deprived eye in kittens, but this does not occur without concurrent reduction of the visual abilities of the fellow eye [15, 19]. The reciprocal changes in the vision of the two eyes find a close parallelism with the rapid physiological shifts of ocular dominance following reverse occlusion in the visual cortex of both cats [20, 21] and ?monkeys [22].

Other recovery conditions, such as the use of mixed daily visual exposure that include adjacent periods of binocular exposure and occlusion of the nondeprived eye [23], have been explored in an effort to prevent some of the unwanted consequences of reverse occlusion [24, 25]. Although mixed daily visual exposure can promote complete recovery of the visual acuity of the deprived eye to normal levels and without any loss of the acuity of the fellow eye, it is effective only under a restricted set of conditions of deprivation and recovery [23].

A promising new recovery condition has been the use of a 10-day period of total darkness that was originally shown to reverse both the behavioural and physiological consequences of an early period of MD in adult Long-Evans rats [26, 27]. More recently, the same period of darkness was found to either prevent the development of amblyopia or promote recovery from amblyopia in kittens induced by a prior period of MD without any ill effects on the acuity of the fellow eye [28, 29]. For these kitten studies, the effect of the period of darkness was examined either when it was imposed immediately after the 7-day period of MD that was initiated at P30 days, or else 8 weeks later when kittens were about 3 months old. In the first situation, the period of darkness resulted in a profound reduction of the vision of both eyes such that the animals appeared blind temporarily following emergence from the darkroom. Thereafter, a slow but matched visual recovery of the two eyes occurred such that the visual acuity of both eyes achieved normal levels in about 50 days. At no time was the acuity of the deprived eye lower than that of the fellow eye so that darkness imposed immediately after the period of MD prevented the development of amblyopia. By contrast, in the second situation when the period of darkness occurred late, the deprived eye was amblyopic at the time darkness was imposed. Remarkably, the acuity of the deprived eye improved very fast after the period of darkness such that normal age-matched levels were achieved in 7-10 days or even less.

The fivefold faster recovery of the acuity of the deprived eye when darkness occurred 2 months after the period of MD as compared to when it followed immediately afterward raises the possibility that visually driven neural activity generated by the fellow eye may make an important contribution to the visual recovery induced by darkness. It was suggested [28–30] that the remarkable behavioural benefits of darkness arose from its ability to promote changes to various key molecules that collectively increase the level of plasticity in the developing visual cortex so as to effectively reset it to a more juvenile and plastic state. The faster rate of recovery of the acuity of the deprived eye following imposition of darkness well after the period of MD, as opposed to immediately afterwards, runs counter to expectations based on the greater age of the animals in the former situation when the level of plasticity would be expected to be much lower. On the other hand, the potential contribution of neural activity generated in cortical neurons by visual stimulation of the fellow eye to the recovery of the vision of the deprived eye after darkness follows explanations linked to the level of the cortical response to visual stimulation of the fellow eye in the immediate aftermath of darkness in the two recovery situations. When darkness is imposed well after the period of MD, neural activity generated by visual stimulation of the fellow eye may serve as a "scaffold" or otherwise guide the reestablishment of neural connections with the deprived eye. However, when the periods of MD and darkness are contiguous, the latter causes a drastic reduction of the vision of the fellow eye [29], and hence, cortical neural activity generated by visual stimulation of this eye would be too low to serve a leadership role in the recovery of the other eye. In the current study, the potential role of neural activity mediated by the fellow eye to the recovery of the deprived eye induced by darkness has been investigated by occluding the fellow eye for various periods of time after termination of darkness.

2. Materials and Methods

2.1. Animals and Rearing Conditions. The study was conducted on 18 kittens derived from 6 litters that were bred and reared in a closed animal colony at Dalhousie University. The animal colony and all animal procedures followed protocols approved by the Dalhousie University Committee on Laboratory Animals and conformed to the guidelines of the Canadian Council on Animal Care. All 18 animals received a 7-day period of MD at about postnatal day 30 (P30) that was followed in all but 2 animals by a 10-day period of total darkness that began at about 3 months of age (at ~P90). Two animals received a period of occlusion of the fellow eye instead of a period of darkness at an equivalent age. Three control animals chosen from 3 separate litters received a period of darkness without any occlusion of the fellow eye. Table 1 displays the rearing history of all animals, their gender and, litter of origin.

For all but the period spent in darkness, animals were housed in colony rooms that were illuminated usually on a 12 : 12 h light/dark cycle that was changed to as high as a 14 : 10 cycle in some rooms on occasions to promote breeding. During the day, animals ran free in the colony rooms but at night were housed in large interconnected cages within the colony rooms. The behavioural measurements of acuity that we made did not require any reduction in the amount or nature of their daily food. For the 10-day period of total darkness, animals were moved to a large darkroom (3.8×3.5 m) that was part of a darkroom facility that is described in detail elsewhere [31]. The facility contained two adjacent darkrooms that were accessible through

Table 1: Animals and rearing conditions. Timing (postnatal days of age) of the initial period of monocular deprivation (MD), darkness, and subsequent visual exposure (fellow eye occlusion and/or binocular vision) for all 18 kittens. Details are also provided on the 6 litters and the gender of the kittens. Prior to and for the 8+ weeks following the period of MD, all kittens received binocular visual exposure.

Animal	Litter ID	Gender	MD	Darkness	Fellow eye occlusion (no. of days)	Binoc. vision
Control animals						
Darkness only						
C422	D	F	P30-37	P101-111		
C439	E	F	P30-37	P102-112		
C446	F	M	P30-37	P91-101		
Fellow eye occlusion only						
C391	B	M	P29-36		P103-120 (17 d)	
C392	B	M	P29-36		P102-126 (24 d)	
Experimental animals						
Darkness followed by fellow eye occlusion						
C425	C	M	P30-37	P101-111	P111-120 (9 d)	P120-
C390	A	F	P29-36	P92-102	P102-113 (11 d)	P113-
C393	B	F	P29-36	P92-102	P102-113 (11 d)	P113-
C419	D	F	P31-38	P90-100	P100-111 (11 d)	P111-
C420	D	F	P31-38	P91-101	P100-111 (11 d)	
C423	C	M	P30-37	P101-111	P111-115 (4 d)	P115-
C424	C	F	P30-37	P101-111	P111-115 (4 d)	P115-
C445	F	F	P30-37	P91-101	P101-103 (2 d)	P103-
C447	F	F	P30-37	P91-101	P101-103 (2 d)	P103-
C448	F	F	P30-37	P91-101	P101-102 (1 d)	P102-
C438	E	M	P30-37	P102-112	P112-113 (1 d)	P113-
Darkness followed by a short period of binoc. vision then fellow eye occlusion						
C457	G	M	P30-37	P100-110	P112-114 (2 d)	P110-112; P114-
C458	G	F	P30-37	P100-110	P112-122 (10 d)	P110-112; P122-

several small anterooms and doors that ensured that the two darkrooms were light-tight. To entrain an activity cycle, a radio in the darkroom was automatically turned on and off at times that corresponded to the lighting cycle of the colony rooms. In the darkroom, animals were kept in a large cage ($1.5 \times 0.7 \times 0.9$ m) with a 24 cm ledge running the length of the cage. As the animals were 3 months old at the time, they were past the age at which they had been weaned and so were held in the darkroom without their mother. Usually, there was only one or two kittens in the darkroom at the same time and they were held in the same large cage. A second cage was added on the rare occasions in which additional kittens were in the darkroom at the same time.

2.2. Surgical Procedures. Monocular deprivation by eyelid suture of the left eye was achieved by use of a two-stage procedure developed [25] to both achieve a secure eyelid closure and allow fast recovery of a normal patent palpebral aperture to facilitate the behavioural assessment of the vision of this eye after the eyelids were opened. As detailed descriptions of these procedures have been provided in a recent paper [32], only a brief summary is provided here. All surgical procedures were performed under gaseous isoflurane anesthesia (2-3% in oxygen), and an s.c. injection of Anafen for postprocedure analgesia was administered once the animals were anesthetized and local anesthesia was administered with Alcaine sterile ophthalmic solution (proparacaine hydrochloride). The first stage of the procedure was to carefully dissect the palpebral conjunctivae free from the upper and lower eyelids and to suture them together with 6-O Vicryl suture thread. A broad-spectrum topical antibiotic (chloromycetin 1%) was then applied to the sutured conjunctivae. The second stage of the surgical procedure was to oppose and suture the exposed tissue on the underside of the eyelids together with 6-O or 5-O silk.

To open the eyelids after the initial week-long period of MD or a later period of occlusion of the fellow eye, animals were anesthetized with isoflurane and any remaining suture material was removed. The eyelids and underlying conjunctivae were then gently cut and pulled apart to achieve a normal palpebral opening. A broad-spectrum topical antibiotic (chloromycetin 1%) was applied to the cornea and surrounding conjunctivae.

2.3. Behavioural Measurements of Visual Acuity. Measurements of visual acuity for square-wave gratings were made by use of a jumping stand and procedures developed and refined over the last four decades in this laboratory [16, 25, 31]. The training and testing procedures that are used

currently and employed for this study have been described in detail recently [31] and so are summarized only briefly here. The stimuli were adjacent large (19 × 19 cm) horizontal and vertical square-wave gratings of the same period (and, hence, spatial frequency) and with a luminance of 80 cd/m2. Acuity was measured by use of a descending method of limits with jumps to the vertical (positive) stimulus rewarded by food and petting while errors resulted in a denial of these rewards. Because the changes in spatial frequency between blocks of trials were very small and equated on a logarithmic scale with as many as 12 steps/octave change in spatial frequency, only a single trial was provided at the lowest spatial frequencies until an error was made. At this point, the animal had to make 5 consecutively correct responses or a minimum of 7 correct responses out of a maximum 10 trials provided at any spatial frequency, before the spatial frequency was increased. Within about 5 steps of spatial frequency from threshold, the minimum number of trials was increased to 5. Threshold, defined as the highest spatial frequency for which the animal performed at a level of 70% or better, was typically sharp so that performance fell from flawless to chance within 3 step changes of spatial frequency. Kittens exhibited a number of stereotypical behaviours near threshold that included a drastic increase in latency to respond, crying, looks towards nearby objects or to one or both of the people involved in testing, and attempts to back away from the edge of the jumping platform.

Once animals were trained, which usually occurred in the fifth and sixth week, measurements of thresholds were made daily or else every second day. With only a few exceptions, the testing of the acuity was conducted in the morning at about the same time for each individual animal. Two of the authors seated on either side of the jumping platform conducted the tests of acuity with one person providing the food and social reward after each response while the other person recorded the response and prepared the stimuli for the next trial. Tests of the acuity of the deprived eye were made with a hard opaque contact lens occluder placed in the other eye. Six occluders of different base curvatures selected to match the mean corneal curvatures of young kittens of various ages [33] were used as the animals matured. To mitigate against any possible pain, a drop of a local ophthalmic anesthetic (proparacaine hydrochloride 1%) was placed in the eye to be occluded prior to insertion of the contact lens. No signs of any discomfort were evident in the 20 minutes of occlusion of the fellow eye that was typically required for the measurement of the acuity of the deprived eye. Measurement of binocular acuity was used as a substitute for monocular measurement of the grating acuity of the nondeprived eye as in the past, they have been demonstrated to be identical. An additional advantage of this practice was that it enabled measurement to be made of the acuity of the deprived eye immediately afterward as the cornea of this eye would be free from distortion that would accompany the use of the contact lens occluder required for monocular measurement of the nondeprived eye acuity [34]. Following the period of MD, the acuity of the deprived eye gradually improved but eventually reached a stable level that remained so for several weeks prior to the period of darkness. During the time when the acuity of the deprived eye was stable, the starting spatial frequency for each acuity measurement was altered to ensure that the threshold reflected a true visual barrier irrespective of the number of trials or length of the testing session. During the time that the visual acuity of the two eyes had stabilized, the frequency of testing was reduced to once or twice weekly. When possible, more frequent daily tests were reinstated within 10 days of the period of dark exposure.

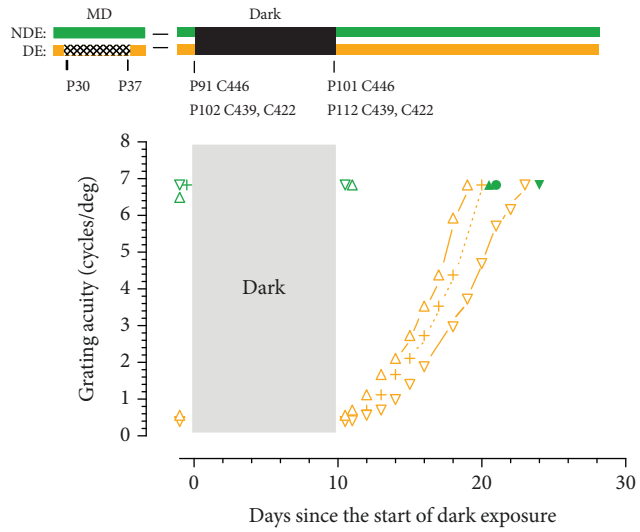

Figure 1: The grating acuity of the two eyes of 3 monocularly deprived kittens immediately prior to and following a 10-day period spent in complete darkness. Each kitten received a 7-day period of MD starting at P30 days and were placed in darkness at either P91 days (C446) or at P102 days (C439, C422). As with subsequent figures, the visual histories and acuity data in the graphs below for the deprived eye (DE) and nondeprived eye (NDE) are depicted in orange and green, respectively. Occlusion of the DE during the early period of MD is shown by crosshatching, and the subsequent period of total darkness is indicated in black. The results of acuity measurements for the 3 animals are depicted by symbols as follows: C422 upright triangles, C446 plus symbols or solid circles (NDE), and C439 inverted triangles. The results of binocular measurements of acuity are shown as open green symbols while monocular measurements of the acuity of the nondeprived eye acuity with which they are equivalent are shown as solid green symbols.

3. Results

3.1. Control Animals. To set the stage for tests of the role of the fellow eye in recovery of the vision of the deprived eye promoted by darkness, two control conditions were necessary. The first of these was a replication of the benefits of darkness conducted on three kittens that were littermates of the animals allocated to the various periods of occlusion of the fellow eye following exposure to darkness. A second control condition was conducted on two animals that had received the same period of MD but had not subsequently been exposed to darkness in order to determine the effects of a period of eyelid occlusion of the fellow eye at an equivalent age to that experienced by the experimental animals. Results from the first of these control conditions in the period immediately prior to and following the 10 days of darkness

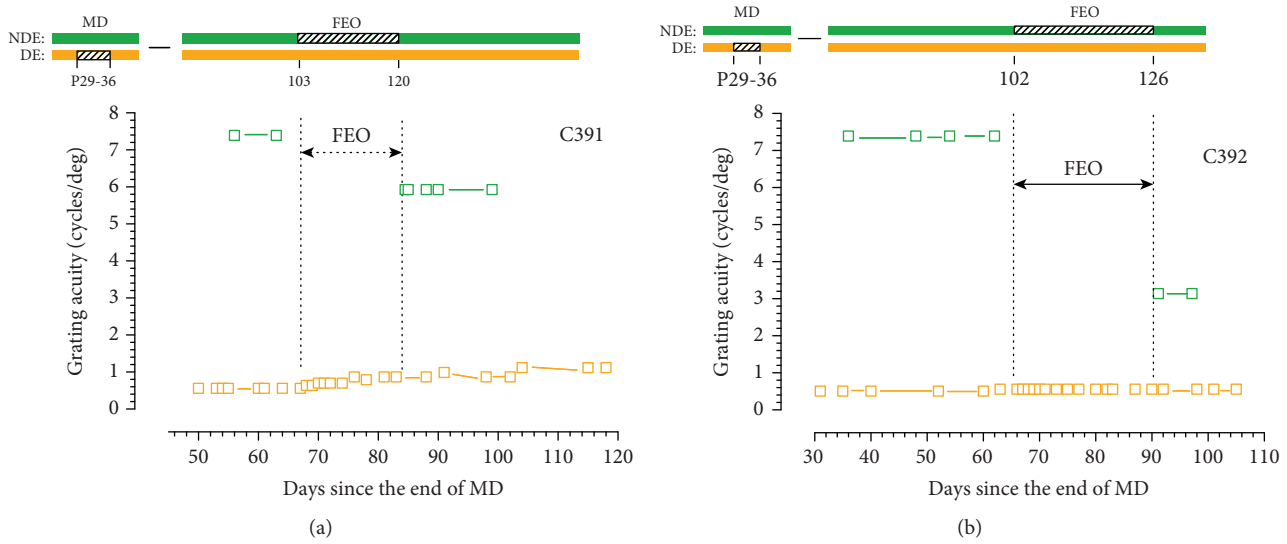

Figure 2: The grating acuity of the deprived eye (orange symbols) and the binocular acuity (green symbols) of 2 monocularly deprived littermate kittens prior to and following 17 (a) (C391) or 24 (b) (C392) days of fellow eye occlusion (FEO). The visual histories of the two animals are depicted above the two graphs.

are displayed together in Figure 1 in order to highlight the similar speed and extent of the darkness-induced recovery of the acuity of the deprived eye observed in all 3 animals. Although two of the animals (C422 and C439) were placed in darkness at almost the same age (at P101 or P102), the third (C446) was so exposed earlier at P91. In agreement with the results obtained in two prior studies [28, 29], the acuity of the deprived eye of all three animals recovered fast to match that of the other eye within either 9 (C422), 10 (C446), or 13 (C439) days. There did not appear to be any simple relationship between the speed of recovery of the deprived eye and the age at which darkness was imposed as one of the animals exposed at P101 recovered almost as fast as the one exposed earliest at P91 (C446). Because all three animals were derived from different litters, it is possible that the slight differences in the rate of recovery could be attributed to differences between litters.

Although it has been known from many earlier studies that occlusion of the fellow eye can result in an improvement of the visual acuity of the deprived eye of kittens following a prior period of MD, in all but a few isolated animals, the manipulation occurred immediately adjacent to the initial period of MD [15, 19, 24]. A similar rearing protocol had been adopted in prior electrophysiological investigations of the ability of fellow eye occlusion to reverse the effects of a preceding period of MD on cortical ocular dominance [20, 21]. Possibly because occlusion of the fellow eye followed immediately after termination of the period of MD in these studies, it was referred to as reverse occlusion. In order to establish the effects of a period of occlusion of the fellow eye made several months *after* the initial period of MD, two littermate control animals were reared with such occlusion imposed at an equivalent age to that of the experimental animals at the end of their period of exposure to darkness. Both animals received an initial 7-day period of MD at P29 that was followed by either a 17- (C391) or 24- (C392) day period of occlusion of the fellow eye at P103 and P102 days,

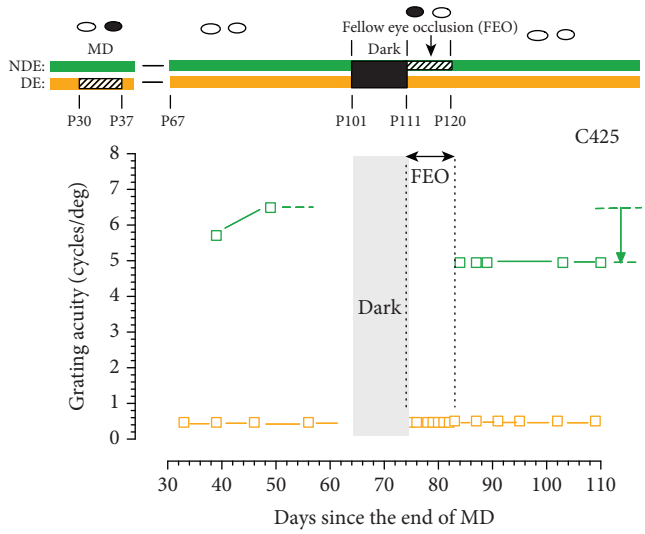

Figure 3: The grating acuity of the deprived eye (orange symbols) and the binocular acuity (green symbols) of a monocularly deprived kitten (C425) surrounding a 10-day period of total darkness followed by a 9-day period of fellow eye occlusion (FEO). As with the previous figures, the visual histories of the two animals are depicted in schematic form by the bars and icons above the two graphs.

respectively. From prior studies, it was anticipated that occlusion of the fellow eye at this late age would not produce substantial improvement of the acuity of the deprived eye or negatively impact the acuity of the fellow eye. The results, displayed in Figure 2, provided only partial support for these expectations. In one animal (C391), occlusion of the fellow eye resulted in a very small improvement of the acuity of the deprived eye, from 0.56 to 0.87 cycles/deg, while for the other animal (C392), the acuity of this eye remained

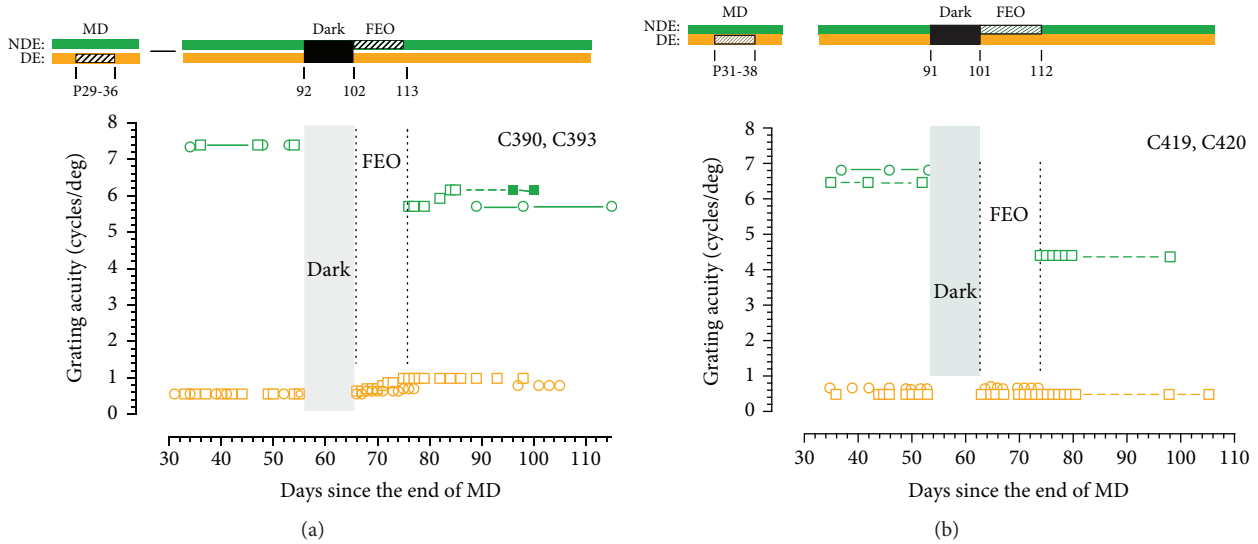

Figure 4: The grating acuity of the deprived (orange symbols) and nondeprived (green solid symbols) eyes as well the binocular acuity (green open symbols) of two pairs of monocularly deprived kittens surrounding 10 days of total darkness followed immediately by an 11-day period of fellow eye occlusion (FEO). As with previous figures, the visual histories of the animals are depicted in schematic form by the bars above the two graphs. (a) Data for C390 (square symbols) and C393 (circle symbols). (b) Data for littermates C419 (square symbols) and C420 (circle symbols). The period of FEO effectively blocked any improvement of the acuity of the deprived eye following the period of darkness but did cause a reduction of the acuity of the nondeprived eye.

unchanged despite a longer period of fellow eye occlusion. On the other hand, the acuity of the fellow eye was reduced in both animals from 7.4 to 5.93 cycles/deg for C391 and to 3.14 cycles/deg for C392 representing losses of 0.32 and 1.23 octaves, respectively. The asymmetric changes in the acuity of the two eyes following fellow eye occlusion that were particularly noteworthy for C392 may reflect physiological changes in the visual cortex reported initially by Mioche and Singer [35] following MD or reverse occlusion. In both situations, the initial change was a decrease of the excitatory response to the newly deprived eye followed by a much slower increase in the response to the other eye. It is not unreasonable to suppose that similar electrophysiological events would be observed in the slightly different situation employed here where occlusion of the fellow eye was delayed with respect to termination of the initial period of MD.

3.2. Experimental Animals. The initial experiments were conducted on five animals with 9-11-day periods of occlusion of the fellow eye immediately following the interval spent in darkness. This occlusion time was chosen as it corresponded to that required for the acuity of the deprived eye to recover to normal levels in two previous studies when both eyes were open following darkness [28, 29]. The results for the animal (C425) that received only 9 days of occlusion of the fellow eye are shown in isolation in Figure 3, while those for the 4 animals that received 11 days occlusion of this eye are displayed as pairs in Figures 4 and 5 in order of the dates when they were tested. For all 5 animals, data are shown beginning about a month prior to the period of darkness. The data for C425 are displayed with elaborate schematic descriptors of the animal's rearing history to aid comprehension of the more sparse representations used in subsequent graphs. For C425, the rearing history is represented both by the icons at the very top and by the horizontal bars that illustrate the four major periods of visual exposure (binocular visual exposure, MD, darkness, and occlusion of the fellow eye) as well as the postnatal ages at which they began and ended. The data for C425 revealed that following darkness, there was no change in the acuity of the deprived eye during the 9-day period of occlusion of the fellow eye. Moreover, following the period of occlusion of the fellow eye, the acuity of this eye was reduced from 6.5 to 4.95 cycles/deg or 0.4 of an octave. There was no change in the visual acuity of either eye in the ensuing month. This result stands in marked contrast to the data of Figure 1 where following the period of darkness, the acuity of the deprived eye recovered from about 0.5 cycles/deg to 6.8 cycles/deg or an improvement of 3.8 octaves without any negative impact on the acuity of the fellow eye.

A very similar pattern of results was observed in the first two kittens that received a slightly longer 11-day period of occlusion of the fellow eye immediately following dark exposure. For C390 (Figure 4(a)), the combination of darkness and fellow eye occlusion resulted in only a very slight overall improvement of the acuity of the deprived eye from 0.56 to 1.0 cycles/deg or 0.84 octaves that was accompanied by a small reduction of the acuity of the fellow eye. During the period of occlusion of the fellow eye following darkness, the acuity of the deprived eye improved very little, from 0.55 to 0.7 cycles/deg or 0.35 octaves. It was not possible to measure the acuity of the deprived eye of the other animal (C393; Figure 4(a)) for almost 3 weeks following the period of occlusion of the fellow eye due to persistent conjunctival inflammation of this eye. Following treatment with ophthalmic topical antibiotics, all signs of inflammation disappeared so

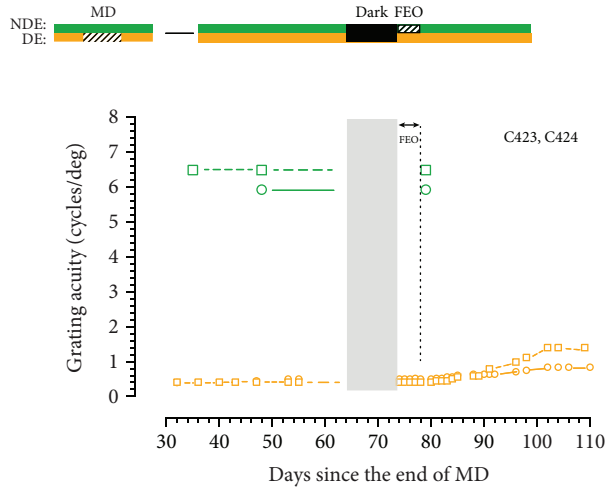

Figure 5: The grating acuity of the deprived eye acuity (orange symbols) and the binocular acuity (green symbols) of two monocularly deprived littermates C423 (square symbols) and C424 (circle symbols) surrounding 10 days of total darkness followed immediately by a 4-day period of fellow eye occlusion (FEO). Whereas the period of FEO effectively blocked any improvement of the acuity of the deprived eye following the period of darkness, it did not result in any reduction of the acuity of the nondeprived eye.

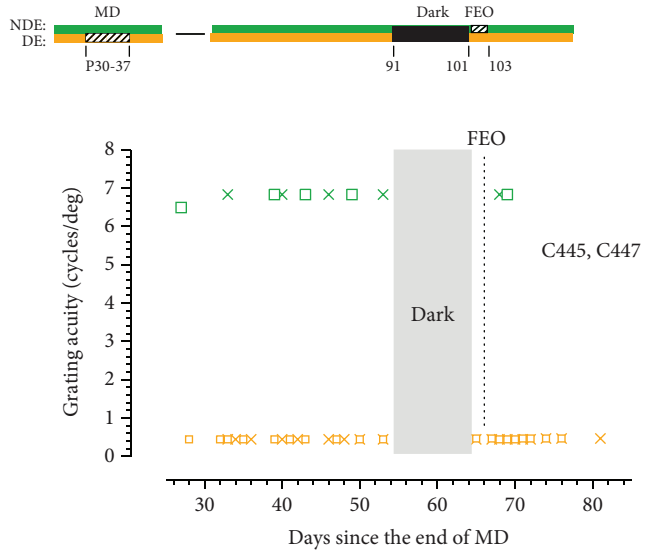

Figure 6: The grating acuity of the deprived eye acuity (orange symbols) and the binocular acuity (green symbols) of two monocularly deprived littermates C445 (square symbols) and C447 (cross symbols) surrounding 10 days of total darkness followed immediately by a 2-day period of fellow eye occlusion (FEO). Whereas the period of FEO effectively blocked any improvement of the acuity of the deprived eye following the period of darkness, it did not result in any reduction of the acuity of the nondeprived eye.

that short-term occlusion of this eye with an opaque contact lens could be resumed to allow measurements of the acuity of the deprived eye once more. However, the acuity of this eye did not change appreciably in the ensuing weeks. The period of occlusion of the fellow eye following darkness resulted in a similar decline of the acuity of the nondeprived eye to that observed for C390. Fellow eye occlusion of the two animals reared most recently; C419 and C420 (Figure 4(b)) also blocked any recovery of the acuity of the deprived eye following darkness. One animal (C420) was found dead early on the morning of the penultimate day of intended occlusion of the fellow eye, and the necropsy performed by the university veterinarian revealed that the presumptive cause of death was a congenital ventricular septal defect. Although the unexpected premature death of C420 prevented assessment of the effect of the period of fellow eye occlusion on the acuity of this eye, the consequences of fellow eye occlusion for its littermate C419 were substantial as the acuity of this eye was reduced from 6.5 to 4.38 cycles/deg or 0.57 octaves.

Occlusion of the fellow eye for 9-11 days blocked any recovery of the acuity of the deprived eye following the period of darkness in all 5 animals, not just during the period of occlusion but in the days that followed. The absence of any change in the acuity of the deprived eye following fellow eye occlusion implies that any heightened plasticity induced in the central visual pathway by exposure to darkness does not extend beyond 11 days as the acuity of the deprived eye remained unchanged following restoration of binocular visual exposure. This result prompted us to explore the consequence of a much shorter 4-day period of fellow eye occlusion imposed on two littermates. The results displayed in Figure 5 indicate that the short period of fellow eye occlusion blocked any recovery of the acuity of the deprived eye after darkness during the period of occlusion and in its immediate aftermath. However, about 4 days later and for the next month, the acuity of the deprived eye began a slow improvement that was most evident for C423 as the acuity tripled from 0.4 to 1.4 cycles/deg or a change of 1.8 octaves. However, the improvement observed in its littermate, C424, was much smaller. This result suggests that some residual darkness-induced plasticity may have remained after termination of fellow eye occlusion to allow some limited recovery of the acuity of the deprived eye. No decrement in the acuity of the fellow eye was observed after the 4 days of occlusion. Again, the most prominent feature of the results from the two animals was the extent to which occlusion of the fellow eye blocked the benefits for the acuity of the deprived eye of the preceding period of darkness. The result implies that binocular visual input in the immediate aftermath of the period of dark exposure may be essential to the recovery of the acuity of the deprived eye. This possibility was explored on two additional groups of kittens for which the fellow eye was occluded for either 1 day or 2 days.

The results from the two animals (C445 and C447) for which the fellow eye was occluded for 2 days (Figure 6) indicate that this short period of occlusion blocked any recovery of the visual acuity of the deprived eye at all in the next 3 weeks. Also, the short period of occlusion of this eye did not cause any reduction in the acuity of this eye once occlusion was terminated. Two further animals were reared with just one day of occlusion of the fellow eye that was initiated immediately after the period of darkness. Because the two

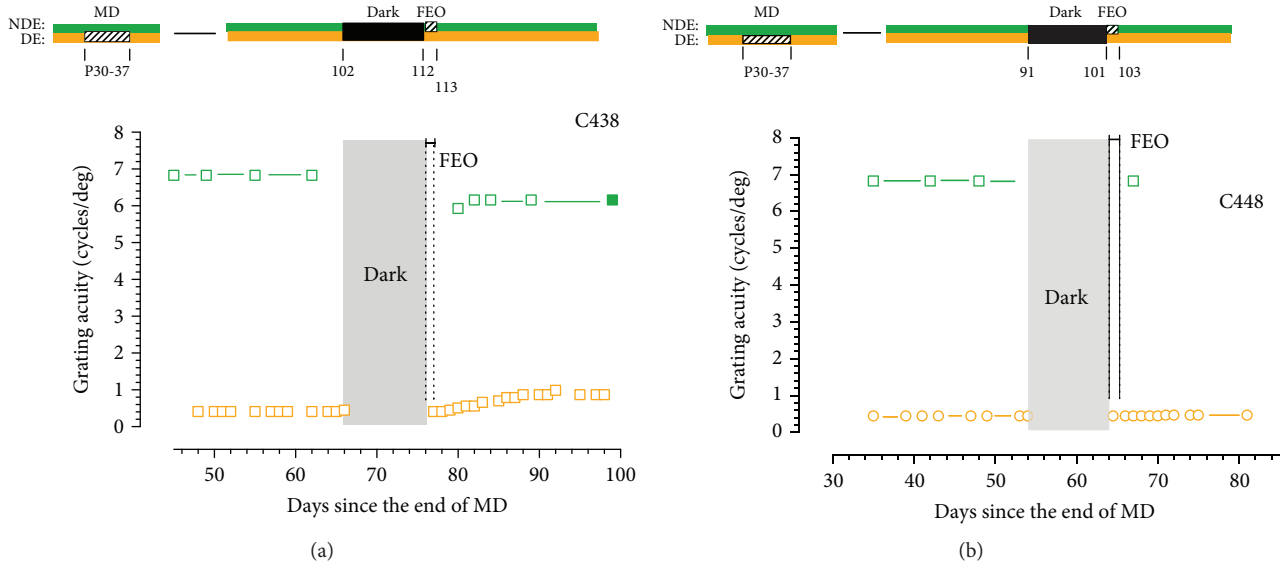

Figure 7: The grating acuity of the deprived eye acuity (orange symbols) and the binocular or nondeprived eye acuity (green symbols) of two monocularly deprived kittens C438 (a) and C448 (b) surrounding 10 days of total darkness followed immediately by a 1-day period of fellow eye occlusion (FEO). The brief period of FEO effectively blocked any improvement of the acuity of the deprived eye following the period of darkness.

animals were exposed to darkness at different ages, their data has been plotted separately in Figure 7. Even one day of occlusion of the fellow eye had an adverse effect on the recovery of the visual acuity of the deprived eye. In one animal, C438, the acuity of the deprived eye recovered a little from 0.4 to 0.9 cycles/deg but the acuity of this eye showed no improvement at all for the other animal (C448). Together, the results from the 11 animals that had the fellow eye occluded immediately upon emergence from the darkroom implied that concordant binocular visual exposure may be essential in the first 24 hours after darkness for the latter to promote recovery of the acuity of the deprived eye.

The increase in deprived eye acuity was poorly correlated with the duration of fellow eye occlusion following darkness ($r^2 = 0.03$; $p = 0.64$). Therefore, the adverse consequence of fellow eye occlusion was summarized in Figure 8 by comparing the final acuity achieved by the amblyopic eye among the 11 animals with fellow eye occlusion following darkness with that of control animals from this and two earlier studies [28, 29] that had both eyes open after darkness. The mean (±s.d.) deprived eye final acuity of the animals in the control group (6.85 ± 0.25 cycles/deg) was substantially higher than that achieved by animals in the fellow eye occlusion group (0.71 ± 0.30 cycles/deg). A permutation test for a difference in the mean final acuity between these two groups was highly significant ($p < 0.00001$).

In a preliminary exploration of the importance for binocular visual input in the immediate aftermath of the 10-day exposure to darkness, two additional animals were reared with a 2-day period of binocular visual exposure interposed immediately prior to either a 2- (C457) or 10- (C458) day period of occlusion of the fellow eye. The different periods of occlusion of the fellow eye employed for these animals dictated that their data be plotted separately in Figure 9.

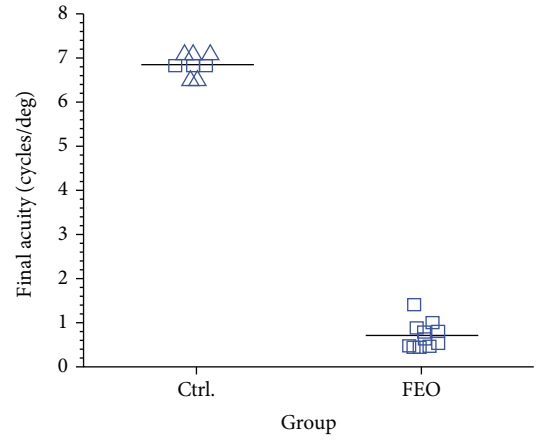

Figure 8: The open square symbols show a comparison of the final acuity achieved by the deprived eye of the 3 animals in the control group (Ctrl) following darkness with that achieved by the deprived eye in the 11 animals that had the fellow eye occluded for various short periods of time after they were removed from the darkroom. The triangle symbols for the control group display the results from animals reared in an identical fashion in two prior studies ([28]; C151, C152, C155, and C157) and [29]; C304).

Despite the different occlusion times for the fellow eye, the pattern of results was very similar. For both animals, the acuity of the deprived eye improved during the short 2-day period of binocular exposure that followed exposure to darkness by an amount similar to that observed in the same period by the 3 control animals of Figure 1 that had both eyes open after 10 days exposure to total darkness. However, occlusion of the fellow eye prevented any further improvement in the acuity of the deprived eye.

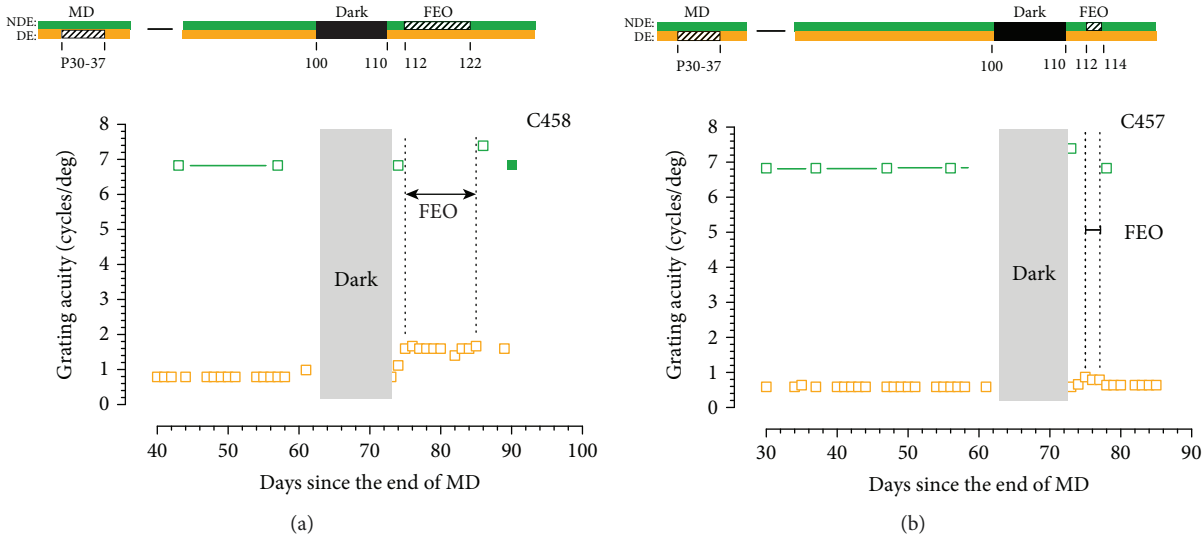

Figure 9: The grating acuity of the deprived eye (orange symbols) and the binocular or nondeprived eye acuity (green symbols) of two monocularly deprived kittens C458 (a) and C457 (b) surrounding 10 days of total darkness followed immediately by a 2-day period of binocular visual exposure that preceded fellow eye occlusion (FEO) for either 10 or 2 days. The period of FEO effectively blocked any further improvement of the acuity of the deprived eye that began during the brief period of binocular visual exposure following the period of darkness.

4. Discussion

As replicated again on three additional animals in this current study (Figure 1), a 10-day period of darkness can promote fast recovery of the visual acuity of the deprived eye of monocularly deprived kittens to match that of the fellow eye. It remains to be seen whether darkness restores other consequences of MD for the vision of the deprived eye such as on contrast sensitivity functions or on vernier acuity. However, there is evidence that darkness can restore normal stereoscopic vision to about a third of kittens following exposure to darkness [29].

Leaving aside for now examination of the ability of darkness to promote complete recovery of all visual functions of the deprived eye, the goal of this study was to investigate the contribution of the fellow eye to the darkness-induced recovery of the visual acuity of the amblyopic eye of monocularly deprived kittens. To test for a crucial role of the fellow eye in this recovery process, the rather blunt intervention of monocular eyelid suture of this eye was used to severely degrade the spatial visual information contained in the retinal image of this eye and so constrain the ability of neural signals from this eye to reinforce signals from the amblyopic eye at synapses in the visual cortex. The results from the first group of animals that received 9-11 days of occlusion of the fellow eye immediately following 10 days exposure to total darkness were very clear as they demonstrated that such occlusion blocked completely any recovery of the acuity of the amblyopic eye. Because the length of the occlusion extended through the time to total recovery of the acuity of the amblyopic eye that is observed when both eyes are open after the period of darkness (Figure 1), it was thought possible that some recovery may occur after shorter periods of fellow eye occlusion due to possible partial persistence of the benefits of the prior dark period. Progressively shorter periods of fellow eye occlusion of 4 days (Figure 5), 2 days (Figure 6), and even one day (Figure 7) effectively blocked any substantial recovery of the acuity of the deprived eye (Figure 8). An obvious conclusion that could be drawn is that binocularly concordant visual input in the immediate aftermath of the period of darkness is essential for the latter to be effective. Stated differently, if neural activity from the fellow eye is discordant with that from the amblyopic eye on the first day after the animal is removed from total darkness, it cannot bootstrap the rapid improvement of the acuity of the amblyopic eye.

The result from the final set of animals displayed in Figure 9 suggests a rather more nuanced conclusion. Here, the fellow eye was occluded two days *after* animals were removed from the darkroom for either 2 (C457) or 10 (C458) days. Nevertheless, occlusion of this eye stopped any further recovery from that achieved over the two days of binocular visual input experienced immediately after the period of darkness. The fact that recovery was blocked by just 2 days of occlusion of the fellow eye (C457) implies that brief occlusion *at any time after darkness* and not just in its immediate aftermath can block recovery and further that normal binocular vision is required throughout the recovery process. Occlusion of the fellow eye appears to be an extremely potent way to disrupt the benefits of darkness for recovery from early monocular deprivation.

Although occlusion of the fellow eye represents a rather blatant way to disrupt the degree of concordance of the visual input to the two eyes, it will be important to investigate whether less severe forms of disrupted binocular visual input such as those introduced by prismatic deviation of the two visual axes or by refractive imbalance can block the benefits of darkness in the same decisive manner as that achieved by fellow eye occlusion. It will also be of interest to determine if recovery following dark exposure

is also prevented by complete elimination of retinal activity from the fellow eye, which can be achieved through intraocular administration of tetrodotoxin [32, 36]. The degradation of normal vision experience through the closed eyelid of the fellow eye may be worse for the recovery of the amblyopic eye than a complete elimination of vision in the fellow eye.

The speed of recovery of the deprived eye that follows a period of darkness suggests that it cannot be explained entirely by the formation of new axonal or dendritic connections with this eye in the visual cortex. Whatever the underlying mechanisms for darkness-induced recovery, it appears to be prompted and guided in some way by neural activity generated by the fellow eye. Upon emergence from the darkroom, the strong cortical neural activity generated by the fellow eye may initially reinforce residual and/or silenced neural connections with the deprived eye in a behaviourally meaningful way that could precipitate further modifications to promote recovery and consolidate gains in visual acuity. The dramatic consequences of occlusion of the fellow eye described here provided strong support for this idea. That this recovery could be blocked by very short periods of occlusion, even after it had begun (Figure 9), deserves further exploration.

4.1. Clinical Implications. The results of fellow eye occlusion may hold important clinical applications with respect to the use of an interval of dark exposure, or possibly binocular retinal inactivation [36], to treat amblyopia in humans. For either treatment to be successful, it is essential that binocular visual input be concordant and remains so in the immediate aftermath of the treatment. In particular, optimal recovery precludes the use of patching of the fellow eye following the period of darkness or possibly binocular retinal inactivation. From a clinical perspective, it is clearly desirable to establish whether darkness or binocular retinal inactivation can prompt recovery from early monocular deprivation in primates. Because of ethical and practical barriers to the use of darkness, it is likely that ?initial attempts will employ brief binocular retinal inactivation. An additional practical barrier to a study on primates, particularly with respect to the consequences of either treatment for vision, is the present lack of methods to provide fast behavioural assessments of visual thresholds. However, it is possible to employ alternative measures such as the use of cortical visually evoked potentials (VEPs) to assess the effects on vision. In addition, the benefits of darkness or binocular retinal inactivation can be assessed in terms of their anatomical effects on the lateral geniculate nucleus [32].

Data Availability

The data used to support the findings of this study are available from the corresponding author upon request.

Conflicts of Interest

The authors declare that there is no conflict of interest regarding the publication of this paper.

Acknowledgments

We thank Rebecca Borchert and Matthew Jacques for their care of the animals. Hector Mantolino assisted with the behavioural testing of 6 kittens (C419, C420, and C422-5). The research was supported by a joint operating grant (PJT-153333) from the Canadian Institutes of Health Research held by KRD, DEM, and NC and by individual NSERC discovery grants to DEM (2015-03819), KRD (2015-05320), and NC (2015-06761).

References

[1] T. N. Wiesel and D. H. Hubel, "Single-cell responses in striate cortex of kittens deprived of vision in one eye," *Journal of Neurophysiology*, vol. 26, no. 6, pp. 1003–1017, 1963.

[2] S. Le Vay, T. N. Wiesel, and D. H. Hubel, "The development of ocular dominance columns in normal and visually deprived monkeys," *Journal of Comparative Neurology*, vol. 191, no. 1, pp. 1–51, 1980.

[3] N. P. Issa, J. T. Trachtenberg, B. Chapman, K. R. Zahs, and M. P. Stryker, "The critical period for ocular dominance plasticity in the ferret's visual cortex," *Journal of Neuroscience*, vol. 19, no. 16, pp. 6965–6978, 1999.

[4] U. C. Drager, "Observations on monocular deprivation in mice," *Journal of Neurophysiology*, vol. 41, no. 1, pp. 28–42, 1978.

[5] M. Fagiolini, T. Pizzorusso, N. Berardi, L. Domenici, and L. Maffei, "Functional postnatal development of the rat primary visual cortex and the role of visual experience: dark rearing and monocular deprivation," *Vision Research*, vol. 34, no. 6, pp. 709–720, 1994.

[6] D. E. Mitchell and B. Timney, "Postnatal development of function in the mammalian visual system," in *Supplement 3: Handbook of Physiology, The Nervous System, Sensory Processes*, I. Darian-Smith, Ed., pp. 507–555, American Physiological Society, Bethesda, MD, USA, 1984.

[7] N. W. Daw, K. Fox, H. Sato, and D. Czepita, "Critical period for monocular deprivation in the cat visual cortex," *Journal of Neurophysiology*, vol. 67, no. 1, pp. 197–202, 1992.

[8] K. R. Jones, P. D. Spear, and L. Tong, "Critical periods for effects of monocular deprivation: differences between striate and extrastriate cortex," *Journal of Neuroscience*, vol. 4, no. 10, pp. 2543–2552, 1984.

[9] C. R. Olson and R. D. Freeman, "Profile of the sensitive period for monocular deprivation in kittens," *Experimental Brain Research*, vol. 39, no. 1, pp. 17–21, 1980.

[10] N. W. Daw, *Visual Development*, Springer, New York, NY, USA, 2nd edition, 2006.

[11] B. M. Hooks and C. Chen, "Critical periods in the visual system: changing views for a model of experience-dependent plasticity," *Neuron*, vol. 56, no. 2, pp. 312–326, 2007.

[12] C. N. Levelt and M. Hübener, "Critical-period plasticity in the visual cortex," *Annual Review of Neuroscience*, vol. 35, no. 1, pp. 309–330, 2012.

[13] H. Morishita and T. K. Hensch, "Critical period revisited: impact on vision," *Current Opinion in Neurobiology*, vol. 18, no. 1, pp. 101–107, 2008.

[14] J. Movshon and L. Kiorpes, "The role of experience in visual development," in *Development of Sensory Systems in Mammals*, J. R. Coleman, Ed., pp. 155–202, Wiley, New York, NY, USA, 1990.

[15] D. E. Mitchell, "The extent of visual recovery from early monocular or binocular visual deprivation in kittens," *The Journal of Physiology*, vol. 395, no. 1, pp. 639–660, 1988.

[16] D. E. Mitchell, M. Cynader, and J. Anthony Movshon, "Recovery from the effects of monocular deprivation in kittens," *Journal of Comparative Neurology*, vol. 176, no. 1, pp. 53–63, 1977.

[17] C. Blakemore, L. J. Garey, and F. Vital-Durand, "The physiological effects of monocular deprivation and their reversal in the monkey's visual cortex," *The Journal of Physiology*, vol. 283, no. 1, pp. 223–262, 1978.

[18] G. K. von Noorden, J. E. Dowling, and D. C. Ferguson, "Experimental amblyopia in monkeys," *Archives of Ophthalmology*, vol. 84, no. 2, pp. 206–214, 1970.

[19] F. Giffin and D. E. Mitchell, "The rate of recovery of vision after early monocular deprivation in kittens," *The Journal of Physiology*, vol. 274, no. 1, pp. 511–537, 1978.

[20] C. Blakemore and R. C. van Sluyters, "Reversal of the physiological effects of monocular deprivation in kittens: further evidence for a sensitive period," *The Journal of Physiology*, vol. 237, no. 1, pp. 195–216, 1974.

[21] J. A. Movshon, "Reversal of the physiological effects of monocular deprivation in the kitten's visual cortex," *The Journal of Physiology*, vol. 261, no. 1, pp. 125–174, 1976.

[22] C. Blakemore, F. Vital Durand, and L. J. Garey, "Recovery from monocular deprivation in the monkey. I. Reversal of physiological effects in the visual cortex," *Proceedings of the Royal Society of London. Series B. Biological Sciences*, vol. 213, no. 1193, pp. 399–423, 1981.

[23] D. E. Mitchell, "The long-term effectiveness of different regimens of occlusion on recovery from early monocular deprivation in kittens," *Philosophical Transactions: Biological Sciences*, vol. 333, pp. 51–79, 1991.

[24] D. E. Mitchell, K. M. Murphy, and M. G. Kaye, "The permanence of the visual recovery that follows reverse occlusion of monocularly deprived kittens," *Investigative Ophthalmology and Visual Science*, vol. 25, no. 8, pp. 908–917, 1984.

[25] K. M. Murphy and D. E. Mitchell, "Reduced visual acuity in both eyes of monocularly deprived kittens following a short or long period of reverse occlusion," *Journal of Neuroscience*, vol. 7, no. 5, pp. 1526–1536, 1987.

[26] H. Y. He, W. Hodos, and E. M. Quinlan, "Visual deprivation reactivates rapid ocular dominance plasticity in adult visual cortex," *Journal of Neuroscience*, vol. 26, no. 11, pp. 2951–2955, 2006.

[27] H. Y. He, B. Ray, K. Dennis, and E. M. Quinlan, "Experience-dependent recovery of vision following chronic deprivation amblyopia," *Nature Neuroscience*, vol. 10, no. 9, pp. 1134–1136, 2007.

[28] K. R. Duffy and D. E. Mitchell, "Darkness alters maturation of visual cortex and promotes fast recovery from monocular deprivation," *Current Biology*, vol. 23, no. 5, pp. 382–386, 2013.

[29] D. E. Mitchell, K. MacNeill, N. A. Crowder, K. Holman, and K. R. Duffy, "Recovery of visual functions in amblyopic animals following brief exposure to total darkness," *The Journal of Physiology*, vol. 594, no. 1, pp. 149–167, 2016.

[30] S. Song, D. E. Mitchell, N. A. Crowder, and K. R. Duffy, "Postnatal accumulation of intermediate filaments in the cat and human primary visual cortex," *Journal of Comparative Neurology*, vol. 523, no. 14, pp. 2111–2126, 2015.

[31] D. E. Mitchell, "A shot in the dark: the use of darkness to investigate visual development and as a therapy for amblyopia," *Clinical and Experimental Optometry*, vol. 96, no. 4, pp. 363–372, 2013.

[32] K. R. Duffy, M. F. Fong, D. E. Mitchell, and M. F. Bear, "Recovery from the anatomical effects of long-term monocular deprivation in cat lateral geniculate nucleus," *Journal of Comparative Neurology*, vol. 526, no. 2, pp. 310–323, 2018.

[33] R. D. Freeman, "Corneal radius of curvature of the kitten and the cat," *Investigative Ophthalmology and Visual Science*, vol. 19, no. 3, pp. 306–308, 1980.

[34] H. A. Dzioba, K. M. Murphy, J. A. Horne, and D. E. Mitchell, "A precautionary note concerning the use of contact lens occluders in developmental studies on kittens, together with a description of an alternative occlusion procedure," *Clinical Vision Sciences*, vol. 1, pp. 191–196, 1986.

[35] L. Mioche and W. Singer, "Chronic recordings from single sites of kitten striate cortex during experience-dependent modifications of receptive-field properties," *Journal of Neurophysiology*, vol. 62, no. 1, pp. 185–197, 1989.

[36] M.-F. Fong, D. E. Mitchell, K. R. Duffy, and M. F. Bear, "Rapid recovery from the effects of early monocular deprivation is enabled by temporary inactivation of the retinas," *Proceedings of the National Academy of Sciences of the United States of America*, vol. 113, no. 49, pp. 14139–14144, 2016.

Hindawi
Neural Plasticity
Volume 2019, Article ID 5157628, 12 pages
https://doi.org/10.1155/2019/5157628

Research Article

Inverse Occlusion: A Binocularly Motivated Treatment for Amblyopia

Jiawei Zhou,[1] **Zhifen He**,[1] **Yidong Wu**,[1] **Yiya Chen**,[1] **Xiaoxin Chen**,[1] **Yunjie Liang**,[1] **Yu Mao**,[1] **Zhimo Yao**,[1] **Fan Lu**,[1] **Jia Qu**,[1] **and Robert F. Hess**[2]

[1]*School of Ophthalmology and Optometry and Eye Hospital, Wenzhou Medical University, Wenzhou, Zhejiang 325003, China*
[2]*McGill University, McGill Vision Research, Department of Ophthalmology, Quebec, Montreal, Canada H3G 1A4*

Correspondence should be addressed to Jiawei Zhou; zhoujw@mail.eye.ac.cn and Robert F. Hess; robert.hess@mcgill.ca

Received 15 September 2018; Revised 23 November 2018; Accepted 8 January 2019; Published 19 March 2019

Guest Editor: Claudia Lunghi

Recent laboratory findings suggest that short-term patching of the amblyopic eye (i.e., inverse occlusion) results in a larger and more sustained improvement in the binocular balance compared with normal controls. In this study, we investigate the cumulative effects of the short-term inverse occlusion in adults and old children with amblyopia. This is a prospective cohort study of 18 amblyopes (10-35 years old; 2 with strabismus) who have been subjected to 2 hours/day of inverse occlusion for 2 months. Patients who required refractive correction or whose refractive correction needed updating were given a 2-month period of refractive adaptation. The primary outcome measure was the binocular balance which was measured using a phase combination task; the secondary outcome measures were the best-corrected visual acuity which was measured with a Tumbling E acuity chart and converted to logMAR units and the stereoacuity which was measured with the Random-dot preschool stereogram test. The average binocular gain was 0.11 in terms of the effective contrast ratio ($z = -2.344$, $p = 0.019$, 2-tailed related samples Wilcoxon Signed Rank Test). The average acuity gain was 0.13 logMAR equivalent ($t(17) = 4.76$, $p < 0.001$, 2-tailed paired samples t-test). The average stereoacuity gain was 339 arc seconds ($z = -2.533$, $p = 0.011$). Based on more recent research concerning adult ocular dominance plasticity, we conclude that inverse occlusion in adults and old children with amblyopia does produce long-term gains to binocular balance and that acuity and stereopsis can improve in some subjects.

1. Introduction

Occlusion of the fixing eye has been the gold standard treatment for amblyopia ever since it was first introduced in 1743 by Conte de Buffon [1]. It has evolved over the years; partial rather than full-time occlusion is now preferred, and filters (i.e., Bangerter filters) [2], lenses (i.e., defocused or frosted), and eye drops (i.e., atropine) [3, 4] have been used instead of opaque patches. It is effective in over 53% of cases in improving acuity in the amblyopic eye by more than 2 lines of logMAR acuity [5]. It does however leave something to be desired in a number of aspects. Compliance can be low [6] because it restricts school-age children to the low vision of their amblyopic eyes for part of the day and also because of its psychosocial side effects [7]. There is a relatively poor binocular outcome even though the acuity of the amblyopic eye is improved [8]. Its effects are age-dependent; effectiveness is much reduced for children over the age of 10 years old [9, 10]. Finally, it is associated with a 25% regression rate once the patch has been removed [11, 12]. It is effective but far from ideal. Interestingly, the basis of this widely accepted therapy is poorly understood. An explanation is often advanced in terms of "forcing the amblyopic to work" by occluding the fixing eye, which prompts the question, *what is stopping the amblyopic eye from working under normal binocular viewing?* This suggests that the problem of improving vision in the amblyopic eye, far from being simply a monocular issue, must have an underlying binocular basis (i.e., involving the fixing eye). Occlusion of the fixing eye must be, in some way, disrupting what is normally preventing the amblyopic eye from working when both eyes are open. Within the clinical literature, this is known as suppression and one supposes that occlusion affects

suppression in a way that is beneficial to the acuity of the amblyopic eye.

Recent laboratory studies have shown that short-term occlusion (i.e., 2 hours) is associated with temporary changes in eye dominance in normal adults. There are two things that are particularly novel about these new finding: first, these changes occur in adults, and secondly, the eye that is patched becomes stronger in its contribution to the binocular sum. In other words, the eye balance is shifted in favour of the previously patched eye. This was first shown by Lunghi et al. [13] using a binocular rivalry measure to quantify eye dominance. Since then, there has been a wealth of information on this form of eye dominance plasticity in normal adults using a wide variety of different approaches [13–27]. Zhou et al. [25] were the first to show that adults with amblyopia also exhibited this form of plasticity and that it tended to be of a larger magnitude and of a more sustained form. They made the novel suggestion that it could provide the basis of a new therapeutic avenue for amblyopes in reestablishing the correct balance between their two eyes. Such a suggestion rests on the assumption that serial episodes of short-term occlusion can lead to sustainable long-term improvements in eye balance. The hallmark of this form of plasticity is that, once the patch has been removed, the patched eye's contribution to binocular vision is strengthened. Zhou et al. [25] suggested that to redress the binocular imbalance that characterizes amblyopia, it is the amblyopic eye that would need to be occluded, opposite to what has been in common practice for hundreds of years to improve the acuity in the amblyopic eye. Such a therapy, in principle, would be primarily binocular in nature (addressing the binocular imbalance as a first step); it would be expected to have much less compliance problems since it is not affecting the day-to-day vision of the patient, and since it has been demonstrated in adults, it could be administered at any age. While this is well and good from a purely binocular perspective, the obvious question is how would occlusion of the amblyopic eye on a long-term basis (e.g., 2 hours or more a day for months) affect the acuity of the patched eye? The ethical basis for such interventions is not in doubt, as there is evidence indicating that such treatment is likely to benefit rather than harm the vision of the amblyopic eye (including children). In the 1960s, so-called inverse occlusion was sometimes used in an attempt to treat eccentric fixation, which accompanies amblyopia in its more severe form. A review of these studies [28–32] leads to two conclusions: first, inverse occlusion did not make the amblyopia worse, and second, acuity improved in the amblyopic eye in a percentage of cases. The percentage of patients whose vision improved was significantly less than that of classical occlusion in most [28, 31, 32], but not all [29, 30] studies, which could arguably be a consequence of the fact that studies on inverse occlusion were restricted to the more severe and resistant forms of amblyopia. Therefore, on the basis of recent laboratory studies on ocular dominance plasticity resulting from short-term monocular occlusion [13–25] and previous clinical studies, on inverse occlusion designed to treat eccentric fixation [28–32], we have two expectations: first that inverse occlusion (i.e., occlusion of the amblyopic eye) should improve the binocular balance in patients with amblyopia and second that improved acuity of the amblyopic eye should also be expected. Two additional benefits of this approach would be the expectation of better compliance, as the fellow eye is not occluded, and its applicability to older children and adults, since ocular dominance plasticity occurs in adults.

To determine whether this radical departure from what is in common practice has any benefit, we studied the effects of inverse occlusion for 2 hours/day for 2 months on a group of 18 anisometropic and strabismic amblyopic teens and adults (10-35 years old), an age range where classical occlusion therapy has low compliance [33]. Our primary outcome measure was the binocular balance or ocular dominance. The second outcome measures were visual acuity and stereoacuity. The results suggest that this approach results in modest gains in both binocular balance and visual acuity within this older age group; no adverse effects were encountered.

2. Materials and Methods

2.1. Participants. Eighteen amblyopes with ($n = 2$) or without ($n = 16$) strabismus participated in our experiment. All of the patients were detected at 10 years old or older or had failed with classical occlusion therapy (i.e., patching the fellow eye). Clinical details of the patients are provided in Table 1. Observers wore their prescribed optical correction, if needed, in the data collection. Written informed consent was obtained from all patients or from the parents or legal guardian of participants aged less than 18 years old, after explanation of the nature and possible consequences of the study. This study followed the tenets of the Declaration of Helsinki and was approved by the Ethics Committee of Wenzhou Medical University.

2.2. Apparatus. The measures of binocular balance were conducted on a PC computer running Matlab (MathWorks Inc., Natick, MA) with PsychToolBox 3.0.9 extensions [34, 35]. The stimuli were presented on a gamma-corrected LG D2342PY 3D LED screen (LG Life Science, Korea) with a 1920×1080 resolution and a 60 Hz refresh rate. Subjects viewed the display dichoptically with polarized glasses in a dark room at a viewing distance of 136 cm. The background luminance was 46.2 cd/m^2 on the screen and 18.8 cd/m^2 through the polarized glasses. A chin-forehead rest was used to minimize head movements during the experiment.

Best-corrected visual acuity was measured using a Tumbling E acuity chart, the Chinese national standard logarithmic vision chart (Wenzhou Xingkang, Wenzhou, China), at 5 meters. This consists of E letters in 4 orientations (up, down, left, or right) on each line in a logarithmic progression from 20/200 to 20/10. The size of the E letters ranges from 1 to -0.3 (logMAR) with a step size of 0.1 log unit per line. Because it is easy to understand and has less requirement of education, this illiterate chart has been recognized as the national standard in China (GB11533-1989). During the measurement, we asked subjects to report the orientation of each optotype in each line, which started from the first line (corresponding to 1 logMAR) and terminated at

Table 1: Clinical details of the participants.

Subject	Age/sex	Cycloplegic refractive errors (OD/OS)	Squint (OD/OS)	Balance point (OD/OS)		logMAR visual acuity			RDS (arc seconds)		History
				Preinverse occlusion	Postinverse occlusion	Before refractive adaptation	Preinverse occlusion	Postinverse occlusion	Preinverse occlusion	Postinverse occlusion	
S1	26/F	Plano	Ø	0.15	0.15	—	0.07	-0.03	1200	1200	Detected at 10 years old, patched occasionally for half year, no surgery
		Plano	ET5°			—	0.77	0.68			
S2	12/M	+0.50	Ø	0.10	0.91	—	-0.22	-0.22	1200	200	Detected at 10 years old, glasses since thereafter, no patching history
		+5.00 +0.50 × 80	Ø			—	0.77	0.47			
S3	35/M	-5.50 -0.75 × 85	Ø	0.15	0.42	—	-0.03	-0.03	800	200	Detected at 21 years old, glasses since thereafter, no patching history
		+0.75	Ø			—	0.18	0.18			
S4	21/F	-1.50	Ø	0.45	0.49	—	-0.03	0.07	100	40	Detected at 19 years old, glasses since thereafter, no patching history
		+3.50	Ø			—	0.18	0.07			
S5	11/F	+4.00 × 95	Ø	0.43	0.52	0.37	0.18	0.07	40	40	Detected at 11 years old, glasses for 2 months, no patching history
		Plano	Ø			0.07	0.07	-0.03			
S6	23/F	+2.25	Ø	0.33	0.20	—	0.98	0.77	1200	1200	Detected at 13 years old, glasses since 18 years old, no patching history
		-2.5 -1.25 × 175	Ø			—	-0.01	-0.03			
S7	12/M	+7.00	Ø	0.40	0.52	0.98	0.98	0.77	1200	1200	Detected at 12 years old, glasses for 2 months, no patching history
		Plano	Ø			-0.03	-0.03	-0.03			
S8	13/M	Plano	Ø	0.14	0.40	—	-0.12	-0.03	1200	40	Detected at 12 years old, glasses since thereafter, patching occasionally for 2 months
		+6.00	Ø			—	0.27	0.18			
S9	11/M	+4.00	Ø	0.71	0.85	0.68	0.68	0.47	200	60	Detected at 11 years old, glasses for 2 months, no patching history
		Plano	Ø			-0.03	-0.03	-0.03			
S10	17/M	+3.25	Ø	0.20	0.44	0.85	0.57	0.57	1200	1200	Detected at 17 years old, glasses for 2 months, no patching history
		Plano	Ø			-0.03	-0.03	-0.03			
S11	11/M	+6.00	Ø	0.14	0.25	1.37	1.37	0.87	1200	1200	Detected at 11 years old, glasses for 2 months, no patching history
		-0.75	Ø			-0.03	-0.03	-0.03			
S12	20/F	Plano	Ø	0.43	0.42	-0.03	-0.03	-0.03	40	40	Detected at 20 years old, glasses for 2 months, no patching history
		+5.00	Ø			0.47	0.37	0.27			
S13	13/M	-0.50	Ø	0.10	0.13	-0.12	-0.12	-0.12	1200	1200	Detected at 13 years old, glasses for 2 months, no patching history
		+5.00 +1.25 × 5	Ø			1.18	1.18	1.07			
S14	10/F	Plano	ET15°	0.19	0.18	—	-0.12	-0.12	1200	1200	Detected at 14 years old, no patching history, no surgery
		Plano	Ø			—	0.77	0.68			
S15	29/F	+2.50 +1.00 × 100	Ø	0.04	0.04	—	0.57	0.57	1200	200	Detected at 7 years old, glasses since thereafter, patching occasionally for 1 year
		+1.50 +1.00 × 90	Ø			—	0.07	0.07			

Table 1: Continued.

Subject	Age/sex	Cycloplegic refractive errors (OD/OS)	Squint (OD/OS)	Balance point (OD/OS)		logMAR visual acuity			RDS (arc seconds)		History
				Preinverse occlusion	Postinverse occlusion	Before refractive adaptation	Preinverse occlusion	Postinverse occlusion	Preinverse occlusion	Postinverse occlusion	
S16	13/M	+4.50	Ø	0.46	0.48	—	0.68	0.57	1200	60	Detected at 12 years old, glasses since thereafter, patching occasionally for 2 months
		Plano	Ø			—	-0.03	-0.03			
S17	11/M	Plano	Ø	0.18	0.21	-0.03	-0.03	-0.03	1200	200	Detected at 11 years old, glasses for 2 months, no patching history
		+3.50 +1.00 × 100	Ø			0.77	0.77	0.68			
S18	19/F	-5.00	Ø	0.82	0.72	-0.03	-0.03	-0.03	1200	1200	Detected at 19 years old, glasses for 2 months, no patching history
		+2.00	Ø			0.37	0.37	0.27			

F: female; M: male; OD: oculus dexter (right eye); OS: oculus sinister (left eye); DS: dioptre sphere; DC: dioptre cylinder; ET: heterotropia esodeviation at far distance (6 m).

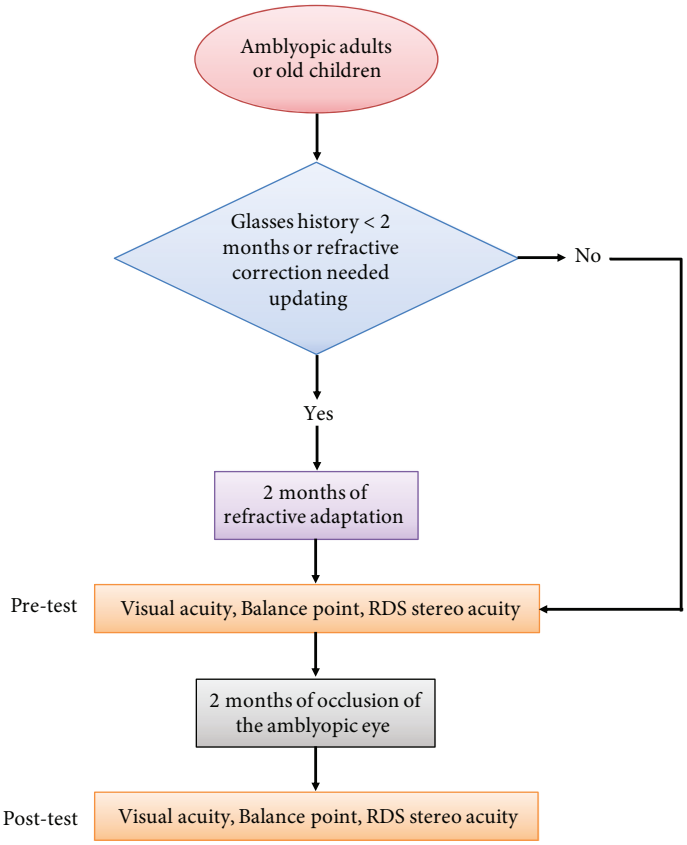

Figure 1: Experimental design. Eighteen amblyopes with ($n = 2$) or without ($n = 16$) strabismus participated in our experiment. Patients' binocular balance (balance point in the binocular phase combination task), visual acuity, and stereoacuity were measured before and after two months of occlusion of the amblyopic eye for 2 hours/day (i.e., the inverse occlusion). For patients who required refractive correction or whose refractive correction needed updating ($n = 9$), a 2-month period of refractive adaptation was provided prior to the inverse occlusion study.

the line where his/her accuracy was less than 75%. Visual acuity was defined as the score associated with 75% correct judgments, which was achieved by using linear interpolation to calculate the score associated with the 75% correct judgments. The measurement of stereoacuity involved the Random-dot preschool stereograms (RDS test; Baoshijia, Zhengzhou, China) at 40 cm. Strabismus angle was measured using the prism cover test.

2.3. Design. Patients' binocular balance (balance point in the binocular phase combination task), visual acuity, and stereoacuity were measured before and after two months of occlusion of the amblyopic eye for 2 hours/day (i.e., the inverse occlusion). For patients who required refractive correction or whose refractive correction needed updating ($n = 9$), a 2-month period of refractive adaptation was provided prior to the inverse occlusion study (Figure 1).

Since this approach is different from that currently used (i.e., classical occlusion therapy), we were careful to conduct follow-up evaluations in accordance with the regulations from the Amblyopia Preferred Practice Pattern® guideline ("PPP" 2017), P124: "If the visual acuity in the amblyopic eye is improved and the fellow eye is stable, the same treatment regimen should be continued." In particular, we conducted weekly visits in the pilot study (in S1 to S13), rather than the 2 to 3 months that "PPP" recommends (P124 in "PPP": "In general, a follow-up examination should be arranged 2 to 3 months after initiation of treatment.") to ensure that the acuity in the amblyopic eye did not deteriorate as a result of patching (Figure 2).

We quantitatively accessed the binocular balance using a binocular phase combination paradigm [36, 37], which measures the contributions that each eye makes to binocular vision. The design was similar as the one we used in previous studies [38, 39], in which observers were asked to dichoptically view two horizontal sine wave gratings having equal and opposite phase shifts of 22.5° (relative to the center of the screen) through polarized glasses; the perceived phase of the grating in the cyclopean percept was measured as a function of the interocular contrast ratio. By this method, we were able to find a specific interocular contrast ratio where the perceived phase of the cyclopean grating was 0 degrees, indicating equal weight to each eye's image. This specific interocular contrast ratio reflects the "balance point" for binocular phase combination since the two eyes under these stimulus conditions contribute equally to binocular vision. For each interocular contrast ratio ($\delta = [0, 0.1, 0.2, 0.4, 0.8, 1.0]$), two configurations were used in the measurement so that any starting potential positional bias will be cancelled out: in one configuration, the phase

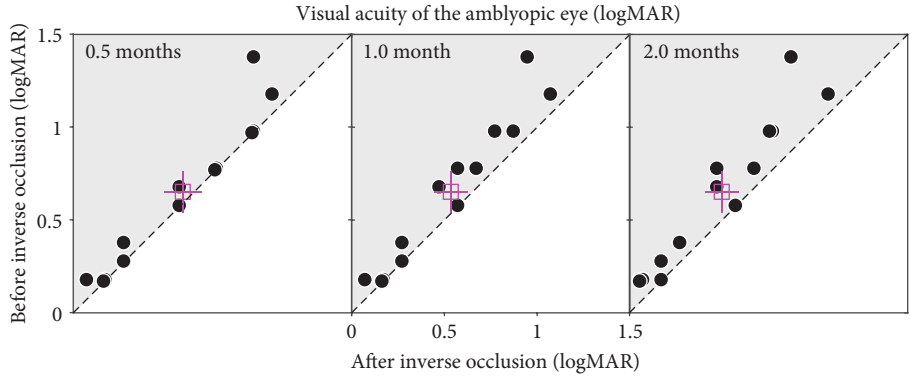

Figure 2: The change of the amblyopic eye's visual acuity after inverse occlusion. S1 to S13 participated in this pilot study. In each panel, each dot represents one patient (jitter points were used to avoid superimposing points). The open square represents the average results. Error bars represent standard errors. Data falling in the shaded area represent improvements; data falling on the sloping line represent no effect. The amblyopic eye's visual acuity improved in 5 of the 13 patients after 2 weeks of treatment; in 9 of the 13 patients after 1 month of treatment; and in 11 of the 13 patients after 2 months of treatment. Fellow eye's visual acuity was stable in all patients. No case of a deterioration of acuity in the amblyopic eye was recorded. The amblyopic eye's visual acuity was significantly different at different follow-up sessions: $F(3, 36) = 11.39$, $p < 0.001$, 2-tailed within-subject repeated measures ANOVA.

shift was +22.5° in the amblyopic eye and -22.5° in the fellow eye, and in the other, the reverse. The perceived phase of the cyclopean grating at each interocular contrast ratio (δ) was quantified by half of the difference between the measured perceived phases in these two configurations. Different conditions (configurations and interocular contrast ratios) were randomized in different trials; thus, adaptation or expectation of the perceived phase would not have affected our results. The perceived phase and its standard error were calculated based on eight measurement repetitions. Before the start of data collection, proper demonstrations of the task were provided by practice trials to ensure observers understood the task. During the test, observers were allowed to take short-term breaks whenever they felt tired.

2.4. Stimuli. In the binocular phase combination measure, the gratings in the two eyes were defined as

$$\begin{aligned} \mathrm{Lum}_{\mathrm{AE}}(y) &= L_0\left[1 - C_0 \cos\left(2\pi f y \pm \frac{\theta}{2}\right)\right], \\ \mathrm{Lum}_{\mathrm{FE}}(y) &= L_0\left[1 - \delta C_0 \cos\left(2\pi f y \mp \frac{\theta}{2}\right)\right], \end{aligned} \quad (1)$$

where L_0 is the background luminance, C_0 is the base contrast in the amblyopic eye, f is the spatial frequency of the gratings, δ is the interocular contrast ratio, and θ is the interocular phase difference.

In our test, $L_0 = 46.2$ cd/m^2 (on the screen), $C_0 = 96\%$, $f = 1$ cycle/°, $\delta = [0, 0.1, 0.2, 0.4, 0.8, 1.0]$, and $\theta = 45°$.

Surrounding the gratings, a high-contrast frame (width, 0.11°; length, 6°) with four white diagonal lines (width, 0.11°; length, 2.83°) was always presented during the test to help observers maintain fusion.

2.5. Procedure. We used the same phase adjustment procedure as used by Huang et al. [37] for measuring the perceived phase of the binocularly combined grating. In each trial, observers were asked firstly to align the stimuli from the two eyes; they were then instructed to adjust the position of a reference line to indicate the perceived phase of the binocularly combined grating. Since the gratings had a period of 2 cycles corresponding to 180 pixels, the phase adjustment had a step size of 4 degrees of phase/pixel (2 cycles × 360 phase degree/cycle/180 pixels).

2.6. Statistical Analysis. Data are presented as mean ± S.E.M. unless otherwise indicated. Sample number (n) indicates the number of observers in each group, which are indicated in the figure. A one-sample Kolmogorov-Smirnov test was performed on each dataset to evaluate normality. A 2-tailed related samples Wilcoxon Signed Rank Test was used for comparison between nonnormally distributed datasets; a 2-tailed paired samples t-test was used for comparison between normally distributed datasets; a within-subject repeated measures ANOVA was used to evaluate the time effect of the inverse occlusion. Differences in means were considered statistically significant at $p < 0.05$. Analyses were performed using the SPSS 23.0 software.

3. Results

In the pilot study, we firstly conducted 0.5 months of inverse occlusion (2 hours/day) in S1 to S13. We found that the amblyopic eye's visual acuity improved in 5 of the 13 patients after 2 weeks of treatment, with no cases of acuity loss in the amblyopic eye. Visual acuity of the fellow eye was stable in all cases. We then extend the occlusion period to 1 month, and 9 of 13 patients were found to exhibit small gains in visual acuity. No cases were recorded where the acuity of the amblyopic eye deteriorated. The visual acuity of the fellow eye remained stable in all cases. We then extended the occlusion period to 2 months and found that 11 of 13 patients showed small improvements in visual acuity in the amblyopic eye at that time. No patients

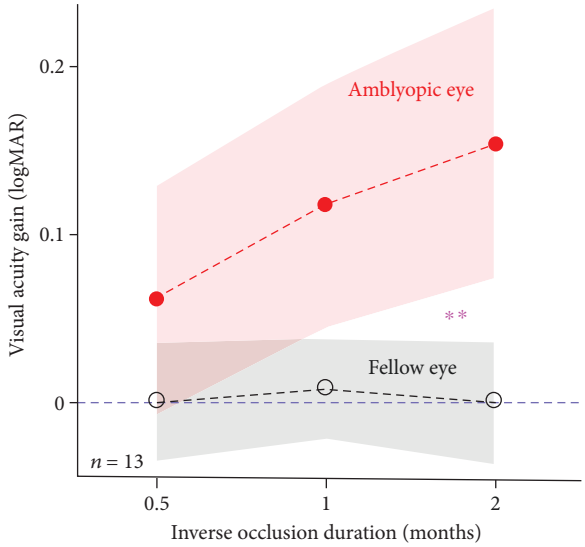

Figure 3: A dose-response relationship for the amblyopic eye. Average visual acuity gains of the amblyopic eye (filled circles) and the fellow eye (open circles) were plotted as a function of the inverse occlusion durations. The areas indicate the 95% confidence interval for the mean. The two curves were significantly different (**): the interaction between the eyes and inverse occlusion durations was significant: $F(2, 24) = 7.98$, $p = 0.002$, 2-tailed repeated measures ANOVA.

exhibited a deterioration of function in the amblyopic eye (Figure 2). A within-subject repeated measures ANOVA verified that the amblyopic eye's visual acuity was significantly different at these different follow-up sessions: $F(3, 36) = 11.39$, $p < 0.001$. This result clearly shows a dose-response relationship for the amblyopic eye in terms of visual acuity.

Since we did not have a control group who were denied any treatment, there is always the possibility that improvements in visual acuity measured at different time points are simply due to learning effects. To test this, we recorded the stability of acuity measured for the untreated fellow eye, as a similar learning effect should apply. In Figure 3, we plot the visual acuity gain as a function of treatment duration for the patched amblyopic eye and the unpatched fellow eye. There is an obvious difference between the two curves. A within-subject repeated measures ANOVA, with eyes and follow-up sessions as within-subject factors, verified that the visual acuity gain was significantly different between eyes ($F(1, 12) = 10.35$, $p = 0.007$) and between follow-up sessions ($F(2, 24) = 10.32$, $p = 0.001$). The interaction between these 2 factors was also significant ($F(2, 24) = 7.98$, $p = 0.002$), indicating that the visual acuity gain of the amblyopic eye is less likely to be accounted for by repeated testing alone. Additionally, any explanation for the acuity gains that are based on learning effects from repeated testing should also apply to the stereo measurements that also showed improvements with inverse occlusion. However, the acuity gains and the stereo gains were not correlated after 2 months of inverse occlusion (Spearman's correlation; $p = 0.79$) across our patient group.

Once we had shown that inverse occlusion can be undertaken in a safe fashion, we added 5 additional patients (S14 to S18) to the original study cohort of 13 (S1 to S13). These additional patients followed similar protocol as the original thirteen (S1 to S13); the only difference was that visual functions were only measured before and after 2 months of treatment. A summary of the main result for all the 18 patients is shown in Figure 4 for the measures of ocular balance, visual acuity, and stereoacuity. Measurements before and after 2 months of treatment are plotted against one another. In terms of ocular balance, the measure used is the interocular contrast that is required to achieve a binocular balance. By binocular balance, we mean that the contributions of each eye's input are equal at the site of binocular combination. For normals with equal eye balance, the effective contrast ratio would be unity. Data falling on the sloping diagonal line represents no change from treatment whereas data falling in the shaded regions represents an improvement in binocular function (Figure 4(a)).

Amblyopes exhibit a range of binocular imbalances ranging from less than 0.04 to 0.82 (Figure 4(a)). Inverse patching for 2 hours/day for 2 months improves some more than others. Six subjects showed no improvement; the other patients showed varying levels of improvement, meaning that their amblyopic eye was contributing more to binocular vision. Overall, the average improvement was a 0.11 change (0.30 ± 0.052 to 0.41 ± 0.058 (mean $\pm$ S.E.M.)) in the effective contrast ratio (square symbol), which was significant based on a 2-tailed related samples Wilcoxon Signed Rank Test: $z = -2.344$, $p = 0.019$. Our patients exhibited a range of acuity deficits ranging from less than 0.18 to close to 1.37 logMAR (Figure 4(b)). As expected, the acuity improvements were of varying degrees. Three patients showed no improvement at all, while all the other patients did exhibit improvements to varying degrees (shaded area). The average improvement (solid symbol) was 0.13 logMAR (from 0.65 ± 0.082 to 0.51 ± 0.068 (mean $\pm$ S.E.M.); Cohen's $d = 0.418$), which was significant based on a 2-tailed paired samples t-test: $t(17) = 4.76$, $p < 0.001$. This magnitude of acuity gain is similar to the results of a recent PEDIG study using classical occlusion of the same duration (i.e., 2 hours/day for 16 weeks) in patients of a similar age range (average improvement of 0.13 logMAR, from 56.1 ± 9.7 to 62.5 ± 11.6 (mean $\pm$ SD) letters; Cohen's $d = 0.599$) [40]. The average stereoacuity gain was 339 arc seconds ($z = -2.533$, $p = 0.011$, 2-tailed related samples Wilcoxon Signed Rank Test). This is a very conservative estimate because 13/18 patients had stereoacuities outside of our measurement range and were conservatively scored at 1200 arc secs, the largest disparity tested. This means that the true stereoacuity gain could be larger than 339 arc seconds.

These changes in binocular balance, visual acuity, and stereoacuity are modest but still impressive considering the fact that the period of occlusion was relatively short (2 hours), the duration of the treatment was limited to 2 months, and it involved an older age group. One interesting finding is that the improvements in balance and visual acuity are not significantly correlated ($p = 0.61$, Spearman's correlation), so it is unlikely they have a common basis.

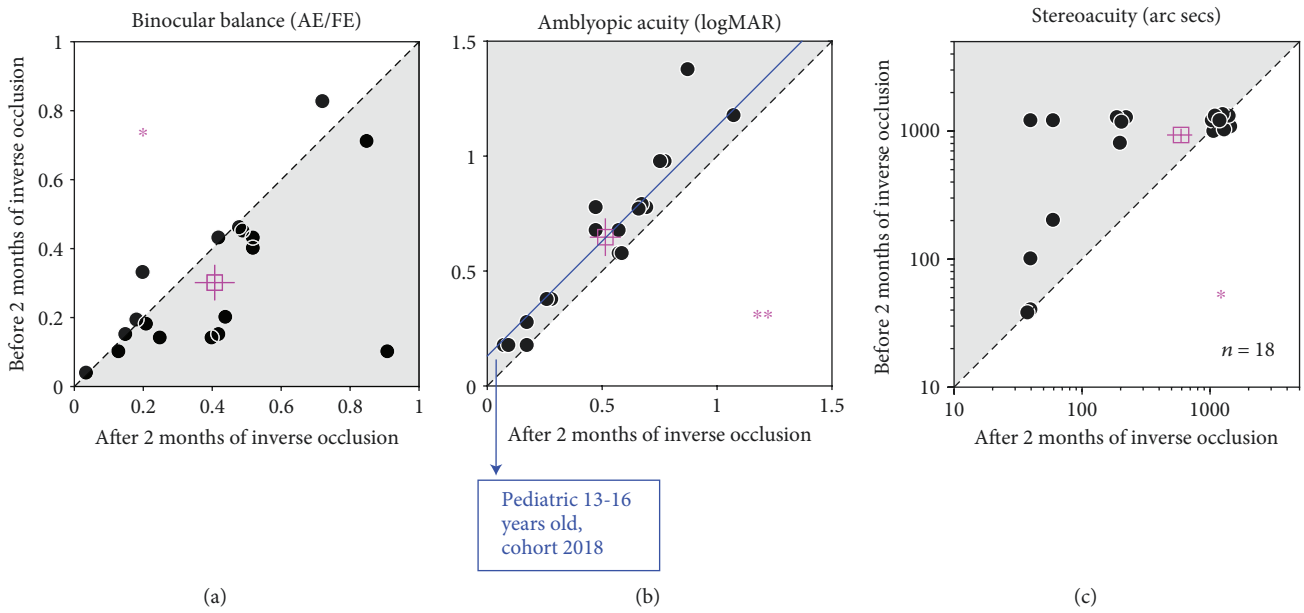

FIGURE 4: Visual outcomes after two months of occlusion of the amblyopic eye for 2 hours/day. Eighteen amblyopes (S1 to S18; 10 to 35 years old), with ($n = 2$) or without ($n = 16$) strabismus, participated. For patients who required refractive correction or whose refractive correction needed updating ($n = 9$), a 2-month period of refractive adaptation was provided before the inverse occlusion. (a) Binocular balance was measured with the binocular phase combination task and expressed as the interocular contrast ratio (amblyopic eye/fellow eye) when the two eyes are balanced. The binocular balance increased from 0.30 ± 0.052 to 0.41 ± 0.058 (mean ± S.E.M.). *: $z = -2.344$, $p = 0.019$, 2-tailed related samples Wilcoxon Signed Rank Test. Error bars represent standard errors. Data falling in the shaded area indicate patients whose two eyes were more balanced; data falling on the sloping line represent no change. (b) Visual acuity was measured with a Tumbling E acuity chart in logMAR units. The visual acuity improved from 0.65 ± 0.082 to 0.51 ± 0.068 (mean ± S.E.M.), effect size: Cohen's $d = 0.418$. **: $t(17) = 4.76$, $p < 0.001$, 2-tailed paired samples t-test. Error bars represent standard errors. Data falling in the shaded area represents better visual acuity; data falling on the sloping line represent no change. Jitter points were used to avoid superimposing points. The blue line indicates a 0.13 logMAR visual acuity improvement (effect size: Cohen's $d = 0.599$) observed from a recent cohort study from the PEDIG group based on 2 hours daily of classical patching treatment for 16 weeks in children aged 13 to 16 years old with amblyopia [40]. (c) Stereoacuity was measured with the Random-dot stereograms. Stereoacuity of 1200 arc secs was assigned for patients (13/18) whose stereoacuity was too bad to be measured. The stereoacuity improved from 932.2 ± 111.00 to 593.3 ± 132.31 (mean ± S.E.M.). *: $z = -2.533$, $p = 0.011$, 2-tailed related samples Wilcoxon Signed Rank Test. Error bars represent standard errors. Data falling in the shaded area represents better stereopsis; data falling on the sloping line represent no change. Jitter points were used to avoid superimposing points.

These improvements were long-lasting as we have followed four patients (S12, S14, S16, and S17) for 1 month and one patient (S9) for 5.5 months after finishing 2 months of the reverse occlusion regime, which showed that the outcomes were sustained (Figure 5). The results at the Post-test2 session were not significantly different from that after the conclusion of 2 months of inverse occlusion: for balance point, $t(4) = -0.72$, $p = 0.51$; for visual acuity, $t(4) = 1.50$, $p = 0.21$; for stereopsis, $z = -1.63$, $p = 0.10$. A larger sample size is needed before it can be definitely concluded that these benefits are sustained; future larger RCT studies are needed to clarify the retention effect.

In our study, the patients' ages ranged from 10 years old to 35 years old. Interestingly, all patients who were younger than 14 years old ($n = 10$) had a visual acuity gain. While for patients older than 14 years old ($n = 8$), only 62.5% of them had a visual acuity gain. However, a Spearman correlation analysis showed that the correlation between the improvement in visual acuity of the amblyopic eye and the patients' age was not significant ($p = 0.10$). The correlations between the patients' age and the binocular balance gain or the RDS stereoacuity gain were also not significant ($p > 0.3$). Future larger RCT studies are needed to clarify the age effect.

The refractive correction needed updating in half of the patients ($n = 9$), and a 2-month period of refractive adaptation was provided before inverse occlusion was commenced. Even though the acuity gains from optical treatments have been shown to be modest after 5-6 weeks of refractive adaptation [41], since those observations were in a much younger age group, there could still be an argument that our findings were due to the refractive correction per se *occurring after our 8-week period*, rather than the inverse occlusion. To assess this, we divided our patients into two subgroups, i.e., those who required refractive adaptation ($n = 9$) and those who did not ($n = 9$). The subgroup that required refractive adaptation was slightly but not significantly younger than the subgroup that did not require refractive adaptation ($z = -0.18$, $p = 0.08$). We found no significant difference of visual outcomes in these two subgroups, in terms of the improvement of the amblyopic eye's visual acuity ($z = -0.71$, $p = 0.49$), binocular balance ($z = -0.13$, $p = 0.93$), and

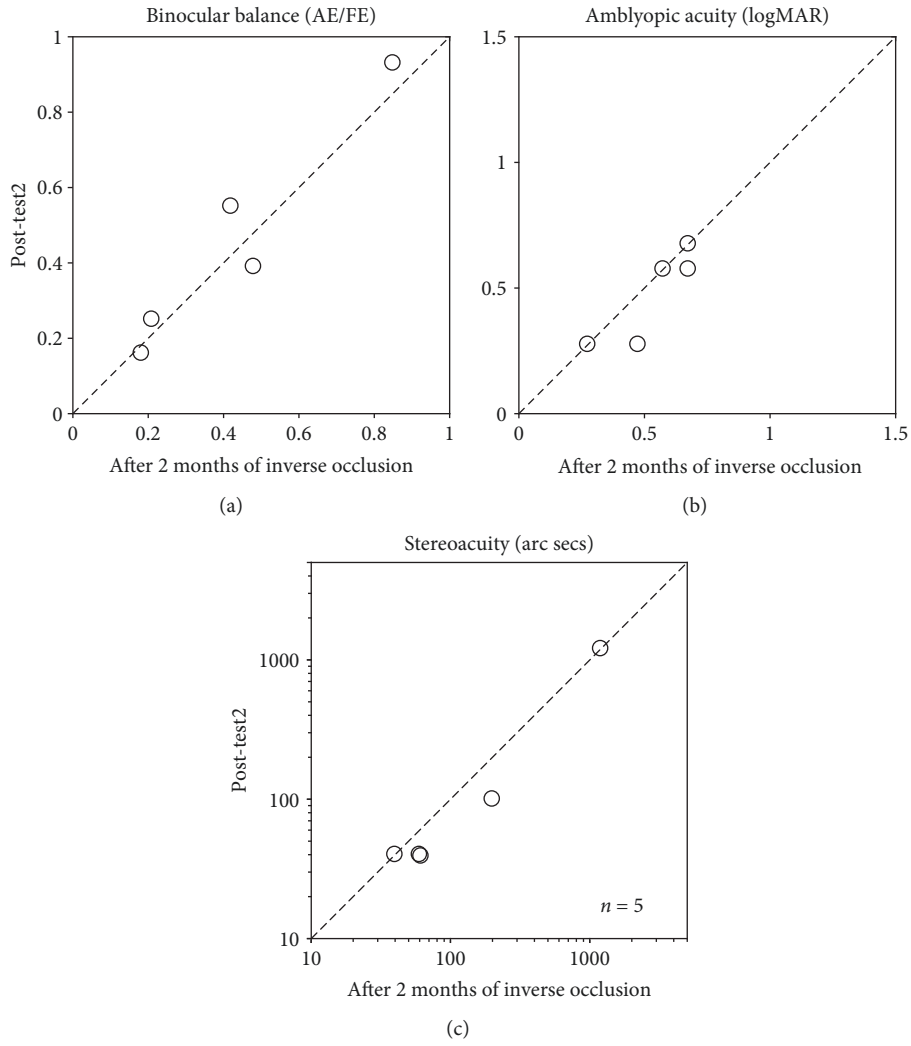

Figure 5: The visual outcomes could be sustained after finishing 2 months of inverse occlusion. Four patients (S12, S14, S16, and S17) were remeasured at 1 month and one patient (S9) at 5.5 months after the completion of 2 months of the reverse occlusion regime. Jitter points were used to avoid superimposing points in panel (c).

stereoacuity ($z = -1.94$, $p = 0.08$). Thus, there is no basis for believing that the gains we show here as the result of inverse occlusion were significantly impacted by refractive adaptation gains in visual acuity occurring beyond our 8-week refractive adaptation period.

4. Discussion

The rationale for this study comes from the recent findings on ocular dominance plasticity in normal and amblyopic adults [13–25]: short-term patching results in a strengthening of the contribution of the previously patched eye to binocular vision. This study, which applies this to amblyopia, raises three interesting issues that are relevant to the treatment of amblyopia. First, it highlights just how poor our understanding of the basis of classical occlusion therapy is. How is it that acuity improves in amblyopia regardless of which eye is occluded? This question does not just come from this study; there is a literature on the acuity improvements that occur as a result of inverse occlusion. While in most cases these improvements are much less than that of classical occlusion, there are studies [29, 30] where it is comparable to that of classical occlusion. The standard explanation of occluding the fixing eye to "force the amblyopic eye to work" is untenable. What is preventing the brain from using information from the amblyopic eye under normal viewing conditions? Whatever it is, occlusion must be preventing it from operating. If what is happening normally involves suppression of information (i.e., inhibition) from the amblyopic eye, then occlusion of the normal eye must be interrupting this process (i.e., disinhibition). The problem must be essentially binocular in nature, which is why it is not critically dependent on which eye is occluded to disrupt the anomalous interaction. We would normally think of this anomalous binocular interaction as a suppression of the amblyopic eye by the fellow eye, but on the basis of the occlusion of either eye being effective, it may be better to think of suppression as simply a reflection of a binocular imbalance. Recent psychophysics [42] and animal neurophysiology [43] suggest that the problem is not because the inhibition from

the fixing to the amblyopic eye is greater but because the matching inhibition from the amblyopic eye is less. It is due to a net imbalance in interocular inhibition. The resulting net imbalance can be disrupted by occluding either eye, and it is the duration of relief from this imbalanced binocular inhibition that may result in an acuity benefit for the amblyopic eye.

Ocular dominance plasticity in normals is an all-or-none, homeostatic process and would not be expected to have accumulated effects over time [44]. In amblyopes, ocular dominance plasticity has different dynamics, being much more sustained [25]. The present results suggest also that it can exhibit accumulated effects in amblyopes that result in long-lasting changes in eye balance. These sustained changes are however modest in size, and it will be necessary to explore how the magnitude of this effect can be increased for it to have significant binocular benefits. Future directions could involve RCT studies with a large number of patients and longer durations of occlusion, potentially with pharmacological enhancement using dopaminergic [45], serotonergic [46], or cholinergic modulations [47] or the combination of binocular training procedures [48–52] and short periods of inverse occlusion.

The finding that the binocular balance and the monocular acuity improvements from inverse patching are not correlated suggests that a simple explanation in terms of reduced suppression is not viable. The two visual improvements are likely to have separate causes and possibly involving different sites in the pathway. The acuity improvement for the amblyopic eye is not dependent on which eye is occluded, as shown here (Figure 4(b)), but the direction of the binocular balance changes is dependent on which eye is occluded [13, 25]. This distinction between binocular balance and monocular visual acuity is an important one and should be incorporated into future clinical treatment studies. Finally, apart from the additional benefit of a better binocular balance, which reflects an important first step in binocular vision restoration and the gains in monocular acuity and stereopsis, its applicability to older children and adults should not be underestimated nor should the better compliance that should follow from the patching of the amblyopic rather than the fixing eye. Application to younger children would necessitate weekly visits to ensure that the acuity in the amblyopic eye did not deteriorate as a result of patching.

4.1. Relevance of a Recently Published Study. During the writing up of this paper, another study was posted on bioRxiv that is highly relevant and supportive of the present approach (Lunghi et al. (2018); doi: 10.1101/360420). Lunghi et al. (2018) undertook a comparable inverse occlusion study in adults based on the similar notion that patching of an eye can improve its contrast gain subsequently, a result that they originally showed in normal humans [13] and we originally demonstrated in humans with amblyopia [25]. However, Lunghi et al. (2018) incorporated physical exercise as well as inverse occlusion and argue, based on a nonexercise control, that the combination of these two factors results in larger improvements when treating amblyopia. This in turn was based on their previous finding that exercise can enhance plasticity in normal adults ([18], but also see [23]). This published study and the current one both suggest that inverse occlusion can provide long-term benefits in visual acuity, stereopsis, and sensory balance. Lunghi et al. find that six 2-hour sessions of inverse occlusion ($n = 10$) combined with exercise result in a visual acuity improvement of 0.15 ± 0.02 logMAR, whereas in our initial experiment of 13 patients (S1 to S13), we find a comparable improvement (0.15 ± 0.04 logMAR) after 2 months of 2 hrs a day of patching. The shortest treatment duration that we used involved 14 days of 2 hrs/day inverse occlusion, and the acuity improvement was 0.06 ± 0.03 logMAR, similar to that found by Lunghi et al. for their nonexercise control (0.06 ± 0.01 logMAR). The exercise enhanced protocol seems to be beneficial over the short treatment duration tested (i.e., 6×2 hrs periods). It will be interesting for future studies to compare the duration-response curves for inverse occlusion with and without exercise to know if they are parallel or whether they converse at longer treatment durations.

4.2. Shortcomings of the Present Study. These are pilot results, which we hope will help power larger RCTs on the potential benefits of inverse occlusion. Most of our patients had anisometropic amblyopia; future studies would need to assess whether the effects are different in different types of amblyopia. The acuity results are modest, and while they are comparable to those found for classical patching for the same short treatment duration [40], it would need to be shown that longer treatment durations result in at least the same extra benefits that have been shown for classical occlusion [53]. The binocular balance changes, while in the right direction, are quite modest in magnitude, and it would need to be shown that longer treatment durations would result in stronger accumulated effects. If this can be shown, inverse occlusion would carry an additional binocular benefit over that of classical occlusion. Finally, no adverse effects were found from this relatively short treatment duration in this older age group; future studies would need to assess this for longer treatment durations and younger age groups.

5. Conclusions

We conclude that patching the amblyopic eye is safe for adults as well as old children with amblyopia and can result in recovery of visual acuity of the amblyopic eye and binocular visual functions.

Data Availability

The data used to support the findings of this study are available from the corresponding author upon request.

Disclosure

The sponsor or funding organization had no role in the design or conduct of this research.

Conflicts of Interest

The authors declare no competing interests.

Authors' Contributions

Jiawei Zhou and Zhifen He are co-first authors.

Acknowledgments

This work was supported by the National Natural Science Foundation of China grant NSFC 81500754, the Qianjiang Talent Project (QJD1702021), the Wenzhou Medical University grant QTJ16005, the Ministry of Human Resources and Social Security, China, grant to JZ, the Canadian Institutes of Health Research Grants CCI-125686 and 228103, the ERA-NET Neuron grant (JTC2015) to RFH, and the Natural Science Foundation of Zhejiang Province Grant (LQ18C090002) to ZY.

References

[1] C. De Buffon, *Disseration sur la cause du strabisme ou des yeux louches*, Me. Acad Roy Sci, Paris, 1743.

[2] Pediatric Eye Disease Investigator Group Writing Committee, "A randomized trial comparing Bangerter filters and patching for the treatment of moderate amblyopia in children," *Ophthalmology*, vol. 117, no. 5, pp. 998–1004.e6, 2010.

[3] The Pediatric Eye Disease Investigator Group, "A randomized trial of atropine vs patching for treatment of moderate amblyopia in children," *Archives of Ophthalmology*, vol. 120, no. 3, pp. 268–278, 2002.

[4] M. X. Repka, R. T. Kraker, J. M. Holmes et al., "Atropine vs patching for treatment of moderate amblyopia follow-up at 15 years of age of a randomized clinical trial," *JAMA Ophthalmology*, vol. 132, no. 7, pp. 799–805, 2014.

[5] Pediatric Eye Disease Investigator Group, "Randomized trial of treatment of amblyopia in children aged 7 to 17," *Archives of Ophthalmology*, vol. 123, no. 4, pp. 437–447, 2005.

[6] M. P. Wallace, C. E. Stewart, M. J. Moseley, D. A. Stephens, and A. R. Fielder, "Compliance with occlusion therapy for childhood amblyopia," *Investigative Ophthalmology & Visual Science*, vol. 54, no. 9, pp. 6158–6166, 2013.

[7] A. Searle, P. Norman, R. Harrad, and K. Vedhara, "Psychosocial and clinical determinants of compliance with occlusion therapy for amblyopic children," *Eye*, vol. 16, no. 2, pp. 150–155, 2002.

[8] E. E. Birch, "Amblyopia and binocular vision," *Progress in Retinal and Eye Research*, vol. 33, pp. 67–84, 2013.

[9] M. Fronius, L. Cirina, H. Ackermann, T. Kohnen, and C. M. Diehl, "Efficiency of electronically monitored amblyopia treatment between 5 and 16 years of age: new insight into declining susceptibility of the visual system," *Vision Research*, vol. 103, pp. 11–19, 2014.

[10] C. E. Stewart, M. J. Moseley, D. A. Stephens, and A. R. Fielder, "Treatment dose-response in amblyopia therapy: the Monitored Occlusion Treatment of Amblyopia Study (MOTAS)," *Investigative Ophthalmology & Visual Science*, vol. 45, no. 9, pp. 3048–3054, 2004.

[11] J. M. Holmes, R. W. Beck, R. T. Kraker et al., "Risk of amblyopia recurrence after cessation of treatment," *Journal of AAPOS*, vol. 8, no. 5, pp. 420–428, 2004.

[12] R. Bhola, R. V. Keech, P. Kutschke, W. Pfeifer, and W. E. Scott, "Recurrence of amblyopia after occlusion therapy," *Ophthalmology*, vol. 113, no. 11, pp. 2097–2100, 2006.

[13] C. Lunghi, D. C. Burr, and C. Morrone, "Brief periods of monocular deprivation disrupt ocular balance in human adult visual cortex," *Current Biology*, vol. 21, no. 14, pp. R538–R539, 2011.

[14] C. Lunghi, M. Berchicci, M. C. Morrone, and F. di Russo, "Short-term monocular deprivation alters early components of visual evoked potentials," *The Journal of Physiology*, vol. 593, no. 19, pp. 4361–4372, 2015.

[15] C. Lunghi, D. C. Burr, and M. C. Morrone, "Long-term effects of monocular deprivation revealed with binocular rivalry gratings modulated in luminance and in color," *Journal of Vision*, vol. 13, no. 6, 2013.

[16] C. Lunghi, U. E. Emir, M. C. Morrone, and H. Bridge, "Short--term monocular deprivation alters GABA in the adult human visual cortex," *Current Biology*, vol. 25, no. 11, pp. 1496–1501, 2015.

[17] C. Lunghi, M. C. Morrone, J. Secci, and R. Caputo, "Binocular rivalry measured 2 hours after occlusion therapy predicts the recovery rate of the amblyopic eye in anisometropic children," *Investigative Ophthalmology & Visual Science*, vol. 57, no. 4, pp. 1537–1546, 2016.

[18] C. Lunghi and A. Sale, "A cycling lane for brain rewiring," *Current Biology*, vol. 25, no. 23, pp. R1122–R1123, 2015.

[19] D. P. Spiegel, A. S. Baldwin, and R. F. Hess, "Ocular dominance plasticity: inhibitory interactions and contrast equivalence," *Scientific Reports*, vol. 7, no. 1, p. 39913, 2017.

[20] J. Zhou, D. H. Baker, M. Simard, D. Saint-Amour, and R. F. Hess, "Short-term monocular patching boosts the patched eye's response in visual cortex," *Restorative Neurology and Neuroscience*, vol. 33, no. 3, pp. 381–387, 2015.

[21] J. Zhou, S. Clavagnier, and R. F. Hess, "Short-term monocular deprivation strengthens the patched eye's contribution to binocular combination," *Journal of Vision*, vol. 13, no. 5, 2013.

[22] J. Zhou and R. F. Hess, "Neutral-density filters are not a patch on occlusion," *Investigative Ophthalmology & Visual Science*, vol. 57, no. 10, pp. 4450-4451, 2016.

[23] J. Zhou, A. Reynaud, and R. F. Hess, "Aerobic exercise effects on ocular dominance plasticity with a phase combination task in human adults," *Neural Plasticity*, vol. 2017, Article ID 4780876, 7 pages, 2017.

[24] J. Zhou, A. Reynaud, Y. J. Kim, K. T. Mullen, and R. F. Hess, "Chromatic and achromatic monocular deprivation produce separable changes of eye dominance in adults," *Proceedings of the Biological Sciences*, vol. 284, no. 1867, p. 20171669, 2017.

[25] J. Zhou, B. Thompson, and R. F. Hess, "A new form of rapid binocular plasticity in adult with amblyopia," *Scientific Reports*, vol. 3, article 2638, pp. 1–5, 2013.

[26] Y. Wang, Z. Yao, Z. He, J. Zhou, and R. F. Hess, "The cortical mechanisms underlying ocular dominance plasticity in adults are not orientationally selective," *Neuroscience*, vol. 367, pp. 121–126, 2017.

[27] Z. Yao, Z. He, Y. Wang et al., "Absolute not relative interocular luminance modulates sensory eye dominance plasticity in adults," *Neuroscience*, vol. 367, pp. 127–133, 2017.

[28] G. Andree, "Der Einfluß der inversen occlusion auf fixation und funktion amblyoper Augen," *Albrecht von Graefes Archiv für klinische und experimentelle Ophthalmologie*, vol. 170, no. 3, pp. 257–264, 1966.

[29] A. Arruga, "Effect of occlusion of amblyopic eye on amblyopia and eccentric fixation," *Transactions of the Ophthalmological Societies of the United Kingdom*, vol. 82, pp. 45–50, 1962.

[30] L. Cibis and C. Windsor, "Clinical results with passive amblyopia treatment," *The American Orthoptic Journal*, vol. 17, pp. 56–61, 1967.

[31] S. R. Malik, A. K. Gupta, S. Choudhry, and D. K. Sen, "Red filter treatment in eccentric fixation," *The British Journal of Ophthalmology*, vol. 52, no. 11, pp. 839–842, 1968.

[32] G. K. von Noorden, "Occlusion therapy in amblyopia with eccentric fixation," *Archives of Ophthalmology*, vol. 73, no. 6, pp. 776–781, 1965.

[33] M. Oliver, R. Neumann, Y. Chaimovitch, N. Gotesman, and M. Shimshoni, "Compliance and results of treatment for amblyopia in children more than 8 years old," *American Journal of Ophthalmology*, vol. 102, no. 3, pp. 340–345, 1986.

[34] D. G. Pelli, "The VideoToolbox software for visual psychophysics: transforming numbers into movies," *Spatial Vision*, vol. 10, no. 4, pp. 437–442, 1997.

[35] D. H. Brainard, "The psychophysics toolbox," *Spatial Vision*, vol. 10, no. 4, pp. 433–436, 1997.

[36] J. Ding and G. Sperling, "A gain-control theory of binocular combination," *Proceedings of the National Academy of Sciences of the United States of America*, vol. 103, no. 4, pp. 1141–1146, 2006.

[37] C. B. Huang, J. Zhou, Z. L. Lu, L. Feng, and Y. Zhou, "Binocular combination in anisometropic amblyopia," *Journal of Vision*, vol. 9, no. 3, p. 17, 2009, 1-16.

[38] J. Zhou, P.-C. Huang, and R. F. Hess, "Interocular suppression in amblyopia for global orientation processing," *Journal of Vision*, vol. 13, no. 5, p. 19, 2013, 1-14.

[39] J. Zhou, W. Jia, C. B. Huang, and R. F. Hess, "The effect of unilateral mean luminance on binocular combination in normal and amblyopic vision," *Scientific Reports*, vol. 3, no. 1, 2013.

[40] V. M. Manh, J. M. Holmes, E. L. Lazar et al., "A randomized trial of a binocular iPad game versus part-time patching in children aged 13 to 16 years with amblyopia," *American Journal of Ophthalmology*, vol. 186, pp. 104–115, 2018.

[41] L. Asper, K. Watt, and S. Khuu, "Optical treatment of amblyopia: a systematic review and meta-analysis," *Clinical & Experimental Optometry*, vol. 101, no. 4, pp. 431–442, 2018.

[42] J. Zhou, A. Reynaud, Z. Yao et al., "Amblyopic suppression: passive attenuation, enhanced dichoptic masking by the fellow eye or reduced dichoptic masking by the amblyopic eye?," *Investigative Ophthalmology & Visual Science*, vol. 59, no. 10, pp. 4190–4197, 2018.

[43] C. Shooner, L. E. Hallum, R. D. Kumbhani et al., "Population representation of visual information in areas V1 and V2 of amblyopic macaques," *Vision Research*, vol. 114, pp. 56–67, 2015.

[44] S. H. Min, A. S. Baldwin, A. Reynaud, and R. F. Hess, "The shift in ocular dominance from short-term monocular deprivation exhibits no dependence on duration of deprivation," *Scientific Reports*, vol. 8, no. 1, article 17083, 2018.

[45] S. Bao, V. T. Chan, and M. M. Merzenich, "Cortical remodelling induced by activity of ventral tegmental dopamine neurons," *Nature*, vol. 412, no. 6842, pp. 79–83, 2001.

[46] M. F. Bear and W. Singer, "Modulation of visual cortical plasticity by acetylcholine and noradrenaline," *Nature*, vol. 320, no. 6058, pp. 172–176, 1986.

[47] J. F. M. Vetencourt, A. Sale, A. Viegi et al., "The antidepressant fluoxetine restores plasticity in the adult visual cortex," *Science*, vol. 320, no. 5874, pp. 385–388, 2008.

[48] E. E. Birch, S. Li, R. M. Jost et al., "Binocular iPad treatment for amblyopia in preschool children," *Journal of American Association for Pediatric Ophthalmology and Strabismus*, vol. 18, no. 4, pp. e1–e2, 2014.

[49] K. R. Kelly, R. M. Jost, L. Dao, C. L. Beauchamp, J. N. Leffler, and E. E. Birch, "Binocular iPad game vs patching for treatment of amblyopia in children: a randomized clinical trial," *JAMA Ophthalmology*, vol. 134, no. 12, pp. 1402–1408, 2016.

[50] J. Li, B. Thompson, D. Deng, L. Y. L. Chan, M. Yu, and R. F. Hess, "Dichoptic training enables the adult amblyopic brain to learn," *Current Biology*, vol. 23, no. 8, pp. R308–R309, 2013.

[51] S. L. Li, A. Reynaud, R. F. Hess et al., "Dichoptic movie viewing treats childhood amblyopia," *Journal of AAPOS*, vol. 19, no. 5, pp. 401–405, 2015.

[52] L. To, B. Thompson, J. R. Blum, G. Maehara, R. F. Hess, and J. R. Cooperstock, "A game platform for treatment of amblyopia," *IEEE Transactions on Neural Systems and Rehabilitation Engineering*, vol. 19, no. 3, pp. 280–289, 2011.

[53] Pediatric Eye Disease Investigator Group, D. K. Wallace, E. L. Lazar et al., "A randomized trial of increasing patching for amblyopia," *Ophthalmology*, vol. 120, no. 11, pp. 2270–2277, 2013.